ROYAUME DU MAROC
Université Mohammed V - RABAT -
جامعة محمد الخامس - الرباط -
Faculté des sciences
كلية العلوم
CENTRE D'ETUDES DOCTORALES - SCIENCES ET TECHNOLOGIES

N° d'ordre : 3845

THÈSE

En vue de l'obtention du : **DOCTORAT**

Structure de Recherche : Physique des Hautes Energie-Modélisation et Simulation

Discipline : Physique.

Spécialité : Physique Théorique.

Présentée et soutenue le 30/09/2023 par :

Fadwa BENABDALLAH

Quantification and Characterization of Non-Classical Correlations: Exploring Beyond Entanglement for Advancements in Quantum Information Theory

JURY

Mohamed BENNAI	PES, Université Hassan II, Faculté des Sciences Ben M'Sik, Casablanca.	Président
Hamid EZ-ZAHRAOUY	PES, Université Mohammed V, Faculté des Sciences, Rabat.	Rapporteur/Examinateur
Morad ELBAZ	PES, Université Mohammed V, Faculté des Sciences, Rabat.	Rapporteur/Examinateur
Nabil HABIBALLAH	PH, Université Ibn Zohr, Faculté des Sciences Appliquée, Ait-Melloul.	Rapporteur/Examinateur
Rachid HOUCA	PH, Université Chouaïb Doukkali, Faculté des Sciences, El Jadida.	Examinateur
Mostafa MANSOUR	PH, Université Hassan II, Faculté des Sciences Aïn Chock, Casablanca.	Examinateur
Bouchra MAROUFI	PH, Université Ibn Tofail, Faculté des Sciences, Kénitra.	Examinateur
Mohammed DAOUD	PES, Université Ibn Tofail, Faculté des Sciences, Kénitra.	Directeur de thèse
Rachid AHL LAAMARA	PH, Université Mohammed V, Faculté des Sciences, Rabat.	Directeur de thèse

Année Universitaire : 2022/2023

DEDICATION

J'ai eu le plaisir et l'honneur d'interagir avec Madame **Amina OUAHMANN** et Monsieur **Najim TAHIRI** aux sujets des travaux pratiques d'électromagnétisme, de mécanique des solides, ainsi que de mécanique analytique et vibrations. Je tiens à les remercier chaleureusement pour leurs conseils avisés.

Je tiens à exprimer mes remerciements à toutes les personnes avec lesquelles j'ai pu discuter durant la préparation de cette thèse et qui m'ont apporté leur aide précieuse lorsque j'en avais besoin. Mes remerciements s'adressent tout particulièrement à **Rafael DRAMPYAN**, **Atta UR RAHMANN**, **Khadija EL ANOUZ**, **Jozef STRECKA**, **Saeed HADDADI** et **Neres ANANIKIAN** pour leur contribution significative. Leur soutien tout au long de ce parcours a été inestimable.

Finalement, je tiens à exprimer ma profonde reconnaissance et gratitude à mes chers parents, **Mohamed BENABDALLAH** et **Khadija ALCRDATE**. Sans leur soutien indéfectible, je ne serais absolument pas là où je suis aujourd'hui. Je les remercie du fond du cœur pour leur soutien constant, leur encouragement inconditionnel, et leur présence réconfortante à chaque étape de ma vie, même à distance. Je leur suis infiniment reconnaissante de tout ce que je suis devenue. Je souhaite également adresser mes sincères remerciements à ma précieuse sœur, **Souad BENABDALLAH**, à mon cher frère, **Othmane BENABDALLAH**. Votre soutien inestimable a été une véritable source de motivation et de réconfort pour moi.

Enfin, je tiens à exprimer ma profonde gratitude envers toutes les personnes, qu'elles soient proches ou éloignées, qui ont contribué de près ou de loin à la réalisation de cette étude. Votre soutien, vos conseils et votre aide précieuse ont été essentiels pour mener à bien ce travail. Je vous suis extrêmement reconnaissante de votre contribution et je vous adresse mes plus sincères remerciements.

REMERCIEMENTS

L'achèvement de cette thèse de doctorat a été une expérience véritablement transformative pour moi, ayant eu un impact profond sur ma vie. Je tiens à exprimer ma profonde gratitude aux nombreuses personnes qui m'ont soutenue et guidée tout au long de ce parcours. Sans leur appui, cette réalisation n'aurait pas été possible. À travers ces remerciements, j'ai maintenant l'occasion d'exprimer toute ma reconnaissance du fond du cœur.

En premier lieu, je tiens à exprimer ma profonde gratitude à Monsieur **El Hassan SAIDI**, Professeur de l'enseignement supérieur à la Faculté des Sciences de l'Université Mohammed V de Rabat. Grâce à son soutien généreux et à ses conseils avisés, j'ai réussi à intégrer avec succès le programme de Master en physique mathématique, qui m'a ouvert la voie à mon inscription au prestigieux programme de doctorat au sein du Laboratoire de Physique des Hautes Énergies, Modélisation et Simulation (LPHE-MS). Je suis très reconnaissante pour les précieux conseils et l'encouragement constant qu'il m'a prodiguée tout au long de mon parcours académique. Son enseignement durant mes années de Licence et de Master Physique Mathématique a été d'une qualité exceptionnelle, nourrissant ma passion pour le sujet et élargissant mes horizons intellectuels.

Mes remerciements vont aussi solennellement à mon parrain scientifique et mon directeur de thèse externe Monsieur **Mohammed DAOUD**, Professeur de l'enseignement supérieur à la Faculté des Sciences de l'Université Ibn Tofail de Kénitra. Il a consacré beaucoup d'efforts pour me guider et m'orienter afin d'achever ce travail de manière exemplaire. C'est avec beaucoup de gentillesse et une large disponibilité que j'en témoigne publiquement en sa faveur. C'est aussi avec beaucoup de patience, d'esprit d'écoute et de discussion constructive qu'il m'a accompagné lors de l'ensemble des étapes de conception et d'élaboration de cette thèse. Au-delà de ses qualités académiques, je suis profondément reconnaissante pour ses qualités humaines. Les preuves d'ouverture, de patience, d'humanité et de modestie qu'il m'a toujours exprimées, m'ont redonné espoir et m'ont encouragé à poursuivre mes travaux et à persévérer pour terminer ma thèse de manière optimale. Sa présence constante, ses encouragements et son soutien indéfectible ont été d'une valeur inestimable pour moi. De plus, il m'a accordé la liberté nécessaire pour développer mes travaux de recherche tout en me prodiguant des conseils éclairés. Je lui suis également reconnaissante pour la qualité de son enseignement lors de la préparation du master, marquée par sa grande compétence et sa passion pour le sujet. Sans son soutien indéfectible, cette thèse n'aurait jamais pu voir le jour. Je lui suis infiniment reconnaissante pour tout ce qu'il a fait pour moi et pour sa contribution significative à mon parcours académique et professionnel.

Je souhaite exprimer mes chaleureux remerciements à mon directeur de thèse interne Monsieur **Rachid AHL LAAMARA**, Professeur Habilité à la Faculté des Sciences de l'Université Mohammed V de Rabat, qui m'a non seulement dirigé vers l'équipe de l'information quan-

tique de LPHE-MS, mais a également accepté avec bienveillance d'être mon directeur de thèse. Je tiens à lui exprimer ma gratitude pour son soutien inconditionnel, sa disponibilité et ses précieux conseils qui m'ont guidée tout au long de cette aventure. Sans ses nombreuses propositions constructives, ce travail n'aurait certainement pas pu aboutir. J'aimerais aussi le remercier chaleureusement de m'avoir donné l'opportunité d'assurer les travaux pratiques sur l'électromagnétisme dans le vide et la mécanique des solides, ainsi que pour son enseignement de bonne qualité durant notre formation dans le Master Physique Mathématique. Sa générosité et son expertise ont indéniablement enrichi ma formation académique et je me sens honorée d'avoir pu bénéficier de ses connaissances.

Mes salutations vont également à Monsieur **Mohamed BENNAI**, Professeur de l'enseignement supérieur à la Faculté des Sciences Ben M'Sik de l'Université Hassan II de Casablanca. Je suis profondément reconnaissante qu'il ait accepté de présider le jury pour mon humble travail. Ses précieux conseils, ses discussions enrichissantes, ses encouragements constants et sa motivation sans faille ont été d'une aide inestimable tout au long de cette expérience.

Je tiens également à remercier Monsieur **Hamid EZ-ZAHRAOUY**, Professeur de l'enseignement supérieur à la Faculté des Sciences de l'Université Mohammed V de Rabat, d'avoir accepté d'être rapporteur de ma thèse malgré ses activités débordantes. De plus, je tiens à le remercier sincèrement pour son enseignement du module de mécanique quantique lors de ma Licence et de mon Master, ainsi que pour avoir été mon encadrant lors du projet de fin d'études de Licence. Sa grande compétence et son expertise ont grandement contribué à enrichir ma compréhension de ce domaine complexe. Je vous prie d'accepter, Monsieur, l'expression de mon respect et de ma profonde gratitude.

Je suis extrêmement reconnaissante envers Monsieur **Morad ELBAZ**, Professeur d'études supérieures à la Faculté des Sciences de Rabat, pour l'honneur qu'il m'a fait en acceptant de faire partie du jury de ma soutenance en tant que rapporteur. Je tiens également à exprimer ma gratitude pour la qualité de son enseignement du module physique statistique tout au long de notre formation en licence. Enfin, je le remercie chaleureusement pour ses précieux conseils.

Je remercie vivement Monsieur **Nabil HABIBALLAH**, Professeur Habilité à la Faculté des Sciences Appliquées Ait-Melloul de l'Université Ibn Zohr d'Agadir, de m'avoir fait l'honneur de participer au jury de ma soutenance en tant que rapporteur, ainsi que d'avoir enduré les difficultés du voyage d'Agadir à Rabat pour accompagner les membres du jury de cette thèse. Je tiens également à le remercier pour ses discussions pertinentes lors des rencontres scientifiques dans le domaine de l'information quantique. Ces échanges enrichissants ont élargi ma perspective et approfondi ma compréhension de ce domaine passionnant. Je suis reconnaissante de pouvoir bénéficier de son expertise et de sa contribution aux avancées scientifiques dans ce domaine.

Mes chaleureux remerciements s'adressent à Monsieur **Mostafa MANSOUR**, Professeur Habilité à la Faculté des Sciences Ain Chock de l'Université Hassan II de Casablanca. Je suis extrêmement reconnaissante qu'il ait accepté d'examiner mon travail de recherche et de faire partie du jury de thèse. Sa participation et son expertise ont été d'une importance cruciale pour l'évaluation de mon travail. De plus, je souhaite exprimer ma gratitude pour la qualité de son enseignement lors de notre formation dans le Master Physique Mathématique. Ses cours ont été extrêmement enrichissants et ont grandement contribué à approfondir mes connaissances dans ce domaine.

Par la même occasion, je suis également reconnaissante à Monsieur **Rachid HOUCA**, Professeur Habilité à la Faculté des Sciences de l'Universiité Chouaib Eldoukali d'El Jadida pour avoir accepté de faire partie des membres du jury de cette thèse. Je le remercie pour son intérêt et sa responsabilité en tant qu'examinateur ainsi que pour avoir supporté les difficultés du voyage d'El Jadida à Rabat pour être avec les membres du jury de cette thèse.

Mes remerciements chaleureux s'adressent à Madame **Bouchra MAROUFI**, Professeur

Habilité à la Faculté des Sciences de l'Université Ibn Tofail de Kénitra, pour avoir accepté d'être membre du jury en tant que examinatrice et pour avoir évalué ce travail. Madame je vous prie d'accepter l'expression de mon respect et de ma profonde gratitude.

Je suis profondément reconnaissante à tous les membres du jury qui ont bien voulu me faire l'honneur d'assister à ma soutenance afin d'évaluer et juger la qualité de ce travail. Je leur suis redevable pour leurs précieux commentaires.

RÉSUMÉ

Le domaine multidisciplinaire de l'informatique quantique et du traitement de l'information vise à comprendre comment l'information peut être traitée selon les lois de la physique quantique. Des ressources non classiques telles que l'intrication, la corrélation quantique et la cohérence sont utilisées dans le calcul, ce qui rend les protocoles d'informatique quantique supérieurs à l'informatique classique traditionnelle. Cependant, des défis subsistent pour améliorer l'efficacité et vaincre les échecs associés à la technologie quantique. Ainsi, l'exploitation de ces ressources dans les systèmes quantiques composites est cruciale pour optimiser et assurer la transmission sécurisée ainsi que la préservation de l'information quantique. Cette thèse propose une étude approfondie sur la théorie des ressources quantiques des corrélations quantiques, y compris le concept d'intrication et les corrélations non classiques au-delà de l'intrication. Il présente divers outils théoriques de quantification de ces ressources et explore les relations intrinsèques entre elles. Une application directe de ces ressources, à savoir la mise en œuvre des protocoles de téléportation quantique est également évoquée. La thèse comprend également des contributions à la dynamique exacte de ces ressources quantiques dans différents modèles de systèmes quantiques ouverts et des stratégies pour éliminer les effets de décohérence et préserver les corrélations quantiques pour améliorer l'information quantique et les protocoles informatiques.

Mots-clés: Intrication quantique, corrélation quantique, discorde quantique, incertitude quantique, cohérence quantique, information de Fisher quantique, téléportation quantique, fidélité, systèmes quantiques ouverts, décohérence.

ABSTRACT

The multidisciplinary field of quantum computing and information processing aims to understand how information can be processed according to the laws of quantum physics. Non-classical resources such as entanglement, quantum correlation, and coherence are used in computation, making quantum computing protocols superior to traditional classical computing. However, several challenges remain in improving the efficiency and overcoming failures associated with quantum technology. Thus, exploiting these resources in composite quantum systems is crucial to optimize and ensure the secure transmission of information. Besides, quantifying as well as characterizing quantum correlations is a key role in relating practical applications to theoretical concepts. However, encoding information in quantum states depends on the nature of the coupling with the environment. This coupling generates entanglement between the system and its environment, leading to the decoherence of the quantum system. Therefore, controlling the environment to minimize decoherence remains a significant challenge for developing robust and evolutionary quantum information processing systems.

This thesis proposes a deeper study of the quantum resource theory of quantum correlations, including the concept of entanglement and quantum coherence. It presents the theoretical tools needed to quantify these resources. For this purpose, various mathematical approaches are discussed to solve associated problems, and analytical results for high-dimensional composite quantum systems are presented. In addition, the intrinsic relationships between these non-classical resources are investigated by extracting the connections that unite the corresponding measurements. A direct application of these quantum correlations is the implementation of quantum teleportation protocols, which require robust information storage to teleport particles with optimal fidelity. In this regard, this thesis provides an overview of quantum teleportation schemes using maximally mixed states as a quantum channel instead of maximally entangled states. This thesis also includes contributions to the exact dynamics of these resources in different models of open quantum systems. A key objective of this study is to investigate the effects of the environment on these non-classical correlations and to obtain techniques to protect them from the destructive effects generated by the environment in quantum systems used for information encoding. By analyzing ways to eliminate decoherence effects and preserve quantum correlations, this study offers concrete strategies to improve quantum information and computing protocols.

Keywords: Quantum entanglement, quantum correlation, quantum discord, quantum uncertainty, quantum coherence, quantum Fisher information, quantum teleportation, fidelity, open quantum systems, decoherence.

RÉSUMÉ DÉTAILLÉ

Le domaine complexe de l'informatique quantique et du traitement de l'information constitue une quête profonde visant à percer les mystères de la manipulation de l'information en harmonie avec les principes fondamentaux de la physique quantique. Il s'agit d'une discipline audacieuse qui repose sur des concepts et des ressources non classiques, tels que l'intrication, les corrélations quantiques et la cohérence, pour réaliser des calculs et des traitements de l'information d'une manière qui transcende les limites de l'information classique traditionnelle.

Ces ressources quantiques confèrent aux protocoles d'information quantique un avantage substantiel, ouvrant la porte à des calculs beaucoup plus puissants et à des protocoles de communication sécurisée révolutionnaires. Cependant, malgré les progrès réalisés, des défis demeurent, et la technologie quantique n'est pas sans imperfections. Les obstacles persistent, entravant l'efficacité des systèmes quantiques et provoquant des échecs technologiques. Par conséquent, l'exploration et l'exploitation continues de ces ressources au sein de systèmes quantiques complexes demeurent essentielles pour perfectionner la transmission sécurisée de l'information.

Une autre dimension cruciale de cette recherche est la quantification et l'identification des corrélations quantiques présentes dans les systèmes quantiques. Cela ne sert pas seulement des fins théoriques, mais crée également des ponts essentiels entre les concepts abstraits et les applications pratiques de l'information quantique.

Cependant, il convient de noter que l'encodage de l'information dans des états quantiques est intrinsèquement lié à l'environnement. L'interaction entre le système quantique et son environnement crée de l'intrication, mais elle génère également la décohérence, ce qui peut perturber le système quantique. Par conséquent, l'art de maîtriser l'environnement pour minimiser la décohérence demeure l'un des défis les plus critiques dans la quête du développement de systèmes de traitement de l'information quantique robustes et évolutifs.

La thèse présentée ici représente un jalon significatif dans cette recherche continue. Elle plonge profondément dans la théorie des ressources quantiques, mettant en lumière les outils théoriques nécessaires pour quantifier ces ressources complexes. Cette exploration se nourrit de diverses approches mathématiques pour résoudre des problèmes ardus. De plus, la thèse offre des résultats analytiques pour des systèmes quantiques de haute dimension, étendant ainsi la portée de la recherche. Elle établit également des liens intrinsèques entre ces ressources quantiques, identifiant les connexions qui relient les mesures correspondantes. Une application directe de ces ressources est la téléportation quantique, un processus qui nécessite un stockage fiable de l'information pour garantir le transfert parfait des particules quantiques.

Dans ce contexte, la thèse explore des schémas de téléportation quantique innovants qui reposent sur des états mélangés au maximum comme ressources quantiques, plutôt que sur des états maximallement intriqués. De plus, elle contribue à la compréhension de la dynamique de

ces ressources quantiques dans divers modèles de systèmes quantiques ouverts, tenant compte des influences de l'environnement.

L'objectif central de cette étude est de mieux comprendre les effets de l'environnement sur les ressources quantiques et de développer des techniques pour les protéger des perturbations environnementales nuisibles. En explorant des moyens de contrer la décohérence et de préserver les précieuses corrélations quantiques, cette étude ouvre la voie à des stratégies concrètes pour améliorer l'information quantique et les protocoles informatiques. Elle nous rapproche ainsi de percées significatives dans le domaine en constante évolution de l'informatique quantique.

Ce travail est structuré en six chapitres, chacun consacré à des aspects spécifiques de la théorie quantique et de ses applications :

Chapitre 1 : Jette les bases en exposant les principes fondamentaux de la théorie quantique, y compris les concepts de qubits, l'entropie de von Neumann, et la théorie de l'information classique. Ce chapitre établit les fondements nécessaires à la compréhension de la théorie de l'information quantique.

Chapitre 2: Plonge dans le concept d'intrication quantique, détaillant les critères pour distinguer les états séparables des états intriqués, ainsi que les techniques de mesure de l'intrication quantique pour les systèmes quantiques.

Chapitre 3 : Ce chapitre se penche sur les corrélations non-classiques qui vont au-delà de l'intrication, en mettant particulièrement l'accent sur la discorde quantique. Il explore diverses métriques pour quantifier ces corrélations.

Chapitre 4 : Il approfondit l'étude des métriques alternatives de type discorde, utilisées pour évaluer les corrélations quantiques dans différents contextes. Ce chapitre discute de leurs propriétés et de leurs applications pratiques, y compris la téléportation quantique.

Chapitre 5 : Ce chapitre traite de la théorie des systèmes quantiques ouverts, qu'ils soient markoviens ou non-markoviens. Il aborde également la décohérence quantique, qui explique la transition du comportement non classique au comportement classique des systèmes quantiques.

Chapitre 6 : Présente nos contributions originales dans le domaine, mettant en valeur nos recherches et leur impact. Enfin, ce manuscrit de thèse se termine par un résumé complet qui met en évidence les principales idées développées tout au long de ce travail. Nous fournissons également des perspectives éclairantes pour des recherches futures, suggérant des domaines potentiels pour des recherches plus approfondies.

Mots-clés: Intrication quantique, corrélation quantique, discorde quantique, incertitude quantique, cohérence quantique, information de Fisher quantique, téléportation quantique, fidélité, systèmes quantiques ouverts, décohérence.

LISTE OF PUBLICATIONS

Publications included in the content of this thesis

1. F. Benabdallah and M. Daoud, *"Dynamics of quantum discord based on linear entropy and negativity of qutrit-qubit system under classical dephasing environments"*, Eur. Phys. J. D **75** (2021) 3.

2. F. Benabdallah, S. Haddadi, H. Arian Zad, M. Reza Pourkarimi, M. Daoud, N. Ananikian, *"Pairwise quantum criteria and teleportation in a spin square complex"*, Sci. Rep. **12** (2022) 6406.

3. F. Benabdallah, K. El Anouz, J. Strecka and M. Daoud, *"Thermal non-classical correlation via skew information, quantum Fisher information, and quantum teleportation of a spin-1/2 Heisenberg trimer system"*, Eur. Phys. J. Plus **137** (2022)1096 432.

4. F. Benabdallah, K. Elanouz and M. Daoud, *"Toward the relationship between local quantum Fisher information and local quantum uncertainty in the presence of intrinsic decoherence"*, Eur. Phys. J. Plus (2022) 548.

5. F. Benabdallah, A. Ur Rahman, S. Haddadi and M. Daoud, *"Long-time protection of thermal correlations in a hybrid-spin system under random telegraph noise"*, Phys. Rev. **E** 106 (2022) 034122.

Publications beyond the scope of this thesis

1. F. Benabdallah, A. Slaoui and M. Daoud, *"Quantum discord based on linear entropy and thermal negativity of qutrit-qubit mixed spin chain under the influence of external magnetic field"*, Quant. Inf. Process **19** (2020) 252.

2. F. Benabdallah, H. Arian Zad. M. Daoud and N. Ananikian, *"Dynamics of quantum correlations in a qubit-qutrit spin system under random telegraph noise"*, Phys. Scr. **96** (2021) 125116.

3. F. Benabdallah, K. El Anouz, A. Ur Rahman, M. Daoud, A. El Allati, and S. Haddadi, *"Witnessing Quantum Correlations in a Hybrid Qubit-Qutrit System Under Intrinsic Decoherence"*, Fortschr. Phys. (2023) 2300032.

LIST OF FIGURES

1.1 Shows a mechanism for broad communication, in a general chematic manner. . . 8

1.2 Binary Shannon entropy $\mathcal{H}(Q)$ plotted versus Q. 9

1.3 (a) Venn diagram for the mutual information $\mathcal{I}(M, N)$. (b) Relationships between the mentioned entropies and mutual information. 12

1.4 Information channel capacity $\mathcal{C}$ of two random variable M and N. 13

1.5 Summary of postulates. 18

1.6 Quantum measurement of a qubit. 20

1.7 A qubit can be represented by any two-level quantum system, for example: electron spin (spin up and down). 22

1.8 Geometric representation of a qubit in a Bloch sphere. 24

2.1 A schematic representation of the PPT and NPT states for the Hilbert spaces $2 \otimes 2$, $2 \otimes 3$, and $3 \otimes 2$ is shown in (a) and for higher dimensions Hilbert spaces in (b). 38

2.2 Schematic illustration of the entanglement witness. (a): The set of all states is divided into a convex set of separable states (Light Blue) and entangled states (Magenta). (b): The witness operator defines a hyperplane (Blue line) for all states that satisfy $\langle W \rangle = 0$. All separable states (Light Blue) as well as some entangled states that are represented by beige stars satisfy the property $\langle W \rangle > 0$. States with negative expectation $\langle W \rangle < 0$ are the quantum states detected by the witness, i.e, the ones represented by yellow stars. 39

2.3 Schematic illustration of the relative entropy entanglement. 45

3.1 Schematic description of the quantum discord based on a distance measurement $\mathcal{D}_p(\rho_{AB}, \rho_{cq})$. 61

4.1 A schematic illustration of the standard quantum teleportation protocol 98

4.2 A schematic illustration of the quantum teleportation protocol using a mixed quantum state ρ_X as a quantum resource. 101

5.1 A schematic representation of the interaction between the system and its environment. 112

5.2 In Markovian dynamics (a), there is only a one-way information flow from system S to environment E, and any encoded information in the system cannot be recovered during its evolution. On the other hand, in non-Markovian dynamics (b), the system can experience information backflow, where the flow of information reverses from environment E to system S for one or more time intervals. This is a unique feature of non-Markovian dynamics. 114
5.3 Schematic illustration showing the action of the quantum dynamical map. 114

LIST OF TABLES

1.1 Properties of entropies. 28

5.1 The basic characteristics of the three pictures, namely Schrödinger, Heisenberg, and interaction pictures as well as the connection between them. 110
5.2 Markovian vs non-Markovian dynamics. 127

CONTENTS

DEDICATION i

REMERCIEMENTS ii

RÉSUMÉ v

ABSTRACT vi

RÉSUMÉ DÉTAILLÉ vii

LISTE OF PUBLICATIONS ix

GENERAL INTRODUCTION 1

1 ELEMENTS OF QUANTUM INFORMATION THEORY 7

1 Classical information theory . . . 8
1.1 Shannon entropy . . . 8
1.2 Relative entropy . . . 9
1.3 Joint entropy and conditional entropy . . . 10
1.4 Mutual information . . . 11
1.5 Channel capacity . . . 12
2 Quantum mechanics . . . 13
2.1 State space description . . . 13
2.2 Density operator formalism . . . 14
2.2.1 Density operator for pure states . . . 14
2.2.2 Density operator for mixed states . . . 14
2.3 Density operator properties . . . 15
2.4 Postulates of quantum mechanics . . . 17
2.5 Reduced density operator . . . 18
2.6 Quantum measurements . . . 19
2.6.1 Projective measurements . . . 19
2.6.2 Positive Operator Valued Measurements . . . 21
3 Quantum information theory . . . 21
3.1 Qubit and Bloch sphere . . . 22
3.1.1 Bit to qubit . . . 22
3.1.2 Geometric demonstration of qubit state . . . 23

3.2 von Neumann entropy . . . 24
3.2.1 Definition . . . 24
3.2.2 von Neumann's entropy properties . . . 25
3.3 Joint, conditional and relative quantum entropy . . . 26
3.4 Quantum mutual information . . . 26
3.5 Tsallis entropy . . . 27
4 Conclusion . . . 28

2 QUANTUM ENTANGLEMENT: A COMPREHENSIVE STUDY OF MEASURES 30
1 Quantum entanglement . . . 31
1.1 Separability and entanglement . . . 31
1.2 Example of entangled states . . . 32
1.3 Local operations and classical communication . . . 33
2 Separability criteria . . . 33
2.1 Seprability criteria for pure states: Schmidt decomposition . . . 34
2.2 Purification . . . 36
2.3 Separability criteria for mixed states . . . 36
2.4 Peres-Horodecki criterion . . . 36
2.5 Entanglement witnesses . . . 38
3 Entanglement measures for bipartite systems . . . 40
3.1 Requirements for entanglement measures . . . 40
3.2 Entanglement entropy . . . 42
3.3 Entanglement of formation . . . 42
3.4 Concurrence . . . 43
3.5 Relative entropy entanglement . . . 45
3.6 Negativity . . . 45
3.7 Logarithmice negativity . . . 47
4 Entanglement measure for tripartite systems . . . 48
4.1 Tripartite Negativity . . . 48
4.2 Tangle . . . 49
5 Conclusion . . . 49

3 QUANTUM DICORD BASED NON-CLASSICAL CORRELATIONS 51
1 Classical and quantum correlated states . . . 52
2 Entropic quantum discord . . . 53
2.1 Defintion and properties . . . 53
3 Analytical expressions of the entropic quantum discord . . . 55
3.1 Quantum discord for X-states . . . 55
3.2 Koashi-Winter relation . . . 58
4 Geometric Quantum Discord . . . 60
4.1 Geometric Quantum Discord based on Hilbert-Schmidt distance . . . 62
4.1.1 For two-qubit quantum states . . . 62
4.1.2 For qubit-qudit quantum states . . . 64
4.2 Geometric quantum discord based on trace-norm . . . 66
5 Linear entropy-based quantum discord . . . 67
5.1 Analytical expression of linear quantum discord for arbitrary two-qubit states . . . 69
5.2 Von Neumann entropy-based quantum discord for rank-2 two-qubit states 71

5.3 Analytical expression of linear quantum discord for arbitrary qudit-qubit states . . . 72
6 Measurement induced disturbance . . . 75
7 Conclusion . . . 77

4 RETHINKING QUANTUM CORRELATIONS AND THE POTENTIAL OF QUANTUM TELEPORTATION 78
1 Skew information . . . 80
1.1 Definition . . . 80
1.2 Skew information properties . . . 81
2 Local quantum uncertainty for arbitrary qubit-qudit systems . . . 82
3 Local quantum uncertainty for multipartite quantum systems . . . 87
4 Uncertainty-induced quantum nonlocality . . . 90
5 Quantum coherence . . . 91
6 Quantum Fisher information . . . 92
6.1 Local quantum Fisher information . . . 93
7 Interplay between local quantum Fisher information and local quantum uncertainty . . . 95
8 Quantum teleportation . . . 97
8.1 Standard quantum teleportation protocol . . . 98
8.2 Scheme of quantum teleportation . . . 100
8.3 Fidelity of Entanglement Teleportation . . . 102
8.4 Quantum teleportation via three-qubit system . . . 103
9 Conclusion . . . 104

5 DYNAMICS OF OPEN QUANTUM SYSTEMS 106
1 Closed quantum systems . . . 107
1.1 For pure states . . . 107
1.2 For mixed states . . . 108
1.3 Interaction picture . . . 109
2 Open quantum systems . . . 111
2.1 Description of open quantum systems . . . 111
2.2 Markovian and non-Markovian dynamics . . . 113
3 Deriving the evolution of open quantum systems using Kraus operators and dynamical maps . . . 114
3.1 Properties of quantum channels with Kraus operators . . . 117
3.2 Kraus representation for general initial conditions . . . 118
3.2.1 For separable states . . . 118
3.2.2 For general initial quantum states . . . 119
4 Standard theory of Markovian open quantum systems . . . 120
4.1 Markovian master equation . . . 120
4.2 Microscopic derivation in the weak coupling limit . . . 121
4.3 Born approximation . . . 122
4.4 Markov approximation . . . 123
4.5 Secular approximation . . . 123
5 Non-Markovian dynamics . . . 126
6 Intrinsic decoherence . . . 127
7 Conclusion . . . 129

6 CONTRIBUTIONS **130**
1 Contribution 1: Dynamics of quantum discord based on linear entropy and negativity of qutrit-qubit system under classical dephasing environments 130
1.1 Summary of contribution 1 130
1.2 Content of contribution 1 130
2 Contribution 2: Pairwise quantum criteria and teleportation in a spin square complex 146
2.1 Summary of contribution 2 146
2.2 Content of contribution 2 146
3 Contribution 3: Thermal non-classical correlation via skew information, quantum Fisher information, and quantum teleportation of a spin-1/2 Heisenberg trimer system 159
3.1 Summary of contribution 3 159
3.2 Content of contribution 3 159
4 Contribution 4: Toward the relationship between local quantum Fisher information and local quantum uncertainty in the presence of intrinsic decoherence . . . 178
4.1 Summary of contribution 4 178
4.2 Content of contribution 4 178
5 Contribution 5: Long-time protection of thermal correlations in a hybrid-spin system under random telegraph noise 197
5.1 Summary of contribution 5 197
5.2 Content of contribution 5 197

GENERAL CONCLUSION AND OUTLOOK **214**

BIBLIOGRAPHY **218**

GENERAL INTRODUCTION

The beauty and wonder of nature have fascinated scientists and philosophers for centuries. From this fascination, a fundamental interest in understanding natural phenomena has driven scientific inquiry. Every physical system and process is subjected to the laws of nature which form the basis of scientific investigation. Quantum physics, developed in the early 20th century, provides a comprehensive framework for understanding the behavior of elementary particles and the fundamental forces that govern their interactions. So far, a remarkable success in making predictions that have been achieved and confirmed by experiments has made it one of the most successful and accomplished theories in the field of physics. At the microscopic scale, the behavior of particles such as atoms and electrons is inherently different from that described by classical physics laws, such as Newtonian mechanics and Maxwell's electromagnetic theory. In classical physics, particles move along deterministic trajectories, and their velocity and acceleration can be determined from their positions. On the other hand, at the microscopic level, particles behave probabilistically, and the wave function that describes the way they move provides the density of the probabilities for identifying a particle at a particular position [1]. This has led to the development of a new set of mathematical tools and conceptual frameworks for understanding quantum phenomena.

Quantum mechanics has not only deepened our understanding of the microscopic world but has also led to a range of technological advancements that have transformed modern society. The development of the transistors, nuclear power, the lasers, magnetic resonance imaging, and the electron microscope are just a few examples of how quantum physics has practical applications. Moreover, quantum mechanics has been instrumental in shaping our understanding of particle physics, quantum field theory, quantum statistical physics, material physics, and other branches of modern physics which form the basis of all modern electronics. Furthermore, quantum science has gone beyond physics to transform our understanding of information, paving the way for new and revolutionary information technologies. The development of quantum computers and the quantum internet has the potential to revolutionize the way we process and communicate information. Despite its tremendous success, the foundations of quantum mechanics remain a subject of scientific and philosophical debate. Ongoing research continues to uncover new and exciting insights into the behavior of quantum systems and to address the challenges of reconciling quantum mechanics with our understanding of the macroscopic world.

On a fundamental level, the peculiar characteristics of quantum systems, such as indeterminacy and nonlocality, continue to pose significant challenges for the scientific community across various domains. The quantum mechanical theory remains relying upon the measurements, which are crucial for both theoretical and experimental investigations in information theory. However, unlike in classical mechanics, quantum measurements can cause disruptions and unavoidably affect the measured system. The concept of indeterminacy emerges from

these unique aspects of quantum systems have profound implications for our understanding of the physical world and presents ongoing research opportunities to deepen our knowledge of quantum mechanics.

Einstein, Podolsky, and Rosen (EPR) argued that quantum measurements have an impact on a system that challenges classical local realism. They recognized that due to the intricate nature of a system, measuring one of its subsystems affects the outcome of measurements made on the other sub-systems. This is in contrast to local realism, which suggests that the quantum states of non-interacting particles that are spatially separated are independent [2]. The contradiction in their argument has led to questioning the completeness of quantum mechanics, and it stems from their adherence to local realism [3]. The concept of entanglement, also known as *"spooky action at a distance"*, arises from the principle of superposition. In an entangled multipartite quantum system, the individual subsystems are strongly correlated with one another, even if they are separated by a significant distance and no longer interact. As a result, the composite quantum system behaves as a single system and can be described by a definite pure state. However, this description is no longer valid for the state of its sub-systems.

Recently, the Nobel Prize in Physics has been awarded to A. Aspect, J.F. Clauser, and A. Zeilinger for quantum entanglement experiments [4]. Entanglement is a unique quantum phenomenon that explores the correlations among separate points of a multipartite system that has no classical analog. It is recognized as a fundamental physical feature in quantum information science, as it enables a range of useful tasks [5, 6]. Experimental achievements have demonstrated the ability to entangle six or eight ions [7, 8], and to entangle six to ten qubits using photons [9, 10]. In addition, nuclear and electronic spins have been entangled in diamonds [11]. These systems have the advantage of allowing for the individual addressing of their constituents. Furthermore, large-scale entangling operations were conducted on 10^5 two-state atoms in optical lattices [12]. Similarly, the entanglement of 10^7 atoms has been accomplished in cold atomic clouds using spin-squeezing techniques [13]. Such systems offer the benefit of collective measurement. With the continuous improvement of quantum control techniques, it is highly likely that even larger systems will be entangled in the near future. It is worth noting that various quantum correlation measuring tools are explored in the previous scientific studies to capture the level of intricacy in the system. The most widely recognized ones include entanglement of formation [14], concurrence [15], and negativity [16].

Up to the last few years, it was widely believed that quantum correlations were strongly connected to the notion of entanglement, and the manipulation of quantum information was considered within the context of *"entanglement-separability"* [6]. However, several studies have shown that the entanglement remains not the only meaningful version of non-classical correlations that can be used for implementing quantum protocols. Recently, it was found that there are quantum correlations that exist beyond entanglement that also offer some advantages, for example, quantum nonlocality without entanglement [17,18]. In addition, it was shown theoretically [19–21], and later experimentally [22], that certain separable states can outperform their classical counterparts in specific tasks. Consequently, there is a growing interest in exploring, characterizing, and quantifying non-classical correlations more broadly.

The first attempts for investigating the notion of quantum correlations beyond entanglement are made by Ollivier and Zurek [23], and later by Henderson and Vedral [24]. They focused on studying these correlations from a measurement perspective and introduced a novel concept known as quantum discord. This metric served as a measure of non-classical correlations [25,26], proving to be an invaluable tool for characterizing the intricate dynamics between quantum systems. This concept has garnered significant attention within the field of quantum theory [21, 27–29]. It quantifies the non-classical correlations between different components of a quantum state [29]. Additionally, it is compatible with the idea of pure-state entanglement, which is acknowledged as an invaluable asset for quantum computing [21]. However, studying

quantum discord poses several challenges and open questions such as the complexity of its quantification. Formally, it is the distinction between complete correlation, also known as quantum mutual information, and the greatest mutual information that a quantum system is capable of gauging. To quantify the classical correlations, an optimization process through all the local measurements is required [25,26]. Calculating the entropic quantum discord is particularly challenging due to the involved optimization procedure [30–32], and analytical solutions are limited to specific families of two-qubit quantum states [33–35]. To address this issue, other alternative metrics are proposed to quantify the level of quantumness. This includes the geometric quantum discord (GQD) [36–38], linear entropy quantum discord (LEQD) [32,39], measurement-induced disturbance (MID) [40], local uantum uncertainty (LQU) [41], uncertainty induced nonlocality (UIN) [42], local quantum Fisher information (LQFI) [43], etc. Although the majority of these quantum correlation quantifiers display comparable behaviors for mixed states and agree for pure states, there are additionally small variations, and their physical meanings vary. Therefore, characterizing the quantum correlations of a system from different perspectives is necessary to fully understand their properties.

Information theory is a fundamental concept that encompasses the storage, transmission and processing of information using physical carriers, which can range from electromagnetic signals to particles such as atoms or photons. When the physical carriers are quantum systems, they form the basis of quantum information theory. This field has opened up new possibilities for information processing and communication. Quantum information science is a fast-growing research discipline, due to the special characteristics of quantum systems, notably quantum superposition and entanglement. Quantum correlations beyond entanglement constitute a fascinating theme that remained a highly debated topic among quantum information and computing analysts [5, 44]. They are recognized as good resources in several areas of quantum information science, including quantum teleportation [45, 46], fractional computations [47], quantum key distribution [48], quantum sensing [49], quantum speed limit time [50], and so forth. For this reason, the quest for such non-classical correlations that exist beyond entanglement remained an amazing new frontier for quantum theorists and experimentalists to explore [51, 52]. Hence, many analytical tools, simulation techniques, and several other methods have been investigated to compute and quantify quantum correlations to explore the separability of bipartite quantum systems [53, 54]. Despite significant progress in quantum information theory, the question of what kinds of correlations are truly quantum remains unanswered. This question underscores the need for continued testing and nourishment of the field. Ultimately, the benefits of quantum information theory are significant, and its continued advancement will undoubtedly lead to exciting new discoveries and innovations in the field of information science.

A promising application of quantum mechanics within the realm of quantum sciences is so-called non-local teleportation. Teleportation involves transferring objects between different locations without physically moving them. Although teleportation has often been depicted in science fiction, it was not until 1993 that Bennett *et al.* demonstrated a process that could occur in the field of quantum mechanics [45]. They demonstrated that it is feasible to transfer a particle's quantum state from one place to a different one using the concept of quantum correlations. This finding holds great potential for quantum information, particularly for the transfer of data between quantum computers. It is crucial to stress that quantum teleportation is unable to produce faster-than-light communication between the parties. This is due to the protocol relying on transferring classical information between two locations, and classical signals are restricted by the speed of light. However, it has been proved that it is possible to contract a quantum computer where qubit operations are performed using teleportation [55,56]. According to the quantum information theory, teleportation highlights the value of entanglement as a valuable resource. Besides, it demonstrated that there is a potential connection between classical information, specifically, the results of measurements, and quantum informa-

tion, which refers to the state of a qubit. Particularly, teleportation shows that by using a shared entangled state and a two-bit classical information channel, two parties can achieve the same result as having a quantum information channel. In other words, they can transfer the original state directly between them [5, 45]. The first successful teleportation of the polarization states of photons was reported in 1997 [57]. Since then, quantum teleportation has been demonstrated using a variety of quantum systems, including photonic qubits [58, 59], trapped ions [60], nuclear spins [61] and solid-state qubits [62]. The distance over which states can be teleported varies greatly for different techniques, ranging from a typical distance of $1\mathring{A}$ for nuclear magnetic resonance (NMR) teleportation [63] to the transfer of photon polarizations between any grounded terminal and a dynamic satellite in 2017 [64]. Although, the distance is a vital factor to take into account when comparing different teleportation schemes, it is also crucial to take into account the efficiency of the different alternatives. The success probability of a teleportation scheme is quantified by efficiency. According to the original teleportation proposal, an effciency of 100% is possible [45], while different implementations have different efficencies.

However, quantum systems are inherently open and sensitive to interactions with their surrounding environments [65]. Even a well-isolated system, its interactions with ancillary or interface systems can cause it to lose its characteristic quantum traits, namely coherence, fidelity, non-classical correlations in the composite systems, and so on [66]. Although these interactions are necessary to store, read, evolve, and a pure state manipulation of the quantum system coherently, eliminating outside noise interference is a difficult task that requires exceptional care. The process of losing coherence due to environmental interactions, known as decoherence, is the primary challenge for realizing quantum information and computation protocols [5]. The preservation and manipulation of quantum states to achieve desired outcomes pose a significant challenge in the field of quantum engineering. Achieving robust storage of quantum states over extended periods and accurately evolving them according to specific targets require sophisticated techniques and technologies. Several investigations have explored quantum correlation dynamics using different classes of decoherence to regulate and control the effect of decoherence [5]. One significant result is the entanglement sudden death (ESD), which is the complete loss of the amount of entanglement within finite time [53, 54]. On the other hand, several decoherence models have investigated the impact of both Markovian and non-Markovian settings on generalized quantum and classical correlation phenomena [53, 54, 67–69]. Their findings reveal that quantum correlation is generally more resilient to the external noise and avoid exhibiting the phenomenon of sudden death in Markovian channels [53, 54, 67–69]. However, quantum discord, which is a general metric of quantum correlation, instantaneously vanishes in non-Markovian environments [70]. Additionally, the freezing dynamics of entanglement is another intriguing phenomenon that occurs in some specific situations [53, 54, 68, 69, 71]. Quantum correlations specifically degrade to a limited, greater than zero level and then abruptly halt, leaving the system to maintain its stable entanglement. The Schrödinger equation cannot adequately capture the dynamics of an open system connected to its environment; therefore, an additional generic solution must be used. Given the various degrees of freedom in the surroundings, the concept of accessible quantum systems permits the construction of a broad group of time-influenced solutions known as master equations [72]. For the sake of simplicity, approximations such as the Markovian approximation are often used to examine and characterize open quantum systems by focusing on two main components: the Born or weak coupling approximation and the Markov approximation [73, 74]. In cases where the open system is strongly coupled with its surroundings and correlations between them are highly presented, the non-Markovian approach is considered, but it should be noted that the non-Markovian dynamic is still not fully understood [75].

Spin-chain frameworks are versatile systems that have been extensively studied for their

ability to shed light on various physical phenomena and their prospective important applications regarding the field of quantum sciences. These applications include studying quantum phases, phase transitions, quantum communication, and so forth. Recently, there has been a particular interest in understanding the Heisenberg spin chain models. For example, in a recent study [76], researchers used this coupling as an effective marker to detect transitions. In addition, the application of this model has shown success in generating entangled networks from partially entangled states, as well as in teleportation as well as dense coding based on thermal entanglement [32, 77–80]. In the realm of quantum information processing, spin chains have garnered significant attention, especially in investigating quantum data transmission over microscopic distances. They are considered powerful entities used for transmitting information between two locations, enabling the construction of quantum buses to relate various computer-hardware parts [81]. The Heisenberg spin chain model is particularly noteworthy, as it is considered the most promising solutions for overcoming the negative impact of decoherance caused by the environment on quantum systems. This is due to its ability to preserve and maintain nonclassical correlations over extended periods, making it a potential solution for addressing the challenges of quantum information processing in practical situations [53, 54, 69, 79, 80].

Nonclassical correlations, or quantum correlations, are unique and indispensable features of quantum systems that set them apart from their classical counterparts. These correlations emerge from the interaction between distinct quantum subsystems and represent a new resource for performing tasks that are either impossible or highly inefficient in the classical world. Consequently, quantum correlations have become the cornerstone of the field of quantum information science, providing the basis for the development of technologies that push the boundaries of classical computing. To date, quantum resources are very important in all quantum information protocols. This thesis focuses mainly on characterizing and quantifying nonclassical correlations, exploring their inherent connections and their roles in enhancing the implementation of quantum information protocols. To achieve these goals, we present our work in a book-like structure that provides technical details for researchers to better understand our results. Along with an overview of the key developments of quantum correlations and understanding their behavior under decoherence, we aim to summarize and reformulate calculations scattered throughout a large body of literature as well as provide our own results. In order to accomplish this purpose, we will structure our thesis as follows:

In the first chapter 1 of this work, an introduction of the fundamental principles of quantum theory is given. We delve into key concepts such as the qubit and its geometric representation, as well as the von Neumann entropy and its entities. To accomplish this, we first review the essentials of classical information theory, including Shannon entropy, joint, relative, and conditional entropy. This allows us to extend our understanding of the quantum framework, where these concepts take on new meaning and relevance. Following this, we then present the mathematical tools of quantum mechanics, specifically the Hilbert space, quantum measurements, and the formalism of the density operator. Through this comprehensive exploration, we aim to equip readers with a solid understanding of the fundamental concepts and mathematical tools necessary to delve deeper into the field of quantum information theory.

In the second chapter 2, the resource-based concept of quantum entanglement is the subject of most attention. We go through different standards for separating separable states from entangled states for both pure and mixed states. Then, we give a thorough analysis of a few parameters that are employed to determine the level of entanglement existing in bipartite and multipartite quantum systems. This phase in the analysis of quantum systems is crucial because it allows us to accurately evaluate the degree of entanglement that exists in a particular quantum state.

In the third chapter 3, our attention turns to non-classical correlations that go beyond quantum entanglement. Specifically, we will delve into the concept of quantum discord, pro-

viding its definition, properties, and analytical expression for some specific cases in two-qubit states. We will explore alternative approaches to handling the analytical difficulties encountered with the optimization process of this metric. This includes using geometric quantum discord based on the Hilbert-Schmidt norm, as well as the Schatten 1-norm. A special interest is devoted to using linear entropy instead of von Neumann entropy for maximizing classical correlations, thus providing a closed formula for quantum discord in an arbitrary qubit-qudit system. Finally, we will discuss another entropic quantum correlation measuring tool, known as a measurement-induced disturbance.

Chapter 4 is dedicated to exploring various discord-like metrics of quantum correlations, which serve as alternative measures for quantifying quantum correlations beyond the quantum discord for arbitrary quantum systems. These measures are based on different notions, such as skew information, quantum coherence, and quantum Fisher information. We provide a thorough analysis of their properties and mathematical methods used in analytical calculations, as well as their practical usefulness in quantum sciences. Furthermore, we investigate quantum teleportation as a direct application of quantum correlations, where we discuss the standard protocol and its implementation. In particular, we focus on how quantum correlations has a crucial part in the successful implementation of quantum teleportation, highlighting the significance of these measures in real-world quantum communication systems.

Chapter 5 presents a comprehensive overview of the accessible quantum systems theory, covering both Markovian and non-Markovian aspects. We examine the mathematical framework and essential properties necessary for presenting dynamical maps that describe open system dynamics in detail, with a specific focus on quantum Markovian systems. The chapter's primary objective is to introduce the theory of quantum decoherence and explain how it can account for the shift between non-classical to classical behavior.

Chapter 6 presents our original contributions to the field, showcasing our research and its impact. Finally, this thesis manuscript concludes with a comprehensive summary that highlights the main ideas developed throughout this work. We also provide insightful perspectives for future research, suggesting potential areas for further investigation.

CHAPTER 1

ELEMENTS OF QUANTUM INFORMATION THEORY

In 1948, Claude Shannon developed the classical information theory, which makes the assumption that information is encoded in physical systems that are evolving in accordance with classical physics laws [82, 83]. In the context of transmitting information via a channel like a telephone communicating wire, Shannon constructed a very basic abstract communication model as the basis for his theory. This paradigm offers a mechanism to quantify the amount of information and may be used in a variety of contexts for all forms of information processing and transmission protocols. Additionally, it allows us to set restrictions on the complexity or expense of operations like information storage or data transmission through noisy channels.

To take advantage of the physical properties of various phenomena in physical systems for information coding, much attention has been devoted to studying them. This is because of the idea that information is believed to be associated with a physical representation and that the storage, manipulation, and transmission of information are all subject to the laws of physics [84].

In contrast, through specific selections of a quantum process and the quantum system's state, it becomes possible to derive the principles of classical mechanics from the underlying principles of quantum mechanics. This implies that, as an approximation, classical theory emerges as a result of quantum theory. In this respect, it would appear more appropriate to inquire, how these quantum physics principles might be applied to measure, communicate and exchange information in the microscopic structures of matter from the relevant non-classical state identified using a set of physical quantities [85].

Quantum information theory was developed to explore the nature of information in the quantum regime and to reveal new information processing capabilities [86]. By preserving information and correlations beyond what is possible in conventional models and incorporating the magical ingredient of non-classical science, specifically the rules of superposition and entanglement. This new theory is of utmost importance for enhancing security and reliably transmitting the information.

To explore the implications of non-classical physics on information theory, it is useful to first establish a foundation in the fundamentals of classical information theory. This will allow us to analyze and determine the necessary modifications required in scenarios where quantum effects play a significant role. Consequently, this chapter begins with an introduction to a few fundamentals of classical information theory. In the second section, we will provide a quick introduction of the fundamental concepts and essential techniques of quantum mechanics used across the whole dissertation. These include the method of measurement used to display the

states and operations of quantum systems on Hilbert spaces. Afterward, we move to provide the concepts and mathematical foundations of quantum theory.

1 Classical information theory

The theory of Classical information was laid by Claude Shannon toward the end of the 40s [82], to study and solve problems of communication or transmission of signals through channels. In this model, the data is defined in the context of ambiguity and is expressed mathematically within a probabilistic paradigm [87–89]. According to this idea, uncertainty arises from how much information a physical system carries. According to Shanon, Fig.1.1 depicts a broad plan for an overall interaction procedure. The communication that will be transmitted to the receiving terminal is created by a source of data. The sender then transforms the data into an electrical impulse that can be transmitted over the medium of the channel. A noise contributor may tamper with the signal throughout transfer, leading the signal that was received to differ from the initial signal. The receiver then estimates the message and delivers it to the intended destination based on the received signal. In classical information theory, bits (classical binary bits) are the most fundamental unit of storage of data in computing and digital communication that could be either "0" or "1" [90]. Throughout this section, we will deal with the concept of classical information, in which we will give a brief review of the well-known Shannon entropy as well as some other useful entropy notions such as joint entropy, mutual information, and conditional entropy. Their important mathematical properties are also discussed to lay the foundation for introducing and discussing quantum information theory.

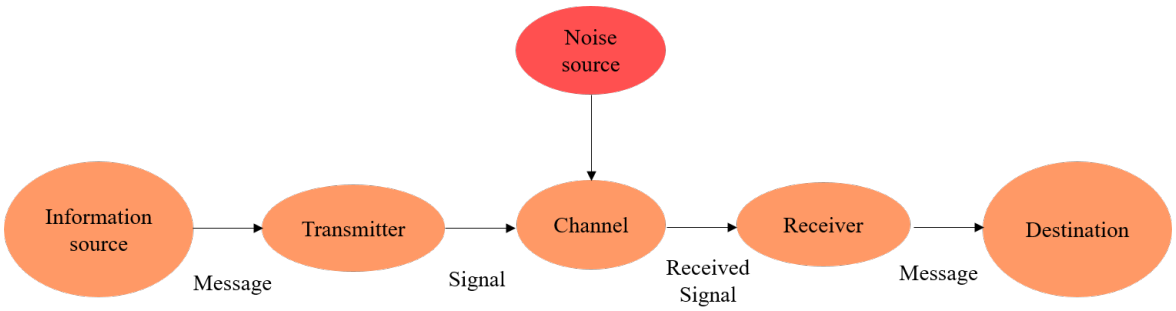


Figure 1.1: Shows a mechanism for broad communication, in a general chematic manner.

1.1 Shannon entropy

Clausius pioneered the concept of entropy in thermodynamic systems for the first time in 1854 [91]. Shannon formulated a statistical entropy in the field of information communication and transmission theory [82]. It is formally analogous to the Boltzmann entropy [92], which can be used to establish a causal explanation based on the statistical description of both macro and microsystems that depart from the dynamics of microscopic components of a system, for example, that of molecules [93]. In addition, Shannon's entropy is a core principle in information theory that characterizes disorder or uncertainty in a random source as well as the average missing information. Assume M is an arbitrary discrete variable taking value in a set $\{m_i\}$ that occurs with corresponding distribution probability function $\{p(m_i)\}$, the relative entropy of the parameter M is formally defined as [82]

$$\mathcal{H}(M) = -\sum_{m_i \epsilon \chi} p(m_i) \log(p(m_i)), \tag{1.1}$$

with the convention $0 \log_2 0 \equiv 0$. Henceforth, the log is taken to be base-2 since the basic unit of information is the bit. We note that the entropy is a non-negative quantity. Moreover, it is independent of the specific values $\{m_i\}$ assumed by the random variable, instead relying particularly on the probability distribution set $\{p(m_i)\}$.

A concrete example of Shannon entropy is the scenario of a binary random variable M, also known as a Bernoulli variable. This variable has two possible outcomes with respective probabilities, namely,

$$M = \begin{cases} 1 & \text{having probability } Q, \\ 0 & \text{having probability } 1-Q. \end{cases}$$

In this situation, Eq.(1.1) simply reduces to the function of binary-entropy defined as

$$\mathcal{H}(M) = -Q \log Q - (1-Q) \log(1-Q) = \mathcal{H}(Q). \tag{1.2}$$

For $Q = \frac{1}{2}$, the entropy reaches its maximum value, while it is zero for $Q = 0$ and $Q = 1$. This appears to be very logical given that there does not exist ambiguity regarding the random factor for $Q = 0$ or $Q = 1$, resulting in no information to disclose its result. Whenever the two occurrences are equivocal, the greatest uncertainty, information, and entropy are attained (see Fig.1.2).

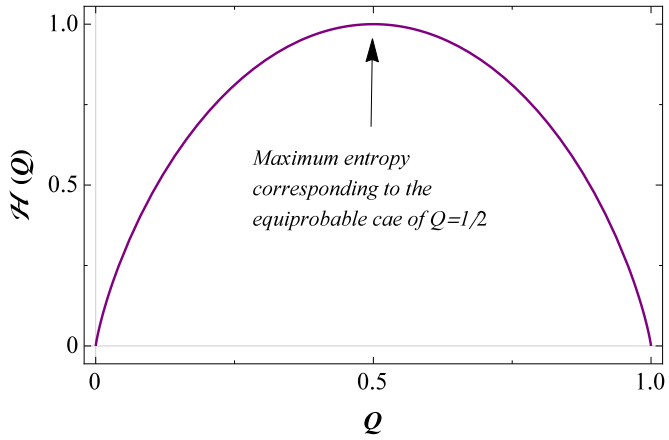


Figure 1.2: Binary Shannon entropy $\mathcal{H}(Q)$ plotted versus Q.

1.2 Relative entropy

Take into account two distinct probabilities distributions, namely $\{p(m_i)\}$ and $\{q(m_i)\}$, over M being a random variable admits values from the set $\{m_i\}$. The so-called relative entropy, also referred to as the Kullback-Leiber divergence [94], is an entropy-like measure of the distance between two probabilities distributions. In addition, it measures the level of information or uncertainty contained in one probability distribution with respect to the other. It is defined as follows:

$$\mathcal{H}(p(m)||q(m)) = -\sum_{m_i \epsilon \chi} p(m_i) \log\left(\frac{q(m_i)}{p(m_i)}\right) = -\mathcal{H}(m) - \sum_{m_i \epsilon \chi} p(m_i) \log\left(q(m_i)\right). \tag{1.3}$$

It is interesting to note that the relative entropy defined in Eq.(1.3) is not necessarily symmetric, that is, $\mathcal{H}(p(m)||q(m)) \neq \mathcal{H}(q(m)||p(m))$. Moreover, it is always a non-negative quantity, i.e., $\mathcal{H}(p(m)||q(m)) \geq 0$ with the equality is achieved only when $p(m) = q(m)$ for all values of $\{m_i\}$.

In order to prove this property, we employ the following inequality: $\log(m)\ln 2 = \ln m \leq m-1$. Thus, we have

$$\begin{aligned}
\mathcal{H}(p(m)||q(m)) &= -\sum_{m_i \epsilon \chi} p(m_i) \log\left(\frac{q(m_i)}{p(m_i)}\right) \\
&\geq \frac{1}{\ln 2}\sum_{m_i \epsilon \chi} p(m_i)\left(1-\frac{q(m_i)}{p(m_i)}\right) \\
&= \frac{1}{\ln 2}\sum_{m_i \epsilon \chi} (p(m_i)-q(m_i)) \\
&= \frac{1}{\ln 2}(1-1) = 0. \qquad (1.4)
\end{aligned}$$

The property discussed above regarding the relative entropy provides an explanation for its recognition as a measure of distance between two distributions in the field of information theory.

1.3 Joint entropy and conditional entropy

Consider a pair of discrete random variables (M, N) that take values from the set $\{m_i\}$ ($\{n_i\}$) with a joint probability distribution denoted as $p(m, n)$. The joint entropy measures the total amount of uncertainty associated with the two random variables M and N taken together [95]. Mathematically, it is defined as follows:

$$\mathcal{H}(M, M) = -\sum_{m\epsilon\chi}\sum_{m\epsilon\gamma} p(m, n)\log_2\left(p(m, n)\right). \qquad (1.5)$$

Notice that it is a symmetric function, that is, $\mathcal{H}(M, N) = \mathcal{H}(N, M)$. Besides, if M and N are not dependent, i.e., $p(m, n) = p(m)p(n)$, then the joint entropy can be written as a sum of Shannon entropies of each variable. Such that

$$\begin{aligned}
\mathcal{H}(M, N) &= -\sum_{m\epsilon\chi}\sum_{n\epsilon\gamma} p(m)p(n)\log_2\left(p(m)p(n)\right) \\
&= -\sum_{m\epsilon\chi}\sum_{n\epsilon\gamma} p(m)p(n)\log_2\left(p(m)\right) - \sum_{m\epsilon\chi}\sum_{n\epsilon\gamma} p(m)p(n)\log_2\left(p(n)\right) \\
&= \sum_{n\epsilon\gamma} p(n)\mathcal{H}(M) + \sum_{m\epsilon\chi} p(m)\mathcal{H}(N) \\
\mathcal{H}(M, N) &= \mathcal{H}(M) + \mathcal{H}(N). \qquad (1.6)
\end{aligned}$$

Likewise, one can determine the average amount of missing information on a random variable M when the information of another random variable N is known perfectly. This average is known as the conditional entropy, which captures the amount of uncertainty that remains about M, given N. It is defined as

$$\mathcal{H}(M|N) = -\sum_{m\epsilon\chi}\sum_{n\epsilon\gamma} p(m, n)\log_2\left(p(m|n)\right), \qquad (1.7)$$

where $p(m, n) = p(m)p(n|m)$ defines conditional probability distribution and it is an antisymmetric function ($\mathcal{H}(M|N) \neq \mathcal{H}(M|N)$). However, the conditional entropy and the joint entropy

are linked via the following entropy chain rule:

$$\begin{aligned}
\mathcal{H}(M,N) &= -\sum_{m\epsilon\chi}\sum_{n\epsilon\gamma} p(m,n)\log_2\left(p(m,n)\right) \\
&= -\sum_{m\epsilon\chi}\sum_{n\epsilon\gamma} p(m,n)\log_2\left(p(m)p(n|m)\right) \\
&= -\sum_{m\epsilon\chi}\sum_{n\epsilon\gamma} p\left(m,n\right)\log_2\left(p(m)\right) - \sum_{m\epsilon\chi}\sum_{n\epsilon\gamma} p(m,n)\log_2\left(p(n|m)\right) \\
&= -\sum_{m\epsilon\chi} p\left(m\right)\log_2\left(p\left(m\right)\right) - \sum_{m\epsilon\chi}\sum_{n\epsilon\gamma} p(m,n)\log_2\left(p(n|m)\right) \\
\mathcal{H}(M,N) &= \mathcal{H}\left(M\right) + \mathcal{H}\left(N|M\right). \qquad (1.8)
\end{aligned}$$

This characteristic holds significant importance in the field of quantum information theory, as it allows us to recover classical concepts within the quantum realm. Moreover, the equation $\mathcal{H}\left(M\right)+\mathcal{H}\left(N|M\right) = \mathcal{H}\left(N\right)+\mathcal{H}\left(M|N\right)$ demonstrates the symmetry of information, highlighting the balanced relationship between the marginal entropies and the conditional entropies.

1.4 Mutual information

Another important concept in classical information theory is mutual information [96, 97]. It measures the mutual dependence between the joint random variables (M, N). More specifically, it measures the reduction of the amount of uncertainty about M having knowledge of N and vice versa. Furthermore, it is defined as the relative entropy (1.3) between the joint probability distribution $p\left(m,n\right)$ and the product probability distribution of each variable $p\left(m\right)p\left(n\right)$. This gives

$$\mathcal{I}\left(M,N\right) = \mathcal{H}\left(p\left(m,n\right)||p(m)p\left(n\right)\right) = \sum_{m\epsilon\chi}\sum_{n\epsilon\gamma} p(m,n)\log_2\left(\frac{p(m,n)}{p(m)p(n)}\right). \qquad (1.9)$$

In this way, the above expression (1.9) can be rewritten in terms of joint entropy and conditional entropy as

$$\begin{aligned}
\mathcal{I}(M,N) &= \sum_{m\epsilon\chi}\sum_{n\epsilon\gamma} p(m,n)\log_2\left(\frac{p(m,n)}{p(m)p(n)}\right) \\
&= \sum_{m\epsilon\chi}\sum_{n\epsilon\gamma} p(m,n)\log_2\left(\frac{p(m|n)}{p(m)}\right) \\
&= -\sum_{m\epsilon\chi}\sum_{n\epsilon\gamma} p(m,n)\log_2\left(p(m)\right) + \sum_{m\epsilon\chi}\sum_{n\epsilon\gamma} p(m,n)\log_2\left(p(m|n)\right) \\
&= -\sum_{m\epsilon\chi} p(m)\log_2\left(p(m)\right) - \left(-\sum_{m\epsilon\chi}\sum_{y\epsilon\gamma} p(m,n)\log_2\left(p(m|n)\right)\right) \\
\mathcal{I}(M,N) &= \mathcal{H}(M) - \mathcal{H}(M|N). \qquad (1.10)
\end{aligned}$$

By using Eq.(1.8), we do have that

$$\mathcal{I}(M,N) = \mathcal{H}(M) + \mathcal{H}(N) - \mathcal{H}(M,N). \qquad (1.11)$$

The mutual information is used to quantify the total correlations between two random variables, namely M and N. It satistifes the following important properties:

- $\mathcal{I}(M,N) = 0$, if M and N are independent;
- symmetry, i.e., $\mathcal{I}(M,N) = \mathcal{I}(N,M)$;

- self-information: $\mathcal{I}(M, M) = \mathcal{H}(M)$;
- non-negativity, i.e., $\mathcal{I}(M, N) \geq 0$.

The connections between the basic measures of Shannon theory: the mutual information $\mathcal{I}(M, N)$, the joint entropy $\mathcal{H}(M, N)$, the conditional entropy $\mathcal{H}(M|N)$ and Shannon entropies $\mathcal{H}(M)$ and $\mathcal{H}(N)$ of the random variables M and N are expressed in the **Venn diagram** (see Fig.1.3). Notice that the overlap between the two circles filled corresponds to the mutual information in M about N and vice versa.

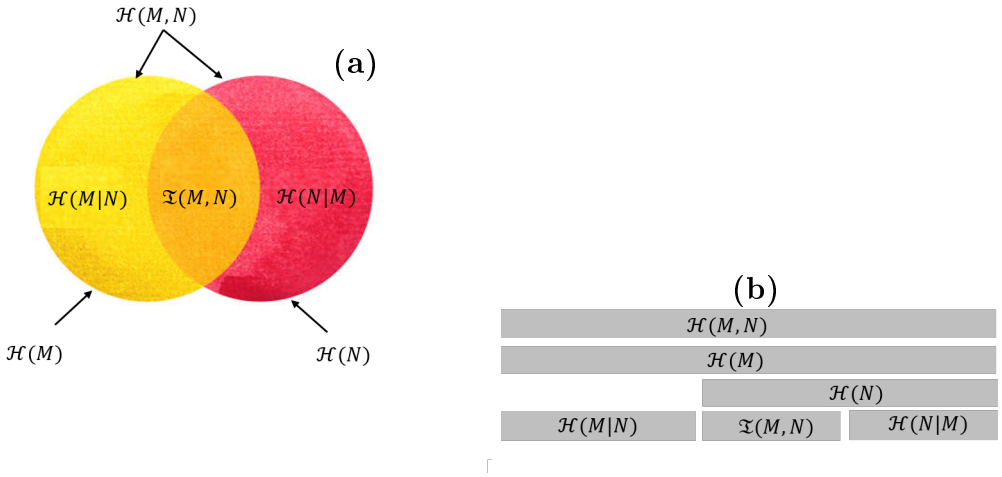


Figure 1.3: (a) Venn diagram for the mutual information $\mathcal{I}(M, N)$. (b) Relationships between the mentioned entropies and mutual information.

1.5 Channel capacity

The determination of the upper and lower bounds of noisy channel capacity is one of the primary goals in the information theory. Indeed, a classical information transfer from sender to receiver in such a way that the channel is memoryless if the transfer is intact and undisturbed. A noisy classical channel develops when the classical system interacts with another system [98]. In this regard, suppose a sender, Alice, intends to deliver classical information to a receiver, Bob, through a classical communication channel with an associated input alphabet M, by presenting all conceivable messages by arranging the channel in various classical states (see Fig.1.4). Then Bob will recover the information by measuring the channel with a related output alphabet N. Therefore, the communication channel possesses a measure of mutual information, denoted as $\mathcal{I}(M, N)$, which quantifies the relationship between the input signal M and the received output N. Consequently, Bob's capacity to retrieve Alice's message accurately is determined by the maximization of mutual information between the input and output channels over all possible input probability distributions $p(m)$. Such that

$$\mathcal{C} = \max_{p(m)} \mathcal{I}(M, N) = \max_{p(m)} \left(\mathcal{H}(M) - \mathcal{H}(M|N)\right), \tag{1.12}$$

where the maximum in Eq.(1.12) is applied over all possible information sources employed as channel input.

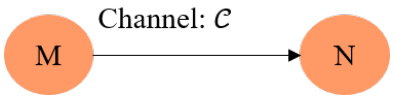


Figure 1.4: Information channel capacity $\mathcal{C}$ of two random variable M and N.

2 Quantum mechanics

On a macroscopic scale, the general descriptive framework for natural occurrences can be built using the fundamental laws of classical physics. In this way, the phenomena that eventually manifest in nature adhere to the classical physics cardinal principles. Quantum mechanics, on the other hand, describes the exchange of energy between matter and energy, as well as the resulting interaction and properties of atoms and subatomic particles, at a microscopic scale. Through this section, we review the basic mathematical tools of quantum mechanics used in this thesis to describe the state of the system such as space state, density matrix formalism and quantum measurements.

2.1 State space description

The state of a system is determined by the information that is accessible regarding its properties. This information can be obtained by measuring relevant physical quantities known as observables, which include energy, position, momentum, spin, and other related quantities. Any isolated physical system in quantum mechanics is connected with a Hilbert space $\mathcal{H}$, often known as the space of states. For an n-dimensional vector space with an orthogonal basis $\{|\mathcal{V}_i\rangle\,, i = 0, \ldots, n-1\}$, the state vectors of these systems are described mathematically by the so-called vector *ket*, which is provided in terms of Dirac notation, denoted by $|\psi\rangle$ [1]. Its dual vector is referred to as $\langle\psi|$ also known as a vector *bra* which belongs to the dual space $\mathcal{H}^*$ of $\mathcal{H}$. In this context, any state vector $|\psi\rangle$ belonging to the Hilbert space $\mathcal{H}$ can be expanded as a linear combination of the vectors that form a complete basis set, such that

$$|\psi\rangle = \textstyle\sum_{i=0}^{n} v_i\,|\mathcal{V}_i\rangle\,, \tag{1.13}$$

where v_i are the probability amplitudes with the normalization condition of $|\psi\rangle$ can be expressed as follows

$$\begin{aligned} \langle\psi|\,\psi\rangle &= \sum_i \sum_j v_i v_j^* \,\langle\mathcal{V}_i|\,\mathcal{V}_j\rangle \\ &= \sum_i |v_i|^2 = 1, \end{aligned} \tag{1.14}$$

where $(*)$ is the complex conjugate. It is crucial to highlight that Hilbert space, as a special vector space, is characterized by several fundamental properties [5]. Among them, we cite the most interesting in this manuscript:

- Linearity: Let $|\varphi\rangle$ and $|\psi\rangle$ represent two vectors in $\mathcal{H}$ and α and β denote two complex numbers. Then any linear combination of these two vectors is also an element in $\mathcal{H}$. Such that

$$\alpha\,|\varphi\rangle + b\,|\psi\rangle \in \mathcal{H}. \tag{1.15}$$

- Inner product: In order to quantitatively distinguish two different state vectors $|\varphi\rangle$ and $|\psi\rangle$, we present the Hermitian inner product defined by

$$\langle\psi|\,\varphi\rangle = \langle\varphi|\,\psi\rangle^* = \sum_i^n \psi_i^* \varphi_i. \tag{1.16}$$

The above expression can also be expressed in the matrix representation of state vectors as follows

$$\langle\psi|\,\varphi\rangle = (\psi_1^*, \psi_2^*, \ldots) \begin{pmatrix} \psi_1^* \\ \psi_2^* \\ \vdots \end{pmatrix}. \tag{1.17}$$

- Norm: It is also known as vector length. It is represented as the square root of an inner product of the vector with itself and it is denoted by $\|\cdot\|$. Mathematically, it is expressed as

$$\|\psi\| = \sqrt{\langle\psi|\,\psi\rangle} \geq 0,$$

where the equality, i.e. $\langle\psi|\,\psi\rangle = 0$, occurs only when $|\psi\rangle = 0$. This effectively implies that the Hilbert space is a positive definite space.

- Orthogonality: Two vector states $|\varphi\rangle$ and $|\psi\rangle$ in $\mathcal{H}$ are said to be orthogonal if they are perpendicular to each other, i.e., their inner product vanishes. Such that

$$\langle\psi|\,\varphi\rangle = \langle\psi|\,\varphi\rangle = 0.$$

2.2 Density operator formalism

In quantum mechanics, the density operator formalism provides an efficient means for characterizing the non-classical state of a physical entity, regardless of whether it is known perfectly or imperfectly. In what follows, we will examine how the statistical ensemble referred to as the density operator, namely ρ, is introduced in both pure and mixed states [5]. Its introduction is intended to redesign non-local theory such that it would completely avoid the notion of state vectors [5]. Besides, to explain the statistical ensemble of a quantum system, it has already been utilized in the non-local theory. It was initially introduced by John von Neumann in 1927 [99], and independently by Lev Landau [100]. It is likewise a density matrix defined by phase-space in statistical physics for determining the probability distribution of a system's position and momentum, for example. A statistical description via density matrices is required for a non-local system to achieve particular quantum procedures like measurement using only states expressed by ket vectors, as in quantum mechanics.

2.2.1 Density operator for pure states

In the context of quantum mechanics, a pure state refers to a quantum state that can be described by a single state vector and has a single non-zero eigenvalue $\{1, |\psi\rangle\}$. Pure states are known for providing the highest level of accessible knowledge about the system. Therefore, the corresponding density operator for a pure state is defined as the projection operator onto the state vector $|\psi\rangle$. It can be expressed as follows

$$\rho = |\psi\rangle\langle\psi|, \tag{1.18}$$

where $|\psi\rangle$ is a normalized vector state, while $\rho_{ij} = \langle\mathcal{V}_i|\,\rho\,|\mathcal{V}_j\rangle$ are the matrix elements of the state ρ. It is worth noting that a quantum system is considered to be in a pure state when its vector state is known with certainty.

2.2.2 Density operator for mixed states

We now consider the situation of mixed quantum states. Assume that a state is prepared in an ensemble of pure quantum states $|\psi_i\rangle$ with probability p_i, where $1 \leq i \leq n$ such that $\sum_{i=1}^{n} p_i = 1$, with each $|\psi_i\rangle$ can be represented by a vector state in the Hilbert space $\mathcal{H}$ as

given in Eq.(1.13). The density operator of a mixed projector state $|\psi_i\rangle\langle\psi_i|$ is thus interpreted as a statistical mixture of the different pure states from the ensemble. Moroever, it describes a quantum state where the knowledge of the state is only partial and the system can take a pure state from among n possible states after measurement. Therefore, the density matrix of the quantum system can be written as the sum of the projectors of each pure state weighted by its probability. It is given as follows

$$\rho = \sum_{i=1}^{n} p_i \rho_i = \sum_{i=1}^{n} p_i |\psi_i\rangle\langle\psi_i|, \quad \sum_{i=1}^{n} p_i = 1 \text{ and } 0 \leq p_i \leq 1 \ \forall i, \tag{1.19}$$

where the p_i's form a probability distribution and the sum is taken on all accessible states to the system. Besides, the pure state (1.18) is only a special case of a mixed state where there is only one non-zero probability p_i equal to 1. It is worth noting that the diagonal elements of the density matrix, also known as populations, give the probabilities of measuring different states of the base in which the density matrix has been defined. While the off-diagonal terms correspond to the coherence caused by a superposition of the different basic states and not due to a statistical mixture. The state is a statistical mixture of the basic states when the coherence terms are all zero, which corresponds to a diagonal matrix. In the case where the state is pure, only one diagonal term must therefore be non-zero when the density matrix is diagonalized.

2.3 Density operator properties

In general, an operator is called a density matrix associated with the set $\{p_i, |\psi\rangle\}$ if and only if it satisfies the following properties [5]:

1. Hermiticity: $\rho = \rho\dagger \Rightarrow p_i = p_i^*$, i.e., the eigenvalues of ρ are reals

$$\begin{aligned} \rho\dagger &= (\sum_{i=1}^{n} p_i |\psi_i\rangle\langle\psi_i|)\dagger \\ &= \sum_{i=1}^{n} p_i^* |\psi_i\rangle\langle\psi_i| = \rho, \end{aligned} \tag{1.20}$$

   where $\dagger$ stands for a transposition conjugate operation.

2. Non-negativity: Assume $|\varphi\rangle$ is an arbitrary vector state on the Hilbert space $\mathcal{H}$, then ρ is a positive operator, i.e., $\langle\varphi|\rho|\varphi\rangle \geq 0, \forall |\varphi\rangle \in \mathcal{H}$. Such that

$$\begin{aligned} \langle\varphi|\rho|\varphi\rangle &= (\sum_{i=1}^{n} p_i \langle\varphi|\psi_i\rangle\langle\psi_i|\varphi\rangle) \\ &= \sum_{i=1}^{n} p_i |\langle\varphi|\psi_i\rangle|^2 \geq 0. \end{aligned} \tag{1.21}$$

3. Trace condition: $\mathrm{Tr}(\rho) = 1$, this also means that ρ is normalized

$$\begin{aligned}
\mathrm{Tr}(\rho) &= \sum_{i=1}^{n} p_i \mathrm{Tr}(\left|\psi_i\right\rangle \left\langle\psi_i\right|) \\
&= \sum_{i,m=1}^{n} p_i \left\langle m\right|\left.\psi_i\right\rangle \left\langle\psi_i\right|\left. m\right\rangle \\
&= \sum_{i=1}^{n} p_i \left\langle\psi_i\right| \sum_{m=1}^{n} \left|m\right\rangle \left\langle m\right|\left.\psi_i\right\rangle \\
&= \sum_{i=1}^{n} p_i \left\langle\psi_i\right|\left.\psi_i\right\rangle \\
&= \sum_{i=1}^{n} p_i = 1,
\end{aligned}$$

with $\sum_{m=1}^{n} \left|m\right\rangle \left\langle m\right| = I$.

4. The expectation value of an arbitrary observable $\langle\mathcal{A}\rangle = \mathrm{Tr}(\mathcal{A}\rho), \forall\mathcal{A} \in \mathcal{H}$.

$$\begin{aligned}
\mathrm{Tr}(\mathcal{A}\rho) &= \mathrm{Tr}(\mathcal{A} \sum_{i=1}^{n} p_i \left|\psi_i\right\rangle \left\langle\psi_i\right|) \\
&= \sum_{m=1}^{n} \sum_{i=1}^{n} p_i \left\langle m\right|\left.\psi_i\right\rangle \left\langle\psi_i\right| \mathcal{A} \left|m\right\rangle \\
&= \sum_{i=1}^{n} p_i \left\langle\psi_i\right| \mathcal{A} \sum_{m=1}^{n} \left|m\right\rangle \left\langle m\right|\left.\psi_i\right\rangle \\
&= \sum_{i=1}^{n} p_i \left\langle\psi_i\right| \mathcal{A} \left|\psi_i\right\rangle = \langle\mathcal{A}\rangle .
\end{aligned} \tag{1.22}$$

5. Purity condition: $0 \leq \mathrm{Tr}(\rho^2) \leq 1$

$$\begin{aligned}
\mathrm{Tr}(\rho^2) &= \sum_{m=1}^{n} \left\langle m\right| \sum_{i,j=1}^{n} p_i p_j \left|\psi_i\right\rangle \left\langle\psi_i\right|\left.\psi_i\right\rangle \left|\psi_j\right\rangle \left|m\right\rangle \\
&= \sum_{i,j=1}^{n} p_i p_j \left\langle\psi_i\right|\left.\psi_j\right\rangle \left\langle\psi_j\right| \sum_{m=1}^{n} \left|m\right\rangle \left\langle m\right|\left.\psi_i\right\rangle \\
&= \sum_{i,j=1}^{n} p_i p_j \left|\left\langle\psi_i\right|\left.\psi_j\right\rangle\right|^2 \\
&= \sum_{i=1}^{n} p_i^2 < \sum_{i=1}^{n} p_i = 1.
\end{aligned} \tag{1.23}$$

The state is said to be pure iff $\rho^2 = \left|\psi\right\rangle \left\langle\psi\right|\left.\psi\right\rangle \left\langle\psi\right| = \rho$ and then $\mathrm{Tr}(\rho^2) = 1$. It follows that the purity verifies the inequality $\mathrm{Tr}(\rho^2) \leq 1$.

The above-mentioned properties ensure that the density matrix correctly describes the mixed state in terms of the probabilities and the pure states in the ensemble. Besides, it plays an important role in various areas, such as quantum information theory and open quantum system theory.

2.4 Postulates of quantum mechanics

According to the definitions stated above, the postulates of quantum mechanics can be reformulated in terms of density operator formalism. Such an alternative approach is mathematically equivalent and analogous to the standard state vector picture. Besides, the density operator approach provides more details and convenient methods to consider different aspects of quantum systems and related phenomena along with greater accuracy and precision [5].

Postulate 1 In quantum mechanics, an isolated or closed physical system is represented by a vector in a Hilbert space, i.e., a complex vector space equipped with an inner product. This vector is also known as the state space of the system. The system is completely defined by its density operator ρ (1.19).

Postulate 2 The time evolution of a closed quantum mechanical system is governed by a unitary operator of the Hilbert space of the system. The density operator ρ describes the system at time t is related to the density operator ρ' describes the system at time t' via a unitary operator U that depends explicitly only on the initial time t and the later time t'. That is

$$\rho' = U\rho U^{\dagger}. \tag{1.24}$$

The Liouville von Neumann equation is an alternative method to describe this kind of evolution. Such that

$$\frac{d\rho(t)}{dt} = -\frac{i}{\hbar}[H(t), \rho(t)], \tag{1.25}$$

where $H(t)$ is the time-dependent Hamiltonian of the total system.

Postulate 3 Quantum measurements are characterized by a set of measurement operators represented as $\{M_k\}$ which act within the state space of the system being measured. The index k corresponds to the possible measurement outcomes in the given experiment. Let us suppose ρ is the state of the quantum system before the measurement, then the probability of getting the results k is

$$p(k) = \mathrm{Tr}(M_k^{\dagger} M_k \rho), \tag{1.26}$$

and the state of the system after the measurement collapses into

$$\rho' = \frac{M_k \rho M_k^{\dagger}}{\mathrm{Tr}(M_k^{\dagger} M_k \rho)}, \tag{1.27}$$

where the measurement operators satisfy the following completeness equation

$$\textstyle\sum_k M_k^{\dagger} M_k = I,$$

with $M_k^{\dagger} M_k$ represents the most general measurement and is known as a Positive Operator-Valued Measure (POVM).

Postulate 4 For any composite physical system, the state space is characterized by the tensor product of all the state spaces of sub-systems. Furthermore, a quantum system $\mathcal{S}_i$ consists of n particles with $i = 1, \ldots, n$ and the system $\mathcal{S}_i$ is prepared in the state ρ_i. Then, the state of the global system is given by

$$\rho = \rho_1 \otimes \rho_2 \otimes \ldots \otimes \rho_n. \tag{1.28}$$

We shall see throughout this thesis that this postulate allows us to define one of the most interesting and counterintuitive phenomena in quantum mechanics such as entanglement.

Fig.1.5 summarizes the postulates of quantum mechanis in terms of the density operator.

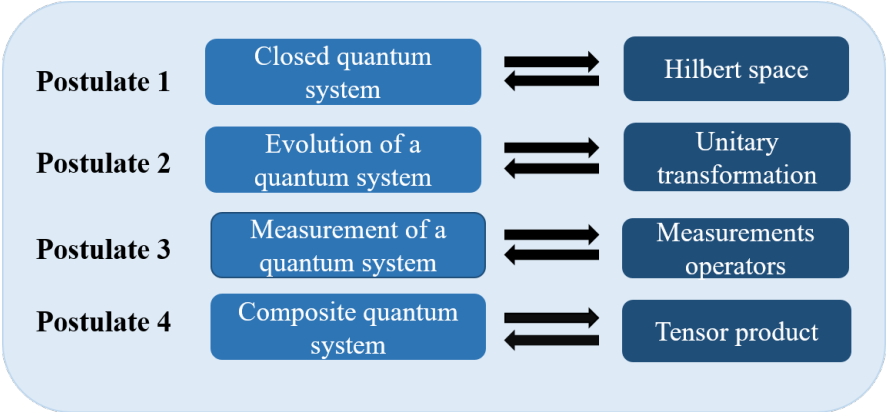


Figure 1.5: Summary of postulates.

2.5 Reduced density operator

One of the deepest advantages of the density operator lies in the description of sub-systems resulting from a composite quantum system. Such a description is provided by using the concept of the reduced density operator. It is therefore indispensable in the analysis of composite quantum systems. Let us consider the case of a composite bipartite quantum state AB consisting of two sub-systems A and B on the bases $\{|m\rangle\}_{m=1}^{d_A} \in \mathcal{H}_A$ and $\{|n\rangle\}_{n=1}^{d_B} \in \mathcal{H}_B$, respectively. If the density operator ρ_{AB} describes the joint system AB acting in the space states $\mathcal{H} = \mathcal{H}_A \otimes \mathcal{H}_B$ of dimension $d = d_A \times d_B$. Then sub-system $A(B)$ is described by the reduced density operator $\rho_A(\rho_B)$. It is given by taking the partial trace of the joint density operator with respect to the degrees of freedom of the other sub-system as [5]

$$\rho_A = \mathrm{Tr}_B(\rho_{AB}) = \sum_n \langle n| \rho_{AB} |n\rangle , \quad \rho_B = \mathrm{Tr}_A(\rho_{AB}) = \sum_m \langle m| \rho_{AB} |m\rangle , \tag{1.29}$$

where $\mathrm{Tr}_{B(A)}$ denotes the partial trace over sub-system $B(A)$. The reduced density operator (1.29) describes a sub-system of the total quantum system. Besides, it satisfies the properties of a density matrix. A trivial example is the maximally entangled Bell state, $|\psi\rangle = \frac{1}{\sqrt{2}}(|00\rangle + |11\rangle)$, to see clearly how one can calculate the partial trace in the case of a bipartite system composed of two sub-systems, namely A and B. The density operator correspond to this Bell state $|\psi\rangle$ is given by

$$\begin{aligned} \rho &= \frac{1}{2}(|00\rangle + |11\rangle)(\langle 00| + \langle 11|) \\ &= \frac{1}{2}(|00\rangle\langle 00| + |00\rangle\langle 11| + |11\rangle\langle 00| + |11\rangle\langle 11|). \end{aligned} \tag{1.30}$$

The above state can be rewritten in the computational basis $\{|00\rangle, |01\rangle, |10\rangle, |11\rangle\}$ as follows

$$\rho = \frac{1}{2}\begin{pmatrix} 1 & 0 & 0 & 1 \\ 0 & 0 & 0 & 0 \\ 0 & 0 & 0 & 0 \\ 1 & 0 & 0 & 1 \end{pmatrix}. \tag{1.31}$$

It is therefore clear that the state (1.31) is a positively defined matrix of trace equal to 1 with eigenvalues 0 and 1/2. However, following definition (1.29), the reduced density operator of the

sub-system A is given by

$$\begin{aligned}\rho_A &= \frac{1}{2}\left(\mathrm{Tr}_B(|00\rangle\langle 00|) + \mathrm{Tr}_B(|00\rangle\langle 11|) + \mathrm{Tr}_B(|11\rangle\langle 00|) + \mathrm{Tr}_B(|11\rangle\langle 11|)\right) \\ &= \frac{1}{2}\left(|0\rangle\langle 0|\langle 0|0\rangle + |1\rangle\langle 0|\langle 0|1\rangle + |0\rangle\langle 1|\langle 1|0\rangle + |1\rangle\langle 1|\langle 1|1\rangle\right) \\ &= \frac{1}{2}\left(|0\rangle\langle 0| + |1\rangle\langle 1|\right) = \frac{1}{2}I. \end{aligned} \tag{1.32}$$

Here, I denotes the 2-order identity operator. Similarly, the reduced density matrix of the second sub-system B is obtained as

$$\rho_B = \frac{1}{2}I. \tag{1.33}$$

The concept of the reduced density matrix plays a significant role in various applications within the field of quantum information, particularly in the study of open quantum systems. In the upcoming chapters, we will delve into these applications and explore how the concept of the reduced density operator contributes to advancing our understanding of quantum information theory.

2.6 Quantum measurements

The problem of measurement continues to be one of the most challenging and controversial topics in the field of QIS and opinions vary widely regarding its importance. Some argue that there is, in fact, no problem at all. Other paradoxes, on the other hand, consider the measurement problem to be one of the major unsolved puzzles of quantum physics. The problem is that quantum physics only provide probabilities for different possible outcomes of an experiment and does not provide any exact mechanism by which the actual outcome observed at the end occurs. In general, the quantum measurement process is essentially what is shown in Fig.1.6; an operation on a qubit, so that the quantum state is in a superposition of the basis vectors, namely $|0\rangle$ and $|1\rangle$, to obtain a classical bit (a completely random process by nature) [101, 102]. In quantum theory, every measurable physical quantity is associated with an observable such as position, momentum and angular momentum, which is represented by an Hermitian operator that is characterized by a set of operators $\{M_k\}_{k=1}^N$ satisfying the completeness relation $\sum_{k=1}^N M_k^\dagger M_k = I$. These operators act on the state space of the system and the state $|\psi\rangle$ after the measurement becomes

$$|\psi\rangle \mapsto |\psi_k\rangle \equiv \frac{M_k|\psi\rangle}{\sqrt{p_k}}, \tag{1.34}$$

where p_k is the probability that outcome k occurs. It is defined by

$$p_k = \langle\psi| M_k^\dagger M_k |\psi\rangle = \|M_k|\psi\rangle\|^2 \geq 0. \tag{1.35}$$

The above formalism of quantum measurement is also called general measurement.

2.6.1 Projective measurements

Projective measurements, also known as von Neuman measurements, are a particular class of generalized measurements [5]. They involve a set of measurement operators $\{M_k\}_{k=1}^N$ that are positive, Hermitian, and orthogonal projectors, where $M\dagger_k = M_k$ such that $\sum_k M_k = I$. Moreover, the number of these operators is precisely equal to the dimension of the Hilbert space. However, they are repeatable in such a way performing a projective measurement once

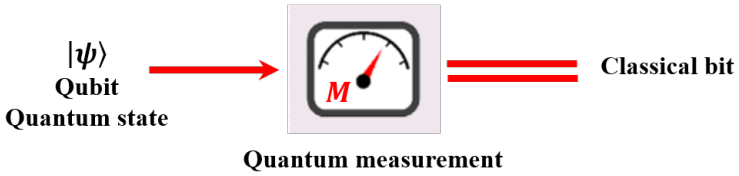


Figure 1.6: Quantum measurement of a qubit.

and obtaining the result μ_k, repeating the measurement yields the same result μ_k without changing the state of the system. Therefore, $M_k = \Pi_k$ where $\Pi_k\Pi_l = \delta_{kl}\Pi_k$ and $\Pi_k^2 = \Pi_k$ with Π_k represents the rank-one projection operators with δ_{kl} stands for the Kronecker delta function. Using this, the probability of observing the outcome k upon measuring the state $|\psi\rangle$ is given as follows

$$p_k = \langle\psi| M_k^\dagger M_k |\psi\rangle = \langle\psi| \Pi_k |\psi\rangle , \tag{1.36}$$

and the state $|\psi_k\rangle$ of the quantum system just after obtaining the outcome k becomes

$$|\psi\rangle \mapsto |\psi_k\rangle \equiv \frac{\Pi_k |\psi\rangle}{\sqrt{p_k}}. \tag{1.37}$$

Moreover, the quantum state does not change if one applies the projective operator Π_k to the state $|\psi_k\rangle$ once again. This is due to the fact that the projective operator Π_k has the property $\Pi_k^2 = \Pi_k$. This means that repeating the measurement produces indeed the same result k each time without affecting the state of the system

$$|\psi_k\rangle \mapsto \left|\psi_k^{'}\right\rangle \equiv \frac{\Pi_k |\psi_k\rangle}{\sqrt{p_k^{'}}}, \tag{1.38}$$

where $p_k^{'} = \langle\psi_k| \Pi_k |\psi_k\rangle$ is explicitly given as

$$p_k^{'} = \left(\langle\psi| \frac{\Pi_k^\dagger}{\sqrt{p_k}}\right) p_k \left(\frac{\Pi_k}{\sqrt{p_k}} |\psi\rangle\right) = \frac{\langle\psi| \Pi_k |\psi\rangle}{p_k}. \tag{1.39}$$

Thus

$$\sqrt{p_k^{'} p_k} = \langle\psi| \Pi_k |\psi\rangle = \sqrt{p_k}. \tag{1.40}$$

If instead of a pure state, one has a mixed state density operator, namely $\rho = \sum_k p_k |\psi_k\rangle \langle\psi_k|$. Then the probability of getting the measurement result k is

$$p_k = \mathrm{Tr}(\Pi_k \rho), \tag{1.41}$$

and the state of the system just after the measurement corresponds to the result k collapses to

$$\rho \mapsto \rho_k = \frac{\Pi_k \rho \Pi_k^\dagger}{\mathrm{Tr}(\Pi_k \rho)}. \tag{1.42}$$

Moreover, the result of a projective measurement on sub-system A of a bipartite quantum system AB is indeed always a pure state. When the measurement is made on sub-system A, the information about the original state of system AB is reduced, but it does not vanish completely. Thus, it is still possible to determine the state of the other sub-system B, and the state of B after the measurement will be a pure state. This is due to the fact that the total system AB is in a pure state and the loss of information about the state of A due to the measurement can be compensated by the information that is obtained about the state of A through the measurement outcome.

2.6.2 Positive Operator Valued Measurements

In general, a quantum system is destroyed during the measurement process, meaning that the description of projective measurements turns out to be restrictive and not always practical. Besides, the repeatability of a projective measurement is violated in cases where the system is measured only once. However, other measurements can be performed on a quantum system that cannot be described within this formalism. This leads us to consider the formalism of generalized quantum measurements also called non-projective measurements, or positive operator-valued measures (POVMs). Specifically, they are defined as a set of Hermitian positive operators $\{M_k\}$ that act on the Hilbert space of a quantum system such that $P_k = M_k^\dagger M_k$ and $P_k^\dagger = M_k^\dagger (M_k^\dagger)^\dagger = P_k$ satisfying the completeness relation $\sum_k P_k = I$. In addition, the corresponding measurement operators are not necessarily orthogonal nor commuting with each other and allow the possibility of measurement outcomes associated with non-orthogonal states. Unlike projective measurement, the number of elements in POVM operators can be greater than the dimension of the Hilbert space. Moreover, they play an important role in many areas of quantum information science [103–105]. For instance, the POVM has been used in the analysis of key distribution in quantum cryptography [106].

It is easy to see that the P_k are non-negative operators, i.e., $\langle\psi| P_k |\psi\rangle \geq 0$ holds for all vector $|\psi\rangle$ in the Hilbert space $\mathcal{H}$. Moreover, the probability associated with the outcome k, knowing that the system is in the state characterized by the density operator ρ, can be expressed as follows

$$p_k = \mathrm{Tr}(P_k \rho). \tag{1.43}$$

In fact, the set of operators P_k is sufficient to define the probabilities of the different measurement outcomes. The complete set of operators $\{P_k\}$ is commonly known as a POVM, and the individual operators P_k are referred to as POVM elements associated with the measurements. By defining $M_k = M_k^\dagger = P_k$, the state after the POVM measurements become

$$\rho \mapsto \rho_k = \frac{\sqrt{P_k}\rho\sqrt{P_k}}{p_k}. \tag{1.44}$$

In general, the POVM framework provides a way to compute the probabilities associated with various measurement outcome, rather than providing enough information about the system's state after measurement. Therefore, the POVM framework is particularly useful for experiments where the main goal is to collect the measurement statistics while knowing the post-measurement states is either impossible or irrelevant to the experiment.

3 Quantum information theory

In the theory of quantum information [5, 103], the non-local principles and Shannon's theory are merged to provide a framework for studying and handling the processing of quantum information. The quantum state variables such as photon polarization, particle spin, energy, and momentum can be used to encode the quantum data and are described by the density operator employed on a Hilbert space. This representation allows for the application of mathematical tools from quantum mechanics and information theory to the manipulation and processing of quantum information. The result of this merger has led to the advancement of modern day quantum procedures, for example, quantum cryptography for secure communication [107], quantum computing for solving complex problems [108] and quantum communication for transmitting information with high efficiency and security [109]. This section will present the main characteristics of quantum information processing. To do this, we start by introducing the notion of qubit which is the smallest unit of storage in quantum theory and then we define a brief description of the von Neuman entropy as well as other entropy notions.

3.1 Qubit and Bloch sphere

3.1.1 Bit to qubit

The classical bit also known as a binary digit is the basic concept of classical computing and classical procedures [90]. This is the most fundamental unit of information and it can only take one of two distinct values, which are characterized as 0 or 1. It can also be represented as true/false, yes/no, +/−, or on/off. By analogy with the classic binary bit, a quantum bit or simply a qubit is the most fundamental unit of quantum information storage [110]. Unlike the classical system where a bit should be in one state or the other, quantum mechanics allows the qubit to be simultaneously in superposition of both states. This means qubits can exist in multiple states at once, allowing for very fast computation and the ability to perform many calculations at once. Several quantum systems can be store in a qubit, such as a spin of the electron in the experiment of Stern and Gerlach [111], in which the separation into two beams of the silver atom reveals that there are two states of possible spins and the two levels can be taken as spin up and spin down (see Fig.1.7). Another example concerns the single

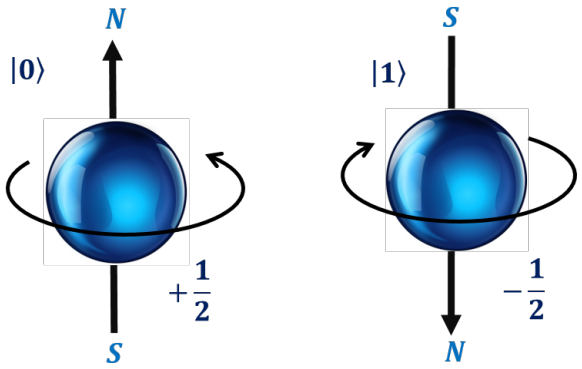


Figure 1.7: A qubit can be represented by any two-level quantum system, for example: electron spin (spin up and down).

photon polarization process, in which the two states can be considered to be vertically and horizontally polarized. In the framework quantum framework, the classical bits: 0 and 1 of the classical computing basis will then be represented by quantum states: $|0\rangle$ and $|1\rangle$. Thus, a general representation of a qubit state is given as a vector in a Hilbert space $\mathcal{H}$ of two dimensions provided with an orthogonal basis $\mathcal{B} = \{|0\rangle, |1\rangle\}$, which will henceforth be named as the standard or the computational basis. It must be noticed that the two basis vectors are denoted as follows

$$|0\rangle \equiv \begin{pmatrix} 1 \\ 0 \end{pmatrix}, \qquad |1\rangle \equiv \begin{pmatrix} 0 \\ 1 \end{pmatrix}. \tag{1.45}$$

The classical bit and a qubit have differences in the fact that the latter can exist in a state other than $|0\rangle$ and $|1\rangle$. In other words, a qubit can be in a continuum of the orthogonal states that include both $|0\rangle$ and $|1\rangle$. Thus, it can be formed by a coherent superposition of the states on the standard basis

$$|\psi\rangle = \alpha\,|0\rangle + \beta\,|1\rangle = \begin{pmatrix} \alpha \\ \beta \end{pmatrix}, \tag{1.46}$$

with α and β being the complex coefficients satisfying the normalization condition $|\alpha|^2 + |\beta|^2 = 1$. When a measurement is performed on the qubit state $|\psi\rangle$ (1.46), it collapses into a definite state, either $|0\rangle$ or $|1\rangle$ with probabilities given by $|\alpha|^2$ and $|\beta|^2$, accordingely. The result of the measurement is then given by a definite state $|0\rangle$ or $|1\rangle$, and the qubit exhibits classical behavior by adopting one of these states after measurement. Besides, outcome probability is determined using the coefficients α and β.

3.1.2 Geometric demonstration of qubit state

The Bloch sphere provides an intriguing geometrical description of a two-level quantum state (qubit) [5]. It is used to describe and understand the characteristics of a quantum state. In fact, the qubit state $|\psi\rangle$ is given as a point on the surface of the sphere. Moreover, the state $|\psi\rangle$ (1.46) is further defined in computational basis vectors, namely $|0\rangle$ and $|1\rangle$, which is associated, respectively, to the north and south poles of the sphere (see Fig.1.8). Therefore, each quantum state is illustrated by a ray coming from the center of the sphere, which is represented by a vector $\overrightarrow{n}$ in $\mathbb{R}^3$ as

$$|\psi\rangle = \cos\left(\frac{\theta}{2}\right)|0\rangle + e^{i\phi}\sin\left(\frac{\theta}{2}\right)|1\rangle\,, \tag{1.47}$$

where $\theta \in [0,\pi]$ and $\phi \in [0,2\pi]$ represent, respectively, the azimuth angle and the polar angle. Moreover, the points on the sphere's surface shows the pure states, the points inside shows the mixed states and the center corresponds to the fully mixed state. In quantum computing, this representation enables the resolution of several operations on single qubits. It is worth noting that the qubit state (1.47) can be reformulated by employing the density operator notion as

$$\begin{aligned}
\rho_{pure} &= |\psi\rangle\langle\psi| \\
&= \begin{pmatrix} \cos^2\left(\frac{\theta}{2}\right) & e^{-i\phi}\sin\left(\frac{\theta}{2}\right)\cos\left(\frac{\theta}{2}\right) \\ e^{i\phi}\sin\left(\frac{\theta}{2}\right)\cos\left(\frac{\theta}{2}\right) & \sin^2\left(\frac{\theta}{2}\right) \end{pmatrix} \\
&= \frac{1}{2}\begin{pmatrix} 1+\cos(\theta) & \sin(\theta)\left(\sin(\phi)-i\sin(\phi)\right) \\ \sin(\theta)\left(\sin(\phi)+i\sin(\phi)\right) & 1-\cos(\theta) \end{pmatrix} \\
&= \frac{1}{2}(I_2 + n_1\sigma_x + n_2\sigma_y + n_3\sigma_z) \\
\rho_{pure} &= \frac{1}{2}(I_2 + \overrightarrow{n}.\overrightarrow{\sigma}),
\end{aligned} \tag{1.48}$$

where I is the 2-dimensional identity matrix, while $\overrightarrow{n} = (n_x, n_y, n_z)$ represents the Bloch vector encoding all the information about the qubit state, which can be determined through $\overrightarrow{n} = \mathrm{Tr}(\rho_{pur}.\overrightarrow{\sigma})$ with $\overrightarrow{\sigma} = (\sigma_x, \sigma_y, \sigma_z)$ are the familiar Pauli matrices that are defined in the standard basis $\mathcal{B} = \{|0\rangle, |1\rangle\}$ as

$$\sigma_x = \begin{pmatrix} 0 & 1 \\ 1 & 0 \end{pmatrix}, \qquad \sigma_y = \begin{pmatrix} 0 & -i \\ i & 0 \end{pmatrix}, \qquad \sigma_z = \begin{pmatrix} 1 & 0 \\ 0 & -1 \end{pmatrix}. \tag{1.49}$$

The above matrices (1.49) are the traceless Hermitian that generate the group $SU(2)$, satisfying $\mathrm{Tr}(\sigma_i\sigma_j) = 2\delta_{ij}$ with $i(j) = (x, y, z)$. By using Eqs. (1.48) and (1.49), the components of the Bloch vector corresponding to the pure state can be written in terms of the angles θ and ϕ as follows

$$n_x = \sin(\theta)\cos(\phi)\,, \qquad n_y = \sin(\theta)\sin(\phi)\,, \qquad n_z = \cos(\theta). \tag{1.50}$$

However, there is no simple generalization of the Bloch sphere known for multiple qubits like that of qudits (d-level quantum systems) [112]. Note that in the case of pure states (1.47), we have $\|\overrightarrow{n}\| = 1$. Thus, the pure states correspond to points on the surface of the Bloch sphere. In general, the Bloch sphere can be used to represent mixed states geometrically. Given a density operator ρ_{mixed} characterizes a qubit's mixed quantum state. Due to its hermeticity, ρ_{mixed} can be decomposed using Eq.(1.48). Assume that $|\phi^+\rangle$ and $|\phi^-\rangle$ are two eigenvectors of the state ρ_{mixed} corresponding to the eigenvalue $\lambda_\pm = (1 \pm \|\overrightarrow{n}\|)/2$. Therefore, the diagonalized density operators ρ_{mixed} can be rewritten as follows:

$$\rho_{mixed} = \frac{1}{2}\left(\lambda_+ |\phi^+\rangle\langle\phi^+| + \lambda_- |\phi^-\rangle\langle\phi^-|\right). \tag{1.51}$$

The above expression (1.51) collapses to the pure state $\left|\phi^{+}\right\rangle$ when $\|\overrightarrow{n}\| = 1$, whose expression is identical to that of $|\psi\rangle$ (1.47). However, when $\|\overrightarrow{n}\| < 1$, we get a statistical mixture of states $\left|\phi^{+}\right\rangle$ and $\left|\phi^{-}\right\rangle$. The Bloch vector in this case describes a point located inside the Bloch sphere. The center of the Bloch sphere, $\|\overrightarrow{n}\| = 0$, corresponds to $I_2/2$ which is a completely mixed state.

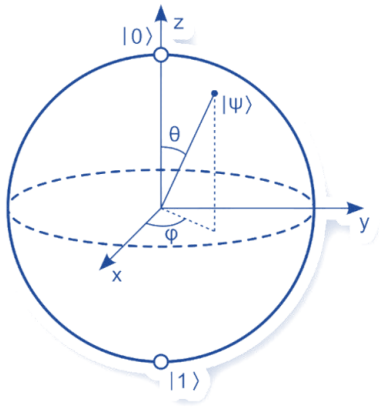


Figure 1.8: Geometric representation of a qubit in a Bloch sphere.

3.2 von Neumann entropy

3.2.1 Definition

von Neumann entropy (VNE) was first explained by John von Neumann in 1932 [113], as analogous to the concept of Shannon information entropy [82]. In non-classical mechanics, physical systems can be described by a Hilbert space, while observables by self-adjoint operators, and statistical operators are tarced back to the density operators. Thus, Shannon entropy is replaced by von Neumann entropy in the quantum regime, in which the eigenvalues of a given density operator ρ form a probability distribution. In other words, the density operators can be considered as a generalization for probability distributions. Therefore, von Neumann entropy $\mathcal{S}(\rho)$ corresponding to a density matrix ρ will be given by [5]

$$\mathcal{S}(\rho) = -\mathrm{Tr}(\rho \log_2 \rho), \tag{1.52}$$

where $\log_2$ introduced in Eq.(1.52) is always taken to base 2 (binary logarithm) to normalize the maximum entropy of the qubit to one. By writing ρ in the following diagonal form

$$\rho = \textstyle\sum_k \lambda_k \left|\lambda_k\right\rangle \left\langle\lambda_k\right|, \tag{1.53}$$

where λ_k denote the eigenvalues of the state ρ and $\left|\lambda_k\right\rangle$ are their associated eigenvectors. Then, $\mathcal{S}(\rho)$ can be re-expressed as follows

$$\begin{aligned}
\mathcal{S}(\rho) &= -\mathrm{Tr}(\rho \log_2 \rho) = -\mathrm{Tr}\left(\textstyle\sum_l \lambda_l \left|\lambda_l\right\rangle \left\langle\lambda_l\right| \log_2 \sum_k \lambda_k \left|\lambda_k\right\rangle \left\langle\lambda_k\right|\right) \\
&= -\textstyle\sum_m \left\langle\lambda_m\right| \left(\sum_l \lambda_l \left|\lambda_l\right\rangle \left\langle\lambda_l\right| \log_2 \sum_k \lambda_k \left|\lambda_k\right\rangle \left\langle\lambda_k\right|\right) \left|\lambda_m\right\rangle \\
&= -\textstyle\sum_{m,l,k} \delta_{ml} \lambda_l \delta_{lk} \log_2 \lambda_k \delta_{km} \\
&= -\textstyle\sum_k \lambda_k \log_2 \lambda_k \\
\mathcal{S}(\rho) &= \mathcal{H}\left(\{\lambda_k\}\right).
\end{aligned} \tag{1.54}$$

The above expression (1.54) is equivalent to the Shannon entropy (1.1) of the probability distribution associated with the diagonalization of the state ρ. Moreover, it is a convenient expression used to evaluate VNE for an arbitrary dimensional quantum state. Similar to the Shannon entropy measuring the level of uncertainty in a classical random variable, VNE quantifies the amount of uncertainty in a given quantum state. Therefore, it is zero for pure states, i.e., $\rho = |\psi\rangle\langle\psi|$, and it provides complete knowledge of the associated quantum system. Mathematically, $\mathcal{S}(|\psi\rangle\langle\psi|) = 0$ means that the state ρ has a non-zero eigenvalue equal to 1 and all the other eigenvalues equal to zero. On the other hand, if one prepares the system in a maximally mixed state I_d/d, i.e., a mixed state where all d corresponding pure states have the same probabilities. Then the mixed state represents the maximal uncertainty of the system with the von Neumann entropy is $\mathcal{S}(I_d/d) = -1/d\mathrm{Tr}\left(\log_2 \frac{1}{d} I_d\right) d = \log_2 d$, which is in accordance with the Shannon entropy.

3.2.2 von Neumann's entropy properties

The von Neumann entropy $\mathcal{S}(\rho)$ defined above possess many properties that can be found in Ref. [5]. For our purpose, we stress here the most important ones:

- Non-negativity: $\mathcal{S}(\rho)$ is always a non-negative function and satisfies $0 \leq \mathcal{S}(\rho) \leq \log_2 d$.
- Invariance: $\mathcal{S}(\rho)$ is invariant under the action of a unitary transformation U, i.e., $\mathcal{S}(U\rho U\dagger) = \mathcal{S}(\rho)$, since $\mathcal{S}(\rho)$ depends only on the eigenvalues of the state ρ.
- Concavity: $\mathcal{S}(\rho)$ is a strictly concave function, i.e., if $\lambda_1, \ldots, \lambda_n \geq 0$ such that $\sum_{i=1}^n \lambda_i = 1$, then one has
$$S(\textstyle\sum_{i=1}^n \lambda_i \rho_i) \geq \sum_{i=1}^n \lambda_i S(\rho_i). \tag{1.55}$$
From this property, we conclude the von Neumann entropy $\mathcal{S}(\rho)$ increases as we know more about how the state was formed.
- Sub-additivity: For a bipartite quantum system described by the state $\rho_{AB} \in \mathcal{H}_{AB}$, the sub-additivity condition of $\mathcal{S}(\rho_{AB})$ holds true:
$$\mathcal{S}(\rho_{AB}) \leq \mathcal{S}(\rho_A) + \mathcal{S}(\rho_B), \tag{1.56}$$
where $\rho_A = \mathrm{Tr}_B \rho_{AB}$ and $\rho_B = \mathrm{Tr}_A \rho_{AB}$. The equality is achieved if and only if ρ_A and ρ_B are independent such that $\rho_{AB} = \rho_A \otimes \rho_B$. Thus, inequality (1.56) means that the entropy is additive for uncorrelated states, while for correlated states the system contains more information than the two sub-systems considered separately. This property is the quantum generalization of the subadditivity of Shannon entropy. However, for tripartite systems characterized by the density operator $\rho_{ABC} \in \mathcal{H}_{ABC}$, the strong sub-additivity of the von Neumann entropy states that
$$\mathcal{S}(\rho_{ABC}) + \mathcal{S}(\rho_B) \leq \mathcal{S}(\rho_{AB}) + \mathcal{S}(\rho_{BC}). \tag{1.57}$$
- Bipartite pure states: For a pure composite state ρ_{AB}, we have
$$\mathcal{S}(\rho_A) = \mathcal{S}(\rho_B), \tag{1.58}$$
since ρ_A and ρ_B have the same eigenvalues.
- Bipartite mixed states: Let p_i be probability distributions with ρ_i being a set of states belonging to orthogonal subspaces, then we can get
$$\mathcal{S}(\textstyle\sum_{i=1}^n p_i \rho_i) \leq \mathcal{H}(\{\lambda_k\}) + \sum_{i=1}^n p_i \mathcal{S}(\rho_i). \tag{1.59}$$

- Triangle inequality: For any bipartite system ρ_{AB}, the triangle inequality also called Araki-Lieb inequality holds that

$$\mathcal{S}(\rho_{AB}) \leq |\mathcal{S}(\rho_A) - \mathcal{S}(\rho_B)|\,, \tag{1.60}$$

  which is in contrast with the analogous property of Shannon entropy.

3.3 Joint, conditional and relative quantum entropy

By analogy with the classical information theory is highly useful to define the quantum version of joint, conditional and relative entropies. Given a bipartite quantum system AB characterized by the density operator ρ_{AB} with $\rho_A(\rho_B)$ shows the reduced density matrix of a subsystem $A(B)$. The quantum mechanical joint entropy $\mathcal{S}(A,B)$ for a bipartite quantum state is defined as the quantum entropy of the joint state ρ_{AB} is given by

$$\mathcal{S}(A,B) = \mathcal{S}(\rho_{AB}) = -\mathrm{Tr}\left(\rho_{AB}\log_2\rho_{AB}\right). \tag{1.61}$$

The quantum conditional entropy (QCE, for short) $\mathcal{S}(A|B)$ measures the uncertainty in sub-system A given the information about the other sub-system B. It is given as follows

$$\mathcal{S}(A|B) = \mathcal{S}(A,B) - \mathcal{S}(B), \tag{1.62}$$

where $\mathcal{S}(A) \equiv \mathcal{S}(\rho_A)$ and $\mathcal{S}(B) \equiv \mathcal{S}(\rho_B)$. It is interpreted as the amount of uncertainty in sub-system A that is not reduced by knowing the state of sub-system B. Unlike the classical conditional entropy given by Eq.(1.7), its quantum counterpart $\mathcal{S}(A|B)$, can be negative, which is a particular characteristic of quantum mechanics that can not be observed in classical case. Moreover, it reaches its minimum value for maximally entangled states.

As a concrete example, let consider a maximally quantum correlated Bell pure state ρ_{BELL} such that $\rho_{BELL} = |\psi_{AB-}\rangle\langle\psi_{AB-}|$ with $|\psi_{AB-}\rangle = \frac{1}{\sqrt{2}}(|01\rangle - |10\rangle)$. In this case, the quantum joint entropy vanishes, i.e., $\mathcal{S}(A,B) = 0$, while the entropies of marginal states are maximum, that is, $\mathcal{S}(A) = \mathcal{S}(B) = 1$. Thus, the QCE takes a negative value $\mathcal{S}(A|B) = -1 < 0$. Therfore, the negative aspect of QCE is a manifestation of the concept of quantum entanglement, which is the key subject of this thesis.

Let for some provided bipartite quantum states, namely ρ and σ, the associated quantum relative entropy (QRE) of the state ρ regarding the state σ is given as [114, 116]

$$\begin{aligned}\mathcal{S}(\rho||\sigma) &= \mathrm{Tr}\left(\rho(\log_2\rho - \log_2\sigma)\right) \\ &= -\mathcal{S}(\rho) - \mathrm{Tr}(\rho\log_2\sigma).\end{aligned} \tag{1.63}$$

It is important to note that the relative quantum entropy $\mathcal{S}(\rho||\sigma)$ (1.63) is always a positive function, namely $\mathcal{S}(\rho||\sigma) \geq 0$. Besides, the equality is achieved only when $\rho = \sigma$. This property is due to the fact that QRE measures the relative distance between the two given states.

3.4 Quantum mutual information

Two equivalent expressions of classical mutual information, namely Eq.(1.10) and Eq.(1.11), can be extended to the quantum regime. Indeed, the quantum version of the expression (1.11) can be easily derived by replacing the Shannon entropy (1.1) with VNE (1.52) and the random variables (M,N), X and Y by the density operators ρ_{AB}, ρ_A and ρ_B, respectively [115, 116]. Thus, it is defined as

$$\mathcal{I}(A:B) = \mathcal{S}(A) + \mathcal{S}(B) - \mathcal{S}(AB). \tag{1.64}$$

However, it could be expressed as QRE of the bipartite state ρ_{AB} with respect to the product form of the quantum states $\rho_A \otimes \rho_B$ as follows

$$\mathcal{I}(A:B) = \mathcal{S}(\rho_{AB}||\rho_A \otimes \rho_B), \tag{1.65}$$

with the fact that $\log_2(\rho_A \otimes \rho_B) = \log_2(\rho_A) \otimes I_B + I_A \otimes \log_2(\rho_B)$. We notice that like its classical counterpart, this quantity (1.64) is also symmetric, namely $\mathcal{I}(A:B) = \mathcal{I}(B:A)$, and it is always a non-negative function, i.e., $\mathcal{I}(A:B) \geq 0$. This is due to the subadditivity property of the VNE and only vanishes for the case of product state, namely $\rho_{AB} = \rho_A \otimes \rho_B$. From now on, we consider the simple notation $\mathcal{I}(\rho_{AB})$ instead of $\mathcal{I}(A:B)$. Moreover, it bears the interpretation of the total correlation between sub-systems A and B of the bipartite state [115–118]. On the other hand, the quantum homolog of Eq.(1.10) is not straightforward as for $\mathcal{I}(\rho_{AB})$ (1.64) since it involves a generalization of the conditional entropy $\mathcal{H}(M|N)$. This latter in quantum theory requires an optimization procedure on one of the components of the quantum system AB. Hence, the two equivalent expressions of mutual information, namely Eq.(1.10) and Eq.(1.11), in the classical setting do not hold for quantum theory since, in general, a measurement disturbs the quantum state of the system.

Let us suppose that we perform a set of POVM measurements performed on sub-system B only. The set of POVM elements is denoted by $\{P_k\} : \{P_k \geq 0, \sum_k P_k = I\}$, where k distinguishes different outcomes of this measurement. The measurements will disturb simultaneously the sub-system B and consequently the whole quantum state AB. The POVM measurements give the statistical set $\{p_k, \rho_{A|k}\}$. Thus, the conditional state of the global system AB related to the measurement $\{P_k\}$ when the outcome k occurs is given as

$$\rho_{AB} \to \rho_{AB|k} = \frac{1}{p_k}\left((I_A \otimes P_k)\,\rho_{AB}\left(I_A \otimes P_k^\dagger\right)\right), \tag{1.66}$$

where $p_k = \mathrm{Tr}\left((I_A \otimes P_k)\,\rho_{AB}\left(I_A \otimes P_k^\dagger\right)\right)$ denotes the probability when the outcome k occurs, while I_A is the identity operator acting on sub-system A. Therefore, the generalization of conditional entropy of the state A with respect to POVM measurements is given by [25]

$$S\left(\rho_{AB}|\{P_k\}\right) = \textstyle\sum_k p_k S\left(\rho_{A|k}\right), \tag{1.67}$$

where $\rho_{A|k} = \mathrm{Tr}_B(\rho_{AB|k})$ is the reduced density operator describing the sub-system A after performing the measurements. Accordingly, the quantum countrepart of the second expression of the classical mutual information Eq.(1.10) yields

$$J\left(\rho_{AB}|\{P_k\}\right) = S(\rho_A) - \textstyle\sum_k p_k S\left(\rho_{A|k}\right), \tag{1.68}$$

which corresponds to the classical mutual information obtained via the POVM $\{P_k\}$ on sub-system B [24]. It is also interpreted as the amount of information gained about sub-system A by measuring sub-system B [24]. Moreover, the total classical correlations of ρ_{AB} are obtained by maximizing $J\left(\rho_{AB}|\{P_k\}\right)$ overall possible POVMs $\{P_k\}$ measurements. In order to quantify the correlations between the components of the bipartite system this optimization is required to isolate the measurement that causes the least amount of disturbance.

3.5 Tsallis entropy

The generalization of the usual notion of quantum entropies beyond those provided by the von Neumann entropy is one of the most fruitful study aspects in quantum information theory [5]. In this sense, several entropy quantities have been introduced and investigated in detail [5]. One of them is a quantity called the Tsallis entropy (TE) which is considered as a measure of

information in quantum key distribution protocols as well as in quantum correlations [119–121]. Therefore, for a given random variable X with a probability distribution p_x, where $p_x \geq 0$ and $\sum_x p_x = 1$, the Tsallis entropy $\mathcal{H}_q(X)$ of order q is a real non-negative quantity defined as [119]

$$\mathcal{H}_q(X) = \frac{1}{1-q}\left(\sum_x p_x^q - 1\right), \tag{1.69}$$

which approaches to the Shannon entropy (1.1) when the parameter q approaches to the unity as

$$\mathcal{H}_1(X) = \lim_{q\to 1} \mathcal{H}_q(X) = \mathcal{H}(X). \tag{1.70}$$

The quantum counterpart of TE (1.69) is then expressed as

$$\mathcal{S}_q(\rho) = \frac{1}{1-q}\left(\mathrm{Tr}(\rho^q) - 1\right). \tag{1.71}$$

However, Tsallis's entropy does not share all the characteristics of von Neumann's entropy. In particular, for bipartite quantum systems, Eq.(1.71) is a non-additive quantity but in contrast, verifies the subadditivity propriety of VNE and it is not strongly subadditive [120]. In addition, like the classical Tsallis entropy, its quantum counterpart (1.71), in the limit $q \to 1$, converges to VNE [120, 121]

$$\mathcal{S}_1(\rho) = \lim_{q\to 1} \mathcal{S}_q(\rho) = \mathcal{S}(\rho). \tag{1.72}$$

Throughout this thesis, we will mainly concentrate on the Tsallis 2-entropy, namely $q = 2$, also known as linear entropy

$$\mathcal{S}_L(\rho) = \mathcal{S}_2(\rho) = 1 - \mathrm{Tr}\left(\rho^2\right).$$

The linear entropy, however, can be computed without diagonalizing the density matrix ρ, which is in contrast to VNE (1.52). However, it holds a great deal of significance for the theory of quantum information since it is directly connected to the purity of a quantum system [122]. The following table(1.1) summarizes the properties of the entropies, namely Shannon entropy, VNE and TE.

Property	Shannon entropy	von Neumann entropy	Tsallis entropy
Non-negativity	Yes	Yes	Yes
Additivity	Yes	Yes	No
Concavity	Yes	Yes	Yes
Monotonicity	Yes	No	Yes, for $q > 1$
Sub-additivity	Yes	Yes	Yes, for $q > 1$
Strong sub-additivity	Yes	Yes	No
Araki-Lieb inequality	Yes	Yes	Yes, when $q \in (0, 1)$

Table 1.1: Properties of entropies.

4 Conclusion

In this chapter, we have mainly introduced the core concept of quantum information theory required for this thesis. Indeed, in the first part, we provided a brief overview of the essential

tools of the classical information theory, namely Shannon entropy, conditional entropy, relative entropy and mutual information. The second part, consists of studying some mathematical background and techniques by means of statistical formulation of quantum mechanics such as the density operator formalism and quantum measurements. Bringing this together we have studied in the last part of this chapter the essential notions of quantum information theory, which are the von Neumann entropy, notion of qubit, and so on. Indeed, all of these preliminaries are essentially used to understand the core aim of quantum correlations including entanglement as well as the theory of open quantum systems as we will see in the next chapters.

CHAPTER 2

QUANTUM ENTANGLEMENT: A COMPREHENSIVE STUDY OF MEASURES

When two or more physical systems interact in the quantum realm, a kind of correlation known as quantum entanglement is generated between them, even if they are spatially separated. The most surprising feature is that, regardless of their distance from one another, a measurement made locally with an observable on one of the sub-systems instantly modifies the state of the others to be consistent with the measurement made on the first one. This means that, despite their spatial separation, the fate of these systems remains linked, a phenomenon known as quantum entanglement. It is a resource that is unique to quantum mechanics which refers to non-classicality and by any classical means, the correlation cannot be defined between the components of a composite quantum system. The concept of entanglement dates back to the early time of the development of quantum theory. It refers to a non-local correlation that was famously dubbed *"spooky action at a distance"* by Albert Einstein, Boris Podolsky and Nathan Rosen (EPR) in their theoretical work [2]. Schrödinger was the first one to describe the phenomenon of entanglement (*"Verschränkung"* in German) in his interaction with the famous EPR work [2, 3, 125], where he characterized a correlation between components of a quantum state that had a non-local nature [3]. Besides, Schrödinger used his legendary cat, known as Schrödinger's cat, as an extreme example to illustrate entanglement [126]. Such a correlation upsets the conceptual frameworks within which the physical world has been thought of until now. In particular, entanglement prompted Einstein and his colleagues to demonstrate a fault in quantum theory. The EPR paradox paradigm concluded that the description of quantum mechanics was either incomplete or non-local. In the case of incompleteness, they believed that there must be some *"hidden variables"* that were ignored by quantum mechanics, whose knowledge would allow for the prediction of measurement results with certainty. On the other hand, if quantum mechanics was non-local, there could be a link between distant parts of a composite system that could not be determined using classical methods.

For over three decades, this problem remained philosophical until J. S. Bell demonstrated in 1964 that no local deterministic theory of hidden variables could reproduce all the statistical predictions of quantum mechanics [127]. In other words, the correlations between measurement results must satisfy certain inequalities, known as Bell inequalities, which constrain local correlations [127]. Bell's theorem has been experimentally verified through a series of experiments known as Bell tests. These experiments have shown that the predictions of quantum mechanics are correct and that the correlations between measurements violate Bell's inequalities. Some of the earliest and most well-known experimental tests of Bell's inequalities were conducted by Freedman et *al* in 1972 [128], and also by Aspect et *al* in 1982 [129]. More recent and highly

cited experimental tests of Bell's inequalities include the work of Rowe et *al* in 2001 [130]. The experimental verification of Bell's theorem has led to the conclusion that quantum mechanics is a non-local theory and that the correlations between measurements can only be explained through entanglement. The practical implications of Bell's theorem for quantum communication and cryptography are discussed by Gisin and Thew in Ref. [109].

In this chapter, we aim to introduce the fundamental concept of quantum entanglement, which is a key ingredient in the work presented in this thesis. The first part of this chapter is devoted to the presentation of quantum entanglement, in which we give the basic concepts and discuss some separability criteria for both pure and mixed states. Afterward, we introduce different measures to quantify the amount of quantum entanglement present in bipartite as well as multipartite quantum systems. This provides a comprehensive understanding of the different ways to measure and quantify entanglement. Overall, by the end of this chapter, readers will have gained a deep understanding of the entanglement and various measures.

1 Quantum entanglement

1.1 Separability and entanglement

This section provides a general overview of determining whether a given state is separable or entangled. To do this objective, we require first a mathematical definition of entanglement versus separability. Let us suppose a bipartite quantum system "AB" consisting of two parts $A(B)$ of dimension $d_A(d_B)$. A pure quantum state $|\psi_{AB}\rangle \in \mathcal{H}_A \otimes \mathcal{H}_B$ is said to be separable or unentangled if and only if it constitutes a product state described in terms of sub-systems, namely A and B, which can be written as [6]

$$|\psi_{AB}\rangle = |\phi_A\rangle \otimes |\chi_B\rangle = |\phi\chi\rangle\,. \tag{2.1}$$

Here, $|\phi_A\rangle \in \mathcal{H}_A$ and $|\chi_B\rangle \in \mathcal{H}_B$ represent the state vectors of sub-systems A and B, respectively. From now on, we will use the simpler notation $|\phi\chi\rangle$ instead of $|\phi_A\rangle \otimes |\chi_B\rangle$. In this circumstance, the reduced density matrices of both sub-systems will also be pure states. Specifically, we have:

$$\rho_A = |\phi_A\rangle\langle\phi_A| \quad \text{and} \quad \rho_B = |\chi_B\rangle\langle\chi_B|\,. \tag{2.2}$$

The above formula (2.2) physically means that the sub-systems A and B are completely independent of each other. This implies that a measurement performed on one sub-system does not affect the state of the other sub-system, as long as they are not non-locally related. Hence, the measurement results obtained from both sub-systems will be uncorrelated. In contrast, if the composed state $|\psi_{AB}\rangle$ cannot be expressed as a product state of sub-systems A and B, i.e., $|\psi_{AB}\rangle \neq |\phi_A\rangle \otimes |\chi_B\rangle$, then the sub-systems A and B are said to be in an entangled state and the whole state $|\psi_{AB}\rangle$ is said to be entangled. In this scenario, the sub-systems A and B are no longer independent from one another and their states are strongly correlated. We can interpret this by the fact that when a measurement is performed on one of the sub-systems, either A or B, the state of the other sub-system will be influenced by the measurement outcome with strongly correlated measurement results, regardless of how far apart they are. This non-local correlation is a fundamental aspect of entanglement. Moreover, the reduced density operators ρ_A and ρ_B corresponding to entangled states will correspond to mixed states. This implies that the reduced density operators will be described by density matrices that are not pure states, but rather a statistical mixture of pure states. As an example of pure entangled and separable states, consider a two-qubit state given by

$$|\psi\rangle = \cos(\theta)\,|01\rangle - \sin(\theta)\,|10\rangle\,. \tag{2.3}$$

The above state $|\psi\rangle$ (2.3) is entangled for all values of θ, except for $\theta = \pi/2$ or π where it becomes separable.

So far, we have only considered the case of pure states. However, this definition can also be extended to mixed states. Specifically, a quantum state described by the density matrix ρ_{AB} is said to be entangled if it cannot be expressed as a convex combination of the product states of its constituent parties [6, 131]

$$\rho_{AB} \neq \sum_i p_i \rho_A^{(i)} \otimes \rho_B^{(i)}, \tag{2.4}$$

where p_i is a probability distribution such that $p_i > 0$ and $\sum_i p_i = 1$ with $\rho_A^{(i)} = \left|\phi_A^{(i)}\right\rangle \left\langle\phi_A^{(i)}\right|$ $\left(\rho_B^{(i)} = \left|\chi_B^{(i)}\right\rangle \left\langle\chi_B^{(i)}\right|\right)$ is the density matrix that describes the sub-system $A(B)$. Indeed, if the above equality holds, the state is separable. It is important to note that separable states do not carry quantum entanglement. However, the definition (2.4) can also be generalized to the case of a multi-partite state, which is an N-partite state acting on $\mathcal{H} = \mathcal{H}_{d_1} \otimes \mathcal{H}_{d_2} \otimes \cdots \otimes \mathcal{H}_{d_N}$. This state is classified as separable or unentangled if it can be expressed as a convex sum of tensor products of its constituent sub-systems as follows:

$$\rho_N = \sum_i p_i \rho_1^{(i)} \otimes \rho_2^{(i)} \otimes \cdots \otimes \rho_N^{(i)}, \quad p_i > 0 \text{ and } \sum_i p_i = 1, \tag{2.5}$$

where p_i is a probability distribution such that $p_i > 0$ and $\sum_i p_i = 1$. While $\rho_j^{(i)}$ denotes the density matrix that describes the sub-system j for the i^{th} term of the convex sum. If the above equality does not hold, the state is said to be entangled.

1.2 Example of entangled states

A prominent example of two-qubit entangled states is the well-known *"Bell states"* [127]. They are named after John S. Bell and they are related to the Bell inequality [132]. Furthermore, they have been implemented in various quantum information science applications, such as superdense coding [133] and quantum teleportation [49]. When two qubits are in the Bell state, they form an EPR pair and are maximally entangled, forming an orthonormal basis for the two-qubit state space. Therefore, they can be distinguished from one another by an appropriate quantum measurement, and one state can be transformed into the other through a local unitary transformation on one of the sub-systems. The four Bell states are explicitly given by [5]

$$|\beta_{00}\rangle = \frac{1}{\sqrt{2}}(|00\rangle + |11\rangle), \tag{2.6}$$

$$|\beta_{01}\rangle = \frac{1}{\sqrt{2}}(|01\rangle + |10\rangle), \tag{2.7}$$

$$|\beta_{10}\rangle = \frac{1}{\sqrt{2}}(|00\rangle - |11\rangle), \tag{2.8}$$

$$|\beta_{11}\rangle = \frac{1}{\sqrt{2}}(|01\rangle - |10\rangle). \tag{2.9}$$

In a compact form, the Bell states (2.6-2.9) can be re-written as

$$\left|\beta_{xy}\right\rangle = \frac{1}{\sqrt{2}}(|0y\rangle + (-1)^x |1\overline{y}\rangle), \quad (x, y = 0, 1) \tag{2.10}$$

where $\overline{y}$ is the negation of y, for example, if $y = 0$, $\overline{y} = 1$ and vice versa. Moreover, these states can be represented on the surface of the Bloch Sphere.

The notion of entanglement is based on the assumption that two partners, namely Alice and Bob, can locally create any given quantum state. Moreover, they have access to a classical communication channel, such as phone, internet and so on. The following density operator, $\rho_{AB} = \sum_i p_i \left|\phi_A^{(i)}\right\rangle \left\langle\phi_A^{(i)}\right| \otimes \left|\chi_B^{(i)}\right\rangle \left\langle\chi_B^{(i)}\right|$, can be then used by the two partners to create any separable state via the following process: Bob is informed of which state Alice produced by her preparation of the corresponding state $\left|\phi_A^{(i)}\right\rangle$ with probability p_i. Then, Bob prepares the corresponding state $\left|\chi_B^{(i)}\right\rangle$ based on Alice's results. However, entangled states such as the singlet state (2.9) cannot be produced in this manner.

1.3 Local operations and classical communication

The above procedure that produces separable states is classified under *"local operations and classical communication"* (LOCC). This approach was initially introduced by Bennett *et al* in Ref. [14]. LOCC is the most comprehensive method used in quantum theory, as long as the partners only employ classical communication. The mathematical explanation of these operations is complicated and remains under investigation. However, Chitambar *et al* in Ref. [134] have significantly contributed to a better understanding of the LOCC approach. The overall concept is straightforward and is explained in the following. A quantum operation Λ^{LOCC} for two parties, namely Alice and Bob, belongs to the class of LOCC if it can be decomposed into the following steps:

Step 1: Alice performs a local measurement on her sub-system.

Step 2: Alice communicates the outcome of her measurement classically to Bob.

step 3: Bob performs a local measurement on his sub-system using the information received from Alice.

step 4: Bob communicates the result of his measurement classically to Alice.

step 5: Alice performs a local measurement on her sub-system according to the information received, and the process restarts at **Step 2**.

In quantum information theory, LOCC plays a crucial role, particularly in the study of the concept of entanglement. As previously explained, any separable state can be produced using LOCC. However, LOCC cannot be used to generate entangled states [6].

2 Separability criteria

To distinguish entangled states from separable ones is a fundamental topic in quantum information theory. However, determining whether a given state can be factored into product states is not a straightforward task due to the lack of constructive criteria provided by the definition of entanglement of a bipartite state. As previously mentioned, entanglement can be considered a non-local phenomenon where the measurement on one sub-system has an immediate impact on the outcome of a measurement on the other sub-system. For bipartite pure states, the Schmidt decomposition is an effective approach to detecting quantum entanglement with certainty. However, for bipartite mixed states, finding a decomposition as in Eq.(2.1) or proving that none exists is a challenging problem. To address this issue, researchers have made significant efforts to examine the separability of mixed states, leading to the development of various operational separability criteria such as the Peres-Horodecki criterion and entanglement

witnesses. Given the complexity of the problem and the importance of the topic in quantum information theory, in this section, we will thoroughly study some widely used disentanglement criteria for both mixed and pure states.

2.1 Seprability criteria for pure states: Schmidt decomposition

In quantum information theory, *"Schmidt decomposition"*, also known as bi-orthogonal expansion or polar expansion [5, 135–137], is a crucial tool for understanding the entanglement properties of bipartite pure quantum states. This decomposition provides a necessary and sufficient criterion for separability, allowing us to represent the state vector of any bipartite quantum system in terms of a single sum rather than double sums. Moreover, it demonstrates that any bipartite pure state can be decomposed into a superposition of orthonormal states. Consider a bipartite quantum system AB composed of two sub-sytems, namely A and B with dimensions $d_A \equiv \dim(\mathcal{H}_A)$ and $d_B \equiv \dim(\mathcal{H}_B)$, respectively, where $d_A \leq d_B$. Let $|\psi_{AB}\rangle$ be a pure state of a composite bipartite system AB in the product Hilbert space $\mathcal{H}_A \otimes \mathcal{H}_B$ and let $\rho_A(\rho_B)$ be the reduced density matrix of the sub-system $A(B)$. According to Schmidt's theorem, there exists an orthonormal basis $\left|u_i^A\right\rangle \in \mathcal{H}_A$ for sub-system A and an orthonormal basis $\left|v_i^A\right\rangle \in \mathcal{H}_B$ for sub-system B, such that the state vector can be expressed as:

$$|\psi_{AB}\rangle = \sum_{i=1}^{n} \sqrt{\lambda_i} \left|u_i^A\right\rangle \otimes \left|v_i^B\right\rangle . \tag{2.11}$$

Here, "n" represents the Schmidt rank of the state vector $|\psi_{AB}\rangle$, satisfying the inequality $n \leq \min\{d_A, d_B\}$, while $\{\lambda_i\}$ are positive real coefficients called Schmidt coefficients, which satisfy the condition $\sum_{i=1}^{n} \lambda_i = 1$. The Schmidt coefficients form the spectrum of the reduced states ρ_A and ρ_B of the sub-systems A and B, respectively, corresponding to the orthonormal states that represent their eigenstates. Thus, the reduced density operators describing each of the sub-systems can be written in the diagonal form as follows:

$$\begin{aligned} \rho_A &= \mathrm{Tr}_B(\left|\psi_{AB}\right\rangle \left\langle\psi_{AB}\right|) = \mathrm{Tr}_B(\sum_{ij} \sqrt{\lambda_i \lambda_j} \left|u_i^A\right\rangle \left\langle u_j^A\right| \otimes \left|v_i^B\right\rangle \left\langle v_j^B\right|) \\ &= \sum_{i=1}^{n} \lambda_i \left|u_i^A\right\rangle \otimes \left|v_i^B\right\rangle , \end{aligned} \tag{2.12}$$

$$\begin{aligned} \rho_B &= \mathrm{Tr}_A(\left|\psi_{AB}\right\rangle \left\langle\psi_{AB}\right|) = \mathrm{Tr}_A(\sum_{ij} \sqrt{\lambda_i \lambda_j} \left|u_i^A\right\rangle \left\langle u_j^A\right| \otimes \left|v_i^B\right\rangle \left\langle v_j^B\right|) \\ &= \sum_{i=1}^{n} \lambda_i \left|u_i^A\right\rangle \otimes \left|v_i^B\right\rangle . \end{aligned} \tag{2.13}$$

The Schmidt coefficients λ_i correspond to the eigenvalues of one of the reduced density matrices ρ_A or ρ_B. Thus, ρ_A and ρ_B have the same non-zero eigenvalues, with the only difference being the degeneracy of the zero eigenvalues. Therefore, the basis vectors of the Schmidt basis are given by the eigenstates of ρ_A and ρ_B. An important aspect is that the Schmidt number allows us to introduce a mathematical definition of bipartite entanglement in pure states. In this regard, it is evident that the state $|\psi_{AB}\rangle = |\phi_A\rangle \otimes |\chi_B\rangle$ is expressed according to the Schmidt decomposition (2.11), with the Shmidt number equal to the unity, i.e., $n = 1$. Therfore, it is a separable state since it is written as a direct product of two states in $\mathcal{H}_A$ and $\mathcal{H}_B$. In other words, a bipartite pure state is said to be separable or unentangled if and only if there is only

one non-zero Schmidt coefficient λ_i. Moreover, the reduced density matrices (2.12) and (2.13) for $n = 1$ have only one element, and as a result, we obtain

$$\mathrm{Tr}(\rho_A^2) = \mathrm{Tr}(\rho_B^2) = 1. \tag{2.14}$$

This implies that the reduced states are pure (see Eq.(1.23)). In contrast, an entangled state, with a Schmidt number that is strictly larger than one, has no such direct product expression, in which case ρ_A and ρ_B are mixed. Moreover, a bipartite pure state is maximally entangled if the Schmidt coefficients λ_i are equal and non-zero. To provide a concrete example of the Schmidt decomposition theorem, let us consider a two-qubit state given by

$$|\psi_1\rangle = \frac{1}{2}(|00\rangle - |01\rangle - |10\rangle + |11\rangle), \tag{2.15}$$

where it is defined in a 4-dimensional Hilbert space $\mathcal{H}_A \otimes \mathcal{H}_B$ with $\mathcal{H}_A$ and $\mathcal{H}_B$ each have two dimensions. The computational basis in this example is not a Schmidt basis for either $\mathcal{H}_A$ or $\mathcal{H}_B$. To determine whether this state is separable or entangled, we must compute first the reduced density matrix ρ_A or ρ_B

$$\rho_B = \frac{1}{2}(|0\rangle\langle 0| - |0\rangle\langle 1| - |1\rangle\langle 0| + |1\rangle\langle 1|) \tag{2.16}$$

$$\rho_B = \frac{1}{2}\begin{pmatrix} 1 & -1 \\ -1 & 1 \end{pmatrix}. \tag{2.17}$$

This state has only one non-zero Schmidt coefficient, namely $\lambda_1 = 1$. Therefore, the state $|\psi\rangle$ is separable and the state (2.15) can be rewritten as

$$|\psi_1\rangle = \left[\frac{1}{\sqrt{2}}\left(|0\rangle_A - |1\rangle_A\right)\right] \otimes \left[\frac{1}{\sqrt{2}}\left(|0\rangle_B - |1\rangle_B\right)\right], \tag{2.18}$$

with the Schmidt bases chosen to be

$$\left|u_1^A\right\rangle = \frac{1}{\sqrt{2}}\left(|0\rangle_A - |1\rangle_A\right), \qquad \left|v_1^B\right\rangle = \frac{1}{\sqrt{2}}\left(|0\rangle_B - |1\rangle_B\right),$$

$$\left|u_2^A\right\rangle = \frac{1}{\sqrt{2}}\left(|0\rangle_A + |1\rangle_A\right), \qquad \left|v_2^B\right\rangle = \frac{1}{\sqrt{2}}\left(|0\rangle_B + |1\rangle_B\right).$$

Another important example defined in the same 4-dimensional space $\mathcal{H}_A \otimes \mathcal{H}_B$ as in the previous example (2.15) is the well-known Bell state (2.9):

$$|\beta_{11}\rangle = \frac{1}{\sqrt{2}}\left(|01\rangle - |10\rangle\right). \tag{2.19}$$

Following the same procedure as in the previous example, the reduced density matrix ρ_A is given as follows

$$\rho_A = \frac{1}{2}\left(|0\rangle\langle 0| + |1\rangle\langle 1|\right) \tag{2.20}$$

$$\rho_A = \frac{1}{2}I_2, \tag{2.21}$$

where I_2 is the 2-dimensional identity operator. In this particular example, we observe that there exist two equal non-zero Schmidt coefficients, namely $\lambda_1 = 1/2$ and $\lambda_2 = 1/2$. This indicates that the state $|\beta_{11}\rangle$ is maximally entangled.

2.2 Purification

A mixed quantum state can be understood as either a statistical mixture of pure quantum states or as part of a higher-dimensional pure state. To turn a mixed state into a pure state, we can introduce another system, called reference system C, in such a way that the total state becomes pure. This process is known as *"purification"* [5]. The resulting pure state exists in a higher-dimensional Hilbert space and has a reduced density matrix identical to the original state. To purify a bipartite mixed state ρ_{AB} on a Hilbert space and derive the pure state $|\psi_{ABC}\rangle$ such that $\rho_{ABC} = |\psi_{ABC}\rangle \langle\psi_{ABC}|$ and $\rho_{AB} = \mathrm{Tr}_C(\rho_{ABC})$, the first step is to diagonalize ρ_{AB} by finding its eigenvalues and eigenvectors. Let $\{\lambda_1, \lambda_2, \lambda_3, \lambda_4\}$ and $\{|\lambda_1\rangle, |\lambda_2\rangle, |\lambda_3\rangle, |\lambda_4\rangle\}$ be the set of eigenvalues and eigenvectors of ρ_{AB}, respectively. Next, we define a set of vectors as a Schmidt basis, such that

$$|1\rangle = \begin{pmatrix} 1 \\ 0 \\ 0 \\ 0 \end{pmatrix}, \quad |2\rangle = \begin{pmatrix} 0 \\ 1 \\ 0 \\ 0 \end{pmatrix}, \quad |3\rangle = \begin{pmatrix} 0 \\ 0 \\ 1 \\ 0 \end{pmatrix}, \quad |4\rangle = \begin{pmatrix} 0 \\ 0 \\ 0 \\ 1 \end{pmatrix}. \tag{2.22}$$

Using this notation, we can express the pure state $|\psi_{ABC}\rangle$ as

$$|\psi_{ABC}\rangle = \sqrt{\lambda_1}\,|\lambda_1\rangle \otimes |1\rangle + \sqrt{\lambda_2}\,|\lambda_2\rangle \otimes |2\rangle + \sqrt{\lambda_3}\,|\lambda_3\rangle \otimes |3\rangle + \sqrt{\lambda_4}\,|\lambda_4\rangle \otimes |4\rangle\,. \tag{2.23}$$

We can easily verify that $\rho_{AB} = \mathrm{Tr}_C(\rho_{ABC})$, where C is the reference system. The dimension of the reference system is determined by the rank of the system. For example, if we have two non-zero eigenvalues, we only require two bases and this is the dimension of the reference system. It is important to note that the reference state is not unique unless the purification is achieved by a unitary operation and the bases can be defined by any set of orthonormal states.

2.3 Separability criteria for mixed states

Schmidt's decomposition theorem is shown to be a necessary criterion for determining whether a given bipartite pure state is factorized or not. However, this theorem is not any further useful for mixed states as the latter describes more complex systems than pure states. To distinguish entangled mixed states from separable ones, we must proceed with alternative strategies for this purpose. Therefore, the investigation of the separability criteria for mixed states has attracted much attention and has been widely studies in a variety of physical contexts [138]. Positive partial transposition and entanglement witnesses are just a few of the commonly used criteria that can be applied to this issue.

2.4 Peres-Horodecki criterion

Positive partial transposition (PPT), also known as the *"Peres-Horodecki criteria"*, is a necessary condition for the separability in arbitrary bipartite mixed states [139, 140]. This criterion was first proposed by Peres in the context of entanglement theory in 1996 [139]. The PPT criterion involves a straightforward algebraic calculation without any optimization procedure since it is based on a partial transposition operation of the density matrix of a given bipartite system. In order to apply the PPT criteria, one should consider a bipartite mixed state ρ_{AB} that acts on the Hilbert space $\mathcal{H}_A \otimes \mathcal{H}_B$. This mixed state can be extended in an arbitrary orthonormal product basis, resulting in the following expression:

$$\rho_{AB} = \textstyle\sum_{ijkl} \rho_{ijkl}\,|i\rangle \langle j| \otimes |k\rangle \langle l|\,. \tag{2.24}$$

In the above expression, $|i\rangle$ and $|j\rangle$ are the state vectors in the Hilbert space $\mathcal{H}_A$ of the first sub-system. Likewise, $|k\rangle$ and $|l\rangle$ are the state vectors of the second sub-system acting on the Hilbert space $\mathcal{H}_B$. The partial transpose operation of a given density matrix ρ_{AB} with respect to the first (second) sub-system $A(B)$ is given by taking the transposition only over the degrees of freedom of sub-system $A(B)$. This operation gives:

$$\rho_{AB}^{T_A} = (T_A \otimes I_B) = \sum_{ij} \sum_{kl} \rho_{ijkl} \left|j\right\rangle \left\langle i\right| \otimes \left|k\right\rangle \left\langle l\right|, \tag{2.25}$$

$$\rho_{AB}^{T_B} = (I_A \otimes T_B) = \sum_{ij} \sum_{kl} \rho_{ijkl} \left|i\right\rangle \left\langle j\right| \otimes \left|l\right\rangle \left\langle k\right|, \tag{2.26}$$

where T indicates the transposition operation and $I_A\,(I_B)$ represents the identity operator of sub-system $A(B)$. According to the Peres-Horodecki criteria, a state ρ_{AB} is separable if its partial transposition with respect to sub-system A is a positive semi-defined density matrix, i.e., $\rho_{AB}^{T_A} \geq 0$. The same procedure naturally holds for $\rho_{AB}^{T_B}$. Conversely, if $\rho_{AB}^{T_A}\left(\rho_{AB}^{T_B}\right)$ has at least one non-positive eigenvalue, then ρ_{AB} is said to be entangled. Therefore, the positivity of the partial transposition (PPT) is necessary for separability [139]. It is important to note that this criterion is independent of the sub-system on which the partial transposition is carried out. This means that $\rho_{AB}^{T_B} = \left(\rho_{AB}^{T_A}\right)^T$, since the positivity of the partially transposed state only depends on its spectrum. Moreover, any separable bipartite state, ρ_{AB}, can be expressed in the form $\rho_{AB} = \sum_i p_i \rho_A^{(i)} \otimes \rho_B^{(i)}$. Therefore, the partial transpose of ρ_{AB} with respect to sub-system A can be written as

$$\rho_{AB}^{T_A} = \sum_i p_i \left(\rho_A^{(i)}\right)^{T_A} \otimes \rho_B^{(i)} \quad \text{and} \quad \rho_{AB}^{T_B} = \sum_i p_i \rho_A^{(i)} \otimes \left(\rho_B^{(i)}\right)^{T_B}. \tag{2.27}$$

Horodecki *et al.* in Ref. [140] have shown that the PPT criterion is a necessary and sufficient condition for inseparability for low-dimensional bipartite systems such as $2 \otimes 2$, $2 \otimes 3$ and $3 \otimes 2$ systems (see Fig.2.1.a). However, this criterion is necessary but not sufficient for higher-dimensional systems (see Fig.2.1.b). It has been established that some entangled states satisfy the positive partial transpose condition ($\rho_{AB}^{T_A} \geq 0$) and are entangled [141]. Such states are referred to as bound entangled since their entanglement cannot be distilled to obtain maximally entangled states [142]. Therefore, the PPT states set includes both non-separable and separable states. Conversely, if a quantum state has a non-positive partial transpose (NPT), the state is inevitably entangled. After taking partial transpose, the density matrix under consideration must have at least one negative eigenvalue, which is known as NPT. While a conjecture exists for the existence of entangled bound states with negative partial transposition [143, 144], a fully rigorous analytical proof remains an open problem [145]. To illustrate the PPT criterion, let us consider the following two-qubit state:

$$\rho_W = \left(\frac{1-r}{4}\right) I_2 \otimes I_2 + r \left|\beta_{11}\right\rangle \left\langle \beta_{11}\right|, \tag{2.28}$$

where r is the purity parameter with $0 < r \leq 1$, while I_2 being the identity matrix in 2-dimension and $|\beta_{11}\rangle$ denotes the maximally entangled Bell state (2.9). Indeed, this class of states (2.28) belongs to the set of well-known Werner-like states [131]. They are significant in several applications of quantum information and computation processing since they can ensure the separability of mixed states and have been classified as generalized maximally entangled mixed states [131]. Besides, they are $(N \times N)$-dimensional bipartite quantum states that are invariant under any local unitary transformation of the form $U \otimes U$ for all unitary operators U, satisfying: $\rho = (U \otimes U)\,\rho\,(U \otimes U)^\dagger$. In the standard basis of two-qubit $\{|00\rangle, |01\rangle, |10\rangle, |11\rangle\}$, the state ρ_W (2.28) can be rewritten as

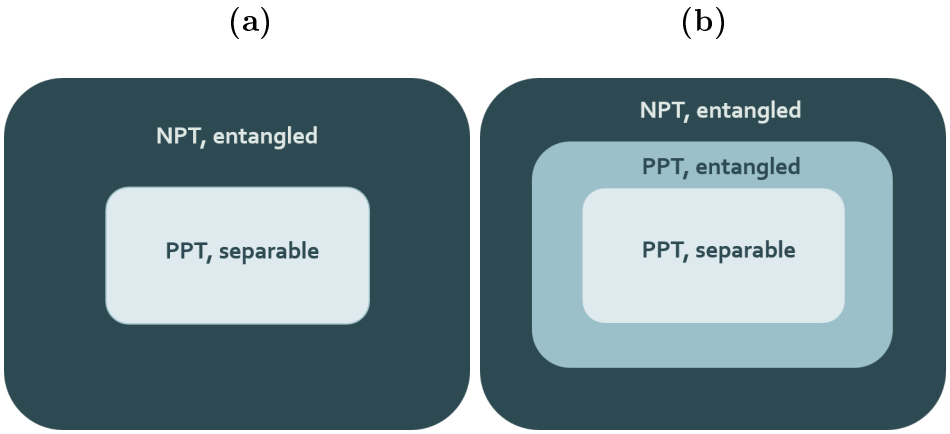


Figure 2.1: A schematic representation of the PPT and NPT states for the Hilbert spaces $2\otimes 2$, $2\otimes 3$, and $3\otimes 2$ is shown in (a) and for higher dimensions Hilbert spaces in (b).

$$\rho_W = \frac{1}{4}\begin{pmatrix} 1-r & 0 & 0 & 0 \\ 0 & 1+r & -2r & 0 \\ 0 & -2r & 1+r & 0 \\ 0 & 0 & 0 & 1-r \end{pmatrix}, \tag{2.29}$$

with respect to the second-qubit B, the partial transposed density matrix becomes

$$\rho_W^{T_B} = (I_A \otimes T_B) = \frac{1}{4}\begin{pmatrix} 1-r & 0 & 0 & -2r \\ 0 & 1+r & 0 & 0 \\ 0 & 0 & 1+r & 0 \\ -2r & 0 & 0 & 1-r \end{pmatrix}. \tag{2.30}$$

By straightforward calculation, the set of eigenvalues of $\rho_W^{T_B}$ (2.30) is $\{\frac{1+r}{4}, \frac{1+r}{4}, \frac{1+r}{4}, \frac{1-3r}{4}\}$. It is obvious that $\frac{1-3r}{4}$ is the lowest eigenvalue which gives a threshold value of the fraction $r^* = 1/3$ such that

$$\begin{cases} -\frac{1}{3} \leq r \leq \frac{1}{3}, & \rho_W \text{ is separable} \\ \frac{1}{3} \leq r \leq 1, & \rho_W \text{ is entangled} \end{cases} \tag{2.31}$$

However, although this criterion is much stronger for detecting the inseparability of a given quantum system, it requires knowledge of the density operator under scrutiny, which is not always possible in experimental settings. An alternative method for detecting separability is the *"entanglement witness"* approach, which is more effective in detecting entanglement both theoretically and experimentally [146].

2.5 Entanglement witnesses

Another useful technique for detecting entanglement in arbitrary quantum systems is the so-called *"entanglement witness"* (EW) [146]. It provides a necessary and sufficient entanglement criterion in terms of directly measurable observable W. This observable is a non-positive definite Hermitian operator acting on the Hilbert space $\mathcal{H}$, where $\mathcal{D}_{sep}(\mathcal{H})$ represents a set of all separable quantum states in Hilbert space $\mathcal{H}$. Specifically, the observable W is referred to as an entanglement witness for a given state ρ if it satisfies the following conditions [6, 140, 147]

$$\text{EW} = \begin{cases} \langle W \rangle \geq 0 & \text{for all separable states } \rho_{sep} \in \mathcal{D}_{sep}(\mathcal{H}) \\ \langle W \rangle < 0 & \text{for at least one entangled state } \rho_{ent} \end{cases} \tag{2.32}$$

where $\langle W \rangle$ is the expectation value. It is given by

$$\langle W \rangle = \mathrm{Tr}(W\rho). \tag{2.33}$$

The observable W is a tool used to detect entanglement in quantum states. If the expectation value of W is non-negative for all possible separable states and has at least one negative eigenvalue, then the state is entangled, i.e., $W \not\geq 0$. This means that the observable W can identify entangled states with high accuracy. However, it is important to note that a positive expectation value of W does not necessarily indicate a separable state, as there are some entangled states that can still have a positive expectation value. One key advantage of using the entanglement witness operator W as a criterion is that it only requires the knowledge of the expectation value of one operator, which makes it computationally efficient and less demanding compared to other entanglement detection methods that require full knowledge of the density operator. An example of such a witness is the Werner state expressed in Eq.(2.28). In this case, the observable W is given by

$$W = \left(|\phi_-\rangle\langle\phi_-|\right)^{T_B} = \frac{1}{2}\begin{pmatrix} 1 & 0 & 0 & 0 \\ 0 & 0 & 1 & 0 \\ 0 & 1 & 0 & 0 \\ 0 & 0 & 0 & 1 \end{pmatrix}, \tag{2.34}$$

where $|\phi_-\rangle = \frac{1}{\sqrt{2}}(|00\rangle + |11\rangle)$ is the eigenstate corresponding to the negative eigenvalue $\left(\frac{1-3r}{4}\right)$ of the partially transposed matrix $\rho_W^{T_B}$ (2.30). Then, the witness operator W is given by taking the partially transposed projector onto this eigenvector $|\phi_-\rangle$. Thus, the expectation value of W (2.34) of the state (2.28) is $\langle W \rangle = \mathrm{Tr}(W\rho) = \left(\frac{1-3r}{4}\right)$, which means that the state is entangled if and only if $r > 1/3$. The same outcome is given using the PPT criterion (2.31).

Moroever, entanglement witness has a clear geometrical significance. The expectation value of an operator depends linearly on the state of the system. Therefore, the set of all states satisfying the condition $\langle W \rangle = 0$ is a hyperplane that divides this set into two areas [146]. The first area with $\langle W \rangle < 0$ is the set of states detected by the witness operator. All of these states are detected by W and entangled. The other area contains the quantum states with $\langle W \rangle > 0$ and includes the set of all separable states $\mathcal{D}_{sep}(\mathcal{H})$ as well as some entangled states. This scheme is shown in Fig.2.2. However, EW is not necessarily invariant under any local unitary transformations, which conflicts with our idea of entanglement which term it as a non-local characteristic of the state ρ.

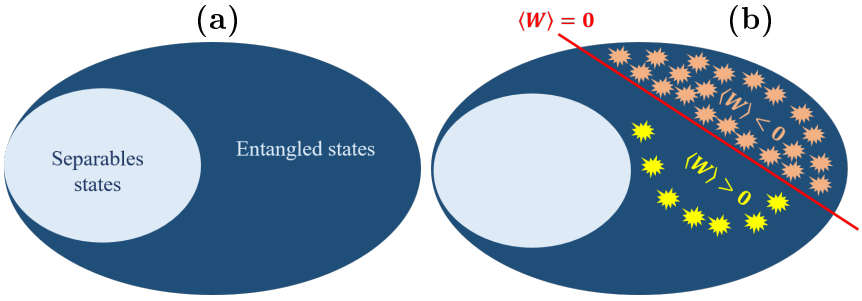


Figure 2.2: Schematic illustration of the entanglement witness. (a): The set of all states is divided into a convex set of separable states (Light Blue) and entangled states (Magenta). (b): The witness operator defines a hyperplane (Blue line) for all states that satisfy $\langle W \rangle = 0$. All separable states (Light Blue) as well as some entangled states that are represented by beige stars satisfy the property $\langle W \rangle > 0$. States with negative expectation $\langle W \rangle < 0$ are the quantum states detected by the witness, i.e, the ones represented by yellow stars.

Entanglement witnesses are an effective method for detecting entangled states in experiments. With some preliminary knowledge about the form of the states, it is possible to engi-

neer or implement some quantum information processing protocols. There are entanglement witnesses in terms of accessible observables that offer a direct approach to test the presence or absence of quantum entanglement in laboratory experiments [8, 9, 148, 149]. Barbieri *et al* in Ref. [148] reported such an experimental realization of the entanglement witnesses. In this experiment, they used parametric down-conversion and linear optics to generate two-qubit Werner states of photons. Moreover, Bourennane *et al* in Ref. [149] performed the first experiment in which a witness for multi-qubit system is utilized. They generated a four-qubit singlet state employing the second-order parametric down-conversion emission along with post-selection, as described in [150].

3 Entanglement measures for bipartite systems

In order to use entangled states for implementing various processes in quantum information sciences and non-local operations, important to determine if the degree of entanglement in a given quantum system is sufficient for a particular task. To accomplish this goal, an appropriate measure of entanglement must first be defined. However, identifying an appropriate measure is a complex task in quantum information theory, as several entanglement measures are not equivalent, and this problem is more challenging than the separability problem. The question of whether a unique measure of entanglement exists but remains unsolved. In this section, we will study in detail some commonly used quantum entanglement quantifiers in the field of quantum information theory, highlighting the advantages and drawbacks of each measure. This will provide a comprehensive understanding of the different measures and aid in determining the appropriate measure for a given situation.

3.1 Requirements for entanglement measures

When considered, a bipartite state ρ_{AB} that acts on the Hilbert space, namely, $\mathcal{H} = \mathcal{H}_A \otimes \mathcal{H}_B$ along with $dim\ \mathcal{H}_A = dim\ \mathcal{H}_B = d$. Entanglement measures or entanglement monotones must, by definition, quantify the degree of entanglement. An appropriate entanglement measure $\mathcal{E}(\rho_{AB})$ must fulfill the required properties [151, 152], which are listed below:

Positivity: An entanglement measure is a function $\mathcal{E}(\rho_{AB})$ that provides to each state a positive real number, $\mathcal{E}(\rho_{AB}) \in \mathbb{R}^+$ of a finite-dimensional bipartite system AB.

Normalisation: A reliable Entanglement quantifier $\mathcal{E}(\rho_{AB})$ remains 0 for any disentangled state, i.e., $\mathcal{E}(\rho_{AB}) = 0$, and reaches its maximum value, namely $\mathcal{E}(\rho_{AB}) = \log_2(d)$, for maximally entangled states in $d \times\ d$ dimension such that $|\Psi\rangle = \frac{1}{\sqrt{d}} \sum_{i=1}^{d} |i\rangle \otimes |i\rangle$.

Invariance: An entanglement measure $\mathcal{E}(\rho_{AB})$ should be invariant under local unitary transformations U_A and U_B that respectively act on $\mathcal{H}_A$ and $\mathcal{H}_B$ for any given quantum states ρ_{AB}, i.e.,

$$\mathcal{E}\left((U_A \otimes U_B)\, \rho_{AB}\, (U_A \otimes U_B)\,\dagger\right) = \mathcal{E}(\rho_{AB}). \tag{2.35}$$

LOCC monotonicity: Since quantum correlation are not induced via LOCC, it is reasonable to require that $\mathcal{E}(\rho_{AB})$ is non-increasing under such operations. In other words, if Λ^{LOCC} is a positive map that LOCC can implement, i.e.,

$$\mathcal{E}\left(\left(\Lambda^{LOCC}\left(\rho_{AB}\right)\right)\right) \leq \mathcal{E}(\rho_{AB}). \tag{2.36}$$

The above condition (2.36) is commonly replaced by a different condition, namely that $\mathcal{E}(\rho_{AB})$ must not exceed on average under LOCC transformations. In other words, if a

LOCC transformation maps ρ_{AB} to states $\rho_{k}{}_{AB}$ with certain probabilities p^k, this means that

$$\sum_k p^k \mathcal{E}(\rho_{k}{}_{AB})) \leq \mathcal{E}(\rho_{AB}). \tag{2.37}$$

The latter condition is considerably robust than Eq.(2.36), but various entanglement measures also satisfy this stronger condition. According to Eq.(2.36), monotonicity under LOCC does indeed imply invariance under local unitary operations. Therefore, the local unitary procedures are a particular set of LOCC transformations. Thus, the previous criterion defined remians a weaker version of this one.

Convexity: Another property that is required and satisfied by most quantum correlation measures is the concept of convexity. In particular, it is required that the entanglement declines under the mixedness of two or more quantum systems such as

$$\mathcal{E}(\sum_k p^k \rho_{k}{}_{AB}) \leq \sum_k p^k \mathcal{E}(\rho_{k}{}_{AB}). \tag{2.38}$$

This inequality states that if one starts from a set $\rho_{k}{}_{AB}$ of states with probabilities p^k, and decays information regarding any single instance $\rho_{k}{}_{AB}$, meaning that the entanglement decreases.

Continuity: For the diminishing of the distance between any two density matrix states, namely ρ_{AB} and σ_{AB} acting on the Hilbert space $\mathcal{H} = \mathcal{H}_A \otimes \mathcal{H}_B$, the difference between the associated entanglement decelerate to zero.

$$\|\rho_{AB} - \sigma_{AB}\| \to 0 \Rightarrow \mathcal{E}(\rho_{AB}) - \mathcal{E}(\sigma_{AB}) \to 0. \tag{2.39}$$

Additivity: For any pair of quantum states ρ_{AB} and σ_{AB}, we have

$$\mathcal{E}(\rho_{AB} \otimes \sigma_{AB}) = \mathcal{E}(\rho_{AB}) + \mathcal{E}(\sigma_{AB}). \tag{2.40}$$

Furthermore, this property is much stronger and is not fulfilled for some entanglement measures, or they are complicated to prove [153]. Nevertheless, it should be true that the entanglement cannot increase if we put two quantum states together.

Sub-additivity: The quantum correlation of a tensor product of a given quantum state pair ρ_{AB} and σ_{AB} cannot be larger than the total sum of the individual state entanglement values.

$$\mathcal{E}(\rho_{AB} \otimes \sigma_{AB}) \leq \mathcal{E}(\rho_{AB}) + \mathcal{E}(\sigma_{AB}). \tag{2.41}$$

However, the additivity requirement holds when $\rho_{AB} = \sigma_{AB}$.

Weak additivity: A certain number N-identical copies of a state ρ_{AB} of a bipartite system AB must have N times the individual subcomponent's entanglement

$$\mathcal{E}(\rho_{AB}^{\otimes N}) = N\mathcal{E}(\rho_{AB}). \tag{2.42}$$

Existence of a regularization: For each quantum state ρ_{AB} the limit exists, we have

$$\mathcal{E}^{\infty}(\rho_{AB}) = \lim_{N\to\infty} \frac{\mathcal{E}(\rho_{AB}^{\otimes N})}{N}. \tag{2.43}$$

An entanglement measure $\mathcal{E}(\rho_{AB})$ satisfying the above-listed requirements is called a monotonic entanglement. Hence, a *"bona fide"* entanglement measure should satisfy at least the first three properties.

3.2 Entanglement entropy

"*Entanglement entropy*" provides the most fundamental approach for quantifying the degree of quantum entanglement in a provided pure quantum state ρ_{AB} of a bipartite state AB [14]. In this sense, it is the only function on the family of states that fulfills certain requirements of an entanglement measure. This quantifier is simply expressed as the von Neumann entropy in Eq.(1.52) of one of the sub-system's reduced density matrices ρ_A and ρ_B. This gives

$$\mathcal{E}_s(\rho_{AB}) = -\mathrm{Tr}(\rho_A \log_2 \rho_A) = -\mathrm{Tr}(\rho_B \log_2 \rho_B), \tag{2.44}$$

where $\rho_{A(B)} = \mathrm{Tr}_{B(A)}(\rho_{AB})$ denotes the partial trace over sub-system $B(A)$. As a trivial example to illustrate the entanglement entropy $\mathcal{E}_s(\rho_{AB})$, consider the following pure Bell state $|\beta_{01}\rangle$ (2.7). The density matrix characterizing this state $|\beta_{01}\rangle$ is given in the computation basis of two-qubit as

$$\rho_{AB} = |\beta_{01}\rangle \langle\beta_{01}| = \frac{1}{2}\begin{pmatrix} 0 & 0 & 0 & 0 \\ 0 & 1 & 1 & 0 \\ 0 & 1 & 1 & 0 \\ 0 & 0 & 0 & 0 \end{pmatrix}. \tag{2.45}$$

Then, ρ_A of the first sub-system A can be written

$$\rho_A = \frac{1}{2}\begin{pmatrix} 1 & 0 \\ 0 & 1 \end{pmatrix}. \tag{2.46}$$

It is evident that ρ_A is a diagonal matrix. Hence, the diagonal entries represent its eigenvalues. Using Eq.(2.44), the entanglement entropy of the state ρ_{AB} (2.45) is

$$\mathcal{E}_s(\rho_{AB}) = -\frac{1}{2}\log_2\left(\frac{1}{2}\right) - \frac{1}{2}\log_2\left(\frac{1}{2}\right) = \log_2 2 = 1. \tag{2.47}$$

The above example clearly shows that the entanglement entropy $\mathcal{E}_s(\rho_{AB})$ takes its maximum value regarding a maximal entangled states while remaining "0" for disentangled states. However, it is easy to verify that the entanglement entropy $\mathcal{E}_s(\rho_{AB})$ of the second sub-system B always takes the same value as that of the first one A. Unfortunately, this quantifier is restricted to the case of bipartite pure states only, and entanglement in mixed quantum systems require a different characterization. This is because their reduced state is generally mixed. In the following, we introduce other metrics for quantifying the degree of entanglement for an arbitrary biqubit mixed state of a quantum system.

3.3 Entanglement of formation

The *"entanglement of formation"* (EOF) concept aims to quantifying the level of resources required to generate an entangled state. This entanglement measure is a generalization of the entanglement entropy $\mathcal{E}_s(\rho_{AB})$ given in Eq.(2.44), in the mixed states [14]. In this inspiration, let us consider a two-qubit mixed state ρ_{AB} that can be decomposed into a convex combination of pure states, such that: $\rho_{AB} = \sum_i p_i |\psi_i\rangle \langle\psi_i|$. For each pure state $|\psi_i\rangle$ in the decomposition, the entanglement entropy is given by $\mathcal{E}_s(|\psi_i\rangle)$(2.44). The EOF of the bipartite type mixed state ρ_{AB} is then given as the averaged entanglement entropy minimized over all the available associated decompositions as follows

$$\mathcal{E}_f(\rho_{AB}) = \min_{\{p_i, |\psi_i\rangle\}} \sum_i p_i \mathcal{E}_s(|\psi_i\rangle), \tag{2.48}$$

where the minimization in Eq.(2.48) is taken over all possible pure state decompositions of ρ_{AB}. Moreover, the EOF tool turns into the von Neumann entropy of the reduced density

statistical ensembles for pure states $\mathcal{E}_s(\rho_{AB})$ (2.44). It provides a way to quantify the amount of entanglement present in a mixed state, which is useful in various applications of quantum information theory. Moreover, this measure (2.48) satisfies all the essential axioms required as a *"bona fide"* entanglement measure, including normalization, convexity, non-increasing under LOCC on average, and invariance under local unitary transformations, as well as asymptotic continuity. However, the question of whether or not EOF is additive is still an open problem [98, 153]. Physically speaking, EOF is interpreted as the smallest number of singlets required to construct a copy of the state [146]. In general, the major difficulty in computing EOF lies in the minimization process involved in the calculation (2.48). This explains why the explicit analytical formula for EOF has only been obtained so far for some special two-qubit quantum states [15, 154].

3.4 Concurrence

"Concurrence" proposed by W.K. Wootters, is the most widely accepted metric of quantum entanglement for a given two-qubit quantum state, whether pure or mixed. It is significantly more effective than the entanglement entropy due to its simplicity [15]. This approach provides a qualitative and quantitative way to distinguish between entangled and unentangled (factorizable) quantum states, which is essential in applications involving quantum information processing (QIP). Indeed the degree of the entanglement based on the concurrence is bounded between zero and a maximum value of 1. The situation reflects $\mathcal{C} = 0$ occurs when the two-qubit state is completely unentangled, whereas $\mathcal{C} = 1$ means the state is maximally entangled. For an arbitrary two-qubit pure state $|\psi_{AB}\rangle$, its concurrence $\mathcal{C}(\,|\psi_{AB}\rangle\,)$ is defined as

$$\mathcal{C}(\,|\psi_{AB}\rangle\,) = \left|\langle\psi_{AB}|\,\tilde{\psi}_{AB}\right\rangle\right|, \tag{2.49}$$

where $\left|\tilde{\psi}_{AB}\right\rangle = (\sigma_y \otimes \sigma_y)\,|\psi^*_{AB}\rangle$ represents the spin-flipped state. While σ_y and $|\psi^*_{AB}\rangle$ are, respectively, the y-component Pauli matrix and the complex conjugate of $|\psi_{AB}\rangle$ in the standard basis. However, there exist some classes of states where the concurrence takes the simplest form. The most basic case is that of an arbitrary two-qubit pure state, which can always be expressed in the computational basis as

$$|\psi_{AB}\rangle = \alpha_{00}\,|00\rangle + \alpha_{01}\,|01\rangle + \alpha_{10}\,|10\rangle + \alpha_{11}\,|11\rangle\,, \tag{2.50}$$

where α_{00}, α_{01}, α_{10} and α_{11} are complex numbers fulfilling the following normalization condition

$$\langle\psi_{AB}|\,\psi_{AB}\rangle = |\alpha_{00}|^2 + |\alpha_{01}|^2 + |\alpha_{10}|^2 + |\alpha_{11}|^2 = 1. \tag{2.51}$$

After some simplifications, the concurrence (2.49) for the considered state (2.50) reduces to

$$\mathcal{C}(\,|\psi_{AB}\rangle\,) = 2\,|\alpha_{00}\alpha_{11} - \alpha_{01}\alpha_{10}|\,. \tag{2.52}$$

We notice that $|\psi_{AB}\rangle$ (2.50) is factorizable if and only if $\alpha_{00}\alpha_{11} = \alpha_{01}\alpha_{10}$. Therefore, in the case of a pure state, we use the difference between $\alpha_{00}\alpha_{11}$ and $\alpha_{01}\alpha_{10}$ as a measure of the degree of entanglement. On the other hand, Rungta *et al* [154–156] generalized the definition of concurrence for higher dimension bipartite systems other than the usual two-qubit system with the name of *"I-concurrence"*. In this sense, we note that the I-concurrence for a pure state of a $d_A \otimes d_B$ system can also be written in terms of the purity of the marginal density matrices as follow:

$$\mathcal{C}(\,|\psi_{AB}\rangle\,) = \sqrt{2\,(1 - \mathrm{Tr}(\rho_A^2))} = \sqrt{2\,(1 - \mathrm{Tr}(\rho_B^2))}. \tag{2.53}$$

The definition of concurrence for pure states (2.49) can be extended to general two-qubit mixed states as the average concurrence of a set of pure states representing $|\psi_{AB}\rangle$, which is obtained by performing a minimization procedure over all possible decompositions of ρ_{AB} into pure states. Such that

$$\mathcal{C}(\rho_{AB}) = \min_{\{p_i, |\psi_i\rangle_{AB}\}} \sum_i p_i \mathcal{C}(\,|\psi_i\rangle_{AB}\,). \tag{2.54}$$

This function (2.54) satisfies the aforementioned axioms, but it is not an additive function [146]. The minimization on all possible pure state decompositions provides a suitable measure of entanglement. For general two-qubit quantum states ρ_{AB}, the concurrence can be expressed as [15]

$$\mathcal{C}(\rho_{AB}) = \max\{0, \sqrt{\lambda_1} - \sqrt{\lambda_2} - \sqrt{\lambda_3} - \sqrt{\lambda_4}\}, \tag{2.55}$$

where $\lambda_i (i = 1, 2, 3, 4)$ are the eigenvalues of the non-Hermitian 4×4 matrix $R = \sqrt{\sqrt{\rho_{AB}}\tilde{\rho}_{AB}\sqrt{\rho_{AB}}}$ in descending order. The matrix $\tilde{\rho}_{AB} = (\sigma_y \otimes \sigma_y)\rho^*_{AB}(\sigma_y \otimes \sigma_y)^\dagger$ is the spin-flipped operator of the state ρ_{AB}. Let us now review the concurrence $\mathcal{C}(\rho_{AB})$ in a particular class of X-states [157]. The term "X-states" refers to a family of two-qubit systems, whose state is formed like the letter "X", that is, $\rho_{11} = \rho_{13} = \rho_{24} = \rho_{34} = 0$ [157]. These states are most commonly encountered in the literature since they generalize several significant classes of mixed quantum states, including maximally entangled Bell states as well as the maximally entangled mixed states such as the well-known Werner states [131]. The specific choice of this type of state can be motivated by their interventions in the implementation of quantum information protocols. In the computational basis $\mathcal{B} = \{|00\rangle, |01\rangle, |10\rangle, |11\rangle\}$, a bipartite state of type X has the following form

$$\rho_X = \begin{pmatrix} \rho_{11} & 0 & 0 & \rho_{14} \\ 0 & \rho_{22} & \rho_{23} & 0 \\ 0 & \rho^*_{23} & \rho_{33} & 0 \\ \rho^*_{14} & 0 & 0 & \rho_{44} \end{pmatrix}, \tag{2.56}$$

with the density matrix elements ρ_{ij} of the state (2.56) are constrained by the normalization and positivity conditions which are respectively given by

$$\mathrm{Tr}(\rho_X) = \rho_{11} + \rho_{22} + \rho_{33} + \rho_{44} = 1, \quad \rho_{11}\rho_{44} \geq |\rho_{14}|^2, \text{ and } \rho_{22}\rho_{33} \geq |\rho_{23}|^2. \tag{2.57}$$

From the expression (2.55), the concurrence $\mathcal{C}(\rho_X)$ of a two-qubit X-state (2.56) leads to

$$\mathcal{C}(\rho_X) = 2\max\{0, \mathcal{C}_1(\rho_X), \mathcal{C}_2(\rho_X)\}, \tag{2.58}$$

where

$$\mathcal{C}_1(\rho_X) = |\rho_{14}| - \sqrt{\rho_{22}\rho_{33}} \text{ and } \mathcal{C}_2(\rho_X) = |\rho_{23}| - \sqrt{\rho_{11}\rho_{44}}. \tag{2.59}$$

The above formula provides a straightforward way to calculate the concurrence for any two-qubit X-state. The well-known Werner state ρ_W (2.28), is a concrete example of an X-shaped state. The concurrence of this state, denoted by $\mathcal{C}(\rho_W)$, can be derived from Eq.(2.58) as

$$\mathcal{C}(\rho_W) = 2\max\left\{0, \frac{1-3r}{4}\right\}. \tag{2.60}$$

Accordingly, when $r > \frac{1}{3}$, the state ρ_W (2.28) is said to be entangled. However, if $r \leq \frac{1}{3}$, the entanglement vanishes and the state ρ_W (2.28) becomes separable (factorizable), resulting in a concurrence of zero.

On the other hand, the entanglement of formation $\mathcal{E}_f(\rho_{AB})$ for a two-qubit system is related to the concurrence $\mathcal{C}(\rho_{AB})$ by the following formula [15]

$$\mathcal{E}_f(\rho_{AB}) = \varepsilon(\mathcal{C}), \tag{2.61}$$

where $\varepsilon(\mathcal{C}) : [0,1] \to [0,1]$ is a strictly increasing function defined by

$$\mathcal{E}_f(\rho_{AB}) = h\left(\frac{1+\sqrt{1-|\mathcal{C}(\rho_{AB})|^2}}{2}\right), \tag{2.62}$$

with $h(x) = -x\log_2 x - (1-x)\log_2(1-x)$ define the binary entropy function. Such a relation, however, does not hold for other dimensions of quantum systems.

3.5 Relative entropy entanglement

Another metric used to quantify the degree of entanglement in a bipartite quantum state is the *"relative entropy of entanglement"* or REE for short [158]. This metric involves determining the smallest distance between the entangled state ρ_{AB} and its closest separable state $\sigma_{AB} \in \mathcal{D}_{sep}(\mathcal{H})$. The relative entropy (1.63) is considered a suitable distance function since it has been shown to be the most physically reasonable choice among all possible distance functions for the purpose of calculating REE [158]. A schematic representation of REE is provided in Fig.2.3. Therefore, it can be mathematically expressed as:

$$\mathcal{E}_r(\rho_{AB}) = \min_{\sigma_{AB}\in\mathcal{D}_{sep}(\mathcal{H})} \mathcal{S}(\rho_{AB}||\sigma_{AB}) = \min_{\sigma_{AB}\in\mathcal{D}_{sep}(\mathcal{H})} \mathrm{Tr}\left(\rho_{AB}\log_2\rho_{AB} - \rho_{AB}\log_2\sigma_{AB}\right), \tag{2.63}$$

where $\mathcal{S}(\rho_{AB}||\sigma_{AB})$ denotes the relative entropy (1.63), while the minimum is carried over all separable states σ_{AB} in $\mathcal{D}_{sep}(\mathcal{H})$. Furthermore, it has been shown that like EOF, $\mathcal{E}_r(\rho_{AB})$ satisfies also all the necessary requirements of a *"bona fide"* measure of quantum entanglement but does not obey the additivity axiom [159]. It is important to note that for pure states, this entanglement metric $\mathcal{E}_r(\rho_{AB})$ coincides with the entanglement of formation $\mathcal{E}_f(\rho_{AB})$, namely $\mathcal{E}_r(\rho_{AB}) = \mathcal{E}_f(\rho_{AB}) = \mathcal{E}_s(\rho_{AB})$ [158, 160], whereas for generic mixed states, the following chain of analytical inequalities holds [160, 161]

$$\mathcal{E}_r(\rho_{AB}) \leq \mathcal{E}_f(\rho_{AB}). \tag{2.64}$$

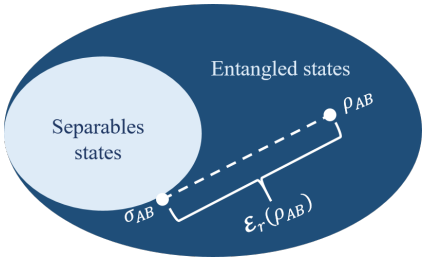


Figure 2.3: Schematic illustration of the relative entropy entanglement.

3.6 Negativity

So far, we have discussed several different entanglement metrics, each with its own set of advantages and disadvantages. However, all of these aforementioned quantifiers required some sort of optimization procedure, making their evaluation a hard task to solve in general. The entanglement in terms of concurrence $\mathcal{C}(\rho_{AB})$ (2.54) is the only exception measure but it is restricted only to the situation of two-qubit entangled states. To introduce a computable measure of entanglement for general bipartite quantum systems with arbitrary dimensional Hilbert

spaces, the concept of *"negativity"* is considered to be one of the most suitable and easiest computable metrics [16, 162], as it does not require a complicated optimization. This quantifier is proposed by Vidal and Werner [16] as the quantitative version of the Peres-Horodecki separability criteria [139, 140]. The entanglement negativity $N(\rho_{AB})$ is expressed through the adding the absolute values of the negative eigenvalues $\{\lambda_i\}$ of $\rho_{AB}^{T_A}$ (2.25) (the same definition is valid for $\rho_{AB}^{T_A}$ (2.26)). Generally, it reads [16]

$$N(\rho_{AB}) = \sum_i |\lambda_i| \,. \tag{2.65}$$

It is worth noting that, similarly to the Peres-Horodecki criterion, the negativity $N(\rho_{AB})$ is also independent of the choice of sub-systems on which the partial transposition is performed. Furthermore, the negativity can also be characterized via the trace norm (Schatten 1-norm) of $\rho_{AB}^{T_A}$ as follows:

$$N(\rho_{AB}) = \frac{\left\|\rho_{AB}^{T_A}\right\|_1 - 1}{2}, \tag{2.66}$$

where $\left\|\rho_{AB}^{T_A}\right\|_1 = \mathrm{Tr}\left(\sqrt{\left(\rho_{AB}^{T_A}\right)^\dagger \rho_{AB}^{T_A}}\right)$ stands for the trace norm of $\rho_{AB}^{T_A}$, which is analogous to the sum of all the absolute values of the negative eigenvalues of $\rho_{AB}^{T_A}$. The negativity, as determined in Eq.(2.65), varies from zero value, $N(\rho_{AB}) = 0$, for completely separable states (PPT states) to half ($N(\rho_{AB}) = 1/2$) for maximally entangled states such as Bell states. However, it is also known that there exist entangled states ρ_{AB} for which the negativity $N(\rho_{AB})$ fulfilling $N(\rho_{AB}) = 0$. For our calculations process, we shall consider here a rescaled form of the negativity function as

$$\mathcal{N}(\rho_{AB}) = 2N(\rho_{AB}). \tag{2.67}$$

Therefore, we will achieve the normalization condition form $0 \leq \mathcal{N}(\rho_{AB}) \leq 1$. In addition, for a two-qubit pure state (2.50) this metric (2.65) is equivalent to the concurrence (2.54), namely $\mathcal{N}(\,|\psi_{AB}\rangle\,) = \mathcal{C}(\,|\psi_{AB}\rangle\,) = 2\,|\alpha_{00}\alpha_{11} - \alpha_{01}\alpha_{10}|$, while the latter can differ from the negativity for a mixed state ρ_{AB} [163]. In general, as proven by Verstraete *et al* in Ref. [164], the negativity $\mathcal{N}(\rho_{AB})$ of a two-qubit mixed state ρ_{AB} cannot exceed its concurrence $\mathcal{C}(\rho_{AB})$, and it adheres to the following inequality

$$\mathcal{N}(\rho_{AB}) \geq \sqrt{\left(1 - \mathcal{C}(\rho_{AB})\right)^2 + \left|\mathcal{C}(\rho_{AB})\right|^2} - \left(1 - \mathcal{C}(\rho_{AB})\right). \tag{2.68}$$

According to Vidal and Werner, negativity is a monotone function for entanglement, including convexity, despite being not additive it can be considered a *"bona fide"* metric to quantify the degree of entanglement in composite systems. Similarly to the concurrence $\mathcal{C}(\rho_W)$ (2.60), the negativity of the state ρ_W (2.28) is given by using the partial transposed density matrix with respect to the second qubit B (2.67) as

$$\mathcal{N}(\rho_W) = \left|\frac{1 - 3r}{2}\right|. \tag{2.69}$$

It is clear that when $r > \frac{1}{3}$ the state ρ_W (2.28) is unseparable (entangled). However, for $r \leq \frac{1}{3}$, the entanglement betwen the two-qubit state vanishes and the state ρ_W becomes unentangled (separable), resulting in a negativity $\mathcal{N}(\rho_W)$ (2.69) of zero value. This is confirmed by the results given by the concurrence $\mathcal{C}(\rho_W)$ (2.60) and the separability criteria, namely PPT (2.31) and EW (2.34).

Another concrete example to illustrate these results, consider a qutrit-qubit quantum state $\rho_{3\otimes 2}$ written in the standard basis $\{|ij\rangle\,,\, i=-1,0,1 \text{ and } j=0,1\}$ as follows

$$\rho_{3\otimes 2}=\begin{pmatrix}\rho_{11} & 0 & 0 & 0 & 0 & 0\\ 0 & \rho_{22} & \rho_{23} & 0 & 0 & 0\\ 0 & \rho_{23} & \rho_{33} & 0 & 0 & 0\\ 0 & 0 & 0 & \rho_{44} & \rho_{45} & 0\\ 0 & 0 & 0 & \rho_{45} & \rho_{55} & 0\\ 0 & 0 & 0 & 0 & 0 & \rho_{66}\end{pmatrix}. \tag{2.70}$$

In order to calculate the negativity of the qutrit-qubit state $\rho_{3\otimes 2}$ (2.70), we require first to derive the negative eigenvalues of the partially transposed density operator $\rho_{3\otimes 2}^{T_A}$ concerning the first sub-system. To achieve this goal, the state $\rho_{3\otimes 2}$ is given in the computational basis as [32]

$$\rho_{3\otimes 2}^{T_A}=\begin{pmatrix}\rho_{11} & 0 & 0 & \rho_{23} & 0 & 0\\ 0 & \rho_{22} & 0 & 0 & 0 & 0\\ 0 & 0 & \rho_{33} & 0 & 0 & \rho_{45}\\ \rho_{23} & 0 & 0 & \rho_{44} & 0 & 0\\ 0 & 0 & 0 & 0 & \rho_{55} & 0\\ 0 & 0 & \rho_{45} & 0 & 0 & \rho_{66}\end{pmatrix}. \tag{2.71}$$

Thus, the negativity of the state $\rho_{3\otimes 2}$ (2.70) is expressed as

$$\mathcal{N}(\rho_{3\otimes 2})=\max\{0,-\vartheta_+\}+\max\{0,-\vartheta_-\}\,. \tag{2.72}$$

where $\vartheta_\pm$ are the negative eigenvalues of the state $\rho_{3\otimes 2}^{T_A}$ (2.71). They are given by

$$\vartheta_+ = \frac{1}{2}\left[(\rho_{11}+\rho_{44})-\sqrt{(\rho_{11}-\rho_{44})^2+4|\rho_{23}|^2}\right], \tag{2.73}$$

$$\vartheta_- = \frac{1}{2}\left[(\rho_{66}+\rho_{33})-\sqrt{(\rho_{66}-\rho_{33})^2+4|\rho_{45}|^2}\right]. \tag{2.74}$$

3.7 Logarithmice negativity

A preferred measure based on the negativity function is the well-known *"logarithmic negativity"* (LN), which is given as:

$$\mathcal{E}_N(\rho_{AB})=\log_2\left[\mathcal{N}(\rho_{AB})+1\right]. \tag{2.75}$$

The monotonicity of the negativity directly indicates that LN is a full entanglement monotone function that remains non-increasing when more restrictive kinds of deterministic LOCC transformations are considered. Despite being non-convex, it is additive regarding the tensor product [165]. Although LN is remains continuous, but except asymptotically. Hence, LN should not reduce the entropy of entanglement of all types of pure states. The fundamental characteristic of $\mathcal{E}_N(\rho_{AB})$ (2.75) is its simplest type of calculation. Using the Eq.(2.72), the logarthimic negativity for the qutrit-qubit $\rho_{3\otimes 2}$ (2.70) can be written as [32]

$$\mathcal{E}_{\mathcal{N}}\left(\rho_{3\otimes 2}\right)=\log_2\left[2\sum_{s=\pm}\max\{0,-\vartheta_s\}+1\right]. \tag{2.76}$$

4 Entanglement measure for tripartite systems

Several quantum entanglement measures have been extensively discussed in the above section can be used to determine the strength of entanglement for composite bipartite quantum systems, particularly in two-qubit states. Moreover, their exact formula was also been provided. However, as the number of qubits in a quantum system increases, the entanglement structure of the system becomes more complicated, making it challenging to analyze the degree of entanglement using simple analytical expressions. Thus, analyzing entanglement in multi-qubit systems is not a trivial issue, and a direct analytical expression to evaluate the inherent entanglement degree is still lacking. For instance, a three-qubit system ABC can have pairwise entanglements such as A with B or C, or two qubits may share some entanglement with the third qubit. Two commonly used measures for quantifying entanglement in multi-qubit systems are the *"tangle"* and *"multi-qubit negativity"*. It is essential to note that other measures of entanglement can be used, and the choice of measure may depend on the specific properties of the system under study.

4.1 Tripartite Negativity

The average associated with bipartite entanglement quantifiers over all possible bi-partitions of the N-qubit quantum system is the most practical and effective metric that is provided to determine the total degree of genuine quantum entanglement in any N-qubit entangled quantum system described by a mixed-state, namely ρ. In fact, for a given multi-qubit system, the explicit analytical formula for negativity has been proven to be [166]

$$N^{(N)}(\rho) = \frac{2}{N}\sum_{k=1}^{N/2}\Big(\frac{1}{n_{bipart}^{(k)}}\sum_{P=1}^{n_{bipart}^{(k)}} N^{P[k|N-k]}(\rho)\Big). \tag{2.77}$$

Here, $k|N-k$ refers to the bi-partitions of the N-qubit quantum system, with $N-k$ qubits in a separate block from the k qubits. While $P[k|N-k]$ is used to establish a combination of k and $N-k$ qubits specifically to construct the $k|N-k$ bipartition. Alternatively, $n_{bipart}^{(k)}$ is the whole set of non-equivalent concrete bi-partitions $P[k|N-k]$ and $N^{P[k|N-k]}(\rho)$ is the negativity corresponding to each specific bipartition of $P[k|N-k]$. Therefore, $N^{P[k|N-k]}(\rho)$ is given as follows:

$$N^{P[k|N-k]}(\rho) = \sum_j \left|\lambda_j(\rho^{T_I})\right|. \tag{2.78}$$

In the expression above, $\lambda_j(\rho^{T_I})$ stands for the non-positive eigenvalues of the partial transposed density matrix ρ^{T_I} with respect to the sub-system I of the whole density matrix ρ, which is made up of the k qubits of the given bi-partition $P[k|N-k]$.

Similar to the case of bipartite negativity (2.65), the quantity(2.77) is also related to the Shatten-norm (trace norm) of ρ^{T_I} via

$$N^{P[k|N-k]}(\rho) = \frac{\left\|\rho^{T_I}\right\| - 1}{2}, \tag{2.79}$$

where the trace norm is defined by $\left\|\rho^{T_I}\right\| = \mathrm{Tr}(\sqrt{\rho^{T_I}\rho^{T_I\dagger}})$. As an example, assume the case of a three-qubit system described by the following density matrix ρ_{ABC}. Hence, the negativity $N^{(N)}(\rho)$ (2.77) can be obtained as follows:

$$N^{(3)}(\rho_{ABC}) = \sqrt[3]{N^{A|BC}(\rho_{ABC})N^{B|AC}(\rho_{ABC})N^{C|AB}(\rho_{ABC})}. \tag{2.80}$$

Let us note that for a three-qubit quantum system with permutation invariance, i.e., interchange between their qubits, the three-qubit negativity $N^{(3)}(\rho_{ABC})$ (2.80) coincide to the bipartite negativity of any included bipartition of the considered system and has the form

$$N^{(3)}(\rho_{ABC}) = N^{A|BC}(\rho_{ABC}) = N^{B|AC}(\rho_{ABC}) = N^{C|AB}(\rho_{ABC}).$$

However, $N^{(N)}(\rho)$ (2.77) fulfills the same axioms as bipartite negativity (2.65). Besides, we will adapt the same notation as in Eq.(2.67), i.e., $\mathcal{N}^{(N)}(\rho) = 2N^{(N)}(\rho)$. Moreover, a zero value of the N-qubit negativity ($\mathcal{N}^{(N)}(\rho) = 0$) signifies that the state is completely factorizable, while it becomes nonzero, $\mathcal{N}^{(N)}(\rho) \neq 0$ for entangled states.

4.2 Tangle

"Tangle" is another entanglement measure in three-qubit systems, that is neither a straightforward generalization nor a direct combination of bipartite metrics [167]. It evaluates the degree of entanglement between three sub-systems that are unable to be characterized or (and) quantified by bipartite entanglement measures. In addition, when one of the sub-systems, namely A, is entangled with the other two sub-systems joined BC, the entanglement can be understood as bipartite entanglement between two $A|BC$ parts. As such, it is quantified using one of the well-known measures for determining bipartite entanglement. In this case, the tangle τ_g of three-qubit systems described by the density matrix ρ_{ABC} is expressed as

$$\tau_g(\rho_{ABC}) = \max_{\{i,j,k\}} \left\{ \mathcal{C}^2(\rho_{i|jk}) - \mathcal{C}^2(\rho_{i|j}) - \mathcal{C}^2(\rho_{i|k}) \right\}, \tag{2.81}$$

where $\mathcal{C}(\rho_{i|jk})$ stands for the bipartite concurrence between the two subsystems i and joined jk. It is given by

$$\mathcal{C}(\rho_{i|jk}) = \sqrt{2(1 - \mathrm{Tr}\,(\rho_i^2))}, \tag{2.82}$$

with $\mathcal{C}(\rho_{i|j})$ $\left(\mathcal{C}(\rho_{i|k})\right)$ refers respectively to the pairwise concurrence between the pairs of qubits i and j and between the qubits i and k, which is determined via equation (2.55). Note that, the tangle $\tau_g(\rho_{ABC})$ (2.81) does not change under permutations of the three qubits, i.e., $\tau_{ABC} = \tau_{BCA} = \tau_{CBA}$. Moreover, the tangle is considered a valid entanglement measure as it is non-decreasing under LOCC operations. It has the unique ability to identify certain forms of entanglement that cannot be detected using bipartite entanglement measures. The tangle is can be traced to the concept of monogamy of entanglement [167–169], which states that the more entangled a system is with one sub-system, the less entangled it can be with another sub-system. This is due to the fact that the tangle remains non-negative for entangled states while equaling zero only when the system is separable.

5 Conclusion

Quantum entanglement has become a crucial resource for new technologies that leverage the unusual properties of the microscopic world. It is being used to enhance the transmission of information, facilitate quantum coding, and has a pivotal role in the design of quantum computers. Despite intensive research efforts, our understanding of entanglement is still incomplete, and many intriguing questions remain unanswered. Measuring and quantifying the non-classical correlation is a significant challenge in the theory of quantum information, and developing new measures to better understand this phenomenon in modern day quantum research. This chapter provides an overview of the concept of quantum entanglement. We have discussed in detail several separability criteria that are used to identify if a state is non-classically correlated or

not. However, these criteria are not such an effective tool, neither for higher-dimensional systems nor arbitrary mixed quantum states. In this regard, we have discussed the fundamental properties of different metrics for detecting the entanglement level that is widely used throughout this thesis, such as the notions of concurrence and negativity. In particular, we have shown that each metric has its own pros and cons while the issue preferably depends on the specific properties of the system under study. However, few entangled quantum states exist which are not detected by certain metrics, such as negativity. This indicates that only entanglement is not the whole story of non-classical correlation that is useful for QIP, and there are other types of quantum correlations beyond entanglement that exist. Hence, the absence of entanglement in the quantum states does not fully imply the lack of quantum characteristics. The latter will be further explored in the next chapter.

CHAPTER 3

QUANTUM DICORD BASED NON-CLASSICAL CORRELATIONS

In the previous chapter, we emphasized the crucial importance of quantum entanglement in the development of quantum information processing. It is a specific type of correlation described by quantum laws that cannot be expressed in the classical framework. It serves as an indispensable resource in quantum information science (QIS) and is a core ingredient for several practical applications of quantum information processing and information-transmitting protocols [5, 6]. However, recent research has revealed that entanglement is not the only significant form of non-classical correlation that can benefit QIS [19,20]. Surprisingly, some disnetangled states can also perform certain quantum tasks more efficiently than their classical analogs [21, 22]. Examples of these tasks include deterministic quantum computing models with only one qubit [170] and quantum non-locality [17], which can be performed via quantum correlations existing beyond entanglement.

One of the major areas of research within QIS is investigating non-classical correlations beyond entanglement. A specific focus is placed on how these correlations can be evaluated, which has attracted significant attention and effort from the scientific community [27, 171]. The first metric used to quantify non-classical correlations is quantum discord (QD), which attracts an impressive deal of attention [27, 28]. This measure enables one to extract all the degrees of non-classical correlations, generally even more than entanglement [23, 24, 29]. Unlike entanglement, QD can exist for mixed separable quantum states [171]. This metric was first described by Ollivier and Zurek [23] and later developed by Henderson and Vedral [24]. It is the most extensively used quantifier of quantum correlations, and several studies have been devoted to this class of measures [21, 27–29]. QD is determined as the difference between the total correlations defined through mutual information and the classical correlations acquired via performing local measurements on one of the subsystems. However, the entropic QD requires a minimization process, which is difficult to solve in general [30–32]. Therefore, investigation of the QD has been restricted to only some particular cases, including interacted two-qubit systems [33–35].

To address the difficulties associated with entropic quantum discord, B. Dakić *et al* in Ref. [36] proposed an alternative approach called geometric quantum discord (GQD). This method uses the Hilbert-Schmidt distance (or Schatten 2-norm) to determine the smallest distance between the quantum state under study and the set of zero-discord states [36]. The geometric measure provided by GQD is mathematically simpler and requires a minimization process that is less complex than the entropic quantum discord. However, it has been noted that the geometric discord based on the Hilbert-Schmidt norm is not a faithful measure of quantum correlations,

as it can increase even under trivial local quantum operations on the unmeasured part [172]. This is due to the Hilbert-Schmidt distance not satisfying the counteractivity property under trace-preserving applications. Various geometric variants have been introduced in the literature, among which the trace norm (the Bures norm or Schatten 1-norm) is the only Schatten norm that can be used to make a geometric measure of quantum correlations [37]. However, closed analytical formulas for trace discord have only been derived for two-qubit X states [38]. The complex algebraic procedures required for this derivation make it evident that this metric is challenging to compute for higher-dimensional quantum systems. Another interesting approach to obtain a closed analytic expression of QD is to use the linear entropy instead of the von Neumann entropy to find analytically the optimal measurements that maximize the conditional mutual information [39,168]. The analytical computation of QD has received a lot of attention, resulting in the development of several discord-like metrics such as the measurement-induced disturbance (MID) [25, 40] and measurement-induced non-locality (MIN) [173].

In the first section of this chapter, we will discuss some preliminaries of classical and quantum-correlated states. Then, we will investigate in detail the concept of entropic quantum discord. We will provide its original definition, as well as some requirements that any measures of quantum correlations must meet. At this step, we will derive a closed formula for some particular quantum states. In the subsequent section, we will give the definition and closed expression for the two geometric versions of quantum discord via the Hilbert-Schmidt norm and the Schatten trace norm. Due to the difficulty of the calculation of the von Neumann entropy based quantum discord, we will provide a reliable algorithm to deal with the analytical expression of quantum correlations in terms of the linear entropy for the arbitrary qudit-qubit system.

1 Classical and quantum correlated states

According to Oppenheim *et al* [27], a quantum composite bipartite quantum system "AB" is locally correlated if the associated density matrix is written as

$$\rho_{cc} = \sum_{ij} p_{ij} \left|i\right\rangle_A \left\langle i\right| \otimes \left|j\right\rangle_B \left\langle j\right|, \tag{3.1}$$

where $\{\left|j\right\rangle\}_A$ and $\{\left|j\right\rangle\}_B$ are the orthogonal states of the sub-systems A and B, correspondingely while p_{ij} denotes the associated joint probability distribution. Conversely, if the density matrix cannot be expressed in this form, the system is said to be quantum correlated.

Take into account that each locally correlated system can be completely separable. Besides this, a separable state, namely $\rho_{AB} = \sum_i p_i \left|\phi_A^{(i)}\right\rangle \left\langle\phi_A^{(i)}\right| \otimes \left|\chi_B^{(i)}\right\rangle \left\langle\chi_B^{(i)}\right|$, is not always classically correlated since the states $\left\{\left|\phi_A^{(i)}\right\rangle\right\}$ and $\left\{\left|\chi_B^{(i)}\right\rangle\right\}$ do not need to be orthogonal. Furthermore, a pure state is quantum correlated if and only if the associated state is entangled, which means that both notions are analogous to pure states.

Moreover, a classical-quantum state is another type of state that can be defined. Let us consider a scenario where the state of the composite system "AB" is quantum for sub-system B but classical for sub-system A, and vice versa. In other words, if $\rho_B^{(i)}$ represents the quantum state of sub-system B and $\{\left|i\right\rangle\}_A$ specifies the orthonormal basis of A, then this type of state is known as a classical-quantum state with respect to sub-system A, and has the following form [174]

$$\rho_{cq} = \sum_i^{d_A} p_i \Pi_i^{(A)} \otimes \rho_i^{(B)}. \tag{3.2}$$

Here, d_A is the dimensionality of sub-system A and $\Pi_i^{(A)} = \left|i\right\rangle_A \left\langle i\right|$ represents its projectors. These preliminaries have been established so far for systems with a d-dimensional Hilbert space,

which are commonly referred to as qudit (d-level quantum system), where $\rho_B^{(i)}$ represents the density operator for sub-system B in the i^{th} basis state.

Let us now focus our attention on composite systems with small dimensions. Specifically, we will investigate a composite system "AB" in which sub-system A is a single classical bit and sub-system B is a single qubit. Notably, the quantum state with respect to sub-system B reflects the density operator ρ_B. The overall classical-quantum state of the entire system "AB" in this case leads to

$$\rho_{cq} = \sum_i p_i \Pi_i^{(A)} \otimes \rho_B^{(i)}. \tag{3.3}$$

Likewise, a density matrix of a quantum-classical turn out to be

$$\rho_{qc} = \sum_i p_i \rho_A^{(i)} \otimes \Pi_i^{(B)}. \tag{3.4}$$

In summary, a given bipartite quantum system described by the density matrix ρ_{AB} is referred to be classical if and only if it fulfills one of the following requirements. We do have

Property 1: ρ_{AB} takes the implicit form of Eq.(3.1) or Eq.(3.2).

Property 2: The state ρ_{AB} must be invariant under the action of a local von Neumann measurement, i.e., projective measurements with regard to sub-system A or B.

Property 3: If a local complete von Neumann measurement is performed on sub-system A (or B), the considered sub-system does not get entangled with an instrument of measurement used during this operation.

Property 4: The total state ρ_{AB} remains invariant with regard to a local unitary operation with a non-degenerate spectrum of A or B.

Property 5: Given a local orthonormal basis related to sub-system A or B, then the total state ρ_{AB} is still incoherent. When an entanglement-breaking channel is invoked on one of the investigated sub-systems, the total state remains invariant.

It should be noted that the aforementioned requirements may also be shown for multipartite states [175].

2 Entropic quantum discord

2.1 Defintion and properties

As previously mentioned, recent research has revealed the existence of quantum correlations beyond quantum entanglement. Historically, the first metric suggested for quantum correlations beyond entanglement is the so-called quantum discord (QD) [23, 24]. It can effectively capture all non-classical correlations present in various quantum systems. Unlike entanglement, QD can be non-zero for some mixed separable quantum states, meaning that the separation of states does not necessarily imply the absence of quantum correlations [116]. In general, the concept of quantum entanglement contains an operational interpretation meaning that separable states can be prepared through LOCC between sub-systems, in contrast to the entangled states. However, this does not hold for quantum discord since classical communication can result in quantum correlations. This occurs when the reduced states of sub-systems are physically mixed and not orthogonal, making it impossible to recover all the information locally [176]. This phenomenon has no classical counterpart, which explains the presence of quantum correlations in separable

states with non-zero discord. Apart from its importance as a quantifier of purely quantum correlations, QD has become increasingly important in several fields and applications in QIP, especially in the absence of entanglement. It can be a good resource for future quantum technologies. Besides, it has been suggested that QD, rather than entanglement, is responsible for the efficiency of quantum computers, which has been confirmed both theoretically [21], and experimentally [22]. Werlang *et al* in Ref. [70] have shown that QD is more robust to decoherence effects than entanglement, making it a promising resource for future quantum technologies. This has been proved for both Markovian and non-Markovian environments by comparing the dynamics of QD with those of concurrence. Unlike entanglement, which is extremely sensitive to environmental impacts, discord is more resilient and can even increase by coupling with an environment. In fact, from an experimental standpoint, this is a fascinating resource [177, 178]. Moreover, Streltsov and Zurek demonstrated that when the measurement device is in a non-classical state, i.e, a state that contains only quantum correlations, the measurement outcomes cannot be perfectly communicated through classical channels [180]. Therefore, meaning that the information decay occurs even when the measuring device is not quantum mechnaically correlated with the studied system. The information lost level remains exactly the same as quantum discord. Ollivier and Zurek [23, 24] defined QD as the difference between the quantum variants of two classically identical expressions of mutual information. Thus, for a general bipartite composite non-local system defined by the density matrix ρ_{AB}, QD has the form

$$\mathcal{Q}_B(\rho_{AB}) = \mathcal{I}(\rho_{AB}) - \mathcal{J}_B(\rho_{AB}). \tag{3.5}$$

Here, the first part on the right-hand side of Eq.(3.5) stands for the quantum mutual information, $\mathcal{I}(\rho_{AB})$, which is defined in Eq.(1.64). This term encompasses all total correlations present in the quantum bipartite state ρ_{AB}, regardless of their classical or quantum nature [115–118]. However, the next part in Eq.(3.5) denotes the classical correlation $\mathcal{J}_B(\rho_{AB})$ of the state ρ_{AB}. It captures all information that can be done via performing classical measurements on sub-system B only. It is written as

$$\begin{aligned} \mathcal{J}_B(\rho_{AB}) &= \max_{\{P_k\}} \Big(J\left(\rho_{AB}|\{P_k\}\right) \Big) \qquad (3.6) \\ &= \max_{\{P_k\}} \Big(S(\rho_A) - \textstyle\sum_k p_k S\left(\rho_{A|k}\right) \Big) \\ \mathcal{J}_B(\rho_{AB}) &= S(\rho_A) - \widetilde{S}_{\min}, \qquad (3.7) \end{aligned}$$

where $\widetilde{S}_{\min} = \min_{\{P_k\}} \sum_k p_k S\left(\rho_{A|k}\right)$ is the minimum value of the conditional entropy. In particular, the quantum discord can be expressed as

$$\mathcal{Q}_B(\rho_{AB}) = S\left(\rho_B\right) - S\left(\rho_{AB}\right) + \widetilde{S}_{\min}, \tag{3.8}$$

where $\mathcal{Q}_B\left(\rho_{AB}\right)$ represents the quantum discord of the state ρ_{AB} when the measurements are performed on sub-system B. Likewise, when the measurements are made on sub-system A, then the corresponding quantum discord is denoted by $\mathcal{Q}_A\left(\rho_{AB}\right)$. However, throughout this thesis, we will consider only the simple form $\mathcal{Q}\left(\rho_{AB}\right)$ instead of $\mathcal{Q}_B\left(\rho_{AB}\right)$ since the measurements are taken on sub-system B. The quantum discord defines the difference between the total correlations $\mathcal{I}\left(\rho_{AB}\right)$ and the classical correlations $\mathcal{J}_B\left(\rho_{AB}\right)$. It also quantifies the absolute degree of quantum correlations in a given quantum system. Similar to entanglement, quantum discord has the following properties:

Property 1: QD is a positive function since $\mathcal{I}\left(\rho_{AB}\right) \geq \mathcal{J}_B\left(\rho_{AB}\right)$ and also a convex quantity. This is the result of the convexity of the conditional entropy.

Property 2: QD is smaller than or completely equivalent to the von Neumann entropy of the unmeasured sub-system (sub-system A in our case). Such that

$$\mathcal{Q}\left(\rho_{AB}\right) \leq S\left(\rho_{A}\right). \tag{3.9}$$

Property 3: For classically correlated states, $\mathcal{Q}\left(\rho_{AB}\right)$ vanishes. In other words, it is equal to zero if the total system is undisturbed by a local measurement on one of the sub-systems, in our case sub-system A.

Property 4: QD is an asymmetric quantity with respect to the exchange of subsystems A and B, due to the non-symmetric nature of the conditional entropy function. This dependency relies on the sub-systems on which the measurements are performed. This reads

$$\mathcal{Q}_{B}\left(\rho_{AB}\right) \neq \mathcal{Q}_{A}\left(\rho_{AB}\right). \tag{3.10}$$

Property 5: QD reduces to the entanglement entropy of the marginal states for pure bipartite states

$$\mathcal{Q}\left(\rho_{AB}\right) = \mathcal{E}_{s}\left(\rho_{AB}\right) = S\left(\rho_{A}\right) = S\left(\rho_{B}\right). \tag{3.11}$$

Property 6: The quantity $\mathcal{Q}\left(\rho_{AB}\right)$ is invariant by performing local unitary operations, such that

$$\mathcal{Q}\left(\rho_{AB}\right) = \mathcal{Q}\Big(\left(U_{A}\otimes U_{B}\right)\rho_{AB}\left(U_{A}\otimes U_{B}\right)^{\dagger}\Big). \tag{3.12}$$

Property 7: The function $\mathcal{Q}\left(\rho_{AB}\right)$ is not-increasing under local operations on the unmesured sub-system A. Such that

$$\mathcal{Q}\left(\rho_{AB}\right) \geq \mathcal{Q}\Big(\left(I_{A}\otimes \Lambda_{B}\right)\rho_{AB}\Big). \tag{3.13}$$

It is important to stress that the main challenge of evaluating analytically the entropic quantum discord (3.8) in terms of von Neumann entropy is, in general, due to the maximization procedure required to optimize classical correlation (3.6) and, consequently, minimize conditional entropy. This explains why the explicit expression of this function has only been derived for some specific classes of two-qubit quantum systems via projective measurements (PM) such as X-states [33–35]. The Werner states and the maximally entangled Bell states are included in this class of states [131]. However, the optimization procedure involved in the computational process is inaccessible for arbitrary bipartite quantum states, and a straightforward formula to compute this quantity for given systems is still lacking. To address this issue, we present alternative methods for computing the degree of quantum discord analytically in the following section.

3 Analytical expressions of the entropic quantum discord

3.1 Quantum discord for X-states

In this study, we provide a brief overview of how to analytically derive the explicit expression of QD for a two-qubit X-state (2.56) using a particular case of the projective measurements (PM) [181]. It is worth noting that Mazhar *et al* in Ref. [26] have also derived the expression of QD for any PM measurements. To begin with, the eigenvalues of the density operator ρ_{X} (2.56) are obtained as follows

$$\lambda_{1,2} = \frac{1}{2}\left[\rho_{11} + \rho_{44} \pm \sqrt{\left(\rho_{11} - \rho_{44}\right)^2 + 4\left|\rho_{14}\right|^2}\right], \tag{3.14}$$

$$\lambda_{3,4} = \frac{1}{2}\left[\rho_{22} + \rho_{33} \pm \sqrt{\left(\rho_{22} - \rho_{33}\right)^2 + 4\left|\rho_{23}\right|^2}\right]. \tag{3.15}$$

From this, the quantum mutual information is given by

$$\mathcal{I}\left(\rho_X\right) = S\left(\rho_A\right) + S\left(\rho_B\right) + \sum_{i=1}^{4} \lambda_i \log_2 \lambda_i. \tag{3.16}$$

Here, the marginal states, namely ρ_A and ρ_B associated with ρ_X (2.56) are respectively given as

$$\rho_A = \mathrm{Tr}_B\left(\rho_X\right) = \begin{pmatrix} \rho_{11} + \rho_{22} & 0 \\ 0 & \rho_{33} + \rho_{44} \end{pmatrix}, \tag{3.17}$$

$$\rho_B = \mathrm{Tr}_A\left(\rho_X\right) = \begin{pmatrix} \rho_{11} + \rho_{33} & 0 \\ 0 & \rho_{22} + \rho_{44} \end{pmatrix}, \tag{3.18}$$

their corresponding quantum entropies are

$$S\left(\rho_A\right) = -\left(\rho_{11} + \rho_{22}\right)\log_2\left(\rho_{11} + \rho_{22}\right) - \left(\rho_{33} + \rho_{44}\right)\log_2\left(\rho_{33} + \rho_{44}\right), \tag{3.19}$$

$$S\left(\rho_B\right) = -\left(\rho_{11} + \rho_{33}\right)\log_2\left(\rho_{11} + \rho_{33}\right) - \left(\rho_{22} + \rho_{44}\right)\log_2\left(\rho_{22} + \rho_{44}\right). \tag{3.20}$$

After extracting the amount of total correlations by means of quantum mutual information $\mathcal{I}\left(\rho_X\right)$, we have to deal next with the classical part $\mathcal{J}\left(\rho_X\right)$. For that, we consider a complete set of orthonormal projection operators that act on sub-system B which are represented by the following operators $\left\{\Pi_k^B = \left|B_k\right\rangle\left\langle B_k\right|, \text{with } k = 1, 2\right\}$, namely

$$\left|B_1\right\rangle = \cos\left(\frac{\theta}{2}\right)\left|1\right\rangle + e^{i\varphi}\sin\left(\frac{\theta}{2}\right)\left|0\right\rangle, \tag{3.21}$$

$$\left|B_2\right\rangle = \sin\left(\frac{\theta}{2}\right)\left|1\right\rangle - e^{i\varphi}\cos\left(\frac{\theta}{2}\right)\left|0\right\rangle, \tag{3.22}$$

where $\left|B_1\right\rangle$ and $\left|B_2\right\rangle$ are described by the angles θ and φ of the Bloch sphere (see Fig.1.47), with $0 \leq \theta \leq \pi/2$ and $0 \leq \varphi < 2\pi$. After performing a local measurement on sub-system B, the state ρ_X will change to the set $\{p_k, \rho_{A|k}\}$. Thus, the conditional state of the state related to this measurement $\{\Pi_k^B\}$ when the outcome k occurs is given as

$$\rho_X \to \rho_{X|k} = \frac{1}{p_k}\Big(\left(I_A \otimes \Pi_k^B\right)\rho_X\left(I_A \otimes \Pi_k^B\right)\Big). \tag{3.23}$$

After measurement, the probability $p_k = \mathrm{Tr}\Big(\left(I_A \otimes \Pi_k^B\right)\rho_X\left(I_A \otimes \Pi_k^B\right)\Big)$ corresponding to the outcome k and the eigenvalues of $\rho_{A|k}$ are respectively written as

$$p_k = \frac{1}{2}\left[1 + (-1)^k \cos\theta\left(1 - 2\rho_{11} - 2\rho_{33}\right)\right], \tag{3.24}$$

and

$$\vartheta_{\pm}(\rho_{A|k}) = \frac{1}{2}\left[1 \pm \frac{\sqrt{\nu_k}}{p_k}\right], \tag{3.25}$$

with the parameter ν_k is defined as follows

$$\begin{aligned}\nu_k &= \frac{1}{4}\left[1-2\left(\rho_{33}+\rho_{44}\right)+(-1)^k\cos\theta\left(1-2\rho_{11}-2\rho_{44}\right)\right]^2 \\ &\quad +\sin^2(\theta)\left[|\rho_{14}|^2+|\rho_{23}|^2-2|\rho_{14}||\rho_{23}|\sin\left(2\varphi+\phi\right)\right],\end{aligned} \tag{3.26}$$

where ϕ is derived from $\cos\phi=\frac{\mathrm{Im}\left(\rho_{14}\rho_{23}^*\right)}{|\rho_{14}\rho_{23}|}$ and $\sin\phi=\frac{\mathrm{Re}\left(\rho_{14}\rho_{23}^*\right)}{|\rho_{14}\rho_{23}|}$, while $\mathrm{Re}(z)$ and $\mathrm{Im}(z)$ represent the real and imaginary parts of a complex number z. Thus, the quantum conditional entropy (1.67) is obtained as

$$S\left(\rho_X|\{\Pi_k^B\}\right)=\sum_{k=1}^{2}p_kS\left(\rho_{A|k}\right)=p_1S\left(\rho_{A|1}\right)p_1S\left(\rho_{A|1}\right)+p_1S\left(\rho_{A|2}\right), \tag{3.27}$$

with $S\left(\rho_{A|k}\right)$ is the entropy of the state $\rho_{A|k}$ that can be expressed as a function of its eigenvalues as follows

$$S\left(\rho_{A|k}\right)=h\left(\vartheta_{\pm}(\rho_{A|k})\right), \tag{3.28}$$

where $h\left(x\right)$ stands for the binary entropy. By setting the first partial derivatives of the conditional entropy (3.27) with respect to θ and φ to zero, allows us to minimize the conditional entropy. Thus, we have

$$\frac{\partial S\left(\rho_{AB}|\{\Pi_k^B\}\right)}{\partial\theta}=0,\qquad \frac{\partial S\left(\rho_{AB}|\{\Pi_k^B\}\right)}{\partial\varphi}=0. \tag{3.29}$$

The expression (3.27) reveals that the conditional entropy is symmetric with respect to $\theta=\frac{\pi}{2}$. When this condition occurs, the obtained conditional entropy (3.27) has one extremum value. In this circumstance, $p_1=p_2$, $\nu_1=\nu_2$ and thus $S\left(\rho_{A|1}\right)=S\left(\rho_{A|2}\right)$. Accordingly, it is only required to minimize $S\left(\rho_{A|1}\right)$ or $S\left(\rho_{A|2}\right)$ when $\theta=\frac{\pi}{2}$. We have the minimum value of $S\left(\rho_{A|1}\right)$ or $S\left(\rho_{A|2}\right)$ derived when $\sin\left(2\varphi+\phi\right)=-1$. Taking into account that $\vartheta_{\pm}(\rho_{A|k})\geq\frac{1}{2}$ in Eq.(3.28) and $h\left(x\right)$ is a decreasing quantity for $x\geq\frac{1}{2}$, hence, the minimum value of the conditional entropy is provided by

$$\xi_1=h\left(\frac{1+\sqrt{\left[1-2\left(\rho_{33}+\rho_{44}\right)\right]^2+4\left(|\rho_{14}|+|\rho_{23}|\right)^2}}{2}\right). \tag{3.30}$$

Another solution of $S\left(\rho_X|\{\Pi_k^B\}\right)$ (3.27) is given when $\theta=0$ for an arbitrary φ. After some computation, one gets another extreme value

$$\xi_2=-\sum_i\rho_{ii}\log_2\rho_{ii}-h\left(\rho_{11}+\rho_{33}\right). \tag{3.31}$$

The above function depends only on the diagonal elements of the state ρ_X (2.56). Substituting Eqs.(3.30-3.31) into Eq.(3.6), one obtains the following minimum conditional entropy as

$$\widetilde{S}_{\min}\equiv\widetilde{S}_{\min}(\theta,\varphi)=\min_{\{\Pi_k^B\}}\sum_k p_kS\left(\rho_{A|k}\right)=\min\left(\xi_1,\xi_2\right), \tag{3.32}$$

which is explicitly expressed as a function of θ and φ. Then, the explicit expression of classical correlation for the state ρ_X (2.56) takes the following form

$$\mathcal{J}(\rho_X)=\max\left(\mathcal{J}_1,\mathcal{J}_2\right), \tag{3.33}$$

where $\mathcal{J}_i=h\left(\rho_{11}+\rho_{22}\right)-\xi_i$. Thus, the analytical formula of the quantum discord for two-qubit X-state is given as

$$\mathcal{Q}(\rho_X)=\min\left(\mathcal{Q}_1,\mathcal{Q}_2\right), \tag{3.34}$$

where $\mathcal{Q}_i = h\left(\rho_{11}+\rho_{33}\right)+\sum_{i=1}^{4}\lambda_i \log_2 \lambda_i+\xi_i$. For this class of local measurements, the minimization of the conditional entropy is performed over the polar and azimuthal angles. Nevertheless, we shall review in what follows that there exists another approach to optimize $\widetilde{S}_{\min}$ in order to reveal the analytical formula of quantum discord Eq.(3.8). This approach is based on the Koashi-Winter relation [182].

3.2 Koashi-Winter relation

The so-called Koashi-Winter relation (KWR) establishes the connection between QD (3.8) and EOF, which is given in Eq.(2.48). This relation allows for the optimization over conditional entropy and, consequently, the classical correlation, to be obtained from EOF through the KWR [182]. However, understanding this connection involves purifying the bipartite state ρ_{AB}. Consider a bipartite system $\rho_{AB} \in \mathcal{H}_A \otimes \mathcal{H}_B$, such that the whole system ABE is characterized by tripartite pure state $\rho_{ABE} = |\psi\rangle_{ABE}\langle\psi| \in \mathcal{H}_A \otimes \mathcal{H}_B \otimes \mathcal{H}_E$, where E represents the environment. To derive the bipartite densities, we trace out the environment sub-system from the tripartite state ρ_{ABE} and obtain $\rho_{AB} = \mathrm{Tr}_E(\rho_{ABE})$ and similarly for $\rho_{AE} = \mathrm{Tr}_B(\rho_{ABE})$. The dimension of the whole space is given by $dim\left(\mathcal{H}_{ABE}\right) = dim\left(\mathcal{H}_A\right).dim\left(\mathcal{H}_B\right).Rank\left(\rho_{AB}\right)$, where $"Rank\left(\rho_{AB}\right)"$ refers to the rank of the bipartite density matrix ρ_{AB}. Importantly, since ABE is a pure tripartite density matrix, the purifying system E consists of the universe minus the sub-systems A and B. The distribution of the correlations of a tripartite purification is controlled by the KWR [182]. This purification generates the quantum correlations between system AB and the attached system E. Koashi and Winter introduced this connection to explain how entanglement is distributed between the two sub-systems. They showed that the classical correlation $\mathcal{J}\left(\rho_{AB}\right)$ (3.6) of the bipartite state ρ_{AB} and the entanglement of formation of its complement state ρ_{AE} are related through a significant monogamy relation. Mathematically, KWR is provided by

$$\mathcal{E}_f\left(\rho_{AE}\right) + \mathcal{J}_B\left(\rho_{AB}\right) = S\left(\rho_A\right). \tag{3.35}$$

It is worth noting that the quantum entropy $S(\rho_A)$ measures how much sub-system A remains in correlation with the external world, regardless of their classical and/or quantum nature. Based on Eq.(3.35), the classical correlation is then expressed as a function of EOF of its complement ρ_{AE} as

$$\mathcal{J}_B\left(\rho_{AB}\right) = S\left(\rho_A\right) - \mathcal{E}_f\left(\rho_{AE}\right), \tag{3.36}$$

in which the minimum value of the conditional entropy $\widetilde{S}_{\min}$ coincides with the entanglement of formation of the state ρ_{AE}. Therfore, we get

$$\widetilde{S}_{\min} = \mathcal{E}_f\left(\rho_{AE}\right). \tag{3.37}$$

Using the above relation will surely reduce the complexity of the optimization process over conditional entropy. By substituting the expression of classical correlation in terms of entanglement of formation Eq.(3.35) back into Eq.(3.8), we find another closed formula of the quantum discord for two-qubit X-states of rank two. The formula is given by

$$\mathcal{Q}\left(\rho_{AB}\right) = S\left(\rho_B\right) - S\left(\rho_{AB}\right) + \mathcal{E}_f\left(\rho_{AE}\right), \tag{3.38}$$

Similarly, when the local measurement is performed on the other sub-system, namely A, then the expression of the quantum discord yields to

$$\mathcal{Q}\left(\rho_{AB}\right) = S\left(\rho_A\right) - S\left(\rho_{AB}\right) + \mathcal{E}_f\left(\rho_{BE}\right), \tag{3.39}$$

To derive the amount of quantum discord using this approach (3.38), the density matrix ρ_X (2.56) can be rewritten in the standard basis $\{|00\rangle, |11\rangle, |01\rangle, |10\rangle\}$ in the following form

$$\rho_X = \begin{pmatrix} \rho_{11} & \rho_{14} & 0 & 0 \\ \rho{*}_{14} & \rho_{44} & 0 & 0 \\ 0 & 0 & \rho_{22} & \rho_{23} \\ 0 & 0 & \rho{*}_{23} & \rho_{33} \end{pmatrix} = (\rho_X)_1 + (\rho_X)_2 , \tag{3.40}$$

where $(\rho_X)_1$ and $(\rho_X)_2$ are, respectively, given by

$$(\rho_X)_1 = \begin{pmatrix} \rho_{11} & \rho_{14} \\ \rho{*}_{14} & \rho_{44} \end{pmatrix}, \qquad (\rho_X)_2 = \begin{pmatrix} \rho_{22} & \rho_{23} \\ \rho{*}_{23} & \rho_{33} \end{pmatrix}. \tag{3.41}$$

In this particular case, the eigenvalues of the density matrix ρ_X are as follows

$$\lambda_{1,2} = \frac{1}{2}\mathrm{Tr}\left((\rho_X)_1\right) \pm \sqrt{\left(\frac{1}{2}\mathrm{Tr}\left((\rho_X)_1\right)\right)^2 - \det\left((\rho_X)_1\right)}, \tag{3.42}$$

$$\lambda_{3,4} = \frac{1}{2}\mathrm{Tr}\left((\rho_X)_2\right) \pm \sqrt{\left(\frac{1}{2}\mathrm{Tr}\left((\rho_X)_2\right)\right)^2 - \det\left((\rho_X)_2\right)}, \tag{3.43}$$

with

$$\det\left((\rho_X)_1\right) = \rho_{11}\rho_{44} - |\rho_{14}|^2 \quad \text{and} \quad \det\left((\rho_X)_2\right) = \rho_{22}\rho_{33} - |\rho_{23}|^2 . \tag{3.44}$$

It is obvious that for the density matrix ρ_X (2.56) having the rank-2, it is sufficient to consider that $\det\left((\rho_X)_1\right)$ and $\det\left((\rho_X)_2\right)$ are both equal to zero. Therefore, the density matrix of ρ_X of rank two has the following non-zero eigenvalues

$$\lambda_1 = \mathrm{Tr}\Big(\,(\rho_X)_1\,\Big) = \rho_{11} + \rho_{44}, \qquad \lambda_3 = \mathrm{Tr}\Big(\,(\rho_X)_2\,\Big) = \rho_{22} + \rho_{33}. \tag{3.45}$$

Through the spectral decomposition of the state ρ_X (2.56), we find

$$\rho_X = \lambda_1 |\psi_1\rangle_{AB} \langle\psi_1| + \lambda_3 |\psi_3\rangle_{AB} \langle\psi_3| , \tag{3.46}$$

where the eigenvectors $|\psi_1\rangle_{AB}$ and $|\psi_3\rangle_{AB}$ are, respectively, given by

$$|\psi_1\rangle_{AB} = \frac{1}{\sqrt{|\rho_{14}|^2 + |\rho_{44}|^2}} \left(\rho_{41}|00\rangle + \rho_{44}|11\rangle\right), \tag{3.47}$$

$$|\psi_3\rangle_{AB} = \frac{1}{\sqrt{|\rho_{23}|^2 + |\rho_{33}|^2}} \left(\rho_{32}|00\rangle + \rho_{33}|11\rangle\right). \tag{3.48}$$

Using the purification procedure (see Chapter 2), the following three-qubit pure state $|\psi\rangle_{ABE}$ is given by

$$|\psi\rangle_{ABE} = \sqrt{\lambda_1}\,|\psi_1\rangle_{AB} \otimes |0\rangle_E + \sqrt{\lambda_3}\,|\psi_3\rangle_{AB} \otimes |1\rangle_E . \tag{3.49}$$

To derive the minimum of condition entropy using the Kaochi-Winter theorem, we need first to evaluate the EOF $\mathcal{E}_f(\rho_{AE})$ of the state ρ_{AE}. After a straightforward calculation, we have

$$\widetilde{S}_{\min} = \mathcal{E}_f(\rho_{AE}) = h\left(\frac{1 + \sqrt{1 - |\mathcal{C}(\rho_{AE})|^2}}{2}\right), \tag{3.50}$$

where $\mathcal{C}(\rho_{AE})$ is the concurrence of the state ρ_{AE}, which is given as

$$|\mathcal{C}(\rho_{AE})|^2 = \frac{4\left(\rho_{11}+\rho_{44}\right)\left(\rho_{22}+\rho_{33}\right)\left(\rho_{41}\rho_{23}-\rho_{33}\rho_{44}\right)}{\left(|\rho_{41}|^2+|\rho_{44}|^2\right)\left(|\rho_{23}|^2+|\rho_{33}|^2\right)}. \tag{3.51}$$

The quantum joint entropy $S(\rho_X)$ of the state ρ_X (2.56) is given as

$$S(\rho_X) = \lambda_1 \log_2 \lambda_1 + \lambda_3 \log_2 \lambda_3, \tag{3.52}$$

and the quantum entropies $S(\rho_A)$ and $S(\rho_B)$ of the marginal states ρ_A and ρ_B of the state ρ_X (2.56) are, respectively, provided by

$$S(\rho_A) = \lambda_1^A \log_2 \lambda_1^A + \lambda_3^A \log_2 \lambda_3^A, \qquad S(\rho_B) = \lambda_1^B \log_2 \lambda_1^B + \lambda_3^B \log_2 \lambda_3^B, \tag{3.53}$$

where the eigenvalues of ρ_A and ρ_B are given as follows

$$\lambda_1^A = \rho_{11}+\rho_{22}, \quad \lambda_3^A = \rho_{33}+\rho_{44}, \quad \lambda_1^B = \rho_{11}+\rho_{33}, \quad \lambda_3^B = \rho_{22}+\rho_{44}. \tag{3.54}$$

Therefore, the closed expression of the QD of the bipartite quantum state ρ_X (2.56) is explicitly written as

$$\begin{aligned} \mathcal{Q}(\rho_X) &= h\left(\rho_{11}+\rho_{22}\right) - h\left(\rho_{11}+\rho_{44}\right) + \\ & h\left(\frac{1}{2}+\frac{1}{2}\sqrt{1-\frac{4\left(\rho_{11}+\rho_{44}\right)\left(\rho_{22}+\rho_{33}\right)\left(\rho_{41}\rho_{23}-\rho_{33}\rho_{44}\right)}{\left(|\rho_{41}|^2+|\rho_{44}|^2\right)\left(|\rho_{23}|^2+|\rho_{33}|^2\right)}}\right). \end{aligned} \tag{3.55}$$

So far, we have derived the quantum discord only for a special case of qubit-qubit states, namely the X-type state, using two different methods. The first approach uses orthogonal projectors to reduce the complexity of the optimization process over the minimization of conditional entropy. In the second approach, we evaluated the quantum discord using the Koashi-Winter theorem. This method provides us with an explicit algorithm to derive the analytical expression of the quantum discord for a two-qubit X-state of rank two, where the minimum of conditional entropy coincides with the EOF of the complementary part. However, a reliable approach to evaluate the quantum discord for an arbitrary bipartite quantum system is still lacking even for general qubit-qubit states. Therfore, deriving an explicit formula for the quantum discord remains an important challenge in QIP. To address this challenge, the following section introduces a geometric alternative version of the entropic quantum discord, known as the *"geometric quantum discord"*.

4 Geometric Quantum Discord

In the previous section, we discussed entropic quantum discord, which allows us to access all the quantum correlations beyond entanglement, which may occur for mixed separable quantum states. However, the complexity involved in calculating QD through the optimization process leads to difficulties in operational quantum tasks [30–32]. As a result, the evaluation of QD has been limited to certain cases, such as interacted bipartite two-qubit systems [33–35]. To avoid these complexities, Dakić *et al* proposed a geometric approach for QD based on the geometric characteristics, known as *"geometric quantum discord"* (GQD) [36]. The latter is used as a useful tool to probe the distance between the given system's state and the set of zero-discord states [36]. The derivation of this alternative measure requires a simple minimization procedure that is analytically achievable for any bipartite quantum state [183, 184]. This is in complete

analogy with geometric measures of entanglement that are defined in terms of distances from the set of separable states. Using this approach, a necessary and sufficient condition for a non-zero quantum discord has been determined, and a geometric method for quantizing quantum discord has been provided. Suppose ρ_{AB} is the density operator of the bipartite system and Ω_{cq} is the set of zero-discord states which is defined as

$$\Omega_{cq} = \sum_k p_k \Pi_k^A \otimes \rho_k^B. \tag{3.56}$$

Here, Π_k^A is the local orthogonal projector in the Hilbert space $\mathcal{H}_A$, while ρ_k^B is an arbitrary density operator in Hilbert space $\mathcal{H}_B$, with $0 \leq p_k \leq 1$ such that $\sum_k p_k = 1$. Moreover, the Hilbert-Schmidt norm (Schatten 2-norm) and the trace norm (Schatten 1-norm), are two specific cases of the Schatten p-norm. The latter is defined for an arbitrary operator X as

$$\|X\|_p = \left[\mathrm{Tr}\left(X^\dagger X\right)^{\frac{p}{2}}\right]^{\frac{1}{p}}, \tag{3.57}$$

where p is a non-negative integer number. Therefore, the geometric quantum discord detects the amount of quantum correlation present in a quantum state based on the Schatten p-norm as the minimal distance between the quantum state under consideration ρ_{AB} and its nearest possible classical-quantum correlated state ρ_{cq}, i.e, $\mathcal{Q}(\rho_{cq}) = 0$. Mathematically, it can be written as

$$\mathcal{Q}_{\mathcal{D}(\rho_{AB},\rho_{cq})}(\rho_{AB}) = \min_{\rho_{cq}\in\Omega_{cq}} \mathcal{D}_p(\rho_{AB}, \rho_{cq}), \tag{3.58}$$

where $\mathcal{D}_p(\rho_{AB}, \rho_{cq}) = \left(\left\|\rho_{AB} - \rho_{cq}\right\|_p\right)^p$ is the proper distance metric between states, while the minimization in the Eq.(3.58) is taken over the set of all states with zero discord.

As depicted in Fig.3.1, the quantity $\mathcal{D}_p(\rho_{AB}, \rho_{cq})$ can be interpreted in terms of the geometry of quantum states. Letting $\mathcal{P}$ denotes the set of all quantum states described by the density operators and Ω_{cq} is the subset of $\mathcal{P}$ containing all the nearest classical-quantum states ρ_{cq} (see Eq.(3.2)). The shortest distance between ρ_{AB} and ρ_{cq} is the geometric quantum discord.

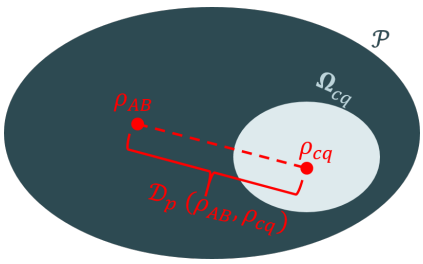


Figure 3.1: Schematic description of the quantum discord based on a distance measurement $\mathcal{D}_p(\rho_{AB}, \rho_{cq})$.

Since $\mathcal{Q}_{\mathcal{D}_p(\rho_{AB},\rho_{cq})}(\rho_{AB})$ given in Eq.(3.58) depends basically on the choice of the proper distance metric of states $\mathcal{D}_p(\rho_{AB}, \rho_{cq})$. Therfore, the GQD must fulfill a variety of requirements to be considered a reliable discord-like metric of quantum correlations:

- $\mathcal{D}_p(\rho_{AB}, \rho_{cq})$ should be monotonic under the action of CPTP map. Such that

$$\mathcal{D}(\rho_{AB}, \rho_{cq}) \geq \mathcal{D}\Big(\Gamma(\rho_{AB}), \Gamma(\rho_{cq})\Big). \tag{3.59}$$

- $\mathcal{D}_p(\rho_{AB}, \rho_{cq})$ must not change under transposition operation, i.e.,

$$\mathcal{D}_p(\rho_{AB}, \rho_{cq}) = \mathcal{D}_p(\rho_{AB}^T, \rho_{cq}^T). \tag{3.60}$$

Considering its striking properties, GQD is typically dependent on the choice of the distance metrics $\mathcal{D}_p(\rho_{AB}, \rho_{cq})$. Once this latter is given, the closest quantum-classical state will be established. For this reason, various reliable geometric discord measures through different distance metrics have been proposed in the literature. Hereafter, we list the most widely used metrics of geometric quantum discord, which are defined by the Hilbert-Schmidt and trace norms.

4.1 Geometric Quantum Discord based on Hilbert-Schmidt distance

The first measure of GQD was proposed by Dakic *et al* [36]. It quantifies the degree of quantum correlations in terms of the Hilbert-Schmidt (or Schatten 2-norm) distance between the considered quantum state and zero quantum discord state. It is given by

$$\mathcal{Q}_{\mathcal{D}_2(\rho_{AB},\rho_{cq})}(\rho_{AB}) = \min_{\rho_{cq}\in\Omega_{cq}} \mathcal{D}_2(\rho_{AB}, \rho_{cq}) = \min_{\rho_{cq}\in\Omega_{cq}} \left\|\rho_{AB} - \rho_{cq}\right\|_2^2, \tag{3.61}$$

where $\left\|\rho_{AB} - \rho_{cq}\right\|_2 = \sqrt{\mathrm{Tr}\left(\rho_{AB} - \rho_{cq}\right)^2}$ denotes the Hilbert-Schmidt norm. Generally, the calculation for this quantifier $\mathcal{Q}_{\mathcal{D}_2(\rho_{AB},\rho_{cq})}(\rho_{AB})$ involves a quite simple minimization procedure compared to the quantum discord based on von Neumann entropy given in Eq.(3.8) [183, 185]. In what follows, we provide an analytical solution to evaluate the GQD based on the Schatten 2-norm for any given two-qubit quantum state as well as for an arbitrary qubit-qudit quantum state.

4.1.1 For two-qubit quantum states

When the measurement is taken on the first sub-system, i.e., the qubit A, the classical-quantum states ρ_{cq} (3.2) for a two-qubit system has the following form

$$\rho_{cq} = p_1 \left|\psi_1\right\rangle \left\langle\psi_1\right| \otimes \rho_1^B + p_2 \left|\psi_2\right\rangle \left\langle\psi_2\right| \otimes \rho_2^B, \tag{3.62}$$

where the set of states $\{\left|\psi_i\right\rangle, i = 1, 2\}$ denotes an orthonormal basis related to the qubit A and ρ_B^i refers to as the marginal density operator of the sub-system B. While p_i denotes the probability distribution that satisfies the condition $p_1 + p_2 = 1$. To reduce the complexity of the calculations, we define:

$$t = p_1 - p_2, \quad \overrightarrow{e} = \left\langle\psi_1\right| \overrightarrow{\sigma} \left|\psi_1\right\rangle, \quad \overrightarrow{s}_{\pm} = \mathrm{Tr}\left(p_1\rho_B^1 \pm p_2\rho_B^2\right) \overrightarrow{\sigma}. \tag{3.63}$$

It is easy to show that $t\ \overrightarrow{e}$ and $\overrightarrow{s}_+$ represent, respectively, the local Bloch vectors of the qubits A and B. While $\overrightarrow{s}$ has a direct connection to the correlation tensor, which takes the form of $T = \overrightarrow{e} \cdot \overrightarrow{s}_-^t$, where t is the transpose operation. Therefore, the zero-discord state ρ_{cq} (3.62) has a Bloch representation that is associated with the triple $\left\{t\overrightarrow{e}, \overrightarrow{s}_+, \overrightarrow{e} \cdot \overrightarrow{s}_-^t\right\}$ with $\|\overrightarrow{e}\|^2 = 1$, $\|\overrightarrow{s}_\pm\|^2 \leq 1$ and $t \in [-1, 1]$. On the other hand, a bipartite two-qubit quantum state ρ_{AB} can be written in the Fano-Bloch form using the triple $\{\overrightarrow{x}, \overrightarrow{y}, T\}$ as follows

$$\rho_{AB} = \frac{1}{4} \sum_{\alpha,\beta=0}^{3} R_{\alpha\beta} \sigma^\alpha \otimes \sigma^\beta \tag{3.64}$$

$$= \frac{1}{4} \left(\sigma^0 \otimes \sigma^0 + \sum_{i=1}^{3} \left(x_i\sigma^i \otimes \sigma^0 + y_i\sigma^0 \otimes \sigma^i\right) + \sum_{i,j=1}^{3} T_{ij}\sigma^i \otimes \sigma^j\right), \tag{3.65}$$

where $R_{\alpha\beta} = \mathrm{Tr}(\rho_{AB}\sigma^\alpha \otimes \sigma^\beta)$. Besides, $x_i = R_{i0} = \mathrm{Tr}(\rho_{AB}\sigma^i \otimes \sigma^0)$ and $y_i = R_{0i} = \mathrm{Tr}(\rho_{AB}\sigma^0 \otimes \sigma^i)$ are the components of the local Bloch vectors. While $T = [R_{ij}] = [T_{ij}] = \mathrm{Tr}(\rho_{AB}\sigma^i \otimes \sigma^j)$ are the components of the correlation tensor associated with ρ_{AB} and $\sigma^i(\sigma^j)(i, j = 1, 2, 3)$ are the

familiar Pauli matrices with σ^0 is the identity matrix of 2-dimensions. Then, by substituting Eq.(3.62) and Eq.(3.62) back into the expression of GQD (3.61), we obtain the following Hilbert-Schmidt distance for two-qubit states between the states ρ_{AB} and ρ_{cq} as

$$\begin{aligned}\left\|\rho_{AB}-\rho_{cq}\right\|_2^2 &= \|\rho_{AB}\|_2^2 - 2\mathrm{Tr}\left(\rho_{AB}\rho_{cq}\right) + \left\|\rho_{cq}\right\|_2^2 \\ &= \frac{1}{4}\left(1+\|\overrightarrow{x}\|_2^2+\|\overrightarrow{y}\|_2^2+\|T\|_2^2\right) \\ &\quad -\frac{1}{2}\left(1+t\,\overrightarrow{x}\,\overrightarrow{e}+\overrightarrow{y}\,\overrightarrow{s}_+ + \overrightarrow{e}T\overrightarrow{s}_-\right) \\ &\quad +\frac{1}{4}\left(1+t^2+\|\overrightarrow{s}_+\|_2^2+\|\overrightarrow{s}_-\|_2^2\right).\end{aligned} \tag{3.66}$$

To obtain the minimal Hilbert-Schmidt distance between the considered state ρ_{AB} and the zero-discord state ρ_{cq}, we first need to optimize the distance $\left\|\rho_{AB}-\rho_{cq}\right\|_2^2$ over the variables t and $\overrightarrow{s}_\pm$. The function involved in this optimization is convex and quadratic with respect to its parameters t and $\overrightarrow{s}_\pm$. It is easy to see that this function has a unique global minimum. In this sense, the minimum arises when the following derivative is zero

$$\frac{\partial\left\|\rho_{AB}-\rho_{cq}\right\|_2^2}{\partial t} = \frac{1}{2}\left(-\overrightarrow{x}\,\overrightarrow{e}+t\right)=0, \tag{3.67}$$

$$\frac{\partial\left\|\rho_{AB}-\rho_{cq}\right\|_2^2}{\partial\overrightarrow{s}_+} = \frac{1}{2}\left(-\overrightarrow{y}+\overrightarrow{s}_+\right)=0, \tag{3.68}$$

$$\frac{\partial\left\|\rho_{AB}-\rho_{cq}\right\|_2^2}{\partial\overrightarrow{s}_-} = \frac{1}{2}\left(-T^t\overrightarrow{e}+\overrightarrow{s}_-\right)=0. \tag{3.69}$$

The solution of the above equations (3.67-3.69) gives $t=\overrightarrow{x}\,\overrightarrow{e}$, $\overrightarrow{s}_+=-\overrightarrow{y}$ and $\overrightarrow{s}_-=T^t\overrightarrow{e}$. Substituting these solutions into Eq (3.66) yields to

$$\left\|\rho_{AB}-\rho_{cq}\right\|_2^2=\frac{1}{4}\left(\|\overrightarrow{x}\|_2^2+\|T\|_2^2-\overrightarrow{e}\left(\overrightarrow{x}\,\overrightarrow{x}^t+TT^t\right)\overrightarrow{e}\right), \tag{3.70}$$

which gives a minimum value when $\overrightarrow{e}$ is an eigenvector of the matrix $K^a=\overrightarrow{x}\,\overrightarrow{x}^t+TT^t$ for the greatest eigenvalue. Therefore, the analytical expression of GQD for general two-qubit quantum states (3.61) is given by

$$\mathcal{Q}_{\mathcal{D}_2(\rho_{AB},\rho_{cq})}(\rho_{AB})=\frac{1}{4}\left(\|x\|_2^2+\|T\|_2^2-K^a_{\max}\right), \tag{3.71}$$

where $x=(x_1,x_2,x_3)^t$ and $K^a_{\max}$ is the maximum eigenvalue of the 3×3 matrix K^a. Similary, when the measurements are made on sub-system B, then x must be replaced by y and TT^t by T^tT. In this case, the expression of GQD turns out to be

$$\mathcal{Q}_{\mathcal{D}_2(\rho_{AB},\rho_{cq})}(\rho_{AB})=\frac{1}{4}\left(\|y\|_2^2+\|T\|_2^2-K^b_{\max}\right), \tag{3.72}$$

where $y=(y_1,y_2,y_3)^t$ and $K^b_{\max}$ is the maximum eigenvalue of the 3×3 matrix $K^b=\overrightarrow{y}\,\overrightarrow{y}^t+T^t$ T. For an arbitrary two-qubit quantum system, the density operator take the following form

$$\rho_{AB}=\begin{pmatrix}\rho_{11}&\rho_{12}&\rho_{13}&\rho_{14}\\ \rho_{21}&\rho_{22}&\rho_{23}&\rho_{24}\\ \rho_{31}&\rho_{32}&\rho_{33}&\rho_{34}\\ \rho_{41}&\rho_{42}&\rho_{43}&\rho_{44}\end{pmatrix}. \tag{3.73}$$

According to the Eq.(3.64), it is straightforward to verified that the total correlation matrix R can be written in terms of the elements of the density matrix ρ_{AB} Eq.(3.73) as

$$\mathrm{R}=\begin{pmatrix} \rho_{11}+\rho_{22}+\rho_{33}+\rho_{44} & \rho_{12}+\rho_{21}+\rho_{34}+\rho_{43} & i\left(\rho_{12}-\rho_{21}+\rho_{34}-\rho_{43}\right) & \rho_{11}-\rho_{22}+\rho_{33}-\rho_{44} \\ \rho_{13}+\rho_{24}+\rho_{31}+\rho_{42} & \rho_{14}+\rho_{23}+\rho_{32}+\rho_{41} & i\left(\rho_{14}-\rho_{23}+\rho_{32}-\rho_{41}\right) & \rho_{13}-\rho_{24}+\rho_{31}-\rho_{42} \\ i\left(\rho_{13}+\rho_{24}-\rho_{31}-\rho_{42}\right) & i\left(\rho_{14}+\rho_{23}-\rho_{32}-\rho_{41}\right) & -\rho_{14}+\rho_{23}+\rho_{32}-\rho_{41} & i\left(\rho_{13}-\rho_{24}-\rho_{31}+\rho_{42}\right) \\ \rho_{11}+\rho_{22}-\rho_{33}-\rho_{44} & \rho_{12}+\rho_{21}-\rho_{34}-\rho_{43} & i\left(\rho_{12}-\rho_{21}-\rho_{34}+\rho_{43}\right) & \rho_{11}-\rho_{22}-\rho_{33}+\rho_{44} \end{pmatrix}. \tag{3.74}$$

Taking these results, we find namely

$$\|x\|_2^2+\|T\|_2^2=\lambda_1+\lambda_2+\lambda_3, \tag{3.75}$$

where λ_1, λ_2 and λ_3 are the eigenvalues of the matrix K^a. These results conduct us to a straightforward expression of GQD in terms of the eigenvalues of the matrix K^a. It is provided by

$$\mathcal{Q}_{\mathcal{D}_2(\rho_{AB},\rho_{cq})}(\rho_{AB})=\frac{1}{4}\min\left\{\lambda_1+\lambda_2,\lambda_2+\lambda_3,\lambda_1+\lambda_3\right\}. \tag{3.76}$$

It should be highlighted that $\mathcal{Q}_{\mathcal{D}_2(\rho_{AB},\rho_{cq})}(\rho_{AB})$ is not normalized to the unity and that its maximum value reflects $\mathcal{Q}_{\mathcal{D}_2(\rho_{AB},\rho_{cq})}(\rho_{AB})=1/2$ occurs when the two-qubit state is maximally entangled. Therefore, in the forthcoming numerical simulations, we shall use the term $2\mathcal{Q}_{\mathcal{D}_2(\rho_{AB},\rho_{cq})}(\rho_{AB})$ as a proper measure for a comparison with other quantum correlation quantifiers. The GQD based on Hilbert-Shmidt distance for qubit-qubit X state ρ_X (2.56), after straithforward claculations reduces to:

$$\mathcal{Q}_{\mathcal{D}_2(\rho_{AB},\rho_{cq})}(\rho_X)=\frac{1}{4}\min\left\{k_1+k_2,k_2+k_3,k_1+k_3\right\}, \tag{3.77}$$

where $k_1=4\left(|\rho_{23}|^2-|\rho_{14}|^2\right)$, $k_2=4\left(|\rho_{23}|^2+|\rho_{14}|^2\right)$ and $k_3=2\left((\rho_{11}-\rho_{33})^2+(\rho_{22}-\rho_{44})^2\right)$. Generally, the geometric quantum discord is connected to the entropic quantum discord (3.8) and the negativity (2.65) for arbitrary bipartite two-qubit quantum systems via the following inequalities [33, 186]:

$$2\mathcal{Q}_{\mathcal{D}_2(\rho_{AB},\rho_{cq})}(\rho_{AB})\geq\mathcal{Q}_A^2(\rho_{AB})\quad\text{ and }\quad 2\mathcal{Q}_{\mathcal{D}_2(\rho_{AB},\rho_{cq})}(\rho_{AB})\geq N^2(\rho_{AB}). \tag{3.78}$$

4.1.2 For qubit-qudit quantum states

Recent studies have revealed that hybrid bipartite quantum systems, such as qubit-qudit or qudit-qubit and multi-qubit system studies, provide useful properties for retaining and preserving quantum correlations over longer periods when compared to the usual two-qubit quantum states. Therefore, we can conclude that increasing the size of quantum systems can be advantageous and superior for future quantum technologies and quantum protocols based on quantum correlations. In this respect, the definition of GQD for any two-qubit states Eq.(3.71) can be generalized for general bipartite quantum systems [183, 184]. However, an exact formula of this quantifier has been established for given bipartite systems of dimensions $m\otimes n$ [183, 184]. Since our discussion is restricted only to qubit-qudit states, we shall focus on the GQD for the case of $2\otimes d$ states with the measurements taken on the qubit sub-systems [187, 188]. This method is also applied for multi-qubit states with the assumption that $d\equiv 2^{N-1}$ [187]. Consider a hybrid density matrix ρ_{AB} acting on the bipartite system $\mathcal{H}_a\otimes\mathcal{H}_b$, with $\dim\mathcal{H}_a=2$ and $\dim\mathcal{H}_b=d$. This density matrix can be written in the Fano-Bloch form as

$$\rho_{AB} = \frac{1}{2d}\sum_{\alpha=0}^{3}\sum_{\beta=0}^{d^2-1}R_{\alpha\beta}\sigma^\alpha\otimes\gamma^\beta \tag{3.79}$$

$$= \frac{1}{2d}\begin{pmatrix}\sigma^0\otimes\gamma^0+\sum_{i=1}^{3}x_i\sigma^i\otimes\gamma^0+\sum_{j=1}^{d^2-1}y_j\sigma^0\otimes\gamma^j \\ +\sum_{i=1}^{3}\sum_{j=1}^{d^2-1}T_{ij}\sigma^i\otimes\gamma^j\end{pmatrix}, \tag{3.80}$$

where γ^i and σ^i are, respectively, the traceless Hermitian generators of $SU(d)$ and $SU(2)$, verifying the orthogonality relation $\mathrm{Tr}\left(\sigma^i\sigma^j\right) = \mathrm{Tr}\left(\gamma^i\gamma^j\right) = 2\delta_{ij}$, with δ_{ij} being the Kronecker symbol. It should be noted that the local Bloch vectors (resp, the correlation tensor) are (3×1)-$((d^2-1)\times 1)$ (resp, $(3\times(d^2-1))$-dimension. They are given through the equations $x_i = R_{i0} = \mathrm{Tr}\left(\rho_{AB}\sigma^i\otimes\gamma^0\right)$, $y_i = R_{0i} = \mathrm{Tr}\left(\rho_{AB}\sigma^0\otimes\gamma^i\right)$ and $T = [R_{ij}] = [T_{ij}] = \mathrm{Tr}\left(\rho_{AB}\sigma^i\otimes\gamma^j\right)$ with γ^0 is the d-dimension identity matrix. As in the case of two-qubit states, the geometric quantum discord based on the Hilbert-Schmidt distance of the qubit-qudit state (3.79) is given by

$$\mathcal{Q}_{\mathcal{D}_2(\rho_{AB},\rho_{cq})}(\rho_{AB}) = \frac{1}{2d}\left(\|x\|_2^2 + \frac{d}{2}\|T\|_2^2 - K^a_{\max}\right), \tag{3.81}$$

where $x = (x_1, x_2, x_3)^t$ and $K^a_{\max}$ is the maximum eigenvalue of the 3×3 matrix $K^a = \overrightarrow{x}\,\overrightarrow{x}^t + \frac{d}{2}TT^t$. It should be emphasized that the analytical expression of the GQD (3.81) for arbitrary qudit-qubit $(d\otimes 2)$ quantum systems can also be obtained in the condition that the local measurements are taken on part B which means the qubit.

In order to illustrate the results concerning the analytical formula of the GQD for qubit-qudit systems, let us consider a qubit-qutrit $(2\otimes 3)$ density matrix given in the standard basis $\{|i,j\rangle,\ i = 0,1 \text{ and } j = -1,0,1\}$ as [53]

$$\rho_{2\times 3} = \begin{pmatrix} \rho_{1,1} & 0 & 0 & 0 & 0 & 0 \\ 0 & \rho_{2,2} & 0 & \rho_{2,4} & 0 & 0 \\ 0 & 0 & \rho_{3,3} & 0 & 0 & 0 \\ 0 & \rho_{2,4} & 0 & \rho_{4,4} & 0 & 0 \\ 0 & 0 & 0 & 0 & \rho_{5,5} & 0 \\ 0 & 0 & 0 & 0 & 0 & \rho_{6,6} \end{pmatrix}. \tag{3.82}$$

To compute the GQD for the qubit-qutrit state (3.82), one needs first to rewrite the above density matrix $\rho_{2\times 3}$ (3.82) in the Fano-Bloch representation as follows

$$\rho_{2\times 3} = \frac{1}{6}\sum_{\alpha=0}^{3}\sum_{\beta=0}^{8} R_{\alpha\beta}\sigma^\alpha\otimes f^\beta \tag{3.83}$$

$$= \frac{1}{6}\left(\begin{array}{c} \sigma^0\otimes f^0 + \sum_{i=1}^{3} x_i\sigma^i\otimes f^0 + \sum_{j=1}^{8} y_j\sigma^0\otimes f^j \\ +\sum_{i=1}^{3}\sum_{j=1}^{8} T_{ij}\sigma^i\otimes f^j \end{array}\right), \tag{3.84}$$

where f^β refers to the generators of $SU(3)$ group which can be characterized via the well-known Gell-Mann matrices. The non-vanishing elements of the total correlation tensor $R_{\alpha\beta}$ of the state under consideration $\rho_{2\times 3}$ (3.82) are provided by

$$R_{00} = \mathrm{Tr}\left(\rho_{2\times 3}\right) = 1, \quad R_{03} = \rho_{1,1} - \rho_{2,2} + \rho_{4,4} - \rho_{5,5}, \tag{3.85}$$

$$R_{11} = R_{22} = 2\rho_{2,4}, \quad R_{30} = \rho_{1,1} + \rho_{2,2} + \rho_{3,3} - \rho_{4,4} - \rho_{5,5} - \rho_{6,6}, \tag{3.86}$$

$$R_{33} = \rho_{1,1} - \rho_{2,2} - 2\rho_{4,4} + \rho_{5,5}, \tag{3.87}$$

$$R_{08} = \frac{1}{\sqrt{3}}\left(\rho_{1,1} + \rho_{2,2} - 2\rho_{3,3} + \rho_{4,4} + \rho_{5,5} - 2\rho_{6,6}\right), \tag{3.88}$$

$$R_{38} = \frac{1}{\sqrt{3}}\left(\rho_{1,1} + \rho_{2,2} - 2\rho_{3,3} - \rho_{4,4} - \rho_{5,5} + 2\rho_{6,6}\right). \tag{3.89}$$

Therefore, the exact expression of GQD described by Eq.(3.81), is given for the qubit–qutrit under discussion (3.82) by

$$\mathcal{Q}_{\mathcal{D}_2(\rho_{AB},\rho_{cq})}(\rho_{2\times 3}) = \frac{1}{2}\left(\frac{1}{3}R_{30}^2 + \frac{1}{2}\left(2R_{11}^2 + R_{33}^2 + R_{38}^2\right)\right) - \max\{k_1,k_2,k_3\}, \tag{3.90}$$

where

$$k_1 = \frac{1}{8}\left(2R_{11}^2 - 2R_{11}\right), \quad k_2 = \frac{1}{8}\left(2R_{11}^2 + 2R_{11}\right), \tag{3.91}$$

$$k_3 = \frac{1}{12}\left(2R_{30}^2 + 3(R_{33}^2 + R_{38}^2)\right). \tag{3.92}$$

However, it has been recently pointed out that despite the easiness of computing this geometric quantifier, this metric suffers from a problem caused by the characteristics of the Hilbert-Schmidt norm. The fact is that this norm can increase even under trivial local reversible operations performed on the unmeasured part, resulting in a bias due to the purity of the global state. It can also be non-contractive under trace-preserving maps [172]. All these facts make this norm and, consequently, this measure unsuitable as a good estimator of quantum correlations. In spite of this drawback, the GQD can yet be considered a suitable indicator for evaluating the quantum correlations in some specific situations. For instance, it can be safely used to examine the degree of quantum correlations between a given quantum system and its environment in open quantum evolutions since these evolutions are globally unitary and do not affect the purity of the state. In this inspiration, we have studied in Ref. [53] the dynamics of the GQD (3.61) of the qubit-qutrit system under both Markovian and non-Markovian noise channels. In this study we have found that this metric behaves similarly to the other mentioned metric of non-classical correlations. However, in order to obtain a proper geometric quantifier of quantum correlations, it is necessary to consider contractible norms. Among these norms is the so-called Schatten 1-norm or trace norm. This norm obeys the contractivity property and is invariant under unitary transformations.

4.2 Geometric quantum discord based on trace-norm

The so-called *"trace distance discord"* or TDD is another quantifier of the GQD. It is a well-defined geometric metric of quantum discord-like measures. TDD is employed to evaluate the degree of quantumness correlations via the Schatten 1-norm (or trace norm) between a given state ρ_{AB} and its nearest classical-quantum state ρ_{cq} belonging to the set Ω_{cq} of zero discord. By using Eq.(3.58) for $p = 1$, the GQD reduces to [37,38]

$$\mathcal{Q}_{\mathcal{D}_1(\rho_{AB},\rho_{cq})}(\rho_{AB}) = \min_{\rho_{cq}\in\Omega_{cq}} \mathcal{D}_1(\rho_{AB},\rho_{cq}) = \min_{\rho_{cq}\in\Omega_{cq}} \left\|\rho_{AB} - \rho_{cq}\right\|_1. \tag{3.93}$$

Here, the term $\left\|\rho_{AB} - \rho_{cq}\right\|_1 = \sqrt{\mathrm{Tr}\left(\rho_{AB} - \rho_{cq}\right) \dagger \mathrm{Tr}\left(\rho_{AB} - \rho_{cq}\right)}$ denotes the trace norm. The analytical expression of the TDD (3.93) has been accomplished only for generic two-qubit X states, and to date, no analytical results have been derived for arbitrary quantum states even for general two-qubit quantum states. According to the results given by Ciccarello *et al* in Ref. [38], the compact expression of the TDD measure for the density matrix ρ_X (2.56) is written as

$$\mathcal{Q}_{\mathcal{D}_1(\rho_{AB},\rho_{cq})}(\rho_X) = \sqrt{\frac{R_{11}^2 \max\left\{R_{33}^2, R_{22}^2 + R_{30}^2\right\} - R_{22}^2 \min\left\{R_{33}^2, R_{11}^2\right\}}{\max\left\{R_{33}^2, R_{22}^2 + R_{30}^2\right\} - \min\left\{R_{33}^2, R_{11}^2\right\} + R_{11}^2 - R_{22}^2}}, \tag{3.94}$$

where $R_{\alpha\beta}$ in Eq.(3.94) are the non-vanishing Fano–Bloch components of the density matrix ρ_X (2.56), which are explicitly given as follows

$$R_{00} = \mathrm{Tr}\rho_X = 1, \quad R_{03} = 1 - 2(\rho_{22} + \rho_{44}), \quad R_{11} = 2\left(|\rho_{23}| + |\rho_{14}|\right), \tag{3.95a}$$

$$R_{22} = 2\left(|\rho_{23}| - |\rho_{14}|\right), \quad R_{33} = 1 - 2\left(\rho_{22} + \rho_{33}\right), \tag{3.95b}$$

$$R_{30} = 2\left(\rho_{11} + \rho_{22}\right) - 1. \tag{3.95c}$$

Despite many efforts made by the scientific community, a closed formula of QD based on von Neumann entropy (3.5) is still not established, even for the simple case of generic qubit-qubit states. Recently, the optimization protocol has been proven for obtaining an analytical expression of the QD is achievable by using the linear entropy instead of von Neumann entropy. This provides a reliable algorithm to deal with the analytical expression of non-classical correlations in terms of linear entropy for arbitrary qudit-qubit systems. This approach will be the aim of the following section.

5 Linear entropy-based quantum discord

As it was already mentioned in the preceding part, we consider here the non-classical correlation through QD in a general qudit–qubit ($d \otimes 2$) state by applying the formalism of linear entropy [32,39,54]. This approach is used to deal with the difficulty of optimizing the classical correlations (see Eq.(3.6)) experienced when the von Neumann entropy is used to evaluate the quantum discord (see Sec.1). Moreover, it has been established that the linear entropy-based quantum discord (LEQD) has a close connection with the original definition of quantum discord Eq.(3.8) in which the average deviation is of the order of 10^{-4} [39]. To derive a close expression of LEQD, one needs to use the expression of the linear entropy $S_2(\rho)$. It is provided for a quantum state ρ by

$$S_2(\rho) = 2\left[1 - \mathrm{Tr}\left(\rho^2\right)\right]. \tag{3.96}$$

In terms of the above expression (3.96), the classical correlation (3.6) is defined for a bipartite state as follows

$$\mathcal{J}_{2B}(\rho_{AB}) = \max_{\{P_k\}} \Big(S_2(\rho_A) - \textstyle\sum_k p_k S_2\left(\rho_{A|k}\right) \Big). \tag{3.97}$$

This arises from Eq.(3.6) when linear entropy is considered instead of von Neumann entropy. In the Bloch representation, an arbitrary qudit state can be characterized as

$$\rho_d = \frac{1}{d}\left[I_d + \mathbf{r}\cdot\boldsymbol{\gamma}\right], \tag{3.98}$$

where I_d is the d-dimension identity matrix and the term $\mathbf{r}$ stands for a (d^2-1)-dimensional real vector. While $\boldsymbol{\gamma} = \left(\gamma_1, \gamma_2, \ldots, \gamma_{d^2-1}\right)^T$ represents the vector whose components can generate $SU(d)$ with T being the transpose of the system. These remain orthogonal to the Hilbert-Schmidt inner product. Hence, the linear entropy of the qudit state (3.98), defined in terms of the Bloch vector $\mathbf{r}$ is provided by

$$S_2(\rho_d) = \frac{1}{d^2}\left(2d^2 - 2d - 4\left|\mathbf{r}\right|^2\right). \tag{3.99}$$

A qudit-qubit ($d \otimes 2$) two-qubit quantum state ρ_{AB} can be represented as follows [168]

$$\rho_{AB} = \Lambda \otimes I_B\left(\left|v_{B'B}\right\rangle\left\langle v_{B'B}\right|\right), \tag{3.100}$$

where I_B represents the identity matrix acting on the sub-system B and $|v_{B'B}\rangle$ denotes the two-qubit symmetric purification of the marginal state ρ_B of the sub-system B on an auxiliary qubit state $B^{'}$. We note that the two-qubit symmetric purification signifies that both reduced density operators are equal, that is, $v_{B'} = v_B = \rho_B$. While Λ reflects a qudit channel or a CPTP map, that maps the qubit state $B^{'}$ to the qudit state A. The procedure of acting on a qudit channel Λ with a single-qubit state $\rho = \left[I_2 + \mathbf{r}_B\cdot\boldsymbol{\sigma}\right]/2$, where $\mathbf{r}_B$ remains for a 3-directional vector, $|\mathbf{r}| \leq 1$ and $\boldsymbol{\sigma}$ refers to the Pauli operator vectors and has the form

$$\Lambda(\rho) = \frac{1}{d}\left[I_d + (\mathbf{Lr} + \mathbf{l})\cdot\boldsymbol{\gamma}\right]. \tag{3.101}$$

Here, $\mathbf{l}$ in Eq.(3.101) denotes a three-dimensional vector, while $\mathbf{L}$ refers to a real matrix of dimension $3 \times (d^2-1)$ whose components are given by

$$\mathbf{L} = [L_{ij}] = \frac{1}{d}\sum_{i=1}^{3}\sum_{j=1}^{d^2-1} \mathrm{Tr}\left(\Lambda\left(\sigma^i\right)\cdot\gamma^j\right). \tag{3.102}$$

To write $|v_{B'B}\rangle = \sum_{i=1,2}\sqrt{\lambda_i}\,|\psi_i\rangle\,|\psi_i\rangle$, one must use the spectral decomposition of the reduced density operator ρ_B, such that: $\rho_B = \sum_{i=1,2}\lambda_i\,|\psi_i\rangle\langle\psi_i|$. The possible decomposition of the state ρ_B into pure states is expressed in this Pauli basis in terms of all possible sets of probabilities $\{p_i\}$ and unit vectors $\{r_i\}$ for which $\mathbf{r}_B = \sum_i p_i r_i$. The action of the qudit map Λ on the state of sub-system B yields

$$\rho_B = \frac{1}{2}\left[I_2 + \mathbf{r}_B\cdot\boldsymbol{\sigma}\right] \qquad \xrightarrow{\Lambda\,:\,\text{qubit-qudit}} \qquad \Lambda(\rho_B) = \frac{1}{d}\left[I_d + (\mathbf{Lr_B} + \mathbf{l})\cdot\boldsymbol{\gamma}\right]. \tag{3.103}$$

Thus, by using Eq.(3.99), the corresponding linear entropy is written as

$$S_2(\Lambda(\rho_B)) = \frac{1}{d^2}\left(2d^2 - 2d - 4\left(\mathbf{Lr_B} + \mathbf{l}\right)^T\left(\mathbf{Lr_B} + \mathbf{l}\right)\right). \tag{3.104}$$

In the same way, we found that the linear entropies of the action of the qudit channel Λ on the pure states $|\psi_i\rangle$, with $i = 1, 2$ are given by

$$S_2(\Lambda(|\psi_i\rangle)) = \frac{1}{d^2}\left(2d^2 - 2d - 4\left(\mathbf{L}r_i + \mathbf{l}\right)^T\left(\mathbf{L}r_i + \mathbf{l}\right)\right). \tag{3.105}$$

Using the above results, it is simple to see that the marginal density operator of the first sub-system ρ_A is equal to the action of the qudit channel on the marginal density operator of the qubit state ρ_B, i.e., $\rho_A = \Lambda(\rho_B)$. Such that

$$\begin{aligned}
\rho_A &= \mathrm{Tr}_B(\rho_{AB}) = \mathrm{Tr}_B\left(\Lambda \otimes I_B\left(|v_{B'B}\rangle\langle v_{B'B}|\right)\right) && (3.106)\\
&= \mathrm{Tr}_B\left(\textstyle\sum_{i,j}\sqrt{\lambda_i\lambda_j}\Lambda\left(|\psi_i\rangle\langle\psi_j|\right)\otimes\left(|\psi_i\rangle\langle\psi_j|\right)\right)\\
&= \langle\psi_k|\left(\textstyle\sum_{i,j}\sqrt{\lambda_i\lambda_j}\Lambda\left(|\psi_i\rangle\langle\psi_j|\right)\otimes\left(|\psi_i\rangle\langle\psi_j|\right)\right)|\psi_k\rangle\\
&= \textstyle\sum_{i,j}\sqrt{\lambda_i\lambda_j}\Lambda\left(|\psi_i\rangle\langle\psi_j|\right)\underbrace{\langle\psi_k|\psi_i\rangle}_{\delta_{kl}}\underbrace{\langle\psi_j|\psi_k\rangle}_{\delta_{jk}}\\
&= \textstyle\sum_i \lambda_i\Lambda\left(|\psi_i\rangle\langle\psi_i|\right) = \Lambda(\rho_B). && (3.107)
\end{aligned}$$

However, Osborne *et al.* have shown that the classical correlation in terms of the linear entropy coincides with the linear Holevo capacity for the qubit channels $\chi_2(\rho_B, \Lambda)$ [168]. It is defined as follows

$$\mathcal{J}_{2B}(\rho_{AB}) = \max_{\{p_i,|\psi_i\rangle\}}\left(S_2(\Lambda(\rho_B)) - \textstyle\sum_i p_i S_2\left(\Lambda\left(|\psi_i\rangle\langle\psi_i|\right)\right)\right), \tag{3.108}$$

where the maximization in Eq.(3.108) is carried out on all pure-state decompositions of the qubit state ρ_B. By substituting Eq.(3.104) and Eq.(3.105) back into Eq.(3.108), we get

$$\mathcal{J}_{2B}(\rho_{AB}) = \frac{4}{d^2}\max_{\{p_i,|\psi_i\rangle\}}\left(p_1\left\|\mathbf{L}r_1+\mathbf{l}\right\|^2 + p_2\left\|\mathbf{L}r_2+\mathbf{l}\right\|^2 - \left\|\mathbf{L}r_B+\mathbf{l}\right\|^2\right). \tag{3.109}$$

By inserting the term $r_i = r_B + X_i$, where $X_i = (X_i^x, X_i^y, X_i^z)$, one can straightforwardly verify that the calculation of the expression $\mathcal{J}_{2B}(\rho_{AB})$ (3.109) reduces to defining the set $\{p_i, X_i\}$ subject to the constraints, namely $\sum_i p_i X_i = 1$ and $\|r_B + X_i\| = 1$. In these circumstances, Eq.(3.109) yields to

$$\mathcal{J}_{2B}(\rho_{AB}) = \frac{4}{d^2} \max_{\{p_i, X_i\}} (\textstyle\sum_i p_i X_i^T \mathbf{L}^T \mathbf{L} X_i). \tag{3.110}$$

without incurring in any loss. Let us suppose that the matrix $\mathbf{L}^T\mathbf{L}$ is diagonal, i.e. $\mathbf{L}^T\mathbf{L} = diag\{\lambda^x, \lambda^y, \lambda^z\}$, with its diagonal components satisfying $\lambda^x \geq \lambda^y \geq \lambda^z$. The conditions $\|r_B + X_i\| = 1$ lead to the identities

$$(X_i^x)^2 = 1 - \|r_B\|^2 - 2r_B^T X_i - (X_i^y)^2 - (X_i^z)^2 . \tag{3.111}$$

By substituting the above quantity back into Eq.(3.110), we get

$$\mathcal{J}_{2B}(\rho_{AB}) = \frac{4}{d^2}\left[\lambda^x \left(1 - \|r_B\|^2\right) + \max_{\{p_i, X_i\}} \textstyle\sum_i p_i((\lambda^y - \lambda^x)(X_i^y)^2 + (\lambda^z - \lambda^x)(X_i^z)^2)\right]. \tag{3.112}$$

Since $\lambda^x \geq \lambda^y \geq \lambda^z$, the second part of the Eq.(3.112) is less than or equal to zero. It is clearly maximized by setting $X_i^y = X_i^z = 0$ for all values of i. As $S_2(\rho_B) = 1 - \|r_B\|^2$, we get therefore the following analytical expression of the classical correlation in terms of the linear entropy for given hybrid qudit-qubit $(d \otimes 2)$ quantum states

$$\mathcal{J}_{2B}(\rho_{AB}) = \frac{4}{d^2} \lambda_{\max}\left(\mathbf{L}^T\mathbf{L}\right) S_2(\rho_B), \tag{3.113}$$

where $\lambda_{\max}\left(\mathbf{L}^T\mathbf{L}\right)$ is the greatest eigenvalue of $\mathbf{L}^T\mathbf{L}$ matrix. It results that the determination of the expression $\mathcal{J}_{2B}(\rho_{AB})$ (3.113) and consequently the linear entropy-based quantum discord requires only the calculation of the matrix $\mathbf{L}$. To do this, we shall provide an overview of how to determine this matrix for common two-qubit states [189] and arbitrary qudit-qubit states [32].

5.1 Analytical expression of linear quantum discord for arbitrary two-qubit states

A generic two-qubit state characterized via the density matrix ρ_{AB} can be rewritten in the standard basis of two-qubit states as

$$\rho_{AB} = \textstyle\sum_{i,j=0}^{1} \beta_{ij} \otimes |i\rangle \langle j| , \tag{3.114}$$

where the term β_{ij} is the 2×2 matrix whose components are given by

$$\beta_{00} = \begin{pmatrix} \rho_{11} & \rho_{13} \\ \rho_{31} & \rho_{33} \end{pmatrix}, \quad \beta_{01} = \begin{pmatrix} \rho_{21} & \rho_{23} \\ \rho_{41} & \rho_{43} \end{pmatrix}, \tag{3.115}$$

$$\beta_{10} = \begin{pmatrix} \rho_{12} & \rho_{14} \\ \rho_{32} & \rho_{34} \end{pmatrix}, \quad \beta_{11} = \begin{pmatrix} \rho_{22} & \rho_{24} \\ \rho_{42} & \rho_{44} \end{pmatrix}. \tag{3.116}$$

The pure state reduced density operator ρ_B can also be reconstructed in this basis as $|\psi_1\rangle = \begin{pmatrix} a_0 & a_1 \end{pmatrix}^T$ and $|\psi_2\rangle = \begin{pmatrix} b_0 & b_1 \end{pmatrix}^T$, where a_i and b_i are real coefficients. The symmetric two-qubit purification $|v_{B'B}\rangle$ of the qubit state ρ_B on an auxiliary qubit system B' leads to the following state

$$\rho_{B'B} = |v_{B'B}\rangle \langle v_{B'B}| = \begin{pmatrix} A\overline{A} & AB & A\overline{B} & AC \\ B\overline{A} & B\overline{B} & B\overline{B} & B\overline{C} \\ B\overline{A} & B\overline{B} & B\overline{B} & B\overline{C} \\ C\overline{A} & C\overline{B} & C\overline{B} & C\overline{C} \end{pmatrix}, \tag{3.117}$$

where

$$A=\sqrt{\lambda_1}a_0^2+\sqrt{\lambda_2}b_0^2,\quad B=\sqrt{\lambda_1}a_0a_1+\sqrt{\lambda_2}b_0b_1,\quad C=\sqrt{\lambda_1}a_1^2+\sqrt{\lambda_2}b_1^2. \tag{3.118}$$

Thus, the elements of the density matrix $\rho_{B'B}$ (3.117) can be described through the components β_{ij} of the density operator ρ_{AB} (3.114) as follows

$$\begin{aligned}
\beta_{00} &= A\overline{A}\Lambda\left(|0\rangle\langle 0|\right)+A\overline{B}\Lambda\left(|0\rangle\langle 1|\right)+B\overline{A}\Lambda\left(|1\rangle\langle 0|\right)+B\overline{B}\Lambda\left(|1\rangle\langle 1|\right), &(3.119)\\
\beta_{01} &= B\overline{A}\Lambda\left(|0\rangle\langle 0|\right)+B\overline{B}\Lambda\left(|0\rangle\langle 1|\right)+C\overline{A}\Lambda\left(|1\rangle\langle 0|\right)+C\overline{B}\Lambda\left(|1\rangle\langle 1|\right), &(3.120)\\
\beta_{10} &= A\overline{B}\Lambda\left(|0\rangle\langle 0|\right)+A\overline{C}\Lambda\left(|0\rangle\langle 1|\right)+B\overline{B}\Lambda\left(|1\rangle\langle 0|\right)+B\overline{C}\Lambda\left(|1\rangle\langle 1|\right), &(3.121)\\
\beta_{11} &= B\overline{B}\Lambda\left(|0\rangle\langle 0|\right)+B\overline{C}\Lambda\left(|0\rangle\langle 1|\right)+C\overline{B}\Lambda\left(|1\rangle\langle 0|\right)+C\overline{C}\Lambda\left(|1\rangle\langle 1|\right). &(3.122)
\end{aligned}$$

The elements of the matrix $\mathbf{L}$ (3.102) for two-qubit states can be determined by solving Eqs.(3.119-3.122) This allows us to get the quantities $\Lambda\left(|i\rangle\langle j|\right)$, from which we derive the components L_{ij} (3.102) in terms of the elements of the density matrix ρ_{AB}. To illustrate these results, we consider the following rank-2 two-qubit Bell-diagonal states [190]

$$\rho_{BELL}=\frac{1}{4}\left(I_{2\times 2}+\textstyle\sum_i c_i\sigma_i\otimes\sigma_i\right), \tag{3.123}$$

where the reals correlation coefficients c_i fulfill the requirement $0\leq|c_i|\leq 1$. In the computational basis, the density matrix ρ (3.123) takes the matrix form

$$\rho_{BELL}=\frac{1}{4}\begin{pmatrix}1+c_3 & 0 & 0 & c_1-c_2\\ 0 & 1-c_3 & c_1+c_2 & 0\\ 0 & c_1+c_2 & 1-c_3 & 0\\ c_1-c_2 & 0 & 0 & 1+c_3\end{pmatrix}. \tag{3.124}$$

In this case, we find that the matrices β_{ij} reduce to

$$\begin{aligned}
\beta_{00} &= \frac{1}{4}\begin{pmatrix}1+c_3 & 0\\ 0 & 1-c_3\end{pmatrix},\quad \beta_{01}=\frac{1}{4}\begin{pmatrix}0 & c_1+c_2\\ c_1-c_2 & 0\end{pmatrix}, &(3.125)\\
\beta_{10} &= \frac{1}{4}\begin{pmatrix}0 & c_1-c_2\\ c_1+c_2 & 0\end{pmatrix},\quad \beta_{11}=\frac{1}{4}\begin{pmatrix}1-c_3 & 0\\ 0 & 1+c_3\end{pmatrix}, &(3.126)
\end{aligned}$$

by solving Eqs.(3.119-3.122), the qubit channel $\Lambda\left(|i\rangle\langle j|\right)$ is provided as

$$\Lambda\left(|0\rangle\langle 0|\right)=2\beta_{00},\quad \Lambda\left(|0\rangle\langle 1|\right)=2\beta_{01},\quad \Lambda\left(|1\rangle\langle 0|\right)=2\beta_{10},\quad \Lambda\left(|1\rangle\langle 1|\right)=2\beta_{11}.$$

After straightforward calculation, we find that the 3×3-matrix $\mathbf{L}$ (3.102) for two-qubit Bell states ρ_{BELL} (3.124) has the following form

$$\mathbf{L}=2\begin{pmatrix}c_1 & 0 & 0\\ 0 & c_2 & 0\\ 0 & 0 & c_3\end{pmatrix}. \tag{3.127}$$

Therfore, the linear entropy based classical correlation for the state ρ_{BELL} (3.124) is

$$\mathcal{J}_{2B}(\rho_{BELL})=\max\{c_1^2,c_2^2,c_2^2\}S_2(\rho_B), \tag{3.128}$$

with the linear entropy of the state ρ_B is $S_2(\rho_B)=1$.

5.2 Von Neumann entropy-based quantum discord for rank-2 two-qubit states

Motivated by the above findings, it is possible to derive another analytical formula of the von Neumann entropy-based quantum discord from $\mathcal{J}_{2B}(\rho_{AB})$ (3.113) for arbitrary rank-2 two-qubit quantum states. To accomplish this, we have to establish first the connection between the entanglement of formation $\mathcal{E}_f(\rho_{AB})$ (2.48), the concurrence $\mathcal{C}(\rho_{AB})$ (2.54), tangle $\tau_g(\rho)$ (2.81), the linear entropy-based classical correlations $\mathcal{J}_{2B}(\rho_{AB})$ (3.113) and the von Neumann entropy-based classical correlations $\mathcal{J}_B(\rho_{AB})$ (3.6). The tangle $\tau_g(\rho_{AB})$ of bipartite quantum states is defined as the minimum across all possible pure-state decompositions $\{p_i, |\varphi_i\rangle\}$ of the state $\rho_{AB} = \sum_i \lambda_i |\psi_i\rangle \langle\psi_i|$. This gives [191]

$$\tau_g(\rho_{AB}) = \min_{\{\lambda_i, |\psi_i\rangle\}} \sum_i p_i S_2(\rho_B^i), \tag{3.129}$$

where $\rho_B^i = \mathrm{Tr}_A(|\varphi_i\rangle \langle\varphi_i|)$. The concurrence of a quantum state ρ_{AB} is related to its tangle $\tau_g(\rho_{AB})$ through the inequality $\mathcal{C}^2(\rho_{AB}) \leq \tau_g(\rho_{AB})$, which holds for arbitrary quantum states due to the convexity of the concurrence. However, the equality only holds for the case of two-qubit states, where the tangle is equal to the square of the concurrence [191]. For pure two-qubit states $|\psi\rangle_{AB}$, the entanglement of formation $\mathcal{E}_f(|\psi\rangle_{AB})$ and the concurrence $\mathcal{C}(|\psi\rangle_{AB})$ are determined via $\mathcal{E}_f(|\psi\rangle_{AB}) = S(\rho_A)$ and $\mathcal{C}(|\psi\rangle_{AB}) = \sqrt{2(1 - \mathrm{Tr}(\rho_A^2))}$, respectively. However, for mixed two-qubit states ρ_{AB}, they are extended by the convex-roof construction, namely $\mathcal{E}_f(\rho_{AB}) = \min_{\{p_i, |\psi_i\rangle\}} \sum_i p_i \mathcal{E}_s(|\psi_i\rangle)$ and $\mathcal{C}(\rho_{AB}) = \min_{\{p_i, |\psi_i\rangle_{AB}\}} \sum_i p_i \mathcal{C}(|\psi_i\rangle_{AB})$, where the minimum is achieved over all possible pure state decompositions of ρ_{AB}. Moreover, we have emphasized the connection between the concurrence and the EOF in Eqs.(2.61-2.62).

Given a rank-2 two-qubit quantum state ρ_{AB} with spectral decomposition $\rho_{AB} = \lambda_1 |\psi_1\rangle \langle\psi_1| + \lambda_2 |\psi_2\rangle \langle\psi_2|$, where λ_j and $|\psi_j\rangle$ are the eigenvalues and eigenvectors of ρ_{AB} (with $j = 1, 2$) and $\sum_i \lambda_j = 1$. By attaching a third qubit system E, the purified tripartite qubit state can be expressed as $|\psi\rangle_{ABC} = \sqrt{\lambda_1} |\psi_1\rangle |0\rangle + \sqrt{\lambda_2} |\psi_2\rangle \langle 1|$, satisfying $\rho_{AB} = \mathrm{Tr}_E(|\psi\rangle_{ABE} \langle\psi|)$. In such a case, we use the Koashi-Winter relation to establish a connection between the von Neumann entropy-based quantum discord and the entanglement of formation (3.38). Therefore, we obtain the following monogamy relation [168]

$$\tau_g(\rho_{AE}) + \mathcal{J}_{2B}(\rho_{AB}) = S_2(\rho_A). \tag{3.130}$$

Since ρ_{AE} is a two-qubit state, then we get $\tau_g(\rho_{AE}) = \mathcal{C}^2(\rho_{AB})$. Moreover, it is easy to see that

$$S(\rho_A) = \mathcal{E}_f(|\psi\rangle_{A|BE}) = f\left(\mathcal{C}^2(|\psi\rangle_{A|BE})\right) = f\left(S_2(\rho_A)\right), \tag{3.131}$$

with

$$\mathcal{E}_f(\rho_{AE}) = f\left(\mathcal{C}^2(\rho_{AE})\right) = f\left(S_2(\rho_A) - \mathcal{J}_{2B}(\rho_{AB})\right), \tag{3.132}$$

where $f(x) = h\left(\frac{1+\sqrt{1-x}}{2}\right)$. By substituting Eq.(3.131) and Eq.(3.132) back into Eq.(3.35) we get

$$\mathcal{J}_B(\rho_{AB}) = S(\rho_A) - f\left(S_2(\rho_A) - \mathcal{J}_{2B}(\rho_{AB})\right). \tag{3.133}$$

Therefore, the von Neumann entropy-based quantum discord for given rank-2 two-qubit quantum states are given by

$$\mathcal{Q}_B(\rho_{AB}) = S(\rho_B) - S(\rho_{AB}) + f\left(S_2(\rho_A) - \mathcal{J}_{2B}(\rho_{AB})\right). \tag{3.134}$$

The above formula provides a direct algorithm to evaluate the von Neumann entropy-based quantum discord for arbitrary rank-2 two-qubit quantum states. It is important to emphasize

that, in contrast to the expression (3.38), one can directly evaluate the QD for rank-2 two-qubit quantum system state ρ_{AB}. For instance, let us consider the rank-2 two-qubit Bell states (3.123). By calculation, we obtain $S(\rho_A) = S(\rho_B) = 1$ and $S_2(\rho_A) = 1$. Then, the von Neumann entropy-based classical correlation for the state (3.123) is given by

$$\mathcal{J}_B(\rho_{BELL}) = 1 - f\left(1 - c^2\right) = \frac{1-c}{2}\log_2(1-c) + \frac{1+c}{2}\log_2(1+c). \tag{3.135}$$

with $c = \max\{c_1, c_2, c_3\}$. Thus, the von Neuman entropy-based quantum discord of the state (3.123) is provided by

$$\mathcal{Q}_B(\rho_{BELL}) = 2 - \textstyle\sum_i \lambda_i \log_2 \lambda_i - \left(\frac{1-c}{2}\log_2(1-c) + \frac{1+c}{2}\log_2(1+c)\right), \tag{3.136}$$

where λ_i are the eigenvalues of the state ρ_{BELL} (3.123). They are given by

$$\lambda_1 = \frac{1}{4}(1 - c_1 - c_2 - c_3), \quad \lambda_2 = \frac{1}{4}(1 + c_1 + c_2 - c_3), \tag{3.137}$$

$$\lambda_3 = \frac{1}{4}(1 + c_1 - c_2 + c_3), \quad \lambda_4 = \frac{1}{4}(1 - c_1 + c_2 + c_3). \tag{3.138}$$

5.3 Analytical expression of linear quantum discord for arbitrary qudit-qubit states

The computation regarding the components of $\mathbf{L}$ matrix was assumed for given two-qubit quantum states. Now we adopt an approach to derive such components for an arbitrary $d \otimes 2$ quantum system. This method focuses mainly on the writing of the density matrix under consideration ρ_{AB} as well as the matrix $\mathbf{L}$ in the Fano-Bloch representation and computing all the elements of these total correlation tensors [32, 54]. To do this, we need first to write the $d \otimes 2$ density matrix ρ_{AB} in the Fano-Bloch representation as

$$\rho_{AB} = \frac{1}{2d}\textstyle\sum_{\alpha=0}^{d^2-1}\sum_{\beta=0}^{3} R_{\alpha\beta}\gamma^\alpha \otimes \sigma^\beta, \tag{3.139}$$

where the coefficients $R_{\alpha\beta} = \frac{d}{2}\mathrm{Tr}\left(\rho_{AB}\gamma^\alpha \otimes \sigma^\beta\right)$ denotes the elements of the total correlation tensor associated with the qudit-qubit state ρ_{AB}(3.139). From the state ρ_{AB} (3.139), the reduced density operator ρ_B can be expressed in terms of Fano-Bloch parameters $R_{\alpha\beta}$ as

$$\rho_B = \mathrm{Tr}_A(\rho_{AB}) = \frac{1}{2}\textstyle\sum_{\beta=0}^{3} R_{0\beta}\sigma^\beta. \tag{3.140}$$

Correspondingly, using the above expression (3.140), the state $\rho_{B'B}$ in (3.100) can be reformulated as

$$\rho_{B'B} = |v_{B'B}\rangle\langle v_{B'B}| = \frac{1}{4}\textstyle\sum_{\alpha,\beta=0}^{3} \mathcal{T}_{\alpha\beta}\sigma^\alpha \otimes \sigma^\beta, \tag{3.141}$$

where $\mathcal{T}_{\alpha\beta}$ represents the elements of the total correlation tensor associated with the state $\rho_{B'B}$ (3.141). They provide as

$$\mathcal{T}_{\alpha\beta} = \mathrm{Tr}\left(\rho_{B'B}\sigma^\alpha \otimes \sigma^\beta\right). \tag{3.142}$$

Moreover, the qudit channel Λ can also be rewritten as follows

$$\Lambda(\sigma^\alpha) = \textstyle\sum_{\alpha=0}^{3}\sum_{\delta=0}^{d^2-1} \mathcal{L}_{\alpha\delta}\gamma^\delta, \tag{3.143}$$

where

$$\mathcal{L}_{\alpha\delta} = \mathrm{Tr}\left(\Lambda(\sigma^\alpha)\cdot\gamma^\delta\right). \tag{3.144}$$

Thus, by employing the state in Eq.(3.141) and Eq.(3.143), we obtain

$$\Lambda \otimes I_B \left(\left| v_{B'B} \right\rangle \left\langle v_{B'B} \right| \right) = \frac{1}{4} \sum_{\delta=0}^{d^2-1} \sum_{\beta=0}^{3} \left(\mathcal{L}^T \mathcal{T} \right)_{\beta\delta} \gamma^{\delta} \otimes \sigma^{\beta}. \tag{3.145}$$

Therfore, from the definition (3.100), it is straightforward to check that

$$\frac{1}{2d} R_{\alpha\beta} = \frac{1}{4} \left(\mathcal{L}^T \mathcal{T} \right)_{\alpha\beta}. \tag{3.146}$$

It follows that the matrix $\mathcal{L}$ describes by (3.144) writes as

$$\mathcal{L} = \frac{2}{d} \left(\mathcal{T}^T \right)^{-1} R^T$$

where R, $\mathcal{T}$ and $\mathcal{L}$ are the matrices whose components are, respectively, $R_{\alpha\beta}$, $\mathcal{T}_{\alpha\beta}$ and $\mathcal{L}_{\alpha\beta}$. In this regard, the matrix $\mathbf{L}$ defined through Eq. (3.113) is a key ingredient to assess the classical correlation (3.113) and consequently the quantum discord for a general bipartite hybrid qudit-qubit state. It is provided by

$$\mathbf{L} = \sum_{i=1}^{3} \sum_{j=1}^{d^2-1} \mathcal{L}_{ij}. \tag{3.147}$$

It is clear that with the matrix $\mathbf{L}$ one can simply compute the classical correlation (3.113). Hence, the closed equation of the linear entropy based quantum discord is obtained for any $d \otimes 2$ system as

$$\mathcal{Q}_2(\rho_{AB}) = \mathcal{I}(\rho_{AB}) - \mathcal{J}_{2B}(\rho_{AB}). \tag{3.148}$$

where $\mathcal{I}(\rho_{AB})$ stands for the quantum mutual information described by Eq.(1.64). As a concrete example to illustrate these results, consider a qutrit-qubit quantum state $\rho_{3\otimes 2}$ in (2.70). In order to calculate the linear entropy-based quantum discord in the qutrit-qubit state $\rho_{3\otimes 2}$ (2.70), one needs first to compute both the correlation matrix components $R_{\alpha\beta}$ of the state ρ_{AB} (see Eq.3.139) and the correlation matrix elements $\mathcal{T}_{\alpha\beta}$ of the state $\rho_{B'B}$ (see Eq.3.141). Hence, the matrix $\rho_{3\otimes 2}$ (2.70) can be rewritten in the Fano-Bloch form as follows

$$\rho_{3\otimes 2} = \frac{1}{6} \sum_{\alpha=0}^{8} \sum_{\beta=0}^{3} R_{\alpha\beta} f^{\alpha} \otimes \sigma^{\beta}, \tag{3.149}$$

where f^{α} refers to the generators of $SU(3)$ group which can be characterized via the well-known Gell-Mann matrices. Generally, for an arbitrary qutrit-qubit quantum state, the total correlation matrix $R = [R_{\alpha\beta}]$ can be expressed in terms of the components of the density matrix ρ_{AB} as

$$\mathrm{R}=\begin{pmatrix} \rho_{11}+\rho_{22}+\rho_{33}+\rho_{44}+\rho_{55}+\rho_{66} & \rho_{12}+\rho_{21}+\rho_{34}+\rho_{43}+\rho_{56}+\rho_{65} & i\left(\rho_{12}-\rho_{21}+\rho_{34}-\rho_{43}+\rho_{56}-\rho_{65}\right) & \rho_{11}-\rho_{22}+\rho_{33}-\rho_{44}+\rho_{55}-\rho_{66} \\ \frac{3}{2}\left(\rho_{13}+\rho_{24}+\rho_{31}+\rho_{42}\right) & \frac{3}{2}\left(\rho_{14}+\rho_{23}+\rho_{32}+\rho_{41}\right) & \frac{3}{2}i\left(\rho_{14}-\rho_{23}+\rho_{32}-\rho_{41}\right) & \frac{3}{2}\left(\rho_{13}-\rho_{24}+\rho_{31}-\rho_{42}\right) \\ \frac{3}{2}i\left(\rho_{13}+\rho_{24}-\rho_{31}-\rho_{42}\right) & \frac{3}{2}i\left(\rho_{14}+\rho_{23}-\rho_{32}-\rho_{41}\right) & \frac{3}{2}\left(-\rho_{14}+\rho_{23}+\rho_{32}-\rho_{41}\right) & \frac{3}{2}i\left(\rho_{13}-\rho_{24}-\rho_{31}+\rho_{42}\right) \\ \frac{3}{2}\left(\rho_{11}+\rho_{22}-\rho_{33}-\rho_{44}\right) & \frac{3}{2}\left(\rho_{12}+\rho_{21}-\rho_{34}-\rho_{43}\right) & \frac{3}{2}i\left(\rho_{12}-\rho_{21}-\rho_{34}+\rho_{43}\right) & \frac{3}{2}\left(\rho_{11}-\rho_{22}-\rho_{33}+\rho_{44}\right) \\ \frac{3}{2}\left(\rho_{15}+\rho_{26}+\rho_{51}+\rho_{62}\right) & \frac{3}{2}\left(\rho_{16}+\rho_{25}+\rho_{52}+\rho_{61}\right) & \frac{3}{2}i\left(\rho_{16}-\rho_{25}+\rho_{52}-\rho_{61}\right) & \frac{3}{2}\left(\rho_{15}-\rho_{26}+\rho_{51}-\rho_{62}\right) \\ \frac{3}{2}i\left(\rho_{15}+\rho_{26}-\rho_{51}-\rho_{62}\right) & \frac{3}{2}i\left(\rho_{16}+\rho_{25}-\rho_{52}-\rho_{61}\right) & \frac{3}{2}\left(-\rho_{16}+\rho_{25}+\rho_{52}-\rho_{61}\right) & \frac{3}{2}i\left(\rho_{15}-\rho_{26}-\rho_{51}+\rho_{62}\right) \\ \frac{3}{2}\left(\rho_{35}+\rho_{46}+\rho_{53}+\rho_{64}\right) & \frac{3}{2}\left(\rho_{36}+\rho_{45}+\rho_{54}+\rho_{63}\right) & \frac{3}{2}i\left(\rho_{36}-\rho_{45}+\rho_{54}-\rho_{63}\right) & \frac{3}{2}\left(\rho_{35}-\rho_{46}+\rho_{53}-\rho_{64}\right) \\ \frac{3}{2}i\left(\rho_{35}+\rho_{46}-\rho_{53}-\rho_{64}\right) & \frac{3}{2}i\left(\rho_{36}+\rho_{45}-\rho_{54}-\rho_{63}\right) & \frac{3}{2}\left(-\rho_{36}+\rho_{45}+\rho_{54}-\rho_{63}\right) & \frac{3}{2}i\left(\rho_{35}-\rho_{46}-\rho_{53}+\rho_{64}\right) \\ \frac{3}{2\sqrt{3}}\left(\rho_{11}+\rho_{22}+\rho_{33}+\rho_{44}-2\rho_{55}-2\rho_{66}\right) & \frac{3}{2\sqrt{3}}\left(\rho_{12}+\rho_{21}+\rho_{34}+\rho_{43}-2\rho_{56}-2\rho_{65}\right) & \frac{3}{2\sqrt{3}}i\left(\rho_{12}-\rho_{21}+\rho_{34}-\rho_{43}-2\rho_{56}+2\rho_{65}\right) & \frac{3}{2\sqrt{3}}\left(\rho_{11}-\rho_{22}+\rho_{33}-\rho_{44}-2\rho_{55}+2\rho_{66}\right) \end{pmatrix}, \tag{3.150}$$

where ρ_{ij} are the elements of the density matrix ρ_{AB} of an arbitrary qutrit-qubit quantum state. This density matrix ρ_{AB} is given in the computational basis of qutrit-qubit as

$$\rho_{AB} = \begin{pmatrix} \rho_{11} & \rho_{12} & \rho_{13} & \rho_{14} & \rho_{15} & \rho_{16} \\ \rho_{21} & \rho_{22} & \rho_{23} & \rho_{24} & \rho_{25} & \rho_{26} \\ \rho_{31} & \rho_{32} & \rho_{33} & \rho_{34} & \rho_{35} & \rho_{36} \\ \rho_{41} & \rho_{42} & \rho_{43} & \rho_{44} & \rho_{45} & \rho_{46} \\ \rho_{51} & \rho_{52} & \rho_{53} & \rho_{45} & \rho_{55} & \rho_{56} \\ \rho_{61} & \rho_{62} & \rho_{63} & \rho_{64} & \rho_{65} & \rho_{66} \end{pmatrix}. \tag{3.151}$$

Thus, the non-zero elements of the total correlation tensor $R_{\alpha\beta}$ (3.150) for the state under scrutiny $\rho_{3\otimes 2}$ (2.70) are provided by

$$R_{00} = \mathrm{Tr}\left(\rho_{3\otimes 2}\right) = 1, \qquad R_{11} = R_{22} = 3\rho_{23}, \qquad R_{61} = R_{72} = 3\rho_{45}, \tag{3.152}$$

$$R_{03} = \rho_{11} - \rho_{22} + \rho_{33} - \rho_{44} + \rho_{55} - \rho_{66}, \tag{3.153}$$

$$R_{30} = \frac{3}{2}\left[\rho_{11} + \rho_{22} - \rho_{33} - \rho_{44}\right], \tag{3.154}$$

$$R_{33} = \frac{3}{2}\left[\rho_{11} - \rho_{22} - \rho_{33} + \rho_{44}\right], \tag{3.155}$$

$$R_{80} = \frac{\sqrt{3}}{2}\left[\rho_{11} + \rho_{22} + \rho_{33} + \rho_{44} - 2\rho_{55} - 2\rho_{66}\right], \tag{3.156}$$

$$R_{83} = \frac{\sqrt{3}}{2}\left[\rho_{11} - \rho_{22} + \rho_{33} - \rho_{44} - 2\rho_{55} + 2\rho_{66}\right]. \tag{3.157}$$

Using the expression (3.140), the reduced density operator ρ_B of the state $\rho_{3\otimes 2}$ (2.70) is given by

$$\rho_B = \frac{1}{2}\begin{pmatrix} R_{00} + R_{03} & 0 \\ 0 & R_{00} - R_{03} \end{pmatrix}. \tag{3.158}$$

Then, using an auxiliary system B', the symmetric two-qubit purification of the reduced density operator ρ_B (3.158) reads as follows.

$$|v_{B'B}\rangle = \sqrt{\frac{(R_{00} + R_{03})}{2}}\,|00\rangle + \sqrt{\frac{(R_{00} - R_{03})}{2}}\,|11\rangle, \tag{3.159}$$

and from (3.141), one has

$$\rho_{B'B} = \frac{1}{2}\begin{pmatrix} (R_{00} + R_{03}) & 0 & 0 & \sqrt{(R_{00}^2 - R_{03}^2)} \\ 0 & 0 & 0 & 0 \\ 0 & 0 & 0 & 0 \\ \sqrt{(R_{00}^2 - R_{03}^2)} & 0 & 0 & (R_{00} - R_{03}) \end{pmatrix} = \frac{1}{4}\sum_{\alpha=0}^{3}\sum_{\beta=0}^{3}\mathcal{T}_{\alpha\beta}\sigma^{\alpha}\otimes\sigma^{\beta}, \tag{3.160}$$

where the non-vanishing correlation matrix components $\mathcal{T}_{\alpha\beta}$ are expressed in terms of the tensor correlation components $R_{\alpha\beta}$ as

$$\mathcal{T}_{00} = \mathcal{T}_{33} = R_{00} = 1, \quad \mathcal{T}_{03} = \mathcal{T}_{30} = R_{03}, \quad \mathcal{T}_{11} = \mathcal{T}_{22} = \sqrt{1 - R_{03}^2}. \tag{3.161}$$

Thus, the matrix $\mathbf{L}$ (3.147) associated with the state $\rho_{3\otimes 2}$ (2.70) writes as

$$L = \frac{2}{3}\begin{pmatrix} \frac{R_{11}}{\sqrt{1-R_{03}^2}} & 0 & 0 & 0 & 0 & \frac{R_{61}}{\sqrt{1-R_{03}^2}} & 0 & 0 \\ 0 & \frac{R_{11}}{\sqrt{1-R_{03}^2}} & 0 & 0 & 0 & 0 & \frac{R_{61}}{\sqrt{1-R_{03}^2}} & 0 \\ 0 & 0 & \frac{R_{33}-R_{03}R_{30}}{1-R_{03}^2} & 0 & 0 & 0 & 0 & \frac{R_{83}-R_{03}R_{80}}{1-R_{03}^2} \end{pmatrix}. \tag{3.162}$$

The associated eigenvalues of the matrix $L^T L$ are given as

$$\lambda_1 = \lambda_3 = \frac{4}{9}\left(\frac{R_{11}^2 + R_{61}^2}{1 - R_{03}^2}\right), \tag{3.163}$$

and

$$\lambda_2 = \frac{4}{9}\left[\frac{\left(R_{33} - R_{03}R_{30}\right)^2 + \left(R_{83} - R_{03}R_{80}\right)^2}{\left(1 - R_{03}^2\right)^2}\right], \tag{3.164}$$

Hence, the linear-entropy based classical correlation (3.113) for the qutrit-qubit state under consideration $\rho_{3\otimes 2}$ (2.70) is provided by

$$\mathcal{J}_{2B}\left(\rho_{3\otimes 2}\right) = \frac{4}{9} S_2(\rho_B) \max\left\{\lambda_1, \lambda_2\right\}, \tag{3.165}$$

with $S_2(\rho_B) = 2\left(1 - (\rho_{66} + \rho_{22} + \rho_{44})^2 - (\rho_{11} + \rho_{55} + \rho_{33})^2\right)$. Therfore, the corresponding expression of the quantum discord (3.148) is obtained as

$$\mathcal{Q}_{2B}\left(\rho_{3\otimes 2}\right) = -\sum_{i=1}^{3} \zeta_i \log_2 \zeta_i - \sum_{j=\pm} \xi_j \log_2 \xi_j + \sum_{k=1}^{6} \mu_k \log_2 \mu_k - \mathcal{J}_2\left(\rho\right), \tag{3.166}$$

where ζ_i (resp, ξ_j) denotes the eigenvalues of the density matrix ρ_A(resp, ρ_B). They are given as

$$\zeta_1 = \rho_{11} + \rho_{22}, \quad \zeta_2 = \rho_{55} + \rho_{66}, \quad \zeta_3 = \rho_{33} + \rho_{44}, \tag{3.167}$$

$$\xi_1 = \rho_{11} + \rho_{33} + \rho_{55}, \tag{3.168}$$

$$\xi_1 = \rho_{66} + \rho_{44} + \rho_{22}, \tag{3.169}$$

and the non-zero eigenvalues μ_k of the density matrix $\rho_{3\otimes 2}$ (2.70) are

$$\mu_{1,2} = \rho_{11}(\rho_{66}), \tag{3.170}$$

$$\mu_{3,4} = \frac{1}{2}\left[(\rho_{22} + \rho_{33}) \pm \sqrt{(\rho_{22} - \rho_{33})^2 + 4|\rho_{23}|^2}\right], \tag{3.171}$$

$$\mu_{5,6} = \frac{1}{2}\left[(\rho_{55} + \rho_{44}) \pm \sqrt{(\rho_{55} - \rho_{44})^2 + 4|\rho_{45}|^2}\right]. \tag{3.172}$$

6 Measurement induced disturbance

Another quantum correlation metric considered is the measurement-induced disturbance (MID). This measure was proposed by Luo in Ref. [40] to find the level of quantumness of correlations between sub-systems within a given bipartite system. This method rely upon the notion that a local state remains undisturbed by classical measurements, and the degree of quantumness in a state is related to how much the state under scrutiny changes after local measurements are performed. In this respect, this quantifier is similar in spirit but not identical to the original quantum discord. As we have seen in the definition of QD (see Eq.(3.8)), the maximization procedure over local measurements are made on one sub-system of the global system. For this metric, the local measurements are taken on both sub-systems. Assume $\{\Pi_i^A\}(\{\Pi_j^B\})$ are complete projective measurements, namely $\Pi_i\Pi_j = \delta_{ij}$ and $\sum_i \Pi_i = 1$, consisting of 1-directional orthogonal projections on subsystem $A(B)$. Accordingly, the state ρ_{AB} after measurement will have the following form

$$\Pi(\rho_{AB}) = \sum_{ij} (\Pi_i^A \otimes \Pi_j^B)\rho_{AB}(\Pi_i^A \otimes \Pi_j^B). \tag{3.173}$$

We note that if $\Pi(\rho_{AB})$ remains unchanged and satisfies the condition $\Pi(\rho_{AB}) = \rho_{AB}$, then the state ρ_{AB} can be considered as a classical state. This is because it remains unperturbed with respect to the local measurement. Unless ρ_{AB} definitely accounts for being a quantum state possessing quantum correlations. Moreover, the set of measurements have been shown that

preserve the reduced density matrices is the same as the spectral resolutions of the marginal state, expressed as: $\rho_A = \sum_i p_i^A \Pi_i^A$ and $\rho_B = \sum_i p_i^B \Pi_i^B$. Such measurement maintains the invariance of the marginal information and is in a certain sense the least perturbing. Hence, the measure of quantum correlations quantified by the MID is given by

$$\mathrm{MID}(\rho_{AB}) = \mathcal{I}(\rho_{AB}) - \mathcal{I}(\Pi(\rho_{AB})). \tag{3.174}$$

where $\mathcal{I}(.)$ is the quantum mutual information given in the Eq.(1.64). It is noteworthy that the MID reduces for pure states to the von Neumann entropy of the marginal states and disappears for the classically correlated states [40]. Moreover, one can easily compute this metric for arbitrary bipartite and multipartite quantum systems in contrast to the von Neumann entropy-based quantum discord [32,53,192]. This is, however, a much easier process compared with the complicated optimization procedure over parameters due to the local measurements and local unitaries [40, 193]. The corresponding drawback is that when the spectrum of the marginal states either ρ_A or ρ_B is degenerate, the MID measure is not necessarily well-defined, as the choice of local eigenbases is no longer unique. As in the previous measure of QCs, we take the qutrit-qubit state $\rho_{3\otimes 2}$ (2.70) as a concrete example to illustrate these results. To do this, we need first to determine the state (2.70) after measurement and the resulting marginal states of the state $\rho_{3\otimes 2}$ (2.70), namely ρ_A and ρ_B. Taking $\Pi_i^A = |i\rangle\langle i|$ $(i = 1, 0, -1)$ and $\Pi_j^B = |j\rangle\langle j|$ $(j = 1, 0)$, and using Eq.(3.173), one obtains

$$\Pi(\rho_{3\otimes 2}) = \begin{pmatrix} \rho_{11} & 0 & 0 & 0 & 0 & 0 \\ 0 & \rho_{22} & 0 & 0 & 0 & 0 \\ 0 & 0 & \rho_{33} & 0 & 0 & 0 \\ 0 & 0 & 0 & \rho_{44} & 0 & 0 \\ 0 & 0 & 0 & 0 & \rho_{55} & 0 \\ 0 & 0 & 0 & 0 & 0 & \rho_{66}^{-} \end{pmatrix}, \tag{3.175}$$

and correspondingly

$$\Pi(\rho_A) = \rho_A = \begin{pmatrix} \rho_{11} + \rho_{22} & 0 & 0 \\ 0 & \rho_{33} + \rho_{4,4} & 0 \\ 0 & 0 & \rho_{66} + \rho_{55} \end{pmatrix}, \tag{3.176}$$

$$\Pi(\rho_B) = \rho_B = \begin{pmatrix} \rho_{11} + \rho_{33} + \rho_{55} & 0 \\ 0 & \rho_{66} + \rho_{44} + \rho_{22} \end{pmatrix}. \tag{3.177}$$

According to the expression (3.174) and (3.175), the MID for the state $\rho_{3\otimes 2}$ (2.70) takes the following from

$$\begin{aligned} \mathrm{MID}(\rho_{3\otimes 2}) &= S(\Pi(\rho_{3\otimes 2})) - S(\rho_{3\otimes 2}) \\ &= \sum_{k=1}^{6} v_k \log_2 v_k - \sum_{k=1}^{6} \mu_k \log_2 \mu_k, \end{aligned} \tag{3.178}$$

with μ_k are the non-vanishing eigenvalues of the state $\rho_{3\otimes 2}$. They are read as

$$\mu_1 = \rho_{11}, \qquad \mu_2 = \rho_{66}, \tag{3.179}$$

$$\mu_{3,4} = \frac{1}{2}\left[(\rho_{22} + \rho_{33}) \pm \sqrt{(\rho_{22} - \rho_{33})^2 + 4|\rho_{24}|^2}\right], \tag{3.180}$$

$$\mu_{5,6} = \frac{1}{2}\left[(\rho_{44} + \rho_{55}) \pm \sqrt{(\rho_{44} - \rho_{55})^2 + 4|\rho_{24}|^2}\right]. \tag{3.181}$$

Analogously, the non-zero eigenvalues v_k of the state $\Pi(\rho_{3\otimes 2})$ are given as

$$v_i = \sum_{i=1}^{6} \rho_{ii}. \tag{3.182}$$

7 Conclusion

In quantum information, non-classical correlations including quantum entanglement, are crucial resources for improving information processing implementations beyond their classical counterparts. It is necessary to emphasize that the expressions of quantum correlation measures are based on bipartite systems. In this sense, we are interested in quantifying quantum correlations of bipartite systems that are the most used in quantum information processing. However, there are various measures of quantum correlations, each capturing different aspects of these correlations, making it challenging to compare them. The choice of measure can depend on the specific task, and different measures can be more or less useful for different applications. Therefore, the study of quantum correlations in a bipartite system is an important area of quantum information research.

In this chapter, we have mainly discussed quantum discord as a reliable metric of non-classical correlations, allowing the classification of states according to their degrees of entanglement. With this inspiration, we derived the analytical expression for the entropic quantum discord, as well as the geometric variants of quantum discord, using the Hilbert-Schmidt distance and Schatten 1-norm for some particular quantum states. Due to the complexity of optimizing this function, we have studied another reliable method for evaluating the entopic quantum discord based on linear entropy for arbitrary qudit-qubit quantum systems. However, a fully rigorous algorithm for calculating quantum discord for an arbitrary bipartite quantum system is still lacking. In this regard, we will examine in detail in the next chapter some discord-like measures of non-classical correlations and their application in quantum teleportation.

CHAPTER 4

RETHINKING QUANTUM CORRELATIONS AND THE POTENTIAL OF QUANTUM TELEPORTATION

Non-classical correlation is an essential tool for implementing quantum protocols, as it offers several advantages over classical information technology [5]. To enable quantum information processing, a quantum system with non-classical correlations is a necessary requirement. Characterizing and quantifying non-classical correlations beyond entanglement in bipartite and multipartite quantum systems have attracted attention in various applications of quantum information science [27, 32, 171]. To understand the role of non-classical correlations in quantum information processing, several quantum correlation witnesses have been investigated, including quantum discord (QD) [23, 24]. This quantity can capture all the quantumness of correlations that exist in various kinds of quantum systems more effectively than quantum entanglement. Despite many efforts by the scientific society, a general analytical algorithm for computing this function is only possible for some specific classes of qubit-qubit states, and the situation is somewhat complex specifically for the case of general quantum states [33–35]. The reason behind this is the optimization procedure on all local generalized measurements [30, 31]. The difficulty in calculating this function led to the introduction of an alternative approach of QD, known as geometric quantum discord [36]. It is determined as the shortest distance between the state under study and the set of zero-discord states [36]. From the analytical point of view, calculating this geometric variant evolves a minimization process much simpler than entropic quantum discord. Although its advantage, this metric cannot be a suitable indicator for estimating non-classical correlations [172].

Nevertheless, a local measurement made on one part of a composite system can disturb the entire system and thus induces uncertainty. This finding resulted in the investigation of the local quantum uncertainty (LQU) and uncertainty-induced non-locality (UIN) as faithful tools to estimate the amount of non-classical correlations in bipartite and multipartite quantum systems [41, 42]. These prominent discord-like correlation measures are based on the concept of Wigner Yanase skew information (WYSI) [194, 195]. Indeed, the LQU is employed to quantify the minimum skew information achievable in a given quantum state and a local non-commuting observable, while UIN serves to assess the maximal skew information between a given quantum state and a local commuting observable. These two related WYSI quantifiers, namely LQU and UIN, are designed to be easier to compute than the original quantum discord. For an arbitrary qubit-qudit system, the closed analytical formulae of LQU [196] and UIN [42] have been derived. Moreover, they meet all the requirements needed for a proper indicator of quantum correlations

[41].

The Wigner-Yanase skew information is closely connected to the notion of quantum coherence [197, 198]. The latter arises from quantum state superposition and it is a fundamental concept in quantum information processing [199]. Quantum coherence is widely used as a crucial resource for quantum technology [200, 201], with relevant applications including quantum optics [199], quantum information science [202], thermodynamics [203] and so on [204, 205]. Moreover, it can be linked to the concept of quantum entanglement [206], entropic uncertainty relations [207, 208], and discord-like correlations [44, 68]. Based on this connection, researchers have proposed a variety of quantum coherence measures, and their properties have been extensively investigated over the years [44, 198]. In this respect, Baumgratz *et al.* [198] formulated a rigorous resource framework for quantifying quantum coherence using the relative entropy of coherence and the l_1-norm quantum coherence as proper quantifiers that are easy to evaluate analytically. Hu *et al.* [44] examined the relationship between discord-like quantum correlations and quantum coherence measures for bipartite and multipartite systems as well in various settings. They reviewed also the resource theory about these correlations and coherence, which are defined based on different distance measures of states.

Surprisingly, the LQU is also closely connected to the concept of quantum Fisher Information (QFI). This connection provides a crucial relation between quantum information theory and quantum estimation theory [195, 209]. Besides, the QFI is a measure of the amount of information that can be extracted from a quantum state about a certain relevant parameter and it is also a measure of the sensitivity of a quantum state to changes in that parameter. It has been also argued that the QFI offers a measure to quantify and characterize the entanglement between the components of multipartite quantum systems [210]. On the other hand, the LQFI is considered as a promising approach to understanding the role of non-classical correlations other than entanglement in enhancing the accuracy and effectiveness of quantum metrology protocols and understanding the role of non-classical correlations in quantum information processing tasks [43, 211, 212]. Mathematically, it is determined as the maximum amount of QFI that can be achieved via employing local measurements on one sub-system of the composite system. Indeed, the evaluation of LQFI can be carried out by optimizing on all the observables of a part of the whole composite system [211, 212]. Since both functions namely, LQU and LQFI, depend on the notion of quantum uncertainty, thus, the LQFI can be used as good non-classical correlations metrics that meet all the requirements required to be a reliable measure of quantum correlations [213]. Overall, the connections between the Wigner-Yanase skew information, quantum coherence, and related concepts have led to a wealth of research on this important topic.

It is commonly accepted that non-classical correlations including quantum entanglement are widely recognized as a crucial resource for implementing various quantum protocols in quantum information science. These protocols include quantum cryptography [107], quantum sensing [49], quantum states merging [214] and quantum teleportation [45, 46, 68]. The latter will be also the subject of interest in this chapter. Quantum teleportation, first proposed by Bennett *et al.* in 1993 [45], allows for the transfer of a quantum state from one particle to another without physically moving the particle itself. Over the years, this concept has been experimentally demonstrated in various settings [57, 59, 215]. Typically, these experiments involve using two entangled photons created through parametric down conversion to form the quantum channel. The polarization state of one of the photons is then teleported from one place to another. The use of quantum teleportation has great potential in quantum communication, where it can be used to transmit quantum cryptographic keys securely [216]. Recently, researchers have explored the use of quantum teleportation in quantum computing, where it can be used to transfer quantum states between qubits. The success of quantum teleportation experiments has led to significant progress in the field of quantum information processing. For instance,

researchers have demonstrated the successful teleportation of complex quantum states, such as multi-photon entangled states, which has the potential to lead to advances in quantum information processing and quantum computing [217]. In 2017, long-distance quantum teleportation was demonstrated with the successful teleportation of a photon from a ground-based telescope in Tibet to a satellite in orbit, over a distance of more than $1,400$ kilometers above the Earth's surface [218]. All these mentioned applications need a strong theoretical background, which is why many attempts have been made to develop rigorous definitions of an entangled state, separability criteria [6], various entanglement measures [153] and several quantum correlations metrics [23,32,36,197].

In this chapter, we will explore the concept of quantum uncertainty, discussing its definition and properties. Inspired by this concept, we will introduce the LQU as a good indicator of quantum correlations. At the same step, we provide its closed analytical expression for an arbitrary qubit–qudit quantum system. We will also investigate how this metric can be extended to multipartite quantum systems. Moreover, the analytical presentation of this non-classical correlation measure is explicitly given in the particular case of qubit-qutrit as well as three-qubit quantum systems. In addition, we will study another faithful indicator of quantum correlations related to the notion of the skew information known as uncertainty-induced non-locality, where we provide a general algorithm for computing it for general bipartite qubit-qudit quantum systems. We also discuss the notion of quantum coherence in terms of the l_1-norm, as well as the quantum Fisher information and its role in quantum metrology and quantum correlations. Moving on, we will study quantum teleportation as a direct application of quantum correlations, where we discuss the standard protocol and its implementation. Specifically, we will focus on how quantum entanglement plays a crucial role in the successful implementation of quantum teleportation.

1 Skew information

Scientists investigate the universe by performing measurements and predicting their outcomes. The error bars in the classical regime are mainly due to technological limits. Therefore, the measurements of a given pair of observables can be made with arbitrary precision. However, this is not always possible in the quantum regime due to the fundamental principle of quantum physics, which states that two incompatible observables cannot be simultaneously measured with arbitrary accuracy, even with a flawless measuring device [219, 220]. Moreover, measuring a quantum system differs significantly from measuring a classical system since not only the result obtained is uncertain, but even the system's state is modified over all the process. The point is to identify the result of this measurement more accurately and the idea of accuracy is directly linked to the uncertainty associated with the result of this measurement. The uncertainty relation gives the statistical nature of the errors in this kind of measurement.

1.1 Definition

In standard practice and within the framework of quantum mechanical formalism, the total uncertainty resulting from the action of a single observable K with a state ρ is generally quantified by a quantity called the variance. It is provided as [221]

$$\mathrm{Var}(\rho, K) \equiv \mathrm{Tr}\left(\rho K_0^2\right) = \mathrm{Tr}\left(\rho K^2\right) - \mathrm{Tr}\left(\rho K\right)^2, \tag{4.1}$$

with $K_0 = K - \mathrm{Tr}\left(\rho K\right)$. In particular, in the case of pure states such that: $\rho = |\psi\rangle\langle\psi|$, the expression (4.1) reduces to

$$\mathrm{Var}(|\psi\rangle\langle\psi|, K) = \langle\psi| K^2 |\psi\rangle - \langle\psi| K |\psi\rangle^2. \tag{4.2}$$

For pure states, the variance-based description of uncertainty is well-suited. However, the scenario gets more complicated and even more subtle for mixed states since the total uncertainty incorporates both the classical ignorances resulting from the mixedness of state and a genuinely quantum portion due to the non-commutativity between the state under scrutiny and the measured observable. Thus, the variance (4.1) combines both classical and quantum uncertainty, i.e., $\mathrm{Var}(\rho, K) \equiv \mathrm{Var}_q(\rho, K) + \mathrm{Var}_c(\rho, K)$. Moroever, the degree of uncertainty can be determined using several methods, such as ones based on entropic quantities [219, 222]. In the theory of quantum information, this class of measures is commonly employed as indicators of uncertainty. However, these quantifiers are always affected by state mixedness, which makes this kind of measure inefficient and restricted.

In the field of quantum information theory, it is indeed extremely important to discriminate quantum contributions from the classical ones. To isolate the quantum contribution of the variance (4.1), Wigner and Yanase established the formalism of the so-called skew information as an effective measure of this uncertainty [194, 195]. It is given as

$$I(\rho, K) = -\frac{1}{2}\mathrm{Tr}\left\{[\sqrt{\rho}, K]^2\right\}, \tag{4.3}$$

in which the brackets $[.,.]$ in the last expression represent the commutator, while $I(\rho, K)$ refers to the skew information associated with the density operator ρ. Unlike the variance (4.1), the Wigner–Yanase skew information (WYSI) is unaffected by classical mixing and reduces to the variance when the state ρ is pure. Moreover, it vanishes only when the state under scrutiny ρ and K commute. The WYSI determines the non-commutativity degree between the quantum state ρ and an observable K, which can be regarded as a Hamiltonian or any other conserved quantity. Besides, it provides an alternative metric of the information content of the quantum state ρ with respect to the non-commutative observables with the conserved quantity K. In particular, it represents the amount of information encoded in the quantum state ρ that is not accessible by the measurement of observable K. Thus, the WYSI provided by Eq.(4.3) can be rewritten in a more concise form as

$$\begin{aligned}
I(\rho, K) &= -\frac{1}{2}\mathrm{Tr}\left\{(\sqrt{\rho}K - K\sqrt{\rho})^2\right\} \\
&= -\frac{1}{2}\mathrm{Tr}\left\{\sqrt{\rho}K\sqrt{\rho}K - \sqrt{\rho}K^2\sqrt{\rho} - K\rho K + K\sqrt{\rho}K\sqrt{\rho}\right\} \\
&= -\frac{1}{2}\left\{\mathrm{Tr}\left(\sqrt{\rho}K\sqrt{\rho}K\right) - \mathrm{Tr}\left(\sqrt{\rho}K^2\sqrt{\rho}\right) - \mathrm{Tr}\left(K\rho K\right) + \mathrm{Tr}\left(K\sqrt{\rho}K\sqrt{\rho}\right)\right\} \\
I(\rho, K) &= \mathrm{Tr}\left(\rho K^2\right) - \mathrm{Tr}\left(\sqrt{\rho}K\sqrt{\rho}K\right).
\end{aligned} \tag{4.4}$$

1.2 Skew information properties

As reported in Ref. [194], the following statements denote the main properties of the skew information:

- The skew information is a non-negative quantity, $I(\rho, K) \geq 0$, due to the minus sign in Eq.(4.3) and it reduces to the variance when the state ρ is pure, i.e.,

$$I(|\psi\rangle\langle\psi|, K) = \mathrm{Var}(|\psi\rangle\langle\psi|, K) = \langle\psi|K^2|\psi\rangle - \langle\psi|K|\psi\rangle^2. \tag{4.5}$$

- For mixed states, $I(\rho, K)$ is always a small function compared to the variance of the

observable K. We have

$$\begin{aligned} I(\rho,K) &= \mathrm{Tr}\left(\rho K^2\right) - \mathrm{Tr}\left(\sqrt{\rho}K\sqrt{\rho}K\right) \\ &\leq \mathrm{Tr}\left(\rho K^2\right) - \mathrm{Tr}\left(\rho K\right)^2 \\ &\equiv \mathrm{Var}(\rho,K). \end{aligned} \tag{4.6}$$

- $I(\rho,K)$ represents a convex function with respect to the quantum state ρ, meaning that it does not increase under classical mixing. That is to say

$$I(\textstyle\sum_i \lambda_i\rho_i,K) \leq \sum_i \lambda_i I(\rho_i,K), \tag{4.7}$$

where λ_i is the probability distribution satisfying the conditions $\sum_i \lambda_i = 1$ and $0 \leq \lambda_i \leq 1$, for any quantum states ρ_i. In contrast, the variance $\mathrm{Var}(\rho,K)$ is a concave quantity in the state ρ.

- It remains unchanged under the action of unitary operations. This holds true only when U commutes with the measured observable K, i.e., $[U,K]=0$. In such cases, we shall have

$$UKU^{-1} = K, \qquad \sqrt{U\rho U^{-1}} = U\sqrt{\rho}U^{-1}. \tag{4.8}$$

Thus, we can show that:

$$\begin{aligned} I(U\rho U^{-1},UKU^{-1}) &= -\frac{1}{2}\mathrm{Tr}\left\{\left[\sqrt{U\rho U^{-1}},UKU^{-1}\right]^2\right\} \\ &= -\frac{1}{2}\mathrm{Tr}\left\{\left[U\sqrt{\rho}U^{-1},UKU^{-1}\right]^2\right\} \\ &= -\frac{1}{2}\mathrm{Tr}\left\{U\left[\sqrt{\rho},K\right]^2U^{-1}\right\} \\ &= -\frac{1}{2}\mathrm{Tr}\left\{\left[\sqrt{\rho},K\right]^2\right\} \\ I(U\rho U^{-1},UKU^{-1}) &= I(\rho,K). \end{aligned} \tag{4.9}$$

- Consider a bipartite state ρ^{AB} defined in the Hilbert space $\mathcal{H}_A \otimes \mathcal{H}_B$ and ρ^A being the reduced density matrix associated with subsystem A. The skew information between the density matrix $\rho^{AB}$and the reduced density matrix ρ^A satisfies the following relation:

$$I(\rho^{AB},K_A\otimes I_B) \geq I(\rho^A,K_A), \tag{4.10}$$

for any local observables K_A that acts on the Hilbert space $\mathcal{H}_A$.

- It is an additive quantity, that is, the amount of information content of a quantum system consisting of two independent parts is equivalent to the sum of the information of the parts.

2 Local quantum uncertainty for arbitrary qubit-qudit systems

Giromali and co-workers recently introduced local quantum uncertainty (LQU, in short) [41]. The latter is considered a promising and faithful discord-like metric for non-classical correlations in any given bipartite non-local states. The reason behind this is the easy computation in comparison and reliability. This metric measures the smallest amount of quantum uncertainty

produced in a quantum state. Based on the notion of Winger-Yanase skew information [194], the LQU quantifies the minimum skew information attainable in the considered quantum state via performing classical von Neumann measurements on a part of the global quantum state. More precisely, let ρ^{AB} denote a state of a bipartite quantum system and $K^{\Lambda} = K_A^{\Lambda} \otimes I_B$ stands for a classical observable, while K_A^{Λ} being a Hermitian operator performing on sub-system A with spectrum Λ. We assume Λ to be non-degenerate, which refers to maximally informative observables on part A. Moreover, I_B refers to the identity matrix that operates on sub-system B. Then, the LQU with respect to sub-system A and optimized on all local observables on part A with non-degenerate spectrum Λ is given by

$$\mathcal{U}_A^{\Lambda}\left(\rho^{AB}\right) = \min_{K^{\Lambda}} I(\rho^{AB}, K^{\Lambda}). \tag{4.11}$$

As reported in Ref. [41], LQU satisfies all the physical requirements for a *"bona fide"* metric of non-classical correlations stated in Sec.2. For instance, it reduces to a monotonic entanglement defined by the marginal entropy of sub-system A, for any bipartite pure states. It becomes zero when the observable and the considered quantum state commute, reflecting the non-existence of any kind of non-classical correlations between the constituents of the quantum bipartite system. Moreover, it remains consistent under the influence of any local unitary operations and does not becoems increase when any classical reversible operations is performed on the non-measured sub-system B. Besides, LQU is inherently an asymmetric function, i.e., $\mathcal{U}_A^{\Lambda}\left(\rho^{AB}\right) \neq \mathcal{U}_B^{\Lambda}\left(\rho^{AB}\right)$, concerning the sub-system exchange since it is dependent on the part on which the local measurements are made. To simplify notation, one can use the simple form $\mathcal{U}\left(\rho^{AB}\right)$ instead of $\mathcal{U}_A^{\Lambda}\left(\rho^{AB}\right)$. Therfore, the local quantum uncertainty provides a reliable discord-type measure, that is, vanishes for all zero-discord (classical-quantum correlated) states.

The expression (4.11) describes a set of Λ-dependent parameters that minimize the skew information for each equivalence class of local Λ-spectral observables. In order to determine the minimum in Eq.(4.11), an essential requirement must be met for optimizing observables on part A. It is necessary for these observables to have a fixed, non-degenerate spectrum. In fact, observables with this spectrum that operate on sub-system A can be parameterized as follows:

$$K_A = V_A \Lambda V_A^{\dagger}, \tag{4.12}$$

where V_A indicates the measurement basis on the special unitary group on part A that can be arbitrarily modified. The non-degenerate fixed-spectrum observables K_A on the first sub-system, i.e., qubit, can be parametrized by choosing $K_A = V_A \sigma_{zA} V_A^{\dagger} = \overrightarrow{n}\,\overrightarrow{\sigma}_A$, where $\|\overrightarrow{n}\| = 1$ and σ_i $(i = x, y, z)$ are the Pauli matrices, describing also the generators of $SU(2)$ group. This is accurate if we focus our analysis on the case of hybrid bipartite qubit-qudit $(2 \otimes d)$ quantum systems. Thus, we remove the superscript Λ for the sake of brevity in the expression (4.11). Consequently, the local quantum uncertainty is normalized to the unity for maximally entangled pure states by choosing this spectrum. In this respect, the expression of the LQU (4.11) becomes

$$\begin{aligned}
\mathcal{U}\left(\rho^{AB}\right) &= \min_{\overrightarrow{n}} I(\rho^{AB}, \overrightarrow{n}\,\overrightarrow{\sigma}_A \otimes I_d) \\
&= \min_{\overrightarrow{n}} \textstyle\sum_{ij} n_i n_j \left[\mathrm{Tr}\left\{\rho^{AB}\sigma_i\sigma_j - \sqrt{\rho^{AB}}\,(\sigma_i \otimes I_d)\sqrt{\rho^{AB}}\,(\sigma_j \otimes I_d)\right\}\right] \\
&= 1 - \min \textstyle\sum_{ij} n_i n_j \left[\mathrm{Tr}\left\{\sqrt{\rho^{AB}}\,(\sigma_i \otimes I_d)\sqrt{\rho^{AB}}\,(\sigma_j \otimes I_d)\right\}\right] \\
&= 1 - \max\left[\overrightarrow{n}\,\mathcal{W}\,\overrightarrow{n}\dagger\right].
\end{aligned} \tag{4.13}$$

Here, $\mathcal{W}$ refers to the 3×3-symmetric matrix whose components are given as the following

$$\mathcal{W} = [w_{ij}] = \mathrm{Tr}\left\{\sqrt{\rho^{AB}}\,(\sigma_i \otimes I_d)\sqrt{\rho^{AB}}\,(\sigma_j \otimes I_d)\right\}, \tag{4.14}$$

where $\sigma_1 \equiv \sigma_x$, $\sigma_2 \equiv \sigma_y$, $\sigma_3 \equiv \sigma_z$, and I_d denotes the identity matrix for the qudit sub-system. Nevertheless, in order to minimize the skew information derived in Eq.(4.3), it is required to maximize the amount of $\overrightarrow{n} \dagger \mathcal{W}\overrightarrow{n}$ in the expression (4.13) on all unit vectors $\overrightarrow{n}$. In this inspiration, the largest value on all unit vectors $\overrightarrow{n}$ coincides with the highest eigenvalues of the matrix $\mathcal{W}$ (4.14). Accordingly, the closed expression of the local quantum uncertainty, which quantifies the amount of non-classical correlation for any given bipartite $2 \otimes d$ quantum state, gives the following

$$\mathcal{U}\left(\rho^{AB}\right) = 1 - \lambda_{\max}\left(\mathcal{W}\right), \tag{4.15}$$

where the quantity $\lambda_{\max}\left(\mathcal{W}\right)$ in Eq.(4.15) designs the greatest eigenvalue of $\mathcal{W}$ (4.14). Unlike the von Neumann entropy-quantum discord, it is clear that by possessing the matrix $\mathcal{W}$, we can straightforwardly and efficiently compute the local quantum uncertainty for hybrid qubit-qudit quantum systems [69]. This is a relatively simple procedure when compared to the complex optimizations over parameters corresponding to the classical measurements [26,32]. It is crucial to state that for some quantum states, QD and LQU capture the same amount of quantum correlations, although they are two different metrics for other states [224]. Moreover, in the case of pure quantum states, $\rho^{AB} = |\psi\rangle\langle\psi|$, LQU coincides with the linear entropy $S_2\left(\rho\right)$ of the marginal state of sub-system A, i.e., $\mathcal{U}\left(|\psi\rangle\langle\psi|\right) = S_2\left(\rho^{AB}\right) = 2\left[1 - \mathrm{Tr}\left\{\rho_A^2\right\}\right]$. This intriguing coincidence arises exclusively for hybrid qubit-qudit quantum systems. However, the expression of LQU for general qubit-qudit quantum systems, as stated in Eq.(4.15), also holds true for the case of arbitrary qudit-qubit $(d \otimes 2)$ quantum systems, provided that the local measurements are carried out on part B (qubit) [225]. Another interesting point to discuss here is the fact that LQU has a geometrical understanding in the case of Hellinger distance $\mathcal{D}_H$, although this only holds to any given $2 \otimes d$ quantum system. This can be geometrically interpreted as the smallest square of Hellinger distance between the state under scrutiny and its least disturbed counterpart after performing a local root-of-unity unitary operation on sub-system A (qubit) [41, 226]. Specifically, the squared Hellinger distance between the states ρ and χ is given by [226]

$$\mathcal{D}_H^2\left(\rho,\chi\right) = \frac{1}{2}\mathrm{Tr}\left\{\left(\sqrt{\rho} - \sqrt{\chi}\right)^2\right\} = 1 - \mathrm{Tr}\left\{\sqrt{\rho\chi}\right\}. \tag{4.16}$$

Thus, LQU is re-expressed in terms of $\mathcal{D}_H$ as follows

$$\begin{aligned}\mathcal{U}\left(\rho^{AB}, K_A\right) &= 1 - \mathrm{Tr}\left\{\sqrt{\rho^{AB}}K_A\sqrt{\rho^{AB}}K_A\right\} = 1 - \mathrm{Tr}\left\{\sqrt{\rho^{AB}}\sqrt{K_A\rho^{AB}K_A}\right\} \\ &= \mathcal{D}_H^2\left(\rho^{AB}, K_A\rho^{AB}K_A\right), \end{aligned} \tag{4.17}$$

where $K_A = \overrightarrow{n}\,\overrightarrow{\sigma}_A$ represents root of unity operation on sub-system A, which means $K_A f\left(\rho^{AB}\right) K_A = f(K_A\rho^{AB}K_A)$ for an arbitrary function f. Moreover, as mentioned in Ref. [41], the trace distance discord (TDD) $\mathcal{Q}_{\mathcal{D}_1(\rho_{AB},\rho_{cq})}(\rho^{AB})$ defined in Eq.(3.93) is always greater or equal to the square Hellinger distance, i.e., $\mathcal{Q}_{\mathcal{D}_1(\rho_{AB},\rho_{cq})}(\rho^{AB}) \geq \mathcal{D}_H^2\left(\rho^{AB}\right)$ [227]. Hence, one can conclude that the TDD is always greater or equal to the LQU. When the quantum system is described by the two-qubit X-state ρ_X (2.56), the non-vanishing elements of the 3×3 matrix $\mathcal{W}$ (4.14) can be expressed in terms of the Fano-Bloch components $R_{\alpha\beta}$ associated with the matrix ρ_X (2.56) as

$$\mathcal{W}_{11} = \left(\sqrt{\lambda_1}+\sqrt{\lambda_4}\right)\left(\sqrt{\lambda_2}+\sqrt{\lambda_3}\right)+\frac{1}{4}\frac{(R_{11}^2-R_{22}^2)+(R_{03}^2-R_{30}^2)}{\sqrt{\left(t_1+2\sqrt{d_1}\right)\left(t_2+2\sqrt{d_2}\right)}}, \tag{4.18}$$

$$\mathcal{W}_{22} = \left(\sqrt{\lambda_1}+\sqrt{\lambda_4}\right)\left(\sqrt{\lambda_2}+\sqrt{\lambda_3}\right)+\frac{1}{4}\frac{(R_{22}^2-R_{11}^2)+(R_{03}^2-R_{30}^2)}{\sqrt{\left(t_1+2\sqrt{d_1}\right)\left(t_2+2\sqrt{d_2}\right)}}, \tag{4.19}$$

$$\begin{aligned}\mathcal{W}_{33} &= \frac{1}{2}\left(\left(\sqrt{\lambda_1}+\sqrt{\lambda_4}\right)^2+\left(\sqrt{\lambda_2}+\sqrt{\lambda_3}\right)^2\right)+\\ &\quad\frac{1}{8}\left(\frac{(R_{03}+R_{30})^2-(R_{11}-R_{22})^2}{\left(t_1+2\sqrt{d_1}\right)}+\frac{(R_{03}-R_{30})^2-(R_{11}+R_{22})^2}{\left(t_2+2\sqrt{d_2}\right)}\right).\end{aligned} \tag{4.20}$$

with $R_{\alpha\beta}=\mathrm{Tr}\left(\rho_X\sigma^\alpha\otimes\sigma^\beta\right)$ are explicitly given in Eqs.(3.95a-3.95c). While $\lambda_i(i=1,...,4)$ represents the eigenvalues of the state ρ_X that can be re-expressed as

$$\lambda_1 = \frac{1}{2}t_1+\frac{1}{2}\sqrt{t_1^2-4d_1},\quad \lambda_2=\frac{1}{2}t_2+\frac{1}{2}\sqrt{t_2^2-4d_2}, \tag{4.21}$$

$$\lambda_3 = \frac{1}{2}t_2-\frac{1}{2}\sqrt{t_2^2-4d_2},\quad \lambda_4=\frac{1}{2}t_1-\frac{1}{2}\sqrt{t_1^2-4d_1}, \tag{4.22}$$

where

$$t_{1,2} = \frac{1}{2}\left(R_{00}\pm R_{03}\right), \tag{4.23}$$

$$d_{1,2} = \frac{1}{16}\left[\left(R_{00}\pm R_{33}\right)^2-\left(R_{30}\pm R_{03}\right)^2-\left(R_{11}\mp R_{22}\right)^2\right]. \tag{4.24}$$

Given that $\mathcal{W}_{12}=\mathcal{W}_{21}=\mathcal{W}_{23}=\mathcal{W}_{32}=\mathcal{W}_{13}=\mathcal{W}_{31}=0$, it is a simplest process to verify that the matrix $\mathcal{W}$ (4.14) in this situation becomes diagonal. This means that we can express its eigenvalues in terms of the diagonal elements $\mathcal{W}_{ii}$ $(i=1,2,3)$. Accordingly, the non-classical correlation in termd of LQU (4.15) can be expressed for state ρ_X (2.56) as

$$\mathcal{U}(\rho_X)=1-\max(\mathcal{W}_{11},\mathcal{W}_{22},\mathcal{W}_{33}). \tag{4.25}$$

It is worth noting that for the state ρ_X (2.56) with non-negative entries, we always have $R_{11}\geq R_{22}$, which implies that $\mathcal{W}_{11}>\mathcal{W}_{22}$. In this case, the local quantum uncertainty (4.25) reduces simply to

$$\mathcal{U}(\rho_X)=1-\max(\mathcal{W}_{11},\mathcal{W}_{33}). \tag{4.26}$$

Therefore, in order to determine the quantum correlations using LQU, we only need to consider separately the following situations: $\mathcal{W}_{11}\geq\mathcal{W}_{33}$ or $\mathcal{W}_{11}\leq\mathcal{W}_{33}$.

Another concrete example to illustrate these results, let us consider a qutrit-qubit quantum state $\rho_{2\otimes3}$ written in the standard basis $\{|ij\rangle,\ i=0,1 \text{ and } j=-1,0,1\}$ as follows [69]

$$\rho_{2\otimes3}=\begin{pmatrix}\rho_{11}&0&0&0&0&0\\0&\rho_{22}&0&\rho_{24}&0&0\\0&0&\rho_{33}&0&\rho_{35}&0\\0&\rho_{42}&0&\rho_{44}&0&0\\0&0&\rho_{53}&0&\rho_{55}&0\\0&0&0&0&0&\rho_{66}\end{pmatrix}. \tag{4.27}$$

In order to obtain derive a closed expression of the LQU (4.15), it is required to compute the eigenvalues of the matrix $\mathcal{W}$ (4.14). To do this, we need first to obtain the eigenvalues and the corresponding eigenvectors of the density matrix $\rho_{2\otimes 3}$ (4.27). They are given as

$$\begin{aligned}\lambda_{1,6} &= \frac{1}{2}(t_1 \pm \sqrt{{t_1}^2 - 4d_1}), \quad \lambda_{2,3} = \frac{1}{2}(t_2 \mp \sqrt{{t_2}^2 - 4d_2}),\\ \lambda_{4,5} &= \frac{1}{2}(t_3 \mp \sqrt{{t_3}^2 - 4d_3}),\end{aligned} \tag{4.28}$$

with t_i and d_i are

$$t_1 = \rho_{11} + \rho_{66}, \quad t_2 = \rho_{22} + \rho_{44}, \quad t_3 = \rho_{33} + \rho_{55}, \tag{4.29}$$

$$d_1 = \rho_{11}\rho_{66}, \quad d_2 = \rho_{22}\rho_{44} - \rho_{24}\rho_{42}, \quad d_3 = \rho_{33}\rho_{55} - \rho_{35}\rho_{53}, \tag{4.30}$$

and the corresponding eigenvectors are, respectively, provided by

$$|\lambda_1\rangle = |12\rangle, \quad |\lambda_{2,3}\rangle = \frac{1}{\sqrt{1 + |\mu_\pm|^2}}(\mu_\pm |02\rangle + |11\rangle), \tag{4.31}$$

$$|\lambda_{4,5}\rangle = \frac{1}{\sqrt{1 + |\eta_\pm|^2}}(\eta_\pm |01\rangle + |10\rangle), \quad |\lambda_6\rangle = |00\rangle, \tag{4.32}$$

where

$$\mu_\pm = \frac{1}{2\rho_{42}}(\rho_{22} - \rho_{44} \pm \sqrt{4|\rho_{24}|^2 + (\rho_{22} - \rho_{44})^2}), \tag{4.33}$$

$$\eta_\pm = \frac{1}{2\rho_{42}}(\rho_{33} - \rho_{55} \pm \sqrt{4|\rho_{35}|^2 + (\rho_{33} - \rho_{55})^2}). \tag{4.34}$$

Moreover, in terms of the related computational basis, the squared root density matrix $\rho_{2\otimes 3}$ (4.27) takes the following form

$$\sqrt{\rho_{2\otimes 3}} = \begin{pmatrix} \alpha_{11} & 0 & 0 & 0 & 0 & 0 \\ 0 & \alpha_{22} & 0 & \alpha_{24} & 0 & 0 \\ 0 & 0 & \alpha_{33} & 0 & 0 & 0 \\ 0 & \alpha_{42} & 0 & \alpha_{44} & 0 & 0 \\ 0 & 0 & 0 & 0 & \alpha_{55} & 0 \\ 0 & 0 & 0 & 0 & 0 & \alpha_{66} \end{pmatrix}, \tag{4.35}$$

where

$$\alpha_{11} = \frac{1}{2}(\sqrt{t_1 + 2\sqrt{d_1}} + \sqrt{t_1 - 2\sqrt{d_1}}), \tag{4.36}$$

$$\alpha_{66} = \frac{1}{2}(\sqrt{t_1 + 2\sqrt{d_1}} - \sqrt{t_1 - 2\sqrt{d_1}}), \tag{4.37}$$

$$\alpha_{22} = \frac{\rho_{22} + \sqrt{d_2}}{\sqrt{t_2 + 2\sqrt{d_2}}}, \quad \alpha_{24} = \frac{\rho_{24}}{\sqrt{t_2 + 2\sqrt{d_2}}}, \quad \alpha_{33} = \frac{\rho_{33} + \sqrt{d_3}}{\sqrt{t_3 + 2\sqrt{d_3}}}, \tag{4.38}$$

$$\alpha_{35} = \frac{\rho_{35}}{\sqrt{t_3 + 2\sqrt{d_3}}}, \quad \alpha_{42} = \frac{\rho_{42}}{\sqrt{t_2 + 2\sqrt{d_2}}}, \quad \alpha_{44} = \frac{\rho_{44} + \sqrt{d_2}}{\sqrt{t_2 + 2\sqrt{d_2}}}, \tag{4.39}$$

$$\alpha_{53} = \frac{\rho_{53}}{\sqrt{t_3 + 2\sqrt{d_3}}}, \quad \alpha_{55} = \frac{\rho_{55} + \sqrt{d_3}}{\sqrt{t_3 + 2\sqrt{d_3}}}. \tag{4.40}$$

Thus, the eigenvalues of the matrix $\mathcal{W}$ (4.14) are given as

$$\begin{aligned} \mathcal{W}_{11} &= \mathcal{W}_{22} = 2(\alpha_{11}\alpha_{44} + \alpha_{22}\alpha_{55} + \alpha_{33}\alpha_{66}), && (4.41) \\ \mathcal{W}_{33} &= \textstyle\sum_{i=1}^{6} \alpha_{ii}^2 - 2(\alpha_{24}\alpha_{42} + \alpha_{35}\alpha_{53}). && (4.42) \end{aligned}$$

Using the formula (4.15), the LQU quantifying the non-classical correlation in the system represented by the state $\rho_{2\otimes 3}$ (4.27) takes the following form

$$\mathcal{U}(\rho_{2\otimes 3}) = 1 - \max(\mathcal{W}_{11}, \mathcal{W}_{33}). \tag{4.43}$$

3 Local quantum uncertainty for multipartite quantum systems

In addition to the N-qubit negativity (see Sec.4), the local multi-particle quantum uncertainty is also viewed as a significant metric for capturing the strength of non-local correlations in multi-qubit quantum systems. However, deriving the LQU for mixed multi-qubit states is a challenging task, since it involves a complicated optimization process that is difficult to solve accurately. For this reason, Ali Mazhar proposed a generalization of the notion of LQU for multi-qubit systems [224]. This was achieved with zero technical consequences since one can always consider the multi-qubit system as a $2 \otimes d$ system, where $d = 2 \otimes 2 \otimes 2 \otimes 2 \otimes \cdots \otimes 2$ denotes the remaining $(N-1)$-qubit as a d-dimensional quantum system [79, 224]. A multi-qubit system exhibits a richer structure compared to a bipartite quantum system. It is possible that certain bipartitions display quantum correlations, although others may possess classical correlations. Hence, we perform the local measurements on each bipartition to investigate only the total non-classical correlation of the whole multi-qubit system. To do this, we assume an arbitrary density operator, denoted as ρ_N, which describes the N-qubit system. We apply local measurements for each qubit $(A, B, \cdots, N)$ with respect to all other qubits. We repeat the same algorithm for each bipartition, and according to the definition given in Eq.(4.14), one can derive the matrix components related to the N symmetric matrices, namely 3×3 symmetric matrices $\widetilde{\mathcal{W}}$. Indeed, we gained the following results [224]:

$$\begin{aligned} \widetilde{\mathcal{W}}^A &= \left(\widetilde{\mathcal{W}}\right)_{ij}^A = \mathrm{Tr}\Big(\sqrt{\rho_N}\,(\sigma_i \otimes I_2 \otimes I_2 \otimes ... \otimes I_2)\,\sqrt{\rho_N}\,(\sigma_j \otimes I_2 \otimes I_2 \otimes ... \otimes I_2)\Big), \\ \widetilde{\mathcal{W}}^B &= \left(\widetilde{\mathcal{W}}\right)_{ij}^B = \mathrm{Tr}\Big(\sqrt{\rho_N}\,(I_2 \otimes \sigma_i \otimes I_2 \otimes ... \otimes I_2)\,\sqrt{\rho_N}\,(I_2 \otimes \sigma_j \otimes I_2 \otimes ... \otimes I_2)\Big), \\ \widetilde{\mathcal{W}}^C &= \left(\widetilde{\mathcal{W}}\right)_{ij}^C = \mathrm{Tr}\Big(\sqrt{\rho_N}\,(I_2 \otimes I_2 \otimes \sigma_i \otimes .... \otimes I_2)\,\sqrt{\rho_N}\,(I_2 \otimes I_2 \otimes \sigma_j \otimes .... \otimes I_2)\Big), \\ &\vdots \\ &\vdots \\ \widetilde{\mathcal{W}}^N &= \left(\widetilde{\mathcal{W}}\right)_{ij}^N = \mathrm{Tr}\Big(\sqrt{\rho_N}\,(I_2 \otimes I_2 \otimes I_2 \otimes .... \otimes \sigma_i)\,\sqrt{\rho_N}\,(I_2 \otimes I_2 \otimes I_2 \otimes .... \otimes \sigma_j)\Big), \end{aligned} \tag{4.44}$$

where σ_i $(i = 0, x, y, z)$ denotes the Pauli matrices. The corresponding eigenvalues of the 3×3 symmetric matrices $\widetilde{\mathcal{W}}^i$ can be obtained via a straightforward calculation. Therefore, the LQU belonging to each bipartition turns out to be

$$
\begin{aligned}
\mathcal{U}_{A/BC\ldots N}\left(\rho_N\right) &= 1-\max\left\{Spectrum\,of\,\widetilde{\mathcal{W}}^{A}\right\},\\
\mathcal{U}_{B/AC\ldots N}\left(\rho_N\right) &= 1-\max\left\{Spectrum\,of\widetilde{\mathcal{W}}^{B}\right\},\\
\mathcal{U}_{C/BC\ldots N}\left(\rho_N\right) &= 1-\max\left\{Spectrum\,of\widetilde{\mathcal{W}}^{C}\right\},\\
&\vdots\\
&\vdots\\
\mathcal{U}_{N/BC\ldots N-1}\left(\rho_N\right) &= 1-\max\left\{Spectrum\,of\,\widetilde{\mathcal{W}}^{N}\right\}. \qquad (4.45)
\end{aligned}
$$

Finally, the LQU for the N-qubit system can be defined as the expectation value of the LQU for each bipartition. This gives

$$\mathcal{U}\left(\rho_N\right)=\frac{1}{N}\sum_{i=1}^{N}\mathcal{U}_{i/N_i}. \qquad (4.46)$$

Now, in order to verify our findings, we shall investigate a concrete paradigm consisting of a three-qubit system [79]. The density operator ρ describing the mentioned system is given in the computational basis $\{|000\rangle,\ |001\rangle,|010\rangle,|011\rangle,|100\rangle,|101\rangle,\ |110\rangle,|111\rangle\}$ as follows:

$$\rho=\begin{pmatrix}
\rho_{11} & 0 & 0 & 0 & 0 & 0 & 0 & 0\\
0 & \rho_{22} & \rho_{23} & 0 & \rho_{25} & 0 & 0 & 0\\
0 & \rho_{32} & \rho_{33} & 0 & \rho_{35} & 0 & 0 & 0\\
0 & 0 & 0 & \rho_{44} & 0 & \rho_{46} & \rho_{47} & 0\\
0 & \rho_{52} & \rho_{53} & 0 & \rho_{55} & 0 & 0 & 0\\
0 & 0 & 0 & \rho_{64} & 0 & \rho_{66} & \rho_{67} & 0\\
0 & 0 & 0 & \rho_{74} & 0 & \rho_{76} & \rho_{77} & 0\\
0 & 0 & 0 & 0 & 0 & 0 & 0 & \rho_{88}
\end{pmatrix}. \qquad (4.47)$$

Furthermore, similar process has been stated above, the matrix components corresponding to each bipartition $A|BC$, $B|AC$ and $C|AB$ are, respectively, obtained as follows

$$\left(\widetilde{\mathcal{W}}\right)_{ij}^{A}=\mathrm{Tr}\Big(\sqrt{\rho}\left(\sigma_i\otimes I_2\otimes I_2\right)\sqrt{\rho}\left(\sigma_j\otimes I_2\otimes I_2\right)\Big), \qquad (4.48)$$

$$\left(\widetilde{\mathcal{W}}\right)_{ij}^{B}=\mathrm{Tr}\Big(\sqrt{\rho}\left(I_2\otimes\sigma_i\otimes I_2\right)\sqrt{\rho}\left(I_2\otimes\sigma_j\otimes I_2\right)\Big), \qquad (4.49)$$

$$\left(\widetilde{\mathcal{W}}\right)_{ij}^{C}=\mathrm{Tr}\Big(\sqrt{\rho}\left(I_2\otimes I_2\otimes\sigma_i\right)\sqrt{\rho}\left(I_2\otimes I_2\otimes\sigma_i\right)\Big), \qquad (4.50)$$

Thus, the non-zero components of the matrices, namely (4.48), (4.49) and (4.50), are given by

$$
\begin{aligned}
\left(\widetilde{\mathcal{W}}\right)_{11}^{A} &= \left(\widetilde{\mathcal{W}}\right)_{22}^{A}=\frac{1}{18}\Big(12\sqrt{\lambda_2}\left(2\sqrt{\lambda_4}+\sqrt{\lambda_5}\right)\\
&+3\left(3\sqrt{\lambda_3}\left(\sqrt{\lambda_6}+3\sqrt{\lambda_7}\right)+2\sqrt{\lambda_1}\left(3\sqrt{\lambda_6}+\sqrt{\lambda_7}+2\sqrt{\lambda_8}\right)\right)\\
&+\left(\sqrt{\lambda_4}+2\sqrt{\lambda_5}\right)\left(3\sqrt{\lambda_6}+\sqrt{\lambda_7}+8\sqrt{\lambda_8}\right)\Big), \qquad (4.51)
\end{aligned}
$$

$$\left(\widetilde{\mathcal{W}}\right)_{33}^{A}=\frac{1}{9}\Big(9\left(\lambda_1+\lambda_2+\lambda_3\right)+\lambda_4+16\sqrt{\lambda_4\lambda_5}+\lambda_5+\left(2\sqrt{\lambda_7}+\sqrt{\lambda_8}\right)^2+6\sqrt{\lambda_6}\left(\sqrt{\lambda_7}+2\sqrt{\lambda_8}\right)\Big), \qquad (4.52)$$

$$\left(\widetilde{\mathcal{W}}\right)^{B}_{11} = \left(\widetilde{\mathcal{W}}\right)^{B}_{22} = \frac{1}{18}\Big(6\sqrt{\lambda_2}\left(3\sqrt{\lambda_3}+\sqrt{\lambda_4}+2\sqrt{\lambda_5}\right)+3\sqrt{\lambda_4\lambda_6}+6\sqrt{\lambda_5\lambda_6}+25\sqrt{\lambda_4\lambda_7} +2\sqrt{\lambda_5\lambda_7}+6\sqrt{\lambda_1}\left(3\sqrt{\lambda_6}+\sqrt{\lambda_7}+2\sqrt{\lambda_8}\right)+3\sqrt{\lambda_3}\left(3\sqrt{\lambda_6}+\sqrt{\lambda_7}+2\sqrt{\lambda_8}\right) +2\left(\sqrt{\lambda_4}+8\sqrt{\lambda_5}\right)\sqrt{\lambda_8}\Big), \tag{4.53}$$

$$\left(\widetilde{\mathcal{W}}\right)^{B}_{33} = \frac{1}{9}\Big(9\left(\lambda_1+\lambda_2\right)+\left(2\sqrt{\lambda_4}+\sqrt{\lambda_5}\right)^2+6\sqrt{\lambda_3}\left(\sqrt{\lambda_4}+2\sqrt{\lambda_5}\right)+\left(2\sqrt{\lambda_7}+\sqrt{\lambda_8}\right)^2+ 6\sqrt{\lambda_6}\left(\sqrt{\lambda_7}+2\sqrt{\lambda_8}\right)\Big), \tag{4.54}$$

$$\left(\widetilde{\mathcal{W}}\right)^{C}_{11} = \left(\widetilde{\mathcal{W}}\right)^{C}_{22} = \frac{1}{18}\Big(6\sqrt{\lambda_2}\left(3\sqrt{\lambda_3}+\sqrt{\lambda_4}+2\sqrt{\lambda_5}\right)+27\sqrt{\lambda_4\lambda_6}+24\sqrt{\lambda_2\lambda_7}+ \sqrt{\lambda_4\lambda_7}+8\sqrt{\lambda_5\lambda_7}+3\sqrt{\lambda_3}\left(3\sqrt{\lambda_6}+\sqrt{\lambda_7}+2\sqrt{\lambda_8}\right)+ 2\sqrt{\lambda_8}\left(6\sqrt{\lambda_2}+\sqrt{\lambda_4}+8\sqrt{\lambda_5}\right)\Big), \tag{4.55}$$

$$\left(\widetilde{\mathcal{W}}\right)^{C}_{33} = \frac{1}{9}\Big(9\left(\lambda_1+\lambda_2\right)+\left(2\sqrt{\lambda_4}+\sqrt{\lambda_5}\right)^2+6\sqrt{\lambda_3}\left(\sqrt{\lambda_4}+2\sqrt{\lambda_5}\right)+9\lambda_6+\lambda_7+16\sqrt{\lambda_7\lambda_8}+\lambda_8\Big). \tag{4.56}$$

where $\lambda_i (i = 1, ..., 8)$ stands for the eigenvalues of the density operator ρ (4.47) that are explicitly provided as following

$$\lambda_1 = \rho_{11}, \quad \lambda_2 = \rho_{33} - \rho_{55}, \tag{4.57}$$

$$\lambda_{3,4} = \frac{1}{2}\left(\rho_{22}+\rho_{33}+\rho_{35} \mp \sqrt{8\rho_{23}^2+\left(\rho_{33}+\rho_{35}-\rho_{22}\right)^2}\right), \tag{4.58}$$

$$\lambda_5 = \rho_{66} - \rho_{67}, \tag{4.59}$$

$$\lambda_{6,7} = \frac{1}{2}\left(\rho_{44}+\rho_{66}+\rho_{67} \mp \sqrt{8\rho_{46}^2+\left(\rho_{66}+\rho_{67}-\rho_{44}\right)^2}\right), \tag{4.60}$$

$$\lambda_8 = \rho_{88}. \tag{4.61}$$

Therefore, the local quantum uncertainties associated with each bipartition have the following form

$$\mathcal{U}_{A/BC}(\rho) = 1 - \max\left\{\widetilde{\mathcal{W}}^A_{11}, \widetilde{\mathcal{W}}^A_{33}\right\}, \tag{4.62}$$

$$\mathcal{U}_{B/AC}(\rho) = 1 - \max\left\{\widetilde{\mathcal{W}}^B_{11}, \widetilde{\mathcal{W}}^B_{33}\right\}, \tag{4.63}$$

$$\mathcal{U}_{C/AB}(\rho) = 1 - \max\left\{\widetilde{\mathcal{W}}^C_{11}, \widetilde{\mathcal{W}}^C_{33}\right\}. \tag{4.64}$$

Hence, the total LQU describing the three-qubit quantum state ρ (4.47) is expressed as

$$\mathcal{U}(\rho) = \frac{\mathcal{U}_{A/BC}(\rho)+\mathcal{U}_{B/AC}(\rho)+\mathcal{U}_{C/AB}(\rho)}{3}. \tag{4.65}$$

4 Uncertainty-induced quantum nonlocality

Inspired by the concept of the WYSI (4.3), the so-called uncertainty-induced quantum nonlocality is another prominent discord-like correlation metric (UIN). This reliable non-classical correlation quantifier was recently proposed as an alternative approach to reveal the degree of quantumness in a bipartite quantum system. It is defined as the maximum skew information achievable in a given quantum state due to a single local observable action [42, 69]. The UIN with regard to sub-system A for any given bipartite quantum state ρ_{AB} can be described in a rigorous way in terms of WYSI as [42]

$$\mathcal{U}_C\left(\rho^{AB}\right) = \min_{K^C} I(\rho^{AB}, K^C), \tag{4.66}$$

where the maximum in Eq.(4.66) is chosen across the set of all observables, $K^C = K_A^C \otimes I_B$, which commutes with the reduced density matrix ρ^A. While K_A^C stands for a Hermitian operator acting on part A admitting a nondegenerate spectrum $\Lambda^{'}$. Besides, I_B is the identity operator acting on part B and $I(\rho^{AB}, K^C)$ is the skew information associated with the density matrix ρ^{AB} which is defined via Eq.(4.3). For a bipartite qubit-qudit $(2 \otimes d)$ quantum system described by the state ρ^{AB}, the marginal state of part A can be represented by

$$\rho^A = \frac{1}{2}\left(I + \mathbf{r}.\boldsymbol{\sigma}^A\right). \tag{4.67}$$

Here, $\mathbf{r} = [r_i]$ stands for the Bloch vector of the state under scrutiny ρ^{AB} whose components are provided by $r_i = \mathrm{Tr}\left(\rho^{AB}\left(\sigma_i^A \otimes I_B\right)\right)$. Similarly to the local traceless observable adopted in the minimization procedure employed in the derivation of the LQU, we directly choose the considered observable $K_A^C = \mathbf{n}.\boldsymbol{\sigma}^A$, where $\|\mathbf{n}\| = 1$ and σ_i $(i = x, y, z)$ are the Pauli matrices. Hence, $\left[K_A^C, \rho^A\right] = 0$ will lead to

$$\mathbf{r} \times \mathbf{n} = \mathbf{0}. \tag{4.68}$$

From the above equation (4.68), two distinct possibilities have to be separately investigated:

- The first possibility corresponds to the case when $\mathbf{r} = 0$. In this situation the marginal state of part A reduces to the identity operator, that is, $\rho^A = \frac{1}{2}I$, which always commute with any given operator. Accordingly, $\mathbf{n}$ can be any given normalized vector, and the UIN for the case when $\mathbf{r} = 0$ is provided as follows

$$\begin{aligned} \mathcal{U}_C\left(\rho^{AB}\right) &= \max\left[1 - \mathbf{n}\mathcal{W}\mathbf{n}^T\right], \\ &= 1 - \lambda_{\min}\left(\mathcal{W}\right). \end{aligned} \tag{4.69}$$

  Here, $\lambda_{\min}\left(\mathcal{W}\right)$ denotes the least eigenvalue of 3×3-symmetric matrix $\mathcal{W}$ (4.14).

- The second possibility corresponds to the situation when $\mathbf{r} \neq 0$. This case will directly lead to $\mathbf{n} = c\mathbf{r}$, where $c \in \mathbb{R}$. Thus, we can obtain

$$\begin{aligned} \mathcal{U}_C\left(\rho^{AB}\right) &= 1 - \mathbf{n}\mathcal{W}\mathbf{n}^T \\ &= 1 - \frac{1}{\|\mathbf{r}\|^2}\mathbf{r}\mathcal{W}\mathbf{r}^T, \end{aligned} \tag{4.70}$$

  where the second equality sign " = " is due to the fact that $\|\mathbf{n}\|^2 = 1$, that is, $\|\mathbf{c}\|^2 = \frac{1}{\|\mathbf{r}\|^2}$, while the superscript T refers to the transposition operation.

Thus, from Eq.(4.69) and Eq.(4.70), the closed form of UIN for any arbitrary $2 \otimes d$ dimensional quantum state ρ^{AB} is given by

$$\mathcal{U}_C\left(\rho^{AB}\right) = \begin{cases} 1 - \lambda_{\min}\left(\mathcal{W}\right), & \mathbf{r} = \mathbf{0} \\ 1 - \frac{1}{\left\|\overrightarrow{r}\right\|^2} \overrightarrow{r} \mathcal{W} \overrightarrow{r}^T. & \mathbf{r} \neq \mathbf{0} \end{cases}$$

Similarly to the LQU, the UIN also satisfies all physical requirements for a genuine indicator of non-classical correlations reported in Sec.2. In the following, we shed light on the main intriguing properties of UIN. In fact, it remains unchanged under any local unitary operations $U_A \otimes U_B$ and non-increasing (contractive) under local operations performed on the unmeasured part B. Besides, UIN vanishes for states with zero quantum discord and it reduces to entanglement monotone for $(2 \otimes d)$-dimension pure states. Nevertheless, UIN has a geometrical meaning in terms of Hellinger distance [42]. This can be geometrically interpreted as the maximal squared Hellinger distance between the state under scrutiny ρ^{AB} and K^C $\rho^{AB} K^C$ [42]. For the qubit-qudit density matrix $\rho_{2\otimes 3}$ represented in (4.27), the analytical expression of UIN is obtained as [69]

$$\mathcal{U}(\rho_{2\otimes 3}) = 1 - \frac{1}{\left\|r_3\right\|^2} r_3 \mathcal{W}_{33} r_3^*, \quad \mathbf{r} \neq \mathbf{0} \tag{4.71}$$

where $r_3 = R_{30} = \rho_{11} + \rho_{22} + \rho_{33} - \rho_{44} - \rho_{55} - \rho_{66}$.

5 Quantum coherence

Quantum coherence is a fundamental property that is essential for quantum information processing. Although it is related to quantum correlations in multipartite states, coherence is an intrinsic quantum trait that underlies all correlations. Therefore, coherence represents a unique quantum resource that is distinct from entanglement and discord-like correlations [44]. Regarding the latter, the amount of non-classical correlations can be estimated using coherence, since the coherence of sub-systems provides an upper bound for the quantum discord-like correlation of the bipartite system. Similar to the method proposed for quantum entanglement, where it can be characterized via the distance between the state under study ρ and a set of states closed under local operations and classical communication (separable states) [6,44,198]. In this sense, Baumgratz *et al.* [198] introduced a mathematical framework for quantifying the degree of quantum coherence in an arbitrary quantum system. Let us consider a d-dimensional Hilbert space, where the coherence can be determined by measuring the shortest distance $\mathcal{D}\left(\rho, \sigma\right)$ between the quantum state ρ and a set of incoherent states $\left\{\sigma = \sum_k^d |k\rangle \langle k| \in \mathcal{I}\right\}$. The reference basis $\{|k\rangle\}_{k=1,\cdots,d}$ can be suitably defined based on the problem under study or the task that necessitates this quantum resource [198,202,228]. In this respect, as the non-zero off-diagonal elements of the density operator ρ represent the superposition of the chosen reference basis [44,198], the authors proposed an accurate measure of quantum coherence using the l_1 trace norm [198]. It is given as

$$\mathcal{C}_{l_1}(\rho) = \min_{\sigma \in \mathcal{I}} \left\|\rho - \sigma\right\|_{l_1} = \sum_{i \neq j} \left|\langle i| \rho |j\rangle\right|. \tag{4.72}$$

It has been demonstrated by Streltsov *et al.* [229] that quantum coherence can serve as a resource for the generation of quantum entanglement. The l_1-norm of coherence serves as an important connection between different measures of coherence and entanglement [230]. However, while quantum coherence can capture quantumness more effectively compared to discord-like measures of quantum correlations, the latter represents an exact basis-independent measure of the former [198].

6 Quantum Fisher information

In the framework of quantum estimation and quantum metrology theory, the concept of quantum Fisher information (QFI) is one of the most crucial resources in the field of quantum information [231]. QFI is considered to be the quantum counterpart of Fisher information in the classical regime [47, 232, 233]. The major goal behind the concept of QFI is to estimate various relevant parameters resulting from the quantum state under consideration, providing a good perspective on parameter estimation settings [47]. It has been argued that the highest degree of Fisher information leads to robust estimation degrees and vice versa, from the viewpoint of quantum estimation theory. It is used to determine the accuracy of a parameter related to a physical quantity encoded in the quantum state. Several attempts have recently been devoted to explore the evolution of QFI in order to identify the intrinsic connection between quantum entanglement and quantum metrology [235]. Entanglement has been shown to enhance the accuracy and efficiency of parameter estimation in unitary processes [236]. From this perspective, it is reasonable to wonder whether quantum correlations beyond entanglement can be related to accuracy in quantum metrology protocols. Let us suppose that $\rho_{\boldsymbol{\varsigma}}$ is an N-dimensional quantum state, where $\boldsymbol{\varsigma} = \{\varsigma_\mu\}$ such that $\mu = 1, \cdots, n$, is an arbitrary parameter to be estimated. In order to reveal the amount of information about the parameter $\boldsymbol{\varsigma}$ from the state $\rho_{\boldsymbol{\varsigma}}$, a set of POVM measurements is performed, namely $P_k = M_k M_k^\dagger$ satisfying $\sum_k P_k = 1$. Then, QFI is defined as follows [237]

$$\mathcal{F}_{\varsigma_\mu \varsigma_\nu}(\rho_{\boldsymbol{\varsigma}}) = \frac{1}{2}\mathrm{Tr}\left(\rho_{\boldsymbol{\varsigma}} \left\{L_{\varsigma_\mu}, L_{\varsigma_\nu}\right\}\right), \tag{4.73}$$

where the notation $\{\cdot,\cdot\}$ stands for the anti-commutator, while the symbols $L_{\varsigma_\mu}\,(L_{\varsigma_\nu})$ denote the symmetric logarithmic derivative (SLD) operators associated with the parameters $\varsigma_\mu\,(\varsigma_\nu)$. Moreover, the SLD operator associated with the parameter ς_ν and the state ρ obeys the following relation:

$$\partial_{\varsigma_\mu}\rho_{\boldsymbol{\varsigma}} = \frac{1}{2}\left(\rho_{\boldsymbol{\varsigma}} L_{\varsigma_\mu} + L_{\varsigma_\mu}\rho_{\boldsymbol{\varsigma}}\right). \tag{4.74}$$

Here, ∂_{ς_μ} represents the partial derivative with respect to the parameter ς_μ. Moreover, it should be noted that the symmetric logarithmic derivative (SLD) operator is hermitian. Therefore, the expression given in Eq.(4.73) turns out to be:

$$\mathcal{F}_{\varsigma_\mu}(\rho_{\boldsymbol{\varsigma}}) = \mathrm{Tr}\left(\rho_{\boldsymbol{\varsigma}} L_{\varsigma_\mu}^2\right) = \mathrm{Tr}\left(\frac{\partial \rho_{\boldsymbol{\varsigma}}}{\partial \varsigma_\mu} L_{\varsigma_\mu}\right). \tag{4.75}$$

By employing the spectral decomposition of the two-qubit state, namely $\rho \equiv \rho_{\boldsymbol{\varsigma}} = \sum_i \lambda_i \left|\lambda_i\right\rangle \left\langle\lambda_i\right|$, where λ_i and $\left|\lambda_i\right\rangle$ such that $i = 1, \cdots, 4$ represents, respectively, the eigenvalues and eigenvectors of the state ρ. Then, the QFI of the estimated parameter $\boldsymbol{\varsigma}$ can be then expressed for a given bipartite two-qubit quantum state as follows [238]

$$\mathcal{F}(\rho) = \mathcal{F}_c(\rho) + \mathcal{F}_q(\rho) - \mathcal{F}_m(\rho). \tag{4.76}$$

The expression of QFI given in Eq.(4.76) is clearly divided into three parts: the first part on the right-hand side of Eq. (4.73) describes the quantum counterpart of classical Fisher information since the probability distributions are simply replaced by the associated eigenvalues of the corresponding state ρ. The second term is regarded as a weighted average of quantum Fisher information on all pure states. The last part always results from the mixture of the first two

terms and therefore reduces the total amount of the QFI. These terms are explicitly written as:

$$\mathcal{F}_c(\rho) = \sum_{i=1}^{4} \frac{(\partial_\zeta \lambda_i)^2}{\lambda_i}, \tag{4.77}$$

$$\mathcal{F}_q(\rho) = 4\sum_{i=1}^{4} \lambda_i[\langle \partial_\zeta \lambda_i | \partial_\zeta \lambda_i\rangle - |\langle \lambda_i | \partial_\zeta \lambda_i\rangle|^2], \tag{4.78}$$

$$\mathcal{F}_m(\rho) = \sum_{i\neq j} \frac{8\lambda_i\lambda_j}{\lambda_i+\lambda_j} |\langle \lambda_i | \partial_\zeta \lambda_i\rangle|^2. \tag{4.79}$$

It is interesting to note that for pure quantum states, the QFI reduces namely to the first two parts of the expression (4.73), namely $\mathcal{F}_c(\rho)$ and $\mathcal{F}_q(\rho)$, while for mixed quantum states, the third term $\mathcal{F}_m(\rho)$ needs to be subtracted. From the aforementioned discussion, it is obvious to see that the QFI of pure states is often larger than that of mixed states.

On the other hand, it has recently been established that the concept of QFI can be generalized for N-dimensional quantum states. Specifically, it is given in the following form [79, 239]

$$\mathcal{F}(\rho) \equiv \mathcal{F}_{\varsigma_\mu}(\rho_\varsigma) = \sum_{i=1}^{N} \frac{(\partial_\zeta \lambda_i)^2}{\lambda_i} + 4\sum_{i=1}^{N} \lambda_i[\langle \partial_\zeta \lambda_i | \partial_\zeta \lambda_i\rangle - |\langle \lambda_i | \partial_\zeta \lambda_i\rangle|^2] - \sum_{i\neq j} \frac{8\lambda_i\lambda_j}{\lambda_i+\lambda_j} |\langle \lambda_i | \partial_\zeta \lambda_j\rangle|^2. \tag{4.80}$$

From a mathematical perspective, the QFI for both arbitrary 4-dimensinal and N-dimensional quantum systems satisfies some useful properties. Among them we can note the following feature: it is an additive function and remains unchanged under the action of unitary transformations [240]. However, the primary goal of evaluating the QFI is to exhibit an elevated and robust estimation accuracy of the relevant parameter of the state under scrutiny. Based on this, as an application of QFI, we have independently estimated the temperature parameters and the external magnetic field, namely T and B, respectively, encoded in the spin-1/2 Heisenberg trimer system described by a thermal quantum state [79]. Roughly speaking, it has been shown that the concept QFI becomes a crucial resource in several area of quantum information theory, in particular, quantum correlation [47]. In this context, we will study a new metric of non-classical correlations based on the concept of QFI, namely local quantum Fisher information (LQFI).

6.1 Local quantum Fisher information

Another concept related to the QFI, known as local quantum Fisher Information (LQFI), has recently attracted a great deal of interest. LQFI defines a discord-type metric of non-classical correlation through performing local measurements on one sub-system of the total quantum state. This metric allows us to gain a better understanding of how quantum correlations are instrumental in setting metrological accuracy. Let us suppose that the initial density matrix $\rho_\zeta(0)$ can be evolved via a unitary evolution transformation namely, $U_\varsigma = e^{iK\varsigma}$, that depends on the parameter ζ and is generated by the Hamiltonian operator K such as such that $\rho_\varsigma = U_\varsigma^\dagger \rho U_\varsigma$. Using the Hermitian operator K, the QFI is therefore given as [232]

$$\mathcal{F}(\rho, K) = \frac{1}{2}\sum_{i\neq j} \frac{(\lambda_i-\lambda_j)^2}{\lambda_i+\lambda_j} |\langle \lambda_i | K | \lambda_j\rangle|^2. \tag{4.81}$$

As already pointed out, the dynamics are regulated by a local transformation, namely $U_\varsigma = e^{iK_A\varsigma}$ of a local Hamiltonian $K_A = K_a \otimes I_B$. In this case, QFI reduces to LQFI via the following expression

$$\mathcal{F}(\rho, K_A) = \text{Tr}\,[\rho K_A^2] - \sum_{i\neq j} \frac{2\lambda_i\lambda_j}{\lambda_i+\lambda_j} |\langle\lambda_i|K_A|\lambda_j\rangle|^2. \tag{4.82}$$

However, the primary advantage of using LQFI is its efficiency as a trustworthy witness of the quantumness of correlations. Specifically, the non-classical correlation captured via employing LQFI is defined as the minimum of QFI on all local observables K_A acting on part A [43]. It is provided by

$$\mathcal{LF}(\rho) = \min_{K_A} \mathcal{F}(\rho, K_A). \tag{4.83}$$

We note that the local observable K_A is expressed using the standard Pauli matrices, i.e. $\sigma^\alpha = (\sigma^1, \sigma^2, \sigma^3)$, and the local observable is set as $K_A = \sigma^\alpha . r^\alpha$, with Bloch vector r^α $(\alpha = x, y, z)$ such that $|r^\alpha| = 1$ [43]. In this case, the first part on the right-hand side of Eq.(4.82) corresponds to the unity, meaning $\text{Tr}\,[\rho K_A^2] = 1$, whereas the second part leads to [80]

$$\begin{aligned}
\sum_{i\neq j} \frac{2\lambda_i\lambda_j}{\lambda_i+\lambda_j} |\langle\lambda_i|K_A|\lambda_j\rangle|^2 &= \sum_{i\neq j} \frac{2\lambda_i\lambda_j}{\lambda_i+\lambda_j} |\langle\lambda_i|K_A|\lambda_j\rangle\langle\lambda_j|K_A|\lambda_i\rangle \\
&= \sum_{i\neq j} \sum_{\alpha=\beta=1}^{3} \frac{2\lambda_i\lambda_j}{\lambda_i+\lambda_j} \langle\lambda_i|(r^\alpha\sigma^\alpha)\otimes I_B|\lambda_j\rangle\langle\lambda_j|(r^\beta\sigma^\beta)\otimes I_B|\lambda_i\rangle \\
&= r^\alpha \sum_{i\neq j} \sum_{\alpha=\beta=1}^{3} \frac{2\lambda_i\lambda_j}{\lambda_i+\lambda_j} \langle\lambda_i|\sigma^\alpha\otimes I_B|\lambda_j\rangle\langle\lambda_j|\sigma^\beta\otimes I_B|\lambda_i\rangle r^\beta \\
&= r^\alpha S_{\alpha\beta} r^\beta \\
&= r^T.S.r,
\end{aligned} \tag{4.84}$$

where $\sigma^1 \equiv \sigma^x$, $\sigma^2 \equiv \sigma^y$ and $\sigma^3 \equiv \sigma^z$. While $S = [S_{ij}]$ refers to a 3×3-symmetric matrix whose components are given as the following

$$(S)_{\alpha\beta} = \sum_{m\neq n} \frac{2\lambda_m\lambda_n}{\lambda_m+\lambda_n} \langle\lambda_m|\sigma^\alpha\otimes I_B|\lambda_n\rangle\langle\lambda_n|\sigma^\beta\otimes I_B|\lambda_m\rangle. \tag{4.85}$$

However, in order to minimize the quantity $\mathcal{F}(\rho, K_A)$ obtained from Eq.(4.73), it is required to maximize the term $r^T.S.r$ in the expression (4.84) on all unit vectors r^α. Here, the largest value on all unit vectors r^α coincides with the highest eigenvalues of the matrix S (4.85). Therefore, the closed expression of the LQFI, which quantifies the degree of non-classical correlation in any given bipartite $2\otimes d$ quantum state, gives the following

$$\mathcal{LF}(\rho) = 1 - \lambda_{\max}^S, \tag{4.86}$$

where the quantity $\lambda_{\max}^S$ in Eq.(4.86) designs the greatest eigenvalue of S (4.85). This metric also satisfies desirable requirements that any genuine indicator of non-classical correlations should meet. It remains unchanged under any local transformation, non-negative and vanishes for states with zero quantum discord, that is, classically correlated states. Furthermore, it coincides with the geometric quantum discord for pure quantum states [43]. This allows us to consider this tool as a reliable metric for non-classical correlations. Thus, measuring only the QFI of local observables can provide a way to detect and quantify the amount of non-classical correlations exist in a quantum system.

After some straightforward algebra and by using the eigenvalues and eigenvectors computed in Eqs.(4.28) and (4.31), the closed formula for LQFI of the bipartite $2\otimes 3$ quantum state $\rho_{2\otimes 3}$ (4.27) is obtained as [69]

$$\mathcal{LF}(\rho_{2\otimes 3}) = 1 - \max(P_{11}, P_{22}, P_{33}), \tag{4.87}$$

where $P_{\alpha\alpha}(\alpha = 1, 2, 3)$ are analytically computed from Eq.(4.85). They are explicitly given by

$$\begin{aligned} P_{11} &= P_{22} = 4\Big(\frac{\lambda_1\lambda_2}{(\lambda_1+\lambda_2)(1+|\upsilon_+|^2)} + \frac{\lambda_1\lambda_3}{(\lambda_1+\lambda_2)(1+|\upsilon_-|^2)} + \\ &\frac{\lambda_2|\upsilon_+|^2}{(1+|\upsilon_+|^2)}\left(\frac{\lambda_4}{(\lambda_2+\lambda_4)(1+|\eta_+|^2)} + \frac{\lambda_5}{(\lambda_2+\lambda_5)(1+|\eta_-|^2)}\right) + \\ &\frac{\lambda_3|\upsilon_-|^2}{(1+|\upsilon_-|^2)}\left(\frac{\lambda_4}{(\lambda_3+\lambda_4)(1+|\eta_+|^2)} + \frac{\lambda_5}{(\lambda_3+\lambda_5)(1+|\eta_-|^2)}\right) + \\ &\frac{\lambda_4\lambda_6|\eta_+|^2}{(\lambda_4+\lambda_6)(1+|\eta_+|^2)} + \frac{\lambda_5\lambda_6|\eta_-|^2}{(\lambda_5+\lambda_6)(1+|\eta_-|^2)}\Big), \end{aligned} \tag{4.88}$$

$$P_{33} = 4\Big(\frac{\lambda_2\lambda_3}{(\lambda_1+\lambda_2)}\frac{|\upsilon_+^*\upsilon_- - 1|^2}{(1+|\upsilon_+|^2)(1+|\upsilon_-|^2)} + \frac{\lambda_4\lambda_5}{(\lambda_4+\lambda_5)}\frac{|\eta_+^*\eta_- - 1|^2}{(1+|\eta_+|^2)(1+|\eta_-|^2)}\Big). \tag{4.89}$$

where λ_i $(i = 1, ...4)$, $\upsilon_\pm$ and $\eta_\pm$ are given in Eq.(4.33) and Eq.(4.34), respectively. Moreover, we have $P_{12} = P_{21} = P_{23} = P_{32} = P_{13} = P_{31} = 0$. On the other hand, the aforementioned discord-like metric of non-classical correlations has a close connection with the notion of LQU, which is defined in Eq.(4.15). Therefore, it is intriguing to determine how these two metrics interplay with one another since they are both related to the concept of quantum uncertainty. This was the main topic that we developed in our contributions [69, 80]. To further elucidate this relationship, we will provide in the next section a detailed analysis of the link and interplay between the LQU (4.15) and the LQFI (4.86) for arbitrary qubit-qudit quantum systems.

7 Interplay between local quantum Fisher information and local quantum uncertainty

Before we can establish the connection between the LQU and the LQFI, we need first to provide the relationship between the skew information defined via Eq.(4.3) and the QFI given in Eq.(4.75) for any given qubit-qudit quantum systems [209]. To do this, let $\rho = \sum_m \lambda_m |\psi_m\rangle\langle\psi_m|$ be a mixed quantum state, where λ_m and $|\psi_m\rangle$ are, respectively, the eigenvalues and eigenvectors of the density matrix ρ. The set of $|\psi_m\rangle$ forms an orthonormal basis such that $\sum_m |\psi_m\rangle\langle\psi_m| = I$. One can easily check that

$$\begin{aligned} \mathrm{Tr}\left(\rho K^2\right) &= \textstyle\sum_m \langle\psi_m|\rho K^2|\psi_m\rangle \\ &= \textstyle\sum_m \lambda_m \langle\psi_m| K^2 |\psi_m\rangle \\ &= \textstyle\sum_m \lambda_m \langle\psi_m| K \sum_n \underbrace{|\psi_n\rangle\langle\psi_n|}_{=I} K |\psi_m\rangle \\ &= \textstyle\sum_{m,n} \lambda_m \langle\psi_m| K |\psi_n\rangle\langle\psi_n| K |\psi_m\rangle \\ &= \textstyle\sum_{m,n} \lambda_m |\langle\psi_m| K |\psi_n\rangle|^2 . \end{aligned} \tag{4.90}$$

The above formula (2.50) can also be rewritten in the symmetric form since $\mathrm{Tr}\left(\rho K^2\right) = \sum_{m,n} \lambda_n |\langle\psi_m| K |\psi_n\rangle|^2$ as follows

$$\mathrm{Tr}\left(\rho K^2\right) = \sum_{m,n} \frac{\lambda_m + \lambda_n}{2} |\langle\psi_m| K |\psi_n\rangle|^2 . \tag{4.91}$$

Likewise, the second part of Eq.(4.4) is given by

$$\begin{aligned}\mathrm{Tr}\left(K\sqrt{\rho}K\sqrt{\rho}\right) &= \sum_m \langle\psi_m| K\sqrt{\rho}K\sqrt{\rho}\,|\psi_m\rangle \\ &= \sum_m \sqrt{\lambda_m}\,\langle\psi_m| K\sqrt{\rho}K\,|\psi_m\rangle \\ &= \sum_{m,n} \sqrt{\lambda_m}\,\langle\psi_m| K\sqrt{\rho}\,|\psi_n\rangle\,\langle\psi_n| K\,|\psi_m\rangle \\ &= \sum_{m,n} \sqrt{\lambda_m\lambda_n}\,\langle\psi_m| K\,|\psi_n\rangle\,\langle\psi_n| K\,|\psi_m\rangle \\ &= \sum_{m,n} \sqrt{\lambda_m\lambda_n}\,|\langle\psi_m| K\,|\psi_n\rangle|^2 . \end{aligned} \tag{4.92}$$

Thus, using the formulae (4.92) and (4.91), the explicit expression of the skew information takes the following form

$$I(\rho,K) = \frac{1}{2}\sum_{m,n}\left(\sqrt{\lambda_m}-\sqrt{\lambda_n}\right)^2 |\langle\psi_m| K\,|\psi_n\rangle|^2 . \tag{4.93}$$

Now, we link the QFI (4.75) to the notion of skew information (4.3). To begin, it is obvious that the density operator ρ_ς fulfills the von Neumann-Landau equation (we take $\hbar = 1$) [209]:

$$i\frac{\partial\rho_\varsigma}{\partial\varsigma} = [K,\rho_\varsigma]. \tag{4.94}$$

By employing the formula (4.74), one obtains

$$\frac{1}{2}\left(L_\varsigma\rho_\varsigma + \rho_\varsigma L_\varsigma\right) = i\left(\rho_\varsigma K - K\rho_\varsigma\right). \tag{4.95}$$

Under the unitary transformation, the SLD operator L_ζ is then independent of the estimated parameter ς if and only if the observable K and the state ρ are assumed to be fixed, that is, $L = \exp\left(i\varsigma K\right) L_\varsigma \exp\left(-i\varsigma K\right)$, meaning

$$\frac{1}{2}\left(L\rho + \rho L\right) = i\left(\rho K - K\rho\right). \tag{4.96}$$

Based on the expression (4.75), it is straightforward to verify that

$$\begin{aligned}\mathrm{Tr}\left(\rho_\varsigma L_\varsigma^2\right) &= \mathrm{Tr}\left(\exp\left(-i\varsigma K\right)\rho\exp\left(i\varsigma K\right)L_\varsigma^2\right) = \mathrm{Tr}\left(\rho\exp\left(i\varsigma K\right)L^2\exp\left(-i\varsigma K\right)\right) \\ &= \mathrm{Tr}\left(\rho L^2\right). \end{aligned} \tag{4.97}$$

Using the spectral decomposition of the state ρ one gets

$$\frac{1}{2}\langle\psi_m|\, L\rho + L\rho\,|\psi_n\rangle = \langle\psi_m|\, i[\rho,K]\,|\psi_n\rangle, \tag{4.98}$$

therefore it is simple to demonstrate that

$$\frac{1}{2}\left(\lambda_m+\lambda_n\right)\langle\psi_m|\, L\,|\psi_n\rangle = i\left(\lambda_m-\lambda_n\right)\langle\psi_m|\, K\,|\psi_n\rangle. \tag{4.99}$$

In this inspiration, the QFI (4.75) is given as follows

$$\begin{aligned}\mathcal{F}(\rho,K) &= \frac{1}{4}\mathrm{Tr}\left(\rho L^2\right) \\ &= \frac{1}{4}\sum_m \langle\psi_m|\,\rho L^2\,|\psi_m\rangle \\ &= \frac{1}{4}\sum_{m,n}\lambda_m\,\langle\psi_m|\, L\,|\psi_n\rangle\,\langle\psi_n|\, L\,|\psi_m\rangle \\ &= \frac{1}{4}\sum_{m,n}\lambda_m\,|\langle\psi_m|\, L\,|\psi_n\rangle|^2 \\ &= \frac{1}{4}\sum_{m,n}\lambda_n\,|\langle\psi_m|\, L\,|\psi_n\rangle|^2 . \end{aligned} \tag{4.100}$$

In terms of the eigenvalues and eigenvectors of the state ρ, the above formula (4.100) can be written as follows

$$\begin{aligned}
\mathcal{F}(\rho, K) &= \sum_{m,n} \frac{\lambda_m + \lambda_n}{8} \left|\langle\psi_m| L |\psi_n\rangle\right|^2 \\
&= \frac{4}{8} \sum_{m,n} (\lambda_m + \lambda_n) \frac{(\lambda_m - \lambda_n)^2}{(\lambda_m + \lambda_n)^2} \left|\langle\psi_m| K |\psi_n\rangle\right|^2 \\
&= \frac{4}{8} \sum_{m,n} \frac{1}{(\lambda_m + \lambda_n)} (\lambda_m - \lambda_n)^2 \left|\langle\psi_m| K |\psi_n\rangle\right|^2 \\
&= \frac{1}{2} \sum_{m,n} \left(\frac{2\sqrt{\lambda_m \lambda_n}}{\lambda_m + \lambda_n} + 1\right) \left(\sqrt{\lambda_m} - \sqrt{\lambda_n}\right)^2 \left|\langle\psi_m| K |\psi_n\rangle\right|^2, \qquad (4.101)
\end{aligned}$$

with

$$0 \leq \frac{2\sqrt{\lambda_m \lambda_n}}{\lambda_m + \lambda_n} \leq 1. \qquad (4.102)$$

Then, the QFI is then majorized by the WYSKI, yielding the following results

$$I(\rho, K) \leq \mathcal{F}(\rho, K) \leq 2I(\rho, K). \qquad (4.103)$$

By minimizing the above inequalities (4.103) under a local observable K_A, we show that the LQFI is bounded by LQU as follows [195, 209]

$$\mathcal{U}(\rho) \leq \mathcal{LF}(\rho) \leq 2\mathcal{U}(\rho).$$

This also means

$$\mathcal{U}(\rho) \leq I(\rho, K) \leq \mathcal{F}(\rho, K), \qquad (4.104)$$

where $\mathcal{U}(\rho)$ and $\mathcal{LF}(\rho)$ are, respectively, the LQU and LQFI defined in Eqs.(4.15) and (4.86). Therfore, we can conclude that the LQU and the LQFI are both useful functions for understanding the effect of non-classical correlations, other than the entanglement, in enhancing the precision and efficiency of quantum metrology protocols. Moreover, they are useful understanding the role of non-classical correlations in quantum information processing tasks, such as quantum cryptography and quantum teleportation. The latter will be the subject of interest in the next section.

8 Quantum teleportation

Quantum correlations is a valuable resource for building quantum technologies, including quantum communication. One such technology is quantum teleportation, which allows for the transfer of the exact properties of a particle encoded in a quantum state between two distant locations without physically transporting the particle itself. This is achieved by destroying the quantum state of a qubit in one location, followed by recreating it on another qubit located at a distance using shared entanglement between the qubits. The concept of quantum entanglement is fundamental to the quantum teleportation protocol. It allows two or more particles to share a single quantum state, regardless of their separation distance. The protocol involves the transmission of quantum information between a sender and a receiver via a pair of entangled particles, local unitary operations and classical communication channels. Bennett and his colleagues first proposed the idea of quantum teleportation in 1993 [45]. The first experimental demonstration of quantum teleportation was conducted in 1997 by Bouwmeester *et al.* in [57]. The experiment used four photons generated through spontaneous parametric down-conversion (SPDC) and teleported the polarization state of the photons. Since then, numerous experiments have been conducted to demonstrate the feasibility and potential applications of this process. In this section, we will provide a full study of quantum teleportation.

8.1 Standard quantum teleportation protocol

In the field of quantum information science, several quantum teleportation protocols have been proposed in the literature. Each protocol has its own strengths and weaknesses and the choice of protocol depends on the specific application and resources available. One such protocol is the *"controlled teleportation"* protocol, which was proposed by Gottesman and Chuang [55]. This protocol involves the use of an additional qubit, which is used to control the teleportation process and can be useful for implementing quantum gates. Another protocol, proposed by Vaidman, is called "*counterfactual teleportation"* [241]. This protocol allows for the transfer of quantum information without any physical particles being transmitted between the sender and receiver, making it an interesting tool for quantum communication with security benefits. There are also protocols that use different types of resources, such as continuous-variable teleportation, which uses continuous variables such as amplitude and phase to represent quantum states [242], and hybrid teleportation, which combines discrete and continuous variables to transfer quantum information [243]. This type of teleportation is essential for quantum communication over continuous channels, such as fiber optics. Hybrid teleportation combines discrete and continuous variables, offering the best of both worlds for transferring quantum information. Despite the differences between these protocols, they all rely on the fundamental principles of quantum entanglement and quantum measurement to transfer quantum information without physically sending the particle itself. In our studies, we were only focused on the standard quantum teleportation protocol provided by Bennett *et al.* in [45]. It is a widely-used and well-studied protocol for quantum teleportation. It is often used as a benchmark for other quantum teleportation protocols due to its simplicity and effectiveness.

Let us consider the scenario where the sender, Alice, wants to transmit an unknown qubit state denoted by $|\psi_1\rangle$ to the receiver, Bob, who is spatially distant from her. However, they can only communicate through classical channels such as phone calls, email and so on. The qubit state, $|\psi_1\rangle$, can be written as a linear combination of two basis states, namely $|0\rangle$ and $|1\rangle$, with complex coefficients, α and β, satisfying the condition $|\alpha|^2 + |\beta|^2 = 1$. Such that

$$|\psi\rangle_1 = \alpha\,|0\rangle_1 + \beta\,|1\rangle_1\,. \tag{4.105}$$

It is important to note that the state $|\psi\rangle_1$ is arbitrary and not necessarily known by either Alice or Bob. A diagram or schematic illustration of the standard quantum teleportation protocol is presented in Fig.4.1.

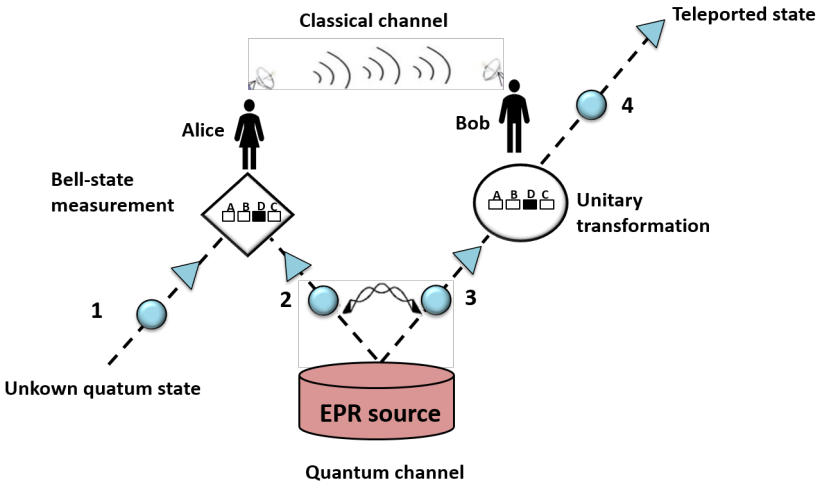


Figure 4.1: A schematic illustration of the standard quantum teleportation protocol

Here, we will provide a brief overview of the main steps involved in this protocol:

- Initialization: Alice and Bob each have their own qubit and they share an entangled pair of qubits known as the Bell pair. It is given by

$$|\beta_{00}\rangle_{23} = \frac{1}{\sqrt{2}}(|00\rangle_{23} + |11\rangle_{23}) \in \mathcal{H}_{23} = \mathcal{H}_2 \otimes \mathcal{H}_3, \tag{4.106}$$

  where qubit 2 belongs to Alice, while qubit 3 belongs to Bob. This state serves as the quantum channel for the teleportation protocol.

- Preparation: This step involves preparing a single particle of the unknown state. This qubit is denoted as "1" and is located in the Hilbert space $\mathcal{H}_1$. Alice has then the qubit that she wants to send and her constituent of the Bell pair, while Bob has only the second constituent. Since Alice cannot send the state of her qubit directly to Bob, she combines it with her half of the entangled pair. The joint state of the three qubits is given as the tensor product below:

$$|\phi\rangle = |\psi\rangle_1 |\beta_{00}\rangle_{23} = \frac{1}{\sqrt{2}} (\alpha |0\rangle_1 + \beta |1\rangle_1) (|00\rangle_{23} + |11\rangle_{23}), \tag{4.107}$$

  where the total Hilbert space of the whole system 123 is $\mathcal{H}_{23} = \mathcal{H}_1 \otimes \mathcal{H}_2 \otimes \mathcal{H}_3$. Distributing terms gives the following equality:

$$|\phi\rangle = \frac{1}{\sqrt{2}} (\alpha |000\rangle_{123} + \beta |100\rangle_{123} + \alpha |011\rangle_{123} + \beta |111\rangle_{123}). \tag{4.108}$$

  Using the Bell states (2.6-2.9), we can represent Alice's qubits in Bell basis as:

$$|\beta_{00}\rangle_{12} = \frac{1}{\sqrt{2}}(|00\rangle + |11\rangle), \quad |\beta_{01}\rangle_{12} = \frac{1}{\sqrt{2}}(|01\rangle + |10\rangle), \tag{4.109}$$

$$|\beta_{10}\rangle_{12} = \frac{1}{\sqrt{2}}(|00\rangle - |11\rangle), \quad |\beta_{11}\rangle_{12} = \frac{1}{\sqrt{2}}(|01\rangle - |10\rangle). \tag{4.110}$$

  The combined state can be expressed in the Bell basis $\{|\beta_{00}\rangle_{12}, |\beta_{01}\rangle_{12}, |\beta_{10}\rangle_{12}, |\beta_{11}\rangle_{12}\}$ as:

$$|\phi\rangle = \frac{1}{2}\Big[|\beta_{00}\rangle_{12} (\alpha |0\rangle_3 + \beta |1\rangle_3) + |\beta_{01}\rangle_{12} (\alpha |0\rangle_3 - \beta |1\rangle_3) \tag{4.111}$$

$$+ |\beta_{10}\rangle_{12} (\alpha |1\rangle_3 + \beta |0\rangle_3) + |\beta_{11}\rangle_{12} (\alpha |1\rangle_3 - \beta |0\rangle_3) \Big]. \tag{4.112}$$

- Measurement: Alice performs a joint Bell-state measurement (BSM) on the two qubits she possesses, namely the qubit $|\psi\rangle_1$ and the first qubit of the entangled pair $|\beta_{00}\rangle_{23}$. According to the decomposition (4.111), the outcome of the measurement will be one of the four states composing the Bell base: $|\beta_{00}\rangle_{12}, |\beta_{01}\rangle_{12}, |\beta_{10}\rangle_{12}$ or $|\beta_{11}\rangle_{12}$, each with the same probability of 1/4. Since the quantum channel was initially made of two entangled qubits, the qubit 3 of Bob will instantaneously be projected into one of the pure states appearing in Eq.(4.111) parameterized by α and β.

- Classical communication: Alice then communicates the result of her measurement to Bob using classical communication channel. This communication requires two bits of classical information to be transmitted since there are four possible measurement outcomes:
  00 for $|\beta_{00}\rangle_{12}$,
  01 for $|\beta_{01}\rangle_{12}$,
  10 for $|\beta_{10}\rangle_{12}$
  and 11 for $|\beta_{11}\rangle_{12}$.

- Correction: Based on the two classical bits received from Alice, Bob performs a corresponding quantum unitary operation on his qubit of the shared entangled pair. The operation depends on the outcome of Alice's measurement as follows:

  If Alice measures $|\beta_{00}\rangle_{12}$, Bob applies the identity operation (I) to his qubit.

  If Alice measures $|\beta_{01}\rangle_{12}$, Bob applies the Pauli-X (σ^x) operation to his qubit.

  If Alice measures $|\beta_{10}\rangle_{12}$, Bob applies the Pauli-Z (σ^z) operation to his qubit.

  If Alice measures $|\beta_{11}\rangle_{12}$, Bob applies the Pauli-X (σ^x) and Pauli-Z (σ^z) operations to his qubit.

- Reconstruction: After Bob applies the correction, his qubit is now in the same state as the unknown quantum state $|\psi\rangle_1$ that Alice wanted to teleport.

Note that the key feature of this protocol is the use of entanglement to teleport the unknown quantum state from Alice to Bob without physically transmitting it. This protocol is secure against eavesdropping because any attempt to measure or copy the unknown quantum state would disturb the entanglement and be detected by Alice and Bob. Based on the protocol described above, we propose a scheme of quantum teleportation using a partial entangled state as the resource for the quantum teleportation process instead of the Bell maximally entangled state given in Eq.(4.106). The advantage of using a partial entangled state is that it requires less entanglement and is easier to implement experimentally compared to a Bell state. However, using a partial entangled state also has drawbacks, including a lower success probability of teleportation and the possibility of a teleported state that is not an exact replica of the original state. In the next part, we will present a scheme for the quantum teleportation process using an arbitrary entangled mixed state as the quantum channel.

8.2 Scheme of quantum teleportation

Bowen *et al.* in Ref. [244], proposed a scheme for implementing quantum teleportation using an entangled mixed state as a resource. This scheme can be interpreted as a general depolarizing quantum channel, allowing the teleportation of any given two-qubit mixed states. One of the significant outcomes of this work is its ability to account for mixed teleported states, except in the case of a maximally entangled channel. As in the standard teleportation protocol, the input entangled state ρ_{in} in the mixed channel is destroyed as depicted in Fig.4.1, and its output state ρ_{out} appears on the other side after implementing a local measurement in the form of linear operators. However, it should be noted that the output state ρ_{out} for the mixed channel differs from that of a maximally entangled channel. The degree of difference between the input and output states depends on the degree of entanglement of the mixed state used as a resource. Let us consider an arbitrary two-qubit pure state as the input state, such as

$$|\psi_{\text{in}}\rangle = \cos\left(\frac{\theta}{2}\right)|10\rangle + e^{i\phi}\sin\left(\frac{\theta}{2}\right)|01\rangle\,. \tag{4.113}$$

Here, $\theta \in [0,\pi]$ and $\phi \in [0,2\pi]$ denote, respectively, the amplitude and the phase of the input state. Using the density operator formalism, the concurrence $\mathcal{C}_{\text{in}}$ of the input state $\rho_{\text{in}} = |\psi_{\text{in}}\rangle\langle\psi_{\text{in}}|$can be expressed as follows

$$\mathcal{C}_{\text{in}} = 2|e^{i\phi}\sin\left(\frac{\theta}{2}\right)\cos\left(\frac{\theta}{2}\right)| = |\sin(\theta)|. \tag{4.114}$$

Mathematically speaking, a mixed quantum channel can be represented as a completely positive and trace-preserving operator (CPTP). This mechanism maps an input density operator

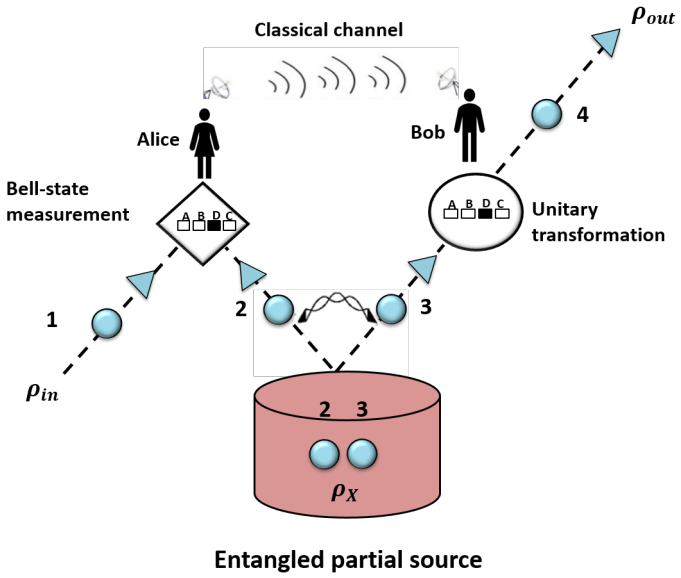


Figure 4.2: A schematic illustration of the quantum teleportation protocol using a mixed quantum state ρ_X as a quantum resource.

to an output density operator ρ_{out} via the function Φ [244], which can be expressed as

$$\rho_{\text{out}} = \Phi\left[\rho_{\text{in}}\right]. \tag{4.115}$$

The concept of CPTP maps will be further elaborated in Chapter 5. When a quantum state is teleported through a mixed channel ρ_{ch}, the resulting output replica state ρ_{out} can be derived by applying simultaneously joint measurements and the local unitary transformations on the input state $\rho_{\text{in}} = |\psi_{\text{in}}\rangle\langle\psi_{\text{in}}|$. This process can be expressed mathematically as follows:

$$\rho_{\text{out}} = \Phi\left[\rho_{\text{in}}\right] = \sum_{\mu,\nu=0}^{3} p_{\alpha\beta}(\sigma^{\mu}\otimes\sigma^{\nu})\rho_{\text{in}}(\sigma^{\mu}\otimes\sigma^{\nu}), \tag{4.116}$$

where $\sigma^0 = I$ is the 2×2 identity operator and σ^i $(i = x, y, z)$ stands for the familiar Pauli matrices. While $p_{\mu\nu} = p_\mu p_\nu$ represents the joint probabilites with $p_\mu = \text{Tr}\left(E^\mu\rho(t)\right)$ satisfy the following condition $\sum_{\mu,\nu} p_{\mu\nu} = 1$. Here, the projective measurements E^j are defined using the well-known Bell states as follows:

$$E^0 = |\beta_{00}\rangle\langle\beta_{00}|, \quad E^1 = |\beta_{01}\rangle\langle\beta_{01}|, \tag{4.117}$$
$$E^2 = |\beta_{10}\rangle\langle\beta_{10}|, \quad E^3 = |\beta_{11}\rangle\langle\beta_{11}|, \tag{4.118}$$

with $|\beta_{00}\rangle, |\beta_{01}\rangle, |\beta_{10}\rangle$ and $|\beta_{11}\rangle$ are given explicitly in Eqs.(2.6-2.9). In order to provide a general overview, we consider an arbitrary two-qubit quantum system described by the density operator in the form of the X-state given in Eq.(2.56) as a quantum channel, i.e., $\rho_{\text{ch}} = \rho_X$. In this case, the output density operator ρ_{out} takes the form:

$$\rho_{\text{out}} = \begin{pmatrix} \widetilde{\rho}_{11} & 0 & 0 & \widetilde{\rho}_{14} \\ 0 & \widetilde{\rho}_{22} & \widetilde{\rho}_{23} & 0 \\ 0 & \widetilde{\rho}_{23}^{*} & \widetilde{\rho}_{33} & 0 \\ \widetilde{\rho}_{14}^{*} & 0 & 0 & \widetilde{\rho}_{44} \end{pmatrix}, \tag{4.119}$$

where the non-zero teleported matrix elements are expressed as

$$\widetilde{\rho}_{11} = \widetilde{\rho}_{44} = (\rho_{11}+\rho_{44})(\rho_{22}+\rho_{33}), \tag{4.120}$$

$$\widetilde{\rho}_{14} = \widetilde{\rho}^{*}_{14} = (\rho_{14}+\rho^{*}_{14})(\rho_{23}+\rho^{*}_{23})\sin(\theta)\cos(\phi), \tag{4.121}$$

$$\widetilde{\rho}_{22} = (\rho_{11}+\rho_{44})^2\cos^2\left(\frac{\theta}{2}\right)+(\rho_{22}+\rho_{33})^2\sin^2\left(\frac{\theta}{2}\right), \tag{4.122}$$

$$\widetilde{\rho}_{33} = (\rho_{11}+\rho_{44})^2\sin^2\left(\frac{\theta}{2}\right)+(\rho_{22}+\rho_{33})^2\cos^2\left(\frac{\theta}{2}\right), \tag{4.123}$$

$$\widetilde{\rho}_{23} = \frac{1}{2}\left[(\rho_{23}+\rho^{*}_{23})^2 e^{i\phi}\sin\theta+(\rho_{14}+\rho^{*}_{14})^2 e^{-i\phi}\sin\theta\right]. \tag{4.124}$$

By knowing the output state, we can characterize the quality of the teleported state ρ_{out} by calculating several quantum corelations quantifiers such as concurrence, quantum discord and so on.

8.3 Fidelity of Entanglement Teleportation

In order to assess the effectiveness of the teleportation process, it is useful to examine the fidelity between the input and the output states. This allows us to evaluate the credibility and reliability of the secure information transmitted between Alice and Bob. For a pure input state, fidelity can be regarded as an effective indicator for evaluating the performance of a quantum channel as it provides information about the closeness of the teleported state to the input state [68,69,245,246]. It is defined as the overlap between the input and the output state, i.e., [5]

$$\mathcal{F} = \left|\langle\psi_{in}|\,\psi_{out}\rangle\right|^2. \tag{4.125}$$

Here, $|\psi_{in}\rangle$ is the input state that Alice wants to teleport, and $|\psi_{out}\rangle$ is the state received by Bob after the teleportation process. However, for a mixed input state ρ_{in}, the fidelity is defined as

$$\mathcal{F} = \langle\psi_{in}|\,\rho_{\text{out}}\,|\psi_{out}\rangle = \left(\text{Tr}\sqrt{\sqrt{\rho_{\text{in}}}\rho_{\text{out}}\sqrt{\rho_{\text{in}}}}\right)^2. \tag{4.126}$$

This quantity ranges from 0 to 1, where $\mathcal{F}=0$ means the input and output states are orthogonal, indicating that the information is completely destroyed during the transmission process and the teleportation fails. Conversely, a fidelity of unity indicates that the input and output states are identical, which is perfect teleportation. When $0<\mathcal{F}<1$, the quantum information is subject to distortions to some extent. However, in practice, fidelity can be affected by factors such as the quality of the quantum channel, the efficiency of the measurements, and the presence of noise or errors, causing the fidelity to be less than 1. Therefore, it is important to optimize these factors to achieve high-fidelity teleportation and reliable transmission of quantum information.

On the other hand, the concept of average fidelity provides a more comprehensive measure of the overall quality of teleportation performance, since it considers both the probability of success and the quality of the teleportation process. It quantifies how well the teleportation protocol can transfer the state of a qubit from one location to another on average. Since the parameters θ and ϕ are unknown, the average fidelity $\mathcal{F}_A$ is calculated over all the points of the Bloch sphere using the formula:

$$\mathcal{F}_A = \frac{1}{4\pi}\int_0^{2\pi} d\phi \int_0^{\pi} d\theta \mathcal{F}\sin\theta, \tag{4.127}$$

by integrating the above formula (4.127), the average fidelity $\mathcal{F}_A$ for our case can be hence written as

$$\mathcal{F}_A = \frac{1}{3}[(\rho_{11} + \rho_{44})^2 + (\rho_{23} + \rho_{23}^*)^2 + 2(\rho_{22} + \rho_{33})^2]. \tag{4.128}$$

It is clear that the average fidelity $\mathcal{F}_A$ depends mainly on the quantum channel parameters. To transmit the input quantum state $\mathcal{F}_A$ with better fidelity than any classical communication protocol, the average fidelity $\mathcal{F}_A$ must exceed $\frac{2}{3}$, which is the maximum achievable for classical communication.

Considering the above quantum teleportation scheme, we have studied in Ref. [80], quantum teleportation using a two-qubit Heisenberg XXZ spin-1/2 chain model as a quantum resource. During this study, we considered the influence of intrinsic decoherence on the transmission of information between the two parties involved in the teleportation process. We have shown that different parameters encoded in the two-qubit Heisenberg XXZ model are efficient to control parameters of quantum communications. Our research has demonstrated that the introduction of decoherence can degrade the quality of teleportation, making it crucial to consider the effects of decoherence when developing quantum communication protocols. In another contribution [68], we have studied the possibility of using a four-qubit square compound on the spin-1/2 Heisenberg XXZ model as a quantum channel for teleportation. Specifically, we have investigated the use of a thermal pairwise quantum state as a resource for quantum teleportation. We examined the impact of various parameters on the quality of the teleported state, such as the temperature, the strength of the magnetic field, and the coupling constants. We found that increasing the strength of the anisotropy parameter can enhance the quality of teleportation. This is because a stronger anisotropy parameter can increase the degree of entanglement between the qubits in the compound, which can lead to a more reliable transfer of quantum information. Overall, our studies contribute to the exploration of the effects of decoherence and thermal noise on quantum teleportation and could potentially lead to the development of more robust and reliable methods for quantum information processing.

8.4 Quantum teleportation via three-qubit system

Based on the standard teleportation process, we will provide an overview of quantum teleportation via the three-qubit quantum system using a given three-qubit mixed state ρ_{ABC} as a quantum resource [79]. This protocol aims to transmit the information encoded in an unknown one-qubit state from Alice, the sender, to two receivers, Bob and Cindy. For successful transmission, Alice possesses two qubits, where the first qubit represents the state to be teleported, namely $|\psi\rangle_u$, while the second qubit represents one of the three proposed qubits. On the other hand, Bob and Cindy hold the remaining two qubits. Bearing this in mind, the overall density operator of the system can be expressed as a compact form:

$$\rho_{uABC} = \rho_u \rho_{ABC}, \tag{4.129}$$

whereby the unknown density matrix is defined as $\rho_u = |\psi\rangle_u\langle\psi|_u$. In the following, we suppose that the unknown density operator has the following matrix form [79]:

$$\rho_u = \frac{1 - 2r_1}{2}|0\rangle\langle 0| + \frac{r_2}{2}(|1\rangle\langle 0| + |0\rangle\langle 1|) + \frac{1 + 2r_1}{2}|1\rangle\langle 1|. \tag{4.130}$$

Here, $0 \leq r_1 \leq 1$ and $r_2 = \sqrt{1 - r_1^2} \geq 0$. To transmit this input state to Cindy and Bob, Alice performs a joint Bell basis measurement on her two qubits. This measurement can be described by the following operators $M_{uA}^i \otimes I_{BC}$, where I_{BC} stands for the identity operator that acts on the combined system BC. The operators M_{uA}^i are given by

$$\begin{aligned} M_{uA}^1 &= |\beta_{00}\rangle_{uA}\langle\beta_{00}|, \quad M_{uA}^2 = |\beta_{01}\rangle_{uA}\langle\beta_{01}|, \\ M_{uA}^3 &= |\beta_{10}\rangle_{uA}\langle\beta_{10}|, \quad M_{uA}^4 = |\beta_{11}\rangle_{uA}\langle\beta_{11}|, \end{aligned} \tag{4.131}$$

where $\{|\beta_{00}\rangle, |\beta_{01}\rangle, |\beta_{10}\rangle, |\beta_{11}\rangle\}$ are the well-known Bell states, which are given explicitly in Eqs.(2.6-2.9). Once Alice obtains her measurement outcome i, she communicates with Bob and Cindy via a classical channel. Then, the combined state of Bob and Cindy's target system BC determined based on Alice's measurement outcomes is given as the following form [247, 248]

$$\rho_{BC}^i = \frac{1}{p_i} \mathrm{Tr}_{uA}[(M_{uA}^i \otimes I_{BC})\rho_{uABC}], \tag{4.132}$$

where p_i is the probability for Alice to obtain the measurement outcome i. It turns out to be

$$p_i = \mathrm{Tr}_{uABC}[(M_{uA}^i \otimes I_{BC})\rho_{uABC}]. \tag{4.133}$$

At this stage, in order to successfully complete this process, Bob and Cindy need perform i-dependent unitary operations $U^i = U_B^i = U_C^i$ on their own qubits B and C, respectively. Then, the output state is given by

$$\rho_{out}^i = U^j \rho^i U^{j\dagger}, \tag{4.134}$$

where U^i is defined as $U^1 = \sigma^x$, $U^2 = \sigma^y$, $U^3 = \sigma^0$, $U^4 = \sigma^z$, while $\rho^i = \mathrm{Tr}_C(\rho_{BC}^i) = \mathrm{Tr}_B(\rho_{BC}^i)$. In order to evaluate the quality of the state shared by Cindy and Bob, namely ρ_{out}^i, at the end of the process of quantum teleportation, compared to the input state ρ_u, one can evaluate the average fidelity. This is done by evaluating the fidelity over all possible Alice's measurement outcomes i and for all unknown states ρ_u on the Bloch sphere. It can be readily proved that the average fidelity can be expressed using a specific formula.

$$\mathcal{F}_A = \frac{1}{4\pi} \int_0^{2\pi} \int_0^{\pi} \sin\theta d\theta d\phi \sum_{i=1}^{4} p_i^i \mathcal{F}^i, \tag{4.135}$$

where $\mathcal{F}^i = \mathrm{Tr}(\rho_{out}^i \rho_u)$. Based on these results, we have studied in detail in Ref. [79] the quantum teleportation via the three-qubit system using a three-qubits mixed quantum state at thermal equilibrium as a quantum channel resource.

9 Conclusion

Due to the complex maximization process involved in the definition of entropic quantum discord, a fully rigorous algorithm for calculating this metric for a general bipartite quantum system, even for a simpler two-qubit quantum system, is still lacking. However, in this chapter, we have investigated alternative metrics of non-classical correlations based on the concept of quantum uncertainty, namely LQU and UIN. Their analytical expressions have been derived explicitly for arbitrary qubit-qudit systems. In the same respect, we have also studied the possibility of generalizing the definition of LQU for multipartite quantum systems. Moving on, we have studied another discord-like metric of non-classical correlation based on quantum coherence. Another concept that has been studied in this chapter is quantum Fisher information, where we have established its role in quantum metrology and quantum correlations. This connection makes it useful in building a bridge between quantum estimation theory and quantum correlations.

This chapter also explores the implications of quantum correlations in quantum information processing. Specifically, we have studied the concept of quantum teleportation, which relies on quantum correlations to transmit information between distant locations without actually physically moving the particles. Our analysis of quantum teleportation has mainly focused on the standard protocol. Despite its limitations in terms of transmission fidelity, quantum teleportation represents a key application of entanglement in modern quantum technologies, and further research in this area may lead to significant advances in quantum communication and computation.

All this makes the characterization and quantification of non-classical correlations in quantum systems an important task in quantum information processing. This is important to understand the decoherence effect. This approach will be the main subject of interest in the next chapter.

CHAPTER 5

DYNAMICS OF OPEN QUANTUM SYSTEMS

Open quantum systems (OQS) dynamics remained a hotspot for physicists and researchers in the case of quantum theory [72]. This field provides a complete and realistic description of a system that interacts with its surrounding environments, where such interaction can lead to undesirable effects such as dissipation and decoherence. These effects can have an impact on various research topics, including quantum information [5], quantum transport [249] and quantum optics [250]. The link connecting system and environment are inevitable and can lead to the deterioration of quantum information, which presents a significant challenge to practical quantum information processing. However, the theory of OQS provides mathematical and practical frameworks that consider the effects of the environment and describe the dynamics of such systems, addressing the challenges posed by these effects.

Decoherence is a significant challenge in understanding the dynamics of OQS [65]. It arises from system-environment correlations and refers to the process by which a quantum system loses coherence due to interactions with its environment [5, 66]. This results in a loss of the ability to observe quantum interference and leads to the appearance of classical behavior. In other words, it provides a mechanism by which quantum information stored in the system gets lost or becomes corrupted due to interactions with the environment [5]. Moreover, it is a major obstacle to the implementation of quantum information processing, as it limits the ability to maintain coherence over long timescales, which is necessary for many quantum computing tasks [5].

Recent advances in open quantum systems have enabled significant progress in the quantum processing, despite the challenges posed by decoherence [5, 72]. One such advance is the development of quantum error correction codes that can protect quantum states from the effects of decoherence [251]. Another important development is the use of quantum feedback control, which actively manipulates quantum systems to mitigate the effects of decoherence [252]. Furthermore, experimental studies of OQS and decoherence have also played a crucial role in advancing our understanding of these phenomena [253]. In particular, the development of quantum computers has provided a testbed for studying the effects of decoherence and identifying strategies for mitigating its effects [254]. By studying the sources of decoherence in quantum computers, researchers have been able to develop new techniques for improving their performance and enhancing their computational capabilities [255]. Overall, these advances have opened up exciting new possibilities for quantum information processing and promise to have a significant impact on a wide range of scientific and technological fields.

Dynamics of OQS remains a challenging task, as its linkage with the environment breaks the system's isolation as well as quantum characteristics, and are not definable using time unitary operations. In general, making the solution of motion's equation for such a system is

a challenging task [72] and the dynamics of OQS could be further assumed into the categories of Markovian or non-Markovian, depending on the nature of the system-environment coupling. In the Markovian process, an inevitable and permanent loss of information occurs from the original system to the linked environment. This loss of information makes the evolution of the system memoryless and independent of its initial state. On the other hand, if the condition of the Markovian process is violated, it leads to a non-Markovian process. In a non-Markovian dynamical maps, an information exchange between the linked environment and relative system occurs where this kind of dynamical maps might have a significant impact on the recovery of information and previous states of the open quantum systems [72, 256].

This chapter provides the readers the fundamental concepts and techniques regarding the dynamics of OQS. This chapter is organized as follows: Sec.1 introduces the relative mathematical as well as physical axioms required for describing closed quantum systems. In Sec.2, we study the framework of the theory of OQS, providing the necessary mathematical tools for a comparative study between the two, including the difference between Markovian and non-Markovian regimes. Further, the universal dynamical maps and their relative relationship with the evolution of open quantum systems are disscussed in Sec.3. Sec.4 presents the microscopic derivation of the Markovian quantum master equation, while Sec.5 defines the Lindblad master equation in non-Markovian dynamics. Finally, Sec.6 derives the time dynamics of the density matrices using the Milburn decoherence scheme.

1 Closed quantum systems

The time-dynamics of a system in the classical framework are typically controlled by several differential equations, including Hamilton's equations, Liouville equation, Euler-Lagrange's equations and so on. However, these methods can exhibit different properties based on the physical system they belong to. In quantum information, the primary subject is to determine the quantum counterpart of these classical approaches using quantum laws. In this inspiration, Erwin Schrödinger provided the initial quantum approach to characterize the time evolution of a quantum closed system with Markovian regime, such as energy and/or matter, with its surroundings [257, 258].

1.1 For pure states

According to the postulate (see Sec.2.2), the dynamics of a quantum state $|\kappa(t)\rangle \in \mathcal{H}$ representing a closed physical system at any given time t, defined by the Schrödinger equation, where $\mathcal{H}$ is the Hilbert space of the total system. It is defined as

$$i\hbar \frac{d}{dt} |\kappa(t)\rangle = H(t) |\kappa(t)\rangle . \tag{5.1}$$

Here, $H(t)$ denotes the total Hermitian Hamiltonian operator of the given system with $H^\dagger(t) = H(t)$. For the remainder of this thesis, we consider $\hbar$ as an energy unit ($\hbar = 1$). Moreover, the Schrödinger equation has an important characteristic of maintaining the norm of quantum states. Indeed, we have

$$\begin{aligned} \frac{d}{dt} \langle \kappa(t) | \kappa(t) \rangle &= \left(\frac{d \langle \kappa(t)|}{dt} \right) |\kappa(t)\rangle + \langle \kappa(t)| \left(\frac{d |\kappa(t)\rangle}{dt} \right) \\ &= i \langle \kappa(t)| H^\dagger(t) |\kappa(t)\rangle - i \langle \kappa(t)| H(t) |\kappa(t)\rangle = 0. \end{aligned} \tag{5.2}$$

Due to the linearity of the Schrödinger equation (5.1), its solution can be expressed in terms of the time unitary operation $U(t, t_0)$ as

$$|\kappa(t)\rangle = U(t, t_0) |\kappa(t_0)\rangle , \tag{5.3}$$

with $|\kappa(t_0)\rangle$ being the initial state. Let us notice that $U(t,t_0)$ is the evolution/propagator/time shift operator, evolves or changes the original state $|\kappa(t_0)\rangle$ to the quantum state $|\kappa(t)\rangle$. Moreover, this operator depends only on the time intervals, $t_0(t)$ initial(later) times. By substituting the state (5.3) back into Eq.(5.1), it therefore follows that the unitary operator $U(t,t_0)$ satisfies the following differential equation:

$$i\frac{d}{dt}U(t,t_0) = H(t)U(t,t_0), \tag{5.4}$$

with $U(t_0,t_0) = I$. The Hermiticity of $H(t)$ ensures the unitarity of $U(t,t_0)$. In fact, the Hamiltonian generates the time evolution through Eq.(5.4) and completely determines everything related to the dynamics of non-open quantum systems with time. By using Dyson expansion [72], one can formally obtain $U(t,t_0)$ acting on $|\kappa(t)\rangle$ from the expression (5.4) as follows:

$$U(t,t_0) = \mathcal{T}_{\leftarrow}\exp\left[-i\int_{t_0}^{t} H\left(t'\right)dt'\right], \tag{5.5}$$

where $\mathcal{T}_{\leftarrow}$ in Eq.(5.5) is the chronological operator for time ordering and is used to make the time-dependent operators in order to increase from the right to the left. However, for the time-independent function $H(t) = H$, $U(t,t_0)$ (5.5) can be simply written as

$$U(t,t_0) = \exp\left[-i\left(t-t_0\right)H\right]. \tag{5.6}$$

The above formula reveals that the time-evolution of $|\kappa(t)\rangle$ in the time-independent Hamiltonian system is simply a unitary rotation governed by the Hamiltonian H and the time interval $(t-t_0)$.

1.2 For mixed states

To discuss the time-evolution of a non-local statistical mixture, a varying approach is required as compared to the previous situation where a pure quantum state was considered. The ensemble of a statistical mixture cannot be characterized by a state vector alone. Instead, we use the density matrix formalism, as described in Sec.2.2, to represent the statistical mixture. To derive the time-dynamics of the closed system's density operator $\rho(t)$, we start with the original state $\rho(t_0)$ represented as [259]

$$\rho(t_0) = \textstyle\sum_i \omega_i \left|\kappa_i(t_0)\right\rangle\left\langle\kappa_i(t_0)\right|, \tag{5.7}$$

where ω_i are the non-negative weights and $|\kappa_i(t_0)\rangle$ denotes the associated initial state vectors. Since these states are time-dependent in accordance with the unitary evolution stated in Eq.(5.3), then the evolved state $\rho(t)$ is expressed by the following formula:

$$\begin{aligned}\rho(t) &= \textstyle\sum_i \omega_i U(t,t_0)\left|\kappa_i(t_0)\right\rangle\left\langle\kappa_i(t_0)\right|U^{\dagger}(t,t_0)\\ &= U(t,t_0)\rho(t_0)U^{\dagger}(t,t_0).\end{aligned} \tag{5.8}$$

The above expression (5.8) takes the form

$$\rho(t) = V(t,t_0)\left[\rho(t_0)\right], \tag{5.9}$$

with $V(t,t_0)$ is referred to as the linear operator which acts as

$$V(t,t_0)\left[X\right] = U(t,t_0)XU^{\dagger}(t,t_0), \tag{5.10}$$

with X is an arbitrary operator that acts on the Hilbert space $\mathcal{H}$. Therefore, the time derivation of the state $\rho(t)$ leads to the so-called Liouville–von Neumann equation, which is given as follows

$$\frac{d\rho(t)}{dt} = -i\left[H(t), \rho(t)\right]. \tag{5.11}$$

This formula is reformulated using for the Liouville operator $\mathcal{L}(t)$ as

$$\frac{d\rho(t)}{dt} = \mathcal{L}(t)\,\rho(t), \tag{5.12}$$

where $\mathcal{L}(X) = -i\,[H(t), X]$. The formula (5.12) shows the time-evolution under study for the density operator and provides a resourceful way to study the dynamical map/behavior of quantum systems. Moreover, the Eq.(5.9) represents the Banach space element regarding the class of traceable self-adjoint operators, namely $\mathcal{B}$. Whilst $V(t, t_0)$ in Eq.(5.10) is the linear operator that acts over this space $\mathcal{B}$ [257, 258]. Therefore, one can study that the evolution operator of pure states projected into the evolution operator for mixed states. Thus, the general solution of Eq.(5.12) is determined as follows

$$\rho(t) = V(t, t_0)\left[\rho(t_0)\right] = \mathcal{T}_{\leftarrow} \exp\left[\int_{t_0}^{t} \mathcal{L}(t')dt'\right] \rho(t_0), \tag{5.13}$$

and by taking the derivative we can immediately arrive at Eq.(5.11).

1.3 Interaction picture

So far, the Liouville-von Neumann equation has been derived using the Schrödinger picture. In this representation, the quantum state evolves in time whilst the operators remain invariant. However, the opposite situation can also be discussed, which corresponds to the Heisenberg picture. In this situation, the quantum state remains fixed and the operators evolve in time. Dividing the total Hamiltonian into two parts, a free part and an interaction part allows for a clear distinction between the evolution of the system caused by the free Hamiltonian and the evolution due to the interaction. This gives rise to another formulation known as the interaction picture or Dirac representation, where both states and operators evolve in time. The characteristics of these three pictures and their interconnection are summarized in table5.1. It is important to emphasize that the Schrodinger and Heisenberg pictures are both limited and do not provide a general description of physical systems (see table5.1). An alternative representation that should be considered is the interaction picture. This approach reflects a more comprehensive description as it takes into account not only the closed system of the Hamiltonian H_0 but also includes the interaction of Hamiltonian H_I between two or more sub-systems, that is,

$$H(t) = H_0 + H_I(t). \tag{5.14}$$

This split provides a powerful tool for the study of quantum mechanics as it facilitates the analysis and comprehension of the effect of interactions on the system under study. Moreover, it enables the determination of the expectation value of any given Schrödinger observable $O(t)$. Such that

$$\langle O(t)\rangle = \mathrm{Tr}\left[O(t)U(t, t_0)\rho(t_0)\,U^{\dagger}(t, t_0)\right]. \tag{5.15}$$

Here, $O(t)$ is assumed to be time-dependent and the operator $U(t, t_0)$ turns out to be

$$U(t, t_0) = U_0(t, t_0)U_I(t, t_0), \tag{5.16}$$

Pictures	Schrödinger	Heisenberg	Interaction
Time-evolution operator	$U_{Sc}(t,t_0) = \mathcal{T}_{\leftarrow}\exp\left[-i\int_{t_0}^{t} H_{Sc}(t')dt'\right]$	$U_{He}(t,t_0) = \mathcal{T}_{\leftarrow}\exp\left[-i\int_{t_0}^{t} H_{He}(t')dt'\right]$	$U_{In}(t,t_0) = \exp\left[-i\left(t-t_0\right)H_{In}\right]$
State vector	$\left\|\kappa(t)\right\rangle_{Sc} = U_{Sc}(t,t_0)\left\|\kappa(t_0)\right\rangle$	$\left\|\kappa(t)\right\rangle_{He} = \left\|\kappa(t_0)\right\rangle$	$\left\|\kappa(t)\right\rangle_{In} = U_{In}^{\dagger}(t,t_0)\left\|\kappa(t)\right\rangle_{Sc}$
Density matrix	$\rho_{Sc}(t) = U_{Sc}(t,t_0)\rho_{Sc}(t_0)\,U_{Sc}^{\dagger}(t,t_0)$	$\rho_{He} = \rho_{Sc}(t_0)$	$\rho_{In}(t) = U_{In}^{\dagger}(t,t_0)\rho_{Sc}(t)\,U_{In}(t,t_0)$
Observables	$O_{Sc} = O_{He}(t_0)$	$O_{He}(t) = U_{He}^{\dagger}(t,t_0)O(t_0)\,U_{He}(t,t_0)$	$O_{In}(t) = U_{In}^{\dagger}(t,t_0)O_{Sc}U_{In}(t,t_0)$
Time derivative	$\frac{d\rho_{Sc}(t)}{dt} = -i\left[H_{Sc}(t),\rho_{Sc}(t)\right]$	$\frac{dO_{He}(t)}{dt} = -i\left[H_{He}(t),O_{He}(t)\right]$	$\frac{d\rho_{In}(t)}{dt} = -i\left[H_{In}(t),\rho_{In}(t)\right]$

Table 5.1: The basic characteristics of the three pictures, namely Schrödinger, Heisenberg, and interaction pictures as well as the connection between them.

with

$$U_0(t,t_0) = \exp\left[-i\left(t-t_0\right)H_0\right]. \tag{5.17}$$

The expectation value provided by Eq.(5.15) can be then expressed using $U_0(t,t_0)$ and $U_I(t,t_0)$ as follows

$$\begin{aligned}\left\langle O(t)\right\rangle &= \mathrm{Tr}\left[U_0^{\dagger}(t,t_0)O(t)U_0(t,t_0)U_I(t,t_0)\rho\left(t_0\right)U_I^{\dagger}(t,t_0)\right]\\ &= \mathrm{Tr}\left[O_I(t)\rho_I\left(t\right)\right],\end{aligned} \tag{5.18}$$

where $O_I(t)$ and $\rho_I\left(t\right)$ are, respectively, the time-dependent observable and the density operator in the interaction representation. They can be expressed as follows

$$O_I(t) = U^{\dagger}(t,t_0)O(t)U(t,t_0), \tag{5.19}$$

$$\rho_I\left(t\right) = U(t,t_0)\rho\left(t_0\right)U^{\dagger}(t,t_0). \tag{5.20}$$

The interesting point to make here is that the interaction picture is regarded as a useful tool in quantum mechanics, since it provides a bridge between the Heisenberg and Schrödinger pictures in different circumstances. When the Hamiltonian is only represented by the free Hamiltonian part, i.e. $H_I(t) = 0$, such that $U(t,t_0) = U_0(t,t_0)\,(U_I(t,t_0) = I)$. In this case, the interaction and Heisenberg representations are both equivalent. Conversely, if the Hamiltonian comprises only the interaction part, $H(t) = H_I(t)$, that is, $U(t,t_0) = U_I(t,t_0)\,(U_0(t,t_0) = I)$, the interaction picture becomes identical to the Schrödinger picture. The evolution operator $U_I(t,t_0)$ in the interaction representation is the solution of the time-dependent differential equation. This gives

$$i\frac{\partial}{\partial t}U_I(t,t_0) = \widehat{H}_I(t)U_I(t,t_0), \qquad U_I(t_0,t_0) = I, \tag{5.21}$$

where $\widehat{H}_I(t)$ refers to the interaction Hamiltonian in the interaction picture. It takes the following form

$$\widehat{H}_I(t) = U^{\dagger}(t,t_0)H_I(t)U(t,t_0). \tag{5.22}$$

Therefore, the corresponding Liouville–von Neumann equation associated with the density operator in the interaction picture $\rho_I(t)$ is given by

$$\frac{d\rho_I\left(t\right)}{dt} = -i\left[\widehat{H}_I(t),\rho_I\left(t\right)\right]. \tag{5.23}$$

The above equation of motion (5.23) may be formally integrated to obtain

$$\rho_I(t) = \rho_I(t_0) - i\int_{t_0}^{t} dt' \left[\widehat{H}_I(t'), \rho_I\left(t'\right)\right], \tag{5.24}$$

where $\rho_I(t_0)$ denotes the initial state of the quantum system at time t_0 in the interaction picture. Moreover, Eq.(5.24) provides a way to study the time evolution of the density matrix in the interaction representation and it is used in quantum mechanics as well as quantum information theory to study the dynamics of open quantum systems. This will be the main topic of the following section.

2 Open quantum systems

A closed quantum system is an ideal quantum system that is completely isolated from its surrounding environments, meaning that it is unaffected by any external interactions or disturbances. In such circumstances, the quantum state evolves following unitary dynamics, ensuring that the total probability is conserved over time and the state remains pure. The unitary evolution is described by a unitary operator, which can be represented mathematically by Eq.(5.11). In contrast, an open quantum system S is coupled to the environment E, leading to a non-unitary evolution of the system state. This non-unitary evolution is caused by the loss of information and the degradation of quantum coherences due to the interaction with the environment. Although the combined system, including both the system and environment, can be considered a closed system and the reduced dynamics of sub-system S alone are non-unitary due to the interaction with the environment [72]. The total state of the system and environment $(S+E)$ can be described using the tensor product of their respective Hilbert spaces $\mathcal{H}_{SE} = \mathcal{H}_S \otimes \mathcal{H}_E$ and the dimension of the whole space is $dim(\mathcal{H}_{SE}) = dim(\mathcal{H}_S).dim(\mathcal{H}_E)$.

2.1 Description of open quantum systems

In general, the total Hamiltonian $H(t)$ of the combined system $(S+E)$ can be considered to be of the following form in time evolution as

$$H(t) = H_S \otimes I_E + I_S \otimes H_E + H_{SE}(t), \tag{5.25}$$

where H_S stands for the self-Hamiltonian of the system, H_E denotes the Hamiltonian of the environment and $H_{SE}(t)$ is the Hamiltonian describing the interaction between both. While $I_S\,(I_E)$ is the identity operator in the Hilbert space $\mathcal{H}_S\,(\mathcal{H}_E)$. For the sake of simplicity, we omit the tensor product symbol " $\otimes$ " and instead we rewrite the total Hamiltonian (5.25) as

$$H(t) = H_S + H_E + H_{SE}(t). \tag{5.26}$$

Moreover, the interaction between these two parts can lead to the generation of correlations between them. A schematic representation is illustrated in Fig.5.1. It is crucial to note that the specific forms of H_S, H_E and $H_{SE}(t)$ depend in the first place on the system and environment under consideration, as well as the nature of the interaction between them. In many physical situations, solving a complete mathematical model of the dynamics of a coupled system can be extremely complex. This complexity is compounded by the presence of the environment, which can be a reservoir or a heat bath with infinitely many degrees of freedom [72]. Solving this type of problem requires an infinite hierarchy of coupled equations of motion, making it challenging to accurately predict the behavior of the system and understand the underlying physical processes. To simplify the problem, researchers often isolate the relevant physical quantities by taking

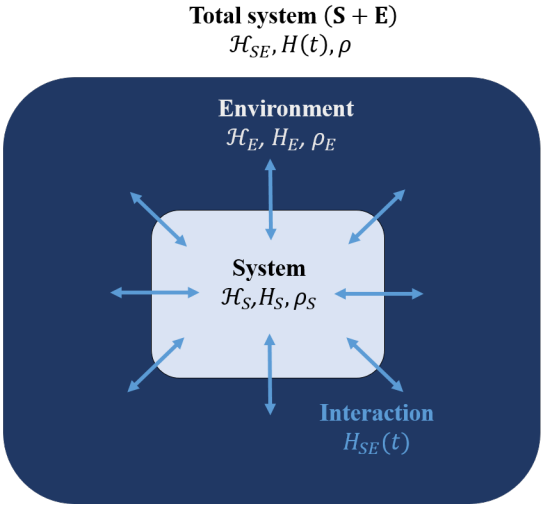


Figure 5.1: A schematic representation of the interaction between the system and its environment.

averages over the remaining, irrelevant degrees of freedom of the environment. However, this task can be complicated when the modes of the environment are unknown or uncontrollable. To address this challenge, researchers develop simpler descriptions of the system in a reduced state space formed by a restricted set of physically relevant variables. This approach is achieved by using various analytical methods and approximation techniques [260]. All observables related to an open system, denoted by S, can be expressed using the form of $\mathcal{O}_S \otimes I_E$. Here, $\mathcal{O}_S$ is referred to as an arbitrary observable acting on the Hilbert space $\mathcal{H}_S$. The expectation value of any observable that acts on the open system's Hilbert space can be obtained via the following expression:

$$\langle \mathcal{O}_S \rangle = \mathrm{Tr}\left[\mathcal{O}_S \rho_S\right], \tag{5.27}$$

where ρ_S stands for the reduced density matrix of the sub-system S, which is derived via the standard technique of tracing out only the degrees of freedom of the environment E from the total state ρ. This gives [72]

$$\rho_S \equiv \mathrm{Tr}_E\left[\rho\right]. \tag{5.28}$$

The formula mentioned above provides a crucial tool for describing the dynamical behavior of open quantum systems. It allows us to derive the time-dependent reduced density matrix $\rho_S(t)$ that describes the open system S at any given time t from the total state $\rho(t)$ of the entire system. Since the state of the combined system $(S+E)$ evolves according to a unitary evolution, we have

$$\rho_S = \mathrm{Tr}_E\left[U(t,t_0)\rho(t_0)\,U^{\dagger}(t,t_0)\right], \tag{5.29}$$

where $\rho(t_0)$ is the initial state of the total system, while $U(t,t_0)$ denotes the time-evolution operator of the total system. Similarly, the partial trace over the environment on both sides of the Liouville-von Neumann equation yields the following equation of motion for the reduced density matrix in the Schrödinger picture:

$$\frac{d}{dt}\rho_S(t) = -i\mathrm{Tr}_E\left[H_S + H_E + H_{SE}(t), \rho(t)\right]. \tag{5.30}$$

In the following, we aim to provide a full description of the most important equations of motion for the reduced density matrix used to explain the dynamical behaviors of open quantum

systems. These equations are employed to reduce the complexity of the exact reduced Liouville-von Neumann equation above while still preserving all of its key features.

2.2 Markovian and non-Markovian dynamics

Open quantum systems (OQS) are classified into two main categories based on how they encode and lose information, namely Markovian and non-Markovian, as illustrated in Fig.5.2. In the Markovian regime (see Fig.5.2.a), the interaction between the system and its surrounding environment causes a one-way flow of information, resulting in the loss of coherence and information from the system to the environment [53, 54, 257]. This kind of information loss is irreversible and the environment does not retain any information that can be used to recover the lost coherence or information later on. Therefore, this regime is known as *"memoryless"*. The evolution of the OQS in this case is solely determined by its current state. Conversely, non-Markovian regimes allow for the partial or complete recovery of lost information during the evolution of OQS (see Fig.5.2.b). This recovery occurs due to the interaction between the system and its environment, which allows the environment to maintain information about the system, leading to a temporary increase in the OQS information known as a *"backflow of information"*. In non-Markovian regimes, the system's past evolution in addition to its present state affects its evolution, making it distinct from Markovian dynamics where the present state is sufficient to predict the system's future evolution. The ability to recover lost information is essential for applications such as quantum computing, where preserving quantum coherence is necessary for implementing quantum algorithms. Non-Markovian dynamics are characterized by non-monotonic changes in the quantifiers of encoded information, such as entropy or fidelity. These changes reflect the intricate interplay between the system and its environment [54,69,72].

To distinguish between the two dynamics, a mathematical framework is employed which relies on the divisibility property of the maps that describe the OQS dynamics. Markovian evolutions possess divisible maps that can be decomposed into smaller maps that describe shorter time intervals [261]. This property enables the interaction between the system and its environment to be treated as a sequence of shorter interactions, resulting in the irreversibility of information flow. Moreover, in Markovian regimes, the dynamical map describes the system's evolution when it is weakly coupled to the environment, meaning that the environment does not significantly affect the system's evolution. This enables us to divide the evolution of the system into smaller, independent steps and describe it using a time-local master equation, which is a differential equation governing the evolution of the system density matrix [72]. On the other hand, in the non-Markovian regime, the dynamical map does not fulfill the divisibility property since the system's evolution is affected by its past states and its interaction history with the environment. Therefore, it cannot be divided into smaller, independent steps. As a result, the system may exhibit memory effects, where lost information is temporarily recovered at one or more time intervals during the evolution. The evolution of the system cannot be described using a time-local master equation, and more general approaches such as integrodifferential equations or non-Markovian quantum stochastic processes are needed to describe the evolution of the system [258].

Understanding Markovian and non-Markovian regimes is critical to the advancement of quantum technologies, including quantum computing and quantum communication. In quantum computing, preserving quantum coherence is essential for implementing quantum algorithms, making it crucial to comprehend the distinctions between Markovian and non-Markovian dynamics [72]. This knowledge is fundamental to developing quantum error correction codes that can safeguard against coherence loss [258]. In quantum communication, non-Markovian dynamics can enhance the security of communication protocols by enabling the recovery of lost information resulting from eavesdropping [262].

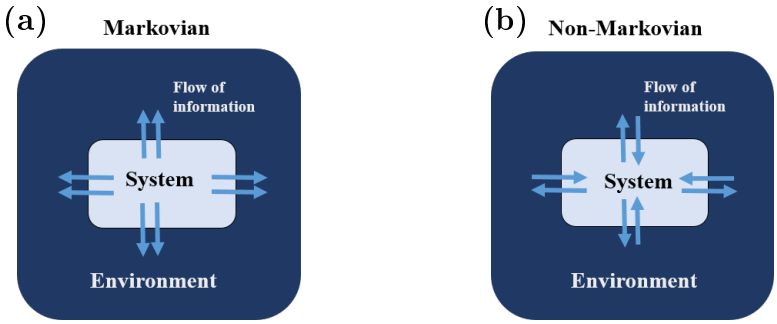


Figure 5.2: In Markovian dynamics (a), there is only a one-way information flow from system S to environment E, and any encoded information in the system cannot be recovered during its evolution. On the other hand, in non-Markovian dynamics (b), the system can experience information backflow, where the flow of information reverses from environment E to system S for one or more time intervals. This is a unique feature of non-Markovian dynamics.

3 Deriving the evolution of open quantum systems using Kraus operators and dynamical maps

Assuming the initial density operator of an open quantum system is represented by $\rho_S(0)$, its evolution over time can be described mathematically as a map from a set of density operators to itself. This map is denoted by $\Phi(t,0)$ and corresponds to time t. To obtain the density operator of the system at any given time t, denoted by $\rho_S(t)$, the map is applied to the initial density operator as follows [72]:

$$\rho_S(0) \to \Phi(t,0)\,\rho_S(0) = \rho_S(t)\,. \tag{5.31}$$

The quantum dynamical map $\Phi(t,0)$ can be fully characterized using operators that are associated with the open system within the Hilbert space $\mathcal{H}_S$, and it maps the set of density operators $\mathcal{S}(\mathcal{H}_S)$ acting on the Hilbert space $\mathcal{H}_S$ to itself (see Fig.5.3). That is

$$\Phi(t,0) : \mathcal{S}(\mathcal{H}_S) \to \mathcal{S}(\mathcal{H}_S). \tag{5.32}$$

Here, $\mathcal{S}(\mathcal{H}_S)$ denotes the standard notation for the algebra of bounded linear operators on a Hilbert space $\mathcal{H}_S$. Moroever, the dynamical map describes a physical process that conserves the properties of the system under evolution. However, this map is called a dynamical map since it describes the change in the state of the system over time [72].

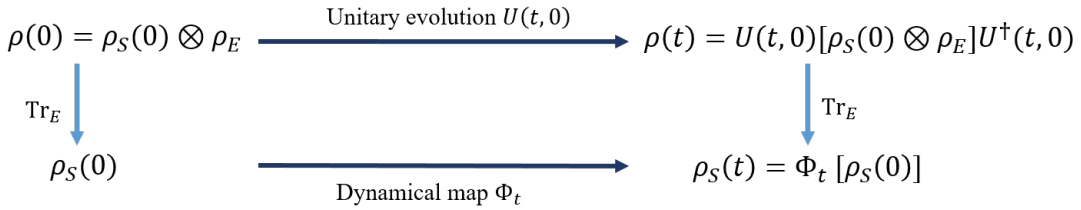


Figure 5.3: Schematic illustration showing the action of the quantum dynamical map.

Assuming that the system and its surrounding environment are initially uncorrelated, i.e., they are separable. The initial state of the entire system in this case $(S+E)$ can be written as a tensor product of the individual states of the system and environment, which is referred to as an uncorrelated product state. This gives

$$\rho(0) = \rho_s(0) \otimes \rho_E, \tag{5.33}$$

where $\rho_s(0)$ represents the initial state of the system S, while $\rho_E \equiv \mathrm{Tr}_S[\rho]$ stands for the state of the environment; which is assumed to be fixed during the evolution. In order to obtain the reduced open system state, one can take the partial trace of the total system-environment state over the degrees of freedom of the environment after evolving the composite system using the unitary time-evolution operator from initial time 0 to time t. This operation is mathematically expressed as:

$$\rho_S(t) = \mathrm{Tr}_E\left[U(t,t_0)\left(\rho_s(0)\otimes\rho_E\right)U^\dagger(t,t_0)\right]. \tag{5.34}$$

The above expression (5.34) allows us to calculate the reduced open system state at any time t, given the initial state of the system and the unitary time-evolution operator of the composite system. It can be rewritten in the following form

$$\rho_S(t) = \Phi(t,0)\,\rho_S(0) = \mathrm{Tr}_E\left[U(t,t_0)\left(\rho_s(0)\otimes\rho_E\right)U^\dagger(t,t_0)\right], \tag{5.35}$$

with $\Phi(t,0)$ depends only on the unitary time-evolution operator $U(t,t_0)$ and the fixed state of the environment ρ_E. Since the state of the environment ρ_E is both positive and normalized, it can be decomposed spectrally on an orthonormal basis consisting of positive eigenvalues. Hence, it follows that

$$\rho_E = \textstyle\sum_\nu \lambda_\nu |\psi_\nu\rangle\langle\psi_\nu|. \tag{5.36}$$

Here, λ_ν stands for the eigenvalues of ρ_E, which satisfy the condition $\sum_\nu \lambda_\nu = 1$, while $|\psi_\nu\rangle$ represents the associated orthonormal eigenvectors. By substituting Eq.(5.36) into expression (5.35), we thus obtain [5]

$$\begin{aligned}
\Phi(t,0)\,\rho_S(0) &= \mathrm{Tr}_E\left[U(t,t_0)\left(\rho_s(0)\otimes\textstyle\sum_\nu \lambda_\nu |\psi_\nu\rangle\langle\psi_\nu|\right)U^\dagger(t,t_0)\right] \\
&= \textstyle\sum_\mu |\psi_\mu\rangle\left[U(t,t_0)\left(\rho_s(0)\otimes\sum_\nu \lambda_\nu |\psi_\nu\rangle\langle\psi_\nu|\right)U^\dagger(t,t_0)\right]\langle\psi_\mu| \\
&= \textstyle\sum_{\mu,\nu} \sqrt{\lambda_\nu}\,\langle\psi_\mu|U(t,t_0)|\psi_\nu\rangle\,\rho_s(0)\sqrt{\lambda_\nu}\,\langle\psi_\nu|U^\dagger(t,t_0)|\psi_\mu\rangle.
\end{aligned} \tag{5.37}$$

The above formula (5.37) yields the following representation

$$\rho_S(t) = \Phi(t,0)\,\rho_S(0) = \textstyle\sum_{\mu,\nu} K_{\mu\nu}(t)\,\rho_s(0)K_{\mu\nu}^\dagger(t), \tag{5.38}$$

where $K_{\mu\nu}(t)$ represents the Kraus operators acting on the state $\rho_S(0)$. They are expressed as [260]

$$K_{\mu\nu}(t) = \sqrt{\lambda_\nu}\,\langle\psi_\mu|U(t,t_0)|\psi_\nu\rangle \tag{5.39}$$

Thus, Eq.(5.38) describes the evolution of the system in terms of Kraus operators [260]. However, it is necessary to ensures the normalization of the system state during its evolution. This condition requires that

$$\mathrm{Tr}\left[\rho_S(t)\right] = \mathrm{Tr}\left[\textstyle\sum_{\mu,\nu} K_{\mu\nu}(t)\,\rho_s(0)K_{\mu\nu}^\dagger(t)\right] = \mathrm{Tr}\left[\sum_{\mu,\nu} K_{\mu\nu}^\dagger K_{\mu\nu}(t)\,\rho_s(0)\right] = 1. \tag{5.40}$$

It is easy to verify that the system state remains normalized if the Kraus operators satisfy the following identity given as follows

$$\textstyle\sum_{\mu,\nu} K_{\mu\nu}^\dagger K_{\mu\nu}(t) = I. \tag{5.41}$$

The above requirement can easily verified by using the definition of Kraus operators given by Eq.(5.39), which leads to

$$\begin{aligned}\sum_{\mu,\nu} K_{\mu\nu}^{\dagger} K_{\mu\nu}(t) &= \sum_{\mu,\nu} \lambda_\nu \langle\psi_\nu| U^{\dagger}(t,t_0) |\psi_\mu\rangle \langle\psi_\mu| U(t,t_0) |\psi_\nu\rangle \\ &= \sum_{\nu} \lambda_\nu \langle\psi_\nu| U^{\dagger}(t,t_0) \underbrace{\Big(\sum_{\mu} |\psi_\mu\rangle \langle\psi_\mu|\Big)}_{I} U(t,t_0) |\psi_\nu\rangle \\ &= \sum_{\nu} \lambda_\nu \langle\psi_\nu| U^{\dagger}(t,t_0) U(t,t_0) |\psi_\nu\rangle \\ &= \sum_{\nu} \lambda_\nu \langle\psi_\nu| \psi_\nu\rangle = \sum_{\nu} \lambda_\nu = I. \end{aligned} \tag{5.42}$$

(5.43)

The references [54, 69] appear to describe the use of Kraus operators to study the evolution of a qubit-qutrit system under random dephasing telegraphic noise. The noise can induce both Markovian and non-Markovian evolutions, and the Kraus operators are employed to describe the corresponding dynamics. Now, let us consider the case where the unitary operator takes the form following form $U(t,t_0) = U_S(t,t_0) \otimes U_E(t,t_0)$, where $U_S(t,t_0)$ acts on the system S and $U_E(t,t_0)$ acts on the environment E. In this case, the Kraus operators can be expressed as

$$\begin{aligned} K_{\mu\nu}(t) &= \sqrt{\lambda_\nu} \langle\psi_\mu| U_S(t,t_0) \otimes U_E(t,t_0) |\psi_\nu\rangle \\ &= U_S(t,t_0) \sqrt{\lambda_\nu} \langle\psi_\mu| U_E(t,t_0) |\psi_\nu\rangle \\ &= U_S(t,t_0) \mathcal{K}_{\mu\nu}(t), \end{aligned} \tag{5.44}$$

where $\mathcal{K}_{\mu\nu}(t) = \sqrt{\lambda_\nu} \langle\psi_\mu| U_E(t,t_0) |\psi_\nu\rangle$ represents the Kraus operators of the environment E. Using the expression (5.44), one can writes the normalization condition as:

$$\begin{aligned}\sum_{\mu,\nu} K_{\mu\nu}^{\dagger}(t) K_{\mu\nu}(t) &= \sum_{\mu,\nu} \Big(U_S(t,t_0)\sqrt{\lambda_\nu}\langle\psi_\mu|U_E(t,t_0)|\psi_\nu\rangle\Big)^{\dagger} \Big(U_S(t,t_0)\sqrt{\lambda_\nu}\langle\psi_\mu|U_E(t,t_0)|\psi_\nu\rangle\Big) \\ &= \sum_{\mu,\nu} \sqrt{\lambda_\mu\lambda_\nu}\langle\psi_\nu|U_E(t,t_0)^{\dagger} U_S(t,t_0)^{\dagger} U_S(t,t_0) U_E(t,t_0)|\psi_\mu\rangle. \end{aligned} \tag{5.45}$$

Since $U(t,t_0) = U_S(t,t_0) \otimes U_E(t,t_0)$ is a unitary operator, we have

$$U_E(t,t_0)^{\dagger} U_S(t,t_0)^{\dagger} U_S(t,t_0) U_E(t,t_0) = I, \tag{5.46}$$

Therefore, the normalization condition simplifies to:

$$\sum_{\mu,\nu} K_{\mu\nu}^{\dagger}(t) K_{\mu\nu}(t) = \sum_{\mu,\nu} \sqrt{\lambda_\mu\lambda_\nu}\langle\psi_\nu|\psi_\mu\rangle = \sum_{\mu} \lambda_\mu = 1, \tag{5.47}$$

where we have used the fact that the states $|\psi_\mu\rangle$ form an orthonormal basis for the Hilbert space of the environment $\mathcal{H}_E$. Hence, the normalization condition in this case is simply that the sum of the eigenvalues of the quantum channel is equal to 1, which in turn gives $\sum_{\mu,\nu} \mathcal{K}_{\mu\nu}^{\dagger}(t) \mathcal{K}_{\mu\nu}(t) = 1$. Therfore, the state that describes the evolution of the system S is given by

$$\begin{aligned}\rho_S(t) &= \sum_{\mu,\nu} \mathcal{K}_{\mu\nu}(t) U_S(t,t_0) \rho_s(0) \mathcal{K}_{\mu\nu}^{\dagger}(t) U\,\dagger_S(t,t_0) \\ &= \sum_{\mu,\nu} U_S(t,t_0) \rho_s(0) U\,\dagger_S(t,t_0) \end{aligned} \tag{5.48}$$

The above formula (5.48) represents the evolution of a closed quantum system. Thus, the Kraus operators provide a more general framework for describing the evolution of a quantum system, which includes the Schrödinger equation as a special case. This equation applies to closed quantum systems, where there is no interaction with an external environment. When there is such interaction, the evolution of the system is described by the more general Lindblad equation, which we will discuss later.

3.1 Properties of quantum channels with Kraus operators

A linear map Φ that admits a Kraus representation has to possess the following set of axiomatic properties [5, 260]:

- Linearity: The map Φ is linear, meaning that it obeys the superposition principle. That is, for any two input states, namely ρ_1 and ρ_2, and complex numbers a and b, we have

$$\begin{aligned}\Phi\left(a\rho_1 + a\rho_2\right) &= \sum_\alpha \mathrm{Tr}\left(K_\alpha a\rho_1 K_\alpha^\dagger\right) + \sum_\alpha \mathrm{Tr}\left(K_\alpha b\rho_2 K_\alpha^\dagger\right) \\ &= a\sum_\alpha \mathrm{Tr}\left(K_\alpha\rho_1 K_\alpha^\dagger\right) + b\sum_\alpha \mathrm{Tr}\left(K_\alpha\rho_2 K_\alpha^\dagger\right) \\ &= a\Phi\left(\rho_1\right) + b\Phi\left(\rho_2\right). \end{aligned} \tag{5.49}$$

- Hermiticity preservation: The quantum channel Φ preserves the property of hermiticity, which means that if the input state is hermitian, then the output state is also hermitian. That is

$$\left(\Phi\left(\rho\right)\right)^\dagger = \left(\sum_\alpha K_\alpha\rho K_\alpha^\dagger\right)^\dagger = \sum_\alpha \left(K_\alpha^\dagger\right)^\dagger \left(\rho\right)^\dagger \left(K_\alpha\right)^\dagger = \sum_\alpha K_\alpha\rho K_\alpha^\dagger = \Phi\left(\rho\right). \tag{5.50}$$

  This is an important property for quantum channels that are used in quantum information processing, as it ensures that certain important physical quantities are preserved when the state is passed through the channel. For example, the expectation values of observables that correspond to hermitian operators are preserved under hermiticity-preserving channels.

- Trace preservation: For any input quantum state ρ, a quantum channel Φ is said to be trace-preserving if it satisfies the following condition:

$$\mathrm{Tr}\left[\Phi\left(\rho\right)\right] = \mathrm{Tr}\left[\sum_\alpha K_\alpha\rho K_\alpha^\dagger\right] = \mathrm{Tr}\left[\underbrace{\sum_\alpha K_\alpha^\dagger K_\alpha}_{I}\rho\right] = \mathrm{Tr}\left[\rho\right] = 1. \tag{5.51}$$

  Therefore, we see that $\mathrm{Tr}\left[\Phi\left(\rho\right)\right] = \mathrm{Tr}\left[\rho\right]$, which means that the quantum channel Φ preserves the trace of the input state ρ. This shows that Φ is a trace-preserving map, which is an important property of a quantum channel as it ensures that probabilities are conserved under the quantum evolution described by the channel.

- Positivity preservation: The quantum channel Φ preserves the property of positivity, which means that if the input state is positive semidefinite, then the output state is also positive semidefinite. That is, if $\rho \geq 0 \Longrightarrow \Phi\left(\rho\right) \geq 0$. This is a crucial requirement for any physical process, as negative eigenvalues in a density matrix correspond to unphysical states. This property ensures that the output density matrix of a quantum channel will always be positive semidefinite, provided the input density matrix is positive semidefinite.

- Complete positivity: The quantum channel Φ is completely positive, which means for any extension $\mathcal{H}_E$ of the initial state space $\mathcal{H}_S$, we require that $\mathcal{H}_S \otimes \mathcal{H}_E \ni \rho_{SE} \geq 0 \Longrightarrow \left[\Phi_S \otimes I_E\right]\left(\rho_{SE}\right)$, independent of the particular dimension of $\mathcal{H}_E$. This condition is physically reasonable since we require not only the local evolution $\rho_S' = \Phi\left(\rho_S\right)$ of some subsystem S to be positivity-preserving but also any combined evolution $\rho_{SE}' = \left[\Phi_S \otimes I_E\right]\left(\rho_{SE}\right)$ which acts trivially on $\mathcal{H}_E$. Otherwise, such a combined evolution could lead to a joint state ρ_{SE}' that is not positive and, hence, not a valid density matrix.

A concrete example of a map that is positive but not completely positive is the transpose map. Let us suppose a two-qubit entangled Bell state

$$\left|\psi^{+}\right\rangle_{AB} = \frac{1}{\sqrt{2}}\left(|00\rangle_{AB} + |11\rangle_{AB}\right). \tag{5.52}$$

By applying the partial transpose with respect to the first qubit, then the partial transposed density matrix, $\rho_{AB} = \left|\psi^{+}\right\rangle_{AB}\left\langle\psi^{+}\right|$, becomes

$$\rho' = \left(T_A \otimes I\right)\rho = \frac{1}{2}\begin{pmatrix} 1 & 0 & 0 & 0 \\ 0 & 0 & 1 & 0 \\ 0 & 1 & 0 & 0 \\ 0 & 0 & 0 & 1 \end{pmatrix}, \tag{5.53}$$

where T_A is partial transposition operator on sub-system A. The eigenvalues of this operator are $1/2, 1/2, 1/2, -1/2$. Since it has a negative eigenvalue, it is not positive definite and therefore not a valid density matrix. This shows that the transpose map is not completely positive.

The set of axiomatic properties represents all necessary conditions for a quantum operation to be completely positive and trace-preserving (CPTP). This means that any dynamical map Φ satisfying these properties represents a valid transformation of quantum states and can be used in various quantum information processing tasks such as quantum error correction, quantum communication, and quantum computation. The Kraus representation is a powerful tool for constructing CPTP quantum operations, and it allows for the systematic design and analysis of quantum information protocols. When the time parameter t is allowed to vary over an interval $[0, T]$ where T can be either finite or infinite, this results in a one-parameter family of quantum dynamical maps denoted by [263]

$$\Phi = \left\{\Phi\left(t, 0\right) | 0 \leq t \leq T,\ \Phi\left(0, 0\right) = I\right\}. \tag{5.54}$$

Here, $\Phi\left(0, 0\right) = I$ represents the unit map or identity map and the density operator ρ_E remains fixed throughout the evolution. The family Φ provides a description of the time evolution of the open system over the interval $[0, T]$ and contains all the necessary information regarding the future evolution of all possible initial states of the system. By applying Φ to the initial state of the system, one can determine the state of the system at any time in the future. This makes the family Φ crucial for studying open quantum systems.

3.2 Kraus representation for general initial conditions

3.2.1 For separable states

Let us consider the case where the initial state is separable and examine how the output state can be expressed using the Kraus representation. Indeed, the separable state can be written as follows

$$\rho\left(0\right) = \sum_i p_i \rho_S^i \otimes \rho_E^i, \tag{5.55}$$

where ρ_S^i and ρ_E^i are, respectively, the states of the system and the environment. The initial state of the system is given as

$$\rho_S\left(0\right) = \mathrm{Tr}_E\left[\rho\left(0\right)\right] = \sum_i p_i \rho_S^i. \tag{5.56}$$

The spectral decomposition of the density matrix of the environment can be written as

$$\rho_E^i = \sum_{\nu_i} \zeta_{\nu_i} |\nu_i\rangle \langle\nu_i| , \tag{5.57}$$

where ζ_{ν_i} and $|\nu_i\rangle$ are the eigenvalues and eigenvectors of the state of the environment ρ_E^i, respectively. By performing the partial trace over the degrees of freedom of the environment, one obtains the reduced density matrix of the system as

$$\begin{aligned} \rho_S(t) &= \sum_{\mu,i,\nu_i} p_i \zeta_{\nu_i} \langle\mu| U(t,t_0) \rho_S^i \otimes |\nu_i\rangle \langle\nu_i| U^\dagger(t,t_0) |\mu\rangle \\ &= \sum_{\mu,i,\nu_i} \zeta_{\nu_i} \langle\mu| U(t,t_0) |\nu_i\rangle p_i \rho_S^i \langle\nu_i| U^\dagger(t,t_0) |\mu\rangle . \end{aligned} \tag{5.58}$$

If we assume that the states ρ_E^i commute, meaning that they are diagonal on the same basis so that $\nu_i \equiv \nu$, $\zeta_{\nu_i} \equiv \zeta_\nu$ and $\rho_E^i = \sum_\nu \zeta_\nu |\nu\rangle \langle\nu|$, then Eq. (5.58) yields

$$\rho_S(t) = \sum_{\mu,\nu} \zeta_\nu \langle\mu| U(t,t_0) |\nu\rangle \sum_i p_i \rho_S^i \langle\nu| U^\dagger(t,t_0) |\mu\rangle , \tag{5.59}$$

and this can be represented as a map acting on the state $\rho_S(0) = \sum_i p_i \rho_S^i$, which brings us back to Eq. (5.39) once again. However, this is only valid when the environment states are identical, i.e., $\rho_E^i = \rho_E$. In the general case, where the environment states are different $\rho_E^i \neq \rho_E$, we cannot express the evolution state of the system using the Kraus representation.

3.2.2 For general initial quantum states

By using a general orthonormal basis for the joint Hilbert space $\mathcal{H}_{S+E}$, we can express the bipartite initial state as follows

$$\rho(0) = \sum_{ijkl} \xi_{ijkl} |i\rangle \langle j| \otimes |k\rangle \langle l| . \tag{5.60}$$

By performing the trace over the environment E, the initial state of the system S is given by

$$\rho_S(0) = \mathrm{Tr}_E[\rho(0)] = \sum_{ijk} \xi_{ijkl} |i\rangle \langle j| . \tag{5.61}$$

The time-evolved state of the system S is then derived using the same procedure as in the derivation of Kraus operators. The result is given by the following formula

$$\begin{aligned} \rho_S(t) &= \sum_\mu \langle\mu| U(t,t_0) \rho_S(0) U^\dagger(t,t_0) |\mu\rangle \\ &= \sum_{\mu ijkl} \xi_{ijkl} \langle\mu| U(t,t_0) |i\rangle \langle j| \otimes |k\rangle \langle l| U^\dagger(t,t_0) |\mu\rangle \\ &= \sum_{\mu k} \langle\mu| U(t,t_0) |k\rangle \left(\textstyle\sum_{ij} \xi_{ijkk} |i\rangle \langle j| \right) \langle k| U^\dagger(t,t_0) |\mu\rangle \\ &\quad + \sum_{\mu,i,j,k\neq l} \langle\mu| U(t,t_0) |k\rangle \left(\textstyle\sum_{ij} \xi_{ijkl} |i\rangle \langle j| \right) \langle l| U^\dagger(t,t_0) |\mu\rangle , \end{aligned} \tag{5.62}$$

where first term on the right-hand side of Eq.(5.62) can be expressed in the Kraus form with Kraus operators $\langle\mu| U(t,t_0) |k\rangle$. However, the second term cannot be written in this form. This implies that there is no completely positive map that can describe the evolution of the system in this case. Therefore, it is not possible to get a map that transforms the initial state $\rho_S(0)$ into the time-evolved state $\rho_S(t)$ using a completely positive map in this case.

4 Standard theory of Markovian open quantum systems

In order to obtain a quantum master equation that depends only on the variables of the reduced system, certain assumptions need to be made. One such assumption is the neglect of the memory effects, which implies that the environment effectively forgets its past interactions with the system as the correlations disperse into the numerous environmental degrees of freedom. Despite being a strong assumption, it is reasonable on a coarse-grained time scale. The Markovian approximation is seen in the microscopic derivation, and can be expressed through the semigroup property for dynamical maps [72]:

$$\Phi\left(t_1+t_2,0\right)=\Phi\left(t_1,0\right)\Phi\left(t_2,0\right), \quad \forall t_1,t_2\geq 0. \tag{5.63}$$

The derivation of the Lindblad master equation will be carried out using both a dynamical semigroup approach and a microscopic theory that will shed light on the approximations used.

4.1 Markovian master equation

A quantum dynamical semigroup is a theoretical framework that aims to describe the behavior of an open quantum system that interacts with its surrounding environment. To achieve this, the framework employs an infinitesimal generator $\mathcal{L}$, which is expressed as [264]

$$\Phi\left(t,0\right)=\exp\left(\mathcal{L}t\right). \tag{5.64}$$

Here, $\mathcal{L}$ is the generator of the semigroup, and it represents a time-independent linear superoperator that acts on $\mathcal{S}(\mathcal{H}_S)$. It is worth noting that the generator $\mathcal{L}$ can be considered a generalization of the Liouvillian operator introduced in Eq.(5.12). The complete positivity of the semigroup has important implications for the structure of the generator. However, using formula (5.64) leads to a first-order differential equation of motion for the reduced density operator of the open system, denoted by $\rho_S\left(t\right)$, which is commonly known as the Markovian quantum master equation [72]. It is given as

$$\frac{d\rho_S\left(t\right)}{dt}=\mathcal{L}\rho_S\left(t\right). \tag{5.65}$$

According to the Gorini-Kossakowski-Sudarshan-Lindblad theorem [73, 74], the operator $\mathcal{L}$ is the generator of a semigroup of completely positive dynamical maps only if it admits the following generalized structure:

$$\frac{d\rho_S\left(t\right)}{dt}=\mathcal{L}\rho_S\left(t\right)=-i\left[H(t),\rho_S\left(t\right)\right]+\sum_i\gamma_i\left(A_i\rho_S\left(t\right)A_i^\dagger-\frac{1}{2}\left\{A_i^\dagger A_i,\rho_S\left(t\right)\right\}\right), \tag{5.66}$$

where $\{X,Y\}$ stands for the anti-commutator of operators X and Y. The above formula (5.66) describes the most general form for the generator of a quantum dynamical semigroup. The first part of the right-hand side of Eq.(5.66) reflects the unitary part of the dynamics generated by the Hamiltonian $H(t)$, which usually denotes the Hamiltonian of the system. Whilst the second part, called the dissipator, represents possible non-unitary effects induced by the environment. Moreover, the operators A_i are usually referred to as Lindblad operators, and the non-negative quantities $\gamma_i\geq 0$ are the associated decay rates, which have the dimension of an inverse time provided the A_i is taken dimensionless [72, 263]. Moreover, the operators A_i and decay rates γ_i describe respectively the types and strength of interactions between the system and its environment. In the absence of the dissipator term, Eq.(5.66) reduces to the von Neumann equation in the Schrödinger picture and produces unitary evolution (5.11). However, in the

presence of the dissipator, the system experiences non-unitary evolution due to its interactions with the environment. Usually, it is more useful to introduce the dissipator term, namely $\mathcal{D}(\rho_S(t))$, which is defined as

$$\mathcal{D}(\rho_S(t)) = \sum_i \gamma_i \left(A_i \rho_S(t) A_i^\dagger - \frac{1}{2} \left\{ A_i^\dagger A_i, \rho_S(t) \right\} \right). \tag{5.67}$$

The expression above provides a way to express the quantum master equation (3.144) in a more convenient form, such that:

$$\mathcal{L}\rho_S(t) = -i\left[H(t), \rho_S(t)\right] + \mathcal{D}(\rho_S(t)). \tag{5.68}$$

Tracing over the environmental degrees of freedom is a commonly used approach for studying the dynamics of open quantum systems at the microscopic level, particularly when the global dynamics of both the system and environment are taken into account. This approach involves making certain approximations, such as assuming a weak coupling between the system and its environment and a Markovian stochastic process. In the following section, we will discuss the microscopic derivation of an open quantum system and its ancillary, with a focus on the weak coupling limit.

4.2 Microscopic derivation in the weak coupling limit

The Markovian stochastic process appears to be a more suitable strategy for studying the dynamics of open systems by making some simplifying assumptions and approximations in a microscopic situation, where the global dynamics of the system and environment are taken into account by tracing out the environmental degrees of freedom [65, 72]. Throughout this section, we will discuss the microscopic derivation method of an open quantum system interacting with its surroundings under the influence of a weak coupling limit. The Hamiltonian of the global quantum system, under this assumption, is assumed to be of the form:

$$\begin{aligned} H_T(t) &= H_S + H_E + H_{SE}(t) \\ &\equiv H_0 + H_{SE}(t), \end{aligned} \tag{5.69}$$

where H_0 represents the free Hamiltonian and decomposes as the sum of the Hamiltonian of the open system H_S and the Hamiltonian of the environment H_E. While $H_{SE}(t)$ denotes the interaction Hamiltonian which describes the interaction between them at time t. The weak coupling assumption implies that the interaction between both is small compared to the free Hamiltonians of the system and environment. This enables us to treat the evolution of the total system as a perturbation from the uncoupled evolution of the system and environment. In this situation, the Liouville-von Neumann equation associated with the total density operator $\rho(t)$ is rewritten in the interaction picture as

$$\frac{d\widehat{\rho}(t)}{dt} = -i\left[\widehat{H}_I(t), \widehat{\rho}(t)\right], \tag{5.70}$$

where $\widehat{\rho}(t)$ and $\widehat{H}_I(t)$ are, respectively, the total density operator and the interaction Hamiltonian in the interaction picture. They are given by

$$\widehat{\rho}(t) = e^{iH_0 t} \rho(t) e^{-iH_0 t}, \tag{5.71}$$

$$\widehat{H}_I(t) = e^{iH_0 t} H_{SE} e^{-iH_0 t}. \tag{5.72}$$

For ease of notation, from now on we will drop the subscript "I" which is used to indicate the interaction picture operators. Moreover, one can formally integrate the equation of motion (5.70) to obtain

$$\widehat{\rho}(t) = \widehat{\rho}(t_0) - i\int_{t_0}^{t} dt'[\widehat{H}(t'), \widehat{\rho}(t')], \tag{5.73}$$

where t_0 is initial time of interaction and $\widehat{\rho}(t_0) \equiv \widehat{\rho}(0) = \rho(0)$. By substituting the expression (5.73) back into the formula (5.70) yields the following equation of motion

$$\frac{d}{dt}\widehat{\rho}(t) = -i[\widehat{H}(t), \rho(0)] - \int_0^t dt' \Big[\widehat{H}(t), [\widehat{H}(t'), \widehat{\rho}(t')]\Big]. \tag{5.74}$$

Then, by taking the trace over the degrees of freedom of the environment and using the expression (5.28), we arrive at

$$\frac{d}{dt}\widehat{\rho}_S(t) = -i\mathrm{Tr}_E\left\{[\widehat{H}(t), \rho(0)]\right\} - \mathrm{Tr}_E\left\{\int_0^t dt' \Big[\widehat{H}(t), [\widehat{H}(t'), \widehat{\rho}(t')]\Big]\right\}. \tag{5.75}$$

Let us suppose that the interaction Hamiltonian in the interaction picture fulfills $\mathrm{Tr}_E\{[\widehat{H}(t), \widehat{\rho}(0)]\} = 0$ as the initial state does not induce any first-order dynamics with regard to its surroundings. It follows that the environment does not play a significant role in the initial dynamics of the system and thus the interaction Hamiltonian only slightly perturbs the environment. This requirement is not restrictive since one can always redefine the free Hamiltonian H_0. In other words, one can add an additional Hamiltonian that only acts on the Hilbert space of the system [265]. This additional Hamiltonian is called a system-environment decoupling Hamiltonian. By choosing an appropriate decoupling Hamiltonian, we can assure that the interaction Hamiltonian in the interaction picture satisfies the condition $\mathrm{Tr}_E\{[\widehat{H}(t), \rho(0)]\} = 0$. If this condition is not satisfied, then the environment will participate significantly in the initial dynamics of the system, which would complicate the analysis and calculations in the interaction picture. Once an appropriate decoupling Hamiltonian is chosen, the first term on the right-hand side of Eq.(5.75) can be ignored, and one can focus only on the second term which is related to the dynamics of the system-environment interaction. This gives

$$\frac{d}{dt}\widehat{\rho}_S(t) = -\mathrm{Tr}_E\left\{\int_0^t dt' \Big[\widehat{H}(t), [\widehat{H}(t'), \widehat{\rho}(t')]\Big]\right\}. \tag{5.76}$$

4.3 Born approximation

An important approximation should be considered at this point called the Born approximation. This approximation assumes that the system is weakly coupled to its environment so that the interaction with the system only slightly perturbs the state of the environment during evolution [250]. This approximation allows us to express the solution of Eq.(5.76) as a product of the state of the system at time t and the state of the environment at the start time, with a correction term $\widehat{\rho}_c(t)$ that accounts for the effects of the interaction. This gives:

$$\widehat{\rho}(t) = \widehat{\rho}_s(t) \otimes \widehat{\rho}_E + \widehat{\rho}_c(t). \tag{5.77}$$

For consistency, we assume that the correction term $\widehat{\rho}_c(t)$ is higher order in the interaction Hamiltonian $\widehat{H}(t)$, which justifies neglecting it in the Born approximation such that $\mathrm{Tr}_E\{\widehat{\rho}_c(t)\} = 0$. This condition ensures that $\widehat{\rho}_S(t)$ has the correct normalization and is a

valid probability distribution over the system's states. By substituting Eq.(5.77) into Eq.(5.76) and after some simplifications, we obtain:

$$\frac{d}{dt}\widehat{\rho}_S(t) = -\mathrm{Tr}_E\left\{\int_0^t dt'\Big[\widehat{H}(t),[\widehat{H}(t'),\widehat{\rho}_s(t')\otimes\widehat{\rho}_E]\Big]\right\}. \tag{5.78}$$

It is crucial to emphasize that this approximation does not necessarily means that correlations produced between the system and environment are ignored, but rather that they are considered to be weak and have a small impact on the dynamics of the reduced system.

4.4 Markov approximation

To obtain a Markovian master equation, it is necessary to make a Markov-like approximation by substituting the state $\widehat{\rho}_s(t')$ in the retarded time with the present state $\widehat{\rho}_s(t)$, which further simplifies the calculation of the dynamics [250]. This approximation requires that the integrand in the calculation of the dynamics is effectively non-zero only for a short time interval around $t' \sim t$. By using these approximations, it is possible to derive an integrodifferential equation that is local in time. This yields

$$\frac{d}{dt}\widehat{\rho}_S(t) = -\mathrm{Tr}_E\left\{\int_0^t dt'\Big[\widehat{H}(t),[\widehat{H}(t'),\widehat{\rho}_s(t)\otimes\widehat{\rho}_E(0)]\Big]\right\}. \tag{5.79}$$

The above equation is known as the *"Redfield equation"*, which is not strictly Markovian since it still contains memory effects that depend on the time difference between the initial and final times and may not conserve the positivity of the density matrix according to the above approximations [265]. To address this, another Markov-like approximation can be performed by substituting t' with $t'-t$ in the integral of the previous equation and extending the upper limit of the integral to infinity [72], that is

$$\frac{d}{dt}\widehat{\rho}_S(t) = -\mathrm{Tr}_E\left\{\int_0^\infty dt'\Big[\widehat{H}(t),[\widehat{H}(t-t'),\widehat{\rho}_s(t)\otimes\widehat{\rho}_E(0)]\Big]\right\}. \tag{5.80}$$

The resulting equation is a strictly Markovian version of Eq.(5.79) that ensure the conservation of the density matrix's positivity. Moreover, it described the behavior of an open quantum system that interacts with its environment over a coarse-grained time interval and is commonly known as the Born-Markov approximation. As an application of the markovian master equation above, we have investigated in detail in one of our contributions the dynamical behavior of several quantum correlations quantifiers in a hybrid bipartite system consisting of a qutrit-qubit coupled to a stochastic noisy environment both separately and collectively [54]. However, it is essential to note that Eq.(5.80) is not necessarily a generator of a dynamical semi-group and does not take the form of the Lindblad equation. Hence, an additional approximation, such as the secular approximation, can be used in conjunction with the Born-Markov approximation to obtain a valid master equation that accounts for CPTP dynamics, which is necessary for a consistent quantum mechanical description. The secular approximation involves averaging over rapidly oscillating terms and is akin to the rotating wave approximation (RWA).

4.5 Secular approximation

Let us assume that the interaction Hamiltonian in Schrödinger representation is of the general form, without any loss of generality [72, 266]

$$H_{SE} = \textstyle\sum_{\alpha=1}^{I} A_\alpha \otimes B_\alpha. \tag{5.81}$$

Here, A_α and B_α $(\alpha = 1, \ldots, I)$ represent Hermitian operators that act on the degrees of freedom of the system and the environment, respectively. Moreover, one can proceed with the decomposition of H_{SE} into a set of eigenoperators belonging to the Hamiltonian of the system. This results in a spectral decomposition of H_S, denoted as $H_S = \sum_i \lambda_i |\lambda_i\rangle \langle\lambda_i| = \sum_i \lambda_i \mathcal{P}_{\lambda_i}$ such that $\mathcal{P}_{\lambda_i} = |\lambda_i\rangle \langle\lambda_i|$. Let us now define

$$A_\alpha(\omega) \equiv \sum_{ij} \delta(\lambda_j - \lambda_i - \omega) \mathcal{P}_{\lambda_i} A_\alpha \mathcal{P}_{\lambda_j}. \tag{5.82}$$

In the above formula, the term $\delta(\lambda_j - \lambda_i - \omega)$ represents the Dirac delta function that identifies all possible transitions in the system's spectrum with a constant energy difference ω. The following statement can be used to characterize the set of operators that satisfy the following requirement:

$$[H_S, A_\alpha(\omega)] = -\omega A_\alpha(\omega), \quad \left[H_S, A_\alpha^\dagger(\omega)\right] = \omega A_\alpha^\dagger(\omega), \tag{5.83}$$

where the operators $A_\alpha(\omega)$ and $A_\alpha^\dagger(\omega)$ are known as the eigenoperators of H_S that, respectively, belong to the frequencies $\pm\omega$. It should be noted that $A_\alpha(\omega)$ does not indicate that A_α is explicitly dependent on ω, but rather indicates that operator A is associated with the frequency ω. It can be shown from Eq.(5.83) that the corresponding operators in the interaction picture have the following form

$$\exp(iH_S t) A_\alpha(\omega) \exp(-iH_S t) = \exp(-i\omega t) A_\alpha(\omega), \tag{5.84}$$

and

$$\exp(iH_S t) A_\alpha^\dagger(\omega) \exp(-iH_S t) = \exp(i\omega t) A_\alpha^\dagger(\omega), \tag{5.85}$$

with $A_\alpha^\dagger(\omega) = A_\alpha(-\omega)$, while $\left[H_S, A_\alpha^\dagger(\omega) A_\alpha(\omega)\right] = 0$. Moreover, they follow the completeness relation $\sum_\omega A_\alpha(\omega) = A_\alpha$. Then, the interaction Hamiltonian (5.81) can be re-expressed as follows:

$$H_{SE} = \sum_{\alpha,\omega} A_\alpha(\omega) \otimes B_\alpha. \tag{5.86}$$

Hence, one can express the interaction Hamiltonian (5.81) in the interaction representation by means of those operators as

$$\widehat{H}(t) = \sum_{\alpha,\omega} \exp(-i\omega t) A_\alpha(\omega) \otimes B_\alpha(t), \tag{5.87}$$

where $B_\alpha(t) = \exp(iH_0 t) B_\alpha \exp(-iH_0 t)$ refers to the environment operators in the interaction representation. When we deal with some physical systems, it is often useful to define the eigenoperator decomposition of the environment observables (5.81) with respect to H_E. By doing this, we can simplify the Hamiltonian (5.81) by neglecting rapidly oscillating terms, yielding a Markovian master equation (5.80) that can be expressed in Lindblad form. This approach is especially useful in problems involving radiation-matter interaction problems that involve the Jaynes-Cummings-Paul model [267,268]. Alternatively, the RWA can be performed within the integrand of Eq.(5.80). This involves introducing Eq.(5.81) into the expression (5.80), which results in [72]:

$$\begin{aligned} \frac{d}{dt}\widehat{\rho}_S(t) &= \int_0^\infty dt' \mathrm{Tr}_E \left\{ \widehat{H}(t-t')\widehat{\rho}_s(t) \otimes \widehat{\rho}_E(0)\widehat{H}(t) - \widehat{H}(t)\widehat{\rho}_s(t) \otimes \widehat{\rho}_E(0)\widehat{H}(t-t') + h.c. \right\} \\ &= \sum_{\omega,\omega'} \sum_{\alpha,\beta} \exp(i(\omega - \omega')t) \Gamma_{\alpha\beta}(\omega) \left(A_\beta(\omega) \widehat{\rho}(t) A_\alpha^\dagger\left(\omega'\right) - A_\alpha^\dagger\left(\omega'\right) A_\beta(\omega) \widehat{\rho}(t) \right) + \\ &\quad h.c., \end{aligned} \tag{5.88}$$

where $h.c.$ represents the Hermitian conjugate expression of the previous term, while $\Gamma_{\alpha\beta}(\omega)$ denotes the one-sided Fourier transform of the environment correlation functions. It is given as

$$\Gamma_{\alpha\beta}(\omega) = \int_0^\infty dt' \exp(i\omega t') \langle B\dagger_\alpha(t) B_\beta(t-t')\rangle, \tag{5.89}$$

where

$$\langle B\dagger_\alpha(t) B_\beta(t-t')\rangle \equiv \mathrm{Tr}_E\{B_\alpha(t) B_\beta(t-t')\widehat{\rho}_E(0)\}, \tag{5.90}$$

and

$$\langle B_\alpha(t)\rangle \equiv \mathrm{Tr}_E\{B_\alpha(t)\widehat{\rho}_E(0)\} = 0, \tag{5.91}$$

with $\langle\ldots\rangle$ denoting an ensemble average. In the case, where ρ_E is a stationary state of the environment, i.e. $[H_B, \rho_E] = 0$. Then, the environment correlation functions are homogeneous in time. Such that

$$\langle B\dagger_\alpha(t) B_\beta(t-t')\rangle = \langle B\dagger_\alpha(t') B_\beta(0)\rangle, \tag{5.92}$$

ensuring that the quantities $\Gamma_{\alpha\beta}(\omega)$ only depend on the time difference $t-t'$ and not on the absolute times t and t'. In the case of homogeneous correlation functions, we can apply the secular approximation. This involves disregarding terms with frequencies that are significantly different from the natural frequency of the system such that $(\omega \neq \omega')$. The validity of this approximation is determined by the time scales of the system and the reservoir. Specifically, the condition $\tau_S \sim \frac{1}{|\omega'-\omega|} << \tau_E$ needs to be satisfied. Here, τ_S represents the time scale of the system, while τ_E is the time scale of the reservoir [72]. This condition ensures that the non-secular terms (with $(\omega \neq \omega')$) oscillate much faster than the secular terms and can be neglected. Thus we have

$$\frac{d}{dt}\widehat{\rho}_S(t) = \sum_\omega \sum_{\alpha,\beta} \Gamma_{\alpha\beta}(\omega)\left(A_\beta(\omega)\widehat{\rho}(t)A^\dagger_\alpha(\omega) - A^\dagger_\alpha(\omega) A_\beta(\omega)\widehat{\rho}(t)\right) + h.c. \tag{5.93}$$

To simplify the analysis, it is convenient to divide the Fourier transforms of the reservoir correlation functions into two components, i.e.

$$\Gamma_{\alpha\beta}(\omega) = \frac{1}{2}\gamma_{\alpha\beta}(\omega) + i\chi_{\alpha\beta}(\omega), \tag{5.94}$$

where the first part is always non-negative, while the second term constitutes the entries of an Hermitian matrix. They are respecively provided as follows:

$$\gamma_{\alpha\beta}(\omega) \equiv \Gamma_{\alpha\beta}(\omega) + \Gamma^*_{\beta\alpha}(\omega) = \int_{-\infty}^\infty dt' \exp(i\omega t') \langle B\dagger_\alpha(t) B_\beta(0)\rangle, \tag{5.95}$$

$$\chi_{\alpha\beta}(\omega) \equiv \frac{1}{2i}\left(\Gamma_{\alpha\beta}(\omega) - \Gamma^*_{\beta\alpha}(\omega)\right). \tag{5.96}$$

Performing this decomposition enables us to express the master equation in the interaction representation. This can be achieved using the following alternative form:

$$\frac{d}{dt}\widehat{\rho}_S(t) = -i[H_{LS}, \widehat{\rho}_S(t)] + \mathcal{D}(\widehat{\rho}_S(t)). \tag{5.97}$$

In the above expression, the term $H_{LS} \equiv \sum_\omega \sum_{\alpha,\beta} \chi_{\alpha\beta}(\omega) A^\dagger_\alpha(\omega) A_\beta(\omega)$ is the Lamb shift Hamiltonian. In general, this Hamiltonian is responsible for causing small renormalization on the non-perturbed energy levels of the open system due to the interaction with its environment. Consequently, we have $[H_S, H_{LS}] = 0$. The second part on the right-hand side of Eq.(5.97) is commonly referred to as the Dissipator, which can be expressed as follows

$$\mathcal{D}(\widehat{\rho}_S(t)) \equiv \sum_\omega \sum_{\alpha,\beta} \gamma_{\alpha\beta}(\omega)\left(A_\beta(\omega)\widehat{\rho}(t)A^\dagger_\alpha(\omega) - \frac{1}{2}\left\{A^\dagger_\alpha(\omega) A_\beta(\omega), \widehat{\rho}(t)\right\}\right). \tag{5.98}$$

It is worth noting that Eq.(5.97) corresponds to a CPTP dynamics, since it can be expressed in the Lindblad form. To achieve this, one can diagonalize matrices $\gamma_{\alpha\beta}(\omega)$ [72]. In the Schrödinger picture, the master equation (5.97) can be written in the form of a CPTP Markovian equation as follows

$$\frac{d}{dt}\widehat{\rho}_S(t) = -i\left[H_S + H_{LS}H_{LS}, \widehat{\rho}_S(t)\right] + \mathcal{D}\left(\widehat{\rho}_S(t)\right). \tag{5.99}$$

The expression given above represents the final form of the CPTP Markovian master equation. In practice, the Lamb shift Hamiltonian H_{LS} is often neglected since the weak coupling limit, which ensures that the energy shift is significantly smaller than the eigenvalues of H_S. An alternative approach is to add a counter-term to the system Hamiltonian that cancels out the Lamb shift contribution. However, precise computation of the Lamb shift Hamiltonian requires the use of relativistic quantum mechanics and renormalization theory [102]. In the next section, we will study non-Markovian behavior, where the assumption of memoryless evolution is relaxed. This leads to richer dynamics, which may have implications for various applications in quantum information processing and beyond.

5 Non-Markovian dynamics

The Lindblad equation is a widely used approach for describing the behavior of an open quantum system. Nonetheless, when the coupling between the system and its surrounding environment is strong, the Lindblad equation (5.65) may not accurately describe the system's dynamics. In such situations, it is possible to generalize Eq.(5.66) to incorporate the effects of strong system-environment coupling. Hence, the dynamics are described by the following master equation at scaled time t [53, 69, 269–271]

$$\frac{d}{dt}\rho_S(t) = \mathcal{K}(t)\,\rho_S(t). \tag{5.100}$$

Here, $\mathcal{K}(t)$ denotes a time-dependent generator of the dynamics, which adheres to the relation

$$\mathcal{K}(t)\,\phi(t) = \int_0^t k(t-t\prime)\,\phi(t')\,dt', \tag{5.101}$$

where $k(t-t\prime)$ denotes the memory kernel function that characterizes the memory of the system and represents the effect of past states on the current state of the system. It regulates the nature of the environment and can significantly impact the dynamics of the system. It is important to note that without applying the time-dependent integral operator $\mathcal{K}(t)$, the master equation (5.66) with Markovian approximation becomes dominant, meaning $k(t-t\prime) = \delta(t-t\prime)\,\mathcal{L}$ (5.65).

To extend the Lindblad equation to describe strongly coupled situations, one approach is to use the so-called *"non-Markovian"* master equation. This equation takes into account the memory effects of the environment on the system's dynamics, which become essential when the system-environment coupling is strong. It is written in terms of a time-dependent density matrix that satisfies a differential equation of the form [272, 273]:

$$\mathcal{K}(t)\,\rho_S(t) = -i\left[H_S(t), \rho_S(t)\right] + \sum_i \gamma_i(t)\left(A_i(t)\,\rho_S(t)\,A_i^\dagger(t) - \frac{1}{2}\left\{A_i^\dagger(t)\,A_i(t), \rho_S(t)\right\}\right). \tag{5.102}$$

We notice this result naturally extends the previous Lindblad structure (3.144) to time-local generators, where the system Hamiltonian $H_S(t)$, decay operators $A_i(t)$, and each of the decay

rates $\gamma_i(t)$ now have the possibility of being time-dependent. These new properties reflect the inclusion of memory effects in the system dynamics. The form of this operator depends on the specific details of the system-environment coupling.

It should be mentioned that the decay rates $\gamma_i(t)$ in the Markovian regime are always non-negative [274, 275], which means that the system loses coherence irreversibly. In other words, the information on the system's state that is lost to the environment is not retrievable. This is because the decay rates depend only on the current state of the system and not on its previous history.

However, in the non-Markovian regime, some of the decay rates can be negative for some i and some $t > 0$. This means that the decay rates can depend not only on the current state of the system but also on its past history [276]. In this case, part of the information on the system's state that is lost to the environment can be retrieved at later times, during the negativity periods of the decay rates. The non-Markovian master equation is more complicated than the Lindblad equation and requires more information about the system-environment coupling. However, it provides a more accurate description of the system's dynamics in strongly coupled situations. This description is essential in understanding the behavior of many physical systems, such as quantum computing and quantum communication protocols, which involve strong system-environment coupling. The table5.2 summarizes the basic differences between Markovian and non-Markovian dynamics.

Markovian dynamics	Non-Markovian dynamics
- No memory effect. - Lindblad master equation. - Lack of correlation. - Loss of information from the system to the environment.	- Memory effect. - Non-Markovian master equation. - The existence of correlation. - Information feedback from the environment to the system.

Table 5.2: Markovian vs non-Markovian dynamics.

So far, we have seen that the primary cause of decoherence in quantum systems is due to environmental interactions such as oscillators and spins bath. The Lindblad master equations, for instance, serve as a useful mathematical framework to describe this type of decoherence. However, it is important to note that there are other causes of decoherence that are inherent to the system's dynamics and not related to its surrounding environment. These causes of decoherence can be described by equations that characterize their nature. They may include, for example, internal interactions between the system's components or fluctuations in the system's Hamiltonian. Understanding these intrinsic causes of decoherence is crucial for developing better quantum technologies and for addressing fundamental questions in quantum mechanics. In this following section, we shed light on the second cause of decoherence.

6 Intrinsic decoherence

The intrinsic decoherence approach was initially introduced by Milburn [277] which modifies standard quantum mechanics by supposing that a system some how does not undergo continuous unitary evolution on sufficiently short time steps. Instead, this process assumes that the system undergoes a stochastic sequence of identical unitary transformations, resulting in the decay of quantum coherence in the energy eigenstate basis that is entirely dependent on phase. Importantly, this decay occurs without the need for an external environment or energy dissipation and is distinct from normal decay. This approximation is very useful since it is applicable to many physically relevant situations. According to Milburn's model [277], the time-dependent

density matrix in the presence of intrinsic decoherence phenomenon takes the following form

$$\frac{d}{dt}\rho(t) = \frac{1}{\Gamma}[\exp(-i\Gamma H)\rho(t)\exp(i\Gamma H) - \rho(t)]. \tag{5.103}$$

Here, $\Gamma = 1/\gamma$ denotes the intrinsic decoherence rate, representing the mean frequency of the unitary step and H refers to as the Hamiltonian of the system under study. By expanding the exponential functions above in a Taylor series and retaining only terms up to the second order, one obtains

$$\frac{d}{dt}\rho(t) = \frac{1}{\Gamma}\Big(\left[1 - \Gamma H - (\Gamma H)^2\right] \rho(t) \left[1 + \Gamma H - (\Gamma H)^2\right] - \rho(t)\Big), \tag{5.104}$$

which can be reformulated in the Lindblad form, which describes the decoherence effect on the system as

$$\frac{d}{dt}\rho(t) = -i[H, \rho(t)] - \frac{\Gamma}{2}[H, [H, \rho(t)]]. \tag{5.105}$$

The above expression (5.105) reduces to the standard von Neumann equation when the condition $\Gamma \longrightarrow 0$ occurs [278]. It also highlights that the first part on the right-hand side of the formula (5.105) provides a coherent unitary time evolution of the system. While the second part, which does not commute with the Hamiltonian reflects the decoherence effect on the system. However, a formal solution of the expression (5.105) is expressed in the operator-sum picture using Kraus operators. This picture provides a useful way to describe the evolution of the system in terms of a set of operations performed on the density operator as follows

$$\rho(t) = \sum_{k=0}^{\infty} M^k(t)\rho(0)(M^k(t))^\dagger, \tag{5.106}$$

where $\rho(0)$ represents the initial state of the system while $M^k(t)$ can be defined as

$$M^k(t) = \frac{(\Gamma t)^k}{k!} H^k \exp(-iHt)\exp(-\Gamma H^2 t/2). \tag{5.107}$$

By using the completeness relation $\sum_n |\psi_n\rangle \langle\psi_n| = 1$, which is satisfied by the eigenvectors of the Hamiltonian H and by inserting it into Eq.(5.106), one can derive a closed formula that describes the time evolution of the system in terms of the eigenvalues and eigenvectors of the Hamiltonian. Such as

$$\rho(t) = \sum_{m,n} \exp(-\frac{\Gamma t}{2}(E_m - E_n)^2 - i(E_m - E_n)t) \times \langle\psi_m| \rho(0) |\psi_n\rangle |\psi_m\rangle \langle\psi_n| . \tag{5.108}$$

Here, E_n and $|\psi_n\rangle$ stands for the eigenvalues and their associated eigenvectors of the Hamiltonian H, respectively. This approach has been applied to physically relevant systems in recent research studies [279, 280]. In this context, in Ref. [80] we have studied the dynamical behavior of several correlation quantifiers including entanglement of two-qubit the Heisenberg spin-1/2 chain model under the effect of Dzyaloshinski–Moriya interaction using the intrinsic decoherence approach.

7 Conclusion

A fundamental concept in quantum physics, open quantum system theory has several applications in quantum simulation, interaction, and computation. It involves observing the number of degrees of freedom around a quantum system in order to investigate its dynamics. Open quantum systems communicate with the environment in real-world situations, hence the system's general dynamics must be unitary. Open systems, nevertheless, are unable to adequately characterised by unitary alterations alone because of these interconnections. Instead, in some cases, evolution equations can be used to express them. We covered a number of key ideas in this chapter in order to better comprehend and analyse the dynamical behaviour of open quantum systems that communicate with their external surroundings. The foundational assumptions for understanding both closed and open quantum systems were presented first. We then looked at the characteristics of universal dynamical maps, a key idea in the concept of open quantum structures. The master equation, which enables us to study both Markovian and non-Markovian dynamics, was then developed. Finally, using Milburn's method, we offer a thorough explanation of the temporal evolution of density operators under intrinsic decoherence.

Quantum devices like quantum dots, superconducting qubits, and ion traps, and their behaviour in various settings, such as quantum sensing, metrology, and imaging, are examples of how open quantum systems may be used. The creation of more effective and dependable quantum systems has shown significant potential in current studies, rendering the concept of open quantum systems a lively and intriguing subject of study.

In conclusion, understanding the behaviour of quantum systems which communicate with their surroundings requires knowledge of the fundamental concepts of open quantum systems. We may apply the theory to a range of domains by examining the fundamental concepts and mathematical structure.

CHAPTER 6

CONTRIBUTIONS

1 Contribution 1: Dynamics of quantum discord based on linear entropy and negativity of qutrit-qubit system under classical dephasing environments

The European Physical Journal D, 75 (2021) 3.

1.1 Summary of contribution 1

The evaluation of the entropic quantum discord (QD) given in Eq.(3.8) is a challenging task in general due to the optimization process of classical correlation over local generalized measurements. This remains an unresolved problem even in the simplest case of a two-qubit state. To address this challenge, our work aims to develop a reliable analytical approach for evaluating QD in arbitrary hybrid qudit-qubit quantum systems using the concept of linear entropy (3.96). The latter provides an alternative tool to overcome the difficulties encountered with the computability of QD based on von Neumann's entropy. This approach is expected to be more efficient and practical for evaluating QD in a wide range of quantum systems.

In real quantum systems, quantum correlations are inevitably affected by the environment, leading to their annihilation. This presents a significant challenge in quantum information science. In this inspiration, we employed the obtained expression of QD to derive the strength of non-classical correlations for a qutrit-qubit quantum system undergoing a global (bilocal + collective) classical dephasing environment noise without considering the memory effect. The master equation (5.80) using the Born-Markov approximations has been solved analytically to control the dynamical behavior of QD. Specifically, we focused on a particular case where the system is initially prepared in a thermal state. The ensuing quantum discord (QD) is compared to the measurement-induced disturbance (MID) and the logarithmic negativity (LN) for each of the three distinct dephasing settings. According to the findings, entanglement by QD and MID appears to be more resistant to the decoherence effect than entanglement by LN. Furthermore, the system exhibits fascinating characteristics such as entanglement sudden death (ESD) and frozen dynamics. We observed that for the chosen system, QD and MID indicate the same amount of quantum correlations. This discovery implies that quantum correlations among multi-component systems in higher-dimensional Hilbert domains may undoubtedly be examined using this type of quantum discord.

1.2 Content of contribution 1

Eur. Phys. J. D
https://doi.org/10.1140/epjd/s10053-020-00022-2

THE EUROPEAN PHYSICAL JOURNAL D

Regular Article - Quantum Information

Dynamics of quantum discord based on linear entropy and negativity of qutrit-qubit system under classical dephasing environments

Fadwa Benabdallah[1,a] and Mohammed Daoud[2,3,b]

[1] LPHE-Modeling and Simulation, Faculty of Sciences, Mohammed V University in Rabat, Rabat, Morocco
[2] Department of Physics, Faculty of Sciences, University Ibn Tofail, Kenitra, Morocco
[3] Abdus Salam International Centre for Theoretical Physics, Miramare, Trieste, Italy

Received 16 August 2020 / Accepted 3 November 2020
© EDP Sciences, SIF and Springer-Verlag GmbH Germany, part of Springer Nature 2021

Abstract. A reliable analytical method to evaluate the non-classical correlations based on linear entropy for an arbitrary qudit-qubit quantum state is proposed. The linear entropy is used to overcome the difficulty encountered with the computability of quantum discord based on von Neumann entropy. The quantum discord based on linear entropy is employed to derive the quantum correlations for a qutrit-qubit system undergoing global (bilocal + collective) classical dephasing environment. Our studies were focused mainly on a particular initial qutrit-qubit state in thermal equilibrium at a temperature T. The obtained amount of quantum discord (QD) is then compared with the measurement-induced disturbance (MID) and logarithmic negativity (LN). The analysis shows that both QD and MID are more robust than entanglement (LN) against the decoherence effect. Besides, the system exhibits interesting behaviors. As for instance, freezing dynamics and entanglement sudden death (ESD). The method developed in this paper to quantify quantum correlations is reliable because it allows us to consider analytically the arbitrary qutrit-qubit quantum states in the classical dephasing environment.

1 Introduction

Quantum entanglement, as one of the most intriguing resources of quantum information theory (QIT), plays valuable roles in several aspects of quantum computation and quantum information processing (QIP) protocols [1,2]. It has attracted growing attention due to wide range of powerful applications, such as quantum teleportation [3], quantum key distribution [4], quantum states merging [5]. Nevertheless, according to various studies [6,7], quantum entanglement is not the only meaningful type of quantum correlations useful for QIP. In fact, there exist some separable quantum states may also contribute to the implementation of certain quantum tasks better than their classical counterparts [8,9]. Thus one of the central topics in QIT became the study of non-classical correlations beyond entanglement with the particular question of how it can be quantified. This approach attracts an impressive amount of attention and effort [10,11]. Among them, quantum discord (QD), was initially introduced by Ollivier and Zurek [12] and independently by Henderson and Vedral [13], can effectively capture all quantum correlations present in various kinds of quantum systems [14]. The quantum discord involves a minimization procedure that is difficult to solve in general [15,16]. Due to this complicated optimization, QD has been calculated explicitly only for limited cases of two-qubit systems [17–19]. Many studies have been devoted also to the problem of quantifying QD from an analytical point of view [20]. These studies were led to introduce various discord-like measures, such as local quantum uncertainty [21], one-way quantum deficit [22], measurement-induced disturbance (MID) [23], and measurement-induced nonlocality (MIN) [24]. Another interesting method for obtaining a closed analytic expression of QD is the use of linear entropy instead of the von Neumann entropy to find analytically the optimal measurements that maximize the conditional mutual information [25,26]. This is important to understand of the decoherence effect [27]. This approach is the subject of interest of this paper. A quantum system is inevitably open and coupled to its environment [28]. During the interaction with ancillary or interface systems, even a well-isolated system has to be at risk of losing its characteristic quantum traits, such as coherence and quantum correlations in composite systems [29]. Such interaction is a prerequisiteto store, evolve, read and manipulate a pure state of the interesting quantum system coherently. Thus the elimination of outside noise interference requires exceptional care. Decoherence is the main challenge for the physical realization of quantum information and com-

[a] e-mail: fadwa_benabdallah@um5.ac.ma (corresponding author)
[b] e-mail: m_daoud@hotmail.com

Published online: 11 January 2021

putation protocols [1]. The robust store of quantum states for a long time and evolve them according to specific targets is a challenging task of quantum engineering. In order to control decoherence effects, various studies were devoted to quantum correlation dynamics under different types of decoherence [1]. One of the most important results is the total loss of entanglement in finite time, which is called the entanglement sudden death (ESD) [30,31]. On the other hand, the influence of both Markovian and non-Markovian environments on dynamics of more general quantum and classical correlation have been studied under various decoherence schemes [32–34]. It has been observed also that quantum correlation is more robust against noise and does not suffer from the phenomenon of sudden death in Markovian environments [32–34]. It has been shown that the discord-like general quantum correlations disappear instantaneously in non-Markovian environments [35]. Another striking phenomenon, known as the freezing dynamics of entanglement, has been shown to occur in some specific situations [27,36]. Indeed, it has been shown that the quantum correlations decay to a finite non-zero value and then suddenly stop the decay and the system maintain its stationary entanglement.

The aim of this paper is to analyze the time evolution of quantum correlations as quantified by logarithmic negativity, measurement-induced disturbance with a special attention to quantum discord for a qutrit-qubit quantum system interacting with a classical dephasing environment [37]. We consider a particular qutrit-qubit state in thermal equilibrium. In addition, the dynamics of these three quantum correlations quantifiers under the effect of global (bilocal + collective) pure dephasing noise are compared. The analysis show that both QD and MID are robust than entanglement against the decoherence effects. Besides, the system exhibits various interesting dynamical behaviors. In particular, QD exhibits the freezing phenomenon, whereas the entanglement of sudden death occurs only for specific values of the temperature T and external magnetic field B. Furthermore, we performed also detailed studies of dynamic behavior of quantum correlations when the qutrit-qubit system is independently subjected to the case of bilocal noise as well to a collective dephasing noise.

This paper is arranged as follows. In Sect. 2, we introduce the decoherence model and the general expression of the state describing an arbitrary qutrit-qubit quantum state in the presence of global dephasing noise. In Sect. 3, we give the analytical expression of the usual quantum correlations quantifiers: the logarithmic negativity, measurement-induced disturbance and the quantum discord based on linear entropy for a given qudit-qubit system. In Sect. 4, the dynamic of these three quantum correlations quantifiers are explicitly given for the special case of a particular initial qutrit-qubit state in thermal equilibrium at a temperature T. Their dynamics behaviors for global, bilocal and collective decoherence noise are also discussed in Sect. 5. The summary and perspectives are given in Sect. 6.

2 Generalized noise model for a qutrit-qubit system

We investigate the time evolution of quantum correlations under the influence of environment noise without considering the memory effect. Thus, in the Markovian approximation we consider a bipartite system, namely qutrit (spin-1) and qubit (spin-$\frac{1}{2}$), coupled to a noisy environment both separately and collectively. In what follows, we shall consider the Hamiltonian which describes the class of interactions generating a pure dephasing process [38,39]. This is given by (we set $\hbar = 1$)

$$H_I(t) = -\frac{1}{2}\mu\left[\Omega_A(t)\, S_z^A + \Omega_B(t)\, s_z^B + \Omega_{AB}(t)\,(S_z^A + s_z^B)\right] \tag{1}$$

where μ is the gyromagnetic ratio, S_z^A corresponds to z -component of three level spin for qutrit and s_z^B is the standard Pauli matrix in z-direction for spin-$\frac{1}{2}$ (qubit)

$$S_z^A = \begin{pmatrix} 1 & 0 & 0 \\ 0 & 0 & 0 \\ 0 & 0 & -1 \end{pmatrix}. \tag{2}$$

In Eq. (1) $\Omega_i(t)$ $(i = A, B, AB)$ are the time-dependent stochastic noise fields which are considered to be statistically independent classical Markov processes. They satisfy the Markov noise conditions given by

$$\langle \Omega_i(t) \rangle = 0, \qquad \langle \Omega_i(t)\Omega_i(s) \rangle = \frac{\Gamma_i}{\mu^2}\delta(t-s), \tag{3}$$

where $\langle \cdots \rangle$ being the ensemble time average and Γ_i stands for the phase damping rates associated with stochastic field $\Omega_i(t)$. The time-dependent density matrix describing the qutrit-qubit system (1) is given by taking ensemble averages over the three stochastic noise fields $\Omega_i(t)$, as follows

$$\rho(t) = \langle\langle\langle \rho_{st}(t) \rangle\rangle\rangle, \tag{4}$$

where $\rho_{st}(t)$ stands for the statistical density operator given by

$$\rho_{st}(t) = U(t)\,\rho(0)\,U^{\dagger}(t), \tag{5}$$

in terms of the stochastic unitary operator $U(t)$ obtained from the stochastic Schrodinger equation as

$$U(t) = \exp\left[-i\int_0^t ds H(s)\right]. \tag{6}$$

Many approaches, such as the master equation [1] and Kraus operator decomposition [40], have been exploited to describe the dynamical behaviors of open quantum systems. For our purpose, we find that it is more convenient to use the master equation approach derived

by invoking the Born–Markov approximation to investigate that the quantum dynamics of the system of interest [40]. The advantage of the Born–Markov approximation is it gives rise to a reliable description of the dynamics of the quantum open system [41]. Next, we assume that the qubit-qutrit syste (S) interacts with a reservoir (R). The system $(S)+(R)$ is described by the composed density operator ρ_{SR}. The reduced density operator for the system ρ_S is given by taking the trace only over the degrees of freedom of the reservoir. This gives

$$\rho_S = \mathrm{Tr}_R(\rho_{SR}). \tag{7}$$

We assume that the qutrit-qubit system (S) and the reservoir (R) are initially uncorrelated. Therfore, the density operator ρ_{SR} factorizes as a direct product, as

$$\rho_{SR}(0) = \rho_S(0) \otimes \rho_R. \tag{8}$$

The derivation of the Markovian master equation can be easily performed in the interaction picture. In this picture, the equation of motion for ρ_{SR} is

$$\dot{\rho}_{SR}(t) = -i[H_I(t), \rho_{SR}(t)]. \tag{9}$$

The equation of motion (9) can be formally integrated to get

$$\rho_{SR}(t) = \rho_{SR}(0) - i\int_0^t ds[H_I(s), \rho_{SR}(s)]. \tag{10}$$

We substitute the expression (10) back into the Eq. (9), we obtain the following equation of motion

$$\begin{aligned}\dot{\rho}_{SR}(t) = &-i[H_I(t), \rho_{SR}(0)] \\ &-\int_0^t ds[H_I(t), [H_I(s), \rho_{SR}(s)]].\end{aligned} \tag{11}$$

The coupling between the system and the reservoir is assumed weak [42]. Therefore, we look for a solution of the Eq. (11) of the form

$$\rho_{SR}(t) \approx \rho_S(t) \otimes \rho_R(0) + \rho_C(t), \tag{12}$$

where $\rho_C(t)$ is higher order than $H_I(t)$ (1). For consistency, we require that $\mathrm{Tr}_R[\rho_C(t)] = 0$. Substituting (12) into (11), we obtain

$$\begin{aligned}\dot{\rho}_{SR}(t) = &-i[H_I(t), \rho_S(0) \otimes \rho_R] \\ &-\int_0^t ds[H_I(t), [H_I(s), \rho_S(s) \otimes \rho_R]].\end{aligned} \tag{13}$$

Taking the trace over the degrees of freedom of the reservoir and using the Eq. (7), we get

$$\begin{aligned}\dot{\rho}_S(t) = &-i\mathrm{Tr}_R[H_I(t), \rho_S(0) \otimes \rho_R] \\ &-\mathrm{Tr}_R\int_0^t ds[H_I(t), [H_I(s), \rho_S(s) \otimes \rho_R]].\end{aligned} \tag{14}$$

The statistical properties of the system can be described by the reduced density operator depending on its past history from the initial state prepared, at time $t = 0$, to the instant s. This is denoted in Eq. (14) by $\rho_S(s)$. In the Markovian regime, the damping destroys the memory of past. In this case it reasonable to replace $\rho_S(s)$ by $\rho_S(t)$ [42,43]. Thus, the Eq. (14) yields to the master equation in the Born–Markov approximation for system described by ρ_S interacting with a reservoir ρ_R as

$$\begin{aligned}\dot{\rho}_S(t) = &-i\mathrm{Tr}_R[H_I(t), \rho_S(0) \otimes \rho_R] \\ &-\mathrm{Tr}_R\int_0^t ds[H_I(t), [H_I(s), \rho_S(t) \otimes \rho_R]].\end{aligned} \tag{15}$$

By inserting the Hamiltonian of interaction (1) into the equation of motion (15) and using the relations (3), we obtain

$$\begin{aligned}&\dot{\rho}_S(t) \\ &= -\frac{1}{4}[\Gamma_A S_z^A S_z^A \rho_S(t) + \Gamma_B \sigma_z^B \sigma_z^B \rho_S(t) \\ &\quad -2\Gamma_A S_z^A \rho_S(t) S_z^A - 2\Gamma_B \sigma_z^B \rho_S(t) \sigma_z^B + \Gamma_A \rho_S(t) S_z^A S_z^A \\ &\quad +\Gamma_B \rho_S(t) \sigma_z^B \sigma_z^B + \Gamma_{AB}(S_z^A S_z^A \rho_S(t) + \sigma_z^B \sigma_z^B \rho_S(t) \\ &\quad -2S_z^A \rho_S(t) S_z^A - 2\sigma_z^B \rho_S(t) \sigma_z^B + \rho_S(t) S_z^A S_z^A \\ &\quad +\rho_S(t) \sigma_z^B \sigma_z^B + S_z^A \sigma_z^B \rho_S(t) + \sigma_z^B S_z^A \rho_S(t) - 2S_z^A \rho_S(t) \sigma_z^B \\ &\quad -2\sigma_z^B \rho_S(t) S_z^A + \rho_S(t) S_z^A \sigma_z^B + \rho_S(t) \sigma_z^B S_z^A)],\end{aligned} \tag{16}$$

After straightforward calculation, the general solution of the resulting time-evolved density matrix of the qutrit-qubit system $\rho_S(t)$ interacting with global (bilocal + collective) environments can be written in the computational basis $\{|i\ j\rangle,\ i = -1, 0, 1 \text{ and } j = 0, 1\}$, as follows

$$\rho_S^{GD}(t)=\begin{pmatrix}\rho_{11} & \gamma_B^4(t)\gamma_{AB}^4(t)\rho_{12} & \gamma_A(t)\gamma_{AB}(t)\rho_{13} & \gamma_A(t)\gamma_B^4(t)\gamma_{AB}^9(t)\rho_{14} & \gamma_A^4(t)\gamma_{AB}^4(t)\rho_{15} & \gamma_A^4(t)\gamma_B^4(t)\gamma_{AB}^{16}(t)\rho_{16}\\ \gamma_B^4(t)\gamma_{AB}^4(t)\rho_{21} & \rho_{22} & \gamma_A(t)\gamma_B^4(t)\gamma_{AB}(t)\rho_{23} & \gamma_A(t)\gamma_{AB}(t)\rho_{24} & \gamma_A^4(t)\gamma_B^4(t)\rho_{25} & \gamma_A^4(t)\gamma_{AB}^4(t)\rho_{26}\\ \gamma_A(t)\gamma_{AB}(t)\rho_{31} & \gamma_A(t)\gamma_B^4(t)\gamma_{AB}(t)\rho_{32} & \rho_{33} & \gamma_B^4(t)\gamma_{AB}^4(t)\rho_{34} & \gamma_A(t)\gamma_{AB}(t)\rho_{35} & \gamma_A(t)\gamma_B^4(t)\gamma_{AB}^9(t)\rho_{36}\\ \gamma_A(t)\gamma_B^4(t)\gamma_{AB}^9(t)\rho_{41} & \gamma_A(t)\gamma_{AB}(t)\rho_{42} & \gamma_B^4(t)\gamma_{AB}^4(t)\rho_{43} & \rho_{44} & \gamma_A(t)\gamma_B^4(t)\gamma_{AB}(t)\rho_{45} & \gamma_A(t)\gamma_{AB}(t)\rho_{46}\\ \gamma_A^4(t)\gamma_{AB}^4(t)\rho_{51} & \gamma_A^4(t)\gamma_B^4(t)\rho_{52} & \gamma_A(t)\gamma_{AB}(t)\rho_{53} & \gamma_A(t)\gamma_B^4(t)\gamma_{AB}(t)\rho_{54} & \rho_{55} & \gamma_B^4(t)\gamma_{AB}^4(t)\rho_{56}\\ \gamma_A^4(t)\gamma_B^4(t)\gamma_{AB}^{16}(t)\rho_{61} & \gamma_A^4(t)\gamma_{AB}^4(t)\rho_{62} & \gamma_A(t)\gamma_B^4(t)\gamma_{AB}^9(t)\rho_{63} & \gamma_A(t)\gamma_{AB}(t)\rho_{64} & \gamma_B^4(t)\gamma_{AB}^4(t)\rho_{65} & \rho_{66}\end{pmatrix}. \tag{17}$$

where the subscript GD (in $\rho_S^{GD}(t)$) stands for global dephasing. $\gamma_i = e^{-\frac{\Gamma_i t}{4}}$ $(i = A, B, AB)$ and ρ_{ij} denotes the elements of the initial density matrix $\rho_S(0)$ of the qutrit-qubit system.

3 Quantum correlations quantifiers

3.1 Entanglement measure: logarithmic negativity

In pure quantum states, the measure of entanglement that is often employed is the entanglement entropy. This quantifier is restricted to a bipartite pure state. In quantum systems comprising three or more subsystems, the entanglement requires other tools to characterize it. This is connected with the fact that their reduced state is usually a mixed state. Various measures have been proposed to quantify the amount of entanglement in mixed states. Among them, the logarithmic negativity $\mathcal{E}_{\mathcal{N}}(\rho)$ has been proven to be one of most suitable quantifiers, because it is easily computable for any mixed state of an arbitrary bipartite system [44]. The logarithmic negativity is based on the definition of negativity $\mathcal{N}(\rho)$ introduced by Vidal and Werner [44] Negativity isdefined as the absolute sum of the negative eigenvalues of the partial transposed density matrix with respect to the first sub-system, i.e.,

$$\mathcal{N}(\rho) = \sum_i |\vartheta_i|, \tag{18}$$

where ϑ_i are the negative eigenvalues of ρ^{T_A} (A denotes the first subsystem). In other words, the negativity is related to the trace norm of ρ^{T_A} defined as

$$\mathcal{N}(\rho) = \frac{||\rho^{T_A}||_1 - 1}{2}, \tag{19}$$

where the trace norm is defined by $||\rho^{T_A}||_1 = \mathrm{Tr}\left(\sqrt{\rho^{T_A}\rho^{T_A\dagger}}\right)$. Then, the logarithmic negativity $\mathcal{E}_{\mathcal{N}}(\rho)$ writes as

$$\mathcal{E}_{\mathcal{N}}(\rho) = \log_2[2\mathcal{N}(\rho) + 1]. \tag{20}$$

$\mathcal{N}(\rho) > 0$ if the state ρ is entangled and $\mathcal{N}(\rho) = 0$ if the state ρ is separable. On the other hand, it is known that there exists a entangle state ρ satisfying $\mathcal{N}(\rho) = 0$. The logarithmic negativity can be used to reveal the amount of entanglement between the components of any bipartite state.

3.2 Quantum discord based on linear entropy

The composite quantum system may have both quantum and classical correlations. They can be jointly quantified by quantum mutual information. Let us consider a composite bipartite quantum system AB described by the density operator ρ_{AB}. The quantum mutual information is defined by

$$\mathcal{I}(\rho_{AB}) = S(\rho_A) + S(\rho_B) - S(\rho_{AB}), \tag{21}$$

where $\rho_{A(B)} = \mathrm{Tr}_{B(A)}\rho_{AB}$ is the reduced density operators of the subsystem $A(B)$; $S(\rho) = -\mathrm{Tr}(\rho\log_2\rho)$ is the von Neumann entropy. The quantum discord $\mathcal{Q}(\rho_{AB})$ is written as the difference between quantum versions of two classically equivalent concepts for mutual information, is defined as

$$\mathcal{Q}(\rho_{AB}) = \mathcal{I}(\rho_{AB}) - \mathcal{J}(\rho_{AB}), \tag{22}$$

with the classical correlation $\mathcal{J}(\rho_{AB})$ of the bipartite state ρ_{AB} writes as

$$\mathcal{J}(\rho_{AB}) = \max_{B_j}[S(\rho_A) - \sum_j p_j S(\rho_{A|j})], \tag{23}$$

where $\{B_j\}$ denotes a set of positive operator-valued measurements (POVM) performed on the subsystem B, with $p_j = \mathrm{Tr}[(I_A \otimes B_j)\rho_{AB}(I_A \otimes B_j^\dagger)]$ and $\rho_{A|j} = \mathrm{Tr}_B[(I_A \otimes B_j)\rho_{AB}(I_A \otimes B_j^\dagger)]/p_j$ are respectively the probability and the conditional state of the system A when the outcome j occurs. I_A is the identity operator acting on the subsystem A. The major difficulty in computing the quantum discord (22) analytically in terms of von Neumann entropy is due to the maximization process for optimizing the classical correlations (23). This is a reason why the explicit expression of QD was obtained only for limited cases of two-qubit systems, for example, X-type and Bell-diagonal states [17–19]. Recently, it has been shown that the optimization procedure to get the quantum discord is possible by replacing von Neumann entropy by linear entropy [26]. This provides a good approach to deal with analytical expression of quantum correlations in an arbitrary qudit-qubit system. In this work, we shall consider the quantum discord in arbitrary qudit-qubit states by employing the formalism of linear entropy to overcome the difficulty encountered with the computability of

quantum discord based on von Neumann entropy. The linear entropy of a quantum state ρ is given by

$$S_2(\rho) = 2[1 - \mathrm{Tr}(\rho^2)]. \tag{24}$$

The classical correlation (23) when the linear entropy (24) is used instead of the von Neumann entropy, leads to

$$\mathcal{J}_2(\rho_{AB}) = \max_{p_j} \left[S_2(\rho_A) - \sum_j p_j S_2\left(\rho_{A|j}\right) \right]. \tag{25}$$

The bipartite quantum state ρ_{AB} may be written as [25]

$$\rho_{AB} = \Lambda \otimes I_B \left(|v_{B'B}\rangle \langle v_{B'B}| \right), \tag{26}$$

where $|v_{B'B}\rangle$ is the symmetric two-qubit purification of the reduced density operator ρ^B with an auxiliary system B'; Λ represents a qudit channel from the qubit state B' to the qudit state A. An arbitary qudit state can be expressed in the Bloch form as $\rho = (I_d + \mathbf{r}\cdot\boldsymbol{\gamma})/d$, where I_d is the $d \times d$ identity matrix, $\mathbf{r}$ is a $\left(d^2-1\right)$ dimensional real vector, $\boldsymbol{\gamma} = (\gamma_1, \gamma_2, \ldots, \gamma_{d^2-1})^T$ denotes the traceless Hermitian generators of $SU(d)$ and T stands for transpose operation. The generators γ are orthogonal with respect to Hilbert-Schmidt inner product. The action of a qudit channel Λ on a single-qubit state $\rho = (I_2 + \mathbf{r_B}\cdot\boldsymbol{\sigma})/2$, where $\mathbf{r_B}$ stands for a three-dimensional vector and $\boldsymbol{\sigma}$ is the vector of Pauli operators, has the following form

$$\Lambda(\rho) = \frac{1}{d}[I_d + (\mathbf{L}\mathbf{r} + \mathbf{l})\cdot\boldsymbol{\gamma}], \tag{27}$$

where L denotes $(3 \times (d^2-1))$ a real matrix whose elements are defined by $L_{ij} = \frac{1}{d}\mathrm{Tr}(\Lambda(\sigma^i)\cdot\gamma^j)$ and $\mathbf{l}$ is a three dimensional vector. Using the spectral decomposition of ρ_B, i.e., $\rho_B = \sum_{i=1,2} \lambda_i |\psi_i\rangle\langle\psi_i|$, one writes $|v_{B'B}\rangle = \sum_{i=1,2} \sqrt{\lambda_i}\,|\psi_i\rangle|\psi_i\rangle$. Thus, based on these results the analytical expression of the classical correlations for any arbitrary $d \otimes 2$ quantum state has the form [26]

$$\mathcal{J}_2(\rho_{AB}) = \frac{4}{d^2}\lambda_{\max}(L^T L) S_2(\rho_B), \tag{28}$$

It follows that the computation of $\mathcal{J}_2(\rho_{AB})$ (28) requires only the determination of the matrix L. To do this, one needs first to write the qudit-qubit density matrix ρ_{AB} in the Fano-Bloch representation as

$$\rho_{AB} = \frac{1}{2d} \sum_{\alpha=0}^{d^2-1} \sum_{\beta=0}^{3} R_{\alpha\beta}\gamma^\alpha \otimes \sigma^\beta, \tag{29}$$

where $R_{\alpha\beta}$ stands for the components of the total correlation tensor associated with ρ_{AB}. They are given by

$$R_{\alpha\beta} = \frac{d}{2}\mathrm{Tr}\left(\rho_{AB}\gamma^\alpha \otimes \sigma^\beta\right) \tag{30}$$

with γ^0 (resp, σ^0) is the identity matrix of d (resp, 2)-dimension. In terms of $R_{\alpha\beta}$ parameters, the reduced density operator ρ_B, writes from the state ρ_{AB} (29), as

$$\rho_B = \mathrm{Tr}_\mathrm{A}\left(\rho_{AB}\right) = \frac{1}{2}\sum_{\beta=0}^{3} R_{0\beta}\sigma^\beta. \tag{31}$$

Using the expression (31), the state $\rho_{B'B}$ (26) can be rewritten, as

$$\rho_{B'B} = |v_{B'B}\rangle\langle v_{B'B}| = \frac{1}{4}\sum_{\alpha,\beta=0}^{3} \mathcal{T}_{\alpha\beta}\sigma^\alpha \otimes \sigma^\beta, \tag{32}$$

where $\mathcal{T}_{\alpha\beta}$ are the components of the total correlation tensor associated with $\rho_{B'B}$. They write as

$$\mathcal{T}_{\alpha\beta} = \mathrm{Tr}\left(\rho_{B'B}\sigma^\alpha \otimes \sigma^\beta\right). \tag{33}$$

The qudit channel Λ can be reformulated as

$$\Lambda(\sigma^\alpha) = \sum_{\alpha=0}^{3}\sum_{\delta=0}^{d^2-1} \mathcal{L}_{\alpha\delta}\gamma^\delta, \tag{34}$$

with

$$\mathcal{L}_{\alpha\beta} = \mathrm{Tr}\left(\Lambda(\sigma^\alpha)\cdot\gamma^\beta\right). \tag{35}$$

By using the state (32) and the Eq. (34), we obtain

$$(\Lambda \otimes 1)\,\rho_{B'B} = \frac{1}{4}\sum_{\delta=0}^{d^2-1}\sum_{\beta=0}^{3}\left(\mathcal{L}^T\,\mathcal{T}\right)_{\delta\beta}\gamma^\delta \otimes \sigma^\beta.$$

Based on the definition (26), it is easy to check that

$$\frac{1}{2d}R_{\alpha\beta} = \frac{1}{4}\left(\mathcal{L}^T\mathcal{T}\right)_{\alpha\beta}. \tag{36}$$

It follows that the matrix $\mathcal{L}$ defined by (35) writes as

$$\mathcal{L} = \frac{2}{d}\left(\mathcal{T}^T\right)^{-1}R^T, \tag{37}$$

where R and $\mathcal{T}$ are the matrices whose elements are $R_{\alpha\beta}$ (30), $\mathcal{T}_{\alpha\beta}$ (33), respectively. In this respect, the matrix L in the Eq. (28) which is the key ingredient to evaluate the classical correlation (28) and the quantum discord for given bipartite qudit-qubit state is given by

$$L = \mathcal{L}_{ij}. \tag{38}$$

Hence, having the matrix L, the classical correlation (28) can readily be computed. Therefore, the quantum discord based on linear entropy for any qudit-qubit system is given

$$\mathcal{Q}_2(\rho_{AB}) = \mathcal{I}(\rho_{AB}) - \mathcal{J}_2(\rho_{AB}). \tag{39}$$

3.3 Measurement-induced disturbance

The third quantum correlations quantifier, which will be considered in this work, is the measurement-induced disturbance (MID). This quantifier was introduced by Luo [23] to quantify the quantumness of correlations for an arbitrary bipartite state. This approach is based on the fact that a classical state is non-disturbed by local measurements. In this approach, the quantumness of a system is defined by how much is changed the associated state after local measurements. Let $\{\Pi_i^A\}$(resp, $\{\Pi_j^B\}$) be complete projective measurements (with $\Pi_i\Pi_j = \delta_{ij}$ and $\sum_i \Pi_i = 1$) consisting of one-dimensional orthogonal projections on the subsystem A(resp, B). Then, the state ρ_{AB} after themeasurement becomes

$$\Pi(\rho_{AB}) = \sum_{ij} (\Pi_i^A \otimes \Pi_j^B)\rho_{AB}(\Pi_i^A \otimes \Pi_j^B). \tag{40}$$

Note that if $\Pi(\rho_{AB})$ (40) remains unchanged (i.e., $\Pi(\rho_{AB}) = \rho_{AB}$) thus ρ_{AB} is called a classical state because this state remains unperturbed with respect to local measurement. Otherwise ρ_{AB} is truly a quantum state and contains quantum correlations. It has been shown in Ref [23] that the choice of measurement that keeps invariant the reduced density matrices, is identical to one induced by the spectral resolutions of the marginal state, namely $\rho_A = \sum_i p_i^A \Pi_i^A$ and $\rho_B = \sum_i p_i^B \Pi_i^B$. Actually, this kind of measurement even keeps the marginal information invariant. Thus, according to Luo's methode [23], the measure of quantum correlations quantified by the measurement-induced disturbance is

$$\mathrm{MID}(\rho_{AB}) = \mathcal{I}(\rho_{AB}) - \mathcal{I}(\Pi(\rho_{AB})). \tag{41}$$

where $\mathcal{I}(.)$ is the quantum mutual information (21). Accordingly, MID (41) is interpreted as difference between the total and classical correlations.

4 Quantum correlations dynamics

4.1 Initial qutrit-qubit state

In order to discuss the dynamics of quantum correlations, we consider a particular initial qutrit-qubit state in thermal equilibrium at a given temperature T [45,46]. The Hamiltonian $H_{qutrit-qubit}$ describes this initial thermal state system writes as

$$H_{qutrit-qubit} = J\left(S_1^x s_2^x + S_1^y s_2^y + S_1^z s_2^z\right) + B s_2^z \tag{42}$$

where J is the strength of the Heisenberg coupling coefficient between the spin-1 (qutrit) and the spin-$\frac{1}{2}$ (qubit) particles. The $J > 0$ case corresponds to the antiferromagnetic phase and the situation where $J < 0$ corresponds to the ferromagnetic phase. B is the external magnetic field acting only on the spin-$\frac{1}{2}$ particle pointing in the z -direction; $S_1^\alpha\,(\alpha = x, y, z)$ denotes three components of the spin-1 operator given by in the standand basis $\{|1,1\rangle, |1,0\rangle, |1,-1\rangle\}$

$$S_1^x = \frac{1}{\sqrt{2}}\begin{pmatrix} 0 & 1 & 0 \\ 1 & 0 & 1 \\ 0 & 1 & 0 \end{pmatrix}, \qquad S_1^y = \frac{1}{\sqrt{2}}\begin{pmatrix} 0 & -i & 0 \\ i & 0 & -i \\ 0 & i & 0 \end{pmatrix},$$
$$S_1^z = \begin{pmatrix} 1 & 0 & 0 \\ 0 & 0 & 0 \\ 0 & 0 & -1 \end{pmatrix}. \tag{43}$$

and s_2^α $(\alpha = x, y, z)$ are the standard Pauli matrices. The eigenvalues and the corresponding eigenstates associated to the Hamiltonian $H_{qutrit-qubit}$ (42) are given by

$$E_1 = (J - B), \quad E_2 = (J + B), \quad E_3^{\pm} = -\frac{1}{2}\delta_{\pm}, \quad E_4^{\pm} = -\frac{1}{2}\gamma_{\pm}, \tag{44}$$

where $\delta_{\pm} = J \pm \sqrt{4B^2 - 4BJ + 9J^2}$ and $\gamma_{\pm} = J \pm \sqrt{4B^2 + 4BJ + 9J^2}$. The corresponding eigenstates are respectively given by

$$|\psi_1\rangle = |-10\rangle, \qquad |\psi_2\rangle = |11\rangle, \tag{45}$$
$$|\psi_3^{\pm}\rangle = \frac{1}{\sqrt{1+\eta_{\mp}^2}}\left(|-11\rangle + \eta_{\mp}|00\rangle\right),$$
$$|\psi_4^{\pm}\rangle = \frac{1}{\sqrt{1+\nu_{\pm}^2}}\left(|01\rangle - \nu_{\pm}|10\rangle\right), \tag{46}$$

where $\eta_{\pm} = (\delta_{\pm} - 2B)/(2\sqrt{2}J)$ and $\nu_{\pm} = (\gamma_{\pm} + 2B)/(2\sqrt{2}J)$. Note that we are working in units, such that B and J are dimensionless. At the thermal equilibrium, the state of the system at temperature T is given by the density operator $\rho_S(0) = \exp(-\beta H)/Z$ where $Z = \mathrm{Tr}[\exp(-\beta H)]$ stands for the canonical ensemble partition function and $\beta = 1/k_B T$. In the computational basis, the initial state of the qutrit-qubit system takes the form

$$\rho_S^{GD}(0,T) = \frac{1}{Z}\begin{pmatrix} a^+ & 0 & 0 & 0 & 0 & 0 \\ 0 & b_1^+ & c^+ & 0 & 0 & 0 \\ 0 & c^+ & b_2^+ & 0 & 0 & 0 \\ 0 & 0 & 0 & b_2^- & c^- & 0 \\ 0 & 0 & 0 & c^- & b_1^- & 0 \\ 0 & 0 & 0 & 0 & 0 & a^- \end{pmatrix}, \tag{47}$$

where

$$a^{\pm} = e^{-(\pm B+J)/k_BT}, \tag{48}$$

$$b_1^{\pm} = e^{J/2k_BT}\left[\cosh\left(\Delta_{\pm}/2k_BT\right) + \frac{(J\pm 2B)}{\Delta_{\pm}}\sinh\left(\Delta_{\pm}/2k_BT\right)\right], \tag{49}$$

$$b_2^{\pm} = e^{J/2k_BT}\left[\cosh\left(\Delta_{\pm}/2k_BT\right) - \frac{(J\pm 2B)}{\Delta_{\pm}}\sinh\left(\Delta_{\pm}/2k_BT\right)\right], \tag{50}$$

$$c^{\pm} = -\frac{2\sqrt{2}}{\Delta_{\pm}}\gamma_A(t)\gamma_B^4(t)\gamma_{AB}(t)e^{J/2k_BT}J\sinh\left(\Delta_{\pm}/2k_BT\right), \tag{51}$$

with $\Delta_{\pm} = \sqrt{9J^2 \pm 4BJ + 4B^2}$. The partition function Z in (47) is given by

$$Z = 2e^{-J/k_BT}\left[\cosh\left(B/k_BT\right) + e^{3J/2k_BT}\left[\cosh\left(\Delta_+/2k_BT\right) + \cosh\left(\Delta_-/2k_BT\right)\right]\right]. \tag{52}$$

Hereafter, the Boltzmann's constant is set to the unit for simplicity, i.e., $k_B = 1$. After having derived the initial state $\rho_S(0)$ (47) from the Hamiltonian $H_{qutrit-qubit}$ (42), the evolved density matrix under global dephasing noise (GD) is obtained by substituting the initial state (47) into the time-evolved density matrix $\rho_S^{GD}(t)$ (17). Thus one gets

$$\rho^{GD}(t) = \frac{1}{Z}\begin{pmatrix} a^+ & 0 & 0 & 0 & 0 & 0 \\ 0 & b_1^+ & \gamma_A(t)\gamma_B^4(t)\gamma_{AB}(t)c^+ & 0 & 0 & 0 \\ 0 & \gamma_A(t)\gamma_B^4(t)\gamma_{AB}(t)c^+ & b_2^+ & 0 & 0 & 0 \\ 0 & 0 & 0 & b_2^- & \gamma_A(t)\gamma_B^4(t)\gamma_{AB}(t)c^- & 0 \\ 0 & 0 & 0 & \gamma_A(t)\gamma_B^4(t)\gamma_{AB}(t)c^- & b_1^- & 0 \\ 0 & 0 & 0 & 0 & 0 & a^- \end{pmatrix}. \tag{53}$$

4.2 Logarithmic negativity

We first consider the time evolution of the logarithmic negativity in the state $\rho_S^{GD}(t)$ (47). In this order, one needs the negative eigenvalues of the partially transposed density matrix $\left(\rho_S^{GD}(t)\right)^{T_A}$. In the computational basis, the time-evolved density matrix $\left(\rho_S^{GD}(t)\right)^{T_A}$ takes the form

$$(\rho^{GD}(t))^{T_A} = \frac{1}{Z}\begin{pmatrix} a^+ & 0 & 0 & \gamma_A(t)\gamma_B^4(t)\gamma_{AB}(t)c^+ & 0 & 0 \\ 0 & b_1^+ & 0 & 0 & 0 & 0 \\ 0 & 0 & b_2^+ & 0 & 0 & \gamma_A(t)\gamma_B^4(t)\gamma_{AB}(t)c^- \\ \gamma_A(t)\gamma_B^4(t)\gamma_{AB}(t)c^+ & 0 & 0 & b_2^- & 0 & 0 \\ 0 & 0 & 0 & 0 & b_1^- & 0 \\ 0 & 0 & \gamma_A(t)\gamma_B^4(t)\gamma_{AB}(t)c^- & 0 & 0 & a^- \end{pmatrix}. \tag{54}$$

The possible negative eigenvalues $\vartheta_{\pm}^{GD}(t)$ of the state (54) are given as

$$\vartheta_{\pm}^{GD}(t) = \frac{1}{2Z}\left[\left(a^{\pm} + b_2^{\mp}\right) - \sqrt{\left(a^{\pm} - b_2^{\mp}\right)^2 + 4|\gamma_A(t)\gamma_B^4(t)\gamma_{AB}(t)c^{\pm}|^2}\right], \tag{55}$$

Based on the Eq. (20), it is easy to check that the logarithmic negativity writes as

$$\mathcal{E}_{\mathcal{N}}\left(\rho_S^{GD}(t)\right) = \log_2\left[2\sum_{s=\pm}\max\left\{0, -\vartheta_s^{GD}(t)\right\} + 1\right]. \tag{56}$$

4.3 Quantum discord based on linear entropy

To illustrate the results of the previous section concerning the analytical expression of quantum discord, one computes first the correlation matrix elements $R_{\alpha\beta}$(resp, $\mathcal{R}_{\alpha\beta}$) of the state $\rho_S^{GD}(t)$(resp, $\rho_{B'B}^{GD}(t)$). Thus, we write the evolved density matrix $\rho_S^{GD}(t)$ (53) in the Fano-Bloch representation as follows

$$\rho_S^{GD}(t) = \frac{1}{6}\sum_{\alpha=0}^{8}\sum_{\beta=0}^{3} R_{\alpha\beta}^{GD}(t) f^{\alpha}\otimes\sigma^{\beta},$$

where f^{α} are the generators of $SU(3)$ group which can be expressed as the Gell-Mann matrices. The non-vanishing components $R_{\alpha\beta}(t)$ are given by

$$R_{00} = \mathrm{Tr}\left(\rho_S^{GD}(t)\right) = 1, \tag{57}$$

$$R_{03} = -\frac{2}{Z}\left[e^{-J/T}\sinh(B/T) + e^{J/2T}\left[\frac{(J+2B)}{\Delta_+}\sinh(\Delta_+/2T) - \frac{(J-2B)}{\Delta_-}\sinh(\Delta_-/2T)\right]\right], \tag{58}$$

$$R_{11}(t) = R_{22}(t) = \frac{3}{Z}\gamma_A(t)\gamma_B^4(t)\gamma_{AB}(t)c^{+},$$
$$R_{61}(t) = R_{72}(t) = \frac{3}{Z}\gamma_A(t)\gamma_B^4(t)\gamma_{AB}(t)c^{-}, \tag{59}$$

$$R_{30} = \frac{3}{2Z}\left[a^{+} + e^{J/2T}\left[2\frac{(J+2B)}{\Delta_+}\sinh(\Delta_+/2T) + \frac{(J-2B)}{\Delta_-}\sinh(\Delta_-/2T) - \cosh(\Delta_-/2T)\right]\right], \tag{60}$$

$$R_{33} = \frac{3}{2Z}\left[a^{+} - e^{J/2T}\left[2\cosh(\Delta_+/2T) + \frac{(J-2B)}{\Delta_-}\sinh(\Delta_-/2T) - \cosh(\Delta_-/2T)\right]\right], \tag{61}$$

$$R_{80} = -\frac{\sqrt{3}}{2Z}\left[2a^{-} + a^{+} - e^{J/2T}\left[2\cosh(\Delta_+/2T) - 3\frac{(J-2B)}{\Delta_-}\sinh(\Delta_-/2T) - \cosh(\Delta_-/2T)\right]\right], \tag{62}$$

$$R_{83} = \frac{\sqrt{3}}{2Z}\left[2a^{-} - a^{+} - e^{J/2T}\left[2\frac{(J+2B)}{\Delta_+}\sinh(\Delta_+/2T) + 3\cosh(\Delta_-/2T) + \frac{(J-2B)}{\Delta_-}\sinh(\Delta_-/2T)\right]\right]. \tag{63}$$

where the non-vanishing components of the correlation matrix are not affected by the decoherence effects, i.e., $R_{\alpha\beta}(t) = R_{\alpha\beta}(0)$ except the components $R_{11}(t)$, $R_{22}(t)$, $R_{61}(t)$ and $R_{72}(t)$. From (31), the reduced density operator $\rho_B^{GD}(t)$ is given by

$$\rho_B^{GD}(t) = \rho_B(0) = \frac{1}{2}\begin{pmatrix} R_{00}+R_{03} & 0 \\ 0 & R_{00}-R_{03}\end{pmatrix}. \tag{64}$$

The symmetric two-qubit purification of the reduced density operator $\rho_B^{GD}(t)$ with an auxiliary system B' writes as follows

$$|v_{B'B}\rangle = \sqrt{\frac{(R_{00}+R_{03})}{2}}|00\rangle + \sqrt{\frac{(R_{00}-R_{03})}{2}}|11\rangle, \tag{65}$$

Using (32), one has

$$\rho_{B'B}^{GD}(t) = \frac{1}{2}\begin{pmatrix} (R_{00}+R_{03}) & 0\,0 & \sqrt{(R_{00}^2-R_{03}^2)} \\ 0 & 0\,0 & 0 \\ 0 & 0\,0 & 0 \\ \sqrt{(R_{00}^2-R_{03}^2)} & 0\,0 & (R_{00}-R_{03})\end{pmatrix} = \frac{1}{4}\sum_{\alpha=0}^{3}\sum_{\beta=0}^{3}\mathcal{T}_{\alpha\beta}(t)\,\sigma^{\alpha}\otimes\sigma^{\beta}, \tag{66}$$

The non-zero correlation matrix elements $\mathcal{T}_{\alpha\beta}(t)$ are given by

$$\mathcal{T}_{00} = \mathcal{T}_{33} = R_{00} = 1,\ \mathcal{T}_{03} = \mathcal{T}_{30} = R_{03},$$
$$\mathcal{T}_{11} = \mathcal{T}_{22} = \sqrt{1-R_{03}^2}, \tag{67}$$

in terms of the tensor correlation components $R_{\alpha\beta}(t)$. Note that the density matrix $\rho_{B'B}^{GD}(t)$ (66) and the correlation matrix elements $\mathcal{T}_{\alpha\beta}(t)$ are not affected by the decoherence effects ($\rho_{B'B}^{GD}(t) = \rho_{B'B}(0)$ and $\mathcal{T}_{\alpha\beta}(t) = \mathcal{T}_{\alpha\beta}(0)$). In this picture, the matrix $L^{GD}(t)$ (38) associated to the evolved matrix density writes ass

$$L^{GD}(t) = \frac{2}{3}\begin{pmatrix} \frac{R_{11}(t)}{\sqrt{1-R_{03}^2}} & 0 & 0 & 0 & 0 & \frac{R_{61}(t)}{\sqrt{1-R_{03}^2}} & 0 & 0 \\ 0 & \frac{R_{11}(t)}{\sqrt{1-R_{03}^2}} & 0 & 0 & 0 & 0 & \frac{R_{61}(t)}{\sqrt{1-R_{03}^2}} & 0 \\ 0 & 0 & \frac{R_{33}-R_{03}R_{30}}{1-R_{03}^2} & 0 & 0 & 0 & 0 & \frac{R_{83}-R_{03}R_{80}}{1-R_{03}^2}\end{pmatrix}. \tag{68}$$

After simple calculations, the eigenvalues of the matrix $\left(L^{GD}(t)\right)^{T}L^{GD}(t)$ are obtained as

$$\lambda_1^{GD}(t) = \lambda_3^{GD}(t) = \frac{1}{h}\left(3\sqrt{2}J\gamma_A(t)\gamma_B^4(t)\gamma_{AB}(t)e^{3J/2T}\right)^2\left(\frac{\sinh^2[\Delta_+/(2T)]}{\Delta_+^2} + \frac{\sinh^2[\Delta_-/(2T)]}{\Delta_-^2}\right),$$

and

$$\lambda_2^{GD}(t) = \lambda_2(0) = \left(\frac{Z^2}{4he^{-2J/T}}\right)^2\left[(R_{33}-R_{03}R_{30})^2 + (R_{83}-R_{03}R_{80})^2\right], \tag{69}$$

with the function $h = \exp(-2J/T)(a^{-}+b_1^{+}+b_2^{-})(a^{+}+b_1^{-}+b_2^{+})$ and the linear entropy $S_2(\rho_B) = h(\frac{2e^{-J/T}}{Z})^2$.

Therefore, the classical correlation (28), is given for the qutrit-qubit under consideration by

$$\mathcal{J}_2\left(\rho_S^{GD}(t)\right) = \frac{4}{9}h(\frac{2e^{-J/T}}{Z})^2 \max\left\{\lambda_1^{GD}(t), \lambda_2(0)\right\}, \quad (70)$$

Thus, the corresponding expression of quantum discord based on linear entropy is

$$\begin{aligned}\mathcal{Q}_2\left(\rho_S^{GD}(t)\right) &= -\sum_{i=1}^{3}\zeta_i\log_2\zeta_i - \sum_{j=\pm}\xi_j\log_2\xi_j \\ &+\sum_{k=1}^{6}\mu_k\log_2\mu_k - \mathcal{J}_2\left(\rho^{GD}(t)\right), \end{aligned} \quad (71)$$

where the eigenvalues ζ_i (ξ_j) of the density matrix $\rho_A^{GD}(t)$ $(\rho_B^{GD}(t))$ are

$$\begin{aligned}\zeta_{1,2} &= \frac{a^{\pm}+b_1^{\pm}}{Z}, \qquad \zeta_3 = \frac{b_2^{+}+b_2^{-}}{Z}, \\ \xi_{\pm} &= \frac{a^{\pm}+b_2^{\pm}+b_1^{\mp}}{Z}, \end{aligned} \quad (72)$$

and the non-vanishing eigenvalues μ_k of the density matrix $\rho_S^{GD}(t)$ (47) are

$$\mu^{GD}{}_{1,2}(t) = \frac{a^{\pm}}{Z}, \quad (73)$$

$$\mu^{GD}{}_{3,4}(t) = \frac{1}{2Z}\left[\left(b_1^{+}+b_2^{+}\right) \pm \sqrt{\left(b_1^{+}-b_2^{+}\right)^2 + 4|\gamma_A(t)\gamma_B^4(t)\gamma_{AB}(t)c^{+}|^2}\right], \quad (74)$$

$$\mu^{GD}{}_{5,6}(t) = \frac{1}{2Z}\left[\left(b_1^{-}+b_2^{-}\right) \pm \sqrt{\left(b_1^{-}-b_2^{-}\right)^2 + 4|\gamma_A(t)\gamma_B^4(t)\gamma_{AB}(t)c^{-}|^2}\right]. \quad (75)$$

4.4 Measurement-induced disturbance

We consider the measurement-induced disturbance quantifier (41) to determine the dynamics of quantum correlations in a qutrit-qubit state $\rho_S^{GD}(t)$ (53) which will be compared to the logarithmic negativity and quantum discord. To do this, one needs to specify the state after a measurement acting on the state (53) and the resulting reduced density matrices $\rho_A^{GD}(t)$ of the first subsystem and $\rho_B^{GD}(t)$ describing the second subsystem. Taking $\Pi_i^A = |i\rangle\langle i|$ $(i = 1, 0, -1)$ and $\Pi_j^B = |j\rangle\langle j|$ $(j = 1, 0)$, and using the expression (40), one gets

$$\Pi(\rho_S^{GD}(t)) = \frac{1}{Z}\begin{pmatrix} a^{+} & 0 & 0 & 0 & 0 & 0 \\ 0 & b_1^{+} & 0 & 0 & 0 & 0 \\ 0 & 0 & b_2^{+} & 0 & 0 & 0 \\ 0 & 0 & 0 & b_2^{-} & 0 & 0 \\ 0 & 0 & 0 & 0 & b_1^{-} & 0 \\ 0 & 0 & 0 & 0 & 0 & a^{-} \end{pmatrix}, \quad (76)$$

and

$$\begin{aligned}\Pi(\rho_A^{GD}(t)) &= \rho_A^{GD}(t) \\ &= \frac{1}{Z}\begin{pmatrix} a^{+}+b_1^{+} & 0 & 0 \\ 0 & b_2^{+}+b_2^{-} & 0 \\ 0 & 0 & a^{-}+b_1^{-} \end{pmatrix}, \end{aligned} \quad (77)$$

$$\begin{aligned}\Pi(\rho_B^{GD}(t)) &= \rho_B^{GD}(t) \\ &= \frac{1}{Z}\begin{pmatrix} a^{+}+b_2^{+}+b_1^{-} & 0 \\ 0 & a^{-}+b_2^{-}+b_1^{+} \end{pmatrix}. \end{aligned} \quad (78)$$

From (41) and (76), the MID takes the following from

$$\begin{aligned}\mathrm{MID}(\rho_S^{GD}(t)) &= S(\Pi(\rho_S^{GD}(t))) - S(\rho_S^{GD}(t)) \\ &= \sum_{k=1}^{6} v_k^{GD}\log_2 v_k^{GD} - \sum_{k=1}^{6}\mu_k^{GD}\log_2\mu_k^{GD} \end{aligned} \quad (79)$$

with μ_k^{GD} are the eigenvalues defined by (73), (74) and (75) of the state $\rho_S^{GD}(t)$ (53) and the non-vanishing eigenvalues v_k^{GD} of the density matrix $\Pi(\rho_S^{GD}(t))$ (76) are

$$v^{GD}{}_{1,2}(t) = \frac{a^{\pm}}{Z},\ v^{GD}{}_{3,4}(t) = \frac{b_1^{\pm}}{Z},\ v^{GD}{}_{5,6}(t) = \frac{b_2^{\pm}}{Z}. \quad (80)$$

5 Analysis of quantum correlations evolution

5.1 Global qutrit-qubit dephasing noise

In order to analyze the effects of the global classical dephasing noise on the behavior of quantum discord (QD), measurement-induced disturbance (MID) and the logarithmic negativity (LN), we first investigate the evolution of QD, MID and LN versus the dimensionless time parameter $(t\Gamma)$ and the exchange coupling coefficient J in the absence of the external magnetic field $(B = 0)$, for a particular temperature value T. For the sake of simplicity, we assume hereafter that all the damping parameters are the same i.e, $\Omega_A(t) = \Omega_B(t) = \Omega_{AB}(t)$. The results are plotted in Fig. 1. These results show that the three quantum correlations quantifiers have different behaviors. Clearly, QD is almost constant for sensitively higher negative values of J and when J is approaching zero QD vanishes (Fig. 1a). We notice that the qutrit and qubit are separable for $J < 0$ (Fig. 1c). MID is symmetric with respect to the axis $J = 0$ and decays monotonically (Fig. 1b). The quantum discord and measurement-induced disturbance disappear completely for $J = 0$. The increase of the coupling coefficient J induces an increase of quantum correlations, including quantum entanglement. This result shows that the exchange coupling coefficient J enhances the amount of quantum cor-

relations in the system. QD decays quickly to a finite non-zero value and reaches an asymptotic constant value. In this situation the quantum discord presents a freezing phenomenon either for the ferromagnetic phase or antiferromagnetic phase. Furthermore, the asymptotic value of QD reached for the antiferromagnetic phase ($J > 0$) is higher that one evaluated for the ferromagnetic phase ($J < 0$). The logarithmic negativity disappears in a finite time which indicates the phenomenon of entanglement sudden death (ESD), except in the interval between $J = 0$ and $J = 1$. Based on the above discussion, we conclude that QD is much robust than MID and LN under global dephasing noise effects.

The effects of the global classical dephasing noise on the behavior of quantum discord (QD), measurementinduced disturbance (MID) and the logarithmic negativity (LN) of the system in antiferromagnetic phase ($J = 1$) for various temperature values T and particular values of the external magnetic field B versus the dimensionless time parameter ($t\Gamma$) are plotted in Figs. 2 and 3. The results of Figs. 2 and 3 show that the QD, MID and LN are maximal for low temperatures and small values of the external magnetic field. Moreover, the quantum discord decays quickly to a finite non-zero value (Figs. 2a, 3a). After this quick decrease, the quantum discord exhibits freezing dynamics (the amount of quantum discord is constant). Figures 2b and 3b show that the measurement-induced disturbance has monotonic decay. For weak values of the temperature, both LN and MID have almost the same behavior, except higher temperatures (for instance, at $T = 1.2$) for which the logarithmic negativity disappears in a finite time. This is entanglement sudden death (ESD) discussed here above. Tuning of the temperature and external magnetic field might increase the value of the critical instant $t\Gamma_c$ and thus avoiding the disappearance of the logarithmic negativity and consequently the intricacy (Figs. 2c, 3c). The global dephasing noise effect is more pronounced when the values of the temperature and magnetic field are high. It must be noticed that the QD shows longer life in comparison with MID and LN. Besides the results reported in Figs. 2 and 3, we have also studied the behavior of quantum correlations measures for other values of B and T. The study shows the same behavior as plotted in Figs. 2 and 3. Therefore, quantum discord is more robust than entanglement under the global dephasing noise effects

Let us now consider the decoherence effect induced by global dephasing noise on the behavior of these different quantifiers of the system in the ferromagnetic phase ($J = -1$) for specific values of temperature T and the external magnetic field B versus the dimensionless time parameter ($t\Gamma$). The results are reported in Fig. 4. Comparing with the dynamics behavior of the system in the antiferromagnetic phase illustrated in Figs. 2 and 3, one can clearly see that the quantum correlation measures have different behavior when the system is changed from antiferromagnetic to ferromagnetic phase. The amount of quantum correlations including entanglement is smaller than that of antiferromagnetic phase. QD and MID have almost the same behavior, namely, decay monotonically with the increasing of temperature, as B increases (Fig. 4). The entanglement sudden death (ESD) also takes places, except for some particular values of temperature and external magnetic field and occurs faster than that of the antiferromagnetic phase (Figs. 2, 3). The duration of ESD depends on the parameters B and T (Fig. 4b, c), and for some small values of T (for instance, at $T = 0.4$) the entanglement reaches to zero (see Fig. 4a). The results of Fig. 4 show that even for the ferromagnetic phase the quantum discord and measurement-induced disturbance are still more robust than quantum entanglement under the global dephasing noise. Therefore, based on the results of Figs. 2, 3 and 4 we get to conclude that the quantum correlation quantifiers for the antiferromagnetic phase ($J = 1$) are more resistant than those in the ferromagnetic phase ($J = -1$) under the decoherence effect. In what follows, we will briefly discuss the dynamic behavior of quantum correlations when the qutrit-qubit system is independently subjected to the case of bilocal (BLD) noise as well for collective dephasing noise (CD).

5.2 Bilocal qutrit-qubit dephasing noise

Under bilocal dephasing noise, qutrit and qubit are only interacting independently and locally with their own noisy environments, i.e., $\Omega_{AB}(t) = 0$. In this case, the negative eigenvalues (55) take the following expression

$$\vartheta_{\pm}^{BLD}(t) = \frac{1}{2Z}\left[\left(a^{\pm}+b_2^{\mp}\right) - \sqrt{\left(a^{\pm}-b_2^{\mp}\right)^2 + 4|\gamma_A(t)\gamma_B^4(t)c^{\pm}|^2}\right], \tag{81}$$

The quantum discord (71), when $\Omega_{AB}(t) = 0$, is now given by

$$\begin{aligned}\mathcal{Q}_2\left(\rho_S^{BLD}(t)\right) &= -\sum_{i=1}^{3}\zeta_i\log_2\zeta_i - \sum_{j=\pm}\xi_j\log_2\xi_j \\ &\quad + \sum_{k=1}^{6}\mu_k^{BLD}(t)\log_2\mu_k^{BLD}(t) - \mathcal{J}_2\left(\rho^{BLD}(t)\right),\end{aligned} \tag{82}$$

with

$$\begin{aligned}\lambda_1^{BLD}(t) &= \left(\frac{2\sqrt{2}J\gamma_A(t)\gamma_B^4(t)e^{(3J)/(2T)}}{\sqrt{h}}\right)^2 \\ &\quad \left(\frac{\sinh^2[\Delta_+/(2T)]}{\Delta_+^2} + \frac{\sinh^2[\Delta_-/(2T)]}{\Delta_-^2}\right).\end{aligned} \tag{83}$$

and the non-vanishing eigenvalues $\mu_k^{BLD}(t)$ become

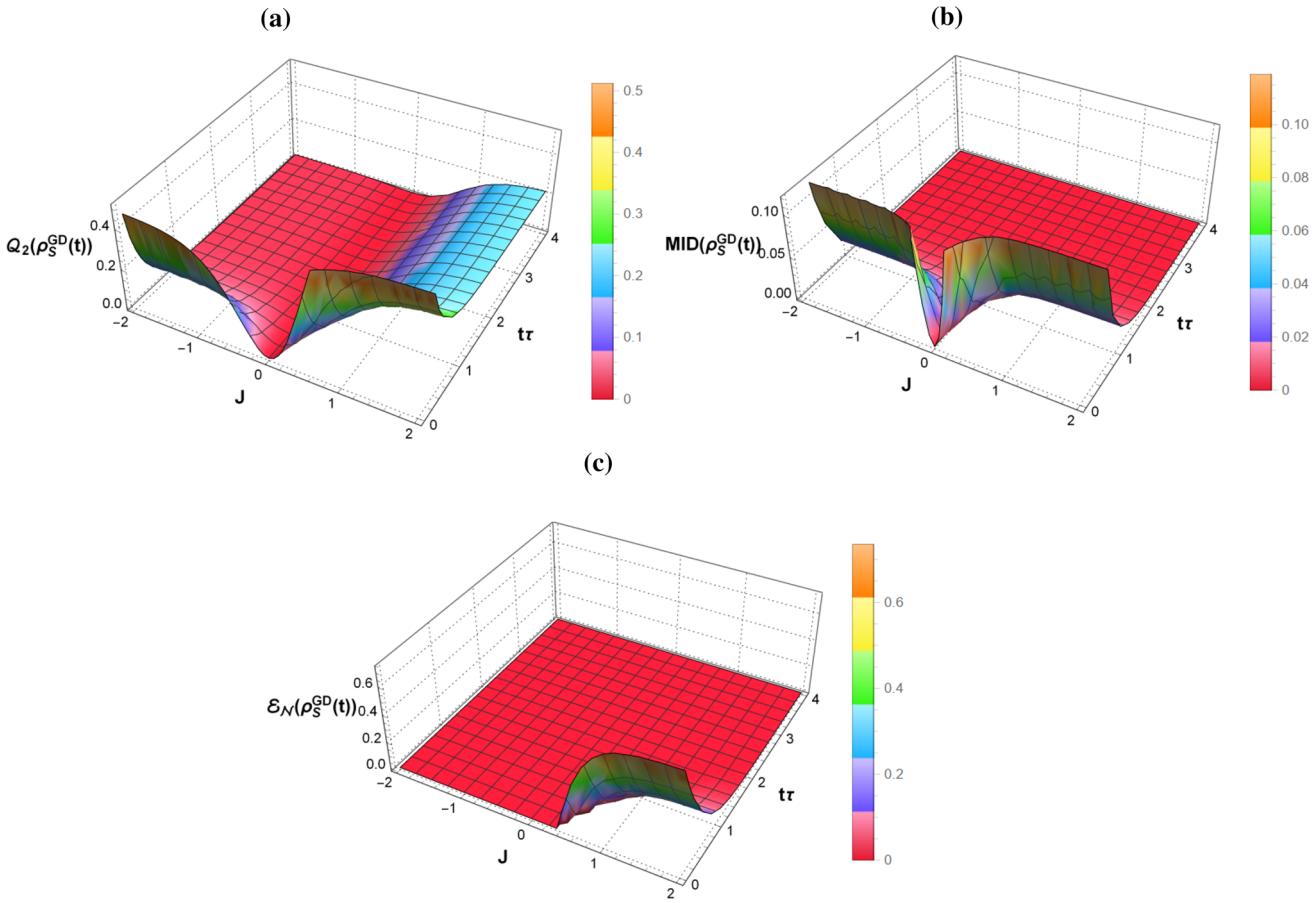


Fig. 1 **a** Dynamics of Quantum discord $\mathcal{Q}_2\left(\rho^{GD}(t)\right)$, **b** measurement-induced disturbance $\mathrm{MID}(\rho^{GD}(t))$ and **c** logarithmic negativity $\mathcal{E}_N\left(\rho^{GD}(t)\right)$ versus the dimensionless parameter $t\Gamma$ and the exchange coupling coefficient J under the effect of global classical dephasing noise for $T = 0.8$ when $B = 0$

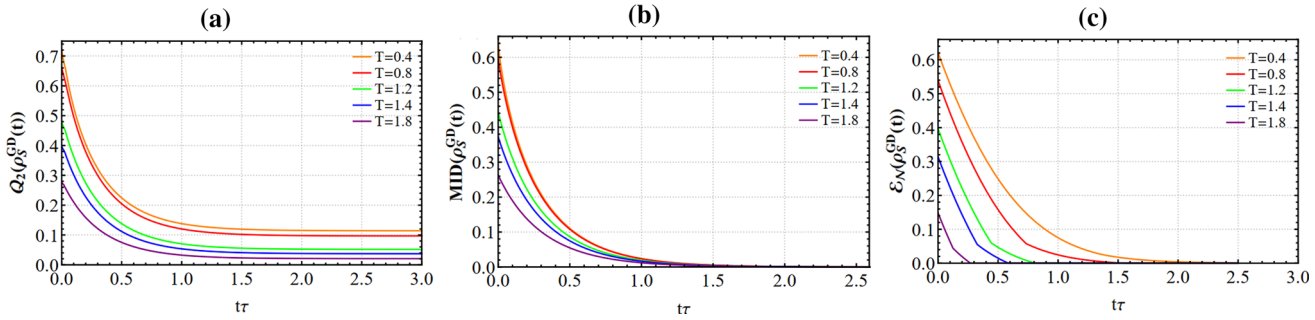


Fig. 2 **a** Dynamics of Quantum discord $\mathcal{Q}_2\left(\rho^{GD}(t)\right)$, **b** measurement-induced disturbance $\mathrm{MID}(\rho^{GD}(t))$ and **c** logarithmic negativity $\mathcal{E}_N\left(\rho^{GD}(t)\right)$ versus the dimensionless parameter $t\Gamma$ under the effect of global classical dephasing noise for different values of temperature T with $B = 1$ in the antiferromagnetic case $J = 1$

$$\mu_{1,2}^{BLD}(t) = \mu_{1,2}^{GD}(t) = \frac{a^{\pm}}{Z},$$
$$\mu_{3,4}^{BLD}(t) = \frac{1}{2Z}\left[\left(b_1^{+}+b_2^{+}\right) \pm \sqrt{\left(b_1^{+}-b_2^{+}\right)^2 + 4|\gamma_A(t)\gamma_B^4(t)c^{+}|^2}\right], \tag{84}$$
$$\mu_{5,6}^{BLD}(t) = \frac{1}{2Z}\left[\left(b_1^{-}+b_2^{-}\right) \pm \sqrt{\left(b_1^{-}-b_2^{-}\right)^2 + 4|\gamma_A(t)\gamma_B^4(t)c^{-}|^2}\right]. \tag{85}$$

The measurement-induced disturbance (79) under bilocal dephasing noise, has the form

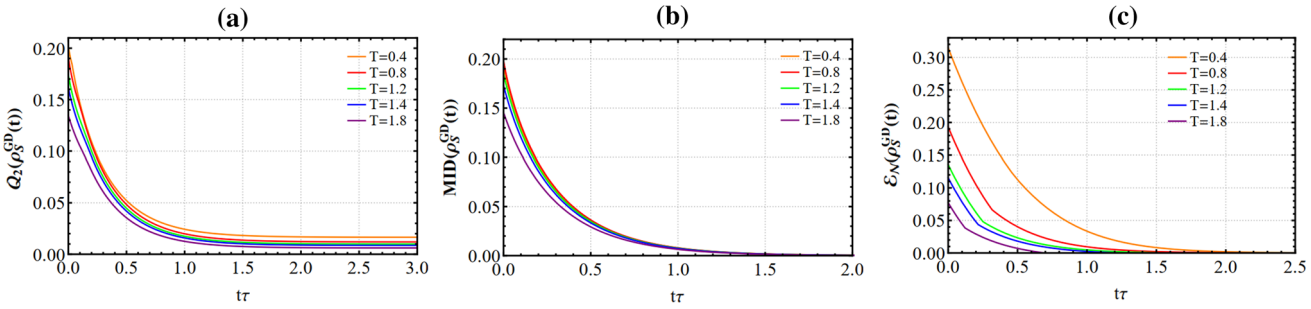


Fig. 3 **a** Dynamics of Quantum discord $\mathcal{Q}_2\left(\rho^{GD}(t)\right)$, **b** measurement-induced disturbance $\mathrm{MID}(\rho^{GD}(t))$ and **c** logarithmic negativity $\mathcal{E}_N\left(\rho^{GD}(t)\right)$ versus the dimensionless parameter $t\Gamma$ under the effect of global classical dephasing noise for different values of temperature T with $B = 3.5$ in the antiferromagnetic case $J = 1$

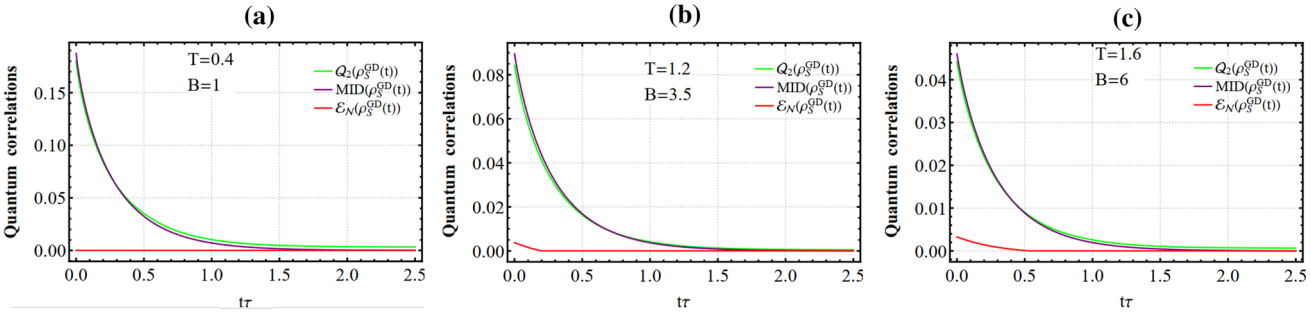


Fig. 4 Dynamics of Quantum correlations versus the dimensionless parameter $t\Gamma$ under the effect of global classical dephasing noise for different values of temperature T and external magnetic field B in the ferromagnetic case $J = -1$

$$MID(\rho_S^{BLD}(t)) = \sum_{k=1}^{6} v_k^{GD} \log_2 v_k^{GD} - \sum_{k=1}^{6} \mu_k^{BLD} \log_2 \mu_k^{BLD} \tag{86}$$

The dynamics of QD, MID, and LN under the bilocal classical dephasing noise is presented in Figs. 5 and 6 for the system either in the antiferromagnetic phase ($J = 1$) or ferromagnetic phase ($J = -1$) respectively. We consider the same simulation parameters reported for the results shown in Figs. 3 and 4. It is clearly seen that the dynamic evolution of the three mentioned quantifiers under the bilocal classical dephasing noise is similar to the behavior described under the global classical dephasing noise, either in the antiferromagnetic (Fig. 3) or ferromagnetic (Fig. 4) phase. The entanglement sudden death also occurs in this case for some particular values of temperature T and external magnetic field B. The quantum d iscord exhibits the freezing dynamics, whereas the measurement-induced disturbance decays monotonously and tends to disappear after a certain time.

5.3 Collective qutrit-qubit dephasing noise

If the local stochastic noise fields are turned off, i.e., $\Omega_A(t) = 0$ and $\Omega_B(t) = 0$, then we obtain a model in which the two-subsystems are interacting with a shared environment collectively (cf. Eq. 1). In this case, the possible negative eigenvalues (55) for collective noise are now of the form

$$\vartheta_{\pm}^{CD}(t) = \frac{1}{2Z}\left[\left(a^{\pm} + b_2^{\mp}\right) - \sqrt{\left(a^{\pm} - b_2^{\mp}\right)^2 + 4|\gamma_{AB}(t)c^{\pm}|^2}\right],$$

Under the collective dephasing noise, the quantum discord (71), become

$$\begin{aligned}\mathcal{Q}_2\left(\rho^{CD}(t)\right) &= -\sum_{i=1}^{3} \zeta_i \log_2 \zeta_i - \sum_{j=\pm} \xi_j \log_2 \xi_j \\ &\quad + \sum_{k=1}^{6} \mu_k^{CD}(t) \log_2 \mu_k^{CD}(t) - \mathcal{J}_2\left(\rho^{CD}(t)\right),\end{aligned} \tag{87}$$

with

$$\begin{aligned}\lambda_1^{CD}(t) &= \left(\frac{2\sqrt{2}J\gamma_{AB}(t)e^{(3J)/(2T)}}{\sqrt{h}}\right)^2 \\ &\quad \left(\frac{\sinh^2[\Delta_+/(2T)]}{\Delta_+^2} + \frac{\sinh^2[\Delta_-/(2T)]}{\Delta_-^2}\right),\end{aligned} \tag{88}$$

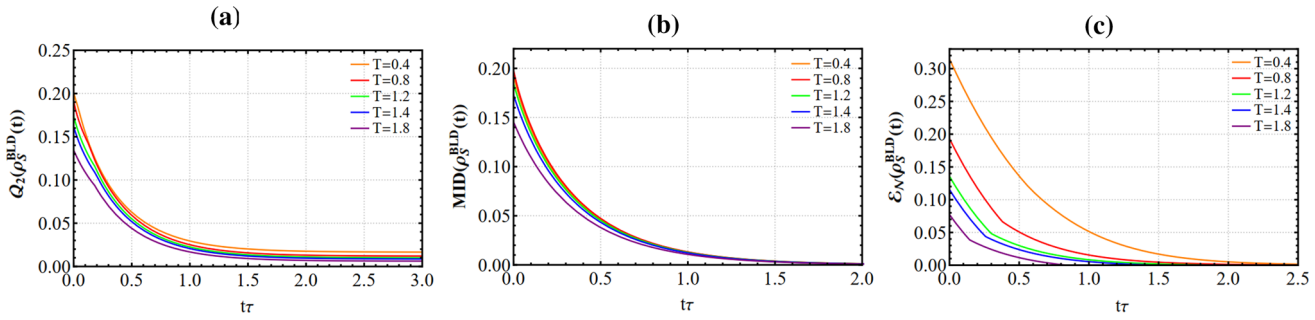


Fig. 5 **a** Dynamics of Quantum discord $\mathcal{Q}_2\left(\rho^{BLD}(t)\right)$, **b** measurement-induced disturbance $\mathrm{MID}(\rho^{BLD}(t))$ and **c** logarithmic negativity $\mathcal{E}_N\left(\rho^{BLD}(t)\right)$ versus the dimensionless parameter $t\Gamma$ under the effect of bilocal classical dephasing noise for different values of temperature T with $B = 3.5$ in the antiferromagnetic case $J = 1$

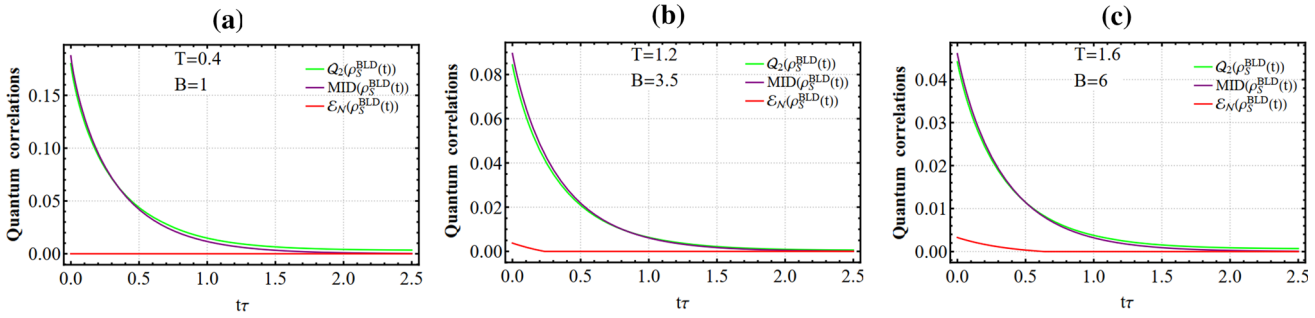


Fig. 6 Dynamics of quantum correlations versus the dimensionless parameter $t\Gamma$ under the effect of bilocal classical dephasing noise for different values of temperature T and external magnetic field B in the ferromagnetic case $J = -1$

The non-vanishing eigenvalues $\mu_k^{CD}(t)$ are

$$\mu_{1,2}^{CD}(t) = \mu_{1,2}^{GD}(t) = \frac{a^{\pm}}{Z},$$
$$\mu_{3,4}^{CD}(t) = \frac{1}{2Z}\left[\left(b_1^{+} + b_2^{+}\right) \pm \sqrt{\left(b_1^{+} - b_2^{+}\right)^2 + 4|\gamma_{AB}(t)c^{+}|^2}\right], \tag{89}$$
$$\mu_{5,6}^{CD}(t) = \frac{1}{2Z}\left[\left(b_1^{-} + b_2^{-}\right) \pm \sqrt{\left(b_1^{-} - b_2^{-}\right)^2 + 4|\gamma_{AB}(t)c^{-}|^2}\right]. \tag{90}$$

The measurement-induced disturbance (79), when $\Omega_A(t) = 0$ and $\Omega_B(t) = 0$, is expressed as

$$\mathrm{MID}(\rho^{CD}(t)) = \sum_{k=1}^{6} v_k^{GD} \log_2 v_k^{GD} - \sum_{k=1}^{6} \mu_k^{CD} \log_2 \mu_k^{CD}$$

The dynamic of QD, MID and LN under the action of the collective dephasing noise is reported in Figs. 7 and 8. A similar behavior is observed for global and bilocal dephasing noise. The only difference is that the three mentioned quantifiers exhibit longer life compared with that depicted for bilocal and global dephasing noises. These results show that the collective dephasing noise increases significantly the survival time of the quantum correlations.

6 Summary and discussion

In conclusion, an analytical method to to evaluate the quantum discord for arbitrary qudit-qubit quantum states is developed. The obtained analytical expression is an alternative tool to overcome the difficulty encountered with the computability of quantum discord based on von Neumann entropy. In the special case of a qubit-qutrit system. We show that QD converges to a non-zero constant (freezing dynamics), MID converges to zero and LN indicates a sudden death (ESD) behavior. Our numerical analysis corroborates the results reported in [11,47,48]. In fact, K.Zyczkowski et al, S.L Braunstein et al and Ferraro et al have proved that for all states, with non zero discord, the interaction with any Markovian bath can never lead to a sudden and permanent vanishing of discord. ESD is then explained by the existence of separability. In particular, we have found that for the chosen system that the quantum discord based on the linear entropy reveals the same amount of quantum correlations as measurement induced disturbance. This result indicates that this type of quantum discord is indeed an useful tool to deal with quantum correlations between multi-component systems in higher-dimensional Hilbert spaces. Another important issue of this work concerns the decoherence dynamics of quantum correlations under the influence of environmental noises. We have demonstrated that quantum discord based on linear entropy reveals a stronge behavior against global noise effects. The

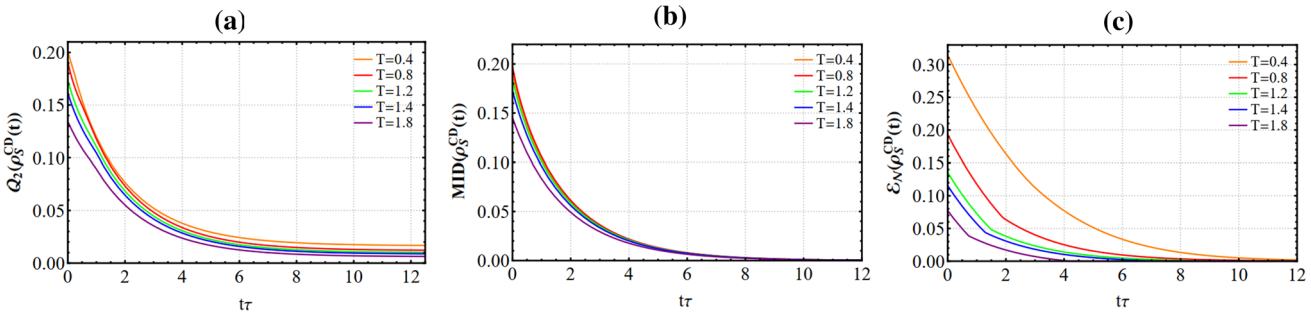


Fig. 7 **a** Dynamics of Quantum discord $\mathcal{Q}_2\left(\rho^{CD}(t)\right)$, **b** measurement-induced disturbance $\mathrm{MID}(\rho^{CD}(t))$ and **c** logarithmic negativity $\mathcal{E}_N\left(\rho^{CD}(t)\right)$ versus the dimensionless parameter $t\Gamma$ under the effect of multi-local classical dephasing noise for different values of temperature T with $B = 3.5$ in the antiferromagnetic case $J = 1$

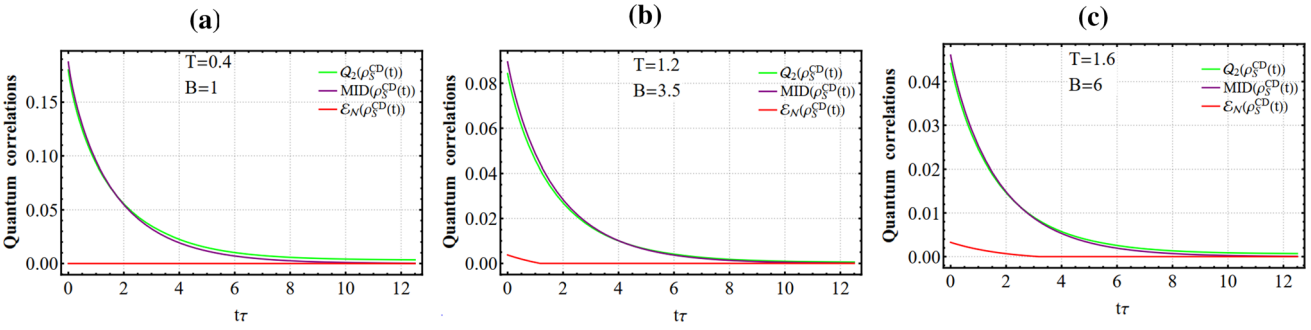


Fig. 8 Dynamics of quantum correlations versus the dimensionless parameter $t\Gamma$ under the effect of multi-local classical dephasing noise for different values of temperature T and external magnetic field B in the ferromagnetic case $J = -1$

investigation of the behavior of quantum discord versus the coupling parameter J, between the qubit and the qutrit, reveals that the dynamics of quantum correlations in the antiferromagnetic phase is more resistant than those in the ferromagnetic phase. It was found also that the quantum discord gradually decays to a finite non-zero value in the antiferromagnetic phase, which indicates the freezing phenomenon of quantum discord based on linear entropy. We demonstrated that the quantum entanglement exhibits the sudden death phenomenon for all three dephasing settings. This indicates clearly that the quantum discord based on linear entropy exhibits more robustness against noise effect, unlike quantum entanglement. Finally, based on the results obtained in this work, it might be interesting to study the survival time of correlations of a qutrit-qubit system by considering non-Markovian environments described by the so-called classical Ornstein–Uhlenbeck noises [49]. We will report on this subject in a forthcoming work.

Data Availability Statement This manuscript has no associated data or the data will not be deposited. [Authors' comment: Because all necessary information can be found in the original manuscript.]

References

1. M.A. Nielsen, I.L. Chuang, *Quantum Computation and Quantum Information* (Cambridge University Press, Cambridge, 2000)
2. R. Horodecki, P. Horodecki, M. Horodecki, K. Horodecki, Rev. Mod. Phys. **81**, 865 (2009)
3. C.H. Bennett, G. Brassard, C. Crepeau, R. Jozsa, A. Peres, W.K. Wooters, Phys. Rev. Lett. **70**, 1895–1899 (1993)
4. T. Jennewein, C. Simon, G. Weihs, H. Weinfurter, A. Zeilinger, Phys. Rev. Lett. **84**, 4729–4732 (2000)
5. M. Horodecki, J. Oppenheim, A. Winter, Nature **436**, 673–676 (2005)
6. A. Datta, A.T. Flammia, C.M. Caves, Phys. Rev. A **72**, 042316 (2005)
7. A. Datta, G. Vidal, Phys. Rev. A **75**, 042310 (2007)
8. A. Datta, A. Shaji, C.M. Caves, Phys. Rev. Lett. **100**, 050502 (2008)
9. B.P. Lanyon, M. Barbieri, M.P. Almeida, A.G. White, Phys. Rev. Lett. **101**, 200501 (2008)
10. J. Oppenheim, M. Horodecki, P. Horodecki, R. Horodecki, Phys. Rev. Lett. **89**, 180402 (2002)
11. A. Ferraro, D. Cavalcanti, F.M. Cucchietti, A. Acín, Phys. Rev. A **81**, 052318 (2010)
12. H. Ollivier, W.H. Zurek, Phys. Rev. Lett. **88**, 017901 (2001)
13. L. Henderson, V. Vedral, J. Phys. A **34**, 6899 (2001)
14. M. Daoud, R. Ahl Laamara, S. Seddik, Int. J. Mod. Phys. B **29**, 1550124 (2015)

15. A. Shabani, D.A. Lidar, Phys. Rev. Lett. **102**, 100402 (2009)
16. F. Galve, G.L. Giorgi, R. Zambrini, Phys. Rev. Lett. **83**, 012102 (2011)
17. D. Girolami, G. Adesso, Phys. Rev. A **83**, 052108 (2011)
18. M. Daoud, R. Ahl Laamara, Int. J. Quantum Inf. **10**, 1250060 (2012)
19. M. Daoud, R. Ahl Laamara, Phys. Lett. A **376**, 2361 (2012)
20. M. Daoud, R. Ahl Laamara, W. Kaydi, Phys. Lett. A **378**, 3501 (2012)
21. D. Girolami, T. Tufarelli, G. Adesso, Phys. Rev. Lett. **110**, 240402 (2013)
22. M. Horodecki, P. Horodecki, R. Horodecki, J. Oppenheim, A. Sen, U. Sen, B. Synak-Radtke, Phys. Rev. A **71**, 062307 (2005)
23. S. Luo, Phys. Rev. A **77**, 022301 (2008)
24. S. Luo, S. Fu, Phys. Rev. Lett. **106**, 120401 (2011)
25. T.J. Osborne, F. Verstraete, Phys. Rev. Lett. **96**, 220503 (2006)
26. Z. Ma, Z. Chen, F.F. Fanchini, S.M. Fei, Sci. Rep. **5**, 10262 (2015)
27. W.H. Zurek, Rev. Mod. Phys. **75**, 715 (2003)
28. C.W. Gardiner, P. Zoller, *Quantum Noise* (Springer, Berlin, 2004)
29. H.M. Wiseman, G.J. Milburn, *Quantum Measurement and Control* (Cambridge University Press, Cambridge, 2009)
30. T. Yu, J.H. Eberly, Phys. Rev. Lett. **93**, 140404 (2004)
31. T. Yu, J.H. Eberly, Opt. Commun. **264**, 393 (2006)
32. F.F. Fanchini, T. Werlang, C.A. Brasil, L.G.E. Arruda, A.O. Caldeira, Phys. Rev. A **81**, 052107 (2010)
33. B. Wang, Z.Y. Xu, M. Feng, Phys. Rev. A **81**, 014101 (2010)
34. F. Altintas, Opt. Commun. **283**, 5264 (2010)
35. T. Werlang, S. Souza, F.F. Fanchini, C.J.V. Boas, Phys. Rev. A **80**, 024103 (2009)
36. M.P. Almeida, F. de Melo, M. Hor-Meyll, A. Salles, S.P. Walborn, Science **316**, 579 (2007)
37. G. Karpat, Z. Gedik, Phys. Lett. A **375**, 4166–4171 (2011)
38. T. Yu, J.H. Eberly, Phys. Rev. B **68**, 165322 (2003)
39. K. Ann, G. Jaeger, Phys. Rev. B **75**, 115307 (2007)
40. H.P. Breuer, F. Petruccione, *The Theory of Open Quantum Systems* (Oxford University Press, Oxford, 2002)
41. C.W. Gardiner, P. Zoller, *Quantum Noise* (Springer, Berlin, 2000)
42. M.O. Scully, M.S. Zubairy, *Quantum Optics* (Cambridge University Press, Cambridge, 1997)
43. A. Mazhar, Braz. J. Phys. **50**(2), 124–135 (2020)
44. G. Vidal, R.F. Werner, Phys. Rev. A **65**, 032314 (2002)
45. G.F. Zhang, Y.C. Hou, A.L. Ji, Solid State Commun. **151**, 790 (2011)
46. F. Benabdallah, A. Slaoui, M. Daoud, Quantum Inf. Process. **19**, 252 (2020)
47. K. Zyczkowski, P. Horodecki, A. Sanpera, M. Lewenstein, Phys. Rev. A **58**, 883 (1998)
48. S.L. Braunstein, C.M. Caves, R. Jozsa, N. Linden, S. Popescu, R. Schack, Phys. Rev. Lett. **83**, 1054 (1999)
49. J.Q. Li, J.Q. Liang, Phys. Lett. A **375**, 1496 (2011)

2 Contribution 2: Pairwise quantum criteria and teleportation in a spin square complex

Scientific Reports, 12 (2022) 6406.

2.1 Summary of contribution 2

As already discussed, characterizing and quantifying entropic quantum discord is a challenging task for implementing quantum technologies. Despite this, an explicit formula for QD in a general bipartite or multipartite quantum system is still lacking. Motivated by this fact, we have studied in this contribution some alternative discord-like quantum correlation metrics, namely concurrence (2.55), local quantum uncertainty (4.15), and l_1-norm coherence (4.72) in a four-qubit square chain. By using a partitioning strategy which can be realized by taking into account the bipartite reduced density matrices whereby one essentially traces across all other systems, retaining just a two-qubit system, we assessed the thermal state of the system under discussion. This makes it possible for us to calculate the various quantum correlations' relevant quantities. The consequences of the intrinsic and extrinsic variables, including the inter-chain XX linking constant, external magnetic field, temperature, and exchange anisotropy, encoded in the thermal state, are thoroughly investigated within a comparative framework on the parameter reliance of the previously mentioned thermal pair-wise quantum correlation measures. Our findings suggest that tuning the anisotropy parameter can enhance thermal quantum correlations and coherence, leading to maximum values. Moreover, we have shown that coherence remains a more efficient correlations than the local quantum uncertainty and concurrence in detecting the quantum characteristics.

Besides, an important aspect of our work was the study of teleportation. Using the aforementioned criteria and the standard quantum teleportation protocol, we have demonstrated the possibility of achieving perfect teleportation of an unknown quantum state between any two qubits in the complex. We analyze the fidelity of the teleportation protocol as a function of parameters, for example, the power of the magnetic field and the temperature effect. Our results show that the fidelity of the protocol can be optimized by tuning these parameters, which could have significant implications for the development of practical quantum communication and computation technologies.

Overall, our study offers a theoretical framework for analyzing pairwise quantum correlations and non-classical teleportation in the spin-square complex, which could prove useful in designing and understanding quantum systems for applications in quantum information processing.

2.2 Content of contribution 2

scientific reports

Check for updates

OPEN

Pairwise quantum criteria and teleportation in a spin square complex

Fadwa Benabdallah[1], Saeed Haddadi[2,3]✉, Hamid Arian Zad[4,5], Mohammad Reza Pourkarimi[6], Mohammed Daoud[7,8] & Nerses Ananikian[4,9]

Thermal non-classical correlations quantified by concurrence entanglement, local quantum uncertainty, and quantum coherence in a four-qubit square chain are exactly examined. The influences of the Hamiltonian parameters on the mentioned pairwise quantum criteria and fidelity of teleportation are studied, and the most interesting findings are discussed in detail. It is found that the tuning anisotropy results in enhancing the thermal quantum correlations and coherence as well as average fidelity until achieving maximum values. We persuasively deduce that quantum coherence is a more efficient criterion than that of concurrence and local quantum uncertainty to detect the quantumness of a thermal state.

During the past two decades, various measures of quantum correlations in bipartite and multipartite systems have been proposed, and their properties have been intensively investigated[1–5]. The most potential resource is quantum entanglement[6,7], which has been considered as the unique form of quantum correlations to enhance the quantum information technology at the time. Indeed, some separable quantum states may also perform better than their classical counterparts for certain quantum tasks[8,9]. Nevertheless, according to various studies[10–14], quantum correlations can not only be limited to quantum entanglement. Inspired by the Wigner-Yanase skew information[15], the local quantum uncertainty (LQU) has been introduced by Girolami et al.[16] as a discord-like quantifier of non-classical correlations in multipartite systems[17]. It quantifies the uncertainty which can arise in a given quantum state due to its noncommutativity with the measured local observable[18]. The LQU is defined as a minimum of the skew information and a closed mathematical expression is available for any bipartite system[16]. Furthermore, beyond its importance as a quantum correlation quantifier, LQU is relatively associated with the notion of quantum Fisher information[19–22], which makes it an easy-to-access key for quantum metrology protocols[16]. Put together, the Wigner-Yanase skew information is also connected with quantum coherence[23–25]. This approach is one of the subjects of interest in this paper. By arising from quantum state superposition, quantum coherence is one of the central concepts for quantum information processing[26,27]. It has been widely used as an important resource for quantum technology[28–32], with further relevant applications including quantum optics[26], quantum information science[33,34], thermodynamics[35,36], and so forth[37–39]. Besides, the quantum coherence could be pleasantly linked to quantum entanglement and entropic uncertainty relations[40–47], and discord-like correlations as well[48]. Motivated by this connection, a wide variety of quantum coherence measurements have been proposed, and their properties have been investigated in detail over the years[25,48]. For instance, Baumgratz et al.[25] formulated a rigorous resource framework for the quantification of quantum coherence. They proposed the relative entropy of coherence and the intuitive l_1 –norm quantum coherence as proper quantifiers of quantum coherence, which take the form of easy to evaluate analytical expressions. Moreover, Hu et al.[48] examined the discord-like quantum correlations and quantum coherence measures for bipartite and multipartite systems, and their relationship in various settings. The authors also provided a full review of the resource theory about the discord-like quantum correlations and quantum coherence, which are defined based on the different distance measures of states.

[1]LPHE-Modeling and Simulation, Faculty of Sciences, Mohammed V University, Rabat, Morocco. [2]Faculty of Physics, Semnan University, P.O.Box 35195-363, Semnan, Iran. [3]Saeed's Quantum Information Group, P.O.Box 19395-0560, Tehran, Iran. [4]A. I. Alikhanyan National Science Laboratory, 0036 Yerevan, Armenia. [5]Department of Theoretical Physics and Astrophysics, Faculty of Science, P.J. Šafárik University, Park Angelinum 9, 041 54 Košice, Slovak Republic. [6]Department of Physics, Salman Farsi University of Kazerun, Kazerun, Iran. [7]Department of Physics, Faculty of Sciences, University Ibn Tofail, Kenitra, Morocco. [8]Abdus Salam International Centre for Theoretical Physics, Strada Costiera 11, 34151 Trieste, Italy. [9]CANDLE Synchrotron Research Institute, Acharyan 31, 0040 Yerevan, Armenia. ✉email: saeed@ssqig.com

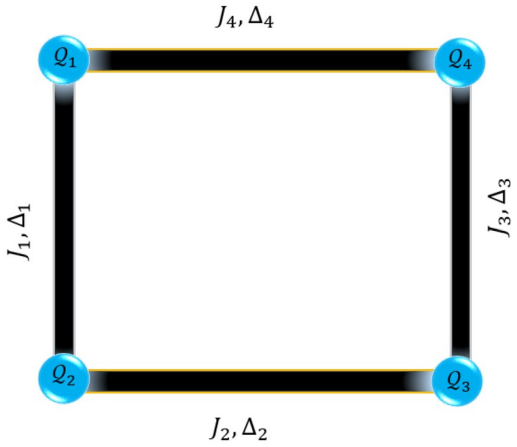


Figure 1. Schematic structure of a four-qubit (Q_1, Q_2, Q_3, and Q_4) square complex on the Heisenberg XXZ model with the corresponding exchange anisotropy and spin interactions.

The exactly solvable spin chains provide notable cornerstones of the quantum theory of magnetism[49–52]. The 1-D ferrimagnetically Heisenberg spin chains have attracted a great deal of attention, for the reason that they naturally bear strong magnetic properties and demonstrate some zero-temperature phase transitions between intriguing ground states that properly coincide with the quantized magnetization plateaus in respective magnetization curves[53–55]. The structural and magnetic properties of the ferromagnetically coupled tetranuclear copper Cu_4^{II} square complex have been experimentally investigated in Ref.[56]. The spin arrangement of this special complex in the crystal lattice leads to the formation of a square structure. Motivated by the considered model and results reported in this reference, in the present paper, we consider a four-qubit square complex to give a detailed investigation of the characteristics of thermal non-classical correlations including bipartite quantum entanglement, LQU, and quantum coherence at finite temperature, as well as, to demonstrate how these quantities behave in such a system at a thermal regime. Difference or similarity between thermal entanglement and other thermal quantum correlation quantifiers will be referred to[57,58]. In this respect, we handle the concurrence, LQU, and the intuitive l_1 –norm quantum coherence for describing the thermal pairwise quantum criteria in a four-qubit square compound on the spin-1/2 Heisenberg XXZ model, under the influence of the external magnetic field, isotropic coupling constant, and exchange anisotropy.

We evaluate the thermal state of the system under consideration by adopting the partitioning scheme, which can be realized by considering the bipartite reduced density matrix whereby one traces over all other systems, leaving effectively only a two-qubit system, which allows us to carry out the calculation of different amounts of quantum correlations related to such a state. Within the comparison framework, the effects of an external magnetic field, inter-chain XX coupling constant and that of the exchange anisotropy in the z-direction on the parameter dependence of the aforementioned thermal pairwise quantum correlation measurements are rigorously examined. Finally, we verify the quantum teleportation of two qubits in an arbitrary pure entangled state through the model under consideration in thermal equilibrium as a quantum channel[59–63]. In fact, we investigate the output quantum correlations, coherence, and average fidelity.

This paper is arranged as follows. In "The model Section", we describe the physical model and its eigenstates with the corresponding eigenvalues. Furthermore, the exact solution of the model via the partitioning scheme is obtained in "Pairwise density operator Section". In "Quantum correlations and coherence Section", a brief review concerning the definition of concurrence entanglement, LQU, quantum coherence and their analytical expressions is given. In "Results and discussion Section", the effects of anisotropy, exchange interaction, and external magnetic field on the quantum correlations and coherence are discussed in detail. By using the standard teleportation protocol, we deal with the evaluation of the fidelity, average fidelity, and the non-classical correlations of teleported state or output state in "Quantum teleportation Section". Finally, the concluding remarks are given in "Concluding remarks and outlook Section".

The model. In this section, let us consider the Hamiltonian of a four-qubit Heisenberg XXZ model as a cluster system, which is under the influence of an external magnetic field (see Fig. 1). The Hamiltonian of the model can be expressed as follows[64,65]

$$H = \sum_{i}^{4} \left[-J_i (S_i^x S_{i+1}^x + S_i^y S_{i+1}^y) + \Delta_i S_i^z S_{i+1}^z \right] - \mu_B g B \sum_{i}^{4} S_i^z, \tag{1}$$

where J_i with $i = \{1, 2, 3, 4\}$ describes the strength of the spin interaction, being ferromagnetic when $J_i > 0$. B is the external magnetic field, which is only applied to the z-direction, while Δ is the exchange anisotropy parameter. Moreover, g is the Landé g-factor with the assumption $g = 2$, and S_i^α ($\alpha = x, y, z$) are the spin-1/2 operators. For convenience, we set $\hbar = 1$ and Bohr magneton μ_B was absorbed into a definition of the magnetic field term. Let us notify that for simplicity, in the forthcoming analytical expressions and simulations, we consider

$J_2 = J_3 = J_4 = J$ and uniform anisotropy $\Delta_1 = \Delta_2 = \Delta_3 = \Delta_4 = \Delta$, assuming $J_1 = 1$ as energy unit for all other parameters with $\{B,\ J,\ \Delta,\ T\}$ being dimensionless parameters. In the next sections, we will assume both pure ferromagnetic interactions ($J > 0$) and mixed ferromagnetic-antiferromagnetic interactions between nearest-neighbor spins by adopting $J < 0$ that means $J_2, J_3, J_4 < 0$ but $J_1 = 1 > 0$. Regarding previous reports, some real magnetic compounds can be plausibly characterized in terms of our modeled spin-1/2 system[66].

By straightforward calculations, one can find the eigenvalues and corresponding eigenstates of the mentioned Hamiltonian (1) in terms of the standard basis, as reported in Methods.

Pairwise density operator. For a system in thermal equilibrium at a temperature T (canonical ensemble), the state of the system is given by the density operator $\rho_{\text{total}}(T) = \exp(-\beta H)/Z$, with $Z = \text{Tr}\left[\exp(-\beta H)\right]$ being the partition function of system and $\beta = 1/k_B T$. Hereafter, the Boltzmann's constant is set to the unit for simplicity, i.e., $k_B = 1$. Hence, the total density operator $\rho_{\text{total}}(T)$ of the described system can be characterized in terms of the eigenstates and eigenvalues of the Hamiltonian (1) as

$$\rho_{\text{total}}(T) = \frac{1}{Z}\sum_{l=1}^{16} \exp(-\beta E_l)|\psi_l\rangle\langle\psi_l|, \tag{2}$$

where E_l and $|\psi_l\rangle$ are the eigenvalues and eigenstates of the Hamiltonian, respectively, as given in Methods. The whole system can be partitioned by considering the bipartite reduced density matrix of two-qubit $\rho_{ij}(T) = \text{Tr}_{kl}\left[\rho_{ijkl}(T)\right]$ with $\rho_{ijkl}(T)$=$\rho_{\text{total}}(T)$, which obtained by tracing over all other systems except subsystems or modes i and j. In total, there are six different density matrices for our considered system. However, we find that the thermal state of $\rho_{12}(T)$ has the highest amount of quantum correlations and coherence. Therefore, from now on, let us consider only this state for analysis. In the standard basis of $\{|00\rangle, |01\rangle, |10\rangle, |11\rangle\}$, the reduced density matrix is given by

$$\rho_{12}(T) \equiv \rho_T = \begin{pmatrix} \rho_{11} & . & . & . \\ . & \rho_{22} & \rho_{23} & . \\ . & \rho_{23} & \rho_{33} & . \\ . & . & . & \rho_{44} \end{pmatrix}, \tag{3}$$

with the dots which are placed instead of zero entries. Since the components of the above matrix are too long to work with conveniently, let us eschew reporting them here.

Quantum correlations and coherence. In this section, let us discuss the main results obtained from the theoretical studies of pairwise density matrix and three described quantum criteria such as entaglement concurrence, LQU, and l_1−norm of quantum coherence.

Entaglement concurrence. In order to describe the thermal quantum entanglement in the reduced density matrix ρ_T, we employ the most widely accepted measure for a two-qubit system ρ called concurrence $C(\rho)$, which has been described by Wootters[7]. The case $C(\rho) = 0$ happens when the system state is separable, whereas $C(\rho) = 1$ reveals maximally entangled state. A straightforward definition of concurrence can be expressed as follow

$$C(\rho) = \max\{0, \sqrt{\lambda_1} - \sqrt{\lambda_2} - \sqrt{\lambda_3} - \sqrt{\lambda_4}\}, \tag{4}$$

where $\lambda_i (i = 1, 2, 3, 4)$ are the eigenvalues in the decreasing order of the 4×4 matrix $R = \rho(\sigma_y \otimes \sigma_y)\rho^*(\sigma_y \otimes \sigma_y)$, in which ρ^* and σ_y are, respectively, the complex conjugate of ρ in the standard basis and the y−component Pauli matrix. Ultimately, the concurrence for our thermal state (3) can be achieved by

$$C(\rho_T) = 2\max\{0, |\rho_{23}| - \sqrt{\rho_{11}\rho_{44}}\}. \tag{5}$$

Local quantum uncertainty. The LQU was recently proposed as a discord-like measure of quantum correlations based on the principle of skew information[16]. It is written as

$$\mathscr{U}(\rho) = \min_{K_A} \mathscr{I}(\rho, K_A \otimes I_B), \tag{6}$$

where K_A is a Hermitian operator (local observable) on the subsystem A admitting a non-degenerate spectrum. I_B being the identity operator acting on the subsystem B, while $\mathscr{I}$ is the Wigner-Yanase skew information associated to the density matrix ρ and defined as[15]

$$\mathscr{I}(\rho, K_A \otimes I_B) = -\frac{1}{2}\text{Tr}[(\sqrt{\rho}, K_A \otimes I_B)^2]. \tag{7}$$

Here, $\mathscr{I}$ is non-negative and non-increasing under classical mixing[17,18]. For a $2 \otimes d$ (qubit-qudit) bipartite quantum systems[16,18], the closed-form of the LQU is given by

$$\mathscr{U}(\rho) = 1 - \lambda_{\max}(\mathscr{W}_{AB}), \tag{8}$$

where $\lambda_{\max}$ stands for the largest eigenvalue of the 3×3 matrix $\mathscr{W}_{AB}$ whose elements are given by[67,68]

$$(\mathscr{W}_{\mathrm{AB}})_{ij} \equiv \mathrm{Tr}[\sqrt{\rho}(\sigma_{\mathrm{A}}^{i} \otimes I_{\mathrm{B}})\sqrt{\rho}(\sigma_{\mathrm{A}}^{j} \otimes I_{\mathrm{B}})], \tag{9}$$

where $\sigma_{\mathrm{A}}^{i(j)}$ with $i(j) = \{x, y, z\}$ represent the Pauli operators of the subsystem A. The LQU provides a reliable quantifier of quantum correlations and it has a geometrical significance in terms of Hellinger distance[16,18]. It is clear that having the matrix $\mathscr{W}_{\mathrm{AB}}$, one can easily evaluate the LQU for qubit-qudit quantum systems contrarily to quantum discord[17]. This is quite an easy task compared with the complicated minimization process over parameters due to the local measurements[13,16,18]. We notice that for a two-qubit pure state, the LQU coincides with the concurrence and vanishes for classically correlated states. Moreover, it is invariant under local unitary operations[16,18].

In the Fano-Bloch representation[69,70], our thermal state ρ_T (3) can be written as follows

$$\rho_T = \frac{1}{4}\sum_{\alpha,\beta=0}^{3} \mathscr{R}_{\alpha\beta}(\sigma^{\alpha} \otimes \sigma^{\beta}), \tag{10}$$

where $\mathscr{R}_{\alpha\beta} = \mathrm{Tr}[\rho_T(\sigma^{\alpha} \otimes \sigma^{\beta})]$ are the components of the total correlation tensor occurring in the Fano-Bloch decomposition associated with bipartite density matrix ρ_T. The non-vanishing components $\mathscr{R}_{\alpha\beta}$ are given as

$$\begin{aligned} \mathscr{R}_{00} &= \mathrm{Tr}[\rho_T] = 1, \quad \mathscr{R}_{03} = 1 - 2(\rho_{22} + \rho_{44}), \quad \mathscr{R}_{11} = \mathscr{R}_{22} = 2\rho_{23}, \\ \mathscr{R}_{30} &= 1 - 2(\rho_{33} + \rho_{44}), \quad \mathscr{R}_{33} = 1 - 2(\rho_{22} + \rho_{33}). \end{aligned} \tag{11}$$

Therefore, in terms of the Fano-Bloch components $\mathscr{R}_{\alpha\beta}$ associated with the matrix ρ_T, the eigenvalues of $(\mathscr{W}_{\mathrm{AB}})_{ij}$ can be expressed as

$$\omega_1 = \omega_2 = \sqrt{\left(t_1 + 2\sqrt{d_1}\right)\left(t_2 + 2\sqrt{d_2}\right)} + \frac{1}{4}\frac{\left(\mathscr{R}_{03}^2 - \mathscr{R}_{30}^2\right)}{\sqrt{\left(t_1 + 2\sqrt{d_1}\right)\left(t_2 + 2\sqrt{d_2}\right)}}, \tag{12}$$

$$\omega_3 = \frac{1}{2}\left[1 + 2\left(\sqrt{d_1} + \sqrt{d_2}\right)\right] + \frac{1}{8}\left[\frac{\left(\mathscr{R}_{03} + \mathscr{R}_{30}\right)^2}{\left(t_1 + 2\sqrt{d_1}\right)} + \frac{\left(\mathscr{R}_{03} - \mathscr{R}_{30}\right)^2 - 4\mathscr{R}_{11}^2}{\left(t_2 + 2\sqrt{d_2}\right)}\right], \tag{13}$$

with

$$t_{1,2} = \frac{1}{2}\left(1 \pm \mathscr{R}_{03}\right), \tag{14}$$

$$d_{1,2} = \frac{1}{16}\left[\left(1 \pm \mathscr{R}_{33}\right)^2 - \left(\mathscr{R}_{30} \pm \mathscr{R}_{03}\right)^2 - \left(\mathscr{R}_{11} \mp \mathscr{R}_{22}\right)^2\right]. \tag{15}$$

Hence, the LQU for the considered thermal state ρ_T is gained from

$$\mathscr{U}(\rho_T) = 1 - \max\{\omega_1, \omega_3\}. \tag{16}$$

Quantum coherence. Quantum coherence is an indisputable physical resource of quantum information processing protocols. Even though quantum coherence in multipartite states is somehow related to quantum correlations, it is a quantum property behind any correlation. Thus, coherence is a quantum resource different from entanglement and discord-like correlations[48]. Regarding the latter, the amount of non-classical correlations is estimated in terms of the coherence, in the sense that coherence of subsystems could act as an upper bound for the quantum discord-like correlation of the total bipartite system.

Herein, we use the intuitive l_1−norm of coherence measure[25], defined as the sum of the absolute off-diagonal elements of a quantum state ρ in the reference basis $\{|i\rangle\}$. It can be calculated as[71]

$$C_{l_1}(\rho) = \sum_{i \neq j} |\langle i|\rho|j\rangle|. \tag{17}$$

Thus, the corresponding l_1−norm of quantum coherence of the our system described by the reduced thermal state ρ_T (3) is given by

$$C_{l_1}(\rho_{\mathcal{T}}) = 2|\rho_{23}|. \tag{18}$$

It has been proved by Streltsov *et al.*[72] that quantum coherence can be used as a resource for quantum entanglement creation. The l_1−norm of coherence is a crucial link between various coherence measurements and entanglement[73]. Although, quantum coherence may capture quantumness more than discord-like measures of quantum correlations, the later is exactly basis-independent measure of the former[25,74].

Results and discussion

To get an insight into the pairwise entanglement, we have plotted the concurrence (5) as a function of the temperature T for several values of the magnetic field B and fixed $\Delta = 1$ as well as $J = 0.02$ in Fig. 2a. It is observed that the concurrence is a decreasing function of T from its maximum value $C(\rho_T) = 1$ for weak values of B, but its

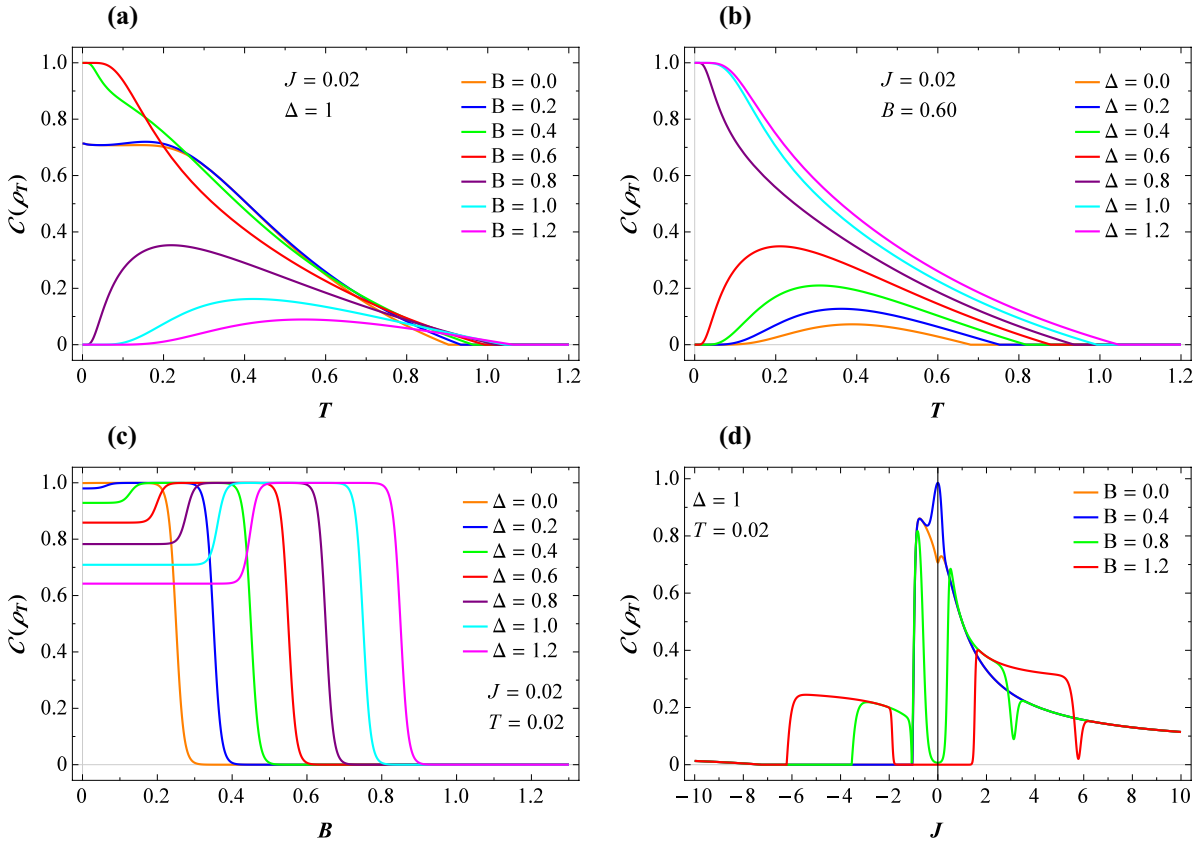


Figure 2. (**a**) Concurrence versus temperature for several fixed values of the magnetic field, taking $J = 0.02$ and $\Delta = 1$. (**b**) Concurrence versus temperature for several fixed values of the exchange anisotropy, taking $J = 0.02$ and $B = 0.6$. (**c**) The same function against magnetic field for various values of the exchange anisotropy at low temperature $T = 0.02$ and fixed $J = 0.02$. (**d**) The exchange coupling dependence of the concurrence at low temperature $T = 0.02$ and fixed $\Delta = 1$, where different values of the magnetic field are assumed.

behavior is different for stronger magnetic fields. Besides, it undergoes substantial changes upon the anisotropy alterations, as seen in Fig. 2b. As a matter of fact, an increase in the Δ strengthens the entanglement. The field dependence of the concurrence is depicted in Fig. 2c at low temperature $T = 0.02$ and low coupling constant $J = 0.02$, where several fixed values of the Δ are considered. One sees that for the finite values of parameters B, J, and T, the concurrence does not reach its maximum as soon as the anisotropy Δ enhances from zero. For $\Delta > 0$, the concurrence remains steady at low magnetic fields, then sharply increases nearby the critical magnetic field and reaches its maximum instantly. Eventually, this quantity shows a steep decrease close to the second critical magnetic field. Fig. 2d displays the concurrence against the exchange coupling J at low temperature $T = 0.02$ and $\Delta = 1$ for various fixed values of the magnetic field. Here, it is evident that the concurrence has an anomalous behavior in the vicinity of some critical points. A sudden death of this measure of entanglement happens nearby the critical point $J = -1$.

Figure 3 illustrates the thermal LQU (16) of the model in different planes. Two plots (a) and (b) depict the temperature dependence of this function for fixed $J = 0.02$, such that Fig. 3a corresponds to the several values of the magnetic field and $\Delta = 1$, whereas the other one corresponds to the case when several values of the anisotropy are assumed at fixed $B = 0.6$. Some differences are evident between LQU and concurrence. For example, the latter reaches its maximum value of 1 at finite low temperatures while the former, under the same conditions, does not. In addition, the concurrence vanishes at a critical temperature, while upon heating, LQU tends to zero but does not vanish. This particular behavior indicates the robustness of LQU against the concurrence at higher temperatures. Fig. 3c displays the LQU as a function of the magnetic field for several values of the exchange anisotropy, supposing low temperature $T = 0.02$ and $J = 0.02$. With the increase of the magnetic field, this function sharply decreases and ultimately vanishes nearby the same critical magnetic point to the concurrence. It is worth mentioning that another notable difference between the magnetic behavior of LQU and concurrence is that, the former behaves anomalously when drops down in height to $\mathcal{U}(\rho_T) = 1/2$. This phenomenon indicated by a horizontal dotted line, however, it was not observed in the concurrence behavior. This is in fact the well-known sudden change behavior for the discord-like quantum correlations, which is caused by the optimization procedure in their respective definitions[75,76]. As a result, the LQU is more sensitive than the concurrence to demonstrate thermal fluctuations or discontinuous phase spectra.

Last but not least, let us also emphasize another important consequence of the LQU analysis with respect to the coupling constant J. Fig. 3d illustrates the LQU versus the coupling constant J at low temperature $T = 0.02$

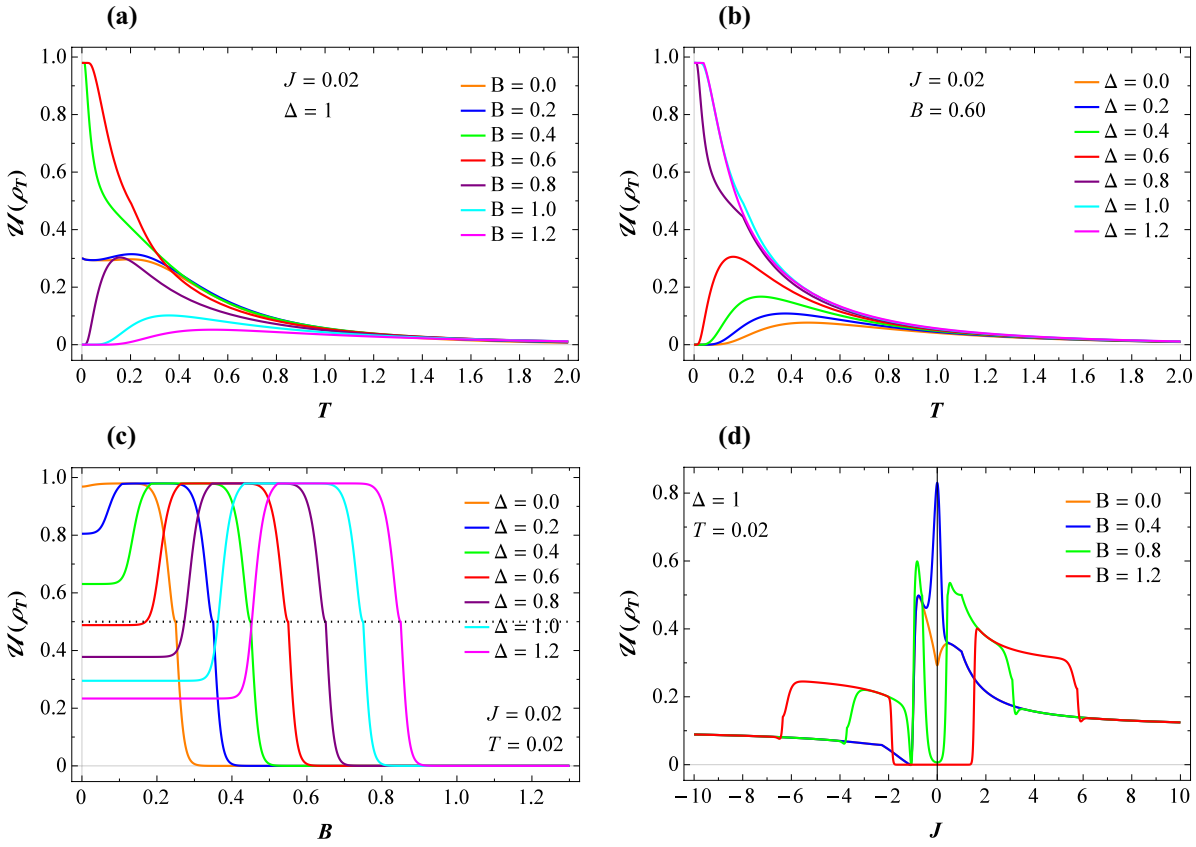


Figure 3. LQU with respect to the same parameter sets in Fig. 2.

and $\Delta = 1$, where four different values of the magnetic field have been taken. For mixed ferromagnetic-antiferromagnetic case $J < 0$, we see that this function does not vanish but tends to $\mathcal{U}(\rho_T) = 0.1$ as J decreases further than critical point $J = -1$. On the other hand, for the ferromagnetic coupling $J > 0$, the LQU falls down close to the critical exchange and it shows a discontinuous alteration at low magnetic field $B = 0.4$ (blue line). Hence, the LQU could be a good witness of the discontinuous thermal behaviors of the model that is more efficient than the concurrence in this medium.

We depict typical thermal variations of the l_1−norm of coherence of our model in Fig. 4. Plots (a) and (b) manifest the temperature dependence of the quantum coherence for the fixed $J = 0.02$ and various values of other parameters. It is evident that $C_{l_1}(\rho_T)$ experiences its maximum at low temperature such as the concurrence. On the other hand, when the temperature increases, at low magnetic fields and low anisotropies such a function gradually decreases and tends to zero but does not vanish neither at higher magnetic fields nor for stronger exchange anisotropies. Returning to Fig. 3, it is observable that the l_1- norm of coherence and LQU have somehow similar behavior to each other at high temperatures.

Figure 4c displays the coherence as a function of the magnetic field at low temperature $T = 0.02$ and low exchange coupling $J = 0.02$, where several fixed values of the anisotropy Δ are assumed. Compared to previous figures, the same behavior to the coherence is evident close to the critical magnetic fields. The l_1−norm of coherence C_{l_1} versus the coupling constant J at low temperature is plotted in Fig. 4d, where fixed value $\Delta = 1$ and four different magnetic fields are selected. It is visible a quite different behavior of this function compared with the LQU and the concurrence. Namely, for the case when $J < 0$, by decreasing the exchange coupling J further than the critical point $J = -1$, the quantum coherence not only does not vanish but also increases notably. Generally speaking, one can deduce from our observations that the l_1- norm of coherence is more efficient than both concurrence and LQU to predict the quantumness of the thermal state even at high temperatures and high magnetic fields.

Quantum teleportation. In this section, we study quantum teleportation for an entangled mixed state as a resource, acts as a generalized depolarizing channel[77–79]. Next, we investigate the effects of the anisotropy and the magnetic field on the possibility of teleportation through the model under verification. Let us assume the input state being an arbitrary unknown two-qubit pure state $|\psi_{\text{in}}\rangle$, such as

$$|\psi_{\text{in}}\rangle = \cos(\theta/2)|10\rangle + e^{i\phi}\sin(\theta/2)|01\rangle, \quad \forall \quad 0 \le \theta \le \pi, \quad 0 \le \phi \le 2\pi. \tag{19}$$

From the mathematical point of view, the quantum channel is known as a completely positive and trace-preserving operator. Via this mechanism, an input density operator is mapped to an output density operator[77]. Generally,

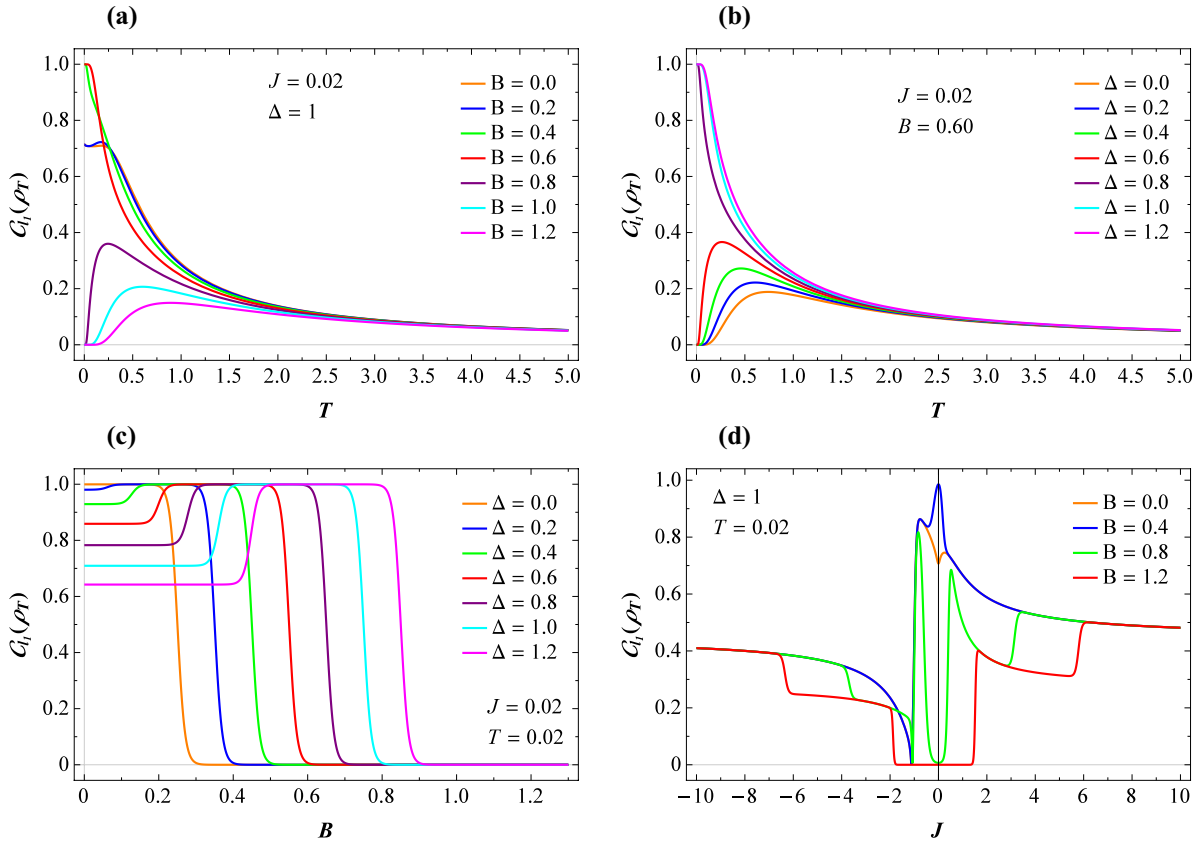


Figure 4. Quantum coherence with respect to the same parameter sets in Figs. 2 and 3.

when the quantum state is teleported through the mixed channel ρ_{ch}, the output replica state ρ_{out} can be obtained by applying joint measurements and the local unitary transformations on the input state $\rho_{in} = |\psi_{in}\rangle\langle\psi_{in}|$, hence

$$\rho_{out} = \sum_{i,j\in\{0,x,y,z\}} p_i p_j (\sigma^i \otimes \sigma^j)\rho_{in}(\sigma^i \otimes \sigma^j), \tag{20}$$

where $\sigma_0 = I$ (I is the 2×2 identity matrix) and $p_i = \mathrm{Tr}(E^i\rho_{ch})$ satisfies the condition $\sum_i p_i = 1$. $E^0 = |\Psi^-\rangle\langle\Psi^-|$, $E^1 = |\Phi^-\rangle\langle\Phi^-|$, $E^2 = |\Psi^+\rangle\langle\Psi^+|$, and $E^3 = |\Phi^+\rangle\langle\Phi^+|$, from which $\{|\Psi^\pm\rangle, |\Phi^\pm\rangle\}$ stand for the well known Bell states. In this paper, we consider the quantum channel as $\rho_{ch} = \rho_T$. Therefore, The output density operator ρ_{out} takes the form

$$\rho_{out} = \begin{pmatrix} \widetilde{\rho}_{11} & . & . & . \\ . & \widetilde{\rho}_{22} & \widetilde{\rho}_{23} & . \\ . & \widetilde{\varrho}_{23} & \widetilde{\rho}_{33} & . \\ . & . & . & \widetilde{\rho}_{11} \end{pmatrix}, \tag{21}$$

where

$$\begin{aligned} \widetilde{\rho}_{11} =& (\rho_{11} + \rho_{44})(\rho_{22} + \rho_{33}), \\ \widetilde{\rho}_{22} =& (\rho_{11} + \rho_{44})^2 \cos^2(\theta/2) + (\rho_{22} + \rho_{33})^2 \sin^2(\theta/2), \\ \widetilde{\rho}_{33} =& (\rho_{11} + \rho_{44})^2 \sin^2(\theta/2) + (\rho_{22} + \rho_{33})^2 \cos^2(\theta/2), \\ \widetilde{\rho}_{23} =& 2e^{i\phi}\rho_{23}^2 \sin\theta. \end{aligned} \tag{22}$$

To describe the quality of the process of teleportation, it is often quite useful to study the fidelity between ρ_{in} and ρ_{out} to characterize the teleported state. When the input state is a pure state, one can apply the concept of fidelity as a useful indicator of the teleportation performance of a quantum channel quantifier[80,81]. The fidelity is defined as[6]

$$\mathscr{F} = \left(\mathrm{Tr}\sqrt{\sqrt{\rho_{in}}\rho_{out}\sqrt{\rho_{in}}}\right)^2. \tag{23}$$

The fidelity is near zero if the input and output states are orthogonal, which means the information is fully destroyed during the transmission process, so the teleportation fails. While it is close to unity, it signifies that the input state is identical to the output state. In the situation when $0 < \mathscr{F} < 1$, the quantum information is

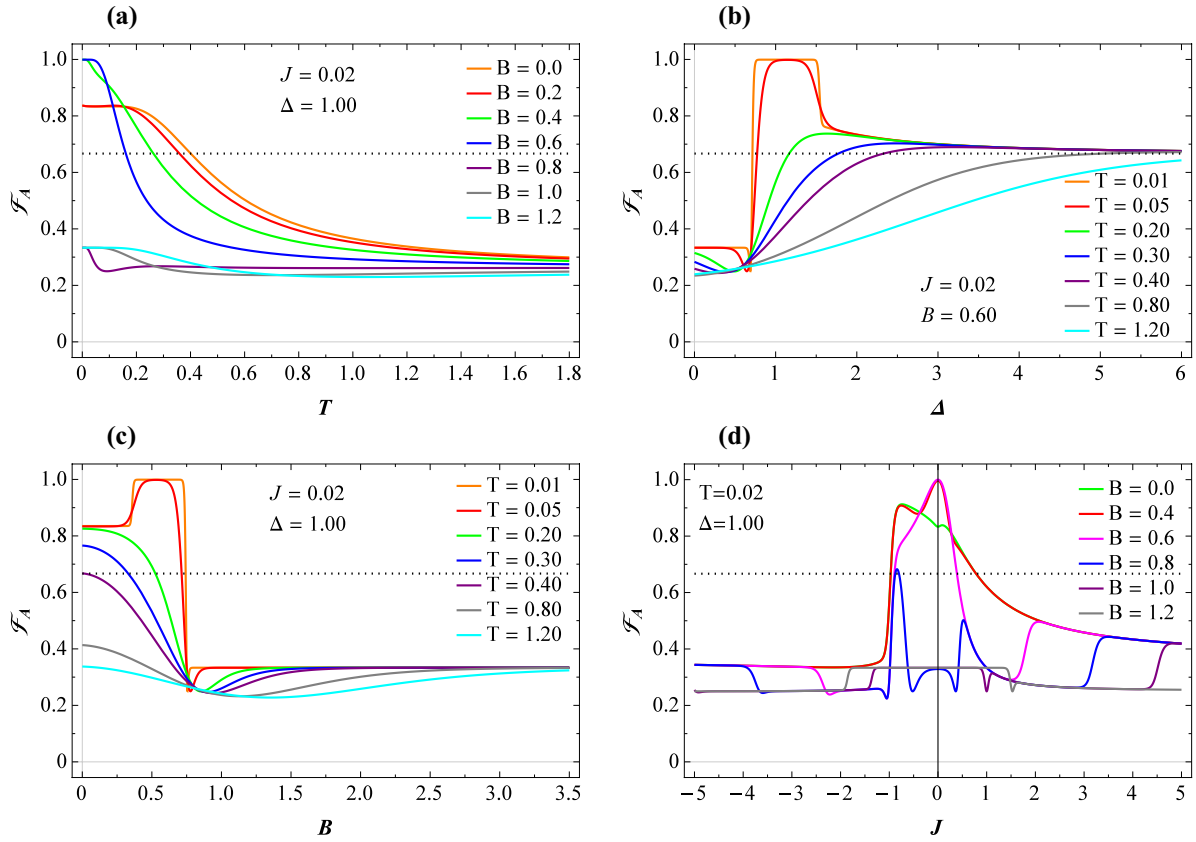


Figure 5. (**a**) The average fidelity $\mathscr{F}_A$ versus temperature, assuming $J = 0.02$, $\Delta = 1$, and several fixed values of the magnetic field. (**b**) $\mathscr{F}_A$ as a function of anisotropy Δ for fixed $J = 0.02$, $B = 0.6$, and different values of the temperature. (**c**) Field dependence of $\mathscr{F}_A$ for various temperatures, where other parameters have been taken as $J = 0.02$ and $\Delta = 1$. (**d**) the same function at low temperature $T = 0.02$ against the coupling constant J when different fixed values of the magnetic field are considered such that $\Delta = 1$. Dotted lines indicate the classical limit of fidelity 2/3.

subjected to distortions after transmitting to some extent. Through a straightforward calculation for our case, one finds

$$\mathscr{F} = \frac{\sin^2\theta}{2}[(\rho_{11}+\rho_{44})^2 + 4\rho_{23}^2 - (\rho_{22}+\rho_{33})^2] + (\rho_{22}+\rho_{33})^2. \tag{24}$$

The average fidelity of teleportation $\mathscr{F}_A$ can be formulated as[82,83]

$$\mathscr{F}_A = \frac{1}{4\pi}\int_0^{2\pi} d\phi \int_0^{\pi} d\theta \mathscr{F} \sin\theta, \tag{25}$$

by integrating Eq. (25), the average fidelity $\mathscr{F}_A$ for our case can be thus expressed as

$$\mathscr{F}_A = \frac{1}{3}[(\rho_{11}+\rho_{44})^2 + 4\rho_{23}^2 + 2(\rho_{22}+\rho_{33})^2]. \tag{26}$$

It is obvious that the average fidelity $\mathscr{F}_A$ depends on the quantum channel (thermal state) parameters in this case. In order to transmit a quantum state better than the classical communication protocols, $\mathscr{F}_A$ must be greater than $\frac{2}{3}$ which is the best fidelity in the classical world. In Fig. 5a, the average fidelity as a function of the temperature for the weak coupling $J = 0.02$ and fixed $\Delta = 1$ is shown, where several fixed values of the magnetic field have been assumed. It is clear from this plot, that $\mathscr{F}_A$ does not reach the limit of quantum fidelities for $B \gtrsim 0.8$, hence the teleportation of information happens for the magnetic field rage $B < 0.8$. An increase in the temperature leads to a decrease in the possibility of teleportation. With looking to Figs. 2a, 3a and 4a, one realizes that for the parameter sets that situation $\mathscr{F}_A < 2/3$ occurs, three functions, i.e., concurrence, LQU, and coherence show a sharp decrease until they vanish at low temperatures and never reach their maximum values under cooling condition. On the other hand, in the parameter regions which $\mathscr{F}_A > 2/3$, all three functions gradually tend towards maximum value under cooling.

In Fig. 5b, we depict the average fidelity versus the anisotropy Δ for several fixed temperatures and parameter sets $J = 0.02$ and $B = 0.6$. A reentrance point is evident in this plot at which a sharp change in the average

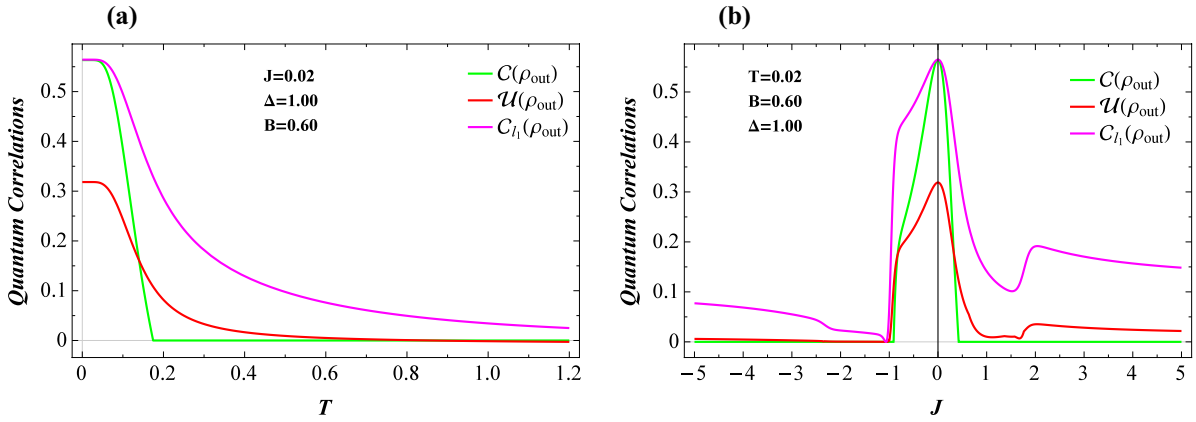


Figure 6. (**a**) Three quantum criteria for the output state versus temperature T and parameter sets $J = 0.02$, $\Delta = 1$, and $B = 0.6$. (**b**) The same quantifiers as functions of the coupling constant J at low temperature $T = 0.02$, assuming $\Delta = 1$ and $B = 0.6$.

fidelity behavior happens and this quantity immediately reaches its maximum $\mathscr{F}_A = 1$ within the anisotropy interval $0.8 \lesssim \Delta \lesssim 1.5$ at extremely low temperatures, accompanying with the achieving maximum value of the concurrence, LQU, and coherence. Generally, the average fidelity tends to limit value 2/3 with increasing the anisotropy. The relevant field dependence of the average fidelity at $J = 0.02$ and $\Delta = 1$ shown in Fig. 5c has also similar behavior. It can be seen from this plot a steep decrease as well as line accumulation in the average fidelity function at low temperatures regime in the vicinity of critical magnetic field. Under heating, $\mathscr{F}_A$ decreases at low magnetic fields. Accordingly, the possibility of teleportation through this model is restricted.

The most interesting finding from the fidelity investigations is manifested in Fig. 5d by which we illustrate the average fidelity with respect to the exchange coupling J at low temperature $T = 0.02$ and $\Delta = 1$. Similar to the other three functions, $\mathscr{F}_A$ anomalously behaves nearby the critical exchange couplings. Surprisingly, in the antiferromagnetic region of J, close to the critical point $J = -1$, the average fidelity sharply drops to its minimum. Consequently, the average fidelity could be an eligible candidate to trace the thermal fluctuations of a typical Heisenberg spin-1/2 square compound possessing either ferromagnetic or mixed ferromagnetic-antiferromagnetic exchange couplings.

Finally, we present our results concerning with the temperature dependence of three discussed quantities for the output state ρ_{out}, i.e., $C(\rho_{out})$, $\mathscr{U}(\rho_{out})$, and $C_{l_1}(\rho_{out})$ for fixed $J = 0.02$, $\Delta = 1$, and $B = 0.6$ in Fig. 6a. All functions decrease from a typical maximum when the temperature increases. The concurrence suddenly vanishes at a critical temperature, while other two functions monotonically decreases. The notable difference between $\mathscr{U}(\rho_{out})$ and $C_{l_1}(\rho_{out})$ is that, the former vanishes at a specific critical temperature while the latter does not reach zero even at high temperatures. Moreover, we plot in Fig. 6b the aforementioned quantities as functions of the exchange coupling J at low temperature $T = 0.02$ and fixed $B = 0.6$ and $\Delta = 1$. By assuming mixed ferromagnetic-antiferromagnetic case ($J < 0$), all three functions sharply decrease and vanish nearby the critical point $J = -1$, reminding the same thermal behaviors of these criteria as well as fidelity at this point. With decrease of the J further than $J = -1$, the concurrence remains zero, while the LQU and quantum coherence arise from zero and reach the non-zero values. On the other side, within the ferromagnetic region ($J > 0$), one can observe the entanglement sudden death at $J \approx 0.5$, whereas the LQU and coherence show a sudden decline at this point, but remain alive even for higher values of J. According to our observations, we generally claim that the l_1−norm of coherence could reveal more quantum information about the system under study, which is consistent with previous results.

Concluding remarks and outlook

We have considered a four-qubit cluster complex on a spin-1/2 Heisenberg XXZ model involving an exchange anisotropy in the presence of a magnetic field along the z-axis. Both pure ferromagnetic and mixed ferromagnetic-antiferromagnetic exchange couplings between nearest-neighbor spins have been verified. We then studied three quantum criteria such as concurrence, local quantum uncertainty, and quantum coherence for a pair of spins. Consequently, we have demonstrated that all three functions behave anomalously close to the critical points. At low temperature and weak coupling constant, we could observe maximum entanglement between selected pair of spins. According to our observations, we convincingly concluded that the quantum coherence is generally more sensitive than the other ones to witnessing the thermal fluctuations in different Hamiltonian parameter sets. We also understood that by tuning the strength of the anisotropy parameter, a significant enhancement on the entanglement and various thermal non-classical correlations and coherence can be achieved. Finally, we have examined the possibility of teleportation through the model under consideration. We found that within a special interval of assumed exchange anisotropy, the average fidelity significantly enhances. However, the average fidelity tends to limit value 2/3 with further increase of the anisotropy. The average fidelity also represented different behaviors such as line accumulation and sharp dropping nearby the critical points.

Investigating aforementioned quantum correlations quantifiers, coherence, and the fidelity of teleportation for similar classes of small spin clusters might enlighten the quantum nature of them that would be applicable

in different subjects such as quantum information processing, quantum communication, and spintronics. Furthermore, we think that our model can pleasantly bring insight into the ground-state phase diagram and several important magnetic and quantum features of some real materials with similar square-shaped structures. Our future activity will concern with this direction.

Methods

Eigenvalues and eigenstates of the Hamiltonian. In this section, we give the eigenvalues and the corresponding eigenstates of Hamiltonian (1) in terms of the standard computational basis $\mathscr{B} = \{|000\rangle, |001\rangle, |010\rangle, |011\rangle, |100\rangle, |101\rangle, |110\rangle, |111\rangle\}$. The eigenvalues of the Hamiltonian are

$$\begin{aligned}
&E_1 = -2B - \tfrac{1}{4}J - \tfrac{1}{4} + \tfrac{1}{4}\sqrt{K}, \quad E_2 = -2B - \tfrac{1}{4}J - \tfrac{1}{4} - \tfrac{1}{4}\sqrt{K}, \quad E_3 = E_4 = 0,\\
&E_5 = 2B - \tfrac{1}{4}J - \tfrac{1}{4} + \tfrac{1}{4}\sqrt{K}, \quad E_6 = 2B - \tfrac{1}{4}J - \tfrac{1}{4} - \tfrac{1}{4}\sqrt{K},\\
&E_7 = 2B + \tfrac{1}{4}J + \tfrac{1}{4} + \tfrac{1}{4}\sqrt{K}, \quad E_8 = 2B + \tfrac{1}{4}J + \tfrac{1}{4} - \tfrac{1}{4}\sqrt{K},\\
&E_9 = \Delta - 4B, \quad E_{10} = -2B + \tfrac{1}{4}J + \tfrac{1}{4} + \tfrac{1}{4}\sqrt{K},\\
&E_{11} = -2B + \tfrac{1}{4}J + \tfrac{1}{4} - \tfrac{1}{4}\sqrt{K}, \quad E_{12} = \Delta + 4B,\\
&E_{13} = -\tfrac{1}{2}\Delta + \tfrac{1}{2}\sqrt{\Delta^2 + J - 2J + 1}, \quad E_{14} = -\tfrac{1}{2}\Delta - \tfrac{1}{2}\sqrt{\Delta^2 + J^2 - 2J + 1},\\
&E_{15} = -\tfrac{1}{2}\Delta + \tfrac{1}{2}\sqrt{\Delta^2 + 5J^2 + 2J + 1}, \quad E_{16} = -\tfrac{1}{2}\Delta - \tfrac{1}{2}\sqrt{\Delta^2 + 5J^2 + 2J + 1},
\end{aligned} \tag{27}$$

with $K = 5J^2 - 2J + 1$. The corresponding eigenstates are given, respectively, by

$$\begin{aligned}
&|\psi_1\rangle = a_+|0001\rangle + b_+|0010\rangle + |0100\rangle + |1000\rangle,\\
&|\psi_2\rangle = a_-|0001\rangle + b_-|0010\rangle + |0100\rangle + |1000\rangle,\\
&|\psi_3\rangle = -|0011\rangle + |1100\rangle,\\
&|\psi_4\rangle = \alpha|0011\rangle + |0101\rangle + |1010\rangle,\\
&|\psi_5\rangle = c_+|0111\rangle + d_+|1011\rangle + |1101\rangle + |1110\rangle,\\
&|\psi_6\rangle = c_-|0111\rangle + d_-|1011\rangle + |1101\rangle + |1110\rangle,\\
&|\psi_7\rangle = c_-|0111\rangle - d_-|1011\rangle - |1101\rangle + |1110\rangle,\\
&|\psi_8\rangle = c_+|0111\rangle - d_+|1011\rangle - |1101\rangle + |1110\rangle,\\
&|\psi_9\rangle = |0000\rangle,\\
&|\psi_{10}\rangle = a_-|0001\rangle - b_-|0010\rangle - |0100\rangle + |1000\rangle,\\
&|\psi_{11}\rangle = a_+|0001\rangle - b_+|0010\rangle - |0100\rangle + |1000\rangle,\\
&|\psi_{12}\rangle = |1111\rangle,\\
&|\psi_{13}\rangle = -|0101\rangle + e_+|0110\rangle - e_+|1001\rangle + |1010\rangle,\\
&|\psi_{14}\rangle = -|0101\rangle + e_-|0110\rangle - e_-|1001\rangle + |1010\rangle,\\
&|\psi_{15}\rangle = |0011\rangle + \beta|0101\rangle + f_+|0110\rangle + f_+|1001\rangle + \beta|1010\rangle + |1100\rangle,\\
&|\psi_{16}\rangle = |0011\rangle + \beta|0101\rangle + f_-|0110\rangle + f_-|1001\rangle + \beta|1010\rangle + |1100\rangle,
\end{aligned} \tag{28}$$

where the following notations are adopted

$$\begin{aligned}
&a_\pm = \frac{2J\left(3J^2 \mp J\sqrt{K} - 2J \pm \sqrt{K} - 1\right)}{\left(2J^2 + J \pm \sqrt{K} - 1\right)\left(J + 1 \mp \sqrt{K} + 1\right)}, \quad \alpha = -\frac{J+1}{J}, \quad \beta = \frac{1}{2}\frac{J+1}{J},\\
&b_\pm = \frac{J\left(J - 3 \pm \sqrt{K}\right)}{\left(2J^2 + J \pm \sqrt{K} - 1\right)}, \quad c_\pm = \frac{2J^2\left(J^2 \mp J\sqrt{K} + 2J \pm \sqrt{K} - 3\right)}{\left(J^3 \mp (J^2 \pm J \pm 1)\sqrt{K} + 1\right)\left(J + 1 \mp \sqrt{K} + 1\right)},\\
&d_\pm = \frac{J(2J^2 - 3J \mp \sqrt{K} - 1)}{\left(J^3 \mp (J^2 \pm J \pm 1)\sqrt{K} + 1\right)}, \quad e_\pm = \frac{J - 1}{\left(\Delta \pm \sqrt{\Delta^2 + J^2 - 2J + 1}\right)},\\
&f_\pm = -\frac{1}{2}\frac{5J^2 + 2J + 1}{J\left(\Delta \pm \sqrt{\Delta^2 + 5J^2 + 2J + 1}\right)}.
\end{aligned} \tag{29}$$

Data availability

All data generated or analyzed during this study are included in this paper.

Received: 16 February 2022; Accepted: 5 April 2022
Published online: 18 April 2022

References

1. Horodecki, R., Horodecki, P., Horodecki, M. & Horodecki, K. Quantum entanglement. *Rev. Mod. Phys.* **81**, 865 (2009).
2. Vedral, V. The role of relative entropy in quantum information theory. *Rev. Mod. Phys.* **74**, 197 (2002).
3. Gühne, O. & Tóth, G. Entanglement detection. *Phys. Rep.* **474**, 1 (2009).
4. Modi, K., Brodutch, A., Cable, H., Paterek, T. & Vedral, V. The classical-quantum boundary for correlations: discord and related measures. *Rev. Mod. Phys.* **84**, 1655 (2012).
5. Haddadi, S. & Bohloul, M. A brief overview of bipartite and multipartite entanglement measures. *Int. J. Theor. Phys.* **57**, 3912 (2018).
6. Nielsen, M. A. & Chuang, I. L. *Quantum Computation and Quantum Information* (Cambridge University Press, Cambridge, 2000).
7. Wootters, W. K. Entanglement of formation of an arbitrary state of two qubits. *Phys. Rev. Lett.* **80**, 2245 (1998).
8. Datta, A., Shaji, A. & Caves, C. M. Quantum discord and the power of one qubit. *Phys. Rev. Lett.* **100**, 050502 (2008).
9. Lanyon, B. P., Barbieri, M., Almeida, M. P. & White, A. G. Experimental quantum computing without entanglement. *Phys. Rev. Lett.* **101**, 200501 (2008).

10. Datta, A., Flammia, A. T. & Caves, C. M. Entanglement and the power of one qubit. *Phys. Rev. A* **72**, 042316 (2005).
11. Datta, A. & Vidal, G. Role of entanglement and correlations in mixed-state quantum computation. *Phys. Rev. A* **75**, 042310 (2007).
12. Benabdallah, F., Slaoui, A. & Daoud, M. Quantum discord based on linear entropy and thermal negativity of qutrit-qubit mixed spin chain under the influence of external magnetic field. *Quantum Inf. Process.* **19**, 252 (2020).
13. Benabdallah, F. & Daoud, M. Dynamics of quantum discord based on linear entropy and negativity of qutrit-qubit system under classical dephasing environments. *Eur. Phys. J. D* **75**, 3 (2021).
14. Benabdallah, F., Arian Zad, H., Daoud, M. & Ananikian, N. Dynamics of quantum correlations in a qubit-qutrit spin system under random telegraph noise. *Phys. Scr.* **96**, 125116 (2021).
15. Wigner, E. P. & Yanase, M. M. Information contents of distributions. *Proc. Nat. Acad. Sci. USA* **49**, 910 (1963).
16. Girolami, D., Tufarelli, T. & Adesso, G. Characterizing nonclassical correlations via local quantum uncertainty. *Phys. Rev. Lett.* **110**, 240402 (2013).
17. Ali, M. Local quantum uncertainty for multipartite quantum systems. *Eur. Phys. J. D.* **74**, 186 (2020).
18. Jebli, L., Benzimoun, B. & Daoud, M. Quantum correlations for two-qubit X states through the local quantum uncertainty. *Int. J. Quantum Inf.* **14**, 1750020 (2017).
19. Luo, S. Wigner-Yanase skew information and uncertainty relations. *Phys. Rev. Lett.* **91**, 180403 (2003).
20. Luo, S. Wigner-Yanase skew information vs .quantum Fisher information. *Proc. Am. Math. Soc.* **132**, 885 (2003).
21. Petz, D. & Ghinea, C. Introduction to quantum Fisher information. *Quantum Probab. Relat. Top.* **1**, 261 (2011).
22. Hu, M. L. & Wang, H. F. Protecting quantum Fisher information in correlated quantum channels. *Ann. Phys. (Berlin)* **532**, 1900378 (2020).
23. Girolami, D. Observable measure of quantum coherence in finite dimensional systems. *Phys. Rev. Lett.* **113**, 170401 (2014).
24. Du, S. P. & Bai, Z. F. The Wigner-Yanase information can increase under phase sensitive incoherent operations. *Ann. Phys.* **359**, 136 (2015).
25. Baumgratz, T., Cramer, M. & Pleino, M. B. Quantifying coherence. *Phys. Rev. Lett.* **113**, 140401 (2014).
26. Ficek, Z. & Swain, S. *Quantum Interference and Coherence: Theory and Experiments* (Springer Series in Optical Sciences, Springer, Berlin, 2005).
27. Xu, X. X. & Hu, M. L. Maximal steered coherence and its conversion to entanglement in multiple bosonic reservoirs. *Ann. Phys. (Berlin)* **534**, 2100412 (2022).
28. Bauch, T. *et al.* Macroscopic quantum tunneling in *d*-wave $YBa_2Cu_3O_{7-\delta}$ Josephson junctions. *Phys. Rev. Lett.* **94**, 087003 (2005).
29. You, J. Q. & Nori, F. Atomic physics and quantum optics using superconducting circuits. *Nature* **474**, 589 (2011).
30. Ferrini, G., Minguzzi, A. & Hekking, F. W. J. Atomic physics and quantum optics using superconducting circuits. *Phys. Rev. A* **78**, 023606 (2008).
31. Giovannetti, V., Lloyd, S. & Maccone, L. Advances in quantum metrology. *Nat. Photonics* **5**, 222 (2011).
32. Fröwis, F. & Dür, W. Stable macroscopic quantum superpositions. *Phys. Rev. Lett.* **106**, 110402 (2011).
33. Streltsov, A., Kampermann, H., Wölk, S., Gessner, M. & Bruß, D. Maximal coherence and the resource theory of purity. *New J. Phys.* **20**, 053058 (2018).
34. Streltsov, A., Adesso, G. & Plenio, M. B. Colloquium: quantum coherence as a resource. *Rev. Mod. Phys.* **89**, 041003 (2017).
35. Brandao, F. G. S. L., Horodecki, M., Oppenheim, J., Renes, J. M. & Spekkens, R. W. Resource theory of quantum states out of thermal equilibrium. *Phys. Rev. Lett.* **111**, 250404 (2013).
36. Naraisimhachar, V. & Gour, G. Low-temperature thermodynamics with quantum coherence. *Nat. Commun.* **6**, 7689 (2015).
37. Hu, M. L., Gao, Y. Y. & Fan, H. Steered quantum coherence as a signature of quantum phase transitions in spin chains. *Phys. Rev. A* **101**, 032305 (2020).
38. Hu, M. L., Fang, F. & Fan, H. Finite-size scaling of coherence and steered coherence in the Lipkin-Meshkov-Glick model. *Phys. Rev. A* **104**, 062416 (2021).
39. Li, B. M., Hu, M. L. & Fan, H. Nonlocal advantage of quantum coherence and entanglement of two spins under intrinsic decoherence. *Chin. Phys. B* **30**, 070307 (2021).
40. Kim, S., Li, L., Kumar, A. & Wu, J. Interrelation between partial coherence and quantum correlations. *Phys. Rev. A* **98**, 022306 (2018).
41. Zhao, F., Wang, D. & Ye, L. Relationship between entanglement and coherence in some two-qubit states. *Int. J. Theor. Phys.* **61**, 10 (2022).
42. Haddadi, S., Pourkarimi, M. R. & Haseli, S. Relationship between quantum coherence and uncertainty bound in an arbitrary two-qubit X-state. *Opt. Quantum Electron.* **53**, 529 (2021).
43. Dolatkhah, H., Haseli, S., Salimi, S. & Khorashad, A. S. Tightening the entropic uncertainty relations for multiple measurements and applying it to quantum coherence. *Quantum Inf. Process.* **18**, 13 (2019).
44. Xie, B. F., Ming, F., Wang, D., Ye, L. & Chen, J. L. Optimized entropic uncertainty relations for multiple measurements. *Phys. Rev. A* **104**, 062204 (2021).
45. Ming, F. *et al.* Improved tripartite uncertainty relation with quantum memory. *Phys. Rev. A* **102**, 012206 (2020).
46. Ding, Z. Y. *et al.* Experimental investigation of entropic uncertainty relations and coherence uncertainty relations. *Phys. Rev. A* **101**, 032101 (2020).
47. Haddadi, S. *et al.* Measurement uncertainty and dense coding in a two-qubit system: combined effects of bosonic reservoir and dipole-dipole interaction. *Results Phys.* **32**, 105041 (2022).
48. Hu, M. L. *et al.* Quantum coherence and geometric quantum discord. *Phys. Rep.* **762**, 1 (2018).
49. Yang, Y. Y. *et al.* Dynamical characteristic of measurement uncertainty under Heisenberg spin models with Dzyaloshinskii-Moriya interactions. *Front. Phys.* **14**, 31601 (2019).
50. Wang, D. *et al.* Quantum-memory-assisted entropic uncertainty relation in a Heisenberg XYZ chain with an inhomogeneous magnetic field. *Laser Phys. Lett.* **14**, 065203 (2017).
51. Hu, M. L., Xi, X. Q., Li, C. X. & Qu, H. Z. Population relaxation effects on entanglement dynamics of the two-qubit spin chains. *Phys. B* **404**, 16 (2009).
52. Haseli, S., Haddadi, S. & Pourkarimi, M. R. Entropic uncertainty lower bound for a two-qubit system coupled to a spin chain with Dzyaloshinskii-Moriya interaction. *Opt. Quantum Electron.* **52**, 465 (2020).
53. Oshikawa, M., Yamanaka, M. & Affleck, I. Magnetization plateaus in spin chains: "Haldane Gap" for half-integer spins. *Phys. Rev. Lett.* **78**, 1984 (1997).
54. Strečka, J. & Karľová, K. Magnetization curves and low-temperature thermodynamics of two spin-1/2 Heisenberg edge-shared tetrahedra. *AIP Adv.* **8**, 101403 (2018).
55. Arian Zad, H., Sabeti, M., Zoshki, A. & Ananikian, N. Electrocaloric effect in the two spin-1/2 XXZ Heisenberg edge-shared tetrahedra and spin-1/2 XXZ Heisenberg octahedron with Dzyaloshinskii-Moriya interaction. *J. Phys.: Condens. Matter* **31**, 425801 (2019).
56. Salmon, L. *et al.* Structural, magnetic and theoretical calculations of a ferromagnetically coupled tetranuclear copper(II) square complex. *New J. Chem.* **38**, 1306 (2014).
57. Ming, F., Shi, W. N., Fan, X. G., Ye, L. & Wang, D. Effective entanglement recovery via operators. *J. Phys. A: Math. Theor.* **54**, 215302 (2021).
58. Ming, F. *et al.* Tradeoff relations in quantum resource theory. *Adv. Quantum Technol.* **4**, 2100036 (2021).

59. Liu, J. M., Weng, B. & Xia, Y. Scheme for teleportation of atomic states within cavities in thermal states. *J. Opt. Soc. Am. B* **23**, 1499 (2006).
60. Yu, P. F., Cai, J. G., Liu, J. M. & Shen, G. T. Teleportation via a two-qubit Heisenberg XYZ model in the presence of phase decoherence. *Phys. A* **387**, 4723 (2008).
61. Freitas, M., Filgueiras, C. & Rojas, M. The effects of an impurity in an Ising-XXZ diamond chain on thermal entanglement, on quantum coherence, and on quantum teleportation. *Ann. Phys.* **531**, 1900261 (2019).
62. Fouokeng, G. C., Tedong, E., Tene, A. G., Tchoffo, M. & Fai, L. C. Teleportation of single and bipartite states via a two qubits XXZ Heizenberg spin chain in a non-Markovian environment. *Phys. Lett. A* **384**, 126719 (2020).
63. Arian Zad, H. & Rojas, M. Quantum coherence, quantum Fisher information and teleportation in the Ising-Heisenberg spin chain model of a heterotrimetallic Fe–Mn–Cu coordination polymer with magnetic impurity. *Phys. E* **126**, 114455 (2020).
64. Jafari, R. & Langari, A. Three-qubit ground state and thermal entanglement of anisotropic Heisenberg (XXZ) and Ising models with Dzyaloshinskii-Moriya interaction. *Int. J. Quantum Inf.* **9**, 1057 (2011).
65. Haddadi, S., Pourkarimi, M. R., Khedif, Y. & Daoud, M. Tripartite measurement uncertainty in a Heisenberg XXZ model. *Eur. Phys. J. Plus* **137**, 66 (2022).
66. Kochem, A. *et al.* Magneto-structural and computational study of a tetranuclear copper complex displaying carbonyl-π interactions. *Eur. J. Inorg. Chem.* **2018**, 5039 (2018).
67. Khedif, Y., Daoud, M. & Sayouty, E. H. Thermal quantum correlations in a two-qubit Heisenberg XXZ spin-1/2 chain under an inhomogeneous magnetic field. *Phys. Scr.* **94**, 125106 (2019).
68. Khedif, Y., Haddadi, S., Pourkarimi, M. R. & Daoud, M. Thermal correlations and entropic uncertainty in a two-spin system under DM and KSEA interactions. *Mod. Phys. Lett. A* **36**, 2150209 (2021).
69. Bloch, F. Nuclear induction. *Phys. Rev.* **70**, 460 (1946).
70. Fano, U. Pairs of two-level systems. *Rev. Mod. Phys.* **55**, 855 (1983).
71. Hu, M. L. & Zhou, W. Enhancing two-qubit quantum coherence in a correlated dephasing channel. *Laser Phys. Lett.* **16**, 045201 (2019).
72. Streltsov, A., Singh, U., Dhar, H. S., Bera, M. N. & Adesso, G. Measuring quantum coherence with entanglement. *Phys. Rev. Lett.* **115**, 020403 (2015).
73. Zhao, M. J., Ma, T., Quan, Q., Fan, H. & Pereira, R. l_1 -norm coherence of assistance. *Phys. Rev. A* **100**, 012315 (2019).
74. Yao, Y., Xiao, X., Ge, L. & Sun, C. P. Quantum coherence in multipartite systems. *Phys. Rev. A* **92**, 022112 (2015).
75. Pinto, J. P. G., Karpat, G. & Fanchini, F. F. Sudden change of quantum discord for a system of two qubits. *Phys. Rev. A* **88**, 034304 (2013).
76. Hu, M. L. & Sun, J. Sudden change of geometric quantum discord in finite temperature reservoirs. *Ann. Phys.* **354**, 265 (2015).
77. Bowen, G. & Bose, S. Teleportation as a depolarizing quantum channel, relative entropy, and classical capacity. *Phys. Rev. Lett.* **87**, 267901 (2001).
78. Yeo, Y. Teleportation via thermally entangled states of a two-qubit Heisenberg XX chain. *Phys. Rev. A* **66**, 062312 (2002).
79. Zhou, Y. & Zhang, G. F. Quantum teleportation via a two-qubit Heisenberg XXZ chain - effects of anisotropy and magnetic field. *Eur. Phys. J. D* **47**, 227 (2008).
80. Jozsa, R. Fidelity for mixed quantum states. *J. Mod. Opt.* **41**, 12 (1994).
81. Rahman, A. U., Haddadi, S., Pourkarimi, M. R. & Ghominejad, M. Fidelity of quantum states in a correlated dephasing channel. *Laser Phys. Lett.* **19**, 035204 (2022).
82. Hu, M. L. Environment-induced decay of teleportation fidelity of the one-qubit state. *Phys. Lett. A* **375**, 2140 (2011).
83. Pourkarimi, M. R. & Haddadi, S. Quantum-memory-assisted entropic uncertainty, teleportation, and quantum discord under decohering environments. *Laser Phys. Lett.* **17**, 025206 (2020).

Acknowledgements

H.A.Z. acknowledges the receipt of the grant from the Abdus Salam International Centre for Theoretical Physics (ICTP), Trieste, Italy. H.A.Z. also acknowledges for the financial support of the National Scholarship Programme of the Slovak Republic (NSP). N. A. acknowledges the support of CS MES RA in the frame of the research project No. SCS 19IT-008 and research project No. SCS 21AG-1C006.

Author contributions

F.B. has put forward the main idea for the model and method and performed the calculations and graphical tasks. S.H. and H.A.Z. have contributed to interpreting the results and writing the manuscript. Thorough checking of the manuscript and confirming the conclusions were done by S.H., M.R.P., M.D., and N.A. The final draft of the manuscript was revised by S.H. and reviewed by all authors.

Competing interests

The authors declare no competing interests.

Additional information

Correspondence and requests for materials should be addressed to S.H.

Reprints and permissions information is available at www.nature.com/reprints.

Publisher's note Springer Nature remains neutral with regard to jurisdictional claims in published maps and institutional affiliations.

Open Access This article is licensed under a Creative Commons Attribution 4.0 International License, which permits use, sharing, adaptation, distribution and reproduction in any medium or format, as long as you give appropriate credit to the original author(s) and the source, provide a link to the Creative Commons licence, and indicate if changes were made. The images or other third party material in this article are included in the article's Creative Commons licence, unless indicated otherwise in a credit line to the material. If material is not included in the article's Creative Commons licence and your intended use is not permitted by statutory regulation or exceeds the permitted use, you will need to obtain permission directly from the copyright holder. To view a copy of this licence, visit http://creativecommons.org/licenses/by/4.0/.

© The Author(s) 2022

3 Contribution 3: Thermal non-classical correlation via skew information, quantum Fisher information, and quantum teleportation of a spin-1/2 Heisenberg trimer system

The European Physical Journal Plus, 137 (2022) 1096.

3.1 Summary of contribution 3

According to recent findings, bipartite systems may not be as effective at comprehending and communicating quantum information as larger quantum systems. These results motivated us to carry out a comprehensive study of non-classical correlations within pure and mixed states of a spin-1/2 Heisenberg trimer, a tripartite quantum system, in the presence and absence of temperature, as well as under the influence of an external magnetic field. Our findings demonstrate that non-classical correlations measured by local quantum uncertainty (4.46) and entanglement measured by negativity (2.80) are strongly influenced by intrinsic parameters such as exchange anisotropy and cyclic three-spin interaction parameters as well as extrinsic parameters such as temperature and magnetic field. Large values of the anisotropy parameter, for instance, greatly enhance the tripartite quantum connections of the proposed system. The statistics also imply that temperature has far stronger adverse impact on negativity than it does on LQU. This demonstrated the LQU's resistance to the effects of temperature. It was shown that LQU is a useful metric for capturing the non-classical linkages in tripartite systems as a consequence.

In the aftermath of this result, we have studied a variety of applications of this model in quantum information theory and quantum estimation using quantum Fisher information and quantum teleportation. Based on the standard quantum teleportation protocol, we investigated the possibility of quantum teleportation using the state under research as a quantum channel.

In fact, we found that at low enough temperatures and coupling constants, the tripartite quantum channel may transport the unknown state. We also concentrated on recognising the generated tripartite magnetic CuII 3 complex system's quantum Fisher information as a quantum metrology application.

This research highlights the importance of studying tripartite quantum systems for quantum communication and information processing. It also sheds light on how intrinsic and extrinsic properties affect non-classical correlations and their potential applications in quantum technologies.

3.2 Content of contribution 3

Eur. Phys. J. Plus (2022) 137:1096
https://doi.org/10.1140/epjp/s13360-022-03297-z

THE EUROPEAN PHYSICAL JOURNAL PLUS

Regular Article

Thermal non-classical correlation via skew information, quantum Fisher information, and quantum teleportation of a spin-1/2 Heisenberg trimer system

Fadwa Benabdallah[1], **Khadija El Anouz**[2,a], **Jozef Strecka**[3], **Mohammed Daoud**[4,5]

[1] LPHE-Modeling and Simulation, Faculty of Sciences, Mohammed V University, Rabat, Morocco
[2] Laboratory of R &D in Engineering Sciences, Faculty of Sciences and Techniques Al-Hoceima, Abdelmalek Essaadi University, Tétouan, Morocco
[3] Department of Theoretical Physics and Astrophysics, Faculty of Science, P. J. Safarik University, Park Angelinum 9, 040 01 Kosice, Slovakia
[4] ICTP, Strada Costiera 11, 34151 Trieste, Italy
[5] Department of Physics, Faculty of Sciences, University Ibn Tofail, Kenitra, Morocco

Received: 20 May 2022 / Accepted: 16 September 2022
© The Author(s), under exclusive licence to Società Italiana di Fisica and Springer-Verlag GmbH Germany, part of Springer Nature 2022

Abstract In the present work, we carry out a description of multi-qubit quantum correlations because of their distinguished physical prominence in quantum information processing and quantum communication. To this end, we have studied quantum correlations within pure and mixed states of a tripartite quantum system which can be referred to as a spin-1/2 Heisenberg trimer with the exchange anisotropy and cyclic three-spin interaction in the presence of the external magnetic field at zero as well as nonzero temperature. Our study reveals that the non-classical correlations quantified by means of local quantum uncertainty and the entanglement quantified in terms of negativity depend decisively on the intrinsic parameters as for instance the exchange anisotropy and cyclic three-spin interaction parameters in addition to extrinsic parameters such as temperature and magnetic field. A variety of applications of this model in quantum information theory and quantum estimation are also studied by means of quantum Fisher information and quantum teleportation. It has been shown that the average fidelity and quantum Fisher information measures are basically enhanced when the temperature and magnetic field parameters vanish.

1 Introduction

Quantum correlations beyond entanglement are a prominent concept in quantum information theory and are of fundamental importance in a modern science. Indeed, since their birth, quantum correlation and entanglement have created an important debate and attracted a great deal of attention in the scientific community for the last decade [1]. For example, the quantum discord is considered as a significant quantifier used to quantify the amount of quantum correlations and it originally arrived from the discrepancy between two different quantities that are classically identical, but from the point of view of quantum mechanics, they are inequivalent [2]. However, the minimization process restrains because of its complexity the computation of quantum discord for all quantum states and it is simply defined only for a few restricted families of states [3, 4]. Indeed, it has been shown that an analytical expression of bipartite quantum discord is obtained for a specific family of states [5]. Moreover, in the case of multi-qubit systems, the quantum discord is also computable [6, 7], and the general formula that is easy to calculate was proposed for $2 \otimes d$ systems [6, 8, 9]. However, for a composite quantum system bipartite, tripartite or multipartite subsystems may be entangled, whereby the entanglement is not the only quantum correlation present in these states. Indeed, there exist some quantum separable states that are quantum-mechanically correlated, i.e., when their quantum discord does not vanish. Recently, multipartite entanglement has been extensively studied and given remarkable attention because, in general, it has a richer structure than the bipartite entanglement. In fact, the need to study the separability of its components has triggered interest in non-classical aspects of multipartite quantum systems [10]. The entanglement as a consequence of the quantum correlations between many quantum parties represents one of the most popular tools used to quantify the non-separability between quantum systems [11]. Various non-classical correlation and entanglement quantifiers have been proposed in the last two decades, which have played a significant role in expanding our appreciation and knowledge of the quantum world [12]. For bipartite and tripartite quantum systems, for example, the negativity is proposed as a good measure of entanglement [13, 14]. Moreover, the local quantum uncertainty (LQU) is known as a very active quantifier of non-classical correlations [15]. Interestingly enough, M. Ali improves an explicit formula of LQU for multipartite quantum systems, where he evaluates the LQU of various three- and four-qubit quantum states, namely W, Dicke, GHZ, singlet and cluster states [16].

Recently, it has been evidenced that the measures of quantum correlations not only touch upon some fundamental tasks in quantum information theory [17], but they are also crucial to many issues in quantum estimation theory [18–20], quantum information pro-

[a] e-mail: elanouzkhadija1994@gmail.com (corresponding author)

Published online: 29 September 2022

cessing and modern communications, etc [21–26]. Moreover, it has been demonstrated that the so-called quantum Fisher information (QFI) is considered as a useful measure in quantum estimation theory, which can detect the entanglement of a composite quantum system [27, 28]. Another concept referred to as the local quantum Fisher information (LQFI), which is founded basically on the QFI, has been investigated as a prominent quantifier of quantum correlations for bipartite quantum states [29, 30]. The idea behind QFI and LQFI starts from the fact that the information encoded in a quantum state is often represented in the form of a set of parameters. Identifying different states through estimating the encoded parameters and by performing measurements allows us to extract the physical information carried by a parameter in the state that exactly defines the QFI. One of the important advantages of studying QFI in this context concerns with its ability to physically guarantee a measure of non-classical correlations, namely LQFI when the dynamics is governed by a local transformation [31]. Inspired by this fact, several quantum spin systems have been suggested in order to study QFI and LQFI under various circumstances. For example, Obada et al. made a comparative study between QFI and the entanglement, where he has showed that the Fisher information may be used as evidence of entanglement [28]. However, A.B.A. Mohamed studied different quantifiers of non-classical correlations, including; QFI and Bures Distance correlations for an open quantum system interacting with its surrounding environment, i.e., a coupled two charge-qubits inside of a coherent cavity in the presence of intrinsic decoherence [32]. Alternatively, in Ref. [31], the authors study the LQU and LQFI in a two-qubit Heisenberg XYZ chain with Dzyaloshinski-Moriya interactions. They showed that LQU and LQFI depend on the temperature and the coupling parameter in the anisotropic XY model.

As it is obvious from the above discussion, the most pronounced features of the aforementioned measures, namely LQU negativity and QFI, are their simplicity and computability. Indeed, the substantial purpose of this paper is to investigate the measures of LQU and the negativity within pure and mixed states of a spin-1/2 Heisenberg trimer with the exchange anisotropy and cyclic three-spin interaction in the presence of a non-uniform magnetic field. In fact, the unconventional enhancement of the tripartite quantum correlations due to the magnetic field can be related to Zeeman's splitting of energy levels, which results in an unexpected abrupt rise of quantum correlations in the spin-1/2 Heisenberg trimer model. The present theoretical study is motivated by the coupled trinuclear Cu_3^{II} triplesalacen complex as a magnetic system [33]. The structural and magnetic properties of this model have been experimentally investigated in Ref. [33]. The spin arrangement of this special complex in the crystal lattice leads to the formation of a pyramid structure. Our results show that large values of the anisotropy parameter Δ strengthen basically the tripartite quantum correlations of the proposed system. Moreover, the outcomes prove that the destructive effects of the temperature are much stronger for the negativity than for the LQU. This emphasizes that the LQU is more robust with respect to temperature effects. This shows that LQU is an appropriate measure capturing the non-classical correlations in tripartite systems. Roughly speaking, in our model, the entanglement sudden death phenomenon does not occur in the tripartite model in contrast of bipartite systems [34–36]. Hence, we can conclude that increasing the size of a quantum system can be superior with respect to bipartite systems in quantum technologies. On the other hand, once the tripartite correlated state is found, one can investigate the quantum teleportation protocol via using this state as a quantum channel during this process. Indeed, we observe that the tripartite quantum channel becomes useful for teleportation of the unknown state for small enough values of the temperature and exchange coupling parameters. Furthermore, as a quantum metrology application, we will concentrate on determining the quantum Fisher information of the obtained tripartite magnetic Cu_3^{II} complex system.

The paper is structured as follows. In Sect.2, we introduce the Hamiltonian describing the proposed model, in which the thermal density operator is investigated. Section 3 contains some preliminaries about negativity and LQU. Their behaviors versus the parameters characterizing the proposed system are analyzed in Sect.4. In Sect.5, a variety of applications in quantum information theory and quantum estimation are also examined by means of quantum Fisher information and quantum teleportation within this model. Finally, a summary of our results and concluding remarks are given in Sect.6.

2 Model and method

Let us consider a spin-1/2 Heisenberg trimer (three-qubit) model developed for the trinuclear copper(II) complex abbreviated by the simple notation Cu_3^{II} [33] (see Fig. 1). This system is represented as a magnetic system with cyclic three-spin interaction under the influence of the external magnetic field. Therefore, the Hamiltonian of the spin-1/2 Heisenberg trimer can be expressed as follows:

$$\begin{aligned} H = &\left[-2J_1(S_1^x S_2^x + S_1^y S_2^y) + \Delta_1 S_1^z S_2^z\right] + \left[-2J_2(S_2^x S_3^x + S_2^y S_3^y) + \Delta_2 S_2^z S_3^z\right] \\ &+ \left[-2J_3(S_3^x S_1^x + S_3^y S_1^y) + \Delta_3 S_3^z S_1^z\right] + \mu_B g B(S_1^z + S_2^z + S_3^z) + K S_1^z S_2^z S_3^z. \end{aligned} \tag{1}$$

The coupling constant J_i with $i = \{1, 2, 3\}$ describes the strength of the exchange interaction within a spin triangle, which is ferromagnetic for $J_i > 0$ and antiferromagnetic and $J_i < 0$. Moreover, B denotes the external magnetic field which is only applied to the z-direction, while the parameter Δ_i with $i = \{1, 2, 3\}$ determines the XXZ exchange anisotropy in the exchange interaction. However, the parameter K is the cyclic three-spin interaction. Finally, the parameter g represents the gyromagnetic Landé g-factor with assumption $g = 2.045$ [33], and μ_B is the Bohr magneton. In such definition, the symbols $S_i^\alpha = \hbar\sigma_i^\alpha/2$ ($\alpha = x, y, z$) correspond to spatial components of the spin- 1/2 operators. For the sake of simplicity, we set $\hbar = 1$ and $\mu_B = 1$.

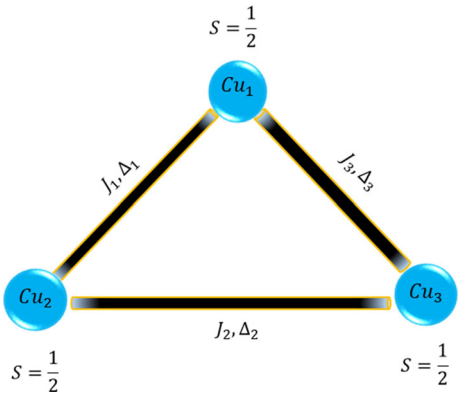


Fig. 1 A schematic structure of the trinuclear Cu_3^{II} complex represented by the spin-1/2 XXZ Heisenberg trimer (three-qubit) model with the corresponding magnetic exchange interactions as indicated in the figure

In contrast, we assume that the spatially isotropic exchange interaction satisfies the constraint $J_1 = J_2 = J_3 = J$ and the unique value of the XXZ exchange anisotropy is considered $\Delta_1 = \Delta_2 = \Delta_3 = \Delta$ in all forthcoming analytical expressions and simulations. In the standard basis formed by the eigenvectors $|\varphi_i\rangle \in \{|000\rangle, |001\rangle, |010\rangle, |011\rangle, |100\rangle, |101\rangle, |110\rangle, |111\rangle\}$ of z-components of the spin-1/2 operators, the matrix representation of the Hamiltonian (1) turns out to be

$$\langle\varphi_i|H|\varphi_j\rangle = \begin{pmatrix} H_{11} & 0 & 0 & 0 & 0 & 0 & 0 & 0 \\ 0 & H_{22} & H_{23} & 0 & H_{25} & 0 & 0 & 0 \\ 0 & H_{23} & H_{33} & 0 & H_{35} & 0 & 0 & 0 \\ 0 & 0 & 0 & H_{44} & 0 & H_{46} & H_{47} & 0 \\ 0 & H_{52} & H_{53} & 0 & H_{55} & 0 & 0 & 0 \\ 0 & 0 & 0 & H_{64} & 0 & H_{66} & H_{67} & 0 \\ 0 & 0 & 0 & H_{74} & 0 & H_{76} & H_{77} & 0 \\ 0 & 0 & 0 & 0 & 0 & 0 & 0 & H_{88} \end{pmatrix}, \tag{2}$$

where the diagonal elements are computed as given bellow

$$\begin{aligned} H_{11} &= \frac{3}{4}\Delta + \frac{3}{2}g\ B + \frac{1}{8}K, \quad H_{22} = H_{33} = H_{55} = -\frac{1}{4}\Delta + \frac{1}{2}g\ B - \frac{1}{8}K, \\ H_{44} &= H_{66} = H_{77} = -\frac{1}{4}\Delta - \frac{1}{2}g\ B + \frac{1}{8}K, \quad H_{88} = \frac{3}{4}\Delta - \frac{3}{2}g\ B - \frac{1}{8}K, \end{aligned} \tag{3}$$

while the off-diagonal elements read

$$\begin{aligned} H_{23} = H_{25} = H_{32} = H_{35} = H_{46} = H_{47} = -J, \\ H_{52} = H_{53} = H_{64} = H_{67} = H_{74} = H_{76} = -J. \end{aligned} \tag{4}$$

The Hamiltonian (2) has a relatively simple block-diagonal form that allows us to obtain a complete set of eigenvalues using an exact analytical diagonalization. Indeed, the eigenvalues of the Hamiltonian (2) are obtained as follows

$$E_{1(4)} = \frac{3\Delta}{4} \mp \frac{3gB}{2} \mp \frac{K}{8}, \quad E_2 = E_3 = \frac{gB}{2} - \frac{\Delta}{4} + J - \frac{K}{8}, \tag{5}$$

$$E_5 = E_6 = -\frac{g\ B}{2} - \frac{\Delta}{4} + J + \frac{K}{8} \quad E_{7(8)} = \pm\frac{g\ B}{2} - \frac{\Delta}{4} - 2J \mp \frac{K}{8}, \quad , \tag{6}$$

whereas the corresponding eigenvectors are given as follows

$$|\psi_1\rangle = |000\rangle, |\psi_2\rangle = \frac{1}{\sqrt{2}}(-|110\rangle + |011\rangle), |\psi_3\rangle = \frac{1}{\sqrt{2}}(-|110\rangle + |101\rangle), \tag{7}$$

$$|\psi_4\rangle = |111\rangle, |\psi_5\rangle = \frac{1}{\sqrt{2}}(-|100\rangle + |001\rangle), |\psi_6\rangle = \frac{1}{\sqrt{2}}(-|100\rangle + |001\rangle), \tag{8}$$

$$|\psi_7\rangle = \frac{1}{\sqrt{3}}(|110\rangle + |101\rangle + |011\rangle), |\psi_8\rangle = \frac{1}{\sqrt{3}}(|100\rangle + |010\rangle + |001\rangle)\ . \tag{9}$$

2.1 Density operator

To gain an overall insight into the quantum properties of the magnetic Cu_3^{II} complex such as thermal entanglement and local quantum uncertainty, it is necessary to obtain the density operator of the system, which can be easily calculated from the eigenvalues (5-6) and the respective eigenvectors (7-9) according to the following formula

$$\rho\,(T) = \frac{1}{Z}\sum_{l=1}^{8}\exp(-\beta E_l)|\psi_l\rangle\langle\psi_l|, \tag{10}$$

which is expressed in terms of the partition function $Z = \mathrm{Tr}\big[\exp(-\beta H)\big]$ with $\beta = 1/(k_B T)$, T is the absolute temperature and k_B is the Boltzmann's constant further to be set to unity. Therefore, in the computational basis, the density matrix corresponding to the density operator (10) at thermal equilibrium (canonical ensemble) has a matrix structure similar to the Hamiltonian matrix (2)

$$\rho(T) = \frac{1}{Z}\begin{pmatrix} \rho_{11} & 0 & 0 & 0 & 0 & 0 & 0 & 0 \\ 0 & \rho_{22} & \rho_{23} & 0 & \rho_{25} & 0 & 0 & 0 \\ 0 & \rho_{32} & \rho_{33} & 0 & \rho_{35} & 0 & 0 & 0 \\ 0 & 0 & 0 & \rho_{44} & 0 & \rho_{46} & \rho_{47} & 0 \\ 0 & \rho_{52} & \rho_{53} & 0 & \rho_{55} & 0 & 0 & 0 \\ 0 & 0 & 0 & \rho_{64} & 0 & \rho_{66} & \rho_{67} & 0 \\ 0 & 0 & 0 & \rho_{74} & 0 & \rho_{76} & \rho_{77} & 0 \\ 0 & 0 & 0 & 0 & 0 & 0 & 0 & \rho_{88} \end{pmatrix}. \tag{11}$$

For the sake of brevity, the elements of the density matrix ρ_{ij} are explicitly given by

$$\begin{aligned}
\rho_{11} &= \exp\left(-\frac{12\,g\,B + K - 6\Delta}{8T}\right),\ \rho_{88} = \exp\left(-\frac{12\,g\,B + K + 6\Delta}{8T}\right),\\
\rho_{22} &= \frac{1}{6}\exp\left(-\frac{-4\,g\,B + 8J + K - 2\Delta}{8T}\right)\left(3 + 2\exp\left(\frac{3J}{2T}\right)\right),\\
\rho_{23} &= \frac{1}{3}\exp\left(\frac{4\,g\,B + 16J - K + 2\Delta}{8T}\right),\\
\rho_{25} &= \frac{1}{6}\exp\left(-\frac{-4\,g\,B + 8J + K - 2\Delta}{8T}\right)\left(-3 + 2\exp\left(\frac{3J}{2T}\right)\right),\\
\rho_{44} &= \frac{1}{6}\exp\left(\frac{-4\,g\,B + 8J + K - 2\Delta}{8T}\right)\left(3 + 2\exp\left(\frac{3J}{2T}\right)\right),\ \rho_{46} = \frac{1}{3}\exp\left(\frac{-4\,g\,B + 16J + K + 2\Delta}{8T}\right),\\
\rho_{55} &= \frac{1}{3}\exp\left(-\frac{-4\,g\,B + 8J + K - 2\Delta}{8T}\right)\left(3 + 2\exp\left(\frac{3J}{2T}\right)\right),\\
\rho_{47} &= \frac{1}{6}\exp\left(\frac{-4\,g\,B - 8J + K + 2\Delta}{8T}\right)\left(-3 + 2\exp\left(\frac{3J}{2T}\right)\right),\\
\rho_{77} &= \frac{1}{3}\exp\left(\frac{-4\,g\,B - 8J + K + 2\Delta}{8T}\right)\left(3 + 2\exp\left(\frac{3J}{2T}\right)\right),
\end{aligned}$$

with

$$\rho_{22} = \rho_{33},\quad \rho_{23} = \rho_{32},\quad \rho_{47} = \rho_{74},\quad \rho_{25} = \rho_{52} = \rho_{35} = \rho_{53},\ \rho_{47} = \rho_{74},$$

The partition function Z emergent (11) can be explicitly written as

$$\begin{aligned}
Z = \exp\left(-\frac{12\,g\,B + 8J + K + 6\Delta}{8T}\right)&\left(\exp\left(\frac{J}{2T}\right)\left(1 + \exp\left(\frac{12Bg + K}{4T}\right)\right)\right.\\
&\left.+\exp\left(\frac{Bg + \Delta}{T}\right)\left(2 + \exp\left(\frac{3J}{2T}\right)\right)\left(\exp\left(\frac{Bg}{T}\right) + \exp\left(\frac{4K}{T}\right)\right)\right).
\end{aligned}$$

The entanglement is called the thermal entanglement because the density operator $\rho(T)$ (11) represents a thermal state. It should be mentioned that the size of the antiferromagnetic exchange interaction $J > 0$ is taken as an energy unit. As a result, in our analysis, the quantities measuring the relative strength of the cyclic three-spin interaction K/J, the magnetic field $\mu_B B/J$, and the temperature $k_B T/J$ could be considered as dimensionless parameters. From now on, we consider the simple form ρ instead of $\rho(T)$.

3 Multi-qubit quantum correlations

In this section, let us restrict our attention to some non-classical correlations quantifiers, namely LQU and entanglement expressed by means of negativity for multi-qubit systems.

3.1 Quantum entanglement: multi-qubit negativity

Apart from bipartite pure states [37, 38] and two-qubit systems in the mixed states [39, 40], an analytical formula required to quantify the entanglement inherent in a multi-qubit system is still lacking. The average of bipartite entanglement measures over all possible bipartitions of the N-qubit system is one of the most popular computable measures used to quantify the global amount of genuine entanglement of an arbitrary N-qubit entangled system in a mixed state ρ [14]. Indeed, the explicit formula of negativity of any multi-qubit system turns out to be [13]

$$\mathcal{N}^{(N)}(\rho)=\frac{2}{N}\sum_{k=1}^{N/2}\left(\frac{1}{n_{bipart}^{(k)}}\sum_{P=1}^{n_{bipart}^{(k)}}\mathcal{N}^{P[k|N-k]}(\rho)\right), \tag{12}$$

where $k|N-k$ denotes the bipartitions of the N-qubit system, with k qubits in one block and the remaining $N-k$ ones in another block. In the bipartition, $k|N-k$, $P[k|N-k]$ is used to specify an exact combination of k and $N-k$ qubits. On the other hand, $n_{bipart}^{(k)}$ represents the total possible non-equivalent concrete bipartitions $P[k|N-k]$ with $\mathcal{N}^{P[k|N-k]}(\rho)$) being the negativity associated with each given bipartition of $P[k|N-k]$ defined as

$$\mathcal{N}^{P[k|N-k]}(\rho)=\sum_{J}\lambda_J(\rho^{T_I})-1. \tag{13}$$

In above, $\lambda_J(\rho^{T_I})$ are the negative eigenvalues of the partially transposed density matrix ρ^{T_I} of the composite system with respect to subsystem I which is constituted by the k qubits of the given bipartition $P[k|N-k]$. In other words, the negativity is related to the trace norm of ρ^{T_I} as

$$\mathcal{N}^{P[k|N-k]}(\rho)=\frac{\left\|\rho^{T_I}\right\|-1}{2}, \tag{14}$$

where the trace norm is defined by $\left\|\rho^{T_I}\right\|=\mathrm{Tr}(\sqrt{\rho^{T_I}\rho^{T_I\dagger}})$. We notice that the zero negativity, namely $\mathcal{N}=0$, corresponds to the completely separable (factorizable) states, while it becomes nonzero, $\mathcal{N}\neq 0$, for entangled (non-separable) states. As a concrete example, let us consider the case of the three-qubit system $\rho(T)$ (11). Therefore, the negativity (12) turns out to be

$$\mathcal{N}^{(3)}(\rho)=\sqrt[3]{\mathcal{N}^{A|BC}\mathcal{N}^{B|AC}\mathcal{N}^{C|AB}}. \tag{15}$$

3.2 Local quantum uncertainty

Recently, Giromali et al. [41] have introduced the notion of the local quantum uncertainty (LQU) as a prominent discord-like measure of a non-classical correlation in bipartite quantum systems. This measure quantifies the uncertainty in a quantum state which can arise due to its non-commutativity with the measured local observable. Based on the definition of Winger-Yanase skew information [42], the LQU is defined as the minimum uncertainty induced by applying measurements on a part of a quantum state as follows

$$\mathcal{U}_A(\rho)=\min_{K_\mathrm{A}}\mathcal{I}(\rho, K_\mathrm{A}\otimes I_\mathrm{B}), \tag{16}$$

where K_A is a hermitian operator (local observable) on subsystem A admitting a non-degenerate spectrum. Moreover, I_B is the identity operator acting on subsystem B, while $\mathcal{I}$ is the skew information associated with the density matrix ρ and it is defined as

$$\mathcal{I}(\rho,\ K)=-\frac{1}{2}\mathrm{Tr}([\sqrt{\rho},\ K]^2), \tag{17}$$

where [., .] is the commutator. It is worth noticing that the Wigner-Yanase skew information (WYSI) is unaffected by classical mixing and it reduces to the variance for pure states. Note that, $\mathcal{I}$ is non-negative and non-increasing under classical mixing [16]. The local quantum uncertainty provides a reliable measure of quantum correlations and it has a geometrical significance in terms of Hellinger distance. Furthermore, it is an asymmetric quantity that remains invariant under local unitary operations and does not increase under local reversible operations on unmeasured part [41]. Moreover, the local quantum uncertainty vanishes for all states with zero discord. It reduces to the linear entropy of the reduced densities of the subsystems for pure bipartite states. From now on, we consider the simple form $\mathcal{U}(\rho)$ instead of $\mathcal{U}_A(\rho)$. For a $2\otimes d$ (qubit-qudit) bipartite quantum systems [41], the compact formula of the local quantum uncertainty turns out to be

$$\mathcal{U}(\rho)=1-\lambda_{\max}(\mathcal{W}), \tag{18}$$

where $\lambda_{\max}$ stands for the largest eigenvalue of the 3×3 matrix $\mathcal{W}$ of the following elements:

$$(\mathcal{W})_{\alpha\beta} = \mathrm{Tr}(\sqrt{\rho}(\sigma^{\alpha} \otimes I_{\mathrm{B}})\sqrt{\rho}(\sigma^{\beta} \otimes I_{\mathrm{B}})), \tag{19}$$

where $\sigma^{\alpha(\beta)}$ with $\alpha(\beta) = \{x, y, z\}$ represents the Pauli operators of subsystem A. It is clear that having the matrix $\mathcal{W}$, one can easily evaluate the local quantum uncertainty for qubit-qudit quantum systems contrarily to the quantum discord based on von Neumann entropy [16]. This is quite an easy task compared with the complicated minimization process over parameters due to the local measurements [34, 41, 43]. It is important to note that for some quantum states, quantum discord and local quantum uncertainty capture the same correlations, whereas they are different measures for others states [16]. Besides, the genuine N-qubit negativity, multi-qubit local quantum uncertainty is another useful indicator of non-classical correlations in multi-qubit systems. However, unlike the genuine N-qubit negativity, its calculation for multi-qubit mixed states is a challenging task since it involves a difficult optimization process, which is very hard to solve exactly. For this purpose, in the ref. [16], Ali Mazhar generalized the concept of LQU for the multi-qubit systems since we can regard the multi-qubit system as a qubit-qudit $(2 \otimes d)$ system such as $d = 2 \otimes 2 \otimes 2 \otimes 2 \otimes .... \otimes 2$ representing the remaining $N - 1$ qubits as d dimensional quantum system. In comparison with bipartite quantum systems, multi-qubit systems have a richer structure. It is possible that some bipartitions are quantum correlated, whereas the others are classically correlated. In order to capture only the purely correlations of quantum nature, we apply the local measurements across each bipartition. To do this, one assumes that ρ_N is an arbitrary density matrix described by N-qubits. For each qubit namely A, B, ...N, we apply the local measurements with respect to the rest of the qubits [16]. Thus, according to Eq. (19), the matrix elements corresponding to the N symmetric matrices belong to each bipartition as

$$\begin{aligned}
(\mathcal{W})^{A}_{ij} &= \mathrm{Tr}(\sqrt{\rho_N}(\sigma_i \otimes I_2 \otimes I_2 \otimes ... \otimes I_2)\sqrt{\rho_N}(\sigma_j \otimes I_2 \otimes I_2 \otimes ... \otimes I_2)),\\
(\mathcal{W})^{B}_{ij} &= \mathrm{Tr}(\sqrt{\rho_N}(I_2 \otimes \sigma_i \otimes I_2 \otimes ... \otimes I_2)\sqrt{\rho_N}(I_2 \otimes \sigma_j \otimes I_2 \otimes ... \otimes I_2)),\\
(\mathcal{W})^{C}_{ij} &= \mathrm{Tr}(\sqrt{\rho_N}(I_2 \otimes I_2 \otimes \sigma_i \otimes .... \otimes I_2)\sqrt{\rho_N}(I_2 \otimes I_2 \otimes \sigma_j \otimes .... \otimes I_2)),\\
&\vdots\\
&\vdots\\
(\mathcal{W})^{N}_{ij} &= \mathrm{Tr}(\sqrt{\rho_N}(I_2 \otimes I_2 \otimes I_2 \otimes .... \otimes \sigma_i)\sqrt{\rho_N}(I_2 \otimes I_2 \otimes I_2 \otimes .... \otimes \sigma_j)).
\end{aligned} \tag{20}$$

Therefore, the local quantum uncertainty associated with each bipartition is given as follows [16]

$$\begin{aligned}
\mathcal{U}_{A/BC...N}(\rho_N) &= 1 - \max\{Spectrum\ of\ \mathcal{W}^{A}\},\\
\mathcal{U}_{B/AC...N}(\rho_N) &= 1 - \max\{Spectrum\ of \mathcal{W}^{B}\},\\
\mathcal{U}_{C/BC...N}(\rho_N) &= 1 - \max\{Spectrum\ of \mathcal{W}^{C}\},\\
&\vdots\\
&\vdots\\
\mathcal{U}_{N/BC...N-1}(\rho_N) &= 1 - \max\{Spectrum\ of\ \mathcal{W}^{N}\}.
\end{aligned} \tag{21}$$

Thus, for a given N-qubits quantum system, the local quantum uncertainty may be defined by

$$\mathcal{U}(\rho_N) = \frac{1}{N}\sum_{i=1}^{N}\mathcal{U}_{i/N_i}. \tag{22}$$

We apply this measure to derive the amount of quantum correlations in a three-qubit Heisenberg spin system (1) in thermal equilibrium at temperature ρ (11). The matrix elements associated with each bipartition $A|BC$, $B|AC$ and $C|AB$ are calculated, respectively, using the formulas

$$(\mathcal{W})^{A}_{ij} = \mathrm{Tr}(\sqrt{\rho}(\sigma_i \otimes I_2 \otimes I_2)\sqrt{\rho}(\sigma_j \otimes I_2 \otimes I_2)), \tag{23}$$

$$(\mathcal{W})^{B}_{ij} = \mathrm{Tr}(\sqrt{\rho}(I_2 \otimes \sigma_i \otimes I_2)\sqrt{\rho}(I_2 \otimes \sigma_j \otimes I_2)), \tag{24}$$

$$(\mathcal{W})^{C}_{ij} = \mathrm{Tr}(\sqrt{\rho}(I_2 \otimes I_2 \otimes \sigma_i)\sqrt{\rho}(I_2 \otimes I_2 \otimes \sigma_i)), \tag{25}$$

where $\sqrt{\rho}$ is given in Appendix 1 (VII A). The non-vanishing matrix elements (23), (24) and (25) are given by

$$\begin{aligned}
(\mathcal{W})^{A}_{11} = (\mathcal{W})^{A}_{22} &= \frac{1}{18}(12\sqrt{\lambda_2}(2\sqrt{\lambda_4} + \sqrt{\lambda_5}) + 3(3\sqrt{\lambda_3}(\sqrt{\lambda_6} + 3\sqrt{\lambda_7}) + 2\sqrt{\lambda_1}(3\sqrt{\lambda_6} + \sqrt{\lambda_7} + 2\sqrt{\lambda_8}))\\
&+ (\sqrt{\lambda_4} + 2\sqrt{\lambda_5})(3\sqrt{\lambda_6} + \sqrt{\lambda_7} + 8\sqrt{\lambda_8})),
\end{aligned} \tag{26}$$

$$(\mathcal{W})^{A}_{33} = \frac{1}{9}(9(\lambda_1+\lambda_2+\lambda_3)+\lambda_4+16\sqrt{\lambda_4\lambda_5}+\lambda_5+(2\sqrt{\lambda_7}+\sqrt{\lambda_8})^2+6(\sqrt{\lambda_6}(\sqrt{\lambda_7}+2\sqrt{\lambda_8})), \tag{27}$$

$$(\mathcal{W})^{B}_{11} = (\mathcal{W})^{B}_{22} = \frac{1}{18}(6\sqrt{\lambda_2}(3\sqrt{\lambda_3}+\sqrt{\lambda_4}+2\sqrt{\lambda_5})+3\sqrt{\lambda_4\lambda_6}+6\sqrt{\lambda_5\lambda_6}+25\sqrt{\lambda_4\lambda_7}+2\sqrt{\lambda_5\lambda_7}+ \\ +6\sqrt{\lambda_1}(3\sqrt{\lambda_6}+\sqrt{\lambda_7}+2\sqrt{\lambda_8})+3\sqrt{\lambda_3}(3\sqrt{\lambda_6}+\sqrt{\lambda_7}+2\sqrt{\lambda_8})+2(\sqrt{\lambda_4}+8\sqrt{\lambda_5})\sqrt{\lambda_8}, \tag{28}$$

$$(\mathcal{W})^{B}_{33} = \frac{1}{9}(9(\lambda_1+\lambda_2)+(2\sqrt{\lambda_4}+\sqrt{\lambda_5})^2+6\sqrt{\lambda_3}(\sqrt{\lambda_4}+2\sqrt{\lambda_5})+(2\sqrt{\lambda_7}+\sqrt{\lambda_8})^2+6(\sqrt{\lambda_6}(\sqrt{\lambda_7}+2\sqrt{\lambda_8})), \tag{29}$$

$$(\mathcal{W})^{C}_{11} = (\mathcal{W})^{C}_{22} = \frac{1}{18}(6\sqrt{\lambda_2}(3\sqrt{\lambda_3}+\sqrt{\lambda_4}+2\sqrt{\lambda_5})+27\sqrt{\lambda_4\lambda_6}+24\sqrt{\lambda_1\lambda_7}+\sqrt{\lambda_4\lambda_7}+8\sqrt{\lambda_5\lambda_7}+ \\ +3\sqrt{\lambda_3}(3\sqrt{\lambda_6}+\sqrt{\lambda_7}+2\sqrt{\lambda_8})+2\sqrt{\lambda_8}(6\sqrt{\lambda_1}+\sqrt{\lambda_4}+8\sqrt{\lambda_5}), \tag{30}$$

$$(\mathcal{W})^{C}_{33} = \frac{1}{9}(9(\lambda_1+\lambda_2)+(2\sqrt{\lambda_4}+\sqrt{\lambda_5})^2+6\sqrt{\lambda_3}(\sqrt{\lambda_4}+2\sqrt{\lambda_5})+9\lambda_6+\lambda_7+16\sqrt{\lambda_7\lambda_8}+\lambda_8). \tag{31}$$

where $\lambda_i (i = 1, ..., 4)$ are the eigenvalues of the density matrix ρ (11) explicitly given in the Appendix 1 (VII A). Hence, the local quantum uncertainties related to each bipartition take the following form:

$$\mathcal{U}_{A/BC}(\rho) = 1 - \max\{\mathcal{W}^{A}_{11}, \mathcal{W}^{A}_{33}\}, \tag{32}$$

$$\mathcal{U}_{B/AC}(\rho) = 1 - \max\{\mathcal{W}^{B}_{11}, \mathcal{W}^{B}_{33}\}, \tag{33}$$

$$\mathcal{U}_{C/AB}(\rho) = 1 - \max\{\mathcal{W}^{C}_{11}, \mathcal{W}^{C}_{33}\}. \tag{34}$$

Therefore, the total local quantum uncertainty describing the three qubits system would be defined as

$$\mathcal{U}(\rho) = \frac{\mathcal{U}_{A/BC}(\rho)+\mathcal{U}_{B/AC}(\rho)+\mathcal{U}_{C/AB}(\rho)}{3}.$$

4 The behavior of quantum correlations

To examine the influence of the cyclic three-spin interaction on the non-classical correlation including the quantum entanglement, some density plots of the negativity $\mathcal{N}$ and LQU are depicted in Fig. 2 in the temperature-field plane by assuming the value of Landé factor $g = 2.045$, two representative values of cyclic three-spin interaction and fixed value of the exchange anisotropy, $\Delta/J = 0.5$ and $\Delta/J = 1.0$. It follows from the displayed density plots that the strongest quantum correlations can be detected simultaneously at low temperature and magnetic field, which gives rise to the highest possible value of the negativity and local quantum uncertainty in the zero-temperature limit. Upon further increase in the temperature and the magnetic field, the quantum correlations decrease, and the state of the model $\rho(T)$ (11) loses its maximum entanglement property. As a matter of fact, an increase in Δ/J significantly strengthens the tripartite quantum correlations in the thermal state $\rho(T)$ (11). For instance, the negativity and LQU are reinforced when Δ/J switches to the unit value (Fig. 2c–d and 2g–h). Moreover, it follows from Fig. 2 that in the absence of the cyclic three-spin interaction $K/J = 0$, both quantum correlations quantifiers are symmetric with respect to zero magnetic field ($\mu_B B/J = 0$). Besides, the cyclic three-spin interaction parameter K/J is responsible for the time-reversal symmetry breaking and the magnetization would not be an odd function of the magnetic field [35]. However, with K/J increase, the symmetry with respect to ($\mu_B B/J = 0$) axis reduces between the three-spin-1/2 particles. In addition, the local quantum uncertainty detects the amount of quantum correlations in the tripartite system (1) much better than the negativity but this last predominate over LQU at some threshold value of the external magnetic field. Moreover, the quantum correlations amounts, regardless of $\mu_B B/J = 0$, are strengthened upon decrease in temperature $k_B T/J$. The difference between both measures is that the negativity vanishes at a certain threshold temperature, above which LQU remains nonzero and it tends to zero just at higher values of temperature (see Fig. 2). Therefore, the destructive effects of the temperature are much stronger for the negativity than the local quantum uncertainty. This confirms a greater robustness of LQU in comparison with thermal entanglement against the temperature effects. This shows that LQU is more suitable to capture the non-classical correlations in tripartite systems.

Now, let us investigate in detail how the tripartite quantum correlations of the spin$-1/2$ XXZ Heisenberg trimer are resistant with respect to thermal fluctuations. The temperature dependence of the negativity (upper panels) and local quantum uncertainty (lower panels) is illustrated in Fig. 3 for specific values of the cyclic three-spin interaction K/J, where the anisotropy parameter Δ/J is assumed to be a tunable term. It is shown that for the zero value of the cyclic three-spin parameter ($K/J = 0$), a maximum of the amount of quantum correlations including negativity is achieved, and the three-qubit system is maximally correlated in contrast the particular case with nonzero K/J. This is explained by the fact that when $K/J = 0$ for both cases ($\Delta/J = 0.5$ and $\Delta/J = 1$), the system is then at zero temperature in the ground state $|\psi_7\rangle$, which means that the ground state $|\psi_7\rangle$ contains more entanglement. For stronger values of K/J (for instance $K/J = 5.5$ and $\Delta/J = 0.5$), the negativity and LQU are null at sufficiently low temperatures ($\mathcal{N} = \mathcal{U} = 0$). This is due to the fact that the ground state is a separable (unentangled) state $|\psi_4\rangle$.

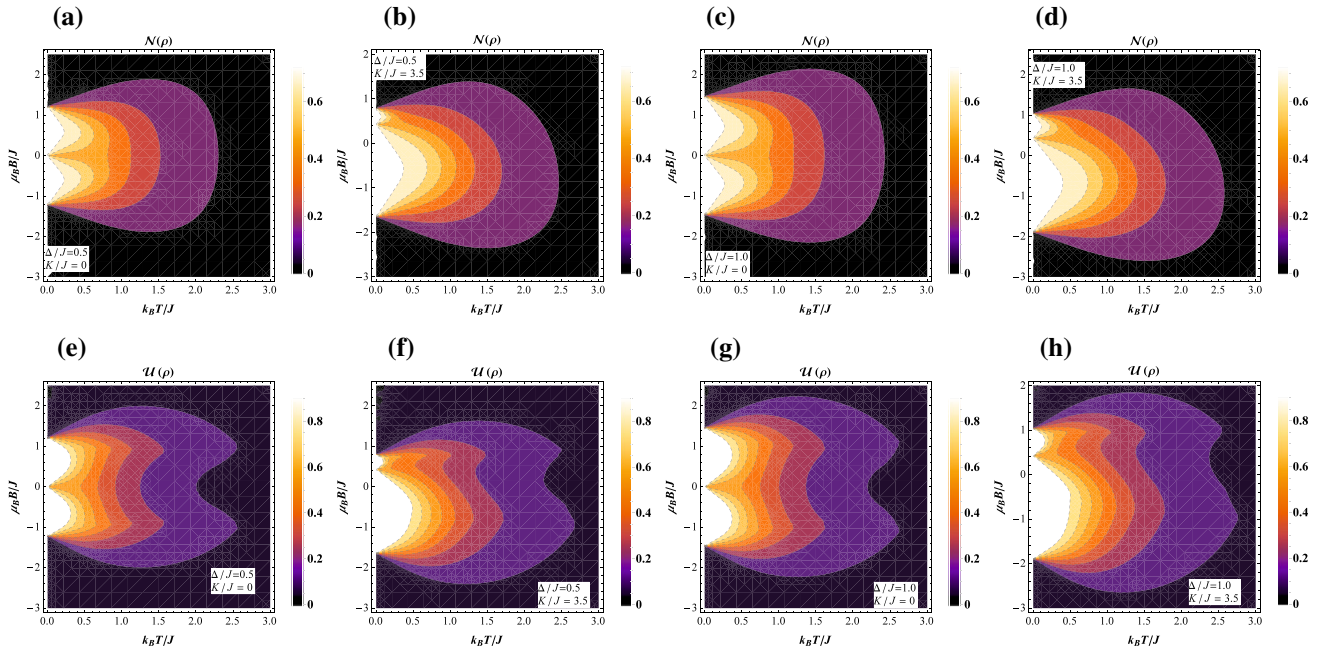


Fig. 2 Upper panels: Density plots of the negativity $\mathcal{N}(\rho(T))$ in the $k_BT/J - \mu_BB/J$ plane for different values of cyclic three-spin interaction K/J specified in the panels and two different values of the exchange anisotropy, $\Delta/J = 0.5$ and $\Delta/J = 1$ with the Landé-g factor fixed to $g = 2.045$. Lower panels: Density plots of the local quantum uncertainty $\mathcal{U}(\rho(T))$ in the $k_BT/J - \mu_BB/J$ plane for different values of cyclic three-spin interaction K/J specified in the panels and two different values of the exchange anisotropy, $\Delta/J = 0.5$ and $\Delta/J = 1$ with the Landé-g factor fixed to $g = 2.045$

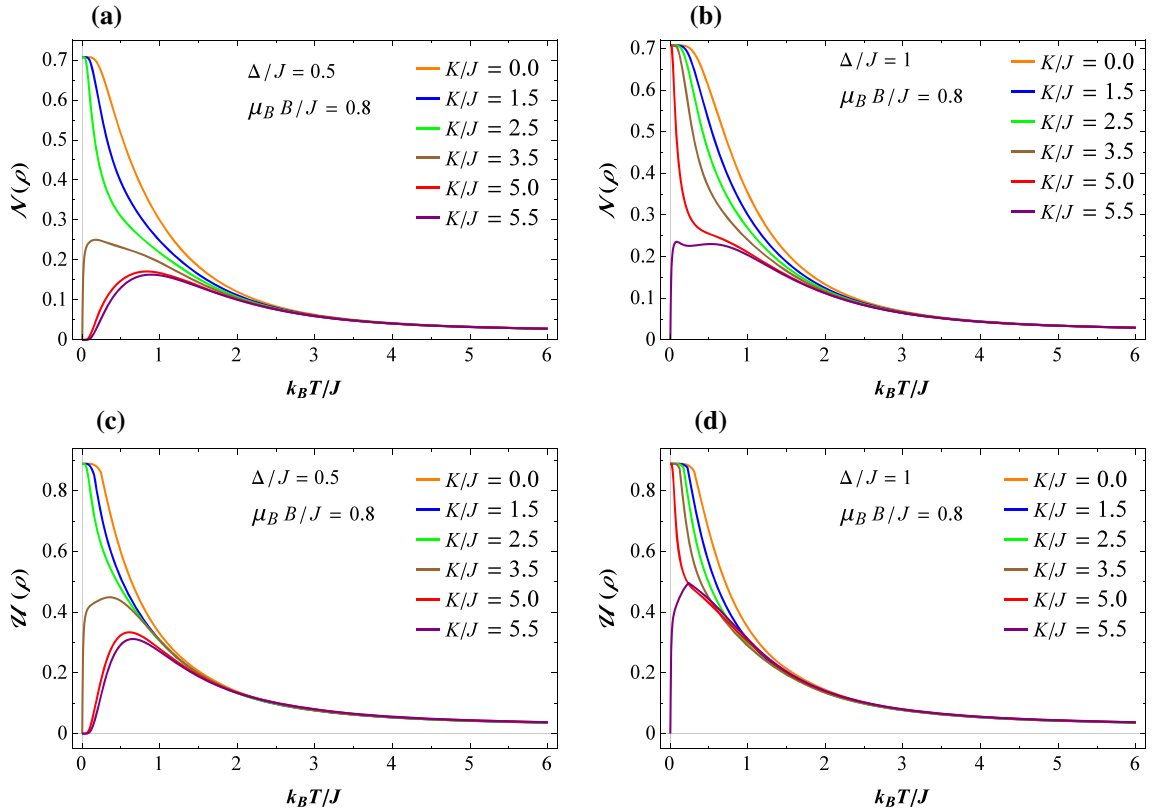


Fig. 3 Upper panels: The thermal dependence of the negativity $\mathcal{N}(\rho(T))$ for several values of the cyclic three-spin interaction K/J with two different values of the exchange anisotropy $\Delta/J = 0.5$ and $\Delta/J = 1$ at $\mu_BB/J = 0.8$ when $g = 2.045$. Lower panels: The thermal dependence of the local quantum uncertainty $\mathcal{U}(\rho(T))$ for several values of the cyclic three-spin interaction K/J with two different values of the exchange anisotropy $\Delta/J = 0.5$ and $\Delta/J = 1$ at $\mu_BB/J = 0.8$ when $g = 2.045$

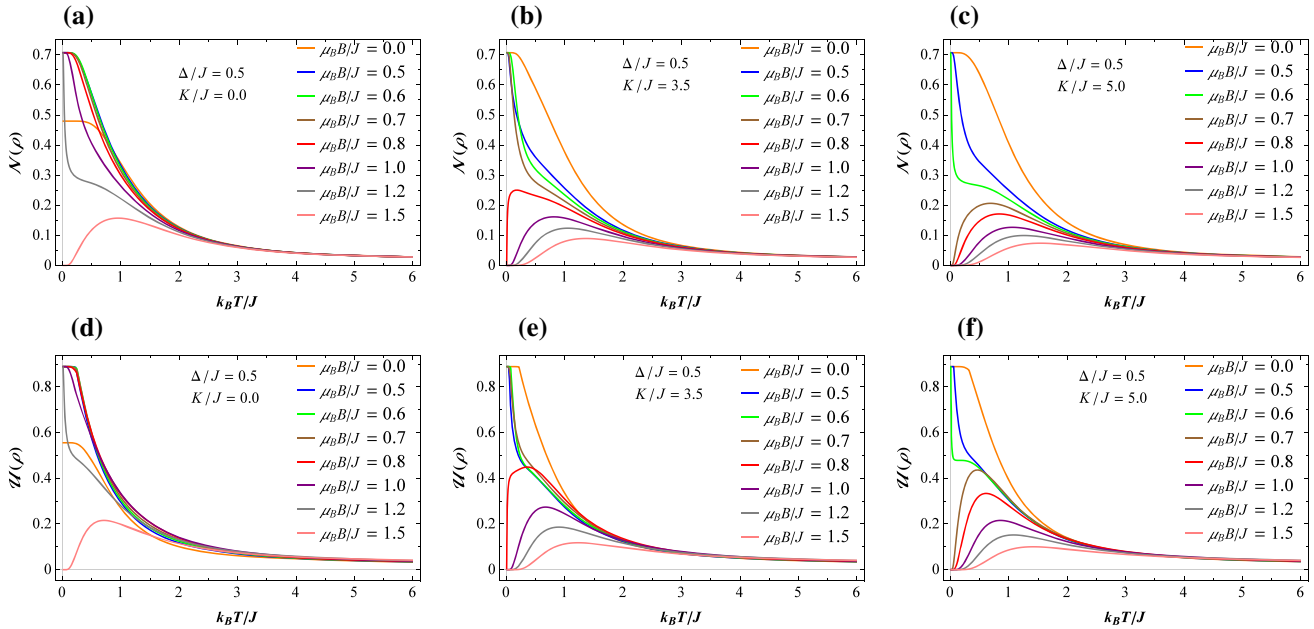


Fig. 4 Upper panels: The thermal dependence of the negativity $\mathcal{N}(\rho(T))$ for several values of the magnetic field $\mu_B B/J$ specified in the panels with different values of the exchange anisotropy ($\Delta/J = 0.5$ and $\Delta/J = 1$) and the cyclic three-spin interaction K/J when the gyromagnetic g-factor $g = 2.045$ is adopted according to Ref. [33]. Lower panels: The thermal dependence of the local quantum uncertainty $\mathcal{U}(\rho(T))$ for several values of the magnetic field $\mu_B B/J$ specified in the panels with different values of the exchange anisotropy ($\Delta/J = 0.5$ and $\Delta/J = 1$) and the cyclic three-spin interaction K/J when the gyromagnetic g-factor $g = 2.045$ is adopted according to Ref. [33]

However, with the temperature increasing, we have a sudden birth of quantum correlations until the maximum value of quantum correlations is achieved by converting the entangled states into the untangled state $|\psi_4\rangle$. Then, they decrease monotonically as soon as the temperature increases. After this decrease, the negativity and LQU exhibit a freezing phenomenon, in which the amount of negativity and local quantum uncertainty are constant during the evolution process. Therefore, the behavior of the negativity and LQU are more robust in the absence of the cyclic three-spin parameter. It should be noticed that the cyclic three-spin interaction reduces the quantum correlations in the tripartite magnetic Cu_3^{II} complex system. It is interesting to notice that the negativity and LQU have the same behavior at low temperatures, but when the temperature increases, the local quantum uncertainty happens to predominate over the thermal entanglement. Besides, when the anisotropy parameter switches to $\Delta/J = 1$, the amount of quantum correlations is enhanced quantitatively by comparing it with the case of easy-plane ($\Delta/J = 0.5$). However, the anisotropy parameter Δ/J enhances the tripartite quantum correlations in the system and thus avoids the sudden birth of quantum correlations at a zero-temperature limit.

The negativity (upper panels) and local quantum uncertainty (lower panels) of the tripartite spin$-1/2$ XXZ Heisenberg trimer with the cyclic three-spin interaction and the gyromagnetic g-factor $g = 2.045$ at a fixed value of the exchange anisotropy $\Delta/J = 0.5$ are plotted in Fig. 4 as a function of temperature for a few selected values of the external magnetic field $\mu_B B/J$. It can be seen from Fig. 4 that both quantum correlation measures show qualitatively similar behavior, except that the LQU is larger than the negativity (LQU captures more information between the subsystems). In the absence of the cyclic three-spin interaction $K/J = 0$ (Fig. 4a and d) at zero magnetic field ($\mu_B B/J = 0$), the model is partially entangled in a zero-temperature limit $k_B T/J \to 0$. The reason is that when $\mu_B B/J = 0$, the system's ground state at zero temperature is a superposition of the entangled states $|\psi_7\rangle$ and $|\psi_8\rangle$ ($\rho(T = 0) = \frac{1}{2}(|\psi_7\rangle\langle\psi_7| + |\psi_8\rangle\langle\psi_8|)$). In fact, the entanglement in a superposition of entangled state is usually less than, or at most equal to the average of the quantum entanglement of the superposed states [34]. For intermediate values of the magnetic field ($0 < \mu_B B/J < 1$), the system captures more quantum correlations in the model (2). This is due to the fact that the system will be in a ground state $|\psi_7\rangle$ ($\rho(T = 0) = |\psi_7\rangle\langle\psi_7|$), which means that the ground state $|\psi_7\rangle$ contains more entanglement. For $\mu_B B/J = 1.2$, the ground state is a classical mixture of separable state $|\psi_4\rangle$ and entangled state $|\psi_7\rangle$ with equal probabilities ($\rho(T = 0) = \frac{1}{2}(|\psi_4\rangle\langle\psi_4| + |\psi_7\rangle\langle\psi_7|)$). For higher values of the magnetic field $\mu_B B/J \geq 1.5$, no thermal quantum correlations occur at the temperature $k_B T/J$ which is very near to zero, even for LQU. This is due to the separable ground state $|\psi_4\rangle$. One can observe that, a sudden birth of the thermal entanglement occurs upon increasing of temperature and the quantifiers reach the maximum amount of quantum correlations achieved (see Fig. 4). We note that with a further increase in the temperature, the amount of quantum correlations captured by the negativity and LQU between the subsystems in the tripartite state decrease asymptotically until the system reaches a steady state (Fig. 4).This is due to the fact that thermal fluctuations only affect quantum correlations at temperatures above the characteristic temperature set by the energy gap, which is nonzero for a finite-sized system [31]. It is obvious from Fig. 4 that the steady-state values are $\mathcal{N}(\rho(\infty)) = 0.022$ and $\mathcal{U}(\rho(\infty)) = 0.024$. We mention that the steady-state value does

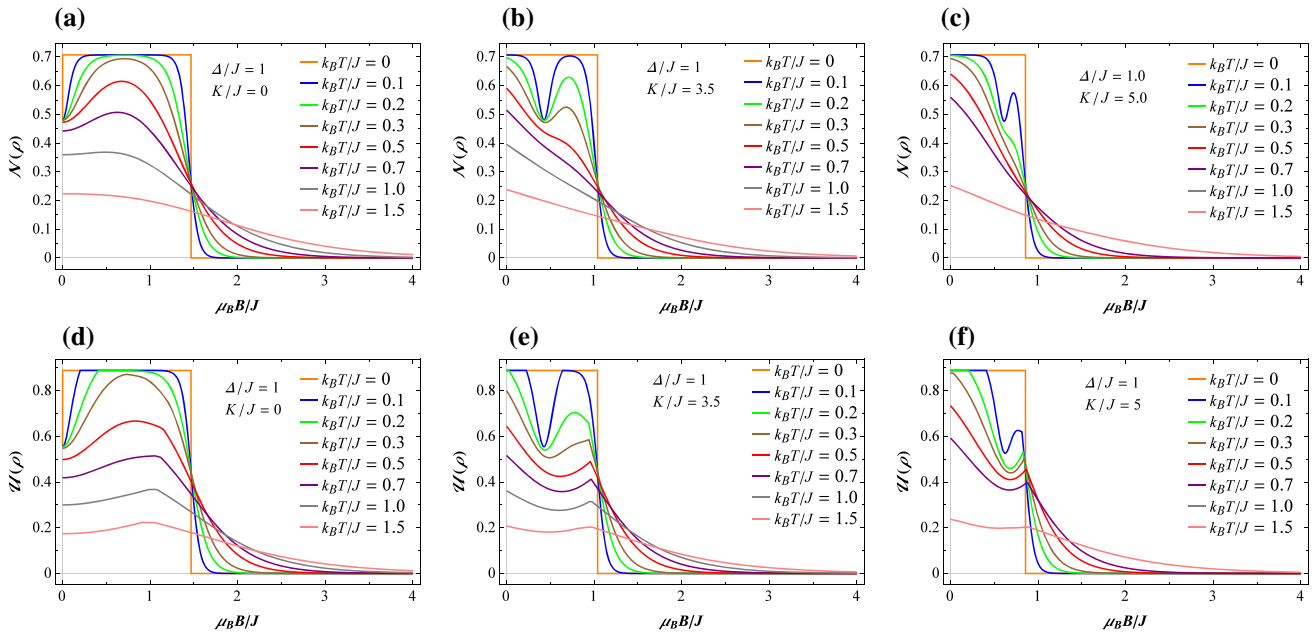


Fig. 5 Upper panels: The behavior of negativity $\mathcal{N}(\rho(T))$ as a function of the external magnetic field $\mu_B B/J$ for different values of temperature and the cyclic three-spin interaction K/J with two selected values of the exchange anisotropy ($\Delta/J = 0.5$ and $\Delta/J = 1$) when $g = 2.045$. Lower panels: The behavior of the local quantum uncertainty $\mathcal{U}(\rho(T))$ as a function of the external magnetic field $\mu_B B/J$ for different values of temperature and the cyclic three-spin interaction K/J with two selected values of the exchange anisotropy ($\Delta/J = 0.5$ and $\Delta/J = 1$) when $g = 2.045$

not depend on parameters that characterize the system. In the presence of the cyclic three-spin interaction $K/J \neq 0$, the quantum correlations show similar behavior as in the absence of $K/J = 0$, the difference is that the system at zero temperature and magnetic field will be in the entangled ground state $|\psi_8\rangle$ (Werner state). This explains the fact that the system is more correlated than in the absence of $K/J = 0$ without the influence of the external magnetic field ($\mu_B B/J = 0$). As the cyclic three-spin interaction increases, the ground state reduces to the separable ground state $|\psi_4\rangle$ even for low values of the magnetic field. This is mainly due to the fact that an increase in the cyclic three-spin interaction produces separable states, which decreases, therefore, the thermal quantum correlations amounts (Fig. 4). As a result, the intervention of the magnetic field and the cyclic three-spin interaction result in a decrease in the entanglement as well as the quantum correlations between the spins of the system. The decrease in LQU and negativity with the increase in the magnetic field implies that the system loses the quantum signature and becomes more classical. On the other hand, the phenomenon of entanglement sudden death does not occur in the tripartite model in comparison with the bipartite system [34, 36]. This indicates that increasing size of the system may be more optimal and robust in comparison with bipartite systems for modern quantum technologies. This confirms the similar conclusions results reported in Ref. [44].

The magnetic field dependence of the tripartite quantum correlations captured by the negativity and LQU are shown in Fig. 5 at a few selected values of the temperature and different values of the cyclic three-spin interaction with fixed values of $g = 2.045$ and $\Delta/J = 1$. In the absence of the cyclic three-spin interaction ($K/J = 0$), both quantifiers are remarkably strengthened when the magnetic field is increased at low temperatures, as indicated by a considerable round maximum of the negativity and LQU observable for sufficiently low temperatures (Fig. 5a,d). The unconventional enhancement of the tripartite quantum correlations due to the magnetic field at sufficiently low but nonzero magnetic fields can be again related to Zeeman's splitting of energy levels, which results in an unexpected abrupt rise of quantum correlations in the spin-1/2 Heisenberg trimer model. This behavior is in agreement with results reported in ref.[45] and it is in contrast with the naive expectation that the magnetic field suppresses the non-classical correlations [34]. However, for higher temperatures, the negativity and LQU show the monotonous variation with respect to the magnetic field $\mu_B B/J$. Upon further increase in the magnetic field $\mu_B B/J$, both quantifiers decrease gradually to zero. In the presence of the cyclic three-spin interaction, a sudden drop of the tripartite quantum correlations can be observed below the saturation field due to the thermal activation of the excited states into the ground state (Fig. 5 b,c,e,f). The relevant field-driven quantum phase transition is manifested at low enough temperature as a sharp narrow minimum of the negativity and LQU that become rounder and wider upon increasing temperature. On the other hand, LQU and negativity disappear in a finite period of time which indicates the phenomenon of entanglement sudden death (ESD). Tuning the temperature and the external magnetic field might increase the value of the critical instant and thus avoiding the disappearance of the quantum correlation measures and consequently the intricacy in the tripartite system (see Fig. 5). This given finding confirms the results obtained in Fig. 4. The temperature effects reduce the quantum correlation in the three-qubit system. Besides, the sudden change of LQU is because of the optimal procedure for choosing the measurement operators [46]. This is in fact the well-known sudden change behavior for the discord-like procedure

in their respective definitions [47, 48]. In fact, from Fig. (5) one can see a sudden change of quantum correlations from separable to bound and free entangled states.

5 Applications in quantum metrology and quantum information theories

5.1 Quantum Fisher information of tripartite quantum systems

The concept of quantum Fisher information known in quantum metrology and quantum estimation theory becomes also a major notion in the field of quantum information [49, 50]. It appears as the quantum version of classical Fisher information. Indeed, the main subject of quantum Fisher information is to estimate different relevant parameters included in a proposed quantum state via extending a view of the parameter estimation settings. Moreover, in the point of view of quantum estimation theory, it has been shown that robust estimation degrees are obtained for large values of Fisher information and vice versa. For the sake of definition, the amount of QFI for a bipartite state, namely ρ_ζ, depending on a parameter ζ is defined as [51]

$$\mathcal{F}_\zeta^\rho = \mathrm{Tr}\,[\rho_\zeta \mathcal{L}_\zeta^2] = \mathrm{Tr}\left[\frac{\partial \rho_\zeta}{\partial \zeta}\mathcal{L}_\zeta\right], \tag{35}$$

where ζ is the parameter to be estimated, while $\mathcal{L}_\zeta$ denotes the Symmetric Logarithmic Derivative (SLD) operator satisfying the condition: $\partial\rho_\zeta/\partial\zeta = (\mathcal{L}_\zeta\rho_\zeta + \rho_\zeta\mathcal{L}_\zeta)/2$. On the other hand, if one makes the spectral decomposition of the bipartite state, then the QFI is defined as given below [52]

$$\mathcal{F}_\zeta^\rho = \sum_{\upsilon=1}^{4}\frac{(\partial_\zeta\kappa_\upsilon)^2}{\kappa_\upsilon} + 4\sum_{\upsilon=1}^{4}\kappa_\upsilon[\langle\partial_\zeta\kappa_\upsilon|\partial_\zeta\kappa_\upsilon\rangle - |\langle\kappa_\upsilon|\partial_\zeta\kappa_\upsilon\rangle|^2] - \sum_{\upsilon\neq\kappa}\frac{8\kappa_\upsilon\kappa\mu}{\kappa_\mu+\kappa_\upsilon}|\langle\kappa_\upsilon|\partial_\zeta\kappa_\mu\rangle|^2, \tag{36}$$

where $\partial_\zeta = \partial/\partial\zeta$. Moreover, κ_υ and $|\kappa_\upsilon\rangle$ such that $\upsilon = 1, ..., 4$ denote the eigenvalues and eigenvectors of ρ_ζ respectively. Interestingly, it has been recently shown that one can generalize this formula for quantum states of N dimension. Indeed, it is defined as the following form [53]

$$\mathcal{F}_\zeta^\rho = \sum_{\upsilon=1}^{N}\frac{(\partial_\zeta\kappa_\upsilon)^2}{\kappa_\upsilon} + 4\sum_{\upsilon=1}^{N}\kappa_\upsilon[\langle\partial_\zeta\kappa_\upsilon|\partial_\zeta\kappa_\upsilon\rangle - |\langle\kappa_\upsilon|\partial_\zeta\kappa_\upsilon\rangle|^2] - \sum_{\upsilon\neq\kappa}\frac{8\kappa_\upsilon\kappa\mu}{\kappa_\mu+\kappa_\upsilon}|\langle\kappa_\upsilon|\partial_\zeta\kappa_\mu\rangle|^2, \tag{37}$$

From the mathematical point of view, the amount of QFI either for 4 -dimension or for N-dimension is an additive function [54]. Moreover, under the action of a unitary operation, the QFI is still invariant [55]. On the other hand, the main idea behind studying QFI is to illustrate an elevated estimation precision of the relevant parameter of a quantum state. Based on this, we shall estimate the temperature parameters as well as the external magnetic field, namely T and B, respectively, encoded in the tripartite magnetic Cu_3^{II} complex system. Roughly speaking, it has been shown that QFI becomes an important resource in different aspects of quantum information theory, in particular, quantum correlation [56]. In this context, we show how much the tripartite correlated state is sensitive to changes in some parameters encoded in it.

In the light of the previous discussion, we plot in Fig. 6 the amount of QFI via estimating the temperature parameter encoded in the tripartite system. It is clear that the state is sensitive with respect to changes in the temperature T, where in general, robust estimation degree of this parameter is obtained for a small interval of k_BT/J as exactly obtained for the logarithmic negativity and local quantum uncertainty. Again as obtained for entanglement and quantum correlation measures, the large values of the temperature allow decreasing the amount of QFI gradually until it completely vanishes for a large interval of T. On the other hand, it is obvious that when the interaction parameters acquire the values $K/J = 0$ and $\mu_B B/J = -0.5$, then, the amount of QFI takes a large amplitude for small numbers of the anisotropy parameter Δ/J. Similarly, as this parameter increases, we lost the possibility to estimate the temperature parameter (see Fig.6 a, b and d), except the zero-field case when $\mu_B B/J$ one obtains a different behavior where small numbers of the three-spin coupling K/J allow small bounds of QFI as illustrated in Fig. 6c.

The quantification and manipulation of QFI via estimating the external magnetic field parameter, namely B, are displayed in Fig. 7 for different initial settings of $K/J, k_BT/J$ and Δ/J. Indeed, Fig. 7a displays the amount of QFI when $K/J = 0$ and $k_BT/J = 0.5$. We observe a close similarity of QFI behavior for all the considered values of $\mu_B B/J$; including positive and negative values. Moreover, it is clear that we can estimate the parameter $\mu_B B/J$ with large bounds in particular for the interval $\mu_B B/J \in [-3, 3]$, while when both parameters K/J and Δ/J vanish then we obtain the maximum possible of the $\mu_B B/J's$ estimation. On the other hand, once we increase the cyclic three-spin interaction parameter, namely K/J, a non-symmetric behavior of QFI clearly appears in Fig. 7b and c. In this situation, the robust estimation degree, i.e., large bounds of QFI becomes significant around the interval $\mu_B B/J \in [0, 1]$. Interestingly, as we have already explained in the behavior of the negativity measure and local quantum uncertainty quantifier, these quantities take large numbers around the same interval, namely $\mu_B B/J \in [0, 1]$, which makes our results substantial since the QFI as a measure of information via estimating the relevant parameters known in quantum estimation theory and the quantum correlation measures known in quantum information theory follows qualitatively the same behavior. One can conclude from Figs. 6 and 7 that one can estimate successfully the tripartite magnetic Cu_3^{II} complex system with robust estimation

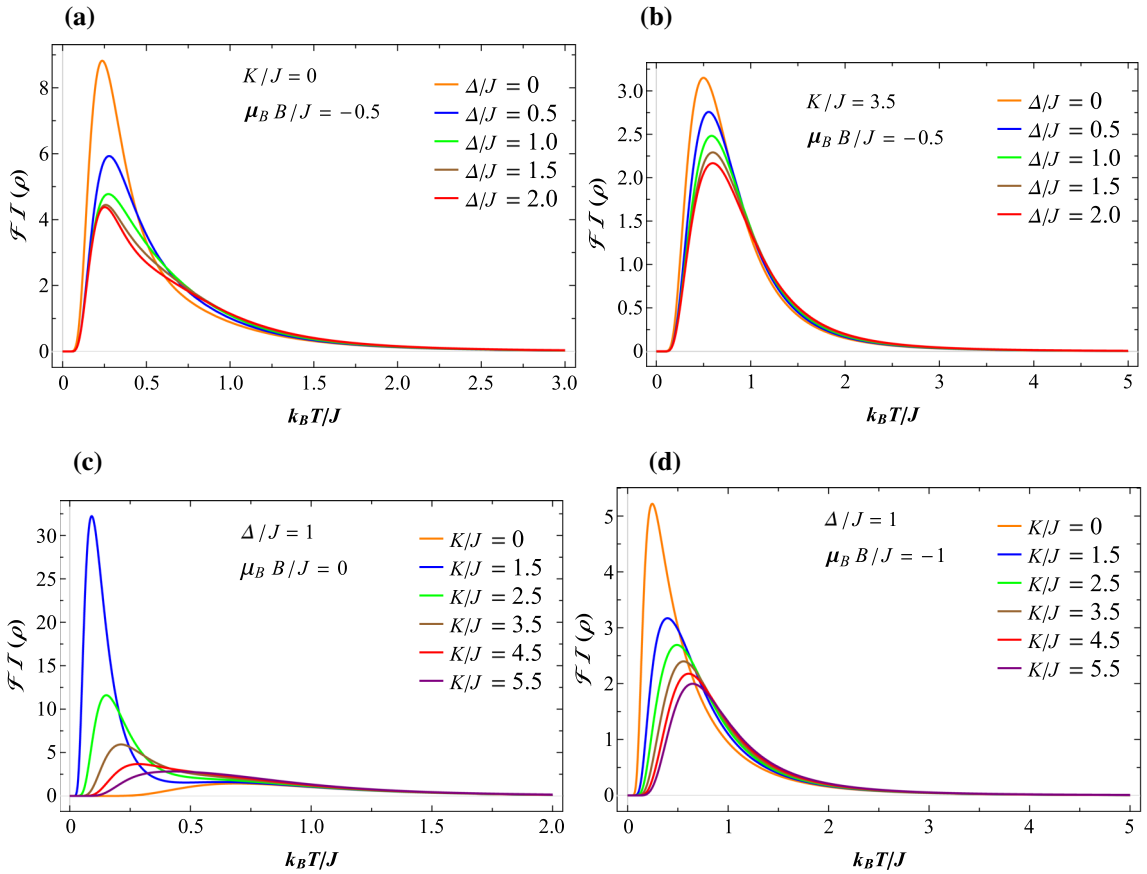


Fig. 6 The amount of QFI with respect to changes the temperature k_BT/J for a few values of Δ/J and K/J and the magnetic fields:(**a**, **b**) $\mu_B B/J = -0.5$, **c** $\mu_B B/J = 0$ and **d** $\mu_B B/J = -1$

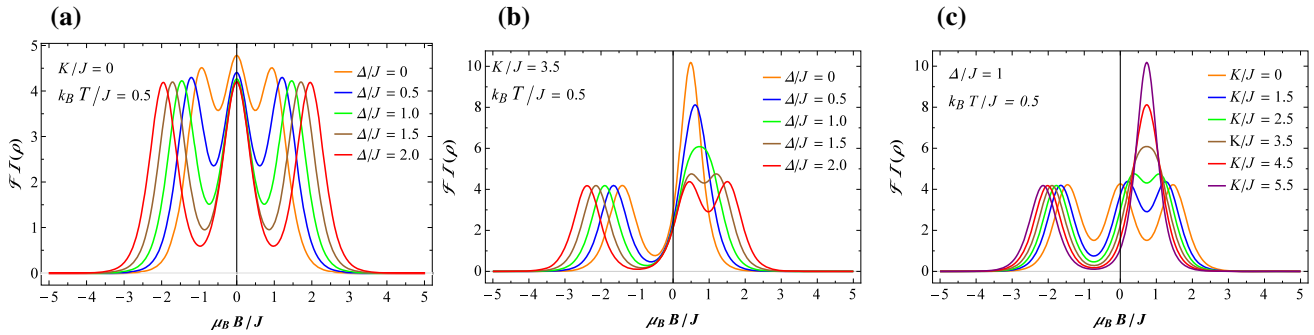


Fig. 7 The amount of QFI with respect to changes of the magnetic field $\mu_B B/J$ for a few different values of Δ/J and K/J and temperatures: **a** $k_BT/J = 0.5$ and **b**, **c** $k_BT/J = 1.5$

for some specific intervals of k_BT/J and $\mu_B B/J$. However, our results show that the amount QFI follows the same behavior as the negativity measure and local quantum uncertainty, which allow us to conclude that QFI can detect entanglement for tripartite quantum systems.

5.2 Quantum teleportation via three-qubit system

Before investigating the effect of changing the interaction parameters encoded in the suggested three-qubit system and their impact on transmitting the information between individual partitions, let us give an overview of quantum teleportation via the three-qubit system. First, let focus our attention to the standard teleportation process [57, 58] using the proposed tripartite state at thermal equilibrium, namely $\rho(T)$ in Eq. (11) as a quantum resource. The main goal of the protocol of quantum teleportation via a three-qubit channel is to transmit the information encoded in an unknown one-qubit state from a sender called Alice and two receivers labeled for example by Bob and Cindy. To achieve this purpose, Alice should hold two qubits. The first qubit is the state to be

teleported, namely $|\psi\rangle_u$, while the other qubit represents one of the three proposed qubits. Meanwhile, Bob and Cindy have the other two qubits. Bearing this in mind, the overall density operator could be given in the following compact form:

$$\rho_{uABC} = \rho_u \rho_{ABC}, \tag{38}$$

whereby the unknown density matrix is defined as $\rho_u = |\psi\rangle_u\langle\psi|_u$. In what follows, we will assume that the unknown density operator is given by the following matrix form:

$$\rho_u = \frac{1-2r_1}{2}|0\rangle\langle 0| + \frac{r_2}{2}(|1\rangle\langle 0| + |0\rangle\langle 1|) + \frac{1+2r_1}{2}|1\rangle\langle 1|, \tag{39}$$

where $0 \leq r_1 \leq 1$ and $r_2 = \sqrt{1-r_1^2} \geq 0$. So as to transmit this state to Cindy and Bob, Alice should perform a mutual measurement on her two own qubits. This measurement can be represented by the operators $M_{uA}^i \otimes I_{BC}$, where I_{BC} denotes the identity operator acting on the joint system BC.

$$\begin{aligned} M_{uA}^1 &= |B_1^+\rangle_{uA}\langle B_1^+|, \quad M_{uA}^2 = |B_1^-\rangle_{uA}\langle B_1^-|, \\ M_{uA}^3 &= |B_2^+\rangle_{uA}\langle B_2^+|, \quad M_{uA}^4 = |B_2^-\rangle_{uA}\langle B_2^-|, \end{aligned} \tag{40}$$

where $|B_{1(2)}^{\pm}\rangle_{uA}$ are the well-known Bell states defined as follows:

$$\begin{aligned} |B_1^{\pm}\rangle_{uA} &= \frac{1}{\sqrt{2}}(|00\rangle_{uA} \pm |11\rangle_{uA}), \\ |B_2^{\pm}\rangle_{uA} &= \frac{1}{\sqrt{2}}(|01\rangle_{uA} \pm |10\rangle_{uA}). \end{aligned} \tag{41}$$

At this stage, Alice gets her outcome measurement i and then connects with her partners, namely Cindy and Bob using a classical channel. Therefore, at the end of this process, the teleported state is given as the following form [59, 60]

$$\rho_{out}^i = \frac{1}{p_i}\,\mathrm{Tr}_{uA}[(M_{uA}^i \otimes I_{BC})\rho_{uABC}], \tag{42}$$

where the probability to get the measurement i turns out to be

$$p_i = \mathrm{Tr}_{uABC}[(M_{uA}^i \otimes I_{BC})\rho_{uABC}]. \tag{43}$$

Now, in order to investigate the quality of Cindy and Bob's state, namely ρ_{out}^i at the end of the process of quantum teleportation compared to the input state ρ_u, one can evaluate the fidelity averaged over all possible outcomes i and also over all unknown states ρ_u on the Bloch sphere. It can be readily proved that the average fidelity is given by

$$\mathcal{F}_A = \frac{1}{4\pi}\int_0^{2\pi}\int_0^{\pi} \sin\theta d\theta d\phi \sum_{i=1}^{4} p_i R^i, \tag{44}$$

where $R^i = \mathrm{Tr}\,(\rho_{out}^i \rho_u)$. Based on this definition and after some straightforward calculations, the average fidelity in our model is calculated as follows:

$$\begin{aligned} \mathcal{F}_A = \frac{1}{2}[&\rho_{11} - 4r_1^2\rho_{11} + \rho_{22} + \rho_{33} + \rho_{44} + \rho_{55} + \rho_{66} + \rho_{77} \\ &+ 4r_1^2(-\rho_{22} + \rho_{33} + \rho_{55} + \rho_{66} - \rho_{77} - \rho_{88}) + \rho_{88}], \end{aligned} \tag{45}$$

where ρ_{ii} are the elements of the three-qubit matrix given in Eq. (11).

As we have already mentioned, the average fidelity is a very successful tool exceedingly used for quantifying the quality of the teleportation process even via the three-qubit system. The average fidelity of the quantum teleportation protocol can be obtained by averaging the input and output states defined in Eqs.(39) and (42), respectively, over all possible initial states. Bearing this in mind, we first plot in Fig. 8 the teleportation average fidelities against temperature k_BT/J by considering various initial settings of the external magnetic field $\mu_B B/J$ and the interaction parameters K/J and Δ/J. It is clear that the average fidelity is sensitive to changes in all aforementioned parameters, where in general, the average fidelity takes large bounds for small intervals of k_BT/J and for small values of $\mu_B B/J$ in particular when $\mu_B B/J = 0$. Indeed, for these specific conditions, the average fidelity exceeds the classical limit of fidelity, namely $\mathcal{F}_A = 2/3$, which means that we have succeeded to implement successfully the scheme of a quantum teleportation with robust fidelity by means of the tripartite thermal state defined through Eq. (11) as a quantum channel. In contrast, the teleportation average fidelity is substantially reduced upon increasing temperature.

So far, we have separately considered the evolution of fidelity against the temperature parameter k_BT/J when various considerations of the magnetic field $\mu_B B/J$ are taken into account. Let us now plot the average fidelity versus the temperature in Fig. 10 by considering different values of the cyclic three-spin interaction parameter K/J. It is clear that when the parameters K and T vanish, then, the amount of average fidelity reaches the maximum bound and it is $\mathcal{F}_A > 0.9$, which means that the output

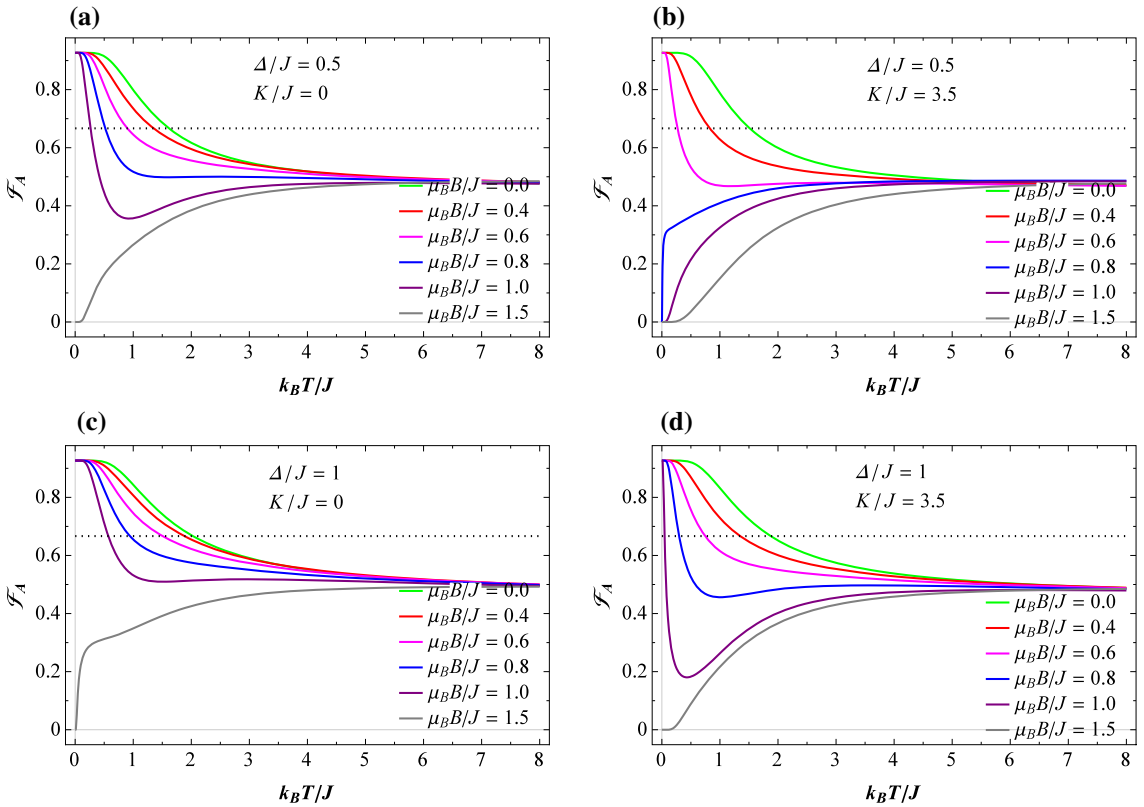


Fig. 8 Upper panels: The average fidelity $\mathcal{F}_A$ as a function of temperature for several fixed values of the external magnetic field $\mu_B B/J$ and parameter set **a** $K/J = 0$, **b** $K/J = 3.5$ assuming $\Delta/J = 0.5$ and $g = 2.045$. Lower panels: The average fidelity $\mathcal{F}_A$ as a function of temperature for several fixed values of the external magnetic field $\mu_B B/J$ and parameter set **c** $K/J = 0$, **d** $K/J = 3.5$ assuming $\Delta/J = 1$ and $g = 2.045$. Dotted lines indicate the classical limit of fidelity 2/3

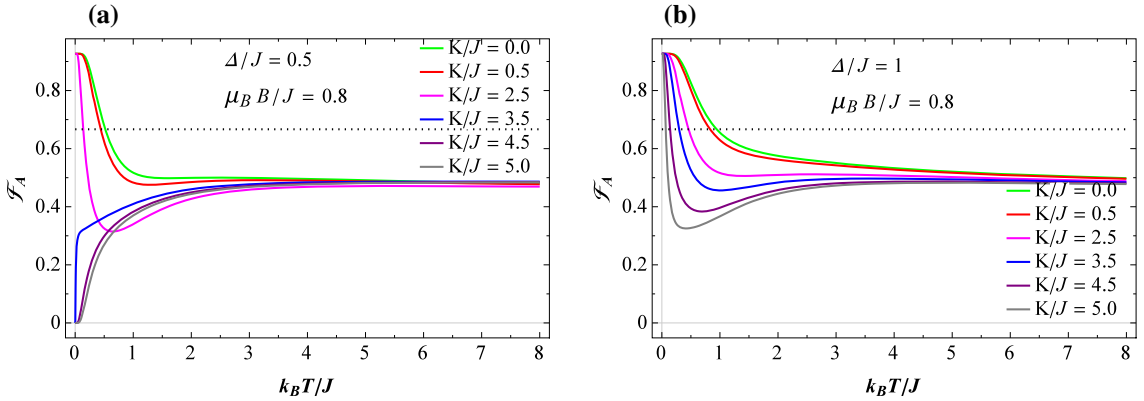


Fig. 9 The average fidelity $\mathcal{F}_A$ as a function of temperature for several values of the cyclic three-spin interaction K/J and parameter set **a** $\Delta/J = 0.5$, **b** $\Delta/J = 1$ assuming $\mu_B B/J = 0.8$ and $g = 2.045$. Dotted lines indicate the classical limit of fidelity 2/3

state is nearly equal to the input state. Moreover, as the temperature increases and when it is restricted to a relatively small values, namely $k_B T/J \in [0, 1.0]$, the average fidelity still exceeds the bound 2/3 for some particular values of the interaction constants K/J and Δ/J, which means that the input state ρ_u was transmitted with much more robust fidelity in comparison with any classical communication protocol. Again this property is lost at higher temperatures.

In Fig. 10, we plot the average fidelity between input and output states for the quantum teleportation, namely $\mathcal{F}_A$ as a function of temperature for several fixed values of the exchange anisotropy Δ/J for fixed numbers of K/J and $\mu_B B/J$. Again, the classical limit is indicated by the horizontal dotted line in the figure. Indeed, we observe again that our quantum channel becomes useful for the teleportation of the unknown state for small enough values of the temperature and exchange coupling parameters. Once these

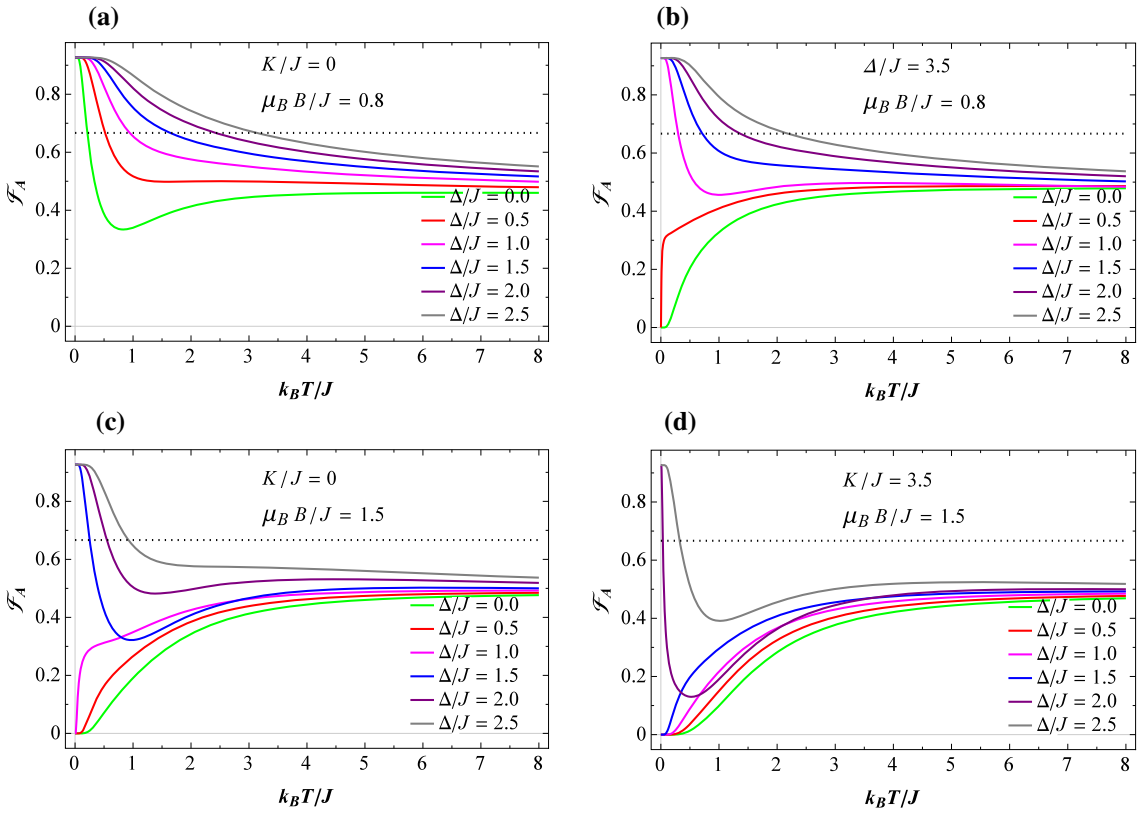


Fig. 10 Upper panels: The average fidelity $\mathcal{F}_A$ as a function of temperature for several fixed values of the exchange coupling coefficient Δ/J and parameter set **a** $K/J = 0$, **b** $K/J = 3.5$ assuming $\mu_B B/J = 0.8$ and $g = 2.045$. Lower panels: The average fidelity $\mathcal{F}_A$ as a function of temperature for several fixed values of the exchange coupling coefficient Δ/J and parameter set **a** $K/J = 0$, **b** $K/J = 3.5$ assuming $\mu_B B/J = 1.5$ and $g = 2.045$. Dotted lines indicate the classical limit of fidelity 2/3

parameters increase, then the fidelity measure substantially decreases. Remarkably, in the case of $K/J = 0$, the amount of fidelity does not vanish, which can be considered a good choice for the proposed tripartite quantum channel.

One can conclude from Figs. (8, 9, 10) that the average fidelity of quantum teleportation using the tripartite state given by Eq. (11) as a quantum channel gives some important results in particular when the temperature takes small enough value and when the other system's parameters K and B vanish. Indeed, it has been shown that the average fidelity is neatly related to the magnetic Cu_3^{II} system used as the quantum channel for the teleportation process.

6 Conclusion

In the present paper, we have examined at a thermal equilibrium the behavior of non-classical correlations by means of local quantum uncertainty along with the thermal entanglement measured by the negativity of the spin-1/2 Heisenberg trimer in the presence of the cyclic three-spin coupling interaction along the z -axis. In this regard, by controlling various parameters; including temperature, magnetic field, etc., the quantum correlations within pure and mixed states of the three-qubit quantum spin system are highlighted. By making a comparative study between the negativity and LQU, we have obtained some interesting outcomes. In particular, it has been shown that both negativity and LQU basically depend on the intrinsic and extrinsic parameters including the exchange anisotropy, cyclic three-spin coupling, magnetic field, and temperature, respectively. On the other hand, the influence of the cyclic three-spin interaction within the quantum correlations has been extensively discussed. Interestingly enough, it has been shown that the robust coupling parameter K/J reduces the amount of non-classical correlations. In contrast, the exchange anisotropy parameter can protect and eventually enhance the quantum correlations in the tripartite magnetic Cu_3^{II} complex system. Hence, we have concluded that the negativity and LQU are sensitive with respect to changes in the cyclic three-spin interaction, which gives rise to breaking of the time-reversal symmetry.

The strongest quantum correlations at zero temperature and zero magnetic fields have been found for the particular case without the cyclic three-spin parameter in $\Delta/J = 1$. The rising magnetic field remarkably reinforces the tripartite quantum correlations due to the Zeeman splitting of energy levels. Hence, the results show that the LQU quantifiers reveal the non-classical correlations in the tripartite system even in absence of the entanglement. This implies that the vanishing of entanglement does not necessarily

mean absence of the quantum correlations. For various initial settings, several phenomena such that sudden death, sudden birth, oscillations, and frozen correlations appear distinctly. In the second part of this paper, we have applied this model to a quantum metrology in order to investigate the sensitivity of the proposed tripartite system with respect to changes in various intrinsic and extrinsic parameters. It is found that it is possible to estimate successfully the temperature and external magnetic field parameters encoded in the tripartite magnetic Cu_3^{II} complex system with robust estimation for some specific intervals. Roughly speaking, the relation between the estimation precisions and the quantum correlations has been pointed out. Moreover, a scheme of quantum teleportation process by using the tripartite state as a quantum channel is also suggested. In this process, we have shown that for sufficiently low temperatures and for a specific value of the magnetic field and cyclic three-spin interaction, in most cases, the corresponding average fidelity is larger than 2/3, which corroborates the success of the teleportation. Therefore, one can conclude that different parameters contained in the tripartite model are efficient to control parameters of quantum communications.

Acknowledgements J.S. acknowledges the financial support of Slovak Research and Development agency provided under the contract No. APVV-20-0150.

Data availability No data availability statement is available.

Declarations

Conflict of interest The authors declare that they have no conflict of interest.

Appendices

1. Appendix I

In this appendix, we provide the parameters needed to compute the local quantum uncertainty for the three-qubit state $\rho(T)$ (11). First, let us introduce the eigenvalues of the density matrix in Eq. (11) as

$$\lambda_1 = \frac{\exp\left(\frac{12Bg+4J+K}{4T}\right)}{\exp\left(\frac{J}{T}\right)\left(1+\exp\left(\frac{12Bg+K}{4T}\right)\right)+\exp\left(\frac{Bg+\Delta}{2T}\right)\left(2+\exp\left(\frac{3J}{2T}\right)\right)\left(\exp\left(\frac{Bg}{T}\right)+\exp\left(\frac{K}{4T}\right)\right)}, \tag{46}$$

$$\lambda_2 = \frac{\exp\left(\frac{J}{T}\right)}{\exp\left(\frac{J}{T}\right)\left(1+\exp\left(\frac{12Bg+K}{4T}\right)\right)+\exp\left(\frac{Bg+\Delta}{2T}\right)\left(2+\exp\left(\frac{3J}{2T}\right)\right)\left(\exp\left(\frac{Bg}{T}\right)+\exp\left(\frac{K}{4T}\right)\right)}, \tag{47}$$

$$\lambda_3 = \frac{\exp\left(\frac{2Bg+\Delta}{T}\right)}{2\left(\exp\left(\frac{J}{T}\right)\left(1+\exp\left(\frac{12Bg+K}{4T}\right)\right)+\exp\left(\frac{Bg+\Delta}{2T}\right)\left(2+\exp\left(\frac{3J}{2T}\right)\right)\left(\exp\left(\frac{Bg}{T}\right)+\exp\left(\frac{K}{4T}\right)\right)\right)}, \tag{48}$$

$$\lambda_4 = \frac{3\exp\left(\frac{Bg+\Delta}{T}\right)}{2\left(\exp\left(\frac{J}{T}\right)\left(1+\exp\left(\frac{12Bg+K}{4T}\right)\right)+\exp\left(\frac{Bg+\Delta}{2T}\right)\left(2+\exp\left(\frac{3J}{2T}\right)\right)\left(\exp\left(\frac{Bg}{T}\right)+\exp\left(\frac{K}{4T}\right)\right)\right)}, \tag{49}$$

$$\lambda_5 = \frac{\exp\left(\frac{2Bg+3J+\Delta}{T}\right)}{\exp\left(\frac{J}{T}\right)\left(1+\exp\left(\frac{12Bg+K}{4T}\right)\right)+\exp\left(\frac{Bg+\Delta}{2T}\right)\left(2+\exp\left(\frac{3J}{2T}\right)\right)\left(\exp\left(\frac{Bg}{T}\right)+\exp\left(\frac{K}{4T}\right)\right)}, \tag{50}$$

$$\lambda_6 = \frac{\exp\left(\frac{4Bg+K+4\Delta}{4T}\right)}{2\left(\exp\left(\frac{J}{T}\right)\left(1+\exp\left(\frac{12Bg+K}{4T}\right)\right)+\exp\left(\frac{Bg+\Delta}{2T}\right)\left(2+\exp\left(\frac{3J}{2T}\right)\right)\left(\exp\left(\frac{Bg}{T}\right)+\exp\left(\frac{K}{4T}\right)\right)\right)}, \tag{51}$$

$$\lambda_7 = \frac{3\exp\left(\frac{4Bg+K+4\Delta}{4T}\right)}{2\left(\exp\left(\frac{J}{T}\right)\left(1+\exp\left(\frac{12Bg+K}{4T}\right)\right)+\exp\left(\frac{Bg+\Delta}{2T}\right)\left(2+\exp\left(\frac{3J}{2T}\right)\right)\left(\exp\left(\frac{Bg}{T}\right)+\exp\left(\frac{K}{4T}\right)\right)\right)}, \tag{52}$$

$$\lambda_8 = \frac{\exp\left(\frac{4Bg+12J+K+4\Delta}{4T}\right)}{\exp\left(\frac{J}{T}\right)\left(1+\exp\left(\frac{12Bg+K}{4T}\right)\right)+\exp\left(\frac{Bg+\Delta}{2T}\right)\left(2+\exp\left(\frac{3J}{2T}\right)\right)\left(\exp\left(\frac{Bg}{T}\right)+\exp\left(\frac{K}{4T}\right)\right)}, \quad , \tag{53}$$

while the corresponding eigenvectors turn out to be

$$|\lambda_1\rangle = |111\rangle, |\lambda_2\rangle = |000\rangle, \tag{54}$$

$$|\lambda_3\rangle = \frac{1}{\sqrt{2}}(-|001\rangle + |010\rangle), |\lambda_4\rangle = \frac{1}{\sqrt{6}}(-|001\rangle - |010\rangle + 2|100\rangle), \tag{55}$$

$$|\lambda_5\rangle = \frac{1}{\sqrt{3}}(|001\rangle + |010\rangle + |100\rangle), |\lambda_6\rangle = \frac{1}{\sqrt{2}}(-|011\rangle + |101\rangle), \tag{56}$$

$$|\lambda_7\rangle = \frac{1}{\sqrt{6}}(-|011\rangle - |101\rangle + 2|110\rangle), |\lambda_8\rangle = \frac{1}{\sqrt{3}}(|011\rangle + |101\rangle + 2|110\rangle). \tag{57}$$

In the computational basis, the square root of the density matrix $\rho(T)$ (11) can be written as follows

$$\sqrt{\rho(T)} = \begin{pmatrix} \sqrt{\lambda_2} & 0 & 0 & 0 & 0 & 0 & 0 & 0 \\ 0 & \frac{1}{6}(3\sqrt{\lambda_3}+\sqrt{\lambda_4}+2\sqrt{\lambda_5}) & \frac{1}{6}(-3\sqrt{\lambda_3}+\sqrt{\lambda_4}+2\sqrt{\lambda_5}) & 0 & \frac{1}{3}(-\sqrt{\lambda_4}+\sqrt{\lambda_5}) & 0 & 0 & 0 \\ 0 & \frac{1}{6}(-3\sqrt{\lambda_3}+\sqrt{\lambda_4}+2\sqrt{\lambda_5}) & \frac{1}{6}(3\sqrt{\lambda_3}+\sqrt{\lambda_4}+2\sqrt{\lambda_5}) & 0 & \frac{1}{3}(-\sqrt{\lambda_4}+\sqrt{\lambda_5}) & 0 & 0 & 0 \\ 0 & 0 & 0 & \frac{1}{6}(3\sqrt{\lambda_6}+\sqrt{\lambda_7}+2\sqrt{\lambda_8}) & 0 & \frac{1}{6}(-3\sqrt{\lambda_6}+\sqrt{\lambda_7}+2\sqrt{\lambda_8}) & \frac{1}{3}(-\sqrt{\lambda_7}+\sqrt{\lambda_8}) & 0 \\ 0 & \frac{1}{3}(-\sqrt{\lambda_4}+\sqrt{\lambda_5}) & \frac{1}{3}(-\sqrt{\lambda_4}+\sqrt{\lambda_5}) & 0 & \frac{1}{3}(2\sqrt{\lambda_4}+\sqrt{\lambda_5}) & 0 & 0 & 0 \\ 0 & 0 & 0 & \frac{1}{6}(-3\sqrt{\lambda_6}+\sqrt{\lambda_7}+2\sqrt{\lambda_8}) & 0 & \frac{1}{6}(3\sqrt{\lambda_6}+\sqrt{\lambda_7}+2\sqrt{\lambda_8}) & \frac{1}{3}(-\sqrt{\lambda_7}+\sqrt{\lambda_8}) & 0 \\ 0 & 0 & 0 & \frac{1}{3}(-\sqrt{\lambda_7}+\sqrt{\lambda_8}) & 0 & \frac{1}{3}(-\sqrt{\lambda_7}+\sqrt{\lambda_8}) & \frac{1}{3}(2\sqrt{\lambda_7}+\sqrt{\lambda_8}) & 0 \\ 0 & 0 & 0 & 0 & 0 & 0 & 0 & \sqrt{\lambda_1} \end{pmatrix}. \tag{58}$$

References

1. R. Lo Franco, B. Bellomo, S. Maniscalco, G. Compagno, Dynamics of quantum correlations in two-qubit systems within non-Markovian environments. Int. J. Mod. Phys. B **27**, 1345053 (2013)
2. H. Ollivier, W..H. Zurek, Quantum discord: a measure of the quantumness of correlations. Phys. Rev. Lett. **88**, 017901 (2001)
3. J. Zhou, X. Hu, N. Jing, Quantum discord of certain two-qubit states. Int. J. Theor. Phys. **59**, 415–425 (2020)
4. B. Li, C.-L. Zhu, X.-B. Liang, B.-L. Ye, S.-M. Fei, Quantum discord for multiqubit systems. Phys. Rev. A **104**, 012428 (2021)
5. M. Ali, Quantum discord for qubit-qudit systems. Phys. A: Math. Theor. **43**, 495303 (2010)
6. M. Mahdian, R. Yousefjani, S. Salimi, Quantum discord evolution of three-qubit states under noisy channels. Eur. Phys. J. D **66**, 133 (2012)
7. J. Xu, Non-Markovian dynamics of spin squeezing. Phys. Lett. A **377**, 238 (2013)
8. F. Buscemi, P. Bordone, Time evolution of tripartite quantum discord and entanglement under local and nonlocal random telegraph noise. Phys. Rev. A **87**, 042310 (2013)
9. F. Benabdallah, H. Arian Zad, M. Daoud, N. Ananikian, Dynamics of quantum correlations in a qubit-qutrit spin system under random telegraph noise. Phys. Scr. **96**, 125116 (2021)
10. P. Hauke, M. Heyl, L. Tagliacozzo, P. Zoller, Measuring multipartite entanglement through dynamic susceptibilities. Nat. Phys. **12**, 778–782 (2016)
11. S. Szalay, Multipartite entanglement measures. Phys. Rev. A **92**, 042329 (2015)
12. J. Li, L. Chen, Detection of genuine multipartite entanglement based on uncertainty relations. Qua. Inf. Proc. **20**, 220 (2021)
13. G. Vidal, R. F. Werner, Computable measure of entanglement. Phys. Rev. A **65**, 032314 (2002)
14. A. Peres, Separability criterion for density matrices. Phys. Rev. Lett. **77**, 1413 (1996)
15. A.V. Fedorova, M.A. Yurischev, Behavior of quantum discord, local quantum uncertainty, and local quantum Fisher information in two-spin-1/2 Heisenberg chain with DM and KSEA interactions. Qua. Inf. Proc. **21**, 92 (2022)
16. M. Ali, Local quantum uncertainty for multipartite quantum systems. Eur. Phys. J. D **74**, 186 (2020)
17. M.A. Nielsen, I.L. Chuang, *Quantum computation and quantum information* (Cambridge University Press, Cambridge, England, 2000)
18. C.-W. Helstrom, *Quantum detection and estimation theory* (Academic, New York, 1976)
19. K. El Anouz, A. El Allati, N. Metwally, T. Mourabit, Estimating the teleported initial parameters of a single-and two-qubit systems. Appl. Phys. B **125**, 1 (2019)
20. K. El Anouz, A. El Allati, Teleporting quantum Fisher information under Davies-Markovian dynamics. Phys. A **596**, 127133 (2022)
21. C. Monroe, Quantum information processing with atoms and photons. Nature **416**, 238–246 (2002)
22. M.-G. Majumdar, Quantum information processing using the exchange interaction. J. Quant. Inf. Sci. **8**, 4 (2018)
23. M.G.A. Paris, Quantum estimation for quantum technology. Int. J. Quant. Inf. **7**, 125 (2009)
24. S.L. Braunstein, C.M. Caves, Statistical distance and the geometry of quantum states. Phys. Rev. Lett. **72**, 3439 (1994)
25. F. Benabdallah, S. Haddadi, H. Arian Zad, M. Reza Pourkarimi, M. Daoud, N. Ananikian, Pairwise quantum criteria and teleportation in a spin square complex. Sci. Rep. **12**, 6406 (2022)
26. S. Kim, L. Li, A. Kumar, J. Wu, Characterizing nonclassical correlations via local quantum Fisher information. Phys. Rev. A **97**, 032326 (2018)
27. K. El Anouz, A. El Allati, A. Salah, F. Saif, Quantum fisher information: probe to measure fractional evolution. Int. J. Theo. Phys. **59**, 5 (2020)
28. A..-S..F. Obada, S. Abdel-Khalek, Entanglement evaluation with atomic fisher information. Phys. A **389**, 891 (2010)
29. Y. Akbari-Kourbolagh, M. Azhdargalam, Entanglement criterion for multipartite systems based on quantum Fisher information. Phys. Rev. A **99**, 012304 (2019)
30. F. Benabdallah, K. El Anouz, M. Daoud, Toward the relationship between local quantum Fisher information and local quantum uncertainty in the presence of intrinsic decoherence. Euro. Phys. J. Plus. **137**, 5 (2022)
31. S. Haseli, Local quantum Fisher information and local quantum uncertainty in two-qubit Heisenberg XYZ chain with Dzyaloshinskii-Moriya interactions. Laser Phys. **30**, 105203 (2020)
32. A.B.A. Mohamed, E. Khalil, M.M. Selim, H. Eleuch, Quantum fisher information and bures distance correlations of coupled two charge-qubits inside a coherent cavity with the intrinsic decoherenceâ. Symmentry **13**, 2 (2021)
33. S. Walleck, H. Theil, M. Heidemeier, G. Heinze-Brü ckner, A. Stammler, H. Bögge, T. Glaser, From triplesalen to triplesalacen: synthesis spectroscopic, redox, and magnetic properties of the trinuclear Cu^{II}_3 triplesalacen complex. Inorg. Chim. Acta **363**, 4287 (2010)
34. F. Benabdallah, A. Slaoui, M. Daoud, Quantum discord based on linear entropy and thermal negativity of qutrit-qubit mixed spin chain under the influence of external magnetic field. Quantum Inf. Process. **19**, 252 (2020)
35. D.C. Mattis, *The theory of magnetism made simple* (World Scientific, Singapore, 2006)

36. M. Freitas, C. Filgueiras, M. Rojas, The effects of an impurity in an Ising-XXZ diamond chain on thermal entanglement, on quantum coherence, and on quantum teleportation. Ann. Phys. **531**, 1900261 (2019)
37. W. K. Wootters, Entanglement of formation of an arbitrary state of two qubits. Phys. Rev. Lett. **80**, 2245 (1998)
38. M.A. Nielsen, I.L. Chuang, *Quantum computation and quantum information* (Cambridge University Press, Cambridge, 2000)
39. W. K. Wootters, Entanglement of Formation for an Arbitrary state of Two Qubits. Phys. Rev. Lett. **80**, 10 (1998)
40. C.H. Bennett, H.J. Brenstein, S. Popescu, B. Schumacher, Concentrating partial entanglement by local operations. Phys. Rev. A **53**, 2046 (1996)
41. D. Girolami, T. Tufarelli, G. Adesso, Characterizing nonclassical correlations via local quantum uncertainty. Phys. Rev. Lett. **110**, 240402 (2013)
42. E. P. Wigner, M. M. Yanasse, Informations contents of distributions. Proc. Nat. Acad. Sci. USA **19**, 910 (1963)
43. F. Benabdallah, M. Daoud, Dynamics of quantum discord based on linear entropy and negativity of qutrit-qubit system under classical dephasing environments. Eur. Phys. J. D **75**, 3 (2021)
44. J. Yang, Y. Huang, Tripartite and bipartite quantum correlations in the XXZ spin chain with three-site interaction. Quantum Inf. Process. **16**, 281 (2017)
45. H. Cencarikova, J. Strecka, Unconventional strengthening of the bipartite entanglement of a mixed spin-(1/2,1) Heisenberg dimer achieved through Zeeman splitting. Phys. Rev. B **102**, 184419 (2020)
46. T. Werlang, G. Rigolin, Thermal and magnetic quantum discord in Heisenberg models. Phys. Rev. A **81**, 044101 (2010)
47. M.L. Hu, J. Sun, Sudden change of geometric quantum discord in finite temperature reservoirs. Ann. Phys. **354**, 265 (2015)
48. J.P.G. Pinto, G. Karpat, F.F. Fanchini, Sudden change of quantum discord for a system of two qubits. Phys. Rev. A **88**, 034304 (2013)
49. C.W. Helstrom, *Quantum detection and estimation theory* (Academic, New York, 1976)
50. A.S. Holevo, *Probabilistic and statistical aspects of quantum theory* (North-Holland, Amsterdam, 1982)
51. M. Genoni, S. Olivares, M.G.A. Paris, Optical phase estimation in the presence of phase diffusion. Phys. Rev. Lett. **106**, 153603 (2011)
52. S. Knysh, V.N. Smelyanskiy, G.A. Durkin, Scaling, laws for precision in quantum interferometry and the bifurcation landscape of the optimal state. Phys. Rev. A **83**, 021804(R) (2011)
53. J. Liu, X. Jing, X. Wang, Phase-matching condition for enhancement of phase sensitivity in quantum metrology. Phys. Rev. A **88**, 042316 (2013)
54. J. Liu, H. Yuan, X.-M. Lu, X. Wang, Quantum Fisher information matrix and multiparameter estimation. J. Phys. A: Math. Theor. **53**, 023001 (2020)
55. G. Tóth, I. Apellaniz, Quantum metrology from a quantum information science perspective. J. Phys. A: Math. Theor. **47**, 424006 (2014)
56. K. El Anouz, A. El Allati, A. Salah et al., Quantum fisher information: probe to measure fractional evolution. Int. J. Theor. Phys. **59**, 1460–1474 (2020)
57. C. H. Bennett, G. Brassard, C. Crépeau, R. Jozsa, A. Peres, W. K. Wootters, Teleporting an unknown quantum state via dual classical and Einstein-Podolsky-Rosen channels. Phys. Rev. Lett. **70**, 1895–1899 (1993)
58. M. Horodecki, P. Horodecki, R. Horodecki, General teleportation channel, singlet fraction, and quasidistillation. Phys. Rev. A **60**, 1888 (1999)
59. Y.-X. Xi, Y.-X. Huang, Quantum teleportation in a three-qubit Heisenberg chain with Dzyaloshinsky Moriya interaction. Mod. Phys. Lett. B **29**, 20 (2015)
60. J.-L. Guo, M. Qing-Xia, H.-S. Song, Magnetic impurity effects on quantum teleportation via the three-qubit Heisenberg XX model. Phys. Scr. **77**, 035004 (2008)

Springer Nature or its licensor holds exclusive rights to this article under a publishing agreement with the author(s) or other rightsholder(s); author self-archiving of the accepted manuscript version of this article is solely governed by the terms of such publishing agreement and applicable law.

4 Contribution 4: Toward the relationship between local quantum Fisher information and local quantum uncertainty in the presence of intrinsic decoherence

The European Physical Journal Plus, 137 (2022) 548.

4.1 Summary of contribution 4

Local quantum Fisher information, which is closely connected to the idea of local quantum uncertainty (4.15), has been described as a useful tool in the investigation of quantum correlations. This work has looked at the complex relationships between the ideas of concurrence (2.55), local quantum uncertainty (4.15), and local quantum Fisher information (4.86). In order to do this, a two-qubit XXZ Heisenberg spin chain system operating in the presence of an external magnetic field is observed for non-classical correlations. By resolving the time-dependent Milburn equation (4.47), we explored a variety of initial states, such as pure, Werner, mixed, and maximally entangled ones.

We were able to investigate a number of phenomena, including sudden death, sudden birth, oscillations, and frozen correlations using local quantum uncertainty, local quantum Fisher information, and concurrence. We discovered that the non-classical quantifiers and entanglement witness fluctuate roughly similarly between their maximum and minimum bounds. We really discovered that these characteristics depend on the system's interaction qualities by altering various interaction parameters that are recorded in the system. Werner and mixed states show a quick, mostly interaction-driven dynamical development of these variables.

Using the conventional quantum teleportation methods, we have also examined the idea of quantum teleportation. In order to carry out this procedure, we examined entanglement in terms of the concurrence of the ultimate teleported state, as well as quantum correlations utilizing LQU and LQFI. The development and examination of quantum connections between the suggested open system and its surroundings offered one of the largest problems in this effort. In light of this, we looked at how the decoherence phenomena affected the quantum teleportation mechanism. In order to demonstrate the believability of communicating the unknown condition, we then looked at faithfulness.

Overall, our study provides valuable insights into the relationship between quantum uncertainty, quantum Fisher information, and entanglement, and how they relate to non-classical correlations in a two-qubit XXZ Heisenberg spin chain system. Our investigation of quantum teleportation protocols also sheds light on the potential impact of decoherence on quantum information processing.

4.2 Content of contribution 4

Eur. Phys. J. Plus (2022) 137:548
https://doi.org/10.1140/epjp/s13360-022-02760-1

THE EUROPEAN PHYSICAL JOURNAL PLUS

Regular Article

Toward the relationship between local quantum Fisher information and local quantum uncertainty in the presence of intrinsic decoherence

Fadwa Benabdallah[1], **Khadija El Anouz**[2,a], **Mohammed Daoud**[3,4]

[1] LPHE-Modeling and Simulation, Faculty of Sciences, Mohammed V University in Rabat, Rabat, Morocco
[2] Laboratory of R&D in Engineering Sciences, Faculty of Sciences and Techniques Al-Hoceima, Abdelmalek Essaadi University, Tétouan, Morocco
[3] ICTP, Strada Costiera 11, 34151 Trieste, Italy
[4] Department of Physics, Faculty of Sciences, University Ibn Tofail, Kenitra, Morocco

Received: 15 September 2021 / Accepted: 23 April 2022
© The Author(s), under exclusive licence to Società Italiana di Fisica and Springer-Verlag GmbH Germany, part of Springer Nature 2022

Abstract The delicate relationship between the concepts of local quantum uncertainty, local quantum Fisher information and concurrence is investigated. This is analyzed by quantifying the non-classical correlations inherent in a two-qubit XXZ open system interacting with its surrounding environment in the presence of an external magnetic field. The second part of this work investigates different kinds of states, namely pure, Werner, mixed, and maximally entangled states via solving the time-dependent Milburn equation. Indeed, by controlling various interaction parameters, it is shown that the non-classical quantifiers and entanglement witness by means of local quantum uncertainty, local quantum Fisher information, and concurrence, respectively, fluctuate approximately similarly between their maximum and minimum bounds, where in general the sudden death, sudden birth, oscillations, and frozen correlations phenomena appear in the case of Werner and maximally entangled states. Finally, a scheme of quantum teleportation protocol is proposed in order to make a comparative study between teleported non-classical correlations and entanglement under the influence of the intrinsic decoherence phenomenon.

1 Introduction

The characterization as well as the quantification of quantum correlations in composite quantum systems have been considered in different areas of quantum information science [1–3] as for instance in quantum computation and quantum estimation theory and stimulated interesting works [4–8]. Now, it is commonly accepted that quantum correlations constitute a key resource in the process of the implementation of various quantum protocols, including: quantum teleportation [8–10], quantum cryptography [11], quantum sensing [12], etc. In this sense, tools were developed in the last two decades to quantify the entanglement rate inherent in a quantum state [13–16]. The most popular one is the concept of the concurrence introduced by Wootters [4,13,17]. Another tool recently introduced in the literature is the concept of the so-called Local Quantum Uncertainty (LQU) that is now considered a reliable tool to quantify quantum correlations in multipartite quantum systems [18,19]. Roughly speaking LQU is investigated as a non-classical correlations quantifier of a multipartite quantum system [19]. It was introduced first time by Girolami et al [18] using the information of the Wigner Yanase Skew information [20]. Indeed, the LQU is originally defined as the minimum of skew information and it is another type of discord-like quantifiers of the uncertainty presented in a quantum state according to its non-commutativity using local observables [18,19,21]. Interestingly enough, the LQU is related directly to the notion of quantum Fisher Information (QFI) and Local quantum Fisher Information (LQFI) and gives an important link between quantum information theory and quantum estimation theory [22–24]. Indeed, it has been shown that quantum Fisher information provides a measure to investigate the entanglement for multipartite entangled systems [25]. Recently, LQFI has been suggested as a very successful tool to quantify quantum correlations in a composite quantum system [26,27]. In fact, the investigation and characterization of LQFI is performed using the optimization over all the observables of one of the subsystems of the whole composite system [26,27]. However, since both quantities, namely LQU and LQFI basically, depend on the quantum uncertainty concept, it might be used as good non-classical correlations quantifiers that satisfy all the conditions needed to be a reliable a measure of quantum correlations [28].

In recent years, the open quantum systems theory have acquired growing importance within the field of quantum information. Indeed, it is at the heart of many physical concepts used to understand and manipulate the interaction between a quantum system and its environment. On the other hand, the interaction of an open quantum system with its surrounding environment as a single composite system can be approached using concurrence, LQU, and LQFI as non-classical quantifiers in order to examine the correlations between its components. Indeed, an open quantum system exhibits the decoherence phenomenon which has been examined for different types of interaction in the literature [29–31]. Indeed, many works paid attention to study non-classical correlations by

[a] e-mail: elanouzkhadija1994@gmail.com (corresponding author)

Published online: 04 May 2022

means of LQU and QFI and examined the dynamics of open systems interact with their environments [27,32–35]. For example, L-P. Chen et al [36] examined the dynamics of LQU and LQFI for a two-qubit system driven by a classical phase noisy laser and they showed that for an open quantum system, the LQU is bounded by LQFI. Similar analyses were reported by B-L. Ye who examined the LQFI as a non-classical correlations quantifier in order to study the quantum phase transition in a spin-1/2 XX Heisenberg chain with three spin interactions [37]. Moreover, M. Ali studied the LQU for a multipartite system and proposed an analytical formula to derive the LQU in multipartite case [19]. Finally, V. Abhignan et al studied a two-qubit spin squeezing model in order to compare the LQU with other quantifiers of quantum correlations, namely trace distance discord and uncertainty-induced quantum nonlocality [33]. They concluded that the entanglement suffers from intrinsic decoherence and exhibits a sudden death phenomenon, while the non-classical quantifiers are more robust against intrinsic decoherence.

The spin-chain frameworks are exemplary systems used to investigate a wide range of physical systems, and various potential applications in quantum information, including: quantum phases, quantum communication, phase transitions, etc. Recently, a particular interest has been devoted to physically understand the Heisenberg spin chain models with Dzyaloshinski–Moriya interaction. For example, in Ref. [38], the authors have used this coupling as a good marker of quantum phase transitions. Moreover, this model is successfully appointed to generate entangled network from partially entangled states, thermal entanglement, teleportation fidelity, and dense coding [39,40]. In particular, the spin chains have acquired an attractive attention within the area of quantum information processing. Indeed, such spin chain has been devoted to investigate quantum data transmission through microscopic distances via considering them as a powerful states used to transfer information between two sites that ensure the building of quantum buses used to connect different computer components [41]. The core idea underlying the first part of this work is to study the dynamics of quantum correlations under intrinsic decoherence [42]. We consider a two-qubit XXZ Heisenberg spin chain subjected to an inhomogeneous magnetic field. We shall employ LQU and LQFI to quantify the quantum correlations in the quantum system, and we shall also use the concurrence as a witness tool to discuss the non-separability. In particular, we examine four different kinds of states, namely pure, mixed, maximally entangled, and Werner states [43]. The last class of states are significant in quantum information and computation processing because they are able to ensure the separability of mixed states since they have been classified as the generalized maximally entangled mixed states [43]. We shall evaluate the joint qubit–qubit state quantum correlations by means of concurrence, local quantum uncertainty, and local quantum Fisher information under the intrinsic decoherence effect. It is shown that these quantities fluctuate approximately in the same manner between their maximum and minimum amplitudes, where we have studied different phenomena, including sudden death, sudden birth, oscillations, and frozen correlations phenomena. The dynamical evolution of these quantities depends basically on the interaction parameters and appears fast in the case of Werner and mixed states. In the second part of this work, we shall focus our attention to quantum teleportation process which is the transmission of the information encoded in an unknown state from a sender named conventionally Alice to another located receiver, Bob using classical and quantum channels [8] . To implement this process of quantum teleportation, we evaluate quantum correlations, by means of LQU and LQFI and entanglement in terms of the concurrence of the final teleported state. Indeed, one of the most challenges of this work is given in the possibility to create and examine local quantum correlations between the proposed open system and its environment. According to this, we shall investigate the impact of the decoherence phenomenon on quantum teleportation protocol. Finally, we examine the fidelity in order to exhibit the credibility of transmitting the unknown state.

The paper is organized as follows. In Sec.2 , we give the Hamiltonian proposed two-qubit Heisenberg XXZ model and the corresponding density operator derived from the exact solution of time-dependent Milburn equation. In Sec.3, we review the definitions and the properties of concurrence, LQU, and LQFI. Their dynamics behaviors versus the interaction parameters for different proposed initial quantum states are considered in Sec.4. By using the standard teleportation protocol, the output state of the two-qubit entangled state is investigated in Sec.5. The evaluation of the fidelity, average fidelity, and the non-classical correlations of teleported state or output state is given in Sec.6 . Finally in Sec.7, we conclude with a summary and some future directions.

2 Theoretical model

2.1 Two-qubit Heisenberg XXZ model

Consider a bipartite quantum system, namely a Heisenberg XXZ spin-1/2 chain interacting with an external magnetic field, B with only nearest-neighbor interactions. The Hamiltonian of this system is given as below

$$H = J(s_1^x s_2^x + s_1^y s_2^y) + \Delta s_1^z s_2^z + (B-b)s_1^z + (B+b)s_2^z. \tag{1}$$

The coupling J describes the spin interaction strength, being anti-ferromagnetic when $J > 0$ while is ferromagnetic when $J < 0$. B is the external magnetic field applied in the z-direction, while b denotes the degree of inhomogeneity of the field. Δ is the exchange anisotropy parameter. For $\Delta = 0$, the model reduces to the isotropic XX, while for $\Delta = J$, the model is simply the isotropic Heisenberg XXX model. The Heisenberg spin-1/2 operators s_i^α ($\alpha = x, y, z$) are expressed in terms of the familiar Pauli matrices σ_i^α, acting on qubit i, as $s_i^\alpha = \hbar\sigma_i^\alpha/2$. For sake of simplicity, we set $\hbar = 1$ so that $\{B,\ J,\ \Delta,\ b\}$ are dimensionless parameters. In

the standard basis, $\mathcal{B} = \{ |00\rangle, |01\rangle, |10\rangle, |11\rangle \}$, the Hamiltonian (1) takes the following matrix form

$$H = \begin{pmatrix} \frac{1}{4}\Delta + B & 0 & 0 & 0 \\ 0 & -\frac{1}{4}\Delta - b & \frac{1}{2}J & 0 \\ 0 & \frac{1}{2}J & -\frac{1}{4}\Delta + b & 0 \\ 0 & 0 & 0 & \frac{1}{4}\Delta - B \end{pmatrix}. \tag{2}$$

By straightforward calculations, one can obtain the eigenvalues of Hamiltonian H as below

$$E_1 = \frac{1}{4}\Delta + B, \quad E_{2,3} = -\frac{1}{4}\Delta \pm \frac{1}{2}\chi, \quad E_4 = \frac{1}{4}\Delta - B, \tag{3}$$

with $\chi = \sqrt{J^2 + 4b^2}$. The corresponding eigenstates by means of the above standard basis are given as follows

$$|\psi_1\rangle = |00\rangle, \quad |\psi_{2,3}\rangle = \frac{1}{\sqrt{1+\eta_\pm^2}} (|10\rangle + \eta_\pm |01\rangle), \quad |\psi_4\rangle = |11\rangle, \tag{4}$$

where $\eta_\pm = \dfrac{J}{2b \pm \chi}$ is the inhomogeneity parameter [44].

2.2 Intrinsic decoherence

In general, any quantum system can be seen as an inevitably open system coupled to its surrounding environment. During the interaction with ancillary or interface systems, even a well-isolated system has to be at risk of losing its characteristic quantum traits, including coherence and quantum correlations. To describe this, Milburn amended the Schrödinger equation by incorporating a decay factor and presented a decoherence model, which is entirely of phase decoherence in the Markovian regime. According to Milburn's model [42], the time-dependent density matrix in the presence of intrinsic decoherence phenomenon is expressed as follows

$$\frac{\mathrm{d}}{\mathrm{d}t}\rho(t) = \frac{1}{\Gamma}[\exp(-i\Gamma H)\rho(t)\exp(i\Gamma H) - \rho(t)], \tag{5}$$

where Γ is the intrinsic decoherence parameter and H being the Hamiltonian of the system. It must be noticed that the master equation describing the intrinsic decoherence effect under Markovian approach writes as

$$\frac{\mathrm{d}}{\mathrm{d}t}\rho(t) = -i[H, \rho(t)] - \frac{\Gamma}{2}[H, [H, \rho(t)]]. \tag{6}$$

which can be derived from (5) for $\Gamma \longrightarrow 0$. Equation (6) corresponds to the standard von Neumann equation [45]. The formal solution of the master equation (6) can be written as

$$\rho(t) = \sum_{k=0}^{\infty} \frac{(\Gamma t)^k}{k!} M^k(t)\rho(0)(M^k(t))^\dagger, \tag{7}$$

where $\rho(0)$ being the initial state of the system and $M^k(t)$ is defined by

$$M^k(t) = H^k \exp(-iHt)\exp(-\Gamma H^2 t/2). \tag{8}$$

By inserting the complete relation $\sum_n ||\psi_n\rangle\rangle \langle\langle\psi_n|| = 1$ satisfied by the eigenvectors of the Hamiltonian (1) into Eq.(7), we obtain the following time-dependent density matrix

$$\rho(t) = \sum_{m,n} \exp(-\frac{\Gamma t}{2}(E_m - E_n)^2 - i(E_m - E_n)t) \times \langle\langle\psi_m||\,\rho(0)\,||\psi_n\rangle\rangle\, ||\psi_m\rangle\rangle\, \langle\langle\psi_n||\,. \tag{9}$$

Here, E_n and $||\psi_n\rangle\rangle$ denote the eigenvalues and eigenvectors of the Hamiltonian (1) given by Eq. (3) and (4), respectively.

2.3 Density operator

In this section, we shall examine the non-classical correlations by means of the so-called local quantum uncertainty and local Fisher information and entanglement measure in terms of concurrence inherent in a two-qubit system using the Heisenberg XXZ model in the presence of intrinsic decoherence phenomenon [42]. Indeed, let us assume that that the qubits are initially prepared in the extended Werner-like state as below [43]:

$$\rho(0) = r\,|\phi\rangle\,\langle\phi| + \frac{1-r}{4} I_4, \tag{10}$$

where r being the purity of the initial state $0 < r \leq 1$ while I is the (4×4) identity matrix and $|\phi\rangle$ is the well-known Bell-like state given by

$$|\phi\rangle = p\,|01\rangle + \sqrt{1-p^2}\,|10\rangle\,, \tag{11}$$

with p is the degree of entanglement. In the standard basis, $\rho(0)$ can be written as

$$\rho(0) = \begin{pmatrix} \rho_{11}(0) & 0 & 0 & 0 \\ 0 & \rho_{22}(0) & \rho_{23}(0) & 0 \\ 0 & \rho_{23}(0) & \rho_{33}(0) & 0 \\ 0 & 0 & 0 & \rho_{44}(0) \end{pmatrix}, \tag{12}$$

where

$$\rho_{11}(0) = \rho_{44}(0) = \frac{1-r}{4},\ \ \rho_{22}(0) = rp^2 + \frac{1-r}{4},\ \rho_{33}(0) = r(1-p^2) + \frac{1-r}{4}, \rho_{23}(0) = rp\sqrt{1-p^2}. \tag{13}$$

From the equation (9), the time evolution of the density matrix can be written as

$$\rho(t) = \begin{pmatrix} \rho_{11}(t) & 0 & 0 & 0 \\ 0 & \rho_{22}(t) & \rho_{23}(t) & 0 \\ 0 & \rho_{*23}(t) & \rho_{33}(t) & 0 \\ 0 & 0 & 0 & \rho_{44}(t) \end{pmatrix}. \tag{14}$$

where the density matrix elements are given by

$$\begin{aligned}
\rho_{11}(t) &= \rho_{11}(0) = \frac{1-r}{4}, \\
\rho_{22}(t) &= \frac{1}{2\chi^2}((8b^2+J^2)\rho_{22}(0) + 4bJ\rho_{23}(0) + J^2\rho_{33}(0) + J\exp(-\frac{1}{2}\chi^2 t\Gamma)(J\rho_{22}(0) - 4b\rho_{23}(0) - J\rho_{33}(0))\cos(\chi t)), \\
\rho_{33}(t) &= \frac{1}{2\chi^2}(J^2\rho_{22}(0) - 4bJ\rho_{23}(0) + (8b^2+J^2)\rho_{33}(0) + J\exp(-\frac{1}{2}\chi^2 t\Gamma)(-J\rho_{22}(0) + 4b\rho_{23}(0) + J\rho_{33}(0))\cos(\chi t)), \\
\rho_{23}(t) &= \frac{1}{2\chi^2}\begin{pmatrix} 2J\exp(\frac{1}{2}\chi^2 t\Gamma)(b\rho_{22}(0) + J\rho_{23}(0) - b\rho_{33}(0)) + 2b(-J\rho_{22}(0) + 4b\rho_{23}(0) \\ +J\rho_{33}(0))\cos(\chi t) + i\chi(J\rho_{22}(0) - 4b\rho_{23}(0) - J\rho_{33}(0))\sin(\chi t) \end{pmatrix}\exp(-\frac{1}{2}\chi^2 t\Gamma), \\
\rho_{44}(t) &= \rho_{44}(0) = \frac{1-r}{4}.
\end{aligned} \tag{15}$$

Note that $\rho_{11}(t)$ and $\rho_{44}(t)$ are not affected by the decoherence phenomenon since $\rho_{11}(t) = \rho_{11}(0)$ and $\rho_{44}(t) = \rho_{44}(0)$. Moreover, the eigenvalues of the density matrix in Eq.(14) are calculated as below:

$$\begin{aligned}
\lambda_1 &= \lambda_2 = \rho_{11}(t), \\
\lambda_3 &= \frac{1}{2}[\rho_{22}(t) + \rho_{33}(t) - \sqrt{(\rho_{22}(t) - \rho_{33}(t))^2 + 4|\rho_{23}(t)|^2}], \\
\lambda_4 &= \frac{1}{2}[\rho_{22}(t) + \rho_{33}(t) + \sqrt{(\rho_{22}(t) - \rho_{33}(t))^2 + 4|\rho_{23}(t)|^2}],
\end{aligned} \tag{16}$$

while the corresponding eigenvectors turn out to be:

$$\begin{aligned}
|\lambda_1\rangle &= |11\rangle\,, \\
|\lambda_2\rangle &= |00\rangle\,, \\
|\lambda_3\rangle &= \frac{1}{\sqrt{1+|\omega|^2}}(\omega\,|01\rangle + |10\rangle), \\
|\lambda_4\rangle &= \frac{1}{\sqrt{1+|\varkappa|^2}}(\varkappa\,|01\rangle + |10\rangle),
\end{aligned} \tag{17}$$

where

$$\begin{aligned}
\omega &= \frac{1}{2\rho_{*23}(t)}[\rho_{22}(t) - \rho_{32}(t) - \sqrt{(\rho_{22}(t) - \rho_{33}(t))^2 + 4|\rho_{23}(t)|^2}], \\
\varkappa &= \frac{1}{2\rho_{*23}(t)}[\rho_{22}(t) - \rho_{32}(t) + \sqrt{(\rho_{22}(t) - \rho_{33}(t))^2 + 4|\rho_{23}(t)|^2}].
\end{aligned} \tag{18}$$

3 Quantum correlations

We begin in this section by introducing some non-classical correlations quantifiers, namely LQU and LQFI and the concurrence.

3.1 Quantum entanglement: concurrence

Various measures have been proposed to quantify the amount of entanglement in bipartite and multipartite quantum systems. The concurrence $\mathcal{C}$ introduced by W.K. Wootters has been proven to be particularly useful and it is the most popular computable measure for arbitrary two-qubit mixed states. This simple approach was developed to distinguish quantum entangled states from separable states qualitatively and quantitatively. Indeed the case reflects $\mathcal{C} = 0$ happens when the system is unentangled (separable), whereas $\mathcal{C} = 1$ reveals a maximally entangled state. The concurrence is given by [17]

$$\mathcal{C} = \max\{0, \sqrt{\delta_1} - \sqrt{\delta_2} - \sqrt{\delta_3} - \sqrt{\delta_4}\}, \tag{19}$$

where $\delta_i (i = 1, 2, 3, 4)$ are the eigenvalues in the decreasing order of the 4×4 matrix $R = \rho(\sigma^y \otimes \sigma^y)\rho^*(\sigma^y \otimes \sigma^y)$, in which ρ^* and σ^y are, respectively, the complex conjugate of ρ in the standard basis and the $y-$component Pauli matrix. For the density matrix (14), the concurrence is given by

$$\mathcal{C}(\rho(t))=2\max\{0, |\rho_{23}(t)| - \sqrt{\rho_{11}(t)\rho_{44}(t)}\}. \tag{20}$$

The concurrence of the initial state $\rho(0)$ (10) can be derived from (20). It writes as

$$\mathcal{C}(\rho(0))=2\max\{0, r(p\sqrt{1-p^2} + \frac{1}{4}) - \frac{1}{4}\}. \tag{21}$$

Hence, the initial state $\rho(0)$ (10) is entangled when $r > r_0 = 1/(1+4p\sqrt{1-p^2})$. However, for $r \leq r_0$, the concurrence (21) is zero and the entanglement vanishes and the initial state $\rho(0)$ (10) becomes separable. For example, when the state of Eq.(11) becomes the Bell state for the value $p = \frac{1}{\sqrt{2}}$, then, in this case $\rho(0)$ is simply the Werner-like state. It is entangled when $r > \frac{1}{3}$.

3.2 Local quantum uncertainty

Due to the probabilistic character of quantum mechanics, two incompatible observables cannot be measured simultaneously with arbitrary precision. The uncertainty principle imposes a fundamental bound on the precision. The total uncertainty due to a single observable K measurement on a quantum state ρ is usually defined by the following variance

$$\mathrm{Var}(\rho, K) = \mathrm{Tr}(\rho K^2) - (\mathrm{Tr}(\rho K))^2. \tag{22}$$

This uncertainty has purely quantum nature for pure states. However, it may include both classical ignorance due to the state mixedness and genuinely quantum part arising by the non-commutativity of a state with an acting observable. In the theory of quantum information, it is essential to distinguish between classical and quantum components. In order to deal only with quantum part of the variance, Wigner and Yanase introduced the notion of the so-called skew information as a good quantifier of this uncertainty [20]. It is defined as follows

$$\mathcal{I}(\rho, K) = -\frac{1}{2}\mathrm{Tr}([\sqrt{\rho}, K]^2), \tag{23}$$

where [., .] is the commutator, while $\mathcal{I}$ is the skew information associated to the density matrix ρ. It is worth nothing that, unlike variance, Wigner–Yanase skew information (WYSI) is unaffected by classical mixing and it reduces to the variance for pure states. Based on the notion of skew information, a discord-like measure of quantum correlations was recently proposed by Girolami et al for arbitrary bipartite quantum systems [18]. This measure called local quantum uncertainty and defined as the minimum skew information achievable with a single local measurement. It is given by

$$\mathcal{U}_A(\rho) = \min_{K_\mathrm{A}} \mathcal{I}(\rho, K_\mathrm{A} \otimes I_\mathrm{B}), \tag{24}$$

where K_A is a Hermitian operator (local observable) on the subsystem A admitting a non-degenerate spectrum. Moreover, I_B being the identity operator acting on the subsystem B. Note that, $\mathcal{I}$ is non-negative and non-increasing under classical mixing [19]. Besides, LQU quantifies the minimum amount of uncertainty in a quantum state and is inherently an asymmetric quantity with respect to subsystem exchange because they depend on which subsystem the measurements are made on [18,21]. From now on, we consider the simple form $\mathcal{U}(\rho)$ instead of $\mathcal{U}_A(\rho)$. For a $2 \otimes d$ (qubit–qudit) bipartite quantum systems [18], the closed-form of the local quantum uncertainty turns out to be,

$$\mathcal{U}(\rho) = 1 - \max(\zeta_1, \zeta_2, \zeta_3), \tag{25}$$

where $\zeta_i (i = 1, 2, 3)$ are the eigenvalue of the 3×3 matrix $\mathcal{W}$ of the following elements:

$$(\mathcal{W})_{\alpha\beta} = \mathrm{Tr}(\sqrt{\rho}\left(\sigma^{\alpha} \otimes I_{\mathrm{B}}\right)\sqrt{\rho}\left(\sigma^{\beta} \otimes I_{\mathrm{B}}\right)), \tag{26}$$

where $\sigma^{\alpha}(\sigma^{\beta})$ with $\alpha(\beta) = \{x, y, z\}$ represent the Pauli operators of the subsystem A. The local quantum uncertainty provides a reliable quantifier of quantum correlations and it has a geometrical significance in terms of Hellinger distance [18]. It is clear that having the matrix $\mathcal{W}$, one can easily evaluate the local quantum uncertainty for qubit–qudit quantum systems contrarily to quantum discord based on von Neumann entropy [19,46]. This is a quite an easy task compared with the complicated minimization process over parameters due to the local measurements [18,29]. It is important to note that for some quantum states, quantum discord and local quantum uncertainty capture the same correlations, whereas, they are different measures for others states [19]. However, for the pure bipartite states, the local quantum uncertainty reduces to the linear entropy of the reduced densities of the subsystems and vanishes for classically correlated state [18]. Moreover, it is invariant under local unitary operations [18].
In the Fano–Bloch representation, the density matrix $\rho(t)$ (14) can be written as follows:

$$\rho(t) = \frac{1}{4}\sum_{\mu,\nu=0}^{3} \mathcal{R}_{\mu\nu}(t)\left(\sigma^{\mu}\otimes\sigma^{\nu}\right), \tag{27}$$

where $\mathcal{R}_{\mu\nu}(t) = \mathrm{Tr}\left(\rho(t)(\sigma^{\mu}\otimes\sigma^{\nu})\right)$ are the total correlation tensor components occurring in the Fano–Bloch decomposition associated with bipartite density matrix $\rho(t)$ with $\sigma^{\mu}(\sigma^{\nu}) = \{\sigma^{0}, \sigma^{\alpha}(\sigma^{\beta})\}$. The non-vanishing components $\mathcal{R}_{\mu\nu}(t)$ are calculated as

$$\begin{aligned}
&\mathcal{R}_{00}(t) = \mathrm{Tr}\rho(t) = 1,\ \mathcal{R}_{03}(t) = 1 - 2(\rho_{22}(t) + \rho_{44}(t)),\ \ \mathcal{R}_{11}(t) = \mathcal{R}_{22}(t) = |\rho_{23}(t)|,\\
&\mathcal{R}_{30}(t) = 1 - 2(\rho_{33}(t) + \rho_{44}(t)),\ \mathcal{R}_{33}(t) = 1 - 2(\rho_{22}(t) + \rho_{33}(t)).
\end{aligned} \tag{28}$$

Therefore, in terms of the Fano–Bloch components $\mathcal{R}_{\mu\nu}(t)$ associated with the matrix $\rho(t)$ (14), the eigenvalues of the 3×3 matrix $(\mathcal{W}(t))_{\alpha\beta}$ (26) can be expressed as

$$\mathcal{W}_{11}(t) = \mathcal{W}_{22}(t) = \sqrt{\left(t_1(t) + 2\sqrt{d_1(t)}\right)\left(t_2(t) + 2\sqrt{d_2(t)}\right)} + \frac{1}{4}\frac{\left(\mathcal{R}_{03}^2(t) - \mathcal{R}_{30}^2(t)\right)}{\sqrt{\left(t_1(t) + 2\sqrt{d_1(t)}\right)\left(t_2(t) + 2\sqrt{d_2(t)}\right)}}, \tag{29}$$

$$\begin{aligned}
\mathcal{W}_{33}(t) = {} & \frac{1}{2}\left(1 + 2\left(\sqrt{d_1(t)} + \sqrt{d_2(t)}\right)\right)\\
& + \frac{1}{8}\left(\frac{(\mathcal{R}_{03}(t) + \mathcal{R}_{30}(t))^2 - (\mathcal{R}_{11}(t) - \mathcal{R}_{22}(t))^2}{\left(t_1(t) + 2\sqrt{d_1(t)}\right)} + \frac{(\mathcal{R}_{03}(t) - \mathcal{R}_{30}(t))^2 - (\mathcal{R}_{11}(t) + \mathcal{R}_{22}(t))^2}{\left(t_2(t) + 2\sqrt{d_2(t)}\right)}\right),
\end{aligned} \tag{30}$$

where

$$\begin{aligned}
t_{1,2}(t) &= \frac{1}{2}\left(\mathcal{R}_{00}(t) \pm \mathcal{R}_{03}(t)\right),\\
d_{1,2}(t) &= \frac{1}{16}\left[(\mathcal{R}_{00}(t) \pm \mathcal{R}_{33}(t))^2 - (\mathcal{R}_{30}(t) \pm \mathcal{R}_{03}(t))^2 - (\mathcal{R}_{11}(t) \mp \mathcal{R}_{22}(t))^2\right].
\end{aligned} \tag{31}$$

Hence, in this case, it is easy to check that the matrix $(\mathcal{W}(t))_{\alpha\beta}$ (26) is diagonal ($\mathcal{W}_{12}(t) = \mathcal{W}_{21}(t) = \mathcal{W}_{23}(t) = \mathcal{W}_{32}(t) = \mathcal{W}_{13}(t) = \mathcal{W}_{31}(t) = 0$). Thus, its eigenvalues are simply reduced to diagonal elements $\mathcal{W}_{ii}(t)$ ($i = 1, 2, 3$). Therefore, the LQU associated with quantum correlation in the system described by $\rho(t)$ (14) takes the form

$$\mathcal{U}(\rho(t)) = 1 - \max(\mathcal{W}_{11}(t), \mathcal{W}_{22}(t), \mathcal{W}_{33}(t)). \tag{32}$$

3.3 Local quantum Fisher information

Quantum Fisher Information has been shown to be an useful concept in quantum estimation theory. It is employed to determine the precision of a parameter associated with a physical quantity encoded in the quantum state. Assume that ρ_{ϵ} is an arbitrary quantum state, where ϵ is the parameter to be estimated, the QFI is defined as follows [47,48]

$$F(\rho) = \frac{1}{4}\mathrm{Tr}[\rho_{\epsilon}\mathcal{L}_{\epsilon}^2], \tag{33}$$

where $\mathcal{L}_{\epsilon}$ denotes the symmetric logarithmic derivative operator that satisfies the following equation :

$$\frac{\partial\rho_{\epsilon}}{\partial\epsilon} = \frac{1}{2}(\mathcal{L}_{\epsilon}\rho_{\epsilon} + \rho_{\epsilon}\mathcal{L}_{\epsilon}). \tag{34}$$

Now, suppose that the initial density operator, namely $\rho(0)$ evolves unitarily and the corresponding unitary operation is $\mathcal{U}_\epsilon = e^{iH\epsilon}$ such as $\rho_\epsilon = \mathcal{U}_\epsilon^\dagger \rho(0)\mathcal{U}_\epsilon$. In this case, the QFI can be expressed in terms of the Hamiltonian H (1) governing the evolution of the system [49]

$$F(\rho, H) = \frac{1}{2}\sum_{i\neq j}\frac{(\lambda_i-\lambda_j)^2}{\lambda_i+\lambda_j}|\langle\lambda_i|H|\lambda_j\rangle|^2, \tag{35}$$

where $\rho = \sum_n \lambda_n|\lambda_n\rangle\langle\lambda_n|$. It follows when the dynamics is governed by a local transformation, namely $e^{-i\epsilon H_A}$ of a local Hamiltonian $H_A = H_a \otimes I_B$, the so-called local quantum Fisher information turns out to be:

$$F(\rho, H_A) = \mathrm{Tr}[\rho H_A^2] - \sum_{i\neq j}\frac{2\lambda_i\lambda_j}{\lambda_i+\lambda_j}|\langle\lambda_i|H_A|\lambda_j\rangle|^2. \tag{36}$$

The main motivation behind the use LQFI is its ability to serve as good witness of quantum correlations. The quantum quantum correlations measured by means of LQFI correspond to the minimum of QFI over all local Hamiltonians H_A acting on the part A [50]. It is given by

$$Q(\rho(t)) = \min_{H_A} F(\rho, H_A). \tag{37}$$

We notice that the local Hamiltonian can be expressed in terms of the Pauli matrices, namely σ^α and Bloch vector r^α ($\alpha = x, y, z$) as $H_A = \sigma^\alpha.r^\alpha$, such that $|r^\alpha| = 1$ [50]. It follows that the first term on the right-hand side of Eq.(36) is equal to one, while the second term leads to:

$$\begin{aligned}
\sum_{i\neq j}\frac{2\lambda_i\lambda_j}{\lambda_i+\lambda_j}|\langle\lambda_i|H_A|\lambda_j\rangle|^2 &= \sum_{i\neq j}\frac{2\lambda_i\lambda_j}{\lambda_i+\lambda_j}|\langle\lambda_i|H_A|\lambda_j\rangle\langle\lambda_j|H_A|\lambda_i\rangle \\
&= \sum_{i\neq j}\sum_{\alpha=\beta=1}^{3}\frac{2\lambda_i\lambda_j}{\lambda_i+\lambda_j}\langle\lambda_i|(r^\alpha\sigma^\alpha)\otimes I_B|\lambda_j\rangle\langle\lambda_j|(r^\beta\sigma^\beta)\otimes I_B|\lambda_i\rangle \\
&= r^\alpha\sum_{i\neq j}\sum_{\alpha=\beta=1}^{3}\frac{2\lambda_i\lambda_j}{\lambda_i+\lambda_j}\langle\lambda_i|\sigma^\alpha\otimes I_B|\lambda_j\rangle\langle\lambda_j|\sigma^\beta\otimes I_B|\lambda_i\rangle r^\beta \\
&= r^\alpha S_{\alpha\beta} r^\beta \\
&= r^T.S.r
\end{aligned} \tag{38}$$

where $\sigma^1 \equiv \sigma^x$, $\sigma^2 \equiv \sigma^y$ and $\sigma^3 \equiv \sigma^z$. Moreover, S denotes a 3×3 symmetric matrix with the following elements

$$(S)_{\alpha\beta} = \sum_{m\neq n}\frac{2\lambda_m\lambda_n}{\lambda_m+\lambda_n}\langle\lambda_m|\sigma^\alpha\otimes I_B|\lambda_n\rangle\langle\lambda_n|\sigma^\beta\otimes I_B|\lambda_m\rangle. \tag{39}$$

The minimum over all unit of vectors r^α which coincide with the maximum eigenvalues of S and the LQFI is obtained as [50]

$$Q(\rho(t)) = 1 - \lambda^S_{\max}. \tag{40}$$

This quantity is invariant under any local unitary operation, non-negative and vanishes for any kind of classically correlated states. Moreover, it coincides the geometric discord for pure quantum states [50]. After some straightforward calculations and using the eigenvalues and eigenvectors calculated in Eqs. (16) and (17), the analytical expression of LQFI is obtained as

$$Q(\rho(t)) = 1 - \max(S_{11}, S_{22}, S_{33}), \tag{41}$$

where $S_{\alpha\alpha}(\alpha = 1, 2, 3)$ are calculated analytically from Eq. (39). They are given by

$$\begin{aligned}
S_{11} = S_{22} &= 4\frac{\lambda_1\lambda_3}{\lambda_1+\lambda_3}|\omega|^2 + 4\frac{\lambda_1\lambda_4}{\lambda_1+\lambda_4}|\varkappa|^2 + 4\frac{\lambda_2\lambda_3}{\lambda_2+\lambda_3} + \frac{\lambda_2\lambda_4}{\lambda_2+\lambda_4}|\omega|^2, \\
S_{33} &= 4\frac{\lambda_3\lambda_4}{\lambda_3+\lambda_4}|\omega^*\varkappa - 1|^2.
\end{aligned} \tag{42}$$

where λ_i ($i = 1, \ldots, 4$), ω and $\varkappa$ are given in Eqs. (16) and (18), respectively. Moreover, we have $S_{12} = S_{21} = S_{23} = S_{32} = S_{13} = S_{31} = 0$. Interestingly enough, one of the most important properties of LQU in relation with LQFI is: given any unitary evolution, the LQU is majorized by LQFI as follows [22,23]

$$\mathcal{U}(\rho(t)) \leq \mathcal{I}(\rho(t), H) \leq Q(\rho(t)), \tag{43}$$

where $\mathcal{U}(\rho(t))$ and $Q(\rho(t))$ are the LQU and LQFI defined in Eqs.(25) and (40) , respectively. Moreover, $\mathcal{I}(\rho(t), H)$ denotes the skew information defined in Eq.(23).

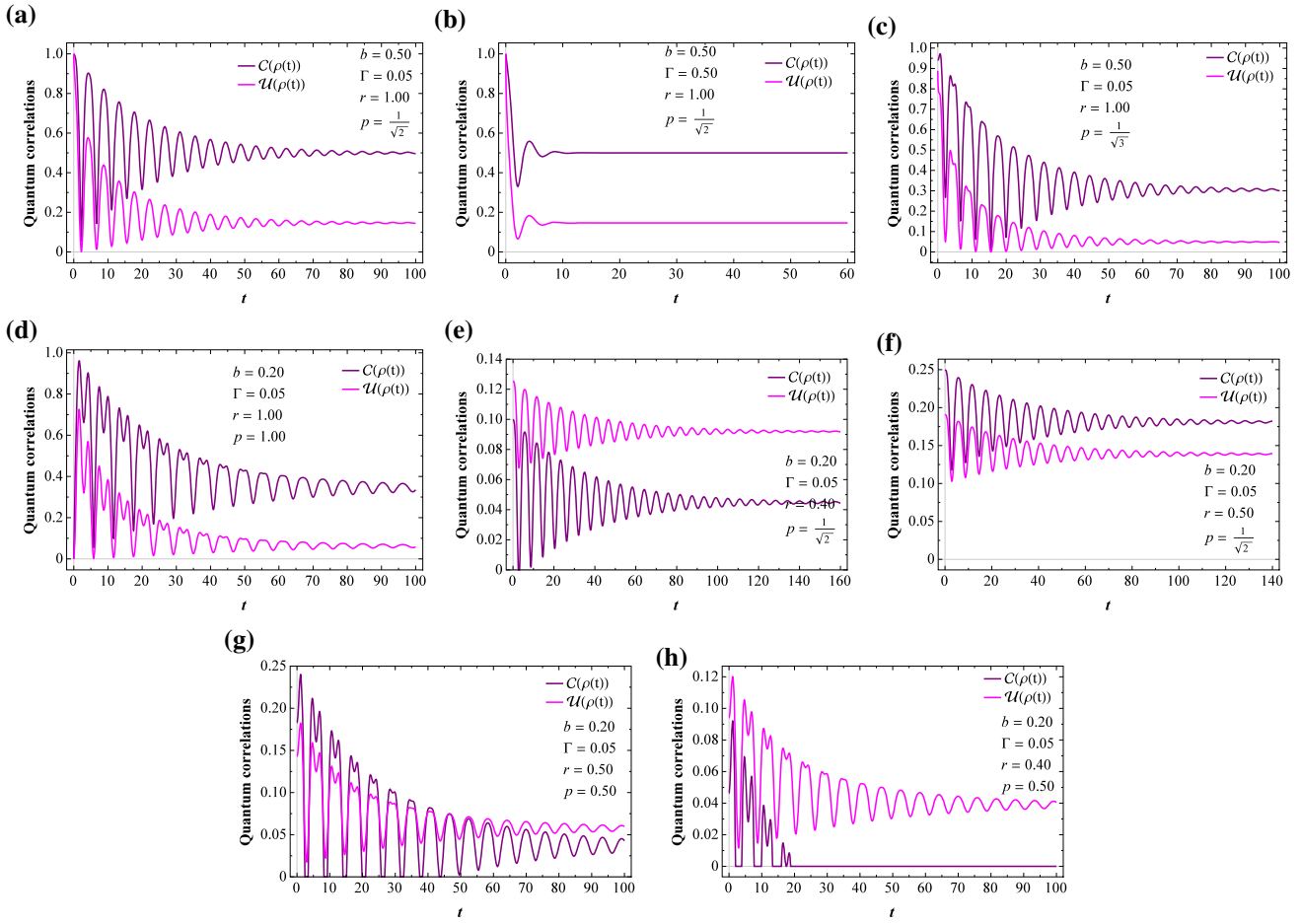


Fig. 1 Dynamics of quantum correlations versus time parameter t for several fixed values of purity parameter p and degree of entanglement r, assuming fixed $J = 1$

4 Analysis of quantum correlations evolution

To get an insight into the dynamics of the bipartite quantum correlations for the model under intrinsic decoherence, we have plotted in Fig. 1 the temporal evolution of the concurrence $\mathcal{C}$ and local quantum uncertainty (LQU) for several values of the purity r and the entanglement degree parameter p and we considered the following value of $J = 1$. Figure 1a, b depicts the behaviors when $r = 1$ and $p = 1/\sqrt{2}$ corresponding to the case where the system is initially prepared in the maximally entangled pure state; $|\phi\rangle = \frac{1}{\sqrt{2}}(|01\rangle + |10\rangle)$. In this case, for $t = 0$, both measures $\mathcal{C}$ and LQU are maximal $\mathcal{C} = 1$ and $\mathcal{U} = 1$, which means that two-qubit are maximally entangled. Moreover, both quantum correlations quantifiers decrease during the decoherence process. When $\Gamma = 0.05$ (Fig. 1a), the LQU shows a set of damping oscillations with series of revival and collapse phenomena over time with an asymptotic limit. All measures reach a steady-state value, which means that the amount of quantum correlation is frozen for specific intervals of time. Note that the time variations for the concurrence $\mathcal{C}$ show large amplitudes compared to those displayed for LQU. Figure 1b shows also that large numbers of the intrinsic decoherence rate ($\Gamma = 0.50$) accelerate the stabilization of correlations at the same steady-state values. Further, the two-qubit state exhibits frozen dynamics for both measures. On the other hand, the oscillatory behavior of parameters is almost disappeared due to the intrinsic decoherence effect. The increment of the decoherence intrinsic rate Γ causes fast correlations measures decay and shows that the intrinsic decoherence plays a destructive effect on the quantum correlations. As we mentioned, the steady-state value does not depend on Γ, but it depends on the system's initial state.

Figure 1c shows the evolution of parameters $\mathcal{C}$ and LQU when the system is initially in a pure Bell-shaped state ($r = 1$) with $p = 1/\sqrt{3}$. This case corresponds to the state $\rho(0) = |\phi\rangle\langle\phi|$ with $|\phi\rangle = \frac{1}{\sqrt{3}}(|01\rangle + \sqrt{2}\,|10\rangle)$. Figure 1c shows that the LQU reaches its maximum value at $t = 0$, whereas the concurrence has a minimum value at which the time parameter t is close to absolute zero. Besides, we can also see that the concurrence has a sharp maximum positioned around $t \approx 1$. However, the maximum bound of the concurrence is higher than LQU. When the dynamic is switched on, both quantifiers decrease following the same behaviors as plotted in Fig. 1a, b but with many oscillations frequencies of the amount of quantum correlations between the two-qubit. It is clear, the robust value of the amplitude of those functions asymptotically decreases. Moreover, the frozen phenomenon appears also in

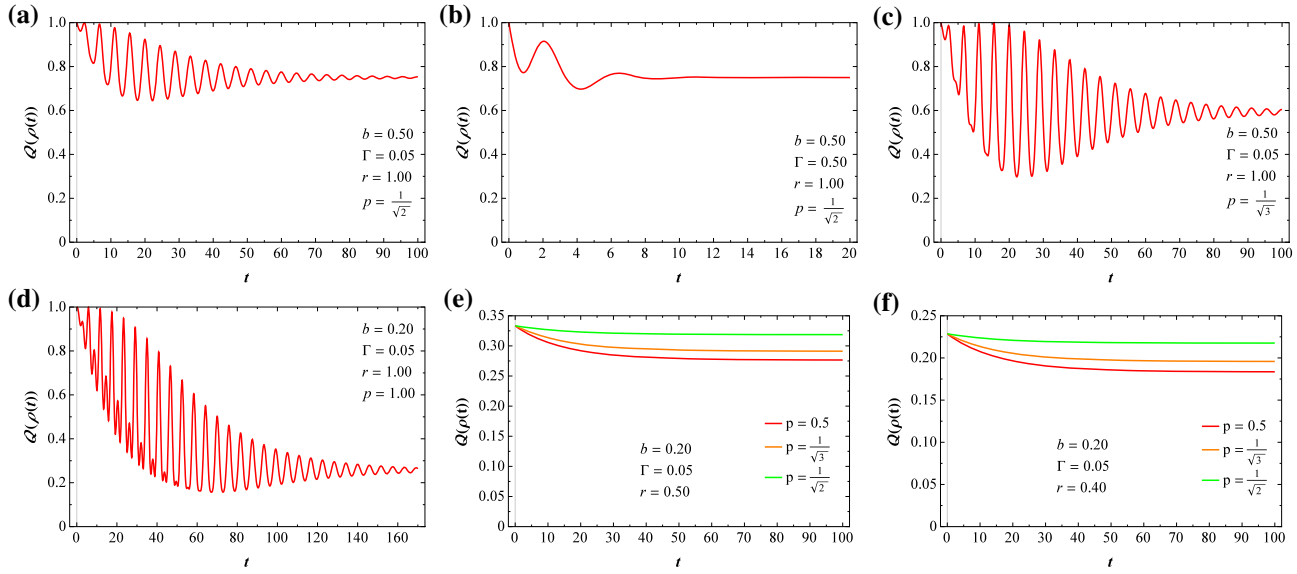


Fig. 2 Dynamics of local Fisher information versus the time parameter t for several fixed values of purity parameter p and degree of entanglement r, assuming fixed $J = 1$

this pure state. Figure 1d shows the evolution of $\mathcal{C}$ and LQU versus the time, when the system is initially separable $p = 1$ (i.e., $\rho(0) = |01\rangle\langle 01|$), at $t = 0$ there are no quantum correlations between the qubits. However, with time increasing, the quantum correlations between two spin-1/2 qubits can be generated by the time evolution of the state under the Hamiltonian (1), implying that the spin–spin interaction is responsible for the induced correlation between the qubits by a series of entanglement revival and collapse phenomena. This conclusion is also similar to the results reported in Ref. [51] where the generation of non-classical correlations is due to the coupling parameter between an atomic system interacting with a single mode of radiation field inside a quantum electrodynamics cavity, in such a way large numbers of the coupling parameter allow in general to increase gradually quantum correlations. Further, the dynamics of concurrence differ from the LQU. The amplitudes of the concurrence $\mathcal{C}$ are always larger than those obtained for LQU. Moreover, the LQU stabilizes for a particular time interval, which means that the LQU is frozen. The LQU correlations are more stable than the concurrence (the LQU stabilizes at a steady-state value lower than the concurrence). By fixing the degree of entanglement at the value $p = 1/\sqrt{2}$, the state (10) turns out to be the Werner state. From equation (21), one can see that when the purity r is ranging between 0.3 and 1, the system is initially entangled, otherwise it is disentangled. We notice that even if the system is separable ($\mathcal{C} = 0$ for $0 \leq r \leq 1/3$), the LQU remains nonzero. It implies that quantum entanglement is only a special kind of quantum correlation and even separable states possess the quantum correlations.

Figure 1e, f shows the time evolution of the concurrence and LQU for $r = 0.4$ and $r = 0.5$, respectively, when the Werner state is considered as the initial state. Figure 1e, f indicates that the LQU takes a maximum bound comparing to the concurrence when $r = 0.4$, but when the purity switches to $r = 0.5$ the concurrence is larger than the LQU. At $t = 0$, both qubits are partially entangled. When the dynamics is switched on the quantum correlations decrease until reaching a constant value. From Fig. 1e, it is clear that the concurrence vanishes instantly for particular time values. For these particular values, the disentangled two qubits have non-zero LQU. The amplitudes of the parameter $\mathcal{C}$ are always larger than those displayed for the LQU, even if the LQU predominates over $\mathcal{C}$. By comparing the results of Fig. 1f with Fig. 1e, we can conclude that the increase of the purity r leads to the correlations enhancement as well as their robustness against the decoherence. The oscillations frequencies become more prominent for the two-qubit system as the purity strength r decreases. The time evolution of the concurrence and LQU, when the system is initially prepared in the mixed state, are shown in Fig. 1g, h, respectively, in the case when $r = 0.4$ and $r = 0.5$. They show different behaviors compared to those shown for concurrence and LQU in the previous cases. For the initially mixed state, we observed that the dynamics under intrinsic decoherence cause entanglement sudden death, while LQU quantity is more robust than entanglement. This indicates that there exists locality by means of LQU even in the absence of entanglement between the subsystems. The amplitudes of the concurrence are always larger than those of the LQU. The phenomena of sudden death and growth of entanglement appear in the behavior of the concurrence entanglement, where the two qubits have a non-zero LQU correlation. Both quantifiers reach a steady-state demonstrating the frozen phenomenon. Interestingly, when the purity switches to $r = 0.4$, the entanglement oscillates at a particular time interval and after some time the entanglement between the qubits remains zero and it is known as the sudden death of entanglement. On the other hand, the LQU keeps the same behavior as plotted in Fig. 1g. Thus, from Fig. 1, we conclude that the LQU correlation is more stable than the concurrence. The stability of the generated correlations is enhanced. The frozen LQU and $\mathcal{C}$ show a robust feature against the intrinsic decoherence.

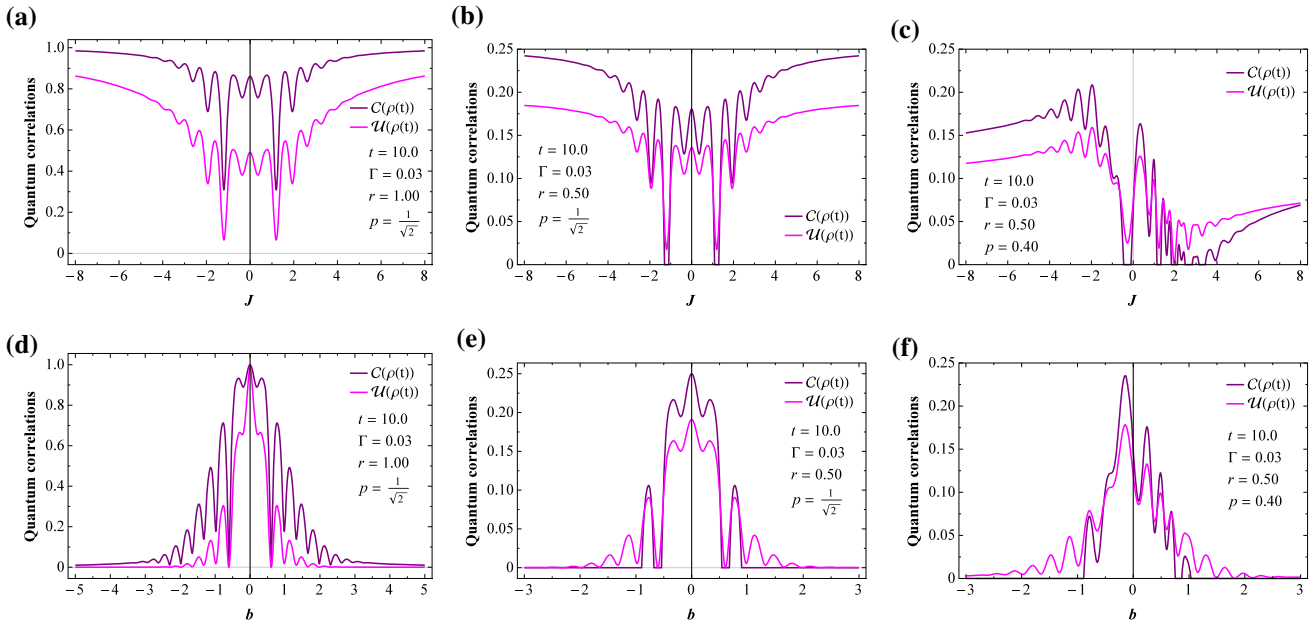


Fig. 3 Upper panels: dynamics of quantum correlations as a function of the exchange coupling parameter J when the system is initially prepared in the maximally entangled state (**a**), in the Werner state (**b**), and in the mixed state (**c**), taking $b = 0.20$, $t = 10$ and $\Gamma = 0.03$. Lower panels: dynamics of quantum correlations as a function of the inhomogeneous magnetic field b when the system is initially prepared in the maximally entangled state (**d**), in the Werner state (**e**), and in the mixed state (**f**), taking $J = 1$, $t = 10$ and $\Gamma = 0.03$

Figure 2 displays the dynamical evolution of LQFI versus the time t for different initial settings of b, r, p and Γ. In the case when $r = 1$ and $p = \frac{1}{\sqrt{2}}$, corresponding to a maximally entangled state, the state $\rho(t)$ defined in Eq.(14) is initially maximally entangled state since the LQFI reaches its maximum for $t = 0$. Under decoherence effects, the LQFI decreases gradually to stabilize for a specific interval of time which means that the LQFI becomes frozen. Moreover, it is clear that for small values of decoherence parameter Γ (Fig. 2a) gives oscillating variation of quantum correlations similar to those displayed for higher values of Γ (See Fig. 2b) which allows to enhance the stability of quantum correlations by means of LQFI. On the other hand, it is clear that even in the presence of decoherence phenomenon, the sudden death phenomenon does not occur. In Fig. 2c, d, we analyze the LQFI quantifier for a pure state, namely $r = 1$ and $p \neq \frac{1}{\sqrt{2}}$. As it can be seen, the LQFI follows the same behaviors as in Fig. 2a, b but with many oscillations frequencies of the quantum correlations between the two-qubit system. Again, it is clear that the presence of decoherence phenomenon doesn't possess the sudden death phenomenon but leads to froze the LQFI for large values of t. However, Fig. 2e, f shows the evolution of non-classical correlations by means of LQFI for different values of p. Indeed, for $p = \frac{1}{\sqrt{2}}$, the state is simply the Werner state. In this case, it is clear that both the oscillation correlations and the sudden death phenomena don't occur while the frozen phenomenon appears fast. The entanglement sudden death does not necessarily mean the loss of all quantum correlations. As separate states nevertheless have an advantage over classical states, thus they are still relevant for protocols that exploit quantum correlations other than entanglement. However, an efficient information processing protocol based on the local quantum Fisher information offers more resistance to the effect of intrinsic decoherence and is completely different from that of entanglement.

From Figs. 1 and 2, it is clear that in most of the above-cited cases, the non-classical correlations quantified by means of LQFI and LQU and the entanglement measure in terms of concurrence follow the same behavior but different upper bounds and various oscillations correlations. Moreover, it is obvious that the sudden death and the sudden growth phenomena appear in the LQU and concurrence behaviors while they don't occur for LQFI. On the other hand, the amplitudes of LQFI are always robust than those displayed for LQU and concurrence. The results discussed above show that the local quantum Fisher information is always greater than the LQU and the concurrence. This agrees with the results given by the inequality (40).

An interesting topic is to investigate an overall insight into the influence of the inhomogeneous magnetic field and the coupling coefficients, namely b and J, respectively, on the dynamics of concurrence and local quantum uncertainty. Indeed, in Fig. 3a–c and Fig. 3e–g, we investigate the evolution of the $\mathcal{C}$ and LQU for the system which is initially prepared in the maximally entangled state, in the Werner state, and in the mixed state as a function of parameters and J, respectively. The time and the intrinsic rate have been fixed at $t = 10$ and $\Gamma = 0.03$. When the system is initially prepared in the maximally entangled state, it is clear from Fig. 3a that the concurrence and LQU are symmetric with respect to $J = 0$. As $|J|$ increases, both quantifiers show oscillations until reaching a maximal asymptotic constant value. This shows that the coupling J enhances the amount of quantum correlations in the system. We notice that both measures have similar behavior but with different amplitudes; therefore, they can give the same information about

the correlations of the qubits and they present a freezing phenomenon for higher values of $|J|$ (the amount of quantum correlations is constant).

From Fig. 3a, it is quite clear that the concurrence is more robust than LQU when the initial states of qubits are maximally entangled. For the case of the Werner state Fig. 3b when $r = 0.5$ and $p = 1/\sqrt{2}$, the entanglement quantified by the concurrence and LQU have similar behavior as shown in Fig. 3a. For particular values of J ($|J| = 1.5$), the concurrence exhibits the phenomena of sudden death and growth entanglement, while the two qubits have non-zero LQU. The concurrence and LQU present an unusual behavior (see Fig. 3c) when the system is initially prepared in the mixed state. First, both measures are not symmetric with respect to $J = 0$. Both quantifiers have more oscillations frequencies in the antiferromagnetic phase ($J > 0$). The concurrence shows the death and growth phenomena with an increase of coupling constant until it reaches a steady state, while the LQU decreases gradually with a tendency of stabilization. Note that the maximum values achieved by LQU are larger than those displayed for entanglement. In the ferromagnetic phase ($J < 0$), for a particular point, $\mathcal{C}$ shows the death and growth phenomenon and then continues to oscillate until it stabilizes. The asymptotic value reached for the antiferromagnetic phase ($J > 0$) is higher than one evaluated for the ferromagnetic phase ($J < 0$). This is due to the ground-state phase transition in the Heisenberg XXZ spin chain H (1) [3,29]. As a result, the quantum correlations in the ferromagnetic phase are most robust than those given in the anti-ferromagnetic phase, when the system is initially prepared in the mixed state. The ferromagnetic property enhances the quantum correlations in the two-qubit system. On the other hand, introducing J into a constructive domain could generate and improve the quantum correlations in the system. This result can be understood as follows: the information between two spin-1/2 qubits is controlled by different parameters in Heisenberg spin chain systems. Some proportionally while some negatively affect the information as well as other correlations between them. One of the parameters, regulating the exchange coupling, directly increases the information transfer rate between the two qubits. Thus, the two qubits become more entangled and correlated as the exchange coupling parameter strength increase and vice versa.

Figure 3d presents the effect of the inhomogeneous magnetic field on the concurrence and LQU for $r = 1$ and $p = 1/\sqrt{2}$. It is clear that the $\mathcal{C}$ and LQU reach their maximum ($\mathcal{C} = 1$ and $\mathcal{U} = 1$) for $b = 0$ and the qubits are maximally correlated. Both quantifiers exhibit sudden revival and collapse phenomena which manifests themselves in increasingly weak peaks as $|b|$ increases. LQU collapses faster than $\mathcal{C}$, which decreases very slowly. This indicates that the LQU is more sensitive to the inhomogeneous magnetic field than $\mathcal{C}$ when the system is prepared in the maximally entangled state. When the system is prepared in the Werner state (Fig. 3e), the concurrence and LQU have nearly the same behavior as plotted in Fig. 3d, except that the concurrence collapses fast for a small period of time which indicates the phenomenon of entanglement sudden death (ESD). This surprising behavior was reported in [52]. The LQU keeps a non-zero value, decreases with oscillations, and becomes zero with an increase of $|b|$, but without any revival. It is attractive that when $r = 0.5$ and $p = 1/\sqrt{2}$ (Werner case), the LQU is more robust than entanglement. Indeed, our numerical analysis corroborates the results reported in Refs [53–55]. In fact the authors showed that that for all states, with non zero discord, the interaction with any Markovian bath can never lead to a sudden and permanent vanishing of discord and the entanglement sudden death phenomenon is then explained by the existence of separability.

Figure 3e shows that the inhomogeneous magnetic files b have a destructive effect on the quantum correlations. When the system is initially prepared in the mixed state Fig. 3f, the concurrence and LQU are not symmetric relative to $b = 0$. The height of the amplitude of these functions considerably decreases as $|b|$ increases. When $b > 0$, the concurrence exhibits a death and revival process for a certain interval of b. Then for large values of $|b|$ indicates the phenomenon of entanglement sudden death. In the negative range of b, the concurrence oscillates gradually as $|b|$ decrease and then suddenly disappears. The LQU continues with tiny oscillations without death and revival phenomena until the system reaches a steady state at a value very close to zero. Besides, the bipartite quantum correlations are more robust in the region when $b < 0$. This is due to the fact that in the negative regimes of the external inhomogeneous magnetic field, the relative effects will be such that the correlations between the sub-systems of the composite state are disturbed the least as compared to that in the positive regimes of the field. Thus, the optimal value of the magnetic field strength where the system remains more correlated is $b < 0$. This sudden change in quantum correlations behavior in the two-qubits state can be used to achieve optimal procedure for choosing the measurement operators [56,57] to investigate specific regions of interest where the system will remain less disturbed and thus more correlated. In the case when the system is initially prepared in the mixed state, we observed less deformation in quantum correlations in the two-qubits system in the region $b < 0$. Therefore, Fig. 3 shows the destructive effect of the inhomogeneous magnetic field b on the correlations of the system. This behavior is predictable since the dynamics of the concurrence and LQU are severely affected by the inhomogeneous magnetic field and intrinsic decoherence which play a negative role in inhibiting decoherence. Very particularly, the external degree of freedom (magnetic field, environment coupling) degrades the property of the quantum system.

In Fig. 4, the LQFI is plotted against the spin interaction strength parameter J including: the anti-ferromagnetic range ($J > 0$) and ferromagnetic range ($J < 0$) and also versus the degree the field inhomogeneity b. Similarly to the LQU and concurrence behaviors, in the first region ($J < 0$) the LQFI decreases gradually to reaches its minimum values at $J = 0$, while in the second region ($J > 0$), it increases suddenly to achieve again the maximum value for large numbers of J. However, the oscillating behavior of quantum correlations appears only for maximally entangled state, namely $r = 1$ and $p = \frac{1}{\sqrt{2}}$ (See Fig. 4a, d), while for the Werner state ($p = \frac{1}{\sqrt{2}}$), then the oscillation correlations disappears totally. However, the evolution of LQFI against the parameter b is given in the plots Fig. 4d–f. Obviously, in the case of a maximally entangled state (Fig. 4d), the plot shows many the oscillations of correlations. Roughly speaking, in the first region, namely ($b < 0$) the amount of LQFI are reduced asymptotically from its

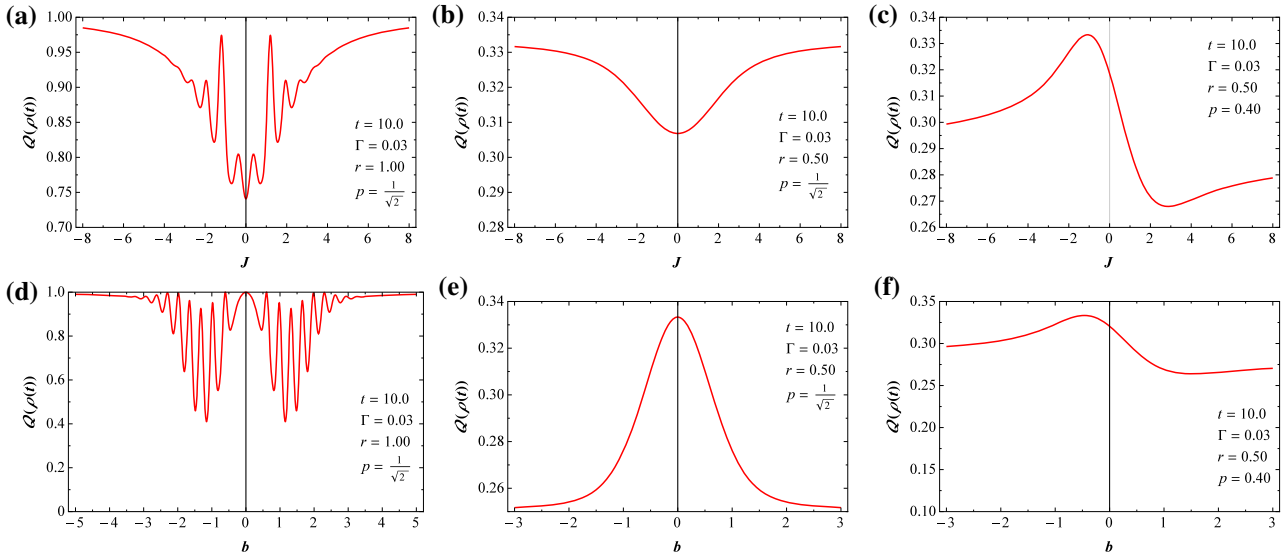


Fig. 4 Upper panels: dynamics of local quantum Fisher information as a function of the exchange coupling parameter J when the system is initially prepared in the maximally entangled state (**a**), in the Werner state (**b**), and in the mixed state (**c**), taking $b = 0.20$, $t = 10$ and $\Gamma = 0.03$. Lower panels: dynamics of local quantum Fisher information as a function of the inhomogeneous magnetic field b when the system is initially prepared in the maximally entangled state (**d**), in the Werner state (**e**), and in the mixed state (**f**), taking $J = 1$, $t = 10$ and $\Gamma = 0.03$

Table 1 A comparative study between LQU, LQFI, and concurrence

Initial states	Sudden death	Sudden birth	Oscillations correlations	Frozen correlations
Pure state	LQU	None	LQU, C and LQFI	LQU, C and LQFI
Werner state	LQU and C	LQU and C	LQU and C	LQU, C and LQFI
Maximally entangled state	LQU	LQU, C and LQFI	LQU, C and LQFI	LQU, C and LQFI
Mixed state	LQU and C	LQU and C	LQU, C and LQFI	LQU, C and LQFI

maximum bound and suddenly increases to achieve again the maximum value for $b = 0$. In the second region, namely $b > 0$ the LQFI decreases gradually and achieve the maximum peak for large numbers of the parameter b. Again in the case of Werner state, the oscillations of the correlations and sudden-death phenomena don't occur and the maximum correlations are obtained around $b = 0$. The frozen LQFI phenomenon occurs for small values of p (See Fig. 4f). As it can be seen from this figure, the LQFI bounds are always greater than LQU and concurrence. From the discussion above, we conclude that the exchange coupling parameter induces quantum correlations between two qubits in contrast to the inhomogeneous magnetic field as well as the intrinsic decoherence rate loss of the quantum correlations. This means that there exists a competition between the Heisenberg exchange coupling coefficient and the inhomogeneous magnetic field as well as the intrinsic decoherence.

The influences of the initial states, the exchange coupling parameter, inhomogeneous magnetic field, and the intrinsic decoherence rate on the dynamics of non-classical correlations have been investigated in detail. Our findings show that the dynamics of the entanglement termed by the concurrence, local quantum uncertainty, and local quantum Fisher information are strongly dependent on the forms of initial states. Our numerical results corroborate the results reported in [34,58]. When the system is initially prepared in a Werner-like state (10), the dynamical behaviors of these quantum correlation measures are independent of the external magnetic field B and the exchange anisotropy parameter Δ. The dynamical behaviors of the mentioned quantifiers exhibit damped oscillations with respect to time. While for initial product state (i.e., $\rho(0) = |01\rangle\langle 01|$), the concurrence and LQU can be created due to the spin–spin coupling interaction.

The following Table 1 summarizes the four generated phenomena already pointed out, namely sudden death, sudden birth, oscillation correlations, and frozen correlations phenomena in the case pure, Werner, maximally entangled, and mixed states.

Finally, since the density operator $\rho(t)$ is an entangled and maximally entangled state for some critical values of t, b and J, namely $t = 0$ and large numbers of J and b, then it would be very motivated to consider it as a quantum channel in order to implement a protocol of quantum teleportation under local-time dynamics and in the presence of intrinsic decoherence effect. In this sense, we shall examine in the next session the non-classical correlations by means of LQFI and LQU and the entanglement measure in terms of concurrence of the teleported state, namely $\rho_{out}(t)$ given by Eq.(47).

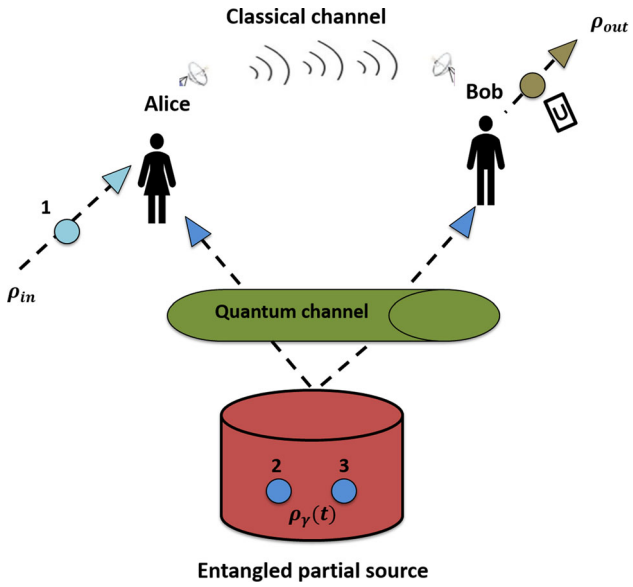


Fig. 5 The scheme of quantum teleportation using $\rho(t)$ as an entangled partial source, where U is the unitary operation required to restore the input state $\rho_{\text{in}}(t)$. The teleported output state is denoted by $\rho_{\text{out}}(t)$

5 Quantum teleportation

In this section, we implement a scheme of quantum teleportation using, as a resource, an entangled mixed state. Indeed, according to Bowen et al [59–61], the scheme of quantum teleportation with arbitrary two-qubit mixed states can be regarded as a general depolarizing quantum channel. The significant results of this work are shown in the ability to take into account the mixed teleported states, except in the case of a maximally entangled channel. Next, we investigate the effects of the intrinsic decoherence phenomenon on the transmission of information shared between a two-partners, namely Alice and Bob using the obtained density operator $\rho(t)$ in Eq.(14) as a quantum channel (See Fig. 5). Assume that the input state being the following arbitrary unknown two-qubit pure state $||\psi_{in}\rangle\rangle$

$$||\psi_{\text{in}}\rangle\rangle = \cos\left(\frac{\theta}{2}\right)||10\rangle\rangle + e^{i\phi}\sin\left(\frac{\theta}{2}\right)||01\rangle\rangle\,, \tag{44}$$

where $\theta \in [0,\pi]$ and $\phi \in [0,2\pi]$ denote the amplitude and the phase of the input state, respectively. After some straightforward calculations, the concurrence of the input state $\rho_{in} = ||\psi_{in}\rangle\rangle\,\langle\langle\psi_{in}||$ turns out to be

$$\mathcal{C}_{\text{in}} = |\sin(\theta)|. \tag{45}$$

From the mathematical point of view, the quantum channel is known as a completely positive and trace-preserving operator. Via this mechanism, an input density operator is mapped to an output density operator [59–61]. When the quantum state is teleported through the mixed channel ρ_{ch}, the output replica state ρ_{out} can be obtained by applying a joint measurement and local unitary transformation to the input state ρ_{in} [59–62], hence

$$\rho_{\text{out}} = \sum_{\mu,\nu=0}^{3} p_{\alpha\beta}(\sigma^{\mu}\otimes\sigma^{\nu})\rho_{\text{in}}(\sigma^{\mu}\otimes\sigma^{\nu}), \tag{46}$$

where $\sigma^0 = I$ (I defining 2×2 identity matrix). The joint probabilities are $p_{\mu\nu} = p_\mu p_\nu$,where $p_\mu = \text{Tr}(E^\mu\rho(t))$ satisfy the condition $\sum_{\mu,\nu} p_{\mu\nu} = 1$. The projective measurements are defined by; $E^0 = \big||\Psi^-\rangle\big\rangle\big\langle\langle\Psi^-|\big|$, $E^1 = \big||\Phi^-\rangle\big\rangle\big\langle\langle\Phi^-|\big|$, $E^2 = \big||\Psi^+\rangle\big\rangle\big\langle\langle\Psi^+|\big|$, and $E^3 = \big||\Phi^+\rangle\big\rangle\big\langle\langle\Phi^+|\big|$, where $\{\big||\Psi^\pm\rangle\big\rangle, \big||\Phi^\pm\rangle\big\rangle\}$ are the well-known Bell states. Therefore, the density operator of the output state ρ_{out} can be calculated straightforwardly from Eq.(46). Indeed, it takes the following matrix form

$$\rho_{\text{out}}(t) = \begin{pmatrix} \widetilde{\rho}_{11}(t) & 0 & 0 & 0 \\ 0 & \widetilde{\rho}_{22}(t) & \widetilde{\rho}_{23}(t) & 0 \\ 0 & \widetilde{\rho}^{*}_{23}(t) & \widetilde{\rho}_{33}(t) & 0 \\ 0 & 0 & 0 & \widetilde{\rho}_{11}(t) \end{pmatrix}, \tag{47}$$

where

$$\widetilde{\rho}_{11}(t) = (\rho_{11}(t)+\rho_{44}(t))(\rho_{22}(t)+\rho_{33}(t)),$$

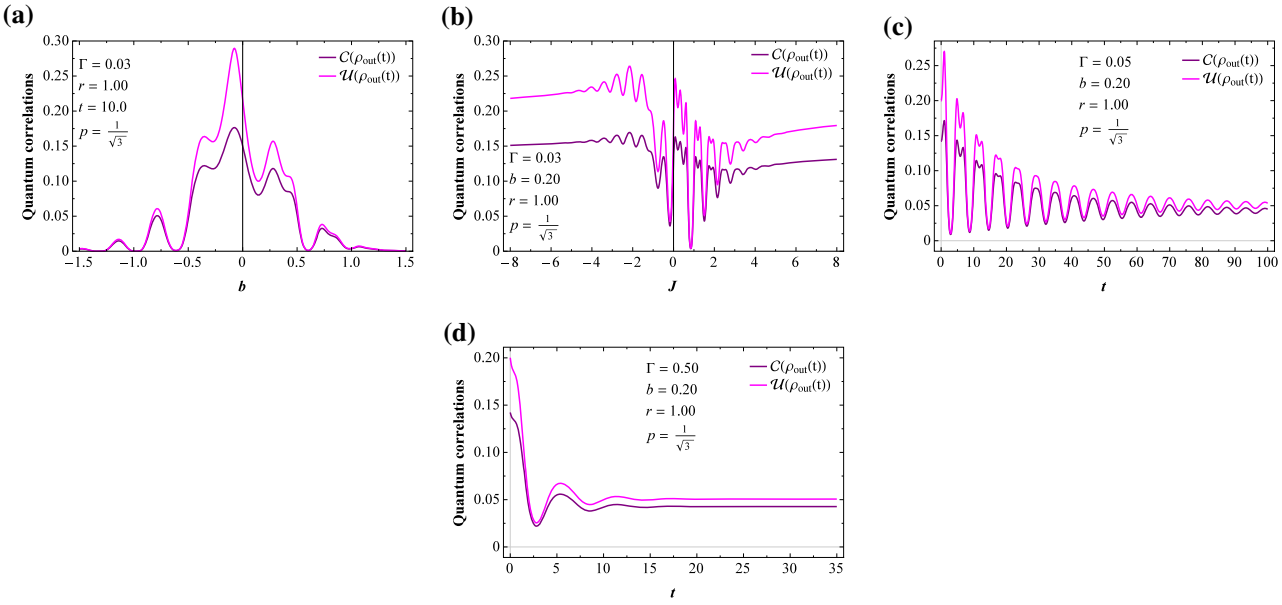


Fig. 6 The dynamics of quantum correlation quantifiers for the output state ρ_{out} versus the inhomogeneous magnetic field b for the parameter set $J = 1$, $t = 10$, and $\Gamma = 0.03$ when the system is initially prepared in the pure state (**a**). The exchange coupling dependence of the dynamics of quantum correlation and fixed $b = 0.20$. The same quantifiers as a function of the time parameter t by assuming $J = 1$ and $b = 0.20$ when $\Gamma = 0.05$ (**c**) and $\Gamma = 0.5$ (**d**)

$$\widetilde{\rho}_{22}(t) = (\rho_{11}(t) + \rho_{44}(t))^2 \cos^2\left(\frac{\theta}{2}\right) + (\rho_{22}(t) + \rho_{33}(t))^2 \sin^2\left(\frac{\theta}{2}\right),$$
$$\widetilde{\rho}_{33}(t) = (\rho_{11}(t) + \rho_{44}(t))^2 \sin^2\left(\frac{\theta}{2}\right) + (\rho_{22}(t) + \rho_{33}(t))^2 \cos^2\left(\frac{\theta}{2}\right),$$
$$\widetilde{\rho}_{23}(t) = 2e^{i\phi}\rho_{23}(t)\sin\theta.$$

We first consider the dynamical evolution of quantum correlations quantifiers of the output state ρ_{out}, i.e., concurrence $\mathcal{C}(\rho_{\text{out}})$ and $\mathcal{U}(\rho_{\text{out}})$ when the system is in the pure entangled state ($r = 1$ and $p = 1/\sqrt{3}$) for fixed $J = 1$ and $\Delta = 0.5$ which are presented in Fig. 6. We plot in Fig. 6a the above-mentioned quantum correlations quantifiers as functions of the inhomogeneous magnetic field for $t = 10$. Both quantifiers have the same behavior, namely, they decrease from a typical maximum with the increase of $|b|$. The phenomena of sudden death and growth of entanglement also occur in the behavior of the concurrence and LQU in the output state. For higher values of the inhomogeneous magnetic field $|b|$, the output concurrence and LQU vanish indicating that there are no quantum correlations (the information between two-qubit is destroyed). Thus, in this situation ($|b| < 0.5$), the concurrence and LQU of the teleported state reach large amplitudes which are good for the success of the quantum teleportation protocol. However, for a sufficiently strong inhomogeneous magnetic field, the output concurrence and LQU gradually decrease, and the entangled state teleportation will not succeed anymore. We plot in Fig. 6b the concurrence and LQU versus the exchange coupling parameter J for $b = 0.20$. The quantum correlations in the output state behave like the results shown for the input state in Fig. 3c. Besides, as $|J|$ increases, both quantifiers oscillate with a tendency to reach a steady state. The frozen phenomenon appears in the output state, which means that information between two-qubit is secured. The output quantum correlations in the ferromagnetic phase predominate over the antiferromagnetic phase. From Fig. 6c, d, the effect of intrinsic decoherence rate is clearly seen through the oscillating behavior of the correlations as a function of time with large amplitudes for LQU. The sudden death phenomenon can be prevented by increasing Γ and at the early times lead to the same steady-state values of the correlations depicted in Fig. 6c. On the other hand, these results are compatible with the results in Fig. 1a for the input state, except that for the teleported state the LQU captures more information than concurrence. Further, we notice that quantum teleportation can be improved by increasing the intrinsic parameter Γ . Thus, we conclude that parameter Γ is an efficient control parameter of quantum communications. This is illustrated in Fig. 6d. According to our numerical calculations, we conclude that the LQU is more robust than concurrence for either input states or output states. In general, the LQU is a discord-like measure of quantum correlations this explains the robustness in comparison with the entanglement (concurrence) [46]. In this sense, LQU has a relevant application in the field of quantum metrology and quantum information processing. Therefore, it is desirable to investigate, characterize, and quantify quantum correlations more broadly.

Figure 7 examines the LQFI as a measure of non-classical correlations of the teleported state. It is clear that the teleported LQFI shows many oscillations for various values of b and r and the increase of the decoherence parameter, namely Γ allows to enhance the LQFI of the teleported state. Moreover, the frozen teleported LQFI appears again for some special values of J, b and

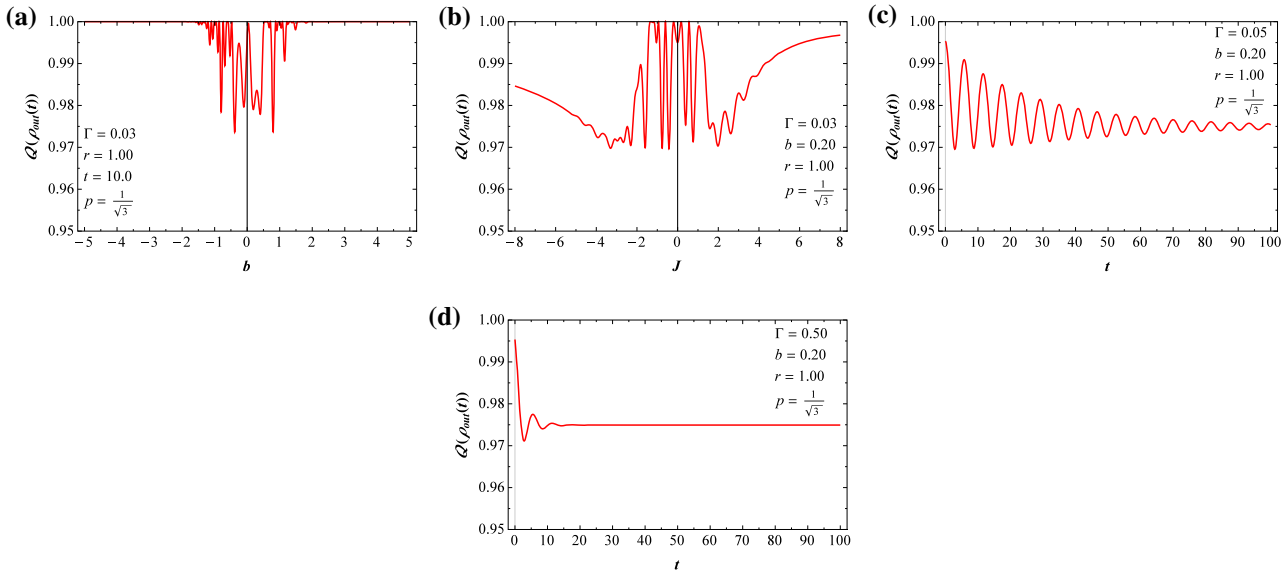


Fig. 7 The dynamics of local fisher information for the output state ρ_{out} versus the inhomogeneous magnetic field b for the parameter set $J = 1$, $t = 10$, and $\Gamma = 0.03$ when the system is initially prepared in the pure state (**a**). The exchange coupling dependence of the dynamics of LQU and fixed $b = 0.20$. The same quantifiers as a function of the time parameter t by assuming $J = 1$ and $b = 0.20$ when $\Gamma = 0.05$ (**c**) and $\Gamma = 0.5$ (**d**)

t. Moreover, it appears fast in the case when Γ takes large values (See Fig. 7d) which indicates an emerging future of frozen LQFI under teleportation protocol in the presence of intrinsic decoherence effects.

6 The fidelity of entanglement teleportation

In order to estimate the quality teleportation process, it is often quite useful to study the fidelity between ρ_{in} and ρ_{out} to characterize the transmission credibility of the secure information shared between Alice and Bob. We note that when the input state is a pure state, we can apply the concept of fidelity as a useful indicator of the teleportation performance of a quantum channel [63]. The fidelity is determined by

$$\mathcal{F} = \left(\text{Tr}\sqrt{\sqrt{\rho_{\text{in}}}\rho_{\text{out}}\sqrt{\rho_{\text{in}}}}\right)^2, \tag{48}$$

We note that the fidelity is near zero if the input and the output state are orthogonal which implying that the information is completely destroyed during the transmission process and the teleportation fails. While it is close to unity if the input state and the output state are identical. In the case when $0 < \mathcal{F} < 1$ the quantum information is subjected to distortions after transmitting to some extent. Using Eq.(47), after a straightforward calculation, the fidelity is given by

$$\mathcal{F} = \frac{\sin^2\theta}{2}[(\rho_{11}(t) + \rho_{44}(t))^2 + 4\rho_{23}^2(t) - (\rho_{22}(t) + \rho_{33}(t))^2] + (\rho_{22}(t) + \rho_{33}(t))^2. \tag{49}$$

Since the parameters θ and ϕ are unknown, we calculate the average of the fidelity $\mathcal{F}_A$ over all the points of Bloch sphere. This is given by

$$\mathcal{F}_A = \frac{1}{4\pi}\int_0^{2\pi} \text{d}\phi \int_0^{\pi} \text{d}\theta \mathcal{F} \sin\theta, \tag{50}$$

which gives

$$\mathcal{F}_A = \frac{1}{3}[(\rho_{11}(t) + \rho_{44}(t))^2 + 4\rho_{23}^2(t) + 2(\rho_{22}(t) + \rho_{33}(t))^2]. \tag{51}$$

Obviously, the average fidelity $\mathcal{F}_A$ depends basically on the quantum channel parameters. To transmit the input state $|\psi_{\text{in}}\rangle$ with better fidelity than any classical communication protocol, $\mathcal{F}_A$ must exceed $\frac{2}{3}$, which is the maximum achievable for classical communication. Figure 8a, b shows the average fidelity against the exchange coupling parameter in the pure state and mixed state, respectively, for mixed values of $b = 0.20$, $\Gamma = 0.03$, and for $t = 10$ where several fixed values of the purity have been considered.

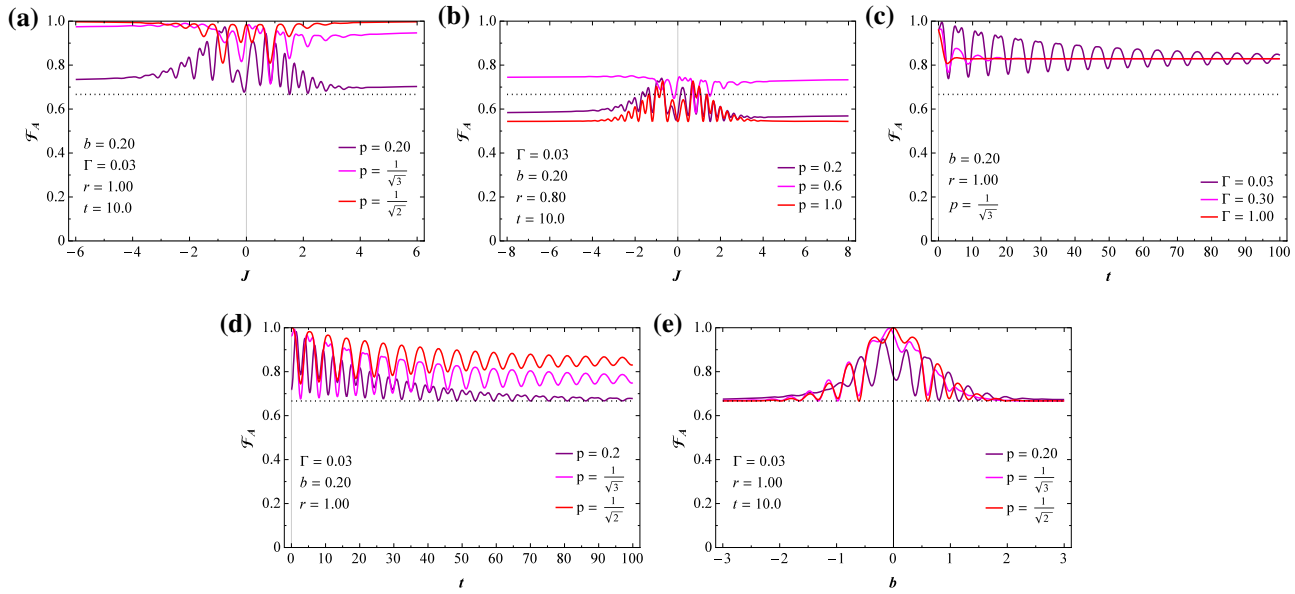


Fig. 8 $\mathcal{F}_A$ versus the exchange coupling coefficient, assuming $b = 0.20$, $t = 10$, and $\Gamma = 0.03$ and several fixed values of the degree of entanglement p, when the system is initially prepared in the pure state (**a**), in the mixed state (**b**). The time dependence of the average fidelity for various values of the intrinsic decoherence parameter (**c**), and the degree of entanglement parameter (**d**), where other parameters have taken as $b = 0.20$ and $r = 1$. $\mathcal{F}_A$ against the inhomogeneous magnetic field b when different fixed values of the magnetic field are considered such that $\Gamma = 0.03$ and $r = 1$

In these figures, the horizontal dashed lines at $\mathcal{F}_A = \frac{2}{3}$ denote the limit of quantum fidelities. When the system is initially prepared in the pure state ($r = 1$) (Fig. 8a), the average fidelity shows many oscillations as the parameter p decreases. Moreover, all curves eventually reach a steady state as the exchange coupling parameter increases, which means that the amount of average fidelity is frozen for a certain time. The inclusion of purity stimulates an increase in the average fidelity until reaching maximum fidelity ($\mathcal{F}_A = 1$). It is also observed that the quantum communication is enhanced with the increase of $|J|$ ($\mathcal{F}_A > 2/3$ represented as a dash-dotted line). In Fig. 8b, the plot shows that the teleportation will not succeed for $\mathcal{F}_A < 2/3$, because the system is initially in the interphase between the entangled state and the separable state in contrast to the situation when the system is prepared in the pure state Fig. 8a, the success of the teleportation depends on the purity parameter. For example, when $r = 0.80$ and $p = 0$, we have a dramatic increase of average fidelity and at lower values of the spin coupling, it reaches the maximum value and then decreases monotonically below $2/3$ as soon as $|J|$ increases. The average fidelity $\mathcal{F}_A$ remains below $2/3$, making it impossible for the existence of quantum teleportation of the information. In Fig. 8c, the evolution of the average fidelity $\mathcal{F}_A$ is plotted for certain values of the intrinsic decoherence parameter when the system is prepared in the pure state. As we can see, the average fidelity oscillates over time and reaches a stable value when time t approaches infinity. Larger the parameter Γ, while the shorter one is the time of reaching the stable values Fig. 8c. Moreover, the stable value remains always above $2/3$, which means that such teleportation through the two-qubit Heisenberg XXZ model is better than any classical communication protocol. When the system is in the initial pure state, the behavior of the average fidelity becomes more robust, enabling the teleportation of information in the regions of large value of intrinsic rate ($\Gamma = 1$). Therefore, the initial state and the parameters of the model are significant factors to determine what kinds of systems are suitable as a quantum channel. From these figures, we can see that the fidelity can reach the unity for $p = 1/\sqrt{2}$, which means that the channel is the two-qubit maximally entangled state, namely $|\phi\rangle = \frac{1}{\sqrt{2}}(|01\rangle + |10\rangle)$, and two-qubit states can always be teleported with a pair of EPR states which agrees with the results reported in [64]. Figure 8e shows the effects of the inhomogeneous magnetic field on the average fidelity when the system is initially prepared in a Bell-like state. The average fidelity achieves the maximum amount at $b = 0$ then gradually decreases as b increases to a critical value of $2/3$. The decay of the average fidelity as a function of b means that the inhomogeneous magnetic field b has unfortunately a destructive effect on the average fidelity. As a result, one conclude that the initial-parameters state of the channel plays an important role in the average fidelity of teleportation. It is found that when the initial state is entangled state $|\phi\rangle = \alpha\,|01\rangle + \beta\,|10\rangle$ the corresponding average fidelity is always larger than $2/3$ (a similar behavior was reported by N. Zidan in Ref. [58]).

7 Conclusions

In this work, we have demonstrated a straightforward analysis of the dynamics of a two-qubit system on the Heisenberg XXZ model under intrinsic decoherence. We first assumed that the system interacts with an external magnetic field, B with only nearest-neighbor

interactions. After exactly solving the time-independent master equation, we have investigated the dynamics of the concurrence, local quantum uncertainty and local quantum Fisher information in order to quantify the quantum correlations of this system. We have concluded that all these quantifiers oscillate similarly between their upper and lower bounds where in general the LQFI is more stable comparing to the LQU and concurrence. The sudden death, sudden birth, oscillations, and frozen correlations phenomena appear clearly for different initial settings. By making a comparative study between the dynamics of $\mathcal{C}$, LQU and LQFI, we have obtained some interesting outcomes. For example, the intrinsic decoherence destroys the oscillations of the correlations between the qubits. For the initially mixed state, we have concluded that the dynamics under intrinsic decoherence causes the sudden death phenomenon for some particular initial state settings, while both LQU and LQFI quantities resist the decoherence effect. This implies that the absence of entanglement does not necessarily mean the absence of non-classical correlations in the quantum states. Besides, the robustness and the generation of the quantum correlations depend on the physical parameters and the initial state as well. Further, our investigations emphasize that efficient information processing based on the LQU and LQFI offers more resistance to the effect of intrinsic decoherence and is completely different from the entanglement. Finally, we have examined the possibility of teleportation process through the model under consideration. We have showed that when the system is initially prepared in entangled state, the corresponding average fidelity is always larger than $2/3$, which means the success of the teleportation in contrast to the case when the system is initially in the interphase between the entangled state and the separable state. Indeed, the initial state of the channel plays an important role in the fully entangled fraction and the average fidelity of teleportation. In particular, we showed that the average fidelity achieves the maximum amount when the degree of inhomogeneity of the field vanishes. Moreover, large numbers of the decoherence parameter allow to enhance different quantities, namely teleported concurrence, LQU, LQFI, and fidelity. Therefore, one can conclude that different parameters encoded in the two-qubit Heisenberg XXZ model are an efficient control parameter of quantum communications.

In summary, it is possible to prepare an entangled mixed state arising from the interaction between a two-qubit open systems interacting with its environments under Markovian dynamics. These results can be used analytically and experimentally in many areas of secure communication, quantum information theory and quantum estimation theory. Our future perspective will concern other types of environments in order to investigate the crucial relationship between entanglement, LQU and LQFI in Markovian and also non-Markovian regimes and to extend the present work higher dimensional. Moreover, it will be motivated for us to take into account the influence of Dzyaloshinski–Moriya interaction on the dynamics of entanglement and quantum correlations. Indeed, in this context, Y-n. Guo et al [34] quantifies the quantum correlations by means of LQU of a two-qubit one-dimensional XYZ Heisenberg chain with Dzyaloshinski–Moriya interaction in thermal equilibrium, where interestingly enough they showed that for an initial separable state, the quantum correlations by means of LQU can be induced due to the Dzyaloshinski–Moriya interaction and Heisenberg anisotropic interaction.

References

1. A. Datta, A.T. Flammia, C.M. Caves, Entanglement and the power of one qubit. Phys. Rev. A **72**, 043216 (2005)
2. A. Datta, G. Vidal, Role of entanglement and correlations in mixed-state quantum computation. Phys. Rev. A **75**, 042310 (2007)
3. F. Benabdallah, A. Slaoui, M. Daoud, Quantum discord based on linear entropy and thermal negativity of qutrit-qubit mixed spin chain under the influence of external magnetic field. Quantum Inf. Process. **19**, 252 (2020)
4. M.A. Nielsen, I.L. Chuang, *Quantum Computation and Quantum Information* (Cambridge University Press, Cambridge, 2000)
5. M. Le Bellac, *A Short Introduction to Quantum Information and Quantum Computation* (Cambridge University Press, Cambridge, 2006)
6. A. Streltsov, H. Kampermann, S. Wölk, M. Gessner, D. Bruß, Efficient quantum state analysis and entanglement detection. New J. Phys. **20**, 053058 (2018)
7. A. Streltsov, G. Adesso, M.B. Plenio, Colloquium: quantum coherence as a resource. Rev. Mod. Phys. **89**, 041003 (2017)
8. C.H. Bennett, G. Brassard, C. Crepeau, R. Jozsa, A. Peres, W.K. Wootters, Teleporting an unknown quantum state via dual classical and Einstein–Podolsky–Rosen channels. Phys. Rev. Lett. **70**, 1895 (1993)
9. H.L. Huang, Quantum teleportation via a two-qubit Ising Heisenberg chain with an arbitrary magnetic field. Int. J. Theor. Phys. **50**, 70–79 (2011)
10. G.C. Fouokeng, E. Tedong, A.G. Tene, M. Tchoffo, L.C. Fai, Teleportation of single and bipartite states via a two qubits XXZ Heisenberg spin chain in a non-Markovian environment Phy. Lett. A **384**, 126719 (2020)
11. A.K. Ekert, Quantum cryptography based on Bell's theorem. Phys. Rev. Lett. **67**, 661 (1991)
12. C.H. Bennett, S.J. Wiesner, Communication via one- and two particle oprators on Einstein–Podolsky–Rosen states. Phys. Rev. Lett. **69**, 20 (1992)
13. R. Horodecki, P. Horodecki, M. Horodecki, K. Horodecki, Quantum etanglement. Rev. Mod. Phys. **81**, 865 (2009)
14. V. Vedral, The role of relative entropy in quantum information theory. Rev. Mod. Phys. **74**, 197 (2002)
15. O. Gühne, G. Tóth, Entanglement detection. Phys. Rep. **474**, 1 (2009)
16. K. Modi, A. Brodutch, H. Cable, T. Paterek, V. Vedral, The classical-quantum boundary for correlations: discord and related measures. Rev. Mod. Phys. **84**, 1655 (2012)
17. W.K. Wootters, Entanglement of formation for an arbitrary state of two qubits. Phys. Rev. Lett. **80**, 10 (1998)
18. D. Girolami, T. Tufarelli, G. Adesso, Characterizing nonclassical correlations via local quantum uncertainty. Phys. Rev. Lett. **110**, 240402 (2013)
19. M. Ali, Local quantum uncertainty for multipartite quantum systems. Eur. Phys. J. D **74**, 186 (2020)
20. E.P. Wigner, M.M. Yanasse, Informations contents of distributions. Proc. Nat. Acad. Sci. USA **19**, 910 (1963)
21. S. Luo, Using measurement-induced disturbance to characterize correlations as classical or quantum. Phys. Rev. A **77**, 022301 (2008)
22. S. Luo, Wigner–Yanase skew information and uncertainty relations. Phys. Rev. Lett. **91**, 180403 (2003)
23. S. Luo, Wigner–Yanase skew information vs. quantum fisher information. Proc. Am. Math. Soc. **132**, 885 (2003)
24. D. Petz, C. Ghinea, Introduction to quantum fisher information. Quantum Probab. Relat. Top. **1**, 261–281 (2011)

25. Y. Akbari-Kourbolagh, M. Azhdargalam, Entanglement criterion for multipartite systems based on quantum Fisher information. Phys. Rev. A **99**, 012304 (2019)
26. S. Haseli, Local quantum Fisher information and local quantum uncertainty in two-qubit Heisenberg XYZ chain with Dzyaloshinskii–Moriya interactions. Laser Phys. **30**, 105203 (2020)
27. A.B.A. Mohamed, E. Khalil, M.M. Selim, H. Eleuch, Quantum Fisher information and bures distance correlations of coupled two charge-qubits inside a coherent cavity with the intrinsic decoherence. Symmetry **13**, 2 (2021)
28. X. Hu, H. Fan, D.L. Zhou, W.-M. Liu, Necessary and sufficient conditions for local creation of quantum correlation. Phys. Rev. A. **85**, 032102 (2012)
29. F. Benabdallah, M. Daoud, Dynamics of quantum discord based on linear entropy and negativity of qutrit–qubit system under classical dephasing environments. Eur. Phys. J. D **75**, 3 (2021)
30. F. Benabdallah, H. Arian Zad, M. Daoud and N. Ananikian, Dynamics of quantum correlations in a qubit-qutrit spin system under random telegraph noise, Phys. Scr. **96** 125116 (2021)
31. K. El Anouz, A. El Allati, N. Metwally, Different indicators for Markovian and non-Markovian dynamics. Phy. Lett. A. **384**, 5 (2019)
32. A.-B.A. Mohamed, N. Metwally, Non-classical correlations based on skew information of entangled two qubit-system with non-mutual interaction under a intrinsic decoherenc. Ann. Phys. **381**, 137–150 (2017)
33. V. Abhignan, R. Muthuganesan, Effects of intrinsic decoherence on discord-like correlation measures of two-qubit spin squeezing model. Phys. Scr. **96**, 125114 (2021)
34. Y.-N. Guo, H.-P. Peng, Q.-L. Tian, Z.-G. Tan, Y. Chen, Local quantum uncertainty in a two-qubit Heisenberg spin chain with intrinsic decoherence. Phys. Scr. **96**, 075101 (2021)
35. A.B.A. Mohamed, A.H. Abdel-Aty, E.G. El-Hadidy, H.A.A. El-Saka, Two-qubit Heisenberg XYZ dynamics of local quantum Fisher information, skew information coherence: Dyzaloshinskii–Moriya interaction and decoherence. Results Phys. **30**, 104777 (2021)
36. L-P. Chen, Y-n. Gu, Dynamics of local quantum uncertainty and local quantum fisher information for a two-qubit system driven by classical phase noisy laser, J. Mod. Opt. **68**, 4 (2021)
37. B.-L. Ye, B. Li, X.-B. Liang, S.-M. Fei, Dynamics of local quantum uncertainty and local quantum Fisher information for a two qubit system driven by classical phase noisy laser. Inte J. Quatum Inf. **18**, 04 (2020)
38. G. Najarbashi, Seifi, B, Quantum phase transition in the Dzyaloshinskiiâ€Moriya interaction with inhomogeneous magnetic field: Geometric approach. Quantum Inf. Process. **16**, 40 (2017)
39. A. Karlsson, M. Bourennane, Quantum teleportation using three-particle entanglement. Phys. Rev. A. **58**, 4394 (1998)
40. J.C. Hao, C.F. Li, G.C. Guo, Controlled dense coding using the Greenberger–Horne–Zeilinger state. Phys. Rev. A. **63**, 054301 (2001)
41. A.-Z. Hamid, M. Hossein, Transferring information through a mixed-five-spin chain channel. Chin. Phys. B. **25**, 080307 (2016)
42. G. Milburn, Intrinsic decoherence in quantum mechanics. Phys. Rev. A **44**(9), 5401 (1991)
43. R.F. Werner, Quantum states with Einstein–Podolsky-Rosen correlations admitting a hidden-variable model. Phys. Rev. A **40**, 4277 (1989)
44. M. Asoudeh, V. Karimipour, Thermal entanglement of spins in an inhomogeneous magnetic field. Phys. Rev. A **71**, 022308 (2005)
45. M. Berman, R. Kosloff, H. Tal-Ezer, Solution of the time-dependent Liouville-von Neumann equation: dissipative evolution. J. Phys. A Math. Gen. **25**, 1283 (1992)
46. M. Ali, A.R.P. Rau, G. Alber, Quantum discord for two-qubit X states. Phys. Rev. A **81**, 042105 (2010)
47. C.W. Helstrom, *Quantum Detection and Estimation Theory* (Academic, New York, 1976)
48. G.A. Matteo, Paris, "Quantum estimation for quantum technology." Int. J. Quant. Inf. **7**, 125 (2009)
49. S.L. Braunstein, C.M. Caves, Statistical distance and the geometry of quantum states. Phys. Rev. Lett. **72**, 3439 (1994)
50. S. Kim, L. Li, A. Kumar, J. Wu, Characterizing nonclassical correlations via local quantum Fisher information. Phys. Rev. A. **97**, 032326 (2018)
51. K. El Anouz, I. El Aouadi, A. El Allati and T. Mourabit, Dynamics of quantum correlations in quantum teleportation, International Journal of Modern Physics B **34**, 10 2050093 (2020)
52. J.L. Guo, H.S. Song, Effects of inhomogeneous magnetic field on entanglement and teleportation in a two-qubit Heisenberg XXZ chain with intrinsic decoherence. Phys. Scr. **78**, 045002 (2008)
53. A. Ferraro, D. Cavalcanti, F.M. Cucchietti, A. Acín, Phys. Rev. A **81**, 052318 (2010)
54. K. Zyczkowski, P. Horodecki, A. Sanpera, M. Lewenstein, Phys. Rev. A **58**, 883 (1998)
55. S.L. Braunstein, C.M. Caves, R. Jozsa, N. Linden, S. Popescu, R. Schack, Phys. Rev. Lett. **83**, 1054 (1999)
56. T. Werlang, G. Rigolin, Thermal and magnetic quantum discord in Heisenberg models. Phys. Rev. A **81**, 044101 (2010)
57. J. Yang, Y. Huang, Tripartite and bipartite quantum correlations in the XXZ spin chain with three-site interaction. Quantum Inf. Process. **16**, 281 (2017)
58. N, Zidan, Quantum teleportation via two-qubit Heisenberg XYZ chain, Can. J. Phys. **92**, 406 (2014)
59. G. Bowen, S. Bose, Teleportation as a depolarizing quantum channel, relative entropy, and classical capacity. Phys. Rev. Lett. **87**, 267901 (2001)
60. Y. Yeo, Teleportation via thermally entangled states of a two-qubit Heisenberg XX chain, Phys. Rev. A **66**, 062312
61. Y. Zhou, G.F. Zhang, Quantum teleportation via a two-qubit Heisenberg XXZ chain-effects of anisotropy and magnetic field. Eur. Phys. J. D **47**, 227 (2008)
62. A. Peres, Separability criterion for density matrices. Phys. Rev. Lett. **77**, 1413 (1996)
63. R. Jozsa, Fidelity for mixed quantum states. J. Mod. Opt. **41**, 12 (1994)
64. L. Qiu, A.M. Wang, X.Q. Su, Effect of Dzyaloshinskill–Moriya anisotropic antisymmetric interaction and intrinsic decoherence on entanglement teleportation. Physica A **387**, 6686 (2008)

5 Contribution 5: Long-time protection of thermal correlations in a hybrid-spin system under random telegraph noise

Physical Review E, 106 (2022) 034122.

5.1 Summary of contribution 5

The properties of the medium that is that carry quantum information and how they affect different aspects of the quantum system have a significant impact on the success of remote protocols. Coupling medium dynamics with dynamics of open quantum systems is essential for good performance. In this study, we investigated the dynamics of quantum correlations in a hybrid qubit-qutrit thermal state using negativity, uncertainty-induced nonlocality, and local quantum Fisher information. We explored how the system was affected by a magnetic field and random telegraph noise while taking into account various system variables in order to ensure that the qubit-qutrit correlations were preserved for longer periods of time.

Our results demonstrate that the initial levels of negative, uncertainty-induced nonlocality, and local quantum Fisher information are inversely related to temperature. In addition, when the magnetic field has different properties, the entanglement, nonlocality, and Fisher information provide a range of dynamical maps that highlight their distinctive character. When the configuration is limited to the non-Markovian regime, qubit-qutrit correlations often reappear. However, an exponential fall with a single minimum is seen when the linked field is in the Markovian domain.

Importantly, our research shows that the current coupled fields can be used to produce quantum dynamical maps with the ideal level of entanglement, nonlocality, and local quantum Fisher information preservation since they provide a number of benefits. Our findings also demonstrate the significance of taking into account the characteristics of transmission mediums when developing nonlocal quantum communication protocols that are more effective and reliable. Overall, this research provides insights into the design of more efficient nonlocal protocols and investigates the impact of transmitting medium properties on the dynamics of quantum correlations.

5.2 Content of contribution 5

Long-time protection of thermal correlations in a hybrid-spin system under random telegraph noise

Fadwa Benabdallah [1], Atta Ur Rahman [2], Saeed Haddadi [3,4,*] and Mohammed Daoud [5,6]

[1] *LPHE-Modeling and Simulation, Faculty of Sciences, Mohammed V University in Rabat, Morocco*

[2] *Key Laboratory of Aerospace Information Security and Trusted Computing, Ministry of Education, School of Cyber Science and Engineering, Wuhan University, Wuhan 430072, China*

[3] *Faculty of Physics, Semnan University, P.O. Box 35195-363, Semnan, Iran*

[4] *Saeed's Quantum Information Group, P.O. Box 19395-0560, Tehran, Iran*

[5] *Department of Physics, Faculty of Sciences, Ibn Tofail University, Kénitra, Morocco*

[6] *Abdus Salam International Centre for Theoretical Physics, Strada Costiera 11, I-34151 Trieste, Italy*

(Received 18 April 2022; accepted 29 August 2022; published 15 September 2022)

The engineering features of transmitting mediums and their impact on different characteristics of a quantum system play a significant role in the efficient performance of nonlocal protocols. For this purpose, the dynamics of open quantum systems and coupling mediums remain a pathway. In this work, we investigate the dynamics of quantum correlations using negativity, uncertainty-induced nonlocality, and local quantum Fisher information in a hybrid qubit-qutrit thermal state when coupled with a magnetic field and influenced by random telegraph noise. Different features of the system parameters are taken into account while designing longer preservation of qubit-qutrit correlations. We show that the temperature has an inverse impact on the initial values of negativity, uncertainty-induced nonlocality, and local quantum Fisher information. When the magnetic field is characterized by different features, the entanglement, nonlocality, and Fisher information show a variety of dynamical maps, assuring their distinct nature. In addition, the qubit-qutrit correlations undergo repeated revivals when the configuration is restricted to the non-Markovian regime. On the other hand, an exponential drop with a single minimum is observed in the Markovian regime of the coupled field. Most importantly, our findings reveal that the present coupled fields have several advantages that can be leveraged to generate the optimal degree of entanglement, nonlocality, and local quantum Fisher information preservation in quantum dynamical maps.

DOI: 10.1103/PhysRevE.106.034122

I. INTRODUCTION

The presence of nonclassical correlations among subcomponents of a quantum state affect the efficacy of its quantum operations [1–3]. Not only the presence but the amount as well as the nature of the correlations present between the submarginal systems of a composite nonlocal system have an impact on the practical implication of nonclassical protocols. Therefore, recognition as well as the estimation of nonlocal correlations have remained a hot topic in quantum information theory [4,5]. In this regard, quantum systems, in general, can have both classical and quantum correlations. Quantum entanglement, the very well known nonclassical occurrence, has been recognized as a critical resource in several quantum information and communication procedures [6–8], including quantum computation [9], teleportation [10], cryptography [11], entanglement swapping [12], quantum private comparison protocols [13], key distribution [14], and dense coding [15], to name a few.

Nonclassical correlations of many-body systems are a rapidly expanding field with a wide range of applications, including phase transitions [16]. Many researchers have investigated quantum entanglement in thermally defined equilibrium states of spin chains exposed to magnetic fields and found interesting results [17]. The interactions of quantum systems with coupled environments usually result in loss of nonclassical correlations between the subsystems of a composite state in this regard. Realizing such decohering effects is critical in the field of quantum information and computing because it allows for efficient information transfer while avoiding the losses that come with it [18]. Decoherence effects in bipartite and tripartite qubit and qutrit systems interacting with various types of environmental strategies have been studied extensively; for example, see Refs. [19–24]. According to recent research, hybrid quantum systems, such as qubit-qutrit studies, have useful properties for preserving quantum correlations when compared to simple bipartite and tripartite states. In this case, the bipartite Heisenberg *XXX* model is one of the most promising candidates for overcoming decoherence effects caused by the environment, as it has demonstrated a high-tolerance capacity for preserving quantum correlations over longer periods [25]. The features of the quantum mixed spin system are also appealing, in addition to the conventional spin-1/2 system. In this regard, a quasi-single-dimensional chain, $A\mathrm{Cu(pbaOH)(H_2O)_3 \cdot 2H_2O}$, with every subunit carrying two different spins $(S, 1/2)$, has been produced for an inorganic compound [26]. The *A*Cu compounds have antiferromagnetic interactions and can be thought of as a Heisenberg mixed spin $(S, 1/2)$ with antiferromagnetic

*Corresponding author: saeed@ssqig.com

 ©2022 American Physical Society

interactions. A mixed spin $(1, 1/2)$ model may be used to represent the bimetallic chain of the NiCu compound [26]. In the present case, we aim to investigate quantum correlations encoded in the thermal qubit-qutrit mixed *XXZ* spin chain model under the influence of an external magnetic field, the Dzyaloshinskii-Moriya (DM) interaction, and exchange coupling constant.

The study of spin chains that are coupled to external magnetic fields, with a focus on magnetic and other related effects, has sparked a lot of interest in recent years [27–32]. This appears to be ideal because the environment in which quantum systems are coupled is typically made up of various types of instabilities. Random telegraph (RT) noise could be caused by charge trapping at the surfaces of thin films; for instance, see Ref. [33]. Thermal fluctuations in various solid-state and superconducting substances cause low-frequency noise, also known as power-law noise [34]. Another instability is fractional Gaussian and Ornstein-Uhlenbeck noises, which are caused by the random motion of particles in a medium [34]. In this case, we will focus on the dephasing effects caused by the RT noise because it is prevalent in many quantum information processing protocols [35,36]. It has also been extensively researched theoretically to characterize system-environment interactions [37–39]. Chemical processes such as molecule fluorescence [39], nonlocal correlation degradation in the presence of low-frequency noise [40], and frequency amplifications [41] have all been investigated using noise. In addition, the experimental study of RT noise revealed dephasing effects in the dynamics of open quantum systems, resulting in rapid nonlocal correlation degradation [42]. In this case, we consider a hybrid environment in which the dynamics of quantum correlations in a Heisenberg *XXZ* spin chain are influenced by both the unstable effects of external magnetic fields and the RT noise. This will not only set us apart from previous research, but it will also lead to more precise results for real-world quantum protocols, such as dephasing effects.

Quantum correlation measures such as entanglement witnesses [43], concurrence [44], and quantum discord have all been developed in recent decades [45]. Quantum correlations between subparticles can be found using any of these metrics [46]. Updated versions or entirely new quantum correlation metrics have recently been derived, which can detect quantum correlations beyond quantum entanglement. Geometric quantum discord [47], local quantum uncertainty [48], local quantum Fisher information (LQFI) [49], and measurement-induced nonlocality [50] are examples of quantum correlation criteria. Recent quantifiers have revealed nonlocal correlations that were heretofore undetectable by previous measures. As a result, quantum operations became more efficient and precise. Thus, in the current study, we aim to include quantum correlation quantifiers such as negativity [51], uncertainty-induced nonlocality (UIN) [52], and LQFI [49], which are more reliable and are easily computable measures. The use of negativity is motivated by the fact that it is one of the most successful entanglement monotones [53,54]. The UIN will help determine the amount of nonlocality in the thermal state [52]. In addition to providing insight into quantum correlation preservation, LQFI can be used to characterize different parameters and their role in quantum correlation preservation [55].

This paper investigates the dynamics of quantum correlations in a hybrid thermal qubit-qutrit system exposed to an external magnetic field influenced by RT noise, temperature, and DM interaction [56]. Quantum systems are generally very sensitive to thermal fluctuations; therefore, the related quantum correlations will be degraded quickly if temperature effects are not controlled precisely. Previous research [57] has mainly focused on the external magnetic field effect and DM interaction strength. However, in the current study, besides DM interaction, we include the effects of exchange coupling, and manipulation of the associated Markovianity and non-Markovianity of the fields to induce longer qubit-qutrit correlations. To estimate the quantum correlations, we plan to use negativity, UIN, and LQFI, and a comparison of each measure to evaluate quantum correlations will also be drawn.

The paper is organized as follows: We describe the physical model in detail in Sec. II. Section III introduces the quantum correlation estimators, and Sec. IV presents the main results and related discussion. We express some final remarks in Sec. V and the conclusion is given in Sec. VI.

II. PHYSICAL MODEL: THE EXACTLY SOLVABLE CASE

In this section, let us consider a qubit-qutrit mixed spin $(1/2, 1)$ Heisenberg *XXZ* chain model under the presence of an inhomogeneous magnetic field, DM interaction, and exchange coupling constant. The self-Hamiltonian describing the mentioned system reads [58]

$$H = H_{XXZ} = J\left[\left(s_1^x S_2^x + s_1^y S_2^y + \Delta s_1^z S_2^z\right) + D_z\left(s_1^x S_2^y - s_1^y S_2^x\right)\right] + \mu_B B\left(s_1^z + S_2^z\right) - b\left(s_1^z - S_2^z\right), \tag{1}$$

where s_1^α and S_2^α $(\alpha = x, y, z)$ denote spatial components of the spin-$1/2$ (qubit) and spin-1 (qutrit) operators, respectively. The coupling constant J denotes the Heisenberg exchange interaction between spin-$1/2$ and spin-1 particles. Positive range $J > 0$ corresponds to the antiferromagnetic interaction between sites of the model while $J < 0$ indicates the ferromagnetic case. Besides, the parameter Δ represents the *XXZ* exchange anisotropy in this exchange interaction, and the parameter D_z refers to the strength of DM interaction oriented along the z direction. The parameter B denotes a static external magnetic field and μ_B is the Bohr magneton [53,54]. Finally, b indicates the degree of inhomogeneity of the magnetic field. By straightforward calculations, the eigenvalues of the bipartite model with self-Hamiltonian (1) are obtained as follows (setting $\hbar = 1$) [58]:

$$\begin{aligned} E_{1,2} &= \tfrac{1}{2}(\mp b \mp 3\mu_B B + J\Delta), \\ E_{3,4} &= \tfrac{1}{4}(2b + 2\mu_B B - J\Delta \mp \omega^-), \\ E_{5,6} &= \tfrac{1}{4}(-2b - 2\mu_B B - J\Delta \mp \omega^+), \end{aligned} \tag{2}$$

with $\omega^\pm = \sqrt{(4b)^2 + 2(2J)^2 + 2(2D_z J)^2 \pm 8bJ\Delta + (J\Delta)^2}$. The corresponding orthogonal eigenstates are respectively given as follows:

$$|\psi_1\rangle = |\uparrow, \Uparrow\rangle,\ |\psi_2\rangle = |\downarrow \Downarrow\rangle,$$

$$|\psi_3\rangle = \frac{1}{\sqrt{1 + |\eta_+|^2}}(\eta_+|\downarrow \bigcirc\rangle + |\uparrow\Downarrow\rangle),$$

$$|\psi_4\rangle = \frac{1}{\sqrt{1+|\eta_-|^2}}(\eta_-|\downarrow\bigcirc\rangle + |\uparrow\Downarrow\rangle),$$
$$|\psi_5\rangle = \frac{1}{\sqrt{1+|\vartheta_+|^2}}(\vartheta_+|\downarrow\Uparrow\rangle + |\uparrow\bigcirc\rangle),$$
$$|\psi_6\rangle = \frac{1}{\sqrt{1+|\vartheta_-|^2}}(\vartheta_-|\downarrow\Uparrow\rangle + |\uparrow\bigcirc\rangle), \tag{3}$$

where $\eta_\pm = \frac{-4b+J\Delta\mp\omega^-}{2\sqrt{2}J(D_z+i)}i$ and $\vartheta_\pm = -\frac{4b+J\Delta\pm\omega^+}{2\sqrt{2}J(D_z+i)}i$. Moreover, $|\uparrow\rangle$ and $|\downarrow\rangle$ represent the eigenbasis of the z component of spin-1/2 operator s^z whereas $|\Uparrow\rangle$, $|\bigcirc\rangle$, and $|\Downarrow\rangle$ are known to be the eigenbasis of spin-1 operators S^z along the z component.

At the equilibrium (canonical ensemble), the initial quantum state of the mixed spin-(1/2, 1) Heisenberg chain (1) can be represented by the density operator, namely $\rho(0, T) = \exp(-\beta H)/Z$, which is expressed in terms of the partition function $Z = \mathrm{Tr}[\exp(-\beta H)]$, where $\beta = 1/k_B T$ is the inverse of the thermodynamic temperature T, and k_B is the Boltzmann constant. For the sake of simplicity, the parameter J is set to be the unit of energy. To investigate the time evolution of temperature-dependent nonclassical correlations, let us consider the well-known local non-Markovian dephasing behavior introduced by Daffer *et al.* [59]. This model has recently been widely used to study the sudden change in the dynamics of quantum correlations [60]. Now, we can consider a colored noise dephasing model with dynamics described by the following master equation at scaled time t [59–61],

$$\dot{\rho}(t) = \mathcal{K}\mathcal{L}\rho(t), \tag{4}$$

where $\mathcal{K}$ is a time-dependent integral operator, satisfying the relation

$$\mathcal{K}\phi = \int_0^t k(t-t')\phi(t')dt', \tag{5}$$

where $k(t-t')$ is the kernel function which regulates the nature of the environment, $\mathcal{L}$ is the Lindblad superoperator that describes the dynamics induced via the interaction with the environment, and $\rho(t)$ is the density operator of the principal system. It is important to note that without applying the time-dependent integral operator $\mathcal{K}$, the master equation (4) with Markovian approximation becomes dominant. Also, the mentioned master equation can be employed if we consider a bipartite qubit-qutrit system interacting with a reservoir having the properties of RT noise. To this end, we can consider the stochastic Hamiltonian as [59–62]

$$\delta H(t) = \delta\omega_A(t)s_A^z + \delta\omega_B(t)S_B^z, \tag{6}$$

where ω_n with $n = \{A, B\}$ are the independent random variables obeying the statistic of a RT signal defined as $\omega_n(t) = a_n(-1)^{m_n(t)}$, where $m_n(t)$ has a Poisson distribution with a mean equal to $t/2\tau_n$, and a_n is known as the switching amplitude taking the values $\pm a_n$. Here, we assume $a_A = a_B = a$ and $\tau_A = \tau_B = \tau$. Using the time-dependent stochastic Hamiltonian (6), the represented correlation function of the RT signal using the stochastic variables reads

$$\langle\omega_n(t)\omega_{n'}(t')\rangle = \delta_{n,n'}a^2\exp(-\gamma|t-t'|), \tag{7}$$

where $\langle\cdots\rangle$ stands for the ensemble average whereas $\gamma = 1/\tau$ is known as the switching rate, which characterizes the spectral width of the coupling with the environment [63]. The time evolution of the density matrix describing the qubit-qutrit system (6) is given by taking ensemble averages over the stochastic noise variables as follows,

$$\rho(t, T) = \langle U(t)\rho(0, T)U^\dagger(t)\rangle, \tag{8}$$

with $\rho(0, T) = \exp(-\beta H)/Z$ and in terms of the unitary operator $U(t)$ obtained from the stochastic Schrödinger equation as

$$U(t) = \mathcal{T}\exp\left[-i\int_0^t H(t')dt'\right], \tag{9}$$

where $\mathcal{T}$ is the time-ordering operator. In general, within the framework of the classical treatment, the environmental effects on a quantum system give rise to the stochastic fluctuations in the Hamiltonian of the quantum system as

$$H(t) = H + \delta H(t). \tag{10}$$

Note that the unitary operator contains both the contributions from the self-Hamiltonian and the stochastic Hamiltonian.

Many approaches have been devoted to studying the dynamical behaviors of a given quantum system such as the master equation [64,65] and decomposition by Kraus operators [66]. In the current case, we find that it is more suitable to use the Kraus operators to probe the quantum dynamics of the model under consideration [66]. The Kraus operators describing the RT noise dynamical map and related effects on the qubit-qutrit system are respectively provided by [60,62]

$$K_1^A = \sqrt{\frac{1+\Lambda(\nu)}{2}}I_A, \quad K_2^A = \sqrt{\frac{1-\Lambda(\nu)}{2}}s_A^z, \tag{11}$$

and

$$K_1^B = \sqrt{\frac{1+\Lambda(\nu)}{2}}I_B, \quad K_2^B = \sqrt{\frac{1-\Lambda(\nu)}{2}}S_B^z,$$
$$K_3^B = \sqrt{\frac{1+\Lambda(\nu)}{2}}\mathcal{S}_B, \tag{12}$$

where K_i satisfies the completeness condition guaranteeing that the evolution is trace-preserving and represents the influence of statistical noise which can be global or local in scope, and where the index runs over the number of elements required for the decomposition. Besides, these operators satisfy the normalization condition $\sum_i K_i^\dagger K_i = I$ with

$$\mathcal{S}_B = \tfrac{1}{2}\left(S_B^x S_B^x + S_B^y S_B^y - S_B^z S_B^z\right), \tag{13}$$

and I_A (I_B) is the identity operator acting on the qubit (qutrit) subspace. The term $\Lambda(\nu)$ is generally called the dephasing function and has the form [59–61]

$$\Lambda(\nu) = \frac{1}{\mu}\exp(-\nu)[\sin(\mu\nu) + \mu\cos(\mu\nu)], \tag{14}$$

in which $\mu = \sqrt{(4a\tau)^2 - 1}$ and $\nu = t/2\tau$ is the scaled time. With no tunneling coupling in the Hamiltonian, the quantum dynamics of a qubit-qutrit system are described by the dephasing function in the form of Eq. (14), which displays the non-Markovian behavior in the strong-coupling regime ($\tau > 2a$) and shows Markovian behavior in the weak-coupling

regime ($\tau < 2a$). Herein, the qubit-qutrit system is equally coupled to all environment frequencies. In the case of RT noise, our system prefers specific frequencies. Accordingly, a is the coupling strength of the qubit-qutrit system with the environment whereas τ determines which frequencies the mentioned system prefers most. Enhancing both a and $\gamma = 1/\tau$ corresponds to a more noisy environment. Hence, the dimensionless quantity $a\tau$ is the significant term that determines the number of fluctuations [59]. From now on, let us consider $a = 1$ for simplicity. As a result, the parameter τ will exclusively be the dominant factor to determine the amount of information exchange between the qubit-qutrit system and the environment.

Now, we derive the density matrix of the system having obvious entanglement as well as the quantum correlation sudden death and birth phenomenon. In order to exhibit entanglement sudden death (ESD) and entanglement sudden birth (ESB) in the qubit-qutrit class state, we consider dephasing RT noise alone acting on subsystems that are dynamically isolated from each other.

The most general time-evolved open-system density matrix expressible in the operator-sum decomposition has the form [60–62]

$$\rho(t,T) = \sum_{i=1}^{2}\sum_{j=1}^{3}\left(K_i^A \otimes K_j^B\right)\rho(0,T)\left(K_i^A \otimes K_j^B\right)^{\dagger}. \quad (15)$$

Note that only when the stochastic Hamiltonian $\delta H(t)$ is commutative with the self-Hamiltonian H and the stochastic Hamiltonian is in the energy eigenvalues of the system, the quantum system undergoes dephasing and the density matrix can be expressed in terms of the dephasing function $\Lambda(\nu)$. Otherwise, the density matrix of the system cannot be generally expressed in the Kraus operator representation in terms of the dephasing function. After straightforward calculation, the time and temperature dependencies of our qubit-qutrit density matrix can be written in the computational basis $\{|\downarrow, \Downarrow\rangle\}, \{|\downarrow, \bigcirc\rangle\}, \{|\downarrow, \Uparrow\rangle\}, \{|\uparrow, \Downarrow\rangle\}, \{|\uparrow, \bigcirc\rangle\}, \{|\uparrow, \Uparrow\rangle\}$ as follows,

$$\rho(t,T) = \frac{1}{Z}\begin{bmatrix} \rho_{1,1} & 0 & 0 & 0 & 0 & 0 \\ 0 & \rho_{2,2} & 0 & \rho_{2,4} & 0 & 0 \\ 0 & 0 & \rho_{3,3} & 0 & \rho_{3,5} & 0 \\ 0 & \rho_{2,4}^{*} & 0 & \rho_{4,4} & 0 & 0 \\ 0 & 0 & \rho_{3,5}^{*} & 0 & \rho_{5,5} & 0 \\ 0 & 0 & 0 & 0 & 0 & \rho_{6,6} \end{bmatrix}, \quad (16)$$

where

$$\rho_{1,1} = \exp(-\beta E_2),\ \rho_{6,6} = \exp(-\beta E_1),$$

$$\rho_{2,2} = \frac{|\eta_+|^2}{1+|\eta_+|^2}\exp(-\beta E_3) + \frac{|\eta_-|^2}{1+|\eta_-|^2}\exp(-\beta E_4),$$

$$\rho_{2,4} = \frac{1}{2}[1+\Lambda(\nu)] \times \left[\frac{\eta_+}{1+|\eta_+|^2}\exp(-\beta E_3) + \frac{\eta_-}{1+|\eta_-|^2}\exp(-\beta E_4)\right],$$

$$\rho_{3,3} = \frac{|\vartheta_+|^2}{1+|\vartheta_+|^2}\exp(-\beta E_5) + \frac{|\vartheta_-|^2}{1+|\vartheta_-|^2}\exp(-\beta E_6),$$

$$\rho_{3,5} = \frac{1}{2}[1+\Lambda(\nu)] \times \left[\frac{\vartheta_+}{1+|\vartheta_+|^2}\exp(-\beta E_5) + \frac{\vartheta_-}{1+|\vartheta_-|^2}\exp(-\beta E_6)\right],$$

$$\rho_{4,4} = \frac{1}{1+|\eta_+|^2}\exp(-\beta E_3) + \frac{1}{1+|\eta_-|^2}\exp(-\beta E_4),$$

$$\rho_{5,5} = \frac{1}{1+|\vartheta_+|^2}\exp(-\beta E_5) + \frac{1}{1+|\vartheta_-|^2}\exp(-\beta E_6), \quad (17)$$

and the partition function Z is given by

$$Z = \sum_{j=1}^{6}\exp(-\beta E_j). \quad (18)$$

Notably, the density matrix of the composite qubit-qutrit system has been expressed as $\rho(t,T)$ given in Eq. (16), implying that the operators s_A^z and S_B^z in the stochastic Hamiltonian are in the energy eigenbasis of the self-Hamiltonian of the qubit and the qutrit subsystems, respectively.

III. QUANTUM CORRELATION INDICATORS

A. Negativity

To investigate the amount of quantum entanglement of a system with spin $S > 1/2$, one may employ a quantity known as negativity $N(\rho)$ [67]. This quantifier has been proven to be one of the most suitable quantifiers, which can be easily computable for any arbitrary pure or mixed state. It is based on the concept of the Peres and Horodecki separability criterion [68,69], in which a negative partial transpose is a necessary condition for the system entanglement. The negativity $N(\rho)$ is defined through the absolute sum of all negative eigenvalues ϑ_i of the partial-transposed density matrix ρ^{T_A} concerning the spin-1/2 subsystem (A denotes the first subsystem). Generally, it reads [67]

$$N(\rho) = \sum_i |\vartheta_i|. \quad (19)$$

The negativity can also be identified via the Schatten 1-norm (trace norm) as below [67],

$$N(\rho) = \frac{||\rho^{T_A}||_1 - 1}{2}, \quad (20)$$

where the term $||X||_1 = \mathrm{Tr}(\sqrt{X^{\dagger}X})$ presents the trace norm for any Hermitian operator X. It is worth mentioning that for maximally entangled states, the negativity is equal to half $[N(\rho) = 1/2]$, whereas $N(\rho) = 0$ corresponds to completely separable (factorizable) states. However, let us consider here a rescaled form of the negativity definition as $\mathcal{N}(\rho) = 2 \times N(\rho)$ for our calculations. Therefore, we will have $0 \leqslant \mathcal{N}(\rho) \leqslant 1$.

In order to evaluate the time and temperature dependencies of the negativity of a qubit-qutrit system $\rho(t,T)$ given in Eq. (16), one needs first to obtain the negative eigenvalues of the partial-transposed density matrix of the total system. To do this, a partial transposition with respect to states of the spin-1/2 gives the partially transposed density matrix $[\rho(t,T)]^{T_A}$. In the computational basis, the thermal-time evolved partial

transposed density matrix $[\rho(t,T)]^{T_A}$ takes the form

$$[\rho(t,T)]^{T_A}=\frac{1}{Z}\begin{pmatrix}\rho_{1,1}&0&0&0&\rho_{2,4}&0\\0&\rho_{2,2}&0&0&0&\rho_{3,5}\\0&0&\rho_{3,3}&0&0&0\\0&0&0&\rho_{4,4}&0&0\\\rho^*_{2,4}&0&0&0&\rho_{5,5}&0\\0&\rho^*_{3,5}&0&0&0&\rho_{6,6}\end{pmatrix}. \tag{21}$$

Now, the possible negative eigenvalues of the state $[\rho(t,T)]^{T_A}$ (21) are gained as

$$\vartheta_1(t,T)=\frac{1}{2Z}[(\rho_{1,1}+\rho_{5,5})-\sqrt{(\rho_{1,1}-\rho_{5,5})^2+4|\rho_{2,4}|^2}], \tag{22}$$

$$\vartheta_2(t,T)=\frac{1}{2Z}[(\rho_{2,2}+\rho_{6,6})-\sqrt{(\rho_{2,2}-\rho_{6,6})^2+4|\rho_{3,5}|^2}], \tag{23}$$

and therefore, the negativity of our state can be expressed as

$$\mathcal{N}(\rho(t,T))=2[\max\{0,-\vartheta_1(t,T)\}+\max\{0,-\vartheta_2(t,T)\}]. \tag{24}$$

B. Uncertainty-induced quantum nonlocality

The UIN is a promising discord-like quantifier linked to the Wigner-Yanase skew information (WYSI) concept [70]. This nonclassical correlation quantifier is defined as the maximal skew information achievable between a given bipartite quantum state ρ and local commuting observable $K^C=K^C_{\rm A}\otimes I_{\rm B}$. The UIN with respect to subsystem A can be expressed in terms of WYSI for a given state ρ as [71,72]

$$\mathcal{U}_C(\rho)=\max_{K^C_{\rm A}\otimes I_{\rm B}}\mathcal{I}\big(\rho,K^C_{\rm A}\otimes I_{\rm B}\big), \tag{25}$$

where the maximum is taken over the set of all observables, $K^C=K^C_{\rm A}\otimes I_{\rm B}$, that commutes with the reduced density matrix ρ^A, where $K^C_{\rm A}$ is a Hermitian operator acting on subsystem A with a nondegenerate spectrum Λ. Moreover, $I_{\rm B}$ is the identity operator acting on subsystem B, while $\mathcal{I}$ is the skew information associated with the density matrix and defined as

$$\mathcal{I}(\rho,K^\Lambda)=-\tfrac{1}{2}{\rm Tr}([\sqrt{\rho},K^\Lambda]^2), \tag{26}$$

which is a measure of the noncommutativity between the state ρ and the observable K^Λ. Note that $\mathcal{I}$ is non-negative and nonincreasing under classical mixing [73]. For a $2\otimes d$ (qubit-qudit) bipartite quantum system, the compact formula of UIN turns out to be

$$\mathcal{U}_C(\rho)=\begin{cases}1-\omega_{\min}(\mathcal{W}_{\rm AB}),\ \vec{r}=\vec{0},\\1-\frac{1}{\|\vec{r}\|^2}\vec{r}\mathcal{W}_{\rm AB}\vec{r}^{\,T},\ \vec{r}\neq\vec{0},\end{cases} \tag{27}$$

where $\vec{r}=[r_i]$ is the Bloch vector of the density matrix ρ, whose elements are calculated by $r_i={\rm Tr}(\rho[\sigma_i\otimes I])$. The superscript T stands for the transpose operation and $\omega_{\min}(\mathcal{W}_{\rm AB})$ stands for the least eigenvalue of the 3×3 symmetric matrix $\mathcal{W}_{\rm AB}$ whose elements are given by

$$(\mathcal{W}_{\rm AB})_{\alpha\beta}={\rm Tr}\big[\sqrt{\rho}\big(\sigma^\alpha_{\rm A}\otimes I_{\rm B}\big)\sqrt{\rho}\big(\sigma^\beta_{\rm A}\otimes I_{\rm B}\big)\big], \tag{28}$$

where $\sigma^{\alpha(\beta)}_{\rm A}$ with $\alpha(\beta)=\{x,y,z\}$ represent the Pauli operators of the subsystem A. The UIN is a reliable quantifier of quantum correlations and it has been demonstrated that this measure satisfies the full physical requirements of a measure of quantum correlations [71,72]. It is clear that having the matrix $\mathcal{W}_{\rm AB}$, one can easily evaluate the UIN for qubit-qutrit quantum systems contrarily to the quantum discord based on von Neumann entropy [73]. This is quite an easy task compared with the complicated minimization process over parameters due to the local measurements [48,65]. However, for the pure bipartite states, the UIN reduces to the linear entropy of the reduced densities of the subsystems and vanishes for classically correlated state [48]. Moreover, it is invariant under local unitary operations and nonincreasing under the local operation on the unmeasured subsystem B [48]. To determine the analytical expression of the UIN (27), it is necessary to compute the eigenvalues of the matrix $\mathcal{W}_{\rm AB}$ (28). For that, one needs to determine both the eigenvalues and the corresponding eigenvectors associated with the density matrix $\rho(t,T)$ in Eq. (16), viz.,

$$\begin{aligned}&\lambda_{1,6}=\tfrac{1}{2}\big(\xi_1\pm\sqrt{\xi_1^2-4d_1}\big),\\&\lambda_{2,3}=\tfrac{1}{2}\big(\xi_2\mp\sqrt{\xi_2^2-4d_2}\big),\ \ \lambda_{4,5}=\tfrac{1}{2}\big(\xi_3\mp\sqrt{\xi_3^2-4d_3}\big),\end{aligned} \tag{29}$$

where

$$\begin{aligned}&\xi_1=\rho_{11}+\rho_{66},\ \ \xi_2=\rho_{22}+\rho_{44},\ \ \xi_3=\rho_{33}+\rho_{55},\\&d_1=\rho_{11}\rho_{66},\ \ d_2=\rho_{22}\rho_{44}-|\rho_{24}|^2,\\&d_3=\rho_{33}\rho_{55}-|\rho_{35}|^2,\end{aligned} \tag{30}$$

and the associated eigenvectors are

$$\begin{aligned}&|\lambda_1\rangle=|\uparrow\Uparrow\rangle,\ \ |\lambda_6\rangle=|\downarrow\Downarrow\rangle,\\&|\lambda_{2,3}\rangle=\frac{1}{\sqrt{1+|\upsilon_\pm|^2}}(\upsilon_\pm|\uparrow\bigcirc\rangle+|\downarrow\Uparrow\rangle),\\&|\lambda_{4,5}\rangle=\frac{1}{\sqrt{1+|\eta_\pm|^2}}(\eta_\pm|\uparrow\Downarrow\rangle+|\downarrow\bigcirc\rangle),\end{aligned} \tag{31}$$

where

$$\upsilon_\pm=\frac{1}{2\rho^*_{2,4}}[\rho_{2,2}-\rho_{4,4}\pm\sqrt{(\rho_{2,2}-\rho_{4,4})^2+4|\rho_{2,4}|^2}], \tag{32}$$

$$\eta_\pm=\frac{1}{2\rho^*_{3,5}}[\rho_{3,3}-\rho_{5,5}\pm\sqrt{(\rho_{3,3}-\rho_{5,5})^2+4|\rho_{3,5}|^2}]. \tag{33}$$

The square root of the density matrix can be written in the computational basis as follows,

$$\sqrt{\rho(t,T)}=\begin{pmatrix}\alpha_{11}&0&0&0&0&0\\0&\alpha_{22}&0&\alpha_{24}&0&0\\0&0&\alpha_{33}&0&\alpha_{35}&0\\0&\alpha^*_{24}&0&\alpha_{44}&0&0\\0&0&\alpha^*_{35}&0&\alpha_{55}&0\\0&0&0&0&0&\alpha_{66}\end{pmatrix}, \tag{34}$$

where

$$\alpha_{11} = \frac{1}{2}(\sqrt{\xi_1 + 2\sqrt{d_1}} + \sqrt{\xi_1 - 2\sqrt{d_1}}),$$
$$\alpha_{66} = \frac{1}{2}(\sqrt{\xi_1 + 2\sqrt{d_1}} - \sqrt{\xi_1 - 2\sqrt{d_1}}),$$
$$\alpha_{22} = \frac{\rho_{22} + \sqrt{d_2}}{\sqrt{\xi_2 + 2\sqrt{d_2}}}, \quad \alpha_{24} = \frac{\rho_{24}}{\sqrt{\xi_2 + 2\sqrt{d_2}}},$$
$$\alpha_{33} = \frac{\rho_{33} + \sqrt{d_3}}{\sqrt{\xi_3 + 2\sqrt{d_3}}}, \quad \alpha_{35} = \frac{\rho_{35}}{\sqrt{\xi_3 + 2\sqrt{d_3}}},$$
$$\alpha_{44} = \frac{\rho_{44} + \sqrt{d_2}}{\sqrt{\xi_2 + 2\sqrt{d_2}}}, \quad \alpha_{55} = \frac{\rho_{55} + \sqrt{d_3}}{\sqrt{\xi_3 + 2\sqrt{d_3}}}. \tag{35}$$

After some straightforward calculations, the eigenvalues of the matrix $\mathcal{W}_{\mathrm{AB}}$ (28) are given as

$$\mathcal{W}_{11} = \mathcal{W}_{22} = 2(\alpha_{11}\alpha_{44} + \alpha_{22}\alpha_{55} + \alpha_{33}\alpha_{66}), \tag{36}$$

$$\mathcal{W}_{33} = \sum_{i=1}^{6} \alpha_{ii}^2 - 2(|\alpha_{24}|^2 + |\alpha_{35}|^2). \tag{37}$$

By using Eq. (27), the UIN for the density matrix $\rho(t, T)$ in Eq. (16) turns out to be (since $\vec{r} \neq \vec{0}$)

$$\mathcal{U}(\rho(t, T)) = 1 - \frac{1}{|r_3|^2} r_3 \mathcal{W}_{33} r_3^*, \tag{38}$$

with $r_3 = \rho_{1,1} + \rho_{2,2} + \rho_{3,3} - \rho_{4,4} - \rho_{5,5} - \rho_{6,6}$.

C. Local quantum Fisher information

Assume a qubit-qutrit quantum state, namely ρ_κ, which depends basically on an arbitrary parameter κ. Now, in order to illustrate the information about κ from ρ_κ, it is enough to perform a set of generalized quantum measurements, that is, positive-operator-valued measures $M = \{M_\theta | M_\theta \geqslant 0\}$, satisfying $\sum_\theta M_\theta = I_d$. Mathematically, the QFI is defined as [74,75]

$$\mathcal{F}(\rho_\kappa) = \tfrac{1}{4}\mathrm{Tr}\big[\rho_\kappa \mathcal{L}_\kappa^2\big], \tag{39}$$

where $\mathcal{L}_\kappa$ denotes the symmetric logarithmic derivative operator such that

$$\frac{\partial \rho_\kappa}{\partial \kappa} = \frac{1}{2}(\mathcal{L}_\kappa \rho_\kappa + \rho_\kappa \mathcal{L}_\kappa). \tag{40}$$

Let us assume that the initial density operator $\rho_\kappa(0)$ can be evolved through a unitary evolution, namely $\mathcal{U}_\kappa = e^{-iH\kappa}$ as $\rho_\kappa = \mathcal{U}_\kappa \rho_\kappa(0) \mathcal{U}_\kappa^\dagger$. Therefore, the QFI employing the Hermitian operator H is defined as [76]

$$\mathcal{F}(\rho_\kappa, H) = \frac{1}{2} \sum_{\alpha \neq \beta} \frac{(\lambda_\alpha - \lambda_\beta)^2}{\lambda_\alpha + \lambda_\beta} |\langle \lambda_\alpha | H | \lambda_\beta \rangle|^2, \tag{41}$$

where $\rho_\kappa = \sum_i \lambda_i |\lambda_i\rangle\langle\lambda_i|$. Recently, another concept, i.e., the LQFI, has been examined based on QFI and it has attracted a great deal of attention since it defines a quantifier of nonclassical correlation using some local measurements applied on one part of the quantum state. Indeed, assume that the dynamics already mentioned is ruled now by a local transformation, that is, $e^{-i\kappa H_A}$, of a local Hamiltonian $H_A = H_a \otimes I_B$. Therefore, the LQFI is defined as [77]

$$\mathcal{F}(\rho_\kappa, H_A) = \mathrm{Tr}\big[\rho H_A^2\big] - \sum_{\alpha \neq \beta} \frac{2\lambda_\alpha \lambda_\beta}{\lambda_\alpha + \lambda_\beta} |\langle \lambda_\alpha | H_A | \lambda_\beta \rangle|^2. \tag{42}$$

As we have already pointed out the central idea behind using the LQFI is to consider it a good quantifier of nonclassical correlations. The LQFI is defined as the minimum of QFI overall local Hamiltonian H_A acting on the part A as

$$\mathcal{Q} = \min_{H_A} \mathcal{F}(\rho_\kappa, H_A). \tag{43}$$

Obviously, if one rewrites the local Hamiltonian in terms of Pauli matrices, that is, $\vec{\sigma} = (\sigma_1, \sigma_2, \sigma_3)$, and choosing the local observable $H_a = \vec{\sigma} \cdot \overrightarrow{r}$ with $|\overrightarrow{r}| = 1$, then the first term on the right-hand side of Eq. (42) is exactly corresponding to the unity, while the second term turns out to be [77–80]

$$\begin{aligned} &\sum_{\alpha \neq \beta} \frac{2\lambda_\alpha \lambda_\beta}{\lambda_\alpha + \lambda_\beta} |\langle \lambda_\alpha | H_A | \lambda_\beta \rangle|^2 \\ &= \sum_{\alpha \neq \beta} \sum_{k=l=1}^{3} \frac{2\lambda_\alpha \lambda_\beta}{\lambda_\alpha + \lambda_\beta} \langle \lambda_\alpha | \sigma_k \otimes I_B | \lambda_\beta \rangle \langle \lambda_\beta | \sigma_l \otimes I_B | \lambda_\alpha \rangle \\ &= \overrightarrow{r}^{\,\dagger} \cdot P \cdot \overrightarrow{r}, \end{aligned} \tag{44}$$

where the elements of the symmetric matrix P are given by

$$P_{k,l} = \sum_{\alpha \neq \beta} \frac{2\lambda_\alpha \lambda_\beta}{\lambda_\alpha + \lambda_\beta} \langle \lambda_\alpha | \sigma_k \otimes I_B | \lambda_\beta \rangle \langle \lambda_\beta | \sigma_l \otimes I_B | \lambda_\alpha \rangle. \tag{45}$$

Hence, the minimum over all unit of vectors $\vec{r}$ coincides with the maximum eigenvalues of P, $\lambda_{\max}^P$. Finally, the LQFI for qubit-qutrit systems is obtained in the following form [49,78–80],

$$\mathcal{Q}(\rho) = 1 - \lambda_{\max}^P. \tag{46}$$

Notice that the above formula is non-negative, invariant under any local unitary operation, and vanishes for classically correlated states. In addition, in the case of pure quantum states, the LQFI coincides with the geometric discord [49]. After some straightforward calculations and using the eigenvalues and eigenvectors calculated in Eqs. (29) and (31), the analytical expression of LQFI for our qubit-qutrit state (16) is obtained as

$$\mathcal{Q}(\rho(t, T)) = 1 - \max\{P_{11}, P_{22}, P_{33}\}, \tag{47}$$

where $P_{ii} (i = 1, 2, 3)$ are calculated analytically from Eq. (45). They are given by

$$P_{11} = P_{22} = 4\Bigg[\frac{\lambda_1\lambda_2}{(\lambda_1 + \lambda_2)(1 + |\upsilon_+|^2)} + \frac{\lambda_1\lambda_3}{(\lambda_1 + \lambda_3)(1 + |\upsilon_-|^2)} + \frac{\lambda_4\lambda_6|\eta_+|^2}{(\lambda_4 + \lambda_6)(1 + |\eta_+|^2)} + \frac{\lambda_5\lambda_6|\eta_-|^2}{(\lambda_5 + \lambda_6)(1 + |\eta_-|^2)}$$

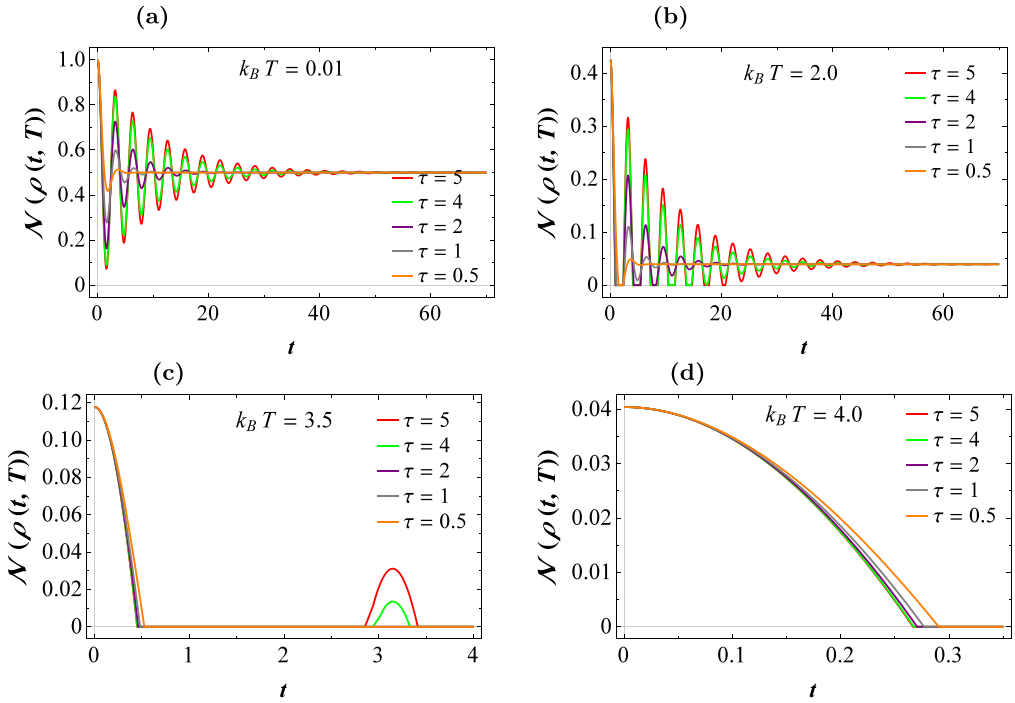


FIG. 1. Dynamics of the negativity versus time parameter t for $a = 1$ by considering a few different values of τ at different values of the temperature $k_B T/J$, assuming fixed $\mu_B B/J = 0.5$, $D_z/J = 6$, $\Delta/J = 0.5$ when $b/J = 0$.

$$+\frac{\lambda_2|\upsilon_+|^2}{(1+|\upsilon_+|^2)}\left(\frac{\lambda_4}{(\lambda_2+\lambda_4)(1+|\eta_+|^2)}+\frac{\lambda_5}{(\lambda_2+\lambda_5)(1+|\eta_-|^2)}\right)$$
$$+\frac{\lambda_3|\upsilon_-|^2}{(1+|\upsilon_-|^2)}\left(\frac{\lambda_4}{(\lambda_3+\lambda_4)(1+|\eta_+|^2)}+\frac{\lambda_5}{(\lambda_3+\lambda_5)(1+|\eta_-|^2)}\right)\Bigg] \tag{48}$$

and

$$P_{33} = 4\left[\frac{\lambda_2\lambda_3}{(\lambda_2+\lambda_3)}\frac{|\upsilon_+^*\upsilon_- - 1|^2}{(1+|\upsilon_+|^2)(1+|\upsilon_-|^2)}+\frac{\lambda_4\lambda_5}{(\lambda_4+\lambda_5)}\frac{|\eta_+^*\eta_- - 1|^2}{(1+|\eta_+|^2)(1+|\eta_-|^2)}\right], \tag{49}$$

where $\upsilon_\pm$ and $\eta_\pm$ are given in Eqs. (32) and (33), respectively. Also, we have $P_{12} = P_{21} = P_{23} = P_{32} = P_{13} = P_{31} = 0$.

IV. ANALYSIS OF QUANTUM CORRELATION DYNAMICS

In this section, we begin by studying the dynamics of quantum correlations characterized by negativity (24), UIN (38), and LQFI (47) for our qubit-qutrit mixed spin chain model under the local dephasing channels exhibiting Markovianity and non-Markovianity.

In Fig. 1, we show the temporal evolution of the negativity for several values of τ and different fixed values of the temperature $k_B T$ in the absence of the inhomogeneous magnetic field ($b/J = 0$). Note that we have set parameter $a = 1$ which acts as a system-environment coupling constant. So, the parameter $\tau > 2$ denotes the non-Markovian regime, whereas $\tau < 2$ corresponds to the Markovian regime. It can be seen that at a low-temperature regime ($k_B T = 0.01$), quantum entanglement estimated by the negativity is maximal [$\mathcal{N}(\rho(t, T)) = 1$] at $t = 0$ [see Fig. 1(a)], which means that the qubit-qutrit state is maximally entangled at the initial moment of interaction. Moreover, the entanglement decreases during the decoherence process until it reaches a steady-state value, which implies that the entanglement is frozen after a specific interval of time. For a smaller value of τ ($\tau = 0.5$ here), the negativity decreases asymptotically with tiny oscillations at a range of time. It is interesting to know that in the Markovian regime $\tau < 2$, we observe tiny revivals in entanglement evolution. As mentioned earlier, the parameter τ regulates the amount of information exchange between the system and the environment. Hence, the oscillations in the dynamical behavior of negativity are mostly controlled by τ. However, the Markovian regime accelerates the stabilization of the negativity. The decrement of the parameter τ causes the negativity to decay faster. With an increase in the temperature ($k_B T = 2$) [see Fig. 1(b)], the phenomena of ESD and ESB appear in the behavior of the negativity with a particular lower damped amplitude and reach a steady state, demonstrating the entanglement freezing phenomenon. Figure 1(c) shows that the dynamics of negativity do not exhibit rebirth for $\tau < 2$ when the temperature $k_B T = 3.5$ is assumed, showing that the system is in the Markovian regime. In this situation,

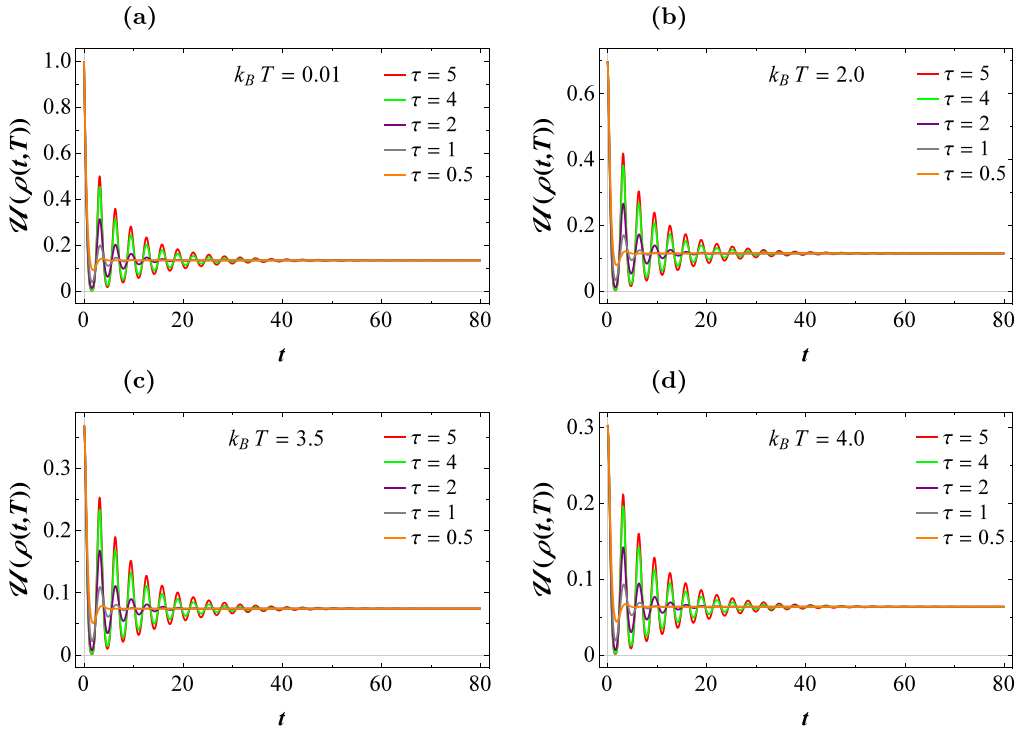


FIG. 2. Dynamics of the UIN versus t by considering a few different values of parameter τ at different values of the temperature $k_B T/J$, assuming fixed $\mu_B B/J = 0.5$, $D_z/J = 6$, $\Delta/J = 0.5$ when $b/J = 0$.

the entanglement between the qubit and qutrit becomes zero after a while, known as the ESD. For $\tau > 2$, the existence of ESD and ESB in the dynamical map of negativity indicates that the qubit-qutrit system and environment exchange information. In addition, such entanglement revivals indicate the usefulness of the parameter τ to convert free states or less entangled states to a more resourceful state (with a high degree of entanglement). In Fig. 1(d), we see that at a higher temperature $k_B T = 4$, for all considered values of τ, the ESD phenomenon appears. It must be noticed that as temperature increases, the entanglement saturates at lower values; specifically when $k_B T > 2$, the state becomes completely separable for the increasing interaction time. Further, we have shown that the lowest temperature values have a significant impact on the maximization of quantum entanglement. The temperature influences not only the initial entanglement of the system but also the non-Markovianity behavior. Lower values of the temperature allow the system to show non-Markovian effects and the entanglement decays with revival character. The presence of ESD and ESB in the current dynamical map of the entanglement estimator reveals that the system and the environment are highly interacting, exhibiting information exchange between them. In addition, practical transmitting channels can be fully fledged by exploiting the parameter τ to design longer entanglement preservation. As can be seen that when τ gets higher, the state's entanglement final saturation levels take time to diminish, hence preventing the state from the separability, in particular, for higher values of $k_B T$. It is noticeable that the magnetic field imposed on the dynamics of quantum systems without environmental noise is not equivalent to the current case with dephasing RT noise [58]. For example, it is intriguing to find that the total time of entanglement negativity becomes extended when injecting the RT noise. As seen in Ref. [58] without RT noise, the entanglement decays in a very short time as compared to that observed under the influence of RT noise. Besides, we observed the monotonic decay in the mentioned paper whereas, in the current case, the entanglement suffers repeated revivals due to the RT environmental dephasing effects, therefore completely contradicting the previous study of the similar system. Physically, this means that the current configuration is best suited for avoiding complete entanglement freezing by the conversion of free states to entangled resource states. However, the dynamics of the thermal entangled state in a qutrit-qubit mixed spin *XXZ* model when coupled to an external magnetic field have been in good agreement with current results by showing longer entanglement preservation along with oscillatory behavior [81].

Figure 2 depicts the dynamics of the mixed qubit-qutrit state using the UIN measure under the presence of an external magnetic field influenced by the RT noise. In the current case, we repeat the parameter values given in Fig. 1. In comparison, the dynamical behavior of UIN seems completely different from the negativity given in Fig. 1, specifically for higher values of the temperature $k_B T$. However, for a higher temperature regime, the UIN shows a set of damping oscillations with a series of revival and collapse phenomena over time with an asymptotic limit. Under the decoherence effects, the UIN decreases gradually to stabilize for a specific interval of time which means that the UIN becomes frozen. On the other hand, it is clear that even under the presence of the decoherence phenomenon, the monotonic decay does not occur in the behavior of UIN even in a high-temperature regime. This indicates the presence of nonlocality even in the absence of entanglement between the qubit and qutrit.

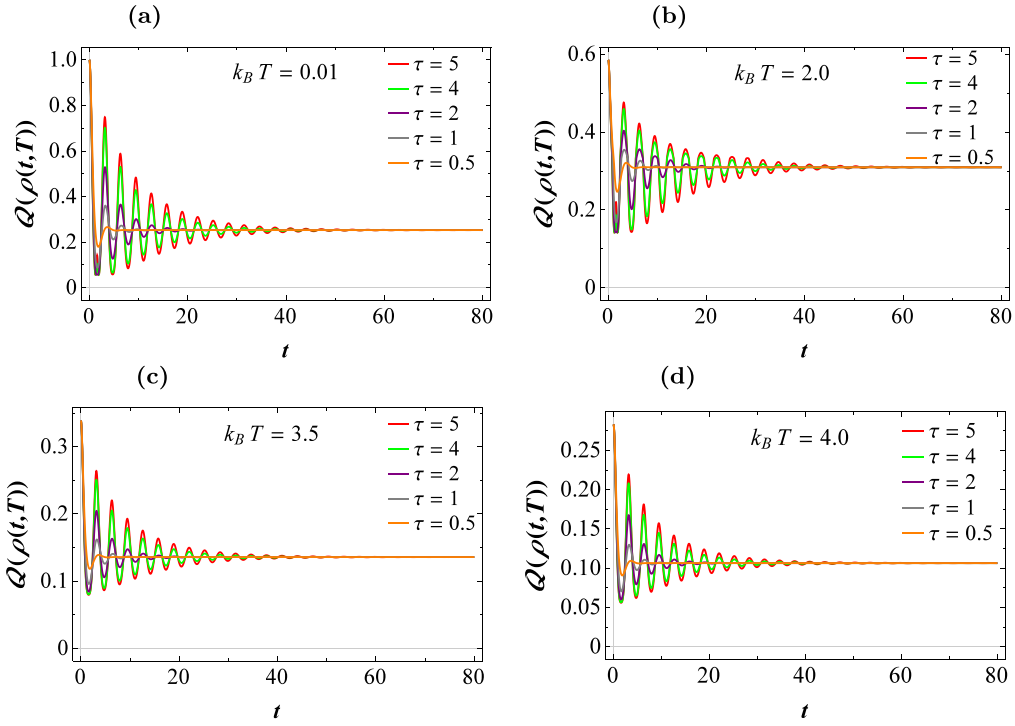


FIG. 3. Dynamics of the LQFI versus t by considering a few different values of parameter τ at different values of the temperature $k_B T/J$, assuming fixed $\mu_B B/J = 0.5$, $D_z/J = 6$, $\Delta/J = 0.5$ when $b/J = 0$.

This also implies that the ESD does not necessarily mean the loss of all quantum correlations. However, the fact remains the same and agrees with Fig. 1(a) that for low-temperature values $k_B T = 0.01$, the state becomes maximally correlated at $t = 0$ [see Fig. 2(a)]. Besides, the nonlocality measured via UIN shows strong resistance to any changes with temperature and nearly remains the same for all temperatures, except in the initial moments of interaction. The revival phenomenon is regulated by the parameter τ and not by any other parameter of the magnetic field in the current setup of parameters. However, slight revivals in the Markovian regime still exist due to the parameter τ which forces the environment to return the information to the system, making some revivals in the dynamical map of UIN. Furthermore, the revival character in the non-Markovian regime ensures the successful exchange of the attributes between the hybrid qubit-qutrit system and environment, which remains the reason to recover the nonlocality after the corresponding loss. The final saturation levels of the UIN measure completely depend upon the relevant temperature, and as temperature increases, the UIN tends to achieve the least values of the saturation levels, suggesting greater loss and vice versa. This is because temperature causes the state to be mixed and increases the entropy of the state, which finally results in greater nonlocality loss. Note that the dynamical maps of quantum correlations investigated under dephasing environments in Refs. [82,83] do not match with our results obtained by UIN, strong evidence of revivals and longer retention of quantum correlations. Besides, the final density matrices of the qubit-qutrit systems obtained in Refs. [82,83] have different structures as compared to that given in Eq. (16), indicating that the comparative configurations have a different amount of quantum correlations.

In Fig. 3, we address the dynamics of quantum correlation in terms of LQFI for a system of qubit-qutrit mixed spin chain coupled with an external magnetic field and superimposed by RT noise. For the current dynamical setup, we repeat the setting of the parameters used to obtain Fig. 1, but for LQFI. The qualitative dynamical outlook of the LQFI measure seems similar to that of the UIN criterion, however, with few slight changes. Namely, the maximum amount of quantum correlation captured by UIN for $t = 0$ is larger than that captured by LQFI. Not only the initial values of the quantum correlations, but the final saturation levels of the LQFI and UIN also do not match. Hence, this ensures that the nonlocality in terms of UIN differs from the quantum correlations quantified by LQFI. In comparison, the UIN and LQFI remain unfrozen and partially lost, which means that these two quantifiers go beyond quantum entanglement captured by negativity. In agreement with UIN, the related revival rate of LQFI increases for the increasing values of τ. Interestingly, the nonmonotonic decay of the LQFI occurs at the least values of τ; for instance, see the orange curves for $\tau = 0.5$. We notice a small revival of quantum correlation, which denotes the presence of feedback phenomenon in the environment causing a fraction of the lost information to flow back to the system at $\tau = 0.5$. Thus, as mentioned before, the low value of τ can also contribute to the behavioral dynamical maps of quantum correlations. The resultant decay in the current case resembles that obtained in the qubit-qutrit system when coupled to the magnetic field in Ref. [58] under the absence of environmental dephasing, where a shorter-lived and monotonic loss has been observed. However, we noticed that certain studies, such as Refs. [17,82,83], indicate that under the environmental dephasing, the decay observed is monotonic which again con-

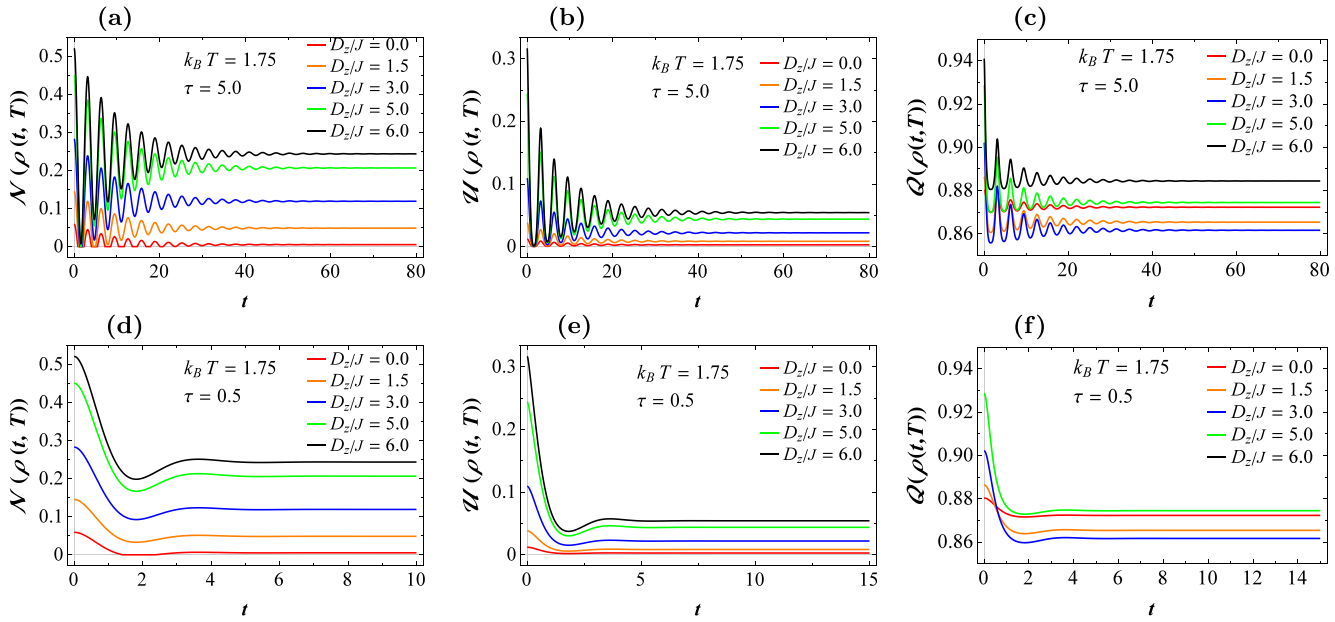


FIG. 4. Upper panels: The dynamics of quantum correlations versus t for several values of DM interaction at $\tau = 5$ when $\mu_B B/J = 0.5$, $k_B T/J = 1.75$, $\Delta/J = 0.5$, and $b/J = 0$. Lower panels: Same as upper panels but for $\tau = 0.5$.

trasts with the current results. Therefore, the longer quantum correlations and the presence of feedback phenomenon in the current system influenced by RT noise remained a more favorable resource for the quantum correlation transmission and preservation. Similarly, the study carried out in Ref. [81] resembles the current results where longer quantum correlation preservation in a qubit-qutrit system is modeled in two bosonic reservoirs regulated by temperature. For the increased efficiency of the quantum mechanical channels, one should increase τ, as it not only controls the revival's character but also regulates the preservation capacity of the system. As seen for higher values of τ, LQFI seems longer preserved. Note that the temperature variations strongly cause the initial quantum correlations to regulate and the two have been witnessed with an inverse relation. Furthermore, for each fixed value of temperature, the saturation level occurs at the same point even for different values of τ.

Figure 4 analyzes the dynamics of quantum correlations using negativity, UIN, and LQFI given in Eqs. (24), (38), and (47) in a mixed hybrid qubit-qutrit state exposed to an external magnetic field with reinforced RT noise. The external magnetic field here is described for different fixed values of DM interaction D_z when $k_B T = 1.75$, non-Markovian regime ($\tau = 5$) upper panel, Markovian regime ($\tau = 0.5$) lower panel, along with the absence of the inhomogeneity ($b = 0$). Because of the interplay of the DM interaction strength, the whole outlook of the comparative dynamics of negativity, UIN, and LQFI became changed. However, the impacts of the non-Markovianity and Markovianity as well as the temperature agree with Figs. 1–3. We observed that in the non-Markovian regime, the coupled fields allowed the quantum correlation quantifiers to decay in an oscillatory manner. Besides, the curves for high τ values took a longer time to saturate than for low values of the same parameter. In the Markovian regime, there occurs a single minimum of negativity, UIN, and LQFI for each parameter setting which then achieves its final saturation level. Also, because of no revivals of quantum phenomena, the loss of information and other attributes of the states will be assumed permanent, as no backflow of information occurs from the environment toward the system. For minimum temperature values, let $k_B T = 0.01$, we witness the state to be maximally correlated and vice versa, as seen in Figs. 1–3. In close connection with previous results, for the high value of temperature $k_B T = 1.75$, we detected the state to be partially entangled. We find the role of DM interaction strength opposite to that of the temperature, where the first one regulates the final saturation levels and the latter one, the initially encoded nonclassical correlations in the qubit-qutrit state. As seen for high values of D_z, the negativity and UIN remains highly preserved; however, for the least values, the forenamed quantities saturate at low values. Note that for $D_z/J = 0.0$, the state becomes completely classical and disentangled at the final interaction times. In contrast, with the LQFI, in the range $0 < D_z/J < 3.0$, we witness a contradicting behavior, where quantum correlations by means of LQFI show lesser loss at low values of D_z as compared to when $D_z/J = 3.0$. Note that for each value of D_z interaction strength, the LQFI initially as well as at final notes remains highly preserved and is not completely lost. This means that the LQFI is more resourceful to resist the dephasing effects of the RT noise and external magnetic field than entanglement and nonlocality, which were easily lost. Indeed, the DM interaction significantly enhances the amount of quantum correlations in the systems. This confirms the results reported in Ref. [62], in which the state become separable at lower values of the temperature in contrast to when the DM interaction is included in the system. Notably, the lower temperature and higher DM interaction strength also contributed to a single

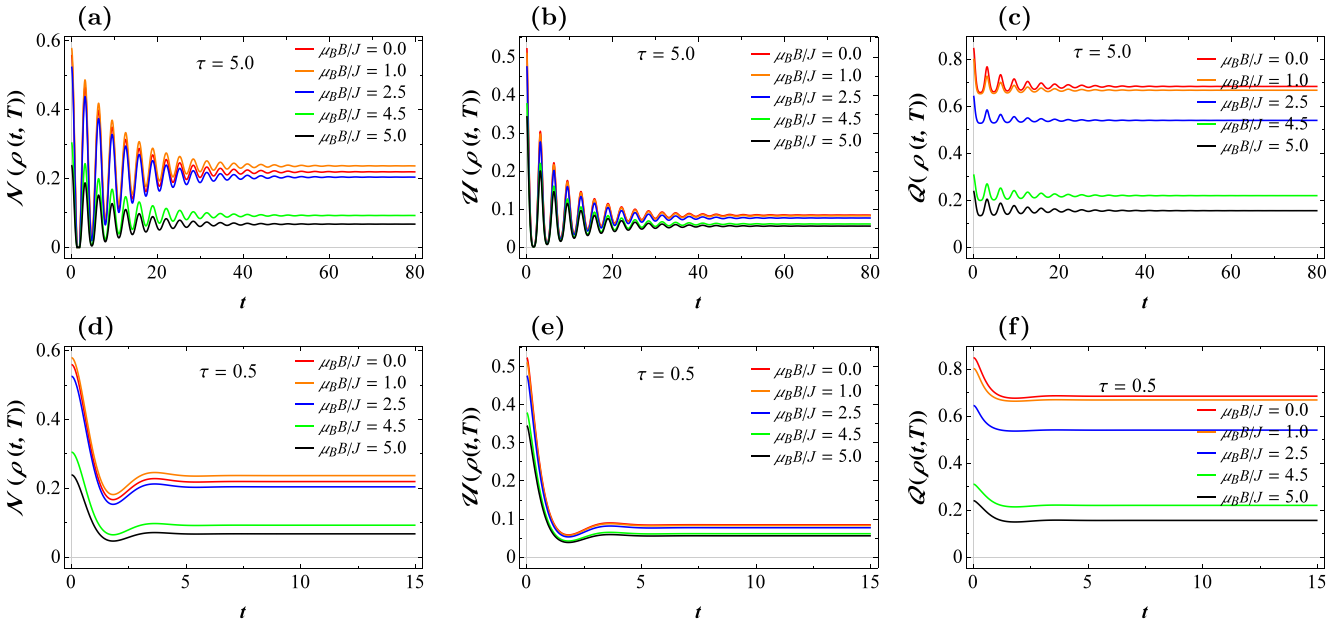


FIG. 5. Upper panels: The dynamics of quantum correlations versus t for several values of the external magnetic field at $\tau = 5$ when $D_z/J = 6$, $k_BT/J = 1.75$, $\Delta/J = 0.5$, and $b/J = 0$. Lower panels: Same as upper panels but for $\tau = 0.5$.

ESB, nonlocality, and LQFI even in the Markovian regime. We see that the negativity and UIN show a single revival after the first death.

Figure 5 illustrates the dynamics of negativity, UIN, and LQFI in a qubit-qutrit mixed entangled state when subjected to an external magnetic field and dephasing RT noise. We repeat the parameter settings shown in Fig. 4; however, we mainly focus on the effects of different fixed values of the magnetic field $\mu_B B/J$ on qubit-qutrit correlations retention in the state. The dynamical outlook of the negativity, UIN, and LQFI against increasing values of B seems opposed to that encountered against increasing D_z and τ values. For low values of $\mu_B B/J$, all quantifiers seemed better preserved. However, as the magnetic field strength increases, the correlations between the qubit-qutrit state become more suppressed. For instance, see the shifting of the red-lined curves to black end for increasing $\mu_B B/J$ values. Not only this, but the related revival rate of the correlation functions is also slightly decreased for the increasing values of B. Moreover, the maximums of the correlation functions against low values of $\mu_B B/J$ remain higher comparatively. We noticed a stronger revival rate in the dynamics of negativity, UIN, and LQFI for the higher values of τ in the non-Markovian regime. A faster decline of the quantum correlations has been witnessed in the Markovian regimes with a single minimum, as one can see that the negativity, UIN, and LQFI achieve the final saturation values quicker compared to that in the non-Markovian regime. Because of the revival phenomenon, the correlations in the system remain preserved for longer intervals in the non-Markovian regime. As compared to the negativity and UIN measures, the LQFI has been found highly impacted by the external magnetic field. The statement is followed by the fact that the revival character of the LQFI vanishes faster compared to that observed for negativity and UIN. Notably, in the Markovian regime, the LQFI fully exhibits an exponential decay before saturating at a constant value, which is comparable to the results of the negativity and UIN. However, it is still noticeable that the LQFI estimator encounters quantum correlations with larger initial values, which are followed by negativity and then UIN. Thus, one can conclude that the current hybrid state has greater initially encoded LQFI than entanglement and nonlocality. Remarkably, in the Markovian regime, a smaller revival character of the entanglement, nonlocality, and LQFI is observed. This is due to the fact that the parameter τ supports a single exchange of information between the system and the environment.

Figure 6 explores the dynamics of nonclassical correlations in a qubit-qutrit hybrid mixed thermal entangled state when an inhomogeneous magnetic field is applied along with RT noise either with Markovian or non-Markovian character. We primarily focus on the impact prevailed by the degree of inhomogeneity on preservation and behavioral dynamics of negativity, UIN, and LQFI. The overall dynamical map of the negativity and LQFI seems opposite in the current case as compared to that observed against B except for UIN. The fact that the increase in homogeneity increases the decay followed the statement. However, the inhomogeneity helps to avoid greater losses and the decay levels become lesser as the related parameter b is increased. In addition, we noticed that the inhomogeneity causes no changes to the revival character of the qubit-qutrit correlations and remained ineffective. The revival character depends upon the parameter τ and the related temperature of the reservoir and agrees with Figs. 1–5. The final decay levels for each inhomogeneous magnetic field strength parameter b are varied and as it increases, the decay levels indicate lesser degradation of the current qubit-qutrit correlations. Nevertheless, UIN remains susceptible to the strength of parameter b and as it grows, the related decay also increases, demonstrating the contradicting behavior to negativity and LQFI. Therefore, we conclude that not all the qubit-qutrit

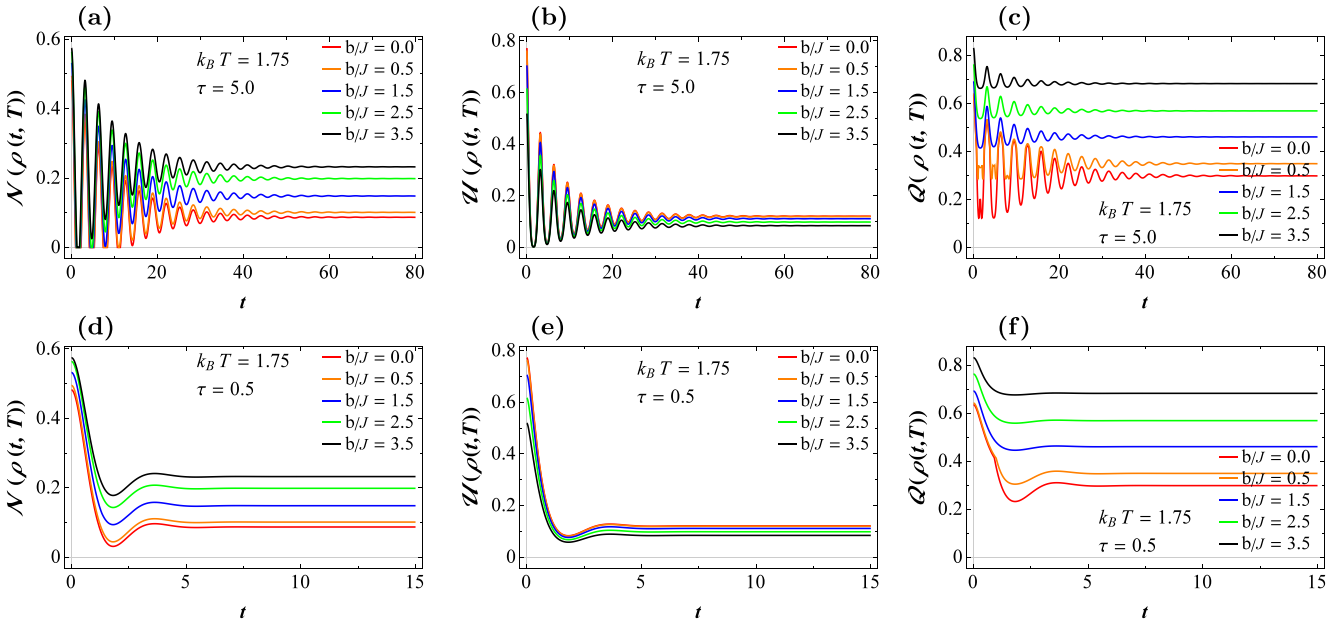


FIG. 6. Upper panels: The dynamics of quantum correlations versus t for several values of an inhomogeneous magnetic field at $\tau = 5$ when $D_z/J = 6$, $k_BT/J = 1.75$, $\Delta/J = 0.5$, and $\mu_B B/J = 0.5$. Lower panels: Same as upper panels but for $\tau = 0.5$.

correlations are equivalent, ensuring their different nature and that similar features of the magnetic field can differently affect them. In the Markovian regime, we notice that for the increasing values of b, the amplitude of the single observed minima increases for the case of negativity and LQFI; however, the opposite occurs in the case of UIN. Note that the mixed entangled state does not become fully separable and attains a final saturation level. The only reason behind this is setting the DM interaction and exchange parameter J to high values which avoid the full separability of the state. The existence of the revival character in the non-Markovian regime indicates the exchange of attributes between the hybrid-spin system and the environment, resulting in temporary information decay for a definite interval. Nonetheless, in the Markovian regime, we witness no revivals which will cause permanent information decay. However, the existence of slight revivals in the Markovian regime is due to the parameter τ, as the width of the Markovian regime is defined by the dimensionless product $a\tau$ (with $a = 1$). Therefore, there are still signs of the revivals in the regime where $\tau < 2$, causing the backflow of information from the environment to the system.

In Fig. 7, we address the time evolution of negativity, UIN, and LQFI for a system of hybrid-spin structure including a qubit-qutrit mixed entangled thermal state coupled with an external magnetic field. In the current case, we mainly focus on the temperature influence on the qubit-qutrit system dynamics. Temperature greatly influenced the initial negativity, UNI, and LQFI values and for the increasing values of T, the initially encoded correlations in the state become suppressed. This means that the rise in temperature makes the system more and more mixed rather than entangled. It is important to note that the initial negativity, UIN, and LQFI varies in magnitudes. In comparison, the initial qubit-qutrit correlations remain more resistant to the temperature effects. More explicitly, the higher values of temperature have negatively influenced the entanglement and it becomes easily lost at high-temperature values. On the other hand, the nonlocality is not completely lost even for the higher values of the temperature. In the case of LQFI, the related final saturation levels show comparatively the least decay because of the higher as well as the lower values of temperature. The results for non-Markovian and Markovian regimes remain in agreement with those defined in Figs. 4–6 and suggest strong revivals in the former and monotonic pattern decay in the latter. In light of the above results, we conclude that characterizing the Hamiltonian parameters by different features can be usefully utilized for practical quantum information processing. In addition, we find the least temperature values more resourceful to induce maximum qubit-qutrit correlations initially. Not only this, but the low-temperature values also contribute to longer quantum correlations preservation in the system. It can be seen that at low temperatures, the non-Markovian behavior is more obvious as compared to that at higher values. Therefore, besides parameter τ, the temperature also severally affects the non-Markovian dynamical maps of quantum correlations. However, some revivals exist in the Markovian regime, due to the system-environment coupling. This causes the information to exchange between the qubit-qutrit system and the environment even in the Markovian regime, implying the non-monotonic oscillatory behavior in negativity, nonlocality, and quantum Fisher information.

V. FINAL REMARKS

Now we consider comparing the current dynamical maps of quantum correlations to that observed for different quantum systems studied previously. In Ref. [84], the dynamics of entanglement and coherence for a system of three qubits, when coupled to external local fields, have been shown under the power-law and RT noises with a higher non-Markovian

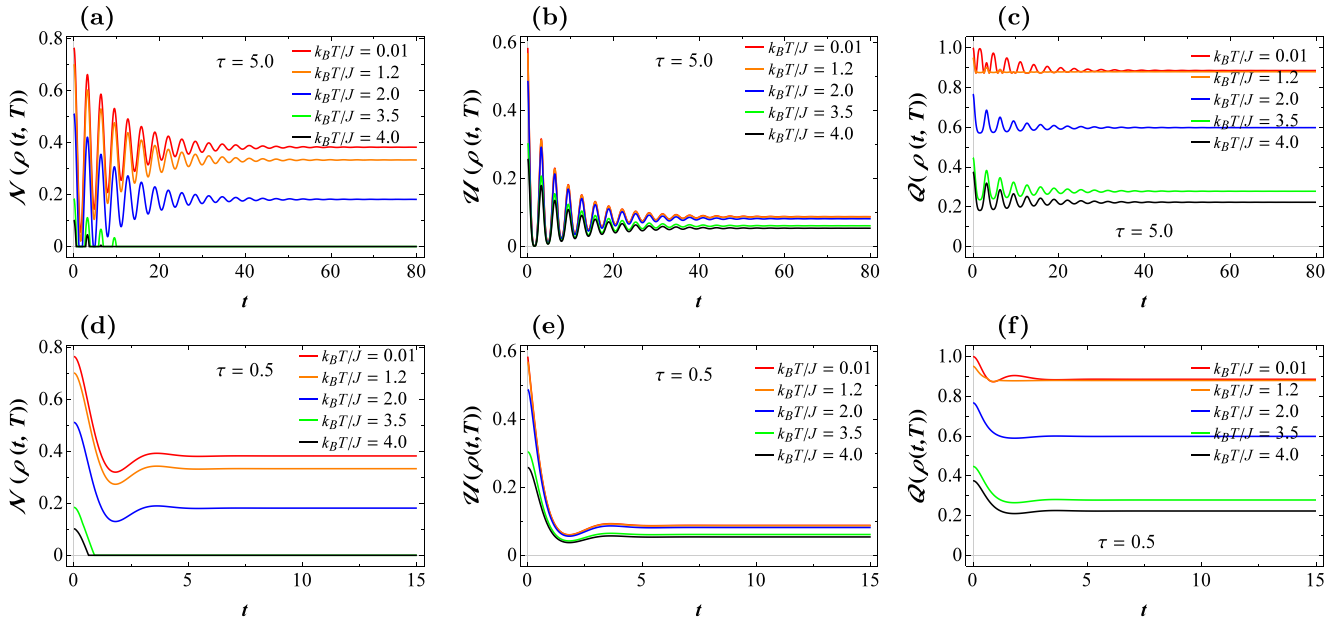


FIG. 7. Upper panels: The dynamics of quantum correlations versus t for several values of the temperature at $\tau = 5$ when $\mu_B B/J = 0.5$, $D_z/J = 6$, $b/J = 3.5$, and $\Delta/J = 0.5$. Lower panels: Same as upper panels but for $\tau = 0.5$.

behavior and preservation capacity as compared to that observed in the current case. Also, in the case of tripartite maximally entangled state when exposed to the classical field and mixed RT and static noise, the resultant exchange capacity and preservation intervals witnessed were comparatively reduced [85]. In the current case, we encountered a smaller exchange of information in the Markovian regime, which was completely absent for different quantum systems under the influence of RT noise in Refs. [38,84,85]. The Markovian and non-Markovian characteristics in the current case were exploited by the different aspects of the magnetic field and the resultant effects were completely changed. For example, in the non-Markovian regime, when the temperature is raised, the oscillatory behavior vanishes, whereas, when the Markovian regime is employed with low temperature, we observed some revivals in quantum correlations. This means that the Markovian and non-Markovian properties can be exploited and can be traced back to the similar results obtained in Ref. [86] for a system of two qubits exposed to mixed dephasing noises. It is important to note that the current qubit-qutrit system performed better at showing greater preservation of quantum correlations as compared to the two-qubit, three-qubit, free, and bound two-qutrit systems studied in Refs. [38,85–88].

In addition, it is also important to note that the current results obtained for negativity, UIN, and LQFI are found matching with other quantum phenomena. For instance, in Ref. [89], the generation of entropic uncertainty is found inversely dependent upon the existence of quantum correlations between the subquantum systems of the neutrino-flavor state. We observed repeated revivals of quantum correlations; therefore, in agreement with Ref. [89], there is a probability of generation of quantum memory in the current qubit-qutrit entangled state also. In Ref. [90], the authors proposed a trade-off scheme that revealed the complementarity relation between first-order coherence and intrinsic concurrence. Hence, providing a theoretical basis for reliable quantum information processing and preservation resources is valuable. Compared to the current case, there is a direct relation between entanglement, nonlocality, and LQFI. Accordingly, it is also a prospect of the current study to demonstrate the relations between first-order coherence and intrinsic concurrence in the qubit-qutrit systems. Furthermore, we find several other quantum criteria influencing each other directly or indirectly. These include the relation of coherence with entropic uncertainty, decoherence effects raised by the rising quantum memory generation values, and the influence of spin chains and related field parameters on the generation of quantum memory in quantum systems [91–93]. In light of these references, we find that the currently studied quantum correlations and related dynamical maps will strengthen bonds with the emerging values of quantum memory assisted entropic uncertainty and coherence [94,95]. Thereby, we believe that all of these studies are strong candidates for the future prospects of the current qubit-qutrit states and might yield interesting results.

VI. CONCLUSION

Quantum information processing and computing require longer preservation of the resources like entanglement, nonlocality, and other quantum correlations. This could be done by investigating different types of external transmitting mediums, related manipulation, and characterization of the parameters. In this study, we are motivated to investigate a thermal hybrid qubit-qutrit mixed entangled state coupled with an external magnetic field and dephasing RT noise. Using negativity, uncertainty-induced nonlocality, and local quantum Fisher information, we analyzed the dynamics and preservation of quantum correlations. With the optimal values of parameters, one can design longer preservation as well as the optimal

dynamical map of quantum correlations in a nonlocal setup. Therefore, we aim to provide optimal values of the related parameters to induce higher preservation of quantum correlations and optimal dynamical behavior.

Our findings show that when characterized by RT dephasing noise, the characteristic behavior of the external magnetic field towards the preservation and dynamics of the qubit-qutrit correlations changes. The characterization of the applied magnetic field by RT noise enables us to induce easy non-Markovian or Markovian dynamics, which seem completely different from conventional magnetic fields and related effects. Moreover, for certain parameters, for example, at high values of DM interaction strength, the non-Markovianity remained the only reason for the entanglement, nonlocality, and quantum correlation preservation in the state. However, this non-Markovianity is detected fragile to the temperature and is suppressed by the related action. Besides this, the temperature has been recorded to regulate the initial quantum correlations in the state and the two have been found in an indirect relation. In particular, characterizing the magnetic field by different parameters affects the qubit-qutrit correlations differently. For instance, the quantum correlations computed by local quantum Fisher information stand as the most effective one and showed the least decay when influenced by DM interaction, magnetic field strength, and temperature. The entanglement and nonlocality measured by negativity and uncertainty-induced nonlocality both remained weaker when exposed to the magnetic field, temperature, and even when DM interaction comes into interplay. According to our results, the optimal parameters which can boost the initial quantum correlations and can preserve them for longer are when the external magnetic field is characterized by the higher DM interaction and inhomogeneity strength at low temperatures. Finally, we found that the current transmitting and preservation channels, i.e., the magnetic field superimposed with RT noise, are vital resources for inducing larger quantum correlation preservation. Most importantly, the current coupled fields have many advantages, which can be used to produce the optimally required kind of dynamical maps of the quantum phenomena.

All data generated or analyzed during this study are included in this paper.

ACKNOWLEDGMENTS

F.B. has put forward the main idea for the model and method and performed the calculations and graphical tasks. A.U.R. and S.H. have contributed to interpreting the results and writing the manuscript. Thorough checking of the manuscript and confirming the conclusions were done by S.H. and A.U.R. The final draft of the manuscript was revised by S.H. and reviewed by all authors.

The authors declare no competing interests.

[1] K. Bu, A. Kumar, L. Zhang, and J. Wu, Cohering power of quantum operations, Phys. Lett. A **381**, 1670 (2017).

[2] K. C. Tan, H. Kwon, C. Y. Park, and H. Jeong, Unified view of quantum correlations and quantum coherence, Phys. Rev. A **94**, 022329 (2016).

[3] D. Beckman, D. Gottesman, M. A. Nielsen, and J. Preskill, Causal and localizable quantum operations, Phys. Rev. A **64**, 052309 (2001).

[4] A. Brodutch and K. Modi, Criteria for measures of quantum correlations, Quantum Inf. Comput. **12**, 721 (2012).

[5] U. Khalid, J. ur Rehman, and H. Shin, Measurement-based quantum correlations for quantum information processing, Sci. Rep. **10**, 2443 (2020).

[6] A. Bokulich and G. Jaeger, *Philosophy of Quantum Information and Entanglement* (Cambridge University Press, Cambridge, 2010).

[7] R. Ursin, F. Tiefenbacher, T. Schmitt-Manderbach, H. Weier, T. Scheidl, M. Lindenthal, and A. Zeilinger, Entanglement-based quantum communication over 144 km, Nat. Phys. **3**, 481 (2007).

[8] G. Arun and V. Mishra, A review on quantum computing and communication, in *2014 2nd International Conference on Emerging Technology Trends in Electronics, Communication and Networking* (IEEE, Surat, India, 2014).

[9] L. Gyongyosi and S. Imre, A survey on quantum computing technology, Comput. Sci. Rev. **31**, 51 (2019).

[10] C. H. Bennett, G. Brassard, C. Crépeau, R. Jozsa, A. Peres, and W. K. Wootters, Teleporting an Unknown Quantum State via Dual Classical and Einstein-Podolsky-Rosen Channels, Phys. Rev. Lett. **70**, 1895 (1993).

[11] H. Zhang, Z. Ji, H. Wang, and W. Wu, Survey on quantum information security, China Commun. **16**, 1 (2019).

[12] R. B. Jin, M. Takeoka, U. Takagi, R. Shimizu, and M. Sasaki, Highly efficient entanglement swapping and teleportation at telecom wavelength, Sci. Rep. **5**, 9333 (2015).

[13] Z. Ji, H. Zhang, and P. Fan, Two-party quantum private comparison protocol with maximally entangled seven-qubit state, Mod. Phys. Lett. A **34**, 1950229 (2019).

[14] Z. Ji, P. Fan, H. Zhang, and H. Wang, Greenberger-Horne-Zeilinger-based quantum private comparison protocol with bit-flipping, Phys. Scr. **96**, 015103 (2021).

[15] S. Bose, M. B. Plenio, and V. Vedral, Mixed state dense coding and its relation to entanglement measures, J. Mod. Opt. **47**, 291 (2000).

[16] A. A. Katanin, A. S. Belozerov, and V. I. Anisimov, Nonlocal correlations in the vicinity of the α-γ phase transition in iron within a DMFT plus spin-fermion model approach, Phys. Rev. B **94**, 161117(R) (2016).

[17] M. Jafarpour, F. K. Hasanvand, and D. Afshar, Dynamics of entanglement and measurement-induced disturbance for a hybrid qubit-qutrit system interacting with a spin-chain environment: A mean field approach, Commun. Theor. Phys. **67**, 27 (2017).

[18] K. K. Sharma and S. N. Pandey, Dynamics of entanglement in qubit-qutrit with x-component of DM interaction, Commun. Theor. Phys. **65**, 278 (2016).

[19] A. U. Rahman, M. Noman, M. Javed, M. X. Luo, and A. Ullah, Quantum correlations of tripartite entangled states under Gaussian noise, Quant. Info. Proc. **20**, 290 (2021).

[20] A. U. Rahman, M. Javed, A. Ullah, and Z. Ji, Probing tripartite entanglement and coherence dynamics in pure and mixed

independent classical environments, Quantum Inf. Process. **20**, 321 (2021).
[21] A. U. Rahman, M. Noman, M. Javed, A. Ullah, and M. X. Luo, Effects of classical fluctuating environments on decoherence and bipartite quantum correlations dynamics, Laser Phys. **31**, 115202 (2021).
[22] A. T. Tsokeng, M. Tchoffo, and L. C. Fai, Dynamics of entanglement and quantum states transitions in spin-qutrit systems under classical dephasing and the relevance of the initial state, J. Phys. Commun. **2**, 035031 (2018).
[23] S. Haddadi, A brief note on the Scott measure as a multipartite entanglement criterion, Laser Phys. Lett. **17**, 075201 (2020).
[24] B. M. Li, M. L. Hu, and H. Fan, Nonlocal advantage of quantum coherence and entanglement of two spins under intrinsic decoherence, Chin. Phys. B **30**, 070307 (2021).
[25] F. Benabdallah, A. Slaoui, and M. Daoud, Quantum discord based on linear entropy and thermal negativity of qutrit-qubit mixed spin chain under the influence of external magnetic field, Quantum Inf. Process. **19**, 252 (2020).
[26] P. J. Van Koningsbruggen, O. Kahn, K. Nakatani, Y. Pei, J. P. Renard, M. Drillon, and P. Legoll, Magnetism of A-Cu^{II} bimetallic chain compounds (A = Fe, Co, Ni): One- and three-dimensional behaviors, Inorg. Chem. **29**, 3325 (1990).
[27] T. Boness, S. Bose, and T. S. Monteiro, Entanglement and Dynamics of Spin Chains in Periodically Pulsed Magnetic Fields: Accelerator Modes, Phys. Rev. Lett. **96**, 187201 (2006).
[28] A. Redwan, A. H. Abdel-Aty, and N. Zidan, Dynamics of classical and quantum information on spin-chains with multiple interactions, Inf. Sci. Lett. **7**, 1 (2018).
[29] M. L. Hu, Y. Y. Gao, and H. Fan, Steered quantum coherence as a signature of quantum phase transitions in spin chains, Phys. Rev. A **101**, 032305 (2020).
[30] S. Haseli, S. Haddadi, and M. R. Pourkarimi, Entropic uncertainty lower bound for a two-qubit system coupled to a spin chain with Dzyaloshinskii-Moriya interaction, Opt. Quantum Electron. **52**, 465 (2020).
[31] S. Haddadi and A. Akhound, Thermal entanglement properties in two qubits one-axis spin squeezing model with an external magnetic field, Int. J. Theor. Phys. **58**, 399 (2019).
[32] D. Wang, F. Ming, A. J. Huang, W. Y. Sun, and L. Ye, Entropic uncertainty for spin-1/2XXX chains in the presence of inhomogeneous magnetic fields and its steering via weak measurement reversals, Laser Phys. Lett. **14**, 095204 (2017).
[33] M. J. Uren, D. J. Day, and M. Kirton, $1/f$ and random telegraph noise in silicon metal-oxide-semiconductor field-effect transistors, Appl. Phys. Lett. **47**, 1195 (1985).
[34] A. U. Rahman, M. Noman, M. Javed, and A. Ullah, Dynamics of bipartite quantum correlations and coherence in classical environments described by pure and mixed Gaussian noises, Eur. Phys. J. Plus **136**, 846 (2021).
[35] S. Daniotti, C. Benedetti, and M. G. Paris, Qubit systems subject to unbalanced random telegraph noise: Quantum correlations, non-Markovianity and teleportation, Eur. Phys. J. D **72**, 208 (2018).
[36] E. Paladino, Y. M. Galperin, G. Falci, and B. L. Altshuler, $1/f$ noise: Implications for solid-state quantum information, Rev. Mod. Phys. **86**, 361 (2014).
[37] X. Cai, Quantum dephasing induced by non-Markovian random telegraph noise, Sci. Rep. **10**, 88 (2020).
[38] A. T. Tsokeng, M. Tchoffo, and L. C. Fai, Quantum correlations and decoherence dynamics for a qutrit-qutrit system under random telegraph noise, Quantum Inf. Process. **16**, 191 (2017).
[39] T. Aoki, Y. Nishikawa, and M. Kuwata-Gonokami, Room-temperature random telegraph noise in luminescence from macroscopic InGaN clusters, Appl. Phys. Lett. **78**, 1065 (2001).
[40] G. Burkard, Non-Markovian qubit dynamics in the presence of $1/f$ noise, Phys. Rev. B **79**, 125317 (2009).
[41] F. Liu and K. L. Wang, Correlated random telegraph signal and low-frequency noise in carbon nanotube transistors, Nano Lett. **8**, 147 (2008).
[42] S. Cialdi, C. Benedetti, D. Tamascelli, S. Olivares, M. G. Paris, and B. Vacchini, Experimental investigation of the effect of classical noise on quantum non-Markovian dynamics, Phys. Rev. A **100**, 052104 (2019).
[43] M. Lewenstein, B. Kraus, J. I. Cirac, and P. Horodecki, Optimization of entanglement witnesses, Phys. Rev. A **62**, 052310 (2000).
[44] W. K. Wootters, Entanglement of formation and concurrence, Quantum Inf. Comput. **1**, 27 (2001).
[45] S. Luo, Quantum discord for two-qubit systems, Phys. Rev. A **77**, 042303 (2008).
[46] S. Haddadi and M. Bohloul, A brief overview of bipartite and multipartite entanglement measures, Int. J. Theor. Phys. **57**, 3912 (2018).
[47] M. L. Hu, X. Hu, J. Wang, Y. Peng, Y. R. Zhang, and H. Fan, Quantum coherence and geometric quantum discord, Phys. Rep. **762–764**, 1 (2018).
[48] D. Girolami, T. Tufarelli, and G. Adesso, Characterizing Nonclassical Correlations via Local Quantum Uncertainty, Phys. Rev. Lett. **110**, 240402 (2013).
[49] S. Kim, L. Li, A. Kumar, and J. Wu, Characterizing nonclassical correlations via local quantum Fisher information, Phys. Rev. A **97**, 032326 (2018).
[50] R. L. Xiao, X. Xiao, and W. J. Zhong, Dynamics of measurement-induced non-locality and geometric discord with initial system–environment correlations, Chin. Phys. B **22**, 080306 (2013).
[51] P. Calabrese, J. Cardy, and E. Tonni, Entanglement Negativity in Quantum Field Theory, Phys. Rev. Lett. **109**, 130502 (2012).
[52] A. B. A. Mohamed and E. M. Khalil, Atomic non-locality dynamics of two moving atoms in a hybrid nonlinear system: Concurrence, uncertainty-induced non-locality and Bell inequality, Opt. Quantum Electron. **53**, 612 (2021).
[53] M. Hagiwara, Y. Narumi, K. Minami, K. Tatani, and K. Kindo, Magnetization process of the $S = 1/2$ and 1 ferrimagnetic chain and dimer, J. Phys. Soc. Jpn. **68**, 2214 (1999).
[54] H. Čenčariková and J. Strečka, Unconventional strengthening of the bipartite entanglement of a mixed spin-(1/2, 1) Heisenberg dimer achieved through Zeeman splitting, Phys. Rev. B **102**, 184419 (2020).
[55] R. Demkowicz-Dobrzański, W. Górecki, and M. Guţă, Multi-parameter estimation beyond quantum Fisher information, J. Phys. A: Math. Theor. **53**, 363001 (2020).
[56] Y. Du, L. Jing, H. Fang, H. Chen, Y. Cai, R. Wang, and Z. Ji, Exploring the impact of random telegraph noise-induced accuracy loss on resistive RAM-based deep neural network, IEEE Trans. Electron Devices **67**, 3335 (2020).
[57] H. T. Lu, Y. J. Wang, S. Qin, and T. Xiang, Zigzag spin chains with antiferromagnetic-ferromagnetic interactions:

Transfer-matrix renormalization group study, Phys. Rev. B **74**, 134425 (2006).
[58] S. Xu, X. K. Song, and L. Ye, Measurement-induced disturbance and negativity in mixed-spin *XXZ* model, Quantum Inf. Process. **13**, 1013 (2014).
[59] S. Daffer, K. Wodkiewicz, J. D. Cresser, and J. K. Mclver, Depolarizing channel as a completely positive map with memory, Phys. Rev. A **70**, 010304(R) (2004).
[60] J. P. G. Pinto, G. Karpat, and F. F. Fanchini, Sudden change of quantum discord for a system of two qubits, Phys. Rev. A **88**, 034304 (2013).
[61] M. Ali, Dynamics of genuine multipartite entanglement under local non-Markovian dephasing, Phys. Lett. A **378**, 2048 (2014).
[62] F. Benabdallah, H. Arian Zad, M. Daoud, and N. Ananikian, Dynamics of quantum correlations in a qubit-qutrit spin system under random telegraph noise, Phys. Scr. **96**, 125116 (2021).
[63] Ł. Cywiński, R. M. Lutchyn, C. P. Nave, and S. D. Sarma, How to enhance dephasing time in superconducting qubits, Phys. Rev. B **77**, 174509 (2008).
[64] M. A. Nielson and I. L. Chuang, *Quantum Computation and Quantum Information* (Cambridge University Press, Cambridge, 2000).
[65] F. Benabdallah and M. Daoud, Dynamics of quantum discord based on linear entropy and negativity of qutrit-qubit system under classical dephasing environments, Eur. Phys. J. D **75**, 3 (2021).
[66] H. P. Breuer and F. Petruccione, *The Theory of Open Quantum Systems* (Oxford University Press, Oxford, 2002).
[67] G. Vidal and R. F. Werner, Computable measure of entanglement, Phys. Rev. A **65**, 032314 (2002).
[68] A. Peres, Separability Criterion for Density Matrices, Phys. Rev. Lett. **77**, 1413 (1996).
[69] M. Horodecki, P. Horodecki, and R. Horodecki, Separability of mixed states: Necessary and sufficient conditions, Phys. Lett. A **223**, 1 (1996).
[70] E. P. Wigner and M. M. Yanase, Information contents of distributions, Proc. Natl. Acad. Sci. USA **49**, 910 (1963).
[71] S. X. Wu, J. Zhang, C. S. Yu, and H. S. Song, Uncertainty-induced quantum nonlocality, Phys. Lett. A **378**, 344 (2014).
[72] Y. Khedif, S. Haddadi, M. R. Pourkarimi, and M. Daoud, Thermal correlations and entropic uncertainty in a two-spin system under DM and KSEA interactions, Mod. Phys. Lett. A **36**, 2150209 (2021).
[73] M. Ali, Local quantum uncertainty for multipartite quantum systems, Eur. Phys. J. D **74**, 186 (2020).
[74] A. Fujiwara and H. Nagaoka, Quantum Fisher metric and estimation for pure state models, Phys. Lett. A **201**, 119 (1995).
[75] M. G. A. Paris, Quantum estimation for quantum technology, Int. J. Quantum Inf. **07**, 125 (2009).
[76] S. L. Braunstein and C. M. Caves, Statistical Distance and the Geometry of Quantum States, Phys. Rev. Lett. **72**, 3439 (1994).
[77] D. Girolami, A. M. Souza, V. Giovannetti, T. Tufarelli, J. G. Filgueiras, R. S. Sarthour, D. O. Soares-Pinto, I. S. Oliveira, and G. Adesso, Quantum Discord Determines the Interferometric Power of Quantum States, Phys. Rev. Lett. **112**, 210401 (2014).
[78] H. S. Dhar, M. N. Bera, and G. Adesso, Characterizing non-Markovianity via quantum interferometric power, Phys. Rev. A **91**, 032115 (2015).
[79] S. Elghaayda, Z. Dahbi, and M. Mansour, Local quantum uncertainty and local quantum Fisher information in two-coupled double quantum dots, Opt. Quantum Electron. **54**, 419 (2022).
[80] F. Benabdallah, K. E. Anouz, and M. Daoud, Toward the relationship between local quantum Fisher information and local quantum uncertainty in the presence of intrinsic decoherence, Eur. Phys. J. Plus **137**, 548 (2022).
[81] L. Chen, X. Q. Shao, and S. Zhang, Measurement-induced disturbance and nonequilibrium thermal entanglement in a qutrit-qubit mixed spin *XXZ* model, Chin. Phys. B **20**, 100311 (2011).
[82] H. Yuan and L. F. Wei, Dynamics of measurement-induced disturbance for a qubit-qutrit system in noninertial frames, Commun. Theor. Phys. **59**, 17 (2013).
[83] A. Basit, H. Ali, F. Badshah, and G. Q. Ge, Enhancement of quantum correlations in qubit-qutrit systems under the non-Markovian environment, Commun. Theor. Phys. **68**, 29 (2017).
[84] A. U. Rahman, S. Haddadi, and M. R. Pourkarimi, Tripartite quantum correlations under power-law and random telegraph noises: Collective effects of Markovian and non-Markovian classical fields, Ann. Phys. (Berlin) **534**, 2100584 (2022).
[85] L. T. Kenfack, M. Tchoffo, G. C. Fouokeng, and L. C. Fai, Dynamics of tripartite quantum correlations in mixed classical environments: The joint effects of the random telegraph and static noises, Int. J. Quantum Inf. **15**, 1750038 (2017).
[86] M. Javed, S. Khan, and S. A. Ullah, The dynamics of quantum correlations in mixed classical environments, J. Russ. Laser Res. **37**, 562 (2016).
[87] A. T. Tsokeng, M. Tchoffo, and L. C. Fai, Free and bound entanglement dynamics in qutrit systems under Markov and non-Markov classical noise, Quantum Inf. Process. **17**, 190 (2018).
[88] S. Haddadi, M. R. Pourkarimi, and D. Wang, Tripartite entropic uncertainty in an open system under classical environmental noise, J. Opt. Soc. Am. B **38**, 2620 (2021).
[89] D. Wang, F. Ming, X. K. Song, L. Ye, and J. L. Chen, Entropic uncertainty relation in neutrino oscillations, Eur. Phys. J. C **80**, 800 (2020).
[90] F. Ming, D. Wang, L. J. Li, X. G. Fan, X. K. Song, L. Ye, and J. L. Chen, Tradeoff relations in quantum resource theory, Adv. Quantum Technol. **4**, 2100036 (2021).
[91] F. Ming, D. Wang, A. J. Huang, W. Y. Sun, and L. Ye, Decoherence effect on quantum-memory-assisted entropic uncertainty relations, Quantum Inf. Process. **17**, 9 (2018).
[92] Y. N. Guo, M. F. Fang, and K. Zeng, Entropic uncertainty relation in a two-qutrit system with external magnetic field and Dzyaloshinskii-Moriya interaction under intrinsic decoherence, Quantum Inf. Process. **17**, 187 (2018).
[93] A. B. A. Mohamed, A. N. Khedr, S. Haddadi, A. U. Rahman, M. Tammam, and M. R. Pourkarimi, Intrinsic decoherence effects on nonclassical correlations in a symmetric spin-orbit model, Results Phys. **39**, 105693 (2022).
[94] F. Ming, D. Wang, W. N. Shi, A. J. Huang, M. M. Du, W. Y. Sun, and L. Ye, Exploring uncertainty relation and its connection with coherence under the Heisenberg spin model with the Dzyaloshinskii-Moriya interaction, Quantum Inf. Process. **17**, 267 (2018).
[95] S. Haddadi, M. R. Pourkarimi, and S. Haseli, Relationship between quantum coherence and uncertainty bound in an arbitrary two-qubit X-state, Opt. Quantum Electron. **53**, 529 (2021).

GENERAL CONCLUSION AND OUTLOOK

The field of quantum information offers a potential revolution in communication and data processing with the development of new methods for encoding information in quantum states. Quantum entanglement is a fundamental and indispensable resource for reliable quantum information processing, and understanding its nature and properties is essential for advancing the field of quantum teleportation. The study of open quantum systems is also crucial for controlling and manipulating quantum systems and gaining a deeper understanding of the fundamental principles of quantum mechanics and the boundary between the classical and quantum worlds. As technology continues to advance, we can expect to see more applications of quantum information in various fields, making the quantification, characterization, and measurement of quantum correlations increasingly important for future research. While focusing on the problem of transmission and security of quantum information, the present thesis has been structured around the following axes.

The primary objective of this thesis is to find more reliable and appropriate non-classical correlation metrics and to understand their behavior in open quantum systems. By achieving this goal, we can pave the way for the realization of practical quantum protocols in the field of quantum information science, such as the successful implementation of quantum teleportation. In this section, we provide a technical summary of the content of the thesis, highlighting the key findings and insights that have emerged from our research. Additionally, we discuss the future of this work, outlining potential avenues for further investigation and development. Finally, we draw general conclusions based on the results we have obtained, summarizing the key contributions of this thesis to the field of quantum information science. Throughout this manuscript, we have endeavored to present our work in a concise manner, with a focus on clarity and accessibility. The thesis is divided into five chapters, each of which builds upon the previous one to provide a comprehensive and coherent exploration of the topic at hand. The general introduction sets the stage for the subsequent chapters, providing a clear and concise overview of the key concepts and ideas that underpin our research.

The first chapter 1 of this thesis provided a comprehensive review of the key introductory concepts of quantum information theory. We began with an explanation of information from the physical point of view, exploring the link between randomness and the lack of information. From there, we delved into the differences between classical and quantum information, providing a brief overview of the corresponding measurements. To aid in this discussion, we also introduced the basic mathematical tools used in the description of quantum states, including the density operator formalism, which is widely useful in both theoretical and experimental levels, the notion of qubits, quantum measurements, and entropy schemes.

Numerous studies focused on the realization of entanglement in quantum states, and significant efforts were dedicated to investigating the dynamics of entanglement, its decoherence, and

its control in diverse systems. Motivated by this, in our second chapter 2 we delved into the phenomenon of quantum entanglement. We discussed various separability criteria that allowed us to qualitatively distinguish quantum entangled states from separable ones, both for pure as well as mixed states. However, to implement the latest technologies based on the concept of quantum entanglement, it was crucial to determine the degree of entanglement encoded in a quantum system. To this end, we delved deeper into different metrics of quantum entanglement in bipartite quantum systems, including concurrence, negativity, logarithmic negativity, and others, examining their advantages and drawbacks. We demonstrated that selecting the appropriate measure depends in the first place on the characteristics of the quantum system under consideration. Moreover, we extended some metrics to multipartite systems, as the latter is advantageous for developing robust technologies.

However, it was demonstrated that even separable states could play an important role in the execution of communication and information protocols they perform better than classical protocols. It was therefore interesting to study the fundamental advantages of quantum correlations beyond entanglement. The third chapter 3 of our study focused on the concept of quantum discord, a widely accepted measure for quantifying the amount of non-classical correlations in a quantum system. We began by presenting a general procedure for deriving the amount of quantum discord in two-qubit quantum states and then explored its relationship between entanglement measures. However, evaluating quantum discord for arbitrary quantum states is challenging due to the complex optimization procedure involved. To address this, we introduced geometric quantum discord, a variant of entropic quantum discord that measures the minimal distance between a quantum state and the closest zero-discord state using the Hilbert-Schmidt norm and trace norm. Our work provided explicit expressions for the geometric quantum discord in both two-qubit and qubit-qudit quantum states. We have shown that the geometric quantum discord is not an appropriate metric of quantumness due to the contractivity under LOCC maps. In this respect, the optimization problem for conditional entropy, and consequently for quantum discord, is the reformulation using linear entropy instead of von Neumann entropy in the classical correlation calculus induced by local measurement. This process yielded two analytical expressions of quantum discord, one for arbitrary qubit-qubit states, and the other for bipartite qudit-qubit states. We have also treated another entropic metric for quantum correlation for a high dimension quantum state known as the measurement induce disturbance.

Despite considerable efforts devoted to quantifying the amount of quantum correlations using quantum discord, a direct algorithm for calculating this metric in any given quantum system remains a challenging task. Motivated by this, we have analytically developed in the fourth chapter 4 some reliable alternative tools allowing for better detection and quantification of discord-like correlations. This approach represents an evolutionary step in characterizing correlations, particularly given the increasing dimension of the Hilbert space as the number of interacting particles increases. To achieve this, we have derived an explicit formula for the local quantum uncertainty and the uncertainty-induced non-locality for qubit-qudit systems using the concept of skew information. We have also extended the definition of local quantum uncertainty to a multipartite quantum system. Moreover, we have studied another metric of non-classical correlations using the concept of quantum coherence. Furthermore, we connected the notion of quantum Fisher information to the analysis of quantum correlations. Specifically, we investigated the characterization of quantum correlations from the perspective of local Fisher quantum information, which is a reasonable measure of quantum correlations. This connection became apparent when we examined the relationship between local quantum Fisher information and local quantum uncertainty, which are both quantifiers of discord-like quantum correlations through quantum uncertainty. This insight was particularly valuable for understanding the role of quantum correlations in determining the high precision of estimated parameters. In the

second part of this chapter, we delved into the topic of quantum teleportation, starting with an investigation of the standard protocol. We then explored the use of a maximally mixed state as a quantum resource to teleport a two-qubit state between two senders, namely Alice and Bob. Additionally, we studied the standard teleportation protocol using a three-qubit state as a quantum resource. Throughout our analysis, we examined the credibility of the quantum teleportation process, mainly by using the concepts of quantum fidelity and average fidelity.

When a quantum system interacts with its surrounding environment, coherence, and quantum characteristics are often destroyed during evolution. However, preserving coherence and quantum correlations is essential for quantum information processing. Therefore, understanding the mechanism of decoherence is crucial for the development of quantum technologies. To design robust protocols against the harmful effects of decoherence, it is important to precisely characterize the noise acting on a quantum system. While the usual approach to studying decoherence is to describe the environment as a quantum reservoir, this description may be difficult or inappropriate in some situations. To address these issues, the fifth chapter 5 of this thesis provides a comprehensive description of the theory of open quantum systems. Specifically, we discussed universal dynamical maps and their relationship with the evolution of open quantum systems. Moreover, we have shown that the dynamics of the reduced system can be obtained from the Liouville-Von Neumann equation. Additionally, we presented Lindblad's master equation, which is derived using the Born-Markov approximations. This master equation is used to study and control decoherence due to the interaction between a quantum system and its environment using Markovian approaches and techniques. We also explore the master equation in the non-Markovian regime and investigate another cause of decoherence that arises from the system's dynamics, rather than its surrounding environment, using the Milburn scheme. By providing a more nuanced understanding of decoherence and its effects on quantum systems, this chapter contributes to the development of more robust and efficient quantum technologies.

In the sixth chapter 6, we have inserted our contributions dedicated to these different significant axes.

- The first contribution 1 of our study focused on optimizing the entropic quantum discord by proposing a reliable approach for computing this metric in an arbitrary qudit-qubit quantum system. This approach involves using linear entropy instead of von Neumann entropy to maximize the classical correlations. To demonstrate the usefulness of this approach, we applied it to a qutrit-qubit system experiencing global classical dephasing environmental noise under the Markovian regime. In order to obtain the time-dependent density matrix, we used the master equation approach via the Born-Markov approximations. Our studies mainly centered on a particular initial qutrit-qubit state in thermal equilibrium at a temperature. We compared the obtained quantum discord (QD) with measurement-induced disturbance (MID) and logarithmic negativity (LN). Our findings revealed that both functions, namely QD and MID, are more robust than entanglement (LN) against the decoherence effect. Additionally, the dynamics of QD exhibited an intriguing behavior known as the freezing phenomenon, confirming that QD is an appropriate metric of non-classical correlation for implementing robust quantum protocols based on the notion of quantum correlations.

- The second contribution 2 is devoted to understanding the relationship between quantum correlation and quantum coherence in quantum systems. In particular, we investigated the evolution of quantum coherence captured via the l_1-norm coherence, quantum correlations based on the local quantum uncertainty and entanglement in terms of concurrence in a pairwise quantum state under thermal conditions. This thermal state is used as a quantum resource to implement quantum teleportation using the standard protocol. Our study examined the effects of various parameters encoded in the quantum system

to enhance both thermal quantum correlations and average fidelity. Our findings demonstrated that quantum coherence is a more efficient metric than concurrence and local quantum uncertainty for detecting the quantumness of the thermal state. Furthermore, by adjusting the anisotropy parameter's strength, we achieved significant enhancements in entanglement, local quantum uncertainty, and coherence. Notably, we observed that within a specific interval of assumed exchange anisotropy, the average fidelity significantly improved. These findings suggest that quantum coherence is an essential aspect of quantum correlation and that it can be used to enhance the performance of quantum protocols such as quantum teleportation.

- Our third contribution 3 presented a comparative study of non-classical correlation metrics, namely the notion of local quantum uncertainty and entanglement in terms of negativity, in a the tripartite magnetic Cu_3^{II} complex system. Our study reveals that both metrics are significantly influenced by the intrinsic parameters, namely the exchange anisotropy and cyclic three-spin interaction parameters, as well as extrinsic parameters such as temperature and magnetic field. Besides, the three-qubit local quantum uncertainty is a good estimator of quantum correlations in this thermal state. We have applied this model to quantum metrology to assess the sensitivity of the proposed tripartite system with respect to changes in various parameters contained in the tripartite model. Our results reveal that it is possible to estimate successfully the temperature and external magnetic field parameters encoded in the mentioned with robust estimation for some specific intervals. Moreover, the relationship between the estimation precisions and the non-classical correlations has been established. Moreover, a scheme of quantum teleportation process by using the tripartite state as a quantum channel is also suggested. Our results showed that, for sufficiently low temperatures and a specific value of the magnetic field and cyclic three-spin interaction, the average fidelity of the corresponding teleportation is greater than 2/3, indicating successful teleportation.

- Our fourth contribution 4 involves analyzing the behavior of several discord-like metrics of quantum correlations, namely local quantum uncertainty (LQU) and local Fisher information (LQFI), and entanglement in terms of concurrence in a Heisenberg XXZ spin-1/2 chain that is affected by intrinsic decoherence. The dynamics are controlled via the Milburn equation. We have studied the behaviors of those metrics for three particular initial states. We investigated the delicate connection between local quantum uncertainty, local quantum Fisher information, and concurrence. We have shown that the generation and robustness of quantum correlations depend on both physical parameters contained in the system and initial states. Our research uncovers that LQU and LQFI are more resistant to intrinsic decoherence and differ from entanglement in terms of information processing. Additionally, we explore the potential for teleportation within this model, as the various parameters of the two-qubit Heisenberg XXZ model serve as effective control parameters for quantum communications.

- The fifth contribution 5 focused on exploring the dynamics of quantum correlations in a hybrid qubit-qutrit thermal state. We used the negativity, uncertainty-induced nonlocality, and local quantum Fisher information to investigate the system's behavior under different conditions. Specifically, we established a connection between uncertainty-induced nonlocality and local quantum Fisher information and examine the impact of magnetic field and random telegraph noise on the qubit-qutrit correlations. We also considered various system parameters to ensure that the correlations are preserved for longer periods. Our results showed that temperature inversely affects the initial values of negativity, uncertainty-induced nonlocality, and local quantum Fisher information. We observed

that entanglement, nonlocality, and Fisher information display distinct dynamics when the magnetic field is characterized by different features. Furthermore, we found that the qubit-qutrit correlations undergo repeated revivals when the configuration is restricted to the non-Markovian regime. However, when the coupled field is in the Markovian regime, we observe an exponential drop with a single minimum.

Overall, we believe that this thesis represents a significant contribution to the field of quantum information science, and we look forward to seeing how our findings and insights will be applied in future research and practical applications. Moving forward, we believe that there are several key areas where future research can build on this work and further advance our understanding of quantum systems. One important area of focus will be further developing and exploring more suitable metrics for capturing the amount of non-classical correlations in higher dimensions quantum systems. This is important because quantum systems with more dimensions are necessary for achieving robust quantum protocols. For example, in quantum communication, higher dimensional systems can increase the amount of information that can be transmitted securely. Furthermore, our future research will focus on understanding the role of quantum correlations under destructive effects, such as decoherence in different environments and temperatures. Specifically, we are interested in exploring the use of more sophisticated quantum systems, such as Heisenberg models and quantum dots, in order to preserve and maintain quantum correlations over longer periods. We aim to gain a deeper understanding of the mechanisms that drive quantum correlations in these systems, and how they can be leveraged to develop more robust and efficient quantum protocols.

BIBLIOGRAPHY

[1] P.A.M. Dirac, *"The principles of quantum mechanics"*, **27**. Oxford University Press (1981).

[2] A. Einstein, B. Podolsky and N. Rosen, *"Can quantum-mechanical description of physical reality be considered complete?"*, Phys. Rev. **47** (1935) 777.

[3] E. Schrödinger, *"Discussion of probability relations between separated systems"*, Proc. Cambridge Phil. Soc. **31** (1935) 555-563.

[4] D. Castelvecchi and E. Gibney, *"'Spooky'quantum-entanglement experiments win physics Nobel"*, Nature **610** (2022) 241.

[5] M.A. Nielsen, I.L. Chuang, *"Quantum computation and quantum information"*, Cambridge University Press, Cambridge (2002).

[6] R. Horodecki, P. Horodecki, M. Horodecki and K. Horodecki, *"Quantum entanglement"*, Rev. Mod. Phys. **81** (2009) 865.

[7] D. Leibfried, E. Knill, S. Seidelin, J. Britton, R.B. Blakestad, J. Chiaverini, D.B. Hume, W.M. Itano, J.D. Jost, C. Langer, R. Ozeri, R. Reichle and D.J. Wineland, *"Creation of a six-atom "Schrödinger cat" state"*, Nature **438** (2005) 639-642.

[8] H. Häffner, W. Hänsel, C.F. Roos, *et al.*, *"Scalable multi-particle entanglement of trapped ions"*, Nature **438** (2005) 643-646.

[9] C.-Y. Lu, X.-Q. Zhou, O. Gühne, *et al.*, *"Experimental entanglement of six photons in graph states"*, Nature Phys. **3** (2007) 91-95.

[10] W.-B. Gao, C.-Y. Lu, X.-C. Yao, *et al.*, *"Experimental demonstration of a hyper-entangled ten-qubit Schrödinger cat state"*, Nature Phys **6** (2010) 331-335 .

[11] P. Neumann, N. Mizuochi, F. Rempp, *et al.*, *"Entanglement among single spins in diamond"*, Science **320** (2008) 1326.

[12] O. Mandel, M. Greiner, A. Widera, *et al.*, *"Controlled collisions for multi-particle entanglement of optically trapped atoms"*, Nature **425** (2003) 937-940.

[13] J. Hald, J.L. Słrensen, C. Schori, E.S. Polzik, *"Spin squeezed atoms: A macroscopic entangled ensemble created by light"*, Phys. Rev. Lett. **83** (1999) 1319.

[14] C.H. Bennett, H. J. Bernstein, S. Popescu and B. Schumacher, *"Concentrating partial entanglement by local operations"*, Phys. Rev. A **53** (1996) 2046.

[15] W.K. Wootters, *"Entanglement of formation of an arbitrary state of two qubits"*, Phys. Rev. Lett. **80** (1998) 2245.

[16] G. Vidal and R. F. Werner, *"Computable measure of entanglement"*, Phys. Rev. A **65** (2002) 032314.

[17] C.H. Bennett, D.P. DiVincenzo, C.A. Fuchs, T. Mor, E. Rains, P.W. Shor, J.A. Smolin, and W.K. Wootters, *"Quantum nonlocality without entanglement"*, Phys. Rev. A **59** (1999) 1070.

[18] M. Horodecki, P. Horodecki, R. Horodecki, J. Oppenheim, A. Sen, U. Sen and B. Synak-Radtke, *"Local versus nonlocal information in quantum-information theory: Formalism and phenomena"*, Phys. Rev. A **71** (2005) 062307.

[19] A. Datta, A.T. Flammia and C.M. Caves, *"Quantum telecloning and multiparticle entanglement"*, Phys. Rev. A. **72** (2005) 042316.

[20] A. Datta and G. Vidal, *"Role of entanglement and correlations in mixed-state quantum computation"*, Phys. Rev. A **75** (2007) 042310.

[21] A. Datta, A. Shaji and C.M Caves, *"Quantum discord and the power of one qubit"*, Phys. Rev. Lett. **100** (2008) 050502.

[22] B.P. Lanyon, M. Barbieri, M.P. Almeida and A.G. White, *"Experimental quantum computing without entanglement"*, Phys. Rev. Lett. **101** (2008) 200501.

[23] H. Ollivier and W.H. Zurek, *"Quantum discord: a measure of the quantumness of correlations"*, Phys. Rev. Lett. **88** (2001) 017901.

[24] L. Henderson and V. Vedral, *"Classical, quantum and total correlations"*, J. Phys. A: Math. Gen. **34** (2001) 6899.

[25] S. Luo, "*Quantum discord for two-qubit systems*", Phys. Rev. A **77** (2008) 042303.

[26] M. Ali, A.R.P. Rau and G. Alber, *"Quantum discord for two-qubit X states"*, Phys. Rev. A **81** 2010 042105.

[27] J. Oppenheim, M. Horodecki, P. Horodecki and R. Horodecki, *"Thermodynamical approach to quantifying quantum correlations"*, Phys. Rev. Lett. **89** (2002) 180402.

[28] C. Wang, Y.Y. Zhang and Q.H. Chen, *"Quantum correlations in collective spin systems"*, Phys. Rev. A **85** (2012) 052112.

[29] L.X. Cen, X.Q. Li, J. Shao and Y.J. Yan, *"Quantifying quantum discord and entanglement of formation via unified purifications"*, Phys. Rev. A **83** (2011) 054101.

[30] A. Shabani and D.A. Lidar, "*Vanishing quantum discord is necessary and sufficient for completely positive maps*", Phys. Rev. Lett. **102** (2009) 100402.

[31] F. Galve, G.L. Giorgi and R. Zambrini, *"Maximally discordant mixed states of two qubits"*, Phys. Rev. A **83** (2011) 012102.

[32] F. Benabdallah, A. Slaoui and M. Daoud, *"Quantum discord based on linear entropy and thermal negativity of qutrit-qubit mixed spin chain under the influence of external magnetic field"*, Quant. Inf. Process **19** (2020) 252.

[33] D. Girolami and G. Adesso, *"Quantum discord for general two-qubit states: analytical progress"*, Phys. Rev. A **83** (2011) 052108.

[34] M. Daoud and R. Ahl Laamara, *"Quantum discord for multipartite coherent states interpolating between werner and greenberger-horne-zeilinger states"*, Int. J. Quant. Inform **10** (2012) 1250060.

[35] M. Daoud and R. Ahl Laamara, *"Geometric measure of pairwise quantum discord for superpositions of multipartite generalized coherent states"*, Phys. Lett. A **376** (2012) 2361.

[36] B. Dakić, V. Vedral and C. Brukner, *"Necessary and sufficient condition for nonzero quantum discord"*, Phys. Rev. Lett. **105** (2010) 190502 .

[37] F.M. Paula, T.R. de Oliveira and M.S. Sarandy, *"Geometric quantum discord through the Schatten 1-norm"*, Phys. Rev. A. **87** (2013) 064101.

[38] F. Ciccarello, T. Tufarelli and V. Giovannetti, *"Toward computability of trace distance discord"*, New J. Phys. **16** (2014) 013038.

[39] Z. Ma, Z. Chen, F.F. Fanchini and S.M. Fei, *"Quantum discord for $d \otimes 2$ systems"*, Sci. Rep. **5** (2015) 10262.

[40] S. Luo, *"Using measurement-induced disturbance to characterize correlations as classical or quantum"*, Phys. Rev. A **77** (2008) 022301.

[41] D. Girolami, T. Tufarelli and G. Adesso, *"Characterizing nonclassical correlations via local quantum uncertainty"*, Phys. Rev. Lett. **110** (2013) 240402.

[42] S.-X. Wu, J. Zhang, C.-S. Yu and H.-S. Song, *"Uncertainty-induced quantum nonlocality"*, Phys. Lett. A **378** (2014) 344.
[43] S. Kim, L. Li, A. Kumar, J. Wu, *"Characterizing nonclassical correlations via local quantum Fisher information"*, Phys. Rev. A. **97** (2018) 032326.
[44] M.L. Hu, X. Hu, J. Wang, Y. Peng, Y.R. Zhang, H. Fan , *"Quantum coherence and geometric quantum discord"*, Phys. Rep. **762** (2018) 1.
[45] C.H. Bennett, G. Brassard, C. Crepeau, R. Jozsa, A. Peres, W.K. Wootters, *"Teleporting an unknown quantum state via dual classical and Einstein–Podolsky–Rosen channels"*, Phys. Rev. Lett. **70** (1993) 1895.
[46] H.L. Huang, *"Quantum teleportation via a two-qubit Ising Heisenberg chain with an arbitrary magnetic field"*, Int. J. Theor. Phys. **50** (2011) 70-79.
[47] K. El Anouz, A. El Allati, A. Salah *et al.*, *"Quantum Fisher information: probe to measure fractional evolution"*, Int. J. Theor. Phys. **59** (2020) 1460-1474.
[48] T. Jennewein, C. Simon, G. Weihs, H. Weinfurter, A. Zeilinger, *"Quantum cryptography with entangled photons"*, Phys. Rev. Lett. **84** (2000) 4729-4732.
[49] C. H. Bennett and S. J. Wiesner, "*Communication via one- and two-particle operators on Einstein-Podolsky-Rosen states*", Phys. Rev. Lett. 69 (1992) 2881.
[50] M. Hadipour, S. Haseli, H. Dolatkhah, S. Haddadi and A. Czerwinski, "*Quantum speed limit for a moving qubit inside a leaky cavity*", Photonics **9** (2022) 875.
[51] G. Adesso, T.R. Bromley and M. Cianciaruso, *"Measures and applications of quantum correlations"*, J. Phys. A: Math.Theor. 49, 473001 (2016).
[52] J.W. Pan, D. Bouwmeester, M. Daniell, H. Weinfurter, and A. Zeilinger, *"Experimental test of quantum nonlocality in three-photon Greenberger-Horne-Zeilinger entanglement"*, Nature 403 (2000) 515.
[53] F. Benabdallah, H. Arian Zad. M. Daoud and N. Ananikian, *"Dynamics of quantum correlations in a qubit-qutrit spin system under random telegraph noise"*, Phys. Scr. **96** (2021) 125116.
[54] F. Benabdallah and M. Daoud, *"Dynamics of quantum discord based on linear entropy and negativity of qutrit-qubit system under classical dephasing environments"*, Eur. Phys. J. D **75** (2021) 3.
[55] D. Gottesman and I.L. Chuang, *"Demonstrating the viability of universal quantum computation using teleportation and single-qubit operations"*, Nature. **402** (1999) 390-393.
[56] E. Knill, R. Laflamme and G.J. Milburn, *"A scheme for efficient quantum computation with linear optics"*, Nature **409** (2001) 46-52.
[57] D. Bouwmeester, J-W Pan, K. Mattle, M. Eibl, H. Weinfurter and A. Zeilinger, *"Experimental quantum teleportation"*, Nature, **390** (1997) 575.
[58] E. Lombardi, F. Sciarrino, S. Popescu and F. De Martini, *" Teleportation of a Vacuum-One-Photon Qubit"*, Phys. Rev. Lett. **88** (2002) 070402.
[59] I. Marcikic, H. De Riedmatten, W. Tittel, H. Zbinden and N. Gisin, *"Long-distance teleportation of qubits at telecommunication wavelengths"*, Nature, **421** (2003) 509.
[60] M. D. Barrett, J. Chiaverini, T. Schaetz, *et al.*, *"Deterministic quantum teleportation of atomic qubits"*, Nature. **429** (2004) 737-739.
[61] M.A. Nielsen, E. Knill and R. Laflamme, *"Complete quantum teleportation using nuclear magnetic resonance"*, Nature. **396** (1998) 52-55.
[62] L. Stefeen, Y. Salathe, M. Oppliger, *et al.*, *"Deterministic quantum teleportation with feed-forward in a solid state system"*, Nature. **500** (2013) 319-322.
[63] S. Pirandola, J. Eisert, C. Weedbrook, A. Furusawa and S.L. Braunstein, "*Advances in quantum teleportation*", Nat. Photon. **9** (2015) 641-652.
[64] J.-G. Ren, P. Xu, H.-L. Yong, et al. "Ground-to-satellite quantum teleportation", Nature. **549** (2017) 70-73.

[65] C.W. Gardiner and P. Zoller, *"Quantum Noise"*, Springer, Berlin, (2004).
[66] H.M. Wiseman and G.J. Milburn, *"Quantum Measurement and Control"*, Cambridge University Press, Cambridge, (2009).
[67] F. Altintas, *"Geometric measure of quantum discord in non-Markovian environments"*, Opt. Commun. **283** (2010) 5264.
[68] F. Benabdallah, S. Haddadi, H. Arian Zad, M. Reza Pourkarimi, M. Daoud, N. Ananikian, *"Pairwise quantum criteria and teleportation in a spin square complex"*, Sci. Rep. **12** (2022) 6406.
[69] F. Benabdallah, A. Ur Rahman, S. Haddadi and M. Daoud, *"Long-time protection of thermal correlations in a hybrid-spin system under random telegraph noise"*, Phys. Rev. **E** 106 (2022) 034122.
[70] T. Werlang, S. Souza, F.F. Fanchini and C.V. Boas, *"Robustness of quantum discord to sudden death"*, Phys. Rev. A. **80** (2009) 024103.
[71] M.P. Almeida, F. de Melo, M. Hor-Meyll, A. Salles, S.P. Walborn, *"Environment-induced sudden death of entanglement"*, Science **316** (2007) 579.
[72] H. P. Breuer and F. Petruccione, *"Theory of open quantum systems"*, Oxford, New York, (2002).
[73] V. Gorini, A. Kossakowski, and E.C.G. Sudarshan, *"Completely positive dynamical semigroups of n-level systems"*, J. Math. Phys. **17** (1976) 821.
[74] G. Lindblad, *"On the generators of quantum dynamical semigroups"*, Commun. Math. Phys. **48** (1976) 119-130.
[75] M.Feng, S. Cai, M. Tang, Y-C. Lai, *"Equivalence and its invalidation between non-Markovian and Markovian spreading dynamics on complex networks"*, Nat. Commun **10** (2019) 3748.
[76] G. Najarbashi, B. Seifi, *"Quantum phase transition in the Dzyaloshinskii-Moriya interaction with inhomogeneous magnetic field: Geometric approach"*, Quantum Inf. Process. **16** (2017) 40.
[77] A. Karlsson, M. Bourennane, *"Quantum teleportation using three-particle entanglement"*, Phys. Rev. A. **58** (1998) 4394.
[78] J.C. Hao, C.F. Li and G.C. Guo, *"Controlled dense coding using the Greenberger-Horne-Zeilinger state"*, Phys. Rev. A. **63** (2001) 054301.
[79] F. Benabdallah, K. El Anouz, J. Strecka and M. Daoud, *"Thermal non-classical correlation via skew information, quantum Fisher information, and quantum teleportation of a spin-1/2 Heisenberg trimer system"*, Eur. Phys. J. Plus **137** (2022)1096 .
[80] F. Benabdallah, K. Elanouz and M. Daoud, *"Toward the relationship between local quantum Fisher information and local quantum uncertainty in the presence of intrinsic decoherence"*, Eur. Phys. J. Plus (2022) 548.
[81] A.-Z. Hamid, M. Hossein, *"Transferring information through a mixed-five-spin chain channel",* Chin. Phys. B. **25** (2016) 080307.
[82] C.E. Shannon, *"A mathematical theory of communication"*, The Bell system technical journal **27** (1948) 379-423.
[83] E.T. Jaynes, *"Information theory and statistical mechanics"*, Phy. Rev. **106** (1957) 620.
[84] M. Keyl, "*Fundamentals of quantum information theory*", Phys. Rep. **369** (2002) 431-548.
[85] M.M. Wilde, "*From classical to quantum Shannon theory*", arXiv: 1106.1445 (2011).
[86] C.G. Timpson, "*Quantum information theory and the foundations of quantum mechanics*", arXiv: 0412063 (2004).
[87] H. Nyquist, "*Certain topics in telegraph transmission theory*", AIEE Trans, **47** (1928) 617-644.
[88] R.V.L. Hartley, "*Transmission of information*", Bell Syst. Techn. J, **7** (1928) 535-563.

[89] S. Verdu, "*Fifty years of shannon theory*", IEEE Transaction on information theory **44** (1998) 2057-2078.
[90] J. Watrous, "*The theory of quantum information*", Cambridge University Press (2018).
[91] R. Clausius, "*Ueber verschiedene für die Anwendung bequeme Formen der Hauptgleichungen der ämechanischen Wärmetheorie*", Ann. Phys, **201** (1865) 353-400.
[92] L. Boltzmann, "*Vorlesungen über Gastheorie*", 2 vols. Barth, Leipzig, 1898 (1896); transl. by S.G. Brush, "*Lectures on gas theory*", Cambridge University Press. London (1964).
[93] J. Honerkamp, "*Statistical physics: an Advanced approach with applications*", Springer (2013).
[94] S. Kullback and R. Leibler, "*On information and sufficiency*", Ann. Math. Statist. **22** (1951) 79-86.
[95] R.M. Gray, "*Entropy and information theory*", Springer (1990) 21-55.
[96] T.M. Cover and J.A. Thomas, "*Elements of information theory*", published by John Wiley and Sons, Inc. Print ISBN 0-471-06259-6 Online ISBN 0-471-20061-1 (1991).
[97] P.E. Griffiths, A. Pocheville, B. Calcott, K. Stotz, H. Kim and R. Knight, "*Measuring causal specificity*", Philos. Sci **82** (2015) 529.
[98] C.H. Bennett, D.P. DiVincenzo and J.A. Smolin, "*Capacities of quantum erasure channels*", Phys. Rev. Lett, **78** (1997) 3217.
[99] J. von Neumann, "*Wahrscheinlichkeitstheoretischer aufbau der quantenmechanik*", Nachr. Ges. Wiss. Göttingen, Mathematisch-Physikalische Klasse, **1** (1927) 245-272.
[100] L. Landau, "*Das dämpfungsproblem in der wellenmechanik*", Z. Physik **45** (1927) 430-441.
[101] V.B. Braginsky, B.B. Vladimir and Y.K. Farid, "*Quantum measurement*", Cambridge University Press, Cambridge (1995).
[102] H.M. Wiseman and J. M. Gerard, "*Quantum measurement and control*", Cambridge University Press, Cambrigde (2009).
[103] M. Le Bellac, "*A short introduction to quantum information and quantum computation*", Cambridge University Press, Cambridge (2006).
[104] H.E. Brandt, "*Positive operator-valued measure in quantum information processing*", Am. J. Phys **67** (1999) 434-439.
[105] S. Hamieh, R. Kobes and H. Zaraket, "*Positive-operator-valued measure optimization of classical correlations*". Phys. Rev. A **70** (2004) 052325.
[106] D. Mayers, "*Unconditional security in quantum cryptography*", J. ACM **48** (2001) 351-406.
[107] A.K. Ekert, "*Quantum cryptography based on Bell's theorem*", Phys. Rev. Lett. **67** (1991) 661.
[108] A. Steane, "*Quantum computing*", Rep. Prog. Phys. **61** (1998) 117.
[109] N. Gisin and R. Thew, "*Quantum communication*", Nat. Photon. **1** (2007) 165-171.
[110] B.W. Schumacher, "*Quantum coding*", Phys. Rev. A **51** (1995) 2738.
[111] B. Friedrich and D. Herschbach, "*Stern and Gerlach: How a bad cigar helped reorient atomic physics*", Phys. Today, **56** (2003) 53-59.
[112] R. Bijukar, "*Representation of qudits on a riemann sphere*", arXiv: 0604210 (2006).
[113] J. von Neuman, "*Mathematische Grundlagen der Quantenmechanik*", Springer, Berlin (1932); transl by E.T. Beyer, " *Mathematical Foundations of Quantum Mechanics*", Princeton University Press, Princeton (1955).
[114] H. Umegaki, "*Conditional expectation in an operator algebra IV. Entropy and information*", Kodai Math. Sem. Rep.**14** (1962) 59-85.
[115] V. Vedral, "*The role of relative entropy in quantum information theory*", Rev. Mod. Phy. **74** (2002) 197.

[116] K. Modi, A. Brodutch, H. Cable, T. Paterek and V. Vedral, "*The classical-quantum boundary for correlations: Discord and related measures*", Rev. Mod. Phys. **84** (2012) 1655-1707.
[117] N.J. Cerf and C. Adami, "*Negative entropy and information in quantum mechanics*", Phys. Rev. Lett. **79** (1997) 5194.
[118] C. Adami and N.J. Cerf, "*von Neumann capacity of noisy quantum channels*", Phys. Rev. A **56** (1997) 3470.
[119] C. Tsallis, "*Possible generalization of Boltzmann-Gibbs statistics*", J. Stat. Phys. **52** (1988) 479-487.
[120] G.A. Raggio, "*Properties of q-entropies*", J. Math. Phys. **36** (1995) 4785-4791.
[121] S. Morelli, C. Klöckl, Ch. Eltschka, J. Siewert and M. Huber, "*Dimensionally sharp inequalities for the linear entropy*", Linear. Algebra. Appl **584** (2020) 294-325.
[122] U. Fano, "*Description of states in quantum mechanics by density matrix and operator techniques*", Rev. Modern Phys. **29** (1957) 74.
[123] A.S. Holevo, "*Bounds for the quantity of information transmitted by a quantum communication channel*", Probl. Inform. Transm. **9** (1973) 177.
[124] C. Weedbrook, S. Pirandola, R. García-Patrón, N.J. Cerf, T.C. Ralph, J.H. Shapiro and S. Lloyd, "*Gaussian quantum information*", Rev. Mod. Phys. **84** (2012) 621.
[125] E. Schrödinger, "*Probability relations between separated systems*", Proc. Cambridge Phil. Soc. **32** (1936) 446-452.
[126] E. Schrödinger, "*Die gegenwärtige Situation in der Quantenmechanik*", Naturwissenschaften **23** (1935) 807-812. English translation by J. D. Trimmer, "*The present situation in quantum mechanics: a translation of Schrödinger's "cat paradox"*", Proc. Am. Philos. Soc. **124** (1980) 323-338. Proc. Am. Philos. Soc. **124** (1980) 323-338.
[127] J. S. Bell, "*On the Einstein-Podolsky-Rosen paradox*", Physics **1** (1964) 195.
[128] S. J. Freedman and J.F. Clauser, "*Experimental test of local hidden-variable theories*", Phys. Rev. Lett. **28** (1972) 938-941.
[129] A. Aspect, J. Dalibard and G. Roger, "*Experimental Test of Bell's Inequalities Using Time-Varying*", Phys. Rev. Lett. **49** (1982) 1804-1807.
[130] M. A. Rowe, D. Kielpinski, V. Meyer, *et al.*, "*Experimental violation of a Bell's inequality with efficient detection*", Nature **409** (2001) 791-794.
[131] R.F. Werner, "*Quantum states with Einstein-Podolsky-Rosen correlations admitting a hidden-variable model*", Phys. Rev. A **40** (1989) 4277.
[132] J. F. Clauser, M. A. Horne, A. Shimony and R. A. Holt, "*Proposed Experiment to Test Local Hidden-Variable Theories*", Phys. Rev. Lett **24** (1970) 549.
[133] D. Bouwmeester, J. W. Pan, K. Mattle, M. Eibl, H. Weinfurter and A. Zeilinger, "*Experimental Quantum Teleportation*", Nature **390** (1997) 575-579.
[134] E. Chitambar, D. Leung, L. Mancinska, M. Ozols and A. Winter, "*Everything You Always Wanted to Know About LOCC (But Were Afraid to Ask)*", Commun. Math. Phys. **328** (2014) 303–326.
[135] A. Peres, 1997, "*Quantum Theory: Concepts and Methods*", Kluwer, Dordrecht, (1997).
[136] A. Ekert and P. L. Knight, "*Entangled quantum systems and the Schmidt decomposition*", Am. J. Phys. **63** (1995) 415-423.
[137] E. Schmidt, "*Zur Theorie der linearen und nichtlinearen Integralgleichungen*", Math. Ann. **63** (1907) 433-476.
[138] C.H. Bennett, D.P. Di Vincenzo, J. Smolin and W.K. Wootters, "*Mixed-state entanglement and quantum error correction*", Phys. Rev. A **54** (1997) 3814.
[139] A. Peres, "*Separability criterion for density matrices*", Phys. Rev. Lett, **77** (1996) 1413.
[140] M. Horodecki, P. Horodecki et R. Horodecki, *"On the necessary and sufficient conditions for separability of mixed quantum states"*, Phy. Lett. A, **223** (1996) 1-8.

[141] P. Horodecki, "Separability criterion and inseparable mixed states with positive partial transposition", Phys. Lett. A **232** (1997) 333-339.
[142] M. Horodecki, P. Horodecki, and R. Horodecki, "Mixed-state entanglement and distillation: Is there a "bound" entanglement in nature?", Phys. Rev. Lett. **80** (1998) 5239.
[143] D.P. DiVincenzo, P.W. Shor, J.A. Smolin, B.M. Terhal and A.V. Thapliyal, "*Evidence for bound entangled states with negative partial transpose*", Phys. Rev. A **61** (2000) 62312.
[144] W. Dür, J. I. Cirac, M. Lewenstein and D. Bruß, "*Distillability and partial transposition in bipartite systems*", Phys. Rev. A **61** (2000) 62313.
[145] O. Krueger and R.F. Werner, "*Some open problems in quantum information theory*", arXiv preprint quant-ph/0504166.
[146] O. Gühne, and G. Tóth, "*Entanglement detection*", Phys. Rep. **474** (2009) 1-75.
[147] B.M. Terhal, "*Bell inequalities and the separability criterion*", Phys. Lett. A **271** (2000) 319-326.
[148] M. Barbieri, F. De Martini, G. Di Nepi, P. Mataloni, G.M. D'Ariano, C. Macchiavello, *Detection of entanglement with polarized photons: Experimental realization of an entanglement witness*, Phys. Rev. Lett. **91** (2003) 227901.
[149] M. Bourennane, M. Eibl, C. Kurtsiefer, S. Gaertner, H. Weinfurter, O. Gühne, P. Hyllus, D. Bruß, M. Lewenstein, A. Sanpera, "*Experimental detection of multipartite entanglement using witness operators*", Phys. Rev. Lett. **92** (2004) 087902.
[150] H. Weinfurter, M. Żukowski, "*Four-photon entanglement from down-conversion*", Phys. Rev. A **64** (2001) 010102.
[151] V. Vedral, M.B. Plenio, M.A. Rippin, P.L. Knight, "*Quantifying entanglement*", Phys. Rev. Lett. **78** (1997) 2275.
[152] C. Eltschka and S. Jens, "*Quantifying entanglement resources*", J. Phys. A : Math. Theor. **47** (2014) 424005.
[153] M.B. Plenio and S. Virmani, "*An introduction to entanglement measures"*, Quantum Inf. Comput. **7** (2007) 1-51.
[154] S. Hill and W.K. Wootters, "*Entanglement of a pair of quantum bits*", Phys. Rev. Lett. **78** (1997) 5022.
[155] P. Rungta, V. Bužek, C.M. Caves, M. Hillery and G.J. Milburn, "*Universal state inversion and concurrence in arbitrary dimensions*", Phys. Rev. A **64** (2001) 042315.
[156] P. Rungta and C.M. Caves, "*Concurrence-based entanglement measures for isotropic states*", Phys. Rev. A **67** (2003) 012307.
[157] T. Yu and J. H. Eberly, "*Evolution from Entanglement to Decoherence of Bipartite Mixed "X" States*", Comput. **7** (2007) 459-468.
[158] V. Vedral, M.B. Plenio, "*Entanglement measures and purification procedures*", Phys. Rev. A **57** (1998) 1619.
[159] K.G.H. Vollbrecht and R.F. Werner, "*Entanglement measures under symmetry*", Phys. Rev. A **64** (2001) 062307.
[160] M.J. Donald, M. Horodecki and O. Rudolph, "*The uniqueness theorem for entanglement measures"*, J. Math. Phys. **43** (2002) 4252.
[161] M. Horodecki, P. Horodecki, and R. Horodecki, "*Limits for entanglement measures*", Phys. Rev. Lett. **84** (2000). 2014 .
[162] G. Vidal, "*Entanglement monotones*", J. Mod. Opt. **47** (2000) 355-376.
[163] A. Miranowic and A. Grudka, "*Ordering two-qubit states with concurrence and negativity*", Phys. Rev. A 70 (2004) 032326.
[164] F. Verstraete, K. M. R. Audenaert, J. Dehaene, and B. De Moor, "*A comparison of the entanglement measures negativity and concurrence*", J. Phys. A **34** (2001) 10327.
[165] M.B. Plenio, "*Logarithmic negativity: a full entanglement monotone that is not convex*", Phys. Rev. Lett. **95** (2005) 090503.

[166] C. Sabin, G. García-Alcaine, "A *classification of entanglement in three-qubit systems*", European Phys. J. D **48** (2008) 435–442.
[167] V. Coffman, J. Kundu and W. K. Wootters, "*Distributed entanglement*", Phys. Rev. A, **61** (2000) 052306.
[168] T.J. Osborne and F. Verstraete, "*General monogamy inequality for bipartite qubit entanglement*", Phys. Rev. Lett. **96** (2006) 220503.
[169] G. Gour, "*Monogamy of quantum entanglement and other correlations",* Phys. Rev. A. **71** (2005) 012318.
[170] E. Knill and R. Laflamme, "*Power of one bit of quantum information*", Phys. Rev. Lett. 81 (1998) 5672.
[171] A. Ferraro, D. Cavalcanti, F.M. Cucchietti and A. Acín, *"Almost all quantum states have nonclassical correlations"*, Phys. Rev. A **81** (2010) 052318.
[172] M. Piani, *"Problem with geometric discord"*, Phys. Rev. A **86** (2012) 034101.
[173] S. Luo, S. Fu, *"Measurement-induced nonlocality"*, Phys. Rev. Lett. **106** (2011) 120401.
[174] M. Piani and G. Adesso, *"Quantumness of correlations revealed in local measurements exceeds entanglement"*, Phys. Rev. A **85** (2012) 040301.
[175] M.S. Tame, M. Paternostro, M.S. Kim and V. Vedral, *"Natural three-qubit interactions in one-way quantum computing"*, Phys. Rev. A 73 (2006) 022309.
[176] K. Berrada, *"Classical and quantum correlations for two-mode coherent-state superposition"*, Opt. Commun. **285** (2011) 2227-2235 .
[177] F. Ciccarello and V. Giovannetti, *"Creating quantum correlations through local nonunitary memoryless channels"*, Phys. Rev. A **85** (2012) 010102.
[178] F. Ciccarello and V. Giovannetti, *"Local-channel-induced rise of quantum correlations in continuous-variable systems"*, Phys. Rev. A **85** (2012) 022108.
[179] S.P. Walborn, D.S. Lemelle, M.P. Almeida and P.H. Souto Ribeiro, "*Quantum Key Distribution with Higher-Order Alphabets Using Spatially Encoded Qudits*", Phys. Rev. Lett. **96** (2006) 090501.
[180] A. Streltsov and W.H. Zurek, *"Quantum discord cannot be shared"*, Phys. Rev. Lett. **111** (2013) 040401.
[181] C.-Z. Wang, C.-X. Li, L.-Y. Nie and J.-F. Li, *"Classical correlation and quantum discord mediated by cavity in two coupled qubits"*, J. Phys. B: At. Mol. Opt. Phys. **44** (2010) 015503.
[182] M. Koachi and A. Winter, *"Monogamy of quantum entanglement and other correlations"*, Phys. Rev. A 69 (2004) 022309.
[183] S. Luo and S. Fu, *"Geometric measure of quantum discord"*, Phys. Rev. A **82** (2010) 034302.
[184] J. Batle, A. Plastino, A.R. Plastino, M. Casas, *"Properties of a geometric measure for quantum discord"*, arXiv:1103.0704v4 (2011).
[185] S. Rana and P. Parashar, *"Tight lower bound on geometric discord of bipartite states"*, Phys. Rev. A 85 (2012) 024102.
[186] D. Girolami and G. Adesso, *"Interplay between computable measures of entanglement and other quantum correlations"*, Phys. Rev. A. **84** (2011) 052110.
[187] S. Vinjanampathy and A.R.P. Rau, *"Quantum discord for qubit–qudit systems"*, J. Phys. A: Math. Theor. **45** (2012) 095303.
[188] A. Bera, T. Das, D. Sadhukhan, S. Singha Roy, A. Sen(De) and U. Sen, *"Quantum discord and its allies: a review of recent progress"*, Rep. Prog. Phys. **81** (2017) 024001.
[189] X.N. Zhu, S.M. Fei and X. Li-Jost, *"Analytical expression of quantum discord for rank-2 two-qubit states"*, Quantum. Inf. Process. **17** (2018) 234.
[190] M.D. Lang and C.M. Caves, *"Quantum discord and the geometry of Bell-diagonal states"*, Phys. Rev. Lett. **105** (2010) 150501.

[191] T.J. Osborne, *"Entanglement measure for rank-2 mixed states"*, Phys. Rev. A. **72** (2005) 022309.

[192] S. Xu, X. Song and L. Ye, *"Measurement-induced disturbance and negativity in mixed-spin XXZ model"*, Quantum. Inf. Process. **13** (2014) 1013–1024.

[193] B.R. Rao, R. Srikanth, C. M. Chandrashekar and S. Banerjee, *"Quantumness of noisy quantum walks: a comparison between measurement-induced disturbance and quantum discord"*, Phys. Rev. A **83** (2011) 064302.

[194] E.P. Wigner, M.M. Yanasse, *"Information contents of distributions"*, Proc. Natl. Acad. Sci. USA **49** (1963) 910-918.

[195] S. Luo, *"Wigner-Yanase skew information and uncertainty relations"*, Phys. Rev. Lett. **91** (2003) 180403.

[196] S. Wang, H. Li, X. Lu, G.-L. Long, *"Closed form of local quantum uncertainty and a sudden change of quantum correlations"*, arXiv:quant-ph/1307.0576v2 (2013).

[197] D. Girolami, *"Observable Measure of Quantum Coherence in Finite Dimensional Systems"*, Phys. Rev. Lett. **113** (2014) 170401.

[198] T. Baumgratz, M. Cramer and M.B. Pleino, *"Quantifying Coherence"*, Phys. Rev. Lett. **113** (2014) 140401.

[199] Z. Ficek and S. Swain, *"Quantum Interference and Coherence: Theory and Experiments"*, Springer Series in Optical Sciences (Springer, Berlin, 2005).

[200] T. Bauch, F. Lombardi, F. Tafuri, A. Barone, G. Rotoli, P. Delsing and T. Claeson, *"Macroscopic Quantum Tunneling in d-Wave $YBa_2Cu_3O_{7-\delta}$ Josephson Junctions"*, Phys. Rev. Lett. **94** (2005) 087003.

[201] J. Q. You and F. Nori, *"Atomic physics and quantum optics using superconducting circuits"*, Nature **474** (2011) 589.

[202] A. Streltsov, G. Adesso and M.B. Plenio, *"Colloquium: quantum coherence as a resource"*, Rev. Mod. Phys. **89** (2017) 041003

[203] F. G. S. L. Brandao, M. Horodecki, J. Oppenheim, J. M. Renes, R. W. Spekkens, *"Resource Theory of Quantum States Out of Thermal Equilibrium"*, Phys. Rev. Lett. **111** (2013) 250404.

[204] M.L. Hu, Y.Y. Gao and H. Fan, *" Steered quantum coherence as a signature of quantum phase transitions in spin chains"*, Phys. Rev. A **101** (2020) 032305.

[205] M.L. Hu, F. Fang and H. Fan, *"Finite-size scaling of coherence and steered coherence in the Lipkin-Meshkov-Glick model"*, Phys. Rev. A **104** (2021) 062416.

[206] F. Zhao, D. Wang and L. Ye, *"Relationship between entanglement and coherence in some two-qubit states"*, Int. J. Theor. Phys. 61 (2022) 10.

[207] H. Dolatkhah, S. Haseli, S. Salimi and A.S. Khorashad, *"Tightening the entropic uncertainty relations for multiple measurements and applying it to quantum coherence"*, Quantum. Inf. Process. **18** (2019) 13.

[208] B.F. Xie, F. Ming, D. Wang, L. Ye and J.L Chen, *"Optimized entropic uncertainty relations for multiple measurements"*, Phys. Rev.A **104** (2021) 062204.

[209] S. Luo, *"Wigner–Yanase skew information vs. quantum fisher information"*, Proc. Am. Math. Soc. **132** (2003) 885.

[210] Y. Akbari-Kourbolagh, M. Azhdargalam, *"Entanglement criterion for multipartite systems based on quantum Fisher information"*, Phys. Rev. A **99** (2019) 012304.

[211] S. Haseli, *"Local quantum Fisher information and local quantum uncertainty in two-qubit Heisenberg XYZ chain with Dzyaloshinskii–Moriya interactions"*, Laser Phys. **30** (2020) 105203.

[212] A.B.A. Mohamed, E. Khalil, M.M. Selim, H. Eleuch, *"Quantum Fisher information and bures distance correlations of coupled two charge-qubits inside a coherent cavity with the intrinsic decoherence"*, Symmetry **13** (2021) 2.

[213] X. Hu, H. Fan, D.L. Zhou, W.-M. Liu, *"Necessary and sufficient conditions for local creation of quantum correlation"*, Phys. Rev. A **85** (2012) 032102.

[214] M. Horodecki, J. Oppenheim, A. Winter, *"Partial quantum information"*, Nature **436** (2005) 673–676.

[215] R. Ursin, T. Jennewein, M. Aspelmeyer, R. Kaltenbaek, M. Lindenthal, P. Walther, and A. Zeilinger, *"Communications: Quantum teleportation across the Danube"*, Nature, **430** (2004) 849.

[216] F. Zhu, W. Zhang, Y. Sheng and Y. Huang, *"Experimental long-distance quantum secure direct communication"*, Sci. Bull. **62** (2017) 1519-1524.

[217] Y Xia, J Song, PM Lu and HS Song, *"Controlled teleportation of a multi-photon GHZ polarization-entangled state using linear optical elements"*, Eur. Phys. J. D **61** (2011) 493-498.

[218] S.K. Liao, W.Q. Cai, W.Y. Liu, L. Zhang, Y. Li, J.G. Ren, J. Yin et al, *"Satellite-to-ground quantum key distribution"*, Nature **549** (2017) 43-47.

[219] W. Heisenberg, *"Über den anschaulichen Inhalt der quanten theoretischen Kinematik und Mechanik"*, Z. Phys. **43** (1927) 172

[220] J. Oppenheim and S. Wehner, *"The uncertainty principle determines the nonlocality of quantum mechanics"*, Science. **330** (2010) 1072.

[221] S. L. Luo, *"Quantum versus classical uncertainty"*, Theor. Math. Phys. **143** (2005) 681-688.

[222] M. Berta, M. Christandl, R. Colbeck, J. M. Renes and R. Renner, *"The uncertainty principle in the presence of quantum memory"*, Nat. Phys. **6** (2010) 659-662 .

[223] N. Li, S. Luo, *"Classical states versus separable states"*, Phys. Rev. A **78** (2008) 024303.

[224] M. Ali, *"Local quantum uncertainty for multipartite quantum systems"*, Eur. Phys. J. D **74** (2020) 186.

[225] I.B. Coulamy, J.H. Warnes, M.S. Sarandy, A. Saguia, *"Scaling of the local quantum uncertainty at quantum phase transitions"*, Phys. Lett. A. **380** (2016) 1724-1728.

[226] S. Luo and Q. Zhang, *"Informational distance on quantum-state space"*, Phys. Rev. A **69** (2004) 032106.

[227] W. Roga, D. Spehner and F. Illuminati, *"Geometric measures of quantum correlations: characterization, quantification, and comparison by distances and operations"*, J. Phys. A: Math. Theor. **49** (2016) 235301.

[228] C. Cruz and M. Anka, *"Quantifying quantum coherence in a metal-silicate framework"*, EPL **130** (2020) 30006.

[229] A. Streltsov, U. Singh, H.S. Dhar, M.N. Bera and G. Adesso, *"Measuring quantum coherence with entanglement"*, Phys. Rev. Lett. **115** (2015) 020403.

[230] M.J. Zhao, T. Ma, Q. Quan, H. Fan and R. Pereira, *"l_1-norm coherence of assistance"*, Phys. Rev. A **100** (2019).

[231] C.W. Helstrom, "Quantum detection and estimation theory", Academic, New York, 1976.

[232] S.L. Braunstein and C.M. Caves, "*Statistical distance and the geometry of quantum states"*, Phys. Rev. Lett. **72** (1994) 3439.

[233] M.G. A. Paris, *"Quantum estimation for quantum technology"*, Int. J. Quantum Inf. **7** (2009) 125.

[234] K. El Anouz, C.P. Onyenegecha, A.I. Opara, A. Salah and A. El Allati, *"Dynamics of quantum Fisher information and quantum coherence of two interacting atoms under time–fractional analysis"*, JOSA. B. **39** (2022) 979-989.

[235] V. Giovannetti, S. Lloyd, L. Maccone, *"Quantum-enhanced measurements: beating the standard quantum limit"*, Science **306** (2004) 1330-1336.

[236] S.F. Huelga, C. Macchiavello, T. Pellizzari, A.K. Ekert, M.B. Plenio, J.I. Cirac, *"Improvement of frequency standards with quantum entanglement"*, Phys. Rev. Lett. **79** (1997) 3865.

[237] H. Strobel, W. Muessel, D. Linnemann, T. Zibold, D. B. Hume, L. Pezzè, A. Smerzi, et M. K. Oberthaler, *"Fisher information and entanglement of non-gaussian spin states"*, Science. **345** (2014) 6195.

[238] S. Knysh, V.N. Smelyanskiy, G.A. Durkin, *"Scaling, laws for precision in quantum interferometry and the bifurcation landscape of the optimal state"*, Phys. Rev. A **83** (2011) 021804 .

[239] J. Liu, X. Jing, X. Wang, *"Phase-matching condition for enhancement of phase sensitivity in quantum metrology"*, Phys. Rev. A **88** (2013) 042316.

[240] J. Liu, H. Yuan, X.-M. Lu, X. Wang, *"Quantum Fisher information matrix and multiparameter estimation"*, J. Phys. A: Math. Theor. **53** (2020) 023001.

[241] L. Vaidman, *"Teleportation of quantum states"*, Phys. Rev. A **49** (1994) 1473.

[242] S.L. Braunstein and H.J. Kimble, *"Teleportation of continuous quantum variables"*, Phys. Rev. Lett. **80** (1998) 869.

[243] A. Furusawa, J.L. SØrensen, S.L. Braunstein, C.A. Fuchs, H.J. Kimble and E.S. Polzik, *"Unconditional quantum teleportation"*, Science. **282** (1998) 706-709.

[244] G. Bowen, S. Bose, *"Teleportation as a depolarizing quantum channel, relative entropy, and classical capacity"*, Phys. Rev. Lett. **87** (2001) 267901.

[245] R. Jozsa, *"Fidelity for mixed quantum states"*, J. Mod. Opt. **41** (1994) 12.

[246] A. Ur Rahman, S. Haddadi, M.R. Pourkarimi and M. Ghominejad, *" Fidelity of quantum states in a correlated dephasing channel"*, Laser. Phys. Lett. **19** (2022) 035204.

[247] Y.-X. Xi, Y.-X. Huang, *"Quantum teleportation in a three-qubit Heisenberg chain with Dzyaloshinsky Moriya interaction"*, Mod. Phys. Lett. B **29** (2015) 20.

[248] J.-L. Guo, M. Qing-Xia, H.-S. Song, *"Magnetic impurity effects on quantum teleportation via the three-qubit Heisenberg XX model"*, Phys. Scr. **77** (2008) 035004.

[249] P. Rebentrost, M. Mohseni, I. Kassal, S. Lloyd and A. Aspuru-Guzik1, "Environment-assisted quantum transport", New J. Phys. **11** (2009) 033003.

[250] M.O. Scully and M.S. Zubairy, *"Quantum Optics"*, Cambridge University Press, Cambridge, (1997).

[251] J. Preskill, *"Quantum computing and the entanglement frontier"*, arXiv:1203.5813 (2012).

[252] P.M. Harrington, E.J. Mueller, K.W. Murch, *"Engineered dissipation for quantum information science"*, Nat. Rev. Phys. **4** (2022) 660–671.

[253] I. Rotter, J.P. Bird, *"A review of progress in the physics of open quantum systems: theory and experiment"*, Rep. Prog. Phys. **78** (2015) 114001.

[254] T. Ladd, F. Jelezko, R. Laflamme, Y. Nakamura, C. Monroe and J.L. O'Brien, *"Quantum computers"*, Nature **464** (2010) 45-53.

[255] M.H. Devoret and R.J. Schoelkopf, *"Superconducting circuits for quantum information: an outlook"*, Science **339** (2013) 1169-1174.

[256] I. de Vega and D. Alonso, *"Dynamics of non-Markovian open quantum systems"*, Rev. Mod. Phys. **89** (2017) 15001.

[257] A. Rivas, A.D. K. Plato, S.F. Huelga and M.B. Plenio, *"Markovian master equations: a critical study"*, New J. Phys. **12** (2010) 113032.

[258] A. Rivas and S.F. Huelga, *"Open quantum systems"*, Springer Berlin. Heidelberg. (2012).

[259] A. Nazir, *"Photon statistics from a resonantly driven quantum dot"*, Phys. Rev. B **78** (2008) 153309.

[260] K. Kraus, A. Böhm, J.D. Dollard and W.H. Wootters, *"States, Effects, and Operations: Fundamental Notions of Quantum Theory (Lecture Notes in Physics)"*, Springer-Verlag, Heidelberg, (1983).

[261] M.M. Wolf and J.I. Cirac, *"Dividing quantum channels"*, Commun. Math. Phys. **279** (2008) 147.
[262] H.P. Breuer, E.M. Laine and J. Piilo , *"Measure for the degree of non-Markovian behavior of quantum processes in open systems"*, Phys. Rev. Lett. **103** (2009) 210401.
[263] H.P. Breuer, E.M. Laine, J. Piilo, B. Vacchini, *"Colloquium: Non-Markovian dynamics in open quantum systems"*, Rev. Mod. Phys. **88** (2016) 021002.
[264] E. B. Davies, *"Quantum Theory of Open Systems"*, Academic Press, New York, (1976).
[265] S. Nakajima, *"On quantum theory of transport phenomena"*, Progr. Theor. Phys. **20** (1958) 948 .
[266] H. Carmichael, *"An open systems approach to quantum optics: Lecture notes in physics"*, Springer-Verlag, Berlin, (1993).
[267] H. Paul, *"Induzierte Emission bei starker Einstrahlung"*, Ann. Phys. (Leipzig) **11** (1963) 411-412.
[268] E.T. Jaynes and F.W. Cummings, *"Comparison of quantum and semiclassical radiation theories with application to the beam maser"*, Proc. IEEE **51** (1963) 89-109.
[269] S. Daffer, K. Wodkiewicz, J. D. Cresser, and J. K. Mclver, *"Depolarizing channel as a completely positive map with memory"*, Phys. Rev. A **70** (2004) 010304(R).
[270] J. P. G. Pinto, G. Karpat and F.F. Fanchini, *"Sudden change of quantum discord for a system of two qubits"*, Phys. Rev. A **88** (2013) 034304.
[271] M. Ali, *"Dynamics of genuine multipartite entanglement under local non-Markovian dephasing"*, Phys. Lett. A **378** (2014) 2048.
[272] H. P. Breuer, "*Foundations and measures of quantum non-Markovianity"*, J. Phys. B: At. Mol. Opt. Phys. **45** (2012) 15.
[273] M.J.W. Hall, J.D. Cresser, L. Li and E. Andersson, *"Canonical form of master equations and characterization of non-Markovianity"*, Phys. Rev. A **89** (2014) 042120.
[274] D. Chruściński and A. Kossakowski, *"Markovianity criteria for quantum evolution"*, J. Phys. B: At. Mol. Opt. Phys. **45** (2012) 154002.
[275] A. Rivas, S.F. Huelga and M.B. Plenio, *"Quantum non-Markovianity: characterization, quantification and detection"*, Rep. Theor. Phys. **77** (2014) 094001.
[276] E.M. Laine, K. Luoma, and J. Piilo, *"Local-in-time master equations with memory effects: applicability and interpretation"*, J. Phys. B: At. Mol. Opt. Phys. **45** (2012) 154004.
[277] G. Milburn, *"Intrinsic decoherence in quantum mechanics"*, Phys. Rev. A **44** (1991) 5401.
[278] M. Berman, R. Kosloff, H. Tal-Ezer, *"Solution of the time-dependent Liouville-von Neumann equation: dissipative evolution"*, J. Phys. A Math. Gen. **25** (1992) 1283.
[279] L. Qiu, A.M. Wang and X.Q. Su, *"Effect of Dzyaloshinskill-Moriya anisotropic antisymmetric interaction and intrinsic decoherence on entanglement teleportation"*, Physica. A **387** (2008) 6686.
[280] A.-B.A. Mohamed and N. Metwally, *"Non-classical correlations based on skew information of entangled two qubit-system with non-mutual interaction under an intrinsic decoherence"*, Ann. Phys. **381** (2017) 137-150.

Résumé

Le domaine multidisciplinaire de l'informatique quantique et du traitement de l'information vise à comprendre comment l'information peut être traitée selon les lois de la physique quantique. Des ressources non classiques telles que l'intrication, la corrélation quantique et la cohérence sont utilisées dans le calcul, ce qui rend les protocoles d'informatique quantique supérieurs à l'informatique classique traditionnelle. Cependant, des défis subsistent pour améliorer l'efficacité et vaincre les échecs associés à la technologie quantique. Ainsi, l'exploitation de ces ressources dans les systèmes quantiques composites est cruciale pour optimiser et assurer la transmission sécurisée ainsi que la préservation de l'information quantique. Cette thèse propose une étude approfondie sur la théorie des ressources quantiques des corrélations quantiques, y compris le concept d'intrication et les corrélations non classiques au-delà de l'intrication. Il présente divers outils théoriques de quantification de ces ressources et explore les relations intrinsèques entre elles. Une application directe de ces ressources, à savoir la mise en œuvre des protocoles de téléportation quantique est également évoquée. La thèse comprend également des contributions à la dynamique exacte de ces ressources quantiques dans différents modèles de systèmes quantiques ouverts et des stratégies pour éliminer les effets de décohérence et préserver les corrélations quantiques pour améliorer l'information quantique et les protocoles informatiques.

Mots-clefs: Intrication quantique, corrélation quantique, cohérence quantique, information de Fisher quantique, téléportation quantique, systèmes quantiques ouverts.

Abstract

The multidisciplinary field of quantum computing and information processing aims to understand how information can be processed according to the laws of quantum physics. Non-classical resources such as entanglement, quantum correlation, and coherence are used in computation, making quantum computing protocols superior to traditional classical computing. However, challenges remain in improving the efficiency and overcoming failures associated with quantum technology. Thus, exploiting these resources in composite quantum systems is crucial to optimize and ensure the secure transmission as well as preservation of quantum information. This thesis proposes a deeper investigation into the quantum resource theory of quantum correlations, including the concept of entanglement and non-classical correlations beyond entanglement. It presents various theoretical tools for quantifying these resources and explores the intrinsic relationships between them. A direct application of these resources, namely the implementation of quantum teleportation protocols is also discussed. The thesis also includes contributions to the exact dynamics of these quantum resources in different models of open quantum systems and strategies to eliminate decoherence effects and preserve quantum correlations to improve quantum information and computing protocols.

Key Words: Quantum entanglement, quantum correlation, quantum uncertainty, quantum coherence, quantum Fisher information, quantum teleportation, open quantum systems.

Année Universitaire : 2022/2023